HERPESVIRUS LATENCY

EDITED BY: Benedikt B. Kaufer, Louis Flamand, Randall J. Cohrs,
Benjamin G. Dewals and Benoit Muylkens

PUBLISHED IN: Frontiers in Microbiology

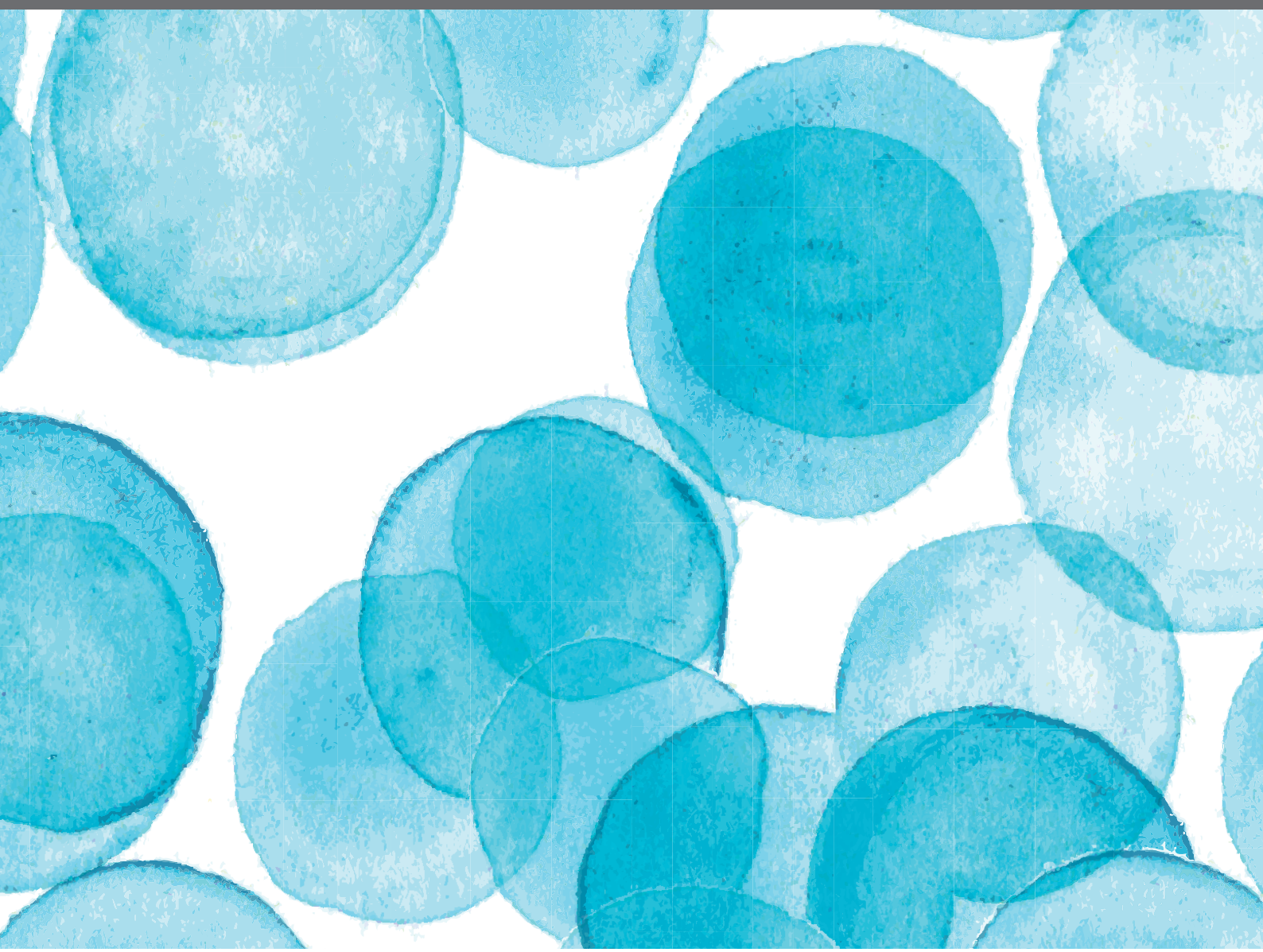

frontiers Research Topics

frontiers

ISSN 1664-8714
ISBN 978-2-88966-001-8
DOI 10.3389/978-2-88966-001-8

About Frontiers

Frontiers is more than just an open-access publisher of scholarly articles: it is a pioneering approach to the world of academia, radically improving the way scholarly research is managed. The grand vision of Frontiers is a world where all people have an equal opportunity to seek, share and generate knowledge. Frontiers provides immediate and permanent online open access to all its publications, but this alone is not enough to realize our grand goals.

Frontiers Journal Series

The Frontiers Journal Series is a multi-tier and interdisciplinary set of open-access, online journals, promising a paradigm shift from the current review, selection and dissemination processes in academic publishing. All Frontiers journals are driven by researchers for researchers; therefore, they constitute a service to the scholarly community. At the same time, the Frontiers Journal Series operates on a revolutionary invention, the tiered publishing system, initially addressing specific communities of scholars, and gradually climbing up to broader public understanding, thus serving the interests of the lay society, too.

Dedication to Quality

Each Frontiers article is a landmark of the highest quality, thanks to genuinely collaborative interactions between authors and review editors, who include some of the world's best academicians. Research must be certified by peers before entering a stream of knowledge that may eventually reach the public - and shape society; therefore, Frontiers only applies the most rigorous and unbiased reviews.
Frontiers revolutionizes research publishing by freely delivering the most outstanding research, evaluated with no bias from both the academic and social point of view. By applying the most advanced information technologies, Frontiers is catapulting scholarly publishing into a new generation.

What are Frontiers Research Topics?

Frontiers Research Topics are very popular trademarks of the Frontiers Journals Series: they are collections of at least ten articles, all centered on a particular subject. With their unique mix of varied contributions from Original Research to Review Articles, Frontiers Research Topics unify the most influential researchers, the latest key findings and historical advances in a hot research area! Find out more on how to host your own Frontiers Research Topic or contribute to one as an author by contacting the Frontiers Editorial Office: researchtopics@frontiersin.org

HERPESVIRUS LATENCY

Topic Editors:
Benedikt B. Kaufer, Freie Universität Berlin, Germany
Louis Flamand, Laval University, Canada
Randall J. Cohrs, University of Colorado, United States
Benjamin G. Dewals, University of Liège, Belgium
Benoit Muylkens, University of Namur, Belgium

Citation: Kaufer, B. B., Flamand, L., Cohrs, R. J., Dewals, B. G., Muylkens, B., eds. (2020). Herpesvirus Latency. Lausanne: Frontiers Media SA.
doi: 10.3389/978-2-88966-001-8

Table of Contents

05 ***Autophagy Quantification and STAT3 Expression in a Human Skin Organ Culture Model for Innate Immunity to Herpes Zoster***
Erin M. Buckingham, James Girsch, Wallen Jackson, Jeffrey I. Cohen and Charles Grose

14 ***Varicella Virus-Host Interactions During Latency and Reactivation: Lessons From Simian Varicella Virus***
Océane Sorel and Ilhem Messaoudi

23 ***"Novel" Triggers of Herpesvirus Reactivation and Their Potential Health Relevance***
Tobias Stoeger and Heiko Adler

27 ***The Critical Role of Genome Maintenance Proteins in Immune Evasion During Gammaherpesvirus Latency***
Océane Sorel and Benjamin G. Dewals

41 ***Herpes Virus Reactivation in Astronauts During Spaceflight and Its Application on Earth***
Bridgette V. Rooney, Brian E. Crucian, Duane L. Pierson, Mark L. Laudenslager and Satish K. Mehta

50 ***Arachidonic Acid Derived Lipid Mediators Influence Kaposi's Sarcoma-Associated Herpesvirus Infection and Pathogenesis***
Jayashree A. Chandrasekharan and Neelam Sharma-Walia

67 ***Comparison of HEp-2 and Vero Cell Responses Reveal Unique Proapoptotic Activities of the Herpes Simplex Virus Type 1 α0 Gene Transcript and Product***
Marie L. Nguyen, Elisabeth Gennis, Kristen C. Pena and John A. Blaho

86 ***Simian Varicella Virus DNA in Saliva and Buccal Cells After Experimental Acute Infection in Rhesus Macaques***
Vicki Traina-Dorge, Satish Mehta, Bridgette Rooney, Brian Crucian, Lara Doyle-Meyers, Arpita Das, Colin Coleman, Maria Nagel and Ravi Mahalingam

93 ***Human Cytomegalovirus Latency and Reactivation in Allogeneic Hematopoietic Stem Cell Transplant Recipients***
Lauren Stern, Barbara Withers, Selmir Avdic, David Gottlieb, Allison Abendroth, Emily Blyth and Barry Slobedman

106 ***Chromatin Profiles of Chromosomally Integrated Human Herpesvirus-6A***
Anthony J. Saviola, Cosima Zimmermann, Michael P. Mariani, Sylvia A. Signorelli, Diana L. Gerrard, Joseph R. Boyd, Darren J. Wight, Guillaume Morissette, Annie Gravel, Isabelle Dubuc, Louis Flamand, Benedikt B. Kaufer and Seth Frietze

118 ***Targeted Promoter Replacement Reveals That Herpes Simplex Virus Type-1 and 2 Specific VP16 Promoters Direct Distinct Rates of Entry Into the Lytic Program in Sensory Neurons*** **in vivo**
Richard L. Thompson and Nancy M. Sawtell

135 ***Modeling Varicella Zoster Virus Persistence and Reactivation – Closer to Resolving a Perplexing Persistent State***
Lillian Laemmle, Ronald S. Goldstein and Paul R. Kinchington

150 ***Persistence of a T Cell Infiltrate in Human Ganglia Years After Herpes Zoster and During Post-herpetic Neuralgia***
Jeremy P. Sutherland, Megan Steain, Michael E. Buckland, Michael Rodriguez, Anthony L. Cunningham, Barry Slobedman and Allison Abendroth

157 ***Epigenetic Regulation of Kaposi's Sarcoma-Associated Herpesvirus Latency***
Mel Campbell, Wan-Shan Yang, Wayne W. Yeh, Chen-Hsuan Kao and Pei-Ching Chang

frontiers in Microbiology

ORIGINAL RESEARCH
published: 05 December 2018
doi: 10.3389/fmicb.2018.02935

Autophagy Quantification and STAT3 Expression in a Human Skin Organ Culture Model for Innate Immunity to Herpes Zoster

*Erin M. Buckingham[1], James Girsch[1], Wallen Jackson[1], Jeffrey I. Cohen[2] and Charles Grose[1]**

[1] Virology Laboratory, Children's Hospital, University of Iowa, Iowa City, IA, United States, [2] Laboratory of Infectious Diseases, National Institute of Allergy and Infectious Diseases, National Institutes of Health, Bethesda, MD, United States

The goal of this project was to document the autophagy response in human neonatal skin organ culture (SOC) after infection with varicella-zoster virus (VZV). The VZV-infected SOC model has attributes of herpes zoster, in that an injection of virus into the skin is analogous to exit of virus from the sensory nerve termini into skin during herpes zoster. Cultures were maintained for 28 days and periodically examined for an autophagy response by quantitation of autophagosomes with Imaris software. Expression of the STAT3 protein was plentiful in the VZV-infected SOC. Abundant autophagy was observed in VZV-infected SOC between 14 and 28 days after infection, while autophagy in mock-infected SOC was minimal (p = 0.0003). The autophagic response after infection of SOC with a recombinant VZV genome containing the herpes simplex virus ICP34.5 neurovirulence gene was similar to wild-type VZV (p = 0.3). These results suggested that the VZV-infected SOC system resembled biopsy data from herpes zoster infection of skin. An enhanced autophagy response has now been reported after infection with two additional alpha herpesviruses besides VZV, namely, pseudorabies virus and duck enteritis herpes virus; both lack the ICP34.5 protein.

Keywords: varicella-zoster virus, pseudorabies virus, herpes simplex virus, interleukin-6, ATG5, autophagosome, HSV ICP34.5, Imaris software

OPEN ACCESS

Edited by:
Anthony Nicola, Washington State University, United States

Reviewed by:
Jennifer Fry Moffat, Upstate Medical University, United States
Paul R. Kinchington, University of Pittsburgh, United States

***Correspondence:**
Charles Grose
Charles-grose@uiowa.edu

Specialty section:
This article was submitted to Virology, a section of the journal Frontiers in Microbiology

Received: *27 August 2018*
Accepted: *14 November 2018*
Published: *05 December 2018*

Citation:
Buckingham EM, Girsch J, Jackson W, Cohen JI and Grose C (2018) Autophagy Quantification and STAT3 Expression in a Human Skin Organ Culture Model for Innate Immunity to Herpes Zoster. Front. Microbiol. 9:2935. doi: 10.3389/fmicb.2018.02935

INTRODUCTION

Herpesviruses are ancient viruses that have retained autophagy as a modulator of innate immune mechanisms (Grose, 2012; Moreau et al., 2015). varicella-zoster virus (VZV) is one of nine human herpesviruses (Davison, 2010).VZV is a human pathogen that causes the primary infection varicella in children and reactivates later in life as zoster or shingles (Weller, 1983). Abundant autophagy has now been detected after infection with VZV and two other alpha herpesviruses: pseudorabies virus (PRV) and duck enteritis herpes virus (Grose et al., 2016; Yin H.C. et al., 2017; Xu et al., 2018).

In earlier studies, we have demonstrated that VZV infection induces both an unfolded protein response (UPR) and an autophagy response (Carpenter et al., 2011; Carpenter and Grose, 2014). We have observed that VZV-induced autophagic flux is easily detectable in infected monolayers, without evidence of a block (Buckingham et al., 2014, 2015). In this manuscript, we describe our adaptation of the human skin organ culture (SOC) model to further assess the innate immune

response to VZV infection (Taylor and Moffat, 2005; Jarosinski et al., 2018). We proposed that VZV infection of human SOC would provide a more accurate representation of innate immunity than analysis solely of infected monolayer cultures. Many earlier VZV studies were carried out after infection of human skin xenografts inserted under the skin of the severe combined immunodeficient mouse (Moffat et al., 1998; Arvin, 2006). The human SOC model is a simpler methodology for VZV infection of human skin that obviates the need for a severe combined immunodeficient mouse (Jarosinski et al., 2018). The chronology of the VZV infectious cycle is very similar in both skin models.

Because of previously documented differences in VZV pathogenesis between cultured cells and skin xenografts in the mouse model, we first examined transcription of antiviral innate immune transcripts in mock-infected SOC and infected SOC. We found unexpectedly that both interleukin-6 (IL-6) transcription as well as protein expression were upregulated following VZV infection (Jarosinski et al., 2018). Recent evidence points to IL-6 as a keystone immunomodulatory cytokine in both healthy and diseased tissues, including its role as a pro-autophagy cytokine in the phosphorylated signal transducer and activator of transcription 3 (STAT3) pathway (Xue et al., 2016). Since elevated IL-6 transcription was not observed in VZV-infected fibroblast monolayers, this discovery would not have been made without the studies in the SOC model. In this report, we further assess and quantify the autophagy response in SOC after infection with wild type VZV and recombinant VZV containing the herpes simplex virus 1 (HSV1) ICP34.5 neurovirulence gene.

MATERIALS AND METHODS

Viruses and Cells

VZV-32 is a low passage laboratory strain; its genome has been completely sequenced (GenBank DQ479961.1) (Peters et al., 2006). rVZV/34.5 is a recombinant virus, in which herpes simplex virus 1 (HSV1) ICP34.5 gene (F strain) previously cloned into a pSG5 expression vector (Stratagene) was cut out along with its SV40 early promoter and poly A signal and inserted into rVZV-Oka (Cohen and Siedel, 1993). MRC-5 human fibroblast cells were grown on coverslips in six well tissue culture plates in Minimum Essential Medium (MEM; Gibco, Life Technologies) supplemented with 7% fetal bovine serum (FBS), L-glutamine, non-essential amino acids, and penicillin/streptomycin. When monolayers were nearly confluent, they were inoculated with trypsin-dispersed VZV-infected cells at a ratio of one infected cell to eight uninfected cells (Grose and Brunel, 1978).

Culture of Explant Skin Samples

De-identified foreskins from circumcision procedures were collected at the University of Iowa Hospital under an exempt Institutional Review Board protocol. As described (Taylor and Moffat, 2005; Jarosinski et al., 2018), we prepared the foreskin for culture by sterilizing the outside of the skin with 1 min incubation in 10% providone-iodine solution followed by rinsing in 70% ethanol and MEM. The skin was then divided into 6 mm round pieces with a biopsy punch and placed onto the mesh bottom of tissue culture inserts in a 12 well plate (Corning) containing 1.4 ml of complete MEM supplemented with nystatin and ciprofloxin. Thereafter, the plate was incubated at 32°C in a humidified incubator with 5% CO_2. We have carried out 9 independent explant procedures.

Infection and Sectioning of Explant Skin Samples

After 24–48 h in culture, pieces of explanted human skin were inoculated with cell associated VZV. A VZV infected monolayer (25 sq. cm.) at 70–80% cytopathology was trypsin-dispersed, sedimented by low speed centrifugation and resuspended into 1 ml of MEM. Each skin piece was pierced to the depth of 1 mm in multiple sites with a hypodermic needle and then an aliquot (500,000 cells in 200 μl) of VZV-infected cells was injected onto the surface of the epidermis and allowed to penetrate into the holes created by piercing the skin surface. Infected skin explants were then incubated for as long as 28 days. Mock infections were handled similarly except for inoculation with uninfected cells. Preparation of the skin samples for cryosectioning and subsequent immunohistochemistry (IHC) protocols have been described in detail (Jarosinski et al., 2018).

Imaging and Quantitative Analysis of Autophagy by Confocal Microscopy

Slides containing the skin samples were prepared for confocal microscopy by published methods (Carpenter et al., 2008). The primary antibody (1:1000) was added for 2 h at ambient temperature and overnight at 4°C; the secondary antibody (1:1250) and Hoechst 33342 DNA stain (1:1000) were added for 2 h. All samples were viewed on a Zeiss 710 confocal fluorescent microscope. Murine monoclonal antibody (MAb) 3B3 against VZV gE, MAb 233 against gC and MAb 251D9 against the capsid protein were produced in this laboratory (Grose et al., 1983; Friedrichs and Grose, 1986; Storlie et al., 2008); rabbit antibody against microtubule-associated protein light chain 3 (LC3) was obtained from Santa Cruz (sc-28266) and mouse MAb against STAT3 was obtained from ThermoFisher Scientific (13-7000). Rabbit monospecific antibody against HSV1 ICP34.5 was given to us by Dr. Ian Mohr (New York University).

Quantitation of autophagosomes by visual inspection of 2D confocal micrographs is highly specific when combined with appropriate controls (Klionsky et al., 2007; Carpenter et al., 2011). Quantitation has been further improved by the Imaris software program (BitPlane), which converts z-stacks of confocal images into 3D animations; the Spot function within Imaris software locates and enumerates autophagosomes within each 3D animation based on size and intensity threshold (Jackson et al., 2013; Lamb et al., 2017). We examined at least 3 separate images from each experimental group in order to determine the number of autophagosomes per cell in each image. The standard error of the mean (SEM) across each set of images was used to generate error bars. The *P* values were determined by unpaired, two-tailed Student's *t* tests, using GraphPad Prism software.

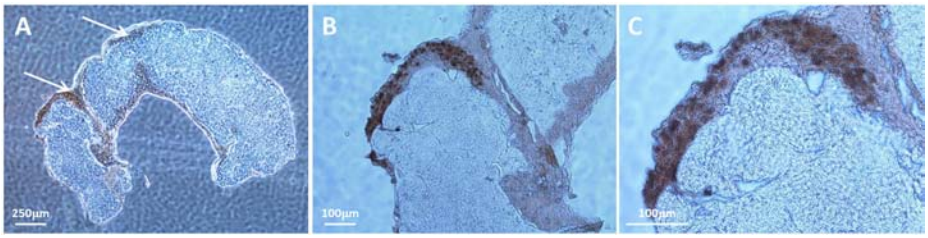

FIGURE 1 | Visualization of a representative VZV-infection within epidermis of human skin explant. Pieces of human skin obtained with a punch that measured 6 mm in diameter were placed in culture medium. As described in Methods, each piece of skin was pierced multiple times with a syringe needle before the infected cell inoculum was layered onto the surface of the same explant. At 14 dpi, infection was analyzed by IHC after labeling with an antibody to a VZV small capsid protein. Since the capsid protein is found mainly in the nuclei of infected cells, the IHC pattern outlined the nuclei within an infectious focus in the SOC epidermis. Two piercing sites in the biopsy are marked with arrows **(A)**. Enlargements of panel **A** are shown in panels **B,C**. The infectious focus contains around 30 nuclei (dark brown color).

RESULTS

Expression of the True Late gC Protein in VZV Infected SOC

A major difference between VZV infection of cultured cells and human skin biopsies during herpes zoster is that mature viral particles are produced in human skin in abundance whereas most viral particles produced in cell culture are aberrant (Tournier et al., 1957; Storlie et al., 2008; Carpenter et al., 2009). A representative example of a VZV-infected SOC is shown in **Figure 1**. In this figure, the cells were prepared for IHC and labeled with an anti-capsid antibody because the nuclei at 14 dpi are filled with capsids. Cell-to-cell virus spread within the epidermis is designated by arrows (**Figure 1A**); higher magnifications of the capsid-labeled infected cells within the SOC are shown in panels B and C.

A marker of the late phase of the alpha herpesvirus infectious cycle is the true late protein gC (Honess and Roizman, 1974). Expression of VZV gC is sparse in cultured cells but plentiful in human skin during herpes zoster (Storlie et al., 2008). Therefore, we investigated the appearance of the gC protein in the VZV infected SOC by confocal microscopy. As seen in the 3D images of the infected SOC, gC expression was easily detected along the linear piercing sites in the skin explant created with the syringe needle (**Figure 2**). As demonstrated by 6 different orientations of the Imaris animation (panels A–F), VZV infection had spread cell-to cell via a piercing site into the epidermis by 14 dpi and then outward from this site. This outward spread into the epidermis was not uniform, rather the spread was meandering.

Expression of STAT3 in the VZV Infected SOC

We previously detected elevated levels of the IL-6 protein in media overlying infected SOC (Jarosinski et al., 2018). A recent report has provided evidence that IL-6 can act as a pro-autophagy cytokine within the IL-6-STAT3 pathway (Xue et al., 2016). Therefore, we looked for evidence of STAT3 expression in the VZV infected SOC. We observed STAT3 immunoreactivity in the VZV-infected skin, in particular, STAT3 expression was found in bystander cells in the near vicinity of an infectious focus as well as within numerous cells of an infectious focus (**Figures 3A–H**). In uninfected skin, only a few randomly distributed STAT3-immunoreactive cells were seen, while no foci of reactivity were observed with the anti-VZV gE antibody (**Figures 3I,J**). The lower panel K represents a landscape image of another infectious focus at a higher magnification (**Figure 3K**).

Quantitation of Autophagosomes in the VZV Infected SOC

We also carried out a series of confocal microscopy experiments on the VZV infected SOC, in order to investigate the

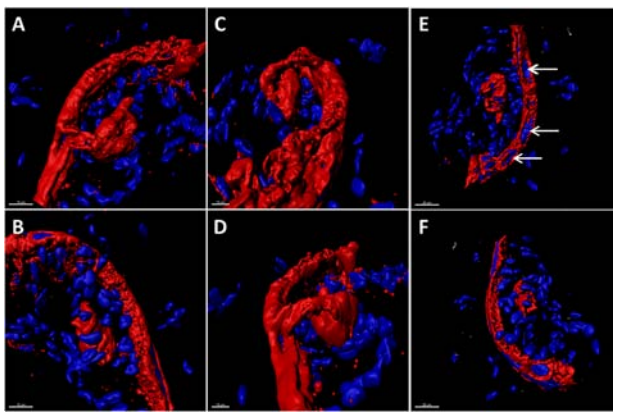

FIGURE 2 | The true late phase of the VZV-infectious cycle in human skin explants. At 14 dpi, VZV infection was analyzed by confocal microscopy with subsequent creation of 3D animations of infected SOC by merging the z-stacks with Imaris software. In order to document that viral replication had entered the late phase of the VZV infectious cycle in human skin, the infectious foci in the skin were immunolabeled with antibody to the true late VZV gC glycoprotein (red color). Six different orientations of the infectious focus are shown in panels **A–F**. In panel **E**, VZV-induced syncytia are visible as clusters of nuclei surrounded by the gC glycoprotein (white arrows). Nuclei are colored blue by the Hoechst dye.

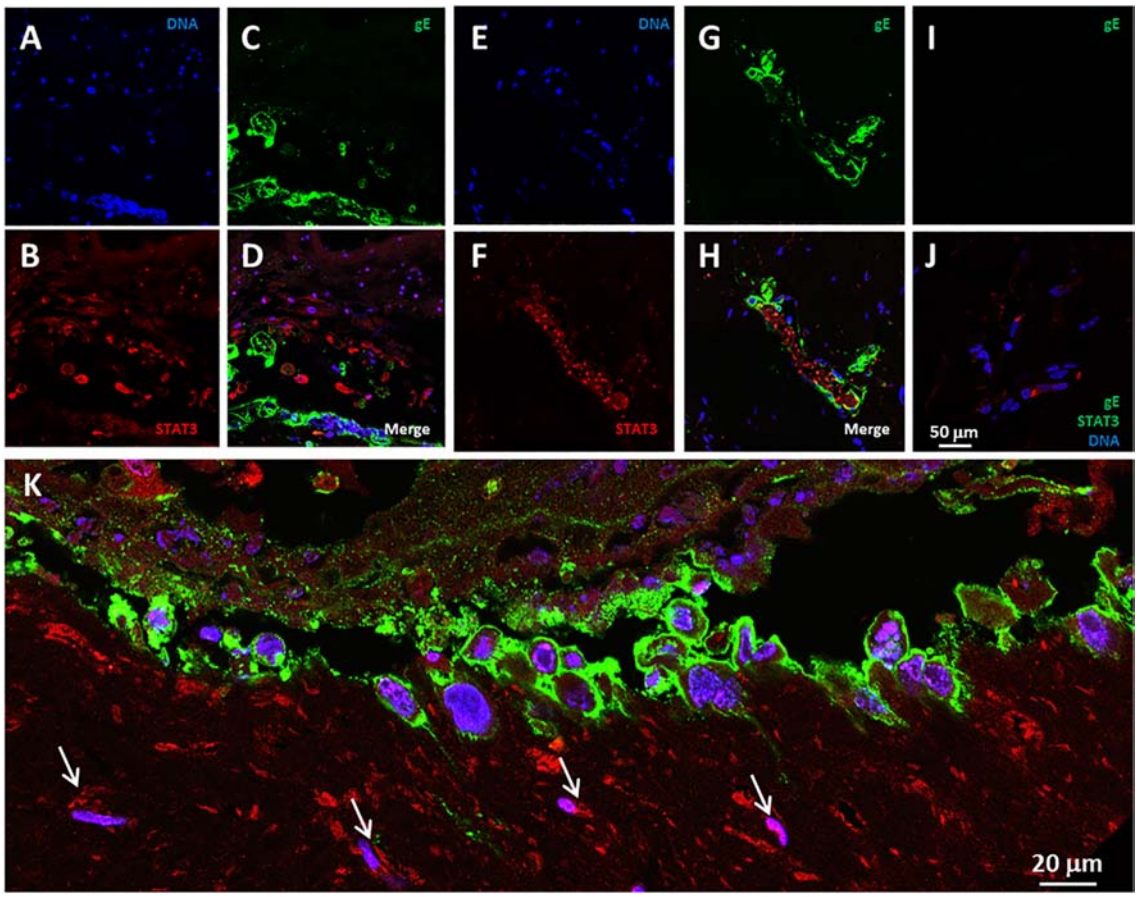

FIGURE 3 | STAT3 expression in VZV infected human skin explants. **(A–H)** STAT3 expression at 14 dpi **(A–D)** and 28 dpi **(E–H)**. The panels show infectious foci outlined by VZV gE immunolabeling mainly in the outer cell membranes, with STAT3 positive cells in the vicinity of the infected cells. **(A,E)** Blue, Hoechst 33342. **(B,F)** Red, STAT3. **(C,G)** VZV gE, green. Panels **D,H** are the merged images of infected explants. **(I,J)** Control images of mock-infected skin explants. The white bar in panel**J** represents all prior panels. **(K)** A higher magnification landscape image of an infectious focus at 14 dpi with a merge of all colors. Arrows designate cells with immunolabeling for STAT3.

degree of autophagy (**Figure 4**). We first examined a mock-infected SOC during each of 6 experiments and observed a minimal number of autophagosomes (**Figure 4A**). After examination of numerous confocal images of VZV infected SOC, we concluded that we had visualized a very robust autophagy response. Measurement of changes in autophagy by enumeration of LC3-positive puncta is one of the most specific assays, especially when combined with analysis by the Imaris software program, which creates a 3D rendering of each z-stack of confocal micrographs as described in Methods. It was apparent that the maximal autophagy response in each cell within VZV-infected human skin was statistically greater than that seen in mock-infected skin (p = 0.0003) (**Figure 4B**). As expected, the number of autophagosomes counted within a 3D image of an infected cell was also greater than the number counted in a single 2D image (**Figures 4C,D**). Finally, we selected two images created by the Imaris animation. There were 3,740 autophagosomes detectable in the cytoplasm above the infectious focus when we set the estimated XY diameter of an autophagosome at 500 nm (**Figure 4**), much higher when performed on 3D renderings of cells rather than on 2D images seen in a confocal micrograph.

Autophagy After SOC Infection With Recombinant VZV/34.5 Virus

After our analyses in SOC described previously as well as the above new data (Jarosinski et al., 2018), we carried out an experiment with a recombinant VZV genome containing the HSV ICP34.5 neurovirulence gene. In our earlier publication, we showed that infection of SOC with wild type VZV closely followed the SCID/human skin model: namely, VZV infection progressed and achieved near maximal distribution by 14 dpi. Although ICP34.5 contributes to HSV neurovirulence in the brain by attaching to Beclin-1 and suppressing autophagy (Orvedahl et al., 2007), the role of ICP34.5 in HSV1-infected non-neuronal tissues has been a subject of debate in the HSV1 literature (Yordy and Iwasaki, 2013). We propose that repeating similar experiments in a VZV/SOC system is an

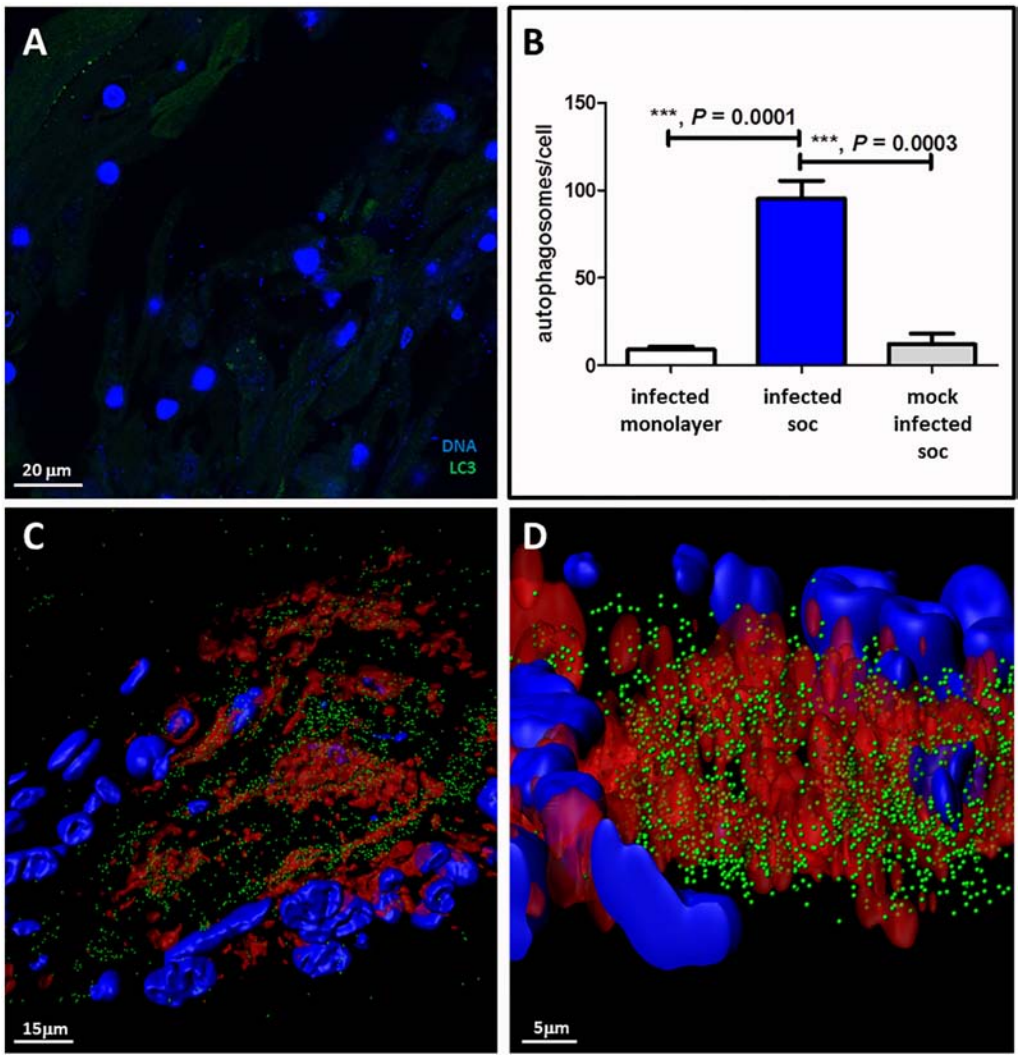

FIGURE 4 | Autophagy in VZV-infected human skin explants. **(A)** Autophagosome formation in mock-infected skin explants. This micrograph is representative of micrographs taken during 6 different experiments. This micrograph includes 27 nuclei in the skin. **(B)** Graph of the number of autophagosomes per cell in infected monolayers versus infected human SOC versus mock-infected human SOC. Data in the infected SOC bar represent 3 separate experiments; data in the uninfected SOC bar represent 6 separate experiments. **(C)** Enumeration of autophagosomes after rendering z-stacks of 2D images of VZV-infected SOC into 3D images by Imaris software. Top-view frame from the 3D animation shows 3740 autophagosomes (green spheres) within the cytoplasm surrounding an infectious focus when the estimated diameter within the Imaris Spot function is set at 500 nm. **(D)** A more enlarged side-view of the prior animation seen in panel **C**. VZV gE, red; LC3, green; Hoechst stain, blue. Three asterisks ***indicates highly significant result.

appropriate control in which to explore the effects of ICP34.5 on autophagy outside of the neuronal system. To this end, the ICP 34.5 gene was cloned into the varicella vaccine genome. We first documented that the ICP34.5 protein was expressed by immunolabeling the protein after rVZV/34.5 infection (**Figure 5A**). As in the SCID model of VZV infection, spread of varicella vaccine virus occurred more slowly in SOC than wild-type VZV (Moffat et al., 1998); at 14 dpi, there were only small foci of infection with the rVZV/34.5 virus (**Figure 5C**).

Thereafter, we examined the infected SOC culture at 28 dpi (**Figures 5D–H**). Time points beyond 21 dpi were not examined often in the SCID model. But at 28 dpi in SOC, we observed that the foci of infection with the rVZV/34.5 virus had enlarged and were similar in size to foci with wild type virus at 14 dpi (compare **Figures 4,5**). Since wild type virus infection does not progress greatly between 14 and 28 dpi, the foci in a control experiment with wild type virus were similar in size to that of rVZV/34.5 at 28 dpi. Then, we obtained images from 6 individual infectious foci in order to quantitate puncta by confocal microscopy combined with Imaris software. Since the samples were labeled with antibody to VZV gE, the predominant VZV glycoprotein, we documented the extensive production of VZV gE throughout the cytoplasm of the infected SOC (**Figures 5E–H**). When we enumerated the puncta within

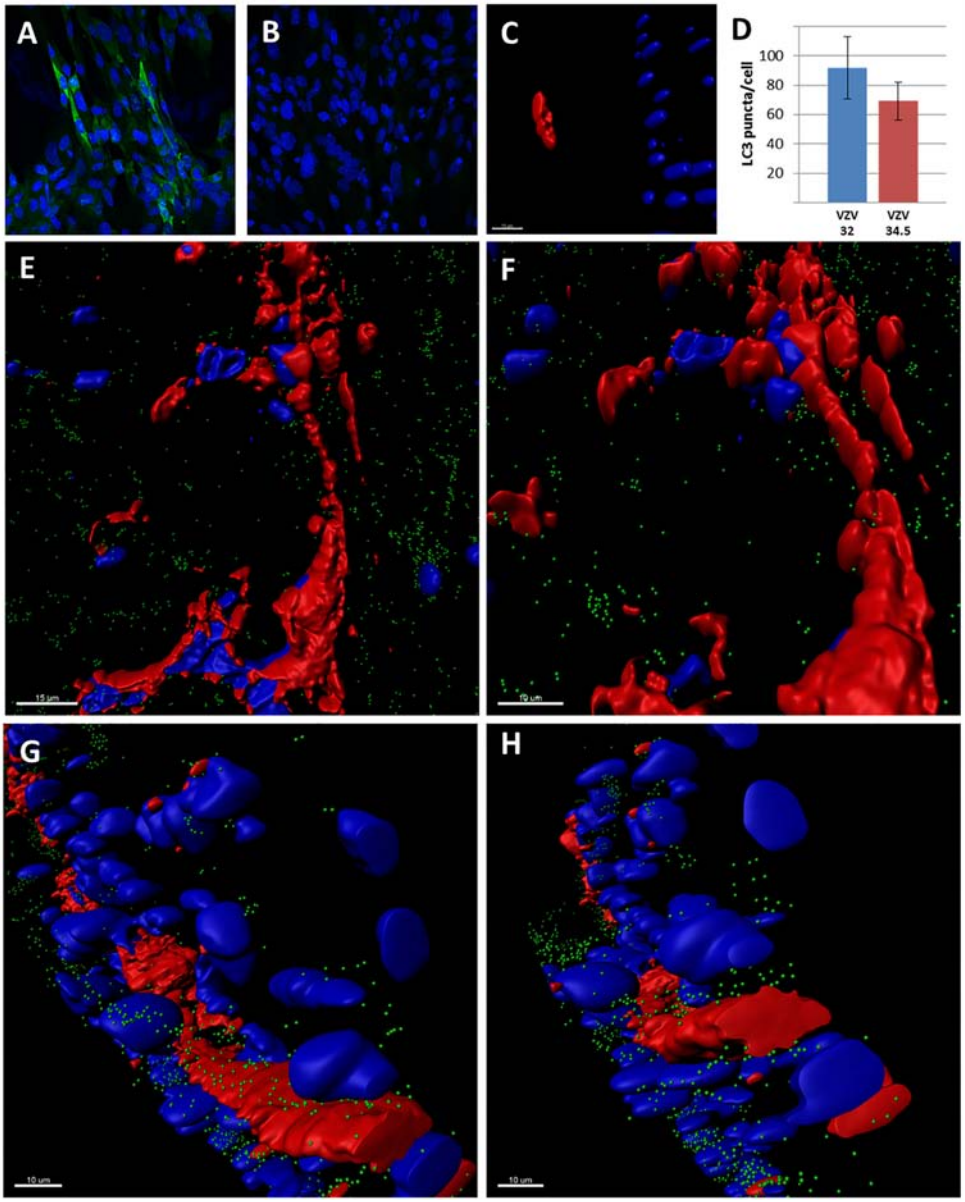

FIGURE 5 | Studies with the recombinant VZV/34.5 virus. **(A)** Immunolabeling of the HSV1 ICP34.5 protein after infection with rVZV/34.5. The ICP34.5 protein is labeled green. **(B)** Control immunolabeling with the anti-ICP34.5 antibody in wild-type VZV infection. No ICP34.5 protein was detected. **(C)** Small focus of VZV/34.5 infection in SOC at 14 dpi. Larger infectious foci were first seen at 28 dpi. **(D)** Graph of autophagosome counts for VZV-32 and VZV/34.5 strains in SOC at 28 dpi. Six individual sections were examined. There was no statistical difference. **(E–H)** Imaris renderings of confocal micrographs in SOC infected with VZV/34.5 for 28 days. VZV-induced syncytia were apparent in each panel because VZV gE immunolabeling was detectable around multiple nuclei without evidence of any barriers by individual cellular membranes. VZV glycoprotein gE is labeled red; autophagic puncta are labeled green; nuclei are labeled blue.

individual infected cells by the Imaris Spot program, we found no significant difference in puncta per infected cell when wild-type and rVZV/34.5 infection were compared (**Figure 5D**; $p = 0.3$). We have previously shown that autophagy and LC3 production were not diminished in cells infected with vaccine virus (Buckingham et al., 2016). This further experiment documented that ICP34.5 when expressed within a VZV genome did not limit autophagosome production in human skin tissue.

DISCUSSION

A goal of the current study was to investigate autophagy in the human SOC model for herpes zoster. A prior investigation in the SOC model documented a dramatic increase in IL-6 transcription in VZV-infected skin explants (Jarosinski et al., 2018). IL-6 has multiple functions that involve both pro-inflammatory and anti-inflammatory effects (Hunter and Jones, 2015). Prior skin studies have shown an induction of IL-6 transcription in

injured human keratinocytes (Sugawara et al., 2001). Our result also supports an earlier report that found IL-6 transcripts in skin biopsies from human subjects with herpes zoster (Uceyler et al., 2014). Increased levels of IL-6 also have been found in the cerebrospinal fluid of patients with vasculopathy in the brain (Jones et al., 2016), and IL-6 inhibits VZV replication in stem-cell derived neuronal cultures (Como et al., 2018). Further, IL-6 transcription is upregulated in the spleen during an avian herpesvirus infection, while increased IL-6 expression is found in the diseased eye after HSV1 infection (Heidari et al., 2010; Bryant-Hudson et al., 2014; Chucair-Elliott et al., 2016). The VZV IL-6 data are strongly supported by an independent investigation of cytokines present in the skin disease called "mad itch" found in animals infected with the closely related PRV, an alpha herpesvirus in the Varicellovirus genus (Laval et al., 2018). The PRV-induced systemic inflammatory response responsible for "mad itch" included elevated IL-6 protein levels in the mouse footpad.

The above VZV IL-6 data are relevant because a recent paper describes a previously unrecognized pathway between elevated IL-6 and autophagy. Hypoxia within a brain tumor stimulated IL-6, which acted upstream as an inducer of autophagy in glioblastoma tumor cells via the IL-6-STAT3-MIR155-3p-CREBRF-CREB3-ATG5 pathway (Xue et al., 2016). In addition to IL-6 studies, we have shown the importance of ATG5 in the VZV induced autophagy pathway (Buckingham et al., 2014). In a prior important study from another laboratory, VZV infection led to increased phosphorylation of STAT3 in skin xenografts; in turn, STAT3 activation was critical for VZV replication in the skin xenograft (Sen et al., 2012).We have confirmed STAT3 activation in infected SOC. Thus, we have now documented the presence of three of the six components of the above autophagy pathway.

Further, our autophagy quantification after infection of SOC with the rVZV/34.5 virus may support HSV1 data that the primary anti-autophagy effects of the ICP34.5 protein are recognized mainly in HSV1-infected neuronal tissues (Yordy and Iwasaki, 2013). A complementary hypothesis is that anti-autophagy effects of ICP34.5 may require or be facilitated by the presence of additional HSV1 proteins not expressed by the smaller VZV genome, for example, US11 (Lussignol et al., 2013). A more recent investigation suggests a non-autophagy mechanism to explain some proviral effects of ICP34.5, namely, that HSV1 ICP34.5 restricts the type 1 interferon response to HSV1 infection indirectly by sustaining expression of the immediate-early HSV1 immunomodulatory gene ICP0 (Manivanh et al., 2017). During VZV infection, the VZV ICP4 homolog (ORF62) is the dominant immediate-early protein, while the VZV ICP0 homolog (ORF61) plays an accessory role (Perera et al., 1992).

When these VZV data about IL-6/STAT3/ATG5 are considered together with the results from the glioblastoma/autophagy study, we conclude that the elevated levels of IL-6 may also facilitate elevated levels of autophagy in VZV-infected skin explants. In support of this hypothesis, we point out the robust autophagosome formation seen in the 3D images of our SOC model of VZV skin infection (**Figure 4**). There were ∼100 autophagosomes per cell in the syncytium with approximately 30 nuclei; this result matches closely with a prior imaging of a biopsy of a human zoster vesicle, where we also enumerated ∼100 autophagosomes per cell (Jackson et al., 2013). In earlier studies using 2D confocal micrographs, we had found a lower range of autophagosomes (10–20) per infected cell, while uninfected and unstressed cells had <4/cell (Carpenter et al., 2011). The number of <4 puncta/cell is generally accepted in the autophagy literature as a standard marker for unstressed cells in 2D images (Klionsky et al., 2007).

Finally, we would like to point out papers that describe enhanced autophagy following infection with two other alpha herpes viruses: PRV and duck enteritis herpes virus (Yin H. et al., 2017; Yin H.C. et al., 2017; Xu et al., 2018). The data within these manuscripts were mutually supportive, for example, the similarities between innate immunity in response to VZV and PRV infection (Jarosinski et al., 2018; Laval et al., 2018). When autophagy was inhibited, viral titers decreased (Grose et al., 2015). With regard to VZV, we note that the abundant autophagy response observed in our SOC model of herpes zoster confirms the abundant autophagy previously reported in skin vesicle biopsies from patients with herpes zoster (Takahashi et al., 2009). We also point out that studies of innate immunity in cultured cells may not always reflect results in human tissue explants, for example, there is no Il-6 production in VZV-infected fibroblast cells while IL-6 production is detected after VZV infection of a human retinal pigment cell line (ARPE-19) (Graybill et al., 2017; Jarosinski et al., 2018). Similar experiments are needed in biopsies of PRV-infected swine and duck tissue infected with duck enteritis virus, in order to validate positive autophagy results in cultured cells.

AUTHOR CONTRIBUTIONS

CG provided overall supervision for the project. EB, JG, and WJ carried out experiments shown in **Figures 1–4**. JC provided the recombinant varicella virus used in **Figure 5**. All authors assembled the data, designed the figures, and contributed to writing the manuscript.

FUNDING

This research project was funded by NIH grants AI89716 and HD94333, as well as the NIAID Intramural Research Program.

ACKNOWLEDGMENTS

A VZV review article cited in the references was written by Thomas Weller, a recipient of the 1954 Nobel Prize in Medicine.

REFERENCES

Arvin, A. M. (2006). Investigations of the pathogenesis of *Varicella zoster* virus infection in the SCIDhu mouse model. *Herpes* 13, 75–80.

Bryant-Hudson, K. M., Gurung, H. R., Zheng, M., and Carr, D. J. (2014). Tumor necrosis factor alpha and interleukin-6 facilitate corneal lymphangiogenesis in response to herpes simplex virus 1 infection. *J. Virol.* 88, 14451–14457. doi: 10.1128/JVI.01841-14

Buckingham, E. M., Carpenter, J. E., Jackson, W., and Grose, C. (2014). Autophagy and the effects of its inhibition on varicella-zoster virus glycoprotein biosynthesis and infectivity. *J. Virol.* 88, 890–902. doi: 10.1128/JVI.02646-13

Buckingham, E. M., Carpenter, J. E., Jackson, W., Zerboni, L., Arvin, A. M., and Grose, C. (2015). Autophagic flux without a block differentiates varicella-zoster virus infection from herpes simplex virus infection. *Proc. Natl. Acad. Sci. U.S.A.* 112, 256–261. doi: 10.1073/pnas.1417878112

Buckingham, E. M., Jarosinski, K. W., Jackson, W., Carpenter, J. E., and Grose, C. (2016). Exocytosis of varicella-zoster virus virions involves a convergence of endosomal and autophagy pathways. *J. Virol.* 90, 8673–8685. doi: 10.1128/JVI.00915-16

Carpenter, J. E., and Grose, C. (2014). Varicella-zoster virus glycoprotein expression differentially induces the unfolded protein response in infected cells. *Front. Microbiol.* 5:322. doi: 10.3389/fmicb.2014.00322

Carpenter, J. E., Henderson, E. P., and Grose, C. (2009). Enumeration of an extremely high particle to Pfu ratio for varicella zoster virus. *J. Virol.* 83, 6917–6921. doi: 10.1128/JVI.00081-09

Carpenter, J. E., Hutchinson, J. A., Jackson, W., and Grose, C. (2008). Egress of light particles among filopodia on the surface of *Varicella-zoster* virus-infected cells. *J. Virol.* 82, 2821–2835. doi: 10.1128/JVI.01821-07

Carpenter, J. E., Jackson, W., Benetti, L., and Grose, C. (2011). Autophagosome formation during varicella-zoster virus infection following endoplasmic reticulum stress and the unfolded protein response. *J. Virol.* 85, 9414–9424. doi: 10.1128/JVI.00281-11

Chucair-Elliott, A. J., Jinkins, J., Carr, M. M., and Carr, D. J. (2016). IL-6 contributes to corneal nerve degeneration after herpes simplex virus type I infection. *Am. J. Pathol.* 186, 2665–2678. doi: 10.1016/j.ajpath.2016.06.007

Cohen, J. I., and Siedel, K. E. (1993). Generation of varicella-zoster virus (VZV) and viral mutants from cosmid DNAs: VZV thymidylate synthetase is not essential for replication in vitro. *PNAS* 90, 7376–7380. doi: 10.1073/pnas.90.15.7376

Como, C. N., Pearce, C. M., Cohrs, R. J., and Baird, N. L. (2018). Interleukin-6 and type 1 interferons inhibit varicella zoster virus replication in human neurons. *Virology* 522, 13–18. doi: 10.1016/j.virol.2018.06.013

Davison, A. J. (2010). Herpesvirus systematics. *Vet. Microbiol.* 143, 52–69. doi: 10.1016/j.vetmic.2010.02.014

Friedrichs, W. E., and Grose, C. (1986). Varicella-zoster virus p32/p36 complex is present in both the viral capsid and the nuclear matrix of the infected cell. *J. Virol.* 57, 155–164.

Graybill, C., Claypool, D. J., Brinton, J. T., Levin, M. J., and Lee, K. S. (2017). Cytokines produced in response to varicella-zoster virus infection of ARPE-19 cells stimulate lymphocyte chemotaxis. *J. Infect. Dis.* 216, 1038–1047. doi: 10.1093/infdis/jix426

Grose, C. (2012). Pangaea and the out-of-Africa model of varicella-zoster virus evolution and phylogeography. *J. Virol.* 86, 9558–9565. doi: 10.1128/JVI.00357-12

Grose, C., and Brunel, P. A. (1978). Varicella-zoster virus: isolation and propagation in human melanoma cells at 36 and 32 degrees C. *Infect. Immun.* 19, 199–203.

Grose, C., Buckingham, E. M., Carpenter, J. E., and Kunkel, J. P. (2016). Varicella-zoster virus infectious cycle: ER stress, autophagic flux, and amphisome-mediated trafficking. *Pathogens* 5:67. doi: 10.3390/pathogens5040067

Grose, C., Buckingham, E. M., Jackson, W., and Carpenter, J. E. (2015). The pros and cons of autophagic flux among herpesviruses. *Autophagy* 11, 716–717. doi: 10.1080/15548627.2015.1017223

Grose, C., Edwards, D. P., Friedrichs, W. E., Weigle, K. A., and McGuire, W. L. (1983). Monoclonal antibodies against three major glycoproteins of varicella-zoster virus. *Infect. Immun.* 40, 381–388.

Heidari, M., Sarson, A. J., Huebner, M., Sharif, S., Kireev, D., and Zhou, H. (2010). Marek's disease virus-induced immunosuppression: array analysis of chicken immune response gene expression profiling. *Viral Immunol.* 23, 309–319. doi: 10.1089/vim.2009.0079

Honess, R. W., and Roizman, B. (1974). Regulation of herpesvirus macromolecular synthesis. I. Cascade regulation of the synthesis of three groups of viral proteins. *J. Virol.* 14, 8–19.

Hunter, C. A., and Jones, S. A. (2015). IL-6 as a keystone cytokine in health and disease. *Nat. Immunol.* 16, 448–457. doi: 10.1038/ni.3153

Jackson, W., Yamada, M., Moninger, T., and Grose, C. (2013). Visualization and quantitation of abundant macroautophagy in virus-infected cells by confocal three-dimensional fluorescence imaging. *J. Virol. Methods* 193, 244–250. doi: 10.1016/j.jviromet.2013.06.018

Jarosinski, K. W., Carpenter, J. E., Buckingham, E. M., Jackson, W., Knudtson, K., Moffat, J. F., et al. (2018). Cellular stress response to varicella-zoster virus infection of human skin includes highly elevated interleukin-6 expression. *Open Forum Infect. Dis.* 5:ofy118. doi: 10.1093/ofid/ofy118

Jones, D., Alvarez, E., Selva, S., Gilden, D., and Nagel, M. A. (2016). Proinflammatory cytokines and matrix metalloproteinases in CSF of patients with VZV vasculopathy. *Neurol. Neuroimmunol. Neuroinflamm.* 3:e246. doi: 10.1212/NXI.0000000000000246

Klionsky, D. J., Cuervo, A. M., and Seglen, P. O. (2007). Methods for monitoring autophagy from yeast to human. *Autophagy* 3, 181–206. doi: 10.4161/auto.3678

Lamb, C. A., Joachim, J., and Tooze, S. A. (2017). Quantifying autophagic structures in mammalian cells using confocal microscopy. *Methods Enzymol.* 587, 21–42. doi: 10.1016/bs.mie.2016.09.051

Laval, K., Vernejoul, J. B., Van Cleemput, J., Koyuncu, O. O., and Enquist, L. W. (2018). Virulent PRV infection induces a specific and lethal systemic inflammatory response in mice. *J. Virol.* doi: 10.1128/JVI.01614-18 [Epub ahead of print].

Lussignol, M., Queval, C., Bernet-Camard, M. F., Cotte-Laffitte, J., Beau, I., Codogno, P., et al. (2013). The herpes simplex virus 1 Us11 protein inhibits autophagy through its interaction with the protein kinase PKR. *J. Virol.* 87, 859–871. doi: 10.1128/JVI.01158-12

Manivanh, R., Mehrbach, J., Knipe, D. M., and Leib, D. A. (2017). Role of herpes simplex virus 1 gamma34.5 in the regulation of IRF3 signaling. *J. Virol.* 91:e1156-17. doi: 10.1128/JVI.01156-17

Moffat, J. F., Zerboni, L., Kinchington, P. R., Grose, C., Kaneshima, H., and Arvin, A. M. (1998). Attenuation of the vaccine Oka strain of varicella-zoster virus and role of glycoprotein C in alphaherpesvirus virulence demonstrated in the SCID-hu mouse. *J. Virol.* 72, 965–974.

Moreau, P., Moreau, K., Segarra, A., Tourbiez, D., Travers, M. A., Rubinsztein, D. C., et al. (2015). Autophagy plays an important role in protecting Pacific oysters from OsHV-1 and Vibrio aestuarianus infections. *Autophagy* 11, 516–526. doi: 10.1080/15548627.2015.1017188

Orvedahl, A., Alexander, D., Talloczy, Z., Sun, Q., Wei, Y., Zhang, W., et al. (2007). HSV-1 ICP34.5 confers neurovirulence by targeting the Beclin 1 autophagy protein. *Cell Host Microbe* 1, 23–35. doi: 10.1016/j.chom.2006.12.001

Perera, L. P., Mosca, J. D., Ruyechan, W. T., and Hay, J. (1992). Regulation of varicella-zoster virus gene expression in human T lymphocytes. *J. Virol.* 66, 5298–5304.

Peters, G. A., Tyler, S. D., Grose, C., Severini, A., Gray, M. J., Upton, C., et al. (2006). A full-genome phylogenetic analysis of varicella-zoster virus reveals a novel origin of replication-based genotyping scheme and evidence of recombination between major circulating clades. *J. Virol.* 80, 9850–9860. doi: 10.1128/JVI.00715-06

Sen, N., Che, X., Rajamani, J., Zerboni, L., Sung, P., Ptacek, J., et al. (2012). Signal transducer and activator of transcription 3 (STAT3) and survivin induction by varicella-zoster virus promote replication and skin pathogenesis. *Proc. Natl. Acad. Sci. U.S.A.* 109, 600–605. doi: 10.1073/pnas.1114232109

Storlie, J., Carpenter, J. E., Jackson, W., and Grose, C. (2008). Discordant varicella-zoster virus glycoprotein C expression and localization between cultured cells and human skin vesicles. *Virology* 382, 171–181. doi: 10.1016/j.virol.2008.09.031

Sugawara, T., Gallucci, R. M., Simeonova, P. P., and Luster, M. I. (2001). Regulation and role of interleukin 6 in wounded human epithelial keratinocytes. *Cytokine* 15, 328–336. doi: 10.1006/cyto.2001.0946

Takahashi, M. N., Jackson, W., Laird, D. T., Culp, T. D., Grose, C., Haynes, J. I., et al. (2009). Varicella-zoster virus infection induces autophagy in both cultured cells and human skin vesicles. *J. Virol.* 83, 5466–5476. doi: 10.1128/JVI.02670-08

Taylor, S. L., and Moffat, J. F. (2005). Replication of varicella-zoster virus in human skin organ culture. *J. Virol.* 79, 11501–11506. doi: 10.1128/JVI.79.17.11501-11506.2005

Tournier, P., Cathala, F., and Bernhard, W. (1957). Ultrastructure and intracellular development of varicella virus observed with electron microscope. *Presse Med.* 65, 1229–1234.

Uceyler, N., Valet, M., Kafke, W., Tolle, T. R., and Sommer, C. (2014). Local and systemic cytokine expression in patients with postherpetic neuralgia. *PLoS One* 9:e105269. doi: 10.1371/journal.pone.0105269

Weller, T. H. (1983). Varicella and herpes zoster. Changing concepts of the natural history, control, and importance of a not-so-benign virus. *N. Engl. J. Med.* 309, 1434–1440. doi: 10.1056/NEJM198312083092306

Xu, C., Wang, M., Song, Z., Wang, Z., Liu, Q., Jiang, P., et al. (2018). Pseudorabies virus induces autophagy to enhance viral replication in mouse neuro-2a cells in vitro. *Virus Res.* 248, 44–52. doi: 10.1016/j.virusres.2018.02.004

Xue, H., Yuan, G., Guo, X., Liu, Q., Zhang, J., Gao, X., et al. (2016). A novel tumor-promoting mechanism of IL6 and the therapeutic efficacy of tocilizumab: Hypoxia-induced IL6 is a potent autophagy initiator in glioblastoma via the p-STAT3-MIR155-3p-CREBRF pathway. *Autophagy* 12, 1129–1152. doi: 10.1080/15548627.2016.1178446

Yin, H., Zhao, L., Jiang, X., Li, S., Huo, H., and Chen, H. (2017). DEV induce autophagy via the endoplasmic reticulum stress related unfolded protein response. *PLoS One* 12:e0189704. doi: 10.1371/journal.pone.0189704

Yin, H. C., Zhao, L. L., Li, S. Q., Niu, Y. J., Jiang, X. J., Xu, L. J., et al. (2017). Autophagy activated by duck enteritis virus infection positively affects its replication. *J. Gen. Virol.* 98, 486–495. doi: 10.1099/jgv.0.000696

Yordy, B., and Iwasaki, A. (2013). Cell type-dependent requirement of autophagy in HSV-1 antiviral defense. *Autophagy* 9, 236–238. doi: 10.4161/auto.22506

Conflict of Interest Statement: The authors declare that the research was conducted in the absence of any commercial or financial relationships that could be construed as a potential conflict of interest.

frontiers in Microbiology

REVIEW
published: 21 December 2018
doi: 10.3389/fmicb.2018.03170

Varicella Virus-Host Interactions During Latency and Reactivation: Lessons From Simian Varicella Virus

*Océane Sorel and Ilhem Messaoudi**

Department of Molecular Biology and Biochemistry, University of California, Irvine, Irvine, CA, United States

Varicella zoster virus (VZV) is a neurotropic alphaherpesvirus and the causative agent of varicella (chickenpox) in humans. Following primary infection, VZV establishes latency in the sensory ganglia and can reactivate to cause herpes zoster, more commonly known as shingles, which causes significant morbidity, and on rare occasions mortality, in the elderly. Because VZV infection is highly restricted to humans, the development of a reliable animal model has been challenging, and our understanding of VZV pathogenesis remains incomplete. As an alternative, infection of rhesus macaques with the homologous simian varicella virus (SVV) recapitulates the hallmarks of VZV infection and thus constitutes a robust animal model to provide critical insights into VZV pathogenesis and the host antiviral response. In this model, SVV infection results in the development of varicella during primary infection, generation of an adaptive immune response, establishment of latency in the sensory ganglia, and viral reactivation upon immune suppression. In this review, we discuss our current knowledge about host and viral factors involved in the establishment of SVV latency and reactivation as well as the important role played by T cells in SVV pathogenesis and antiviral immunity.

Keywords: herpesvirus, viral latency, varicella zoster virus, simian varicella virus, non-human primates, viral reactivation, shingles

OPEN ACCESS

Edited by:
Benedikt B. Kaufer,
Freie Universität Berlin, Germany

Reviewed by:
Donald Scott Schmid,
Centers for Disease Control and Prevention (CDC), United States
Stefan Oliver,
Stanford University, United States

***Correspondence:**
Ilhem Messaoudi
imessaou@uci.edu

Specialty section:
This article was submitted to Virology, a section of the journal Frontiers in Microbiology

Received: *02 October 2018*
Accepted: *07 December 2018*
Published: *21 December 2018*

Citation:
Sorel O and Messaoudi I (2018) Varicella Virus-Host Interactions During Latency and Reactivation: Lessons From Simian Varicella Virus. Front. Microbiol. 9:3170. doi: 10.3389/fmicb.2018.03170

INTRODUCTION AND KNOWLEDGE GAPS

Varicella zoster virus (VZV) is one of the nine human herpesviruses. Primary VZV infection results in varicella (also known as chickenpox), a disease characterized by a vesicular rash, fever, headache, and loss of appetite (Heininger and Seward, 2006). Like other alphaherpesviruses, VZV exhibits neurotropism and establishes latency in sensory ganglia neurons. VZV transmission is thought to occur through either inhalation of saliva droplets containing infectious particles and by direct contact with virus in varicella or zoster skin lesions (Leclair et al., 1980; Sawyer et al., 1994; Suzuki et al., 2004). Subsequently, VZV is presumed to undergo initial replication in the upper respiratory tract and tonsillar lymph nodes before viremia and dissemination to the skin leading to the development of varicella (Zerboni et al., 2014). Although primary VZV infection in immunocompetent individuals usually results in a benign disease, serious complications can occur in immune compromised individuals, including pneumonia, secondary bacterial infection, and stroke (Gnann, 2002; Chiner et al., 2010; Wiegering et al., 2011). Two hypotheses are proposed to explain how VZV reaches the ganglia: (Heininger and Seward, 2006) VZV infects sensory neurons via retrograde axonal transport from the infected skin, and (Suzuki et al., 2004) VZV is carried by infected T cells to the ganglia through the hematogenous route (Depledge et al., 2018b). During

reactivation, VZV travels from the ganglia to the skin via anterograde axonal transport to cause herpes zoster (HZ, also known as shingles), a painful and debilitating disease that primarily affects the elderly and immunocompromised. HZ is characterized by severe prodromal pain followed by a rash restricted to the dermatome innervated by the ganglia from which the virus reactivated (Wareham and Breuer, 2007). The incidence of HZ is estimated to be 3 per 1000 adults between the age of 40 and 50 years old and increases to 11 cases per 1000 adults above the age of 80 years old (Keating, 2016). VZV reactivation can also cause other complications such as HZ ophthalmicus, vasculitis, stroke, as well as pain without development of a rash, referred as zoster sine herpete (Dayan and Peleg, 2017). Routine vaccination of children against chickenpox was implemented in several countries including Japan (1988), the United States (1995), and Canada (1999) using the live attenuated VZV vaccine that was derived from the Oka strain (Gershon, 2017). There are currently two available vaccines to prevent HZ in the elderly: a live-attenuated (Zostavax®, licensed 2005, ∼55% efficacious) and a recombinant (Shingrix®, licensed 2018, 97% efficacious) vaccine (Arnold and Messaoudi, 2017a; James et al., 2018).

Despite extensive studies, our understanding of VZV pathogenesis remains incomplete. First, the mechanisms by which VZV disseminates from the initial site of infection to the skin and ganglia are poorly understood. The prevailing model proposes that VZV initially replicates within mucosal epithelial cells at the sites of entry, followed by spread to tonsils and other regional lymphoid tissues, where VZV gains access to T cells that deliver the virus to cutaneous sites of replication and sensory ganglia (Zerboni et al., 2014). However, this model was constructed primarily using data obtained from *in vitro* studies carried out using the attenuated Oka vaccine strain and *in vivo* studies utilizing a severe-combined immunodeficient (SCID) mouse model implanted with human fetal tissues (SCID-hu) (Moffat et al., 1995; Ku et al., 2004). Moreover, the exact timeline as well as the mechanisms through which the latency is established and maintained following primary infection still remains unclear. In order to address these questions, a reliable animal model that recapitulates the key hallmarks of VZV infection is necessary.

SIMIAN VARICELLA VIRUS INFECTION: AN *IN VIVO* MODEL TO STUDY VARICELLA ZOSTER VIRUS PATHOGENESIS

Numerous attempts have been made to develop a reliable animal model that recapitulates the hallmarks of VZV infection. However, the success of these models remains limited due to the strict human specificity of VZV. Although seroconversion was observed following VZV inoculation in different rodent models including guinea pigs, mice, and rats; no virus was detected in circulation in these models (Haberthur and Messaoudi, 2013). Infection of guinea pigs was rendered possible through the derivation of a guinea pig-adapted VZV strain (by passaging the virus multiple times in fetal guinea pig cells) and injection of peripheral blood mononuclear cells (PBMCs) that are first infected *in vitro* (Gan et al., 2014). Although VZV was shown to establish latency in enteric neurons *in vivo*, the inconsistent development of both viremia and rash in addition to the inability to induce VZV reactivation *in vivo* limits the use of this small animal model (Haberthur and Messaoudi, 2013). Reactivation can be induced *in vitro* through overexpression of VZV ORF61 in latently infected guinea pigs enteric neurons (Gershon et al., 2008). Subcutaneous injection of VZV-infected cells in rats was reported to lead to establishment of a latency-like quiescent state in sensory ganglia although the virus was not shown to be able to reactivate (Annunziato et al., 1998; Sadzot-Delvaux et al., 1990). In addition, footpad inoculation of VZV-infected cells in the rat model has been used to study post-herpetic neuralgia (PHN), long-term chronic pain associated with zoster (Dalziel et al., 2004). Inoculation of non-human primates with VZV also resulted in latency and the development of immunity in the absence of viremia or varicella, suggestive of abortive infection (Felsenfeld and Schmidt, 1979; Meyer et al., 2015a; Myers et al., 1987, Provost et al., 1987; Cohen et al., 1996; Willer et al., 2012). Intradermal inoculation of chimpanzees resulted in a local rash, however, several restrictions have been placed on the use of apes for biomedical research (Myers et al., 1987; Cohen et al., 1996).

In order to overcome the host specificity restriction of VZV, a humanized SCID mouse model was developed using human tissue xenografts. The engraftment of different human fetal tissues (thymus/liver, skin, ganglia, and lung) in this model allowed direct inoculation of VZV and resulted in several important insights into VZV pathogenesis (Moffat et al., 1995; Ku et al., 2004; Zerboni et al., 2005; Reichelt et al., 2008; Wang et al., 2017). However, this model also presents several limitations including: (1) direct inoculation into the human xenografts tissues does not mimic natural route of transmission; (2) the lack of adaptive immunity, which is critical to control viral infection; and (3) the possibility that the strict human host specificity of VZV may alter virus behavior in this model; (4) the use of the attenuated Oka vaccine strain in some of these studies, which compared to the parent wild type strain contains numerous nucleotide substitutions found in multiple open reading frames (ORFs) and may therefore not accurately model the behavior of wild type virus strains (Jones and Arvin, 2003; Yamanishi, 2008; Sen et al., 2015).

To overcome these limitations an alternative animal model was developed where non-human primates are inoculated with Simian varicella virus (SVV), an alphaherpesvirus that causes a vesicular rash in Old World monkeys. SVV and VZV virions have a diameter of 170–200 nm and 80–120 nm, respectively, and are composed of a nucleocapsid of icosahedral symmetry surrounded by a viral envelope (Gray, 2010). The nucleocapsid of both SVV and VZV contains a linear double-stranded DNA genome of 124,138 and 124,884 bp, respectively. The viral genomes of SVV and VZV include a unique long sequence of 104.1 and 104.8 kb, respectively, and a unique short region that comprises a 4.9 and 5.2 kb sequence for SVV and VZV, respectively, as well as internal repeat and terminal repeat

regions (Clarke et al., 1992). SVV and VZV genomes share 70–75% DNA homology (Gray and Oakes, 1984) and an amino acid identity ranging from 27 to 75% (Gray et al., 2001). Both VZV and SVV encode 74 ORFs of which 71 are distinct and 3 (ORFs 69, 70, and 71) are duplicated within the repeat regions (Mahalingam and Gilden, 2007; Zerboni et al., 2014). Despite exhibiting co-linearity with respect to gene organization, SVV ORFA is absent in VZV genome while SVV does not include a gene homolog of VZV ORF2 (Gray et al., 2001).

The first outbreak of a varicella-like disease in non-human primates was reported in 1967 followed by several epizootics in primates facilities worldwide (Clarkson et al., 1967; Gray, 2008). Depending on the non-human species, SVV infection can cause disease that ranges from a mild varicella (in rhesus macaques also called *Macaca mulata*) to a severe and life-threatening disease associated with high morbidity and mortality rates [cynomolgus monkeys (*Macaca fascicularis*) and African green monkeys (*Chlorocebus sabaeus*)] (Gray, 2008). This spectrum of disease outcomes is a hallmark of herpesvirus infection in species that are closely related to the natural host, e.g., Macacine herpesvirus 1 (also known as herpes simian B virus) infection in humans (Elmore and Eberle, 2008), Elephant endotheliotropic herpesvirus infection in Asian elephants (Long et al., 2016), and Alcelaphine herpesvirus 1 in cattle (Sorel et al., 2017). Moreover, SVV infection in cynomolgus monkeys and African green monkeys results in persistent viremia which limits the use of these models to study the adaptive immune response against SVV (White et al., 2002; Mahalingam et al., 2007). In contrast, intra-bronchial inoculation of rhesus macaques with SVV faithfully recapitulates the hallmarks of VZV pathogenesis including: viremia, development of varicella, generation of robust cellular and humoral immune responses, establishment of latency in the sensory ganglia, and viral reactivation following immune suppression (Messaoudi et al., 2009; Meyer et al., 2011; Haberthur et al., 2013, 2014; Arnold et al., 2017; **Figure 1**).

ROLE OF T CELLS IN SVV TRAFFICKING

Data from several studies carried out using the hu-SCID mouse model strongly suggest a critical role for T cells in VZV dissemination. First, direct inoculation of VZV-infected fibroblasts into human fetal thymus and liver xenografts placed under the kidney capsule of SCID mice revealed that T cells support VZV replication (Moffat et al., 1995). Furthermore, injection of VZV-infected T cells into human skin xenografts implanted in the SCID model demonstrated the importance of the type I interferon response in restricting VZV replication in the skin (Ku et al., 2004). More importantly, intravenous injection of VZV-infected T cells but not fibroblasts resulted in vesicular rash of human skin implants suggesting that T cells can traffic the virus to the skin (Ku et al., 2004). These observations gave rise to the current model which stipulates that VZV gains access to T cells that deliver the virus to cutaneous sites of replication (Zerboni et al., 2014). However, given the limitations of this mouse model, findings from these studies cannot be extrapolated to decisively uncover the mechanisms by which VZV hijacks T cells to disseminate to the ganglia in the human host *in vivo*.

In both rhesus macaques and African green monkeys, different subsets of immune cells, including T cells, were shown to reach the ganglia as early as 3 days post intrabronchial inoculation (dpi) during acute infection (Ouwendijk et al., 2013b; Arnold et al., 2016a), prior to the detection of anti-SVV specific T cell immunity, these results suggest that T cells play an important role in SVV dissemination to sensory ganglia. Interestingly, CD8 memory T cells were the most abundant subset of immune cells infiltrating the ganglia of SVV-infected African green monkeys and rhesus macaques (Arnold et al., 2016a; Ouwendijk et al., 2016). In support of the potential role of T cells as Trojan horse for SVV, T cells isolated from bronchial alveolar lavage (BAL) samples during primary infection supported viral replication (Arnold et al., 2016a). Similarly, T cells infiltrate the enteric nervous system during acute SVV infection in African green monkeys (Ouwendijk et al., 2018). These results obtained in the SVV infection model along with the studies reporting that VZV infected T cells can traffic the virus to human xenografts in the SCID-hu mouse model further emphasize the importance played by T cells in varicella viruses dissemination and pathogenesis (Ku et al., 2004; Zerboni et al., 2005).

In order to improve our understanding of the mechanisms by which SVV alters T cells migratory behavior and to in SVV trafficking, a recent study analyzed the transcriptional profile of T cells in BAL samples following SVV infection in rhesus macaques (Arnold and Messaoudi, 2017b). This study reported that multiple cellular processes were dysregulated in T cells upon SVV infection, including genes involved in chromatin assembly, immune response, cell cycle, and cellular metabolism. These results suggest that SVV might alter T cell functions in order to achieve efficient viral replication and allow the virus to spread in the host while evading the immune system. Interestingly, in line with this hypothesis, previous *in vitro* studies using single-cell mass-spectrometry analysis (CyTOF) have reported that VZV infection of human tonsil T cells leads to upregulation of several immune genes including components of the TCR signaling machinery (Sen et al., 2014, 2015).

SVV LATENCY PATTERN IN THE RHESUS MACAQUE MODEL

Transcriptomic analysis of BAL cells collected from rhesus macaques during SVV primary infection showed that all ORFs were expressed between 3 and 7 dpi with increasing intensity that correlated with viremia (Meyer et al., 2011). The most highly expressed SVV ORFs detected at 3 dpi in BAL samples were ORF 57 (unknown function), ORF 41 (capsid protein), ORF 55 (component of the DNA helicase-primase complex), and ORF 63 (transactional activator) (Meyer et al., 2011). At 7 dpi, ORF63, ORF41 as well as ORF49 (structural

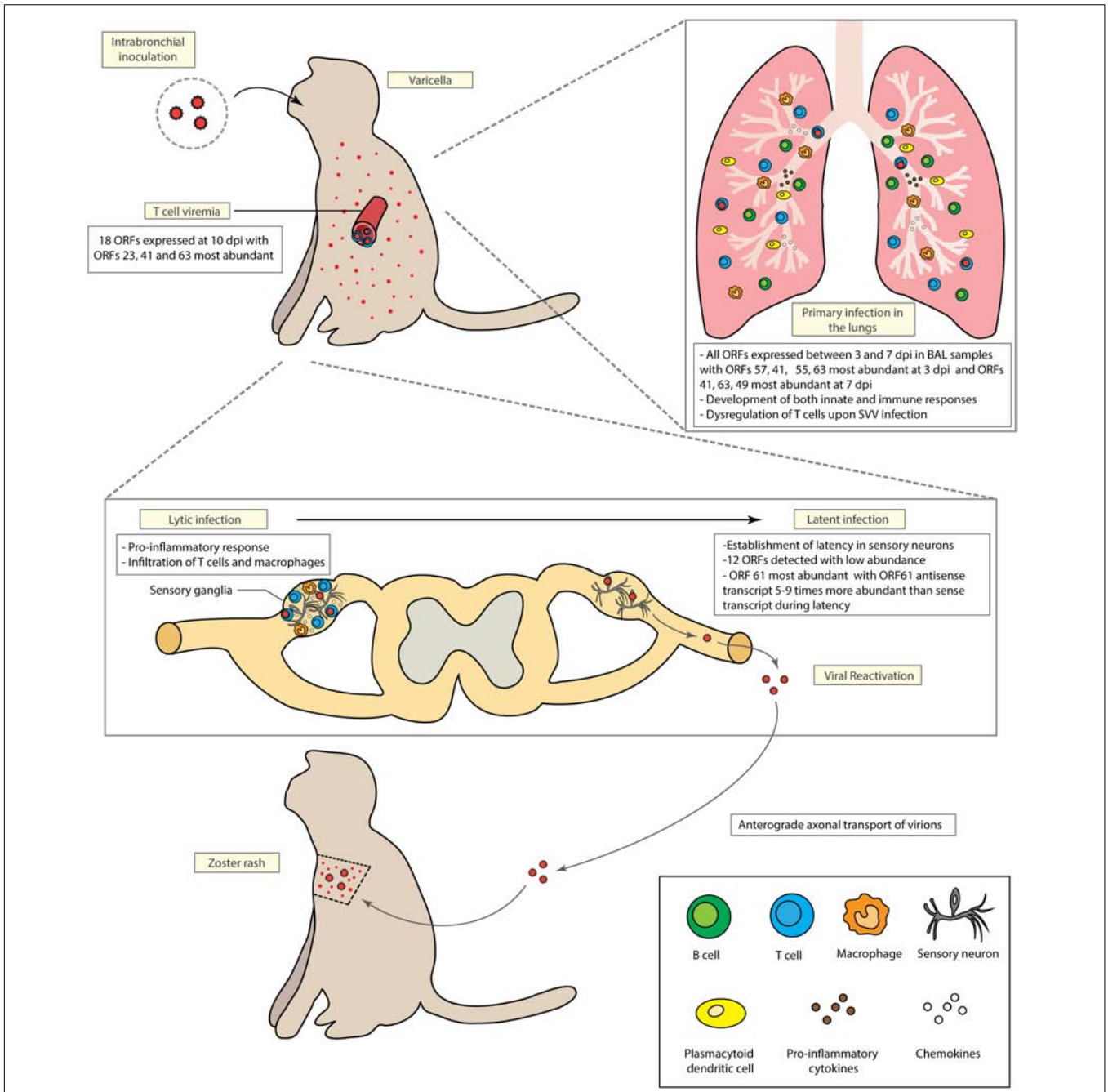

FIGURE 1 | Model of Simian Varicella Virus (SVV) pathogenesis in rhesus macaques following intrabronchial inoculation. Intrabronchial inoculation of rhesus macaques with SVV results in primary infection associated with viral replication in the lung, T cell viremia and the development of varicella. SVV reaches sensory ganglia as early as 3 days post infection. Initial viral replication is followed by the establishment of latency in the sensory ganglia. SVV can reactivate upon immune suppression. Both primary infection and viral reactivation induce robust cellular and humoral immune responses.

protein) were the most abundant transcripts expressed in BAL cells (Meyer et al., 2011). Parallel analysis of the viral transcriptome profiles of PBMCs derived from rhesus macaques infected with SVV revealed that only 18 SVV ORFs were expressed at 10 dpi in these samples, consistent with significantly lower viremia (Meyer et al., 2011). However, similarly to the BAL samples, the most highly expressed viral genes included ORFs 23, 41, and 63 (Meyer et al., 2011).

Latency is a state that is characterized by a restricted viral gene expression pattern. In line with that expectation, only 12 SVV ORFs were detected sporadically during SVV latent infection in the sensory ganglia. Importantly, ORF61 was the most abundant and consistently detected transcript in

the ganglia during latent infection (Meyer et al., 2011). More specifically, the antisense transcript of ORF61 was found to be 5–9 times more abundant than sense transcripts (Messaoudi et al., 2009). Similar findings were reported for latently infected ganglia collected from Vervet and African green monkeys (Ou et al., 2007; Ouwendijk et al., 2013a). Recently, the presence of an ORF61 anti-sense transcript was reported for VZV latent infection (Depledge et al., 2018a). Although multiple isoforms of VZV ORF61 antisense transcripts were detected during lytic infection, only one isoform was predominant during latency and was shown to suppress VZV ORF61 expression (Depledge et al., 2018a). Taken together, these results suggest that cessation of ORF61 expression by the anti-sense transcript may be critical in the establishment and maintenance of latency. Interestingly, establishment of latency was not impaired in animals infected with an SVV mutant deleted of ORF61 (SVVΔORF61) (Meyer et al., 2013c). Since ORF61 is thought to be shut off by the anti-sense transcript in order to prevent reactivation during latency, the lack of the ORF61 anti-sense transcript following infection with SVVΔORF61 would explain why establishment and maintenance of latency are not affected by the deletion.

SVV ORF61 is an immediate early gene that encodes a protein with a RING finger motif at the amino terminus, which is important for potential E3 ubiquitin ligase activity as well as a nuclear localization signal at the N terminus (Gray et al., 2007). Previous *in vitro* studies showed that ORF61 protein can transactivate its own promoter as well as promoters of SVV genes of all kinetic classes (Gray et al., 2007). Although SVV ORF61 is non-essential for SVV lytic cycle *in vitro*, SVVΔORF61 replicates 2- to 5-fold less efficiently compared to the wild-type (WT) virus (Gray et al., 2007). Similarly, *in vivo* infection with SVVΔORF61 was associated to a decreased expression of all viral transcripts and decreased viral loads in rhesus macaques (Meyer et al., 2013c). Infection with SVVΔORF61 also led to increased infiltration of plasmacytoid dendritic cells (pDC) into the lungs and expression of interferon stimulated genes *in vivo* suggesting a potential role of ORF61 in evasion of the host innate immune response (Meyer et al., 2013c). Indeed, both SVV and VZV ORF61 were shown to interfere with NF-κB signaling *in vitro* (Whitmer et al., 2015).

THE IMPORTANT ROLE OF T CELLS IN THE ESTABLISHMENT AND MAINTENANCE OF LATENCY

Intrabronchial infection of rhesus macaques with SVV results in the development of both innate and adaptive immune responses in the lungs concomitant with a decrease in the SVV viral loads observed (Arnold et al., 2016b). The mucosal innate immune response is characterized by a significant production of pro-inflammatory cytokines, chemokines (including T cell chemoattractants) and IFNα into the alveolar space that correlates with increased frequency of pDCs (Haberthur et al., 2014; Arnold et al., 2016b). This initial response is followed by a robust proliferation and infiltration of B and T cells in the lungs (Haberthur et al., 2014). Although CD8 T cells were found to be more abundant, a higher proportion of CD4 T cells were specific to SVV in the BAL (Haberthur et al., 2014). This observation is in line with several studies that reported a critical role for CD4 T cells in controlling both SVV and VZV acute infection (Haberthur et al., 2011; Duncan and Hambleton, 2015; Sen et al., 2015; Sen and Arvin, 2016). Indeed, whereas depletion of B cells and CD8 T cells showed no or limited effect on disease severity, CD4 depletion led to higher viral loads, prolonged viremia, and disseminated varicella (Haberthur et al., 2011). These results explain why children with T cell deficiencies are more prone to developing serious complications following VZV infection whereas children with B cell deficiencies have uncomplicated disease (Arvin et al., 1978; Wilson et al., 1992; Nader et al., 1995; Redman et al., 1997; Zerboni et al., 1998).

The anti-SVV T cell responses during acute infection in rhesus macaques is broad with CD8 T cell responses directed mainly against immediate-early (IE) and early (E) viral proteins whereas CD4 T cell responses were mostly specific to late (L) proteins (Haberthur et al., 2013). During latency, the magnitude of the T cell response decreases dramatically and becomes more restricted (Haberthur et al., 2013). Specifically, T cell responses directed against only 5 ORFs (ORF 4, 11, 19, 31, and 37) were maintained during latency whereas specific T cell responses to ORFs 10, 20, 29, 31, 62, 63, 68 showed a significant decrease compared to primary infection (Haberthur et al., 2013). Amongst these viral antigens, ORF68 (gE) is the most abundant glycoprotein, a critical determinant of VZV pathogenesis (Moffat et al., 2004; Berarducci et al., 2009; Zerboni et al., 2011), and a highly immunogenic viral antigen (Vizoso Pinto et al., 2010). These data suggest that boosting T cell responses against these viral antigens that are highly immunogenic during acute infection but poorly recognized during latency may be a promising direction for HZ vaccine. Indeed, the highly efficacious new recombinant subunit HZ vaccine (Shingrix®) contains an adjuvanted form of VZV gE that was shown to elicit a robust humoral and cell-mediated immunity (Mo et al., 2002; James et al., 2018; Syed, 2018). In contrast, Zostavax™ induces a lower VZV-specific cell-mediated immunity including a reduced gE-specific memory T cell responses compared to Shingrix®(Levin et al., 2018; Weinberg et al., 2018).

The importance of T cell responses during acute infection in the establishment of latency is evidenced by the detection of high level of viral transcription in ganglia of animals depleted of CD4 T cells during acute infection (Meyer et al., 2013b). It should be noted that at the time of ganglia analysis, the animals were no longer viremic. These results strongly suggest that loss of CD4 T cell immunity during acute infection impaired the establishment of a latency in sensory ganglia of infected macaques (Meyer et al., 2013b). In accordance with this observation, SVV infection of aged rhesus macaques was also characterized by dampened T cell responses and high levels of viral transcription inconsistent with latent infection (Meyer et al., 2013b). More recently, direct inoculation of VZV-infected fibroblasts into human fetal dorsal root ganglia (DRG) implanted under the kidney capsule as well as intravenous transfer of VZV-infected

CD4 T cells showed persistent viral replication in the ganglia tissue followed eventually by latency (Zerboni et al., 2005; Reichelt et al., 2008). These data from the hu-SCID mouse suggest that adaptive immune responses may not be critical for the establishment of latency. However, the CD4 T cells were most likely obtained from VZV-seropositive individuals and therefore the fact that they may harbor VZV-specific T cells cannot be dismissed. Similarly to VZV, stress and immune suppression can induce SVV reactivation leading to anterograde axonal transport of virions to the skin causing HZ lesions (Soike et al., 1984; Mahalingam et al., 2007, 2010; Traina-Dorge et al., 2014). Because T cells were shown to be critical in the establishment of latency, a recent study investigated the specific role of T cell immunity in preventing SVV reactivation (Arnold et al., 2017). This study showed that depletion of either CD4 or CD8 T cells in latently infected animals led to subclinical reactivation (defined as viremia detected in the absence of zoster rash) and an increase in the viral loads in the ganglia (Arnold et al., 2017). Moreover, large transcriptional changes of genes involved in inflammation and neuronal functions were reported in the ganglia obtained from animals that experienced subclinical reactivation (Arnold et al., 2017). Taken together, these results support the critical role of T cell immunity in maintaining SVV latency.

IMMUNOLOGICAL OUTCOMES FOLLOWING REACTIVATION

Other studies have attempted to induce reactivation in SVV-latently infected rhesus macaques using a combination of total body irradiation (2–8 Gy) and immune suppressant regimens (cyclosporine and tacrolimus). In some of these studies, cynomolgus and rhesus macaques were irradiated before receiving tacrolimus and prednisone, resulting in clinical reactivation in 25 and 100% of animals, respectively (Mahalingam et al., 2007; Traina-Dorge et al., 2014). In another study, treatment with only immune suppressants resulted in 75% reactivation (Ouwendijk et al., 2013a). The incidence of HZ obtained following these experimental treatments is significantly higher than the reactivation rate reported in humans. Another perplexing outcome of these studies includes the very high incidence of reactivation in the non-treated controls which is often ∼100%. Other groups failed to reproduce these findings using the same approaches (Meyer et al., 2015b), potentially due to a higher level of stress induced by a longer transportation to the irradiation site for the animals in the compared to those housed in the Oregon National Primate Center.

Following reactivation, SVV antigens were detected in multiple tissues, including skin and lymph nodes in rhesus macaques despite the lack of viremia at the time of HZ (Traina-Dorge et al., 2015). In skin tissues, SVV antigens were found mainly in sweat glands, whereas in lymph nodes, they were detected in macrophages, dendritic cells (DCs), and T cells. It is possible that DCs containing SVV antigens are activating T cells in the peripheral lymph nodes or that infected DCs are transferring SVV to T cells as previously described for VZV (Abendroth et al., 2001). Additionally, SVV reactivation in rhesus macaques induces the development of a strong systemic pro-inflammatory response (Traina-Dorge et al., 2014) associated with an overall increased in the number of total T cells compared to latency (James et al., 2014). T cell infiltration was detected in the sensory ganglia of cynomolgus macaques experiencing reactivation where neurons were found to be surrounded mainly by CD8 rather than CD4 T cells (Ouwendijk et al., 2013a). Moreover, as previously reported for post-mortem human sensory ganglia derived from patients who suffered from HZ at the time of death (Steain et al., 2011), the authors detected elevated levels of CXCL10, a chemokine involved in T cell migration (Ouwendijk et al., 2013a). Taken together these results suggest that the pro-inflammatory response play an important role in initiating T cell recruitment to the site of SVV/VZV reactivation. However, the high reactivation rates in the control animals raises concerns about the clinical significance of these findings.

CONCLUSION AND FUTURE PERSPECTIVES

Although studies over the last few decades have led to significant advances in our understanding of VZV pathogenesis, several questions remain unanswered. Specifically, although it is now well established that that T cells play a critical in the pathogenesis of both VZV and SVV, the exact mechanisms by which VZV/SVV modulate T cell functions to alter their migratory properties and confer ability to access into the central nervous system are not known. Furthermore, the viral and cellular factors that control establishment and maintenance of SVV/VZV latency in sensory ganglia remain poorly understood. Notably, the role of the ORF61 anti-sense transcript during the transition from lytic to latent phases has yet to be investigated. Similarly, the role of epigenetic modifications (such as histone/DNA methylation or histone acetylation) in the maintenance of latency remains to be studied. Future studies should uncover the impact of persistent transcriptional changes within the ganglia on neuronal function. SVV infection in rhesus macaques provides a model well-suited to further our knowledge of varicella viruses' pathogenesis. The availability of this model together with a versatile bacterial artificial chromosome (Gray et al., 2011; Meyer et al., 2013a) that facilitates manipulation of the viral genome will play a critical role in addressing these remaining gaps in our knowledge.

AUTHOR CONTRIBUTIONS

OS and IM wrote the manuscript.

FUNDING

This work was supported by NIH award 1UM01AR065705.

REFERENCES

Abendroth, A., Morrow, G., Cunningham, A. L., and Slobedman, B. (2001). *Varicella-zoster virus* infection of human dendritic cells and transmission to T cells: implications for virus dissemination in the host. *J. Virol.* 75, 6183–6192. doi: 10.1128/JVI.75.13.6183-6192.2001

Annunziato, P., LaRussa, P., Lee, P., Steinberg, S., Lungu, O., Gershon, A. A., et al. (1998). Evidence of latent *Varicella-zoster virus* in rat dorsal root ganglia. *J. Infect. Dis.* 178(Suppl. 1)), S48–S51. doi: 10.1086/514261

Arnold, N., Girke, T., Sureshchandra, S., and Messaoudi, I. (2016a). Acute *Simian varicella virus* infection causes robust and sustained changes in gene expression in the sensory ganglia. *J. Virol.* 90, 10823–10843. doi: 10.1128/JVI.01272-16

Arnold, N., Girke, T., Sureshchandra, S., Nguyen, C., Rais, M., and Messaoudi, I. (2016b). Genomic and functional analysis of the host response to acute simian varicella infection in the lung. *Sci. Rep.* 28:34164. doi: 10.1038/srep34164

Arnold, N., and Messaoudi, I. (2017a). Herpes zoster and the search for an effective vaccine. *Clin. Exp. Immunol.* 187, 82–92. doi: 10.1111/cei.12809

Arnold, N., and Messaoudi, I. (2017b). *Simian varicella virus* causes robust transcriptional changes in T cells that support viral replication. *Virus Res.* 15, 226–235. doi: 10.1016/j.virusres.2017.07.004

Arnold, N., Meyer, C., Engelmann, F., and Messaoudi, I. (2017). Robust gene expression changes in the ganglia following subclinical reactivation in rhesus macaques infected with *Simian varicella virus*. *J. Neurovirol.* 23, 520–538. doi: 10.1007/s13365-017-0522-3

Arvin, A. M., Pollard, R. B., Rasmussen, L. E., and Merigan, T. C. (1978). Selective impairment of lymphocyte reactivity to *Varicella-zoster virus* antigen among untreated patients with lymphoma. *J. Infect. Dis.* 137, 531–540. doi: 10.1093/infdis/137.5.531

Berarducci, B., Rajamani, J., Reichelt, M., Sommer, M., Zerboni, L., and Arvin, A. M. (2009). Deletion of the first cysteine-rich region of the *Varicella-zoster virus* glycoprotein E ectodomain abolishes the gE and gI interaction and differentially affects cell-cell spread and viral entry. *J. Virol.* 83, 228–240. doi: 10.1128/JVI.00913-08

Chiner, E., Ballester, I., Betlloch, I., Blanquer, J., Aguar, M. C., Blanquer, R., et al. (2010). *Varicella-zoster virus* pneumonia in an adult population: has mortality decreased? *Scand. J. Infect. Dis.* 42, 215–221. doi: 10.3109/00365540903428166

Clarke, P., Rabkin, S. D., Inman, M. V., Mahalingam, R., Cohrs, R., Wellish, M., et al. (1992). Molecular analysis of *Simian varicella virus* DNA. *Virology* 190, 597–605. doi: 10.1016/0042-6822(92)90897-X

Clarkson, M. J., Thorpe, E., and McCarthy, K. (1967). A virus disease of captive vervet monkeys (*Cercopithecus aethiops*) caused by a new herpesvirus. *Archiv. Gesamte Virusforschung.* 22, 219–234. doi: 10.1007/BF01240517

Cohen, J. I., Moskal, T., Shapiro, M., and Purcell, R. H. (1996). Varicella in Chimpanzees. *J. Med. Virol.* 50, 289–292. doi: 10.1002/(SICI)1096-9071(199612)50:4<289::AID-JMV2>3.0.CO;2-4

Dalziel, R. G., Bingham, S., Sutton, D., Grant, D., Champion, J. M., Dennis, S. A., et al. (2004). Allodynia in rats infected with *Varicella zoster virus*–a small animal model for post-herpetic neuralgia. *Brain Res. Brain Res. Rev.* 46, 234–242. doi: 10.1016/j.brainresrev.2004.07.008

Dayan, R. R., and Peleg, R. (2017). Herpes zoster - typical and atypical presentations. *Postgraduate Med.* 129, 567–571. doi: 10.1080/00325481.2017.1335574

Depledge, D. P., Ouwendijk, W. J. D., Sadaoka, T., Braspenning, S. E., Mori, Y., Cohrs, R. J., et al. (2018a). A spliced latency-associated VZV transcript maps antisense to the viral transactivator gene 61. *Nat. Commun.* 9:1167. doi: 10.1038/s41467-018-03569-2

Depledge, D. P., Sadaoka, T., and Ouwendijk, W. J. D. (2018b). Molecular aspects of *Varicella-zoster virus* latency. *Viruses* 10:E349. doi: 10.3390/v10070349

Duncan, C. J., and Hambleton, S. (2015). *Varicella zoster virus* immunity: a primer. *J. Infect.* 71(Suppl. 1), S47–S53. doi: 10.1016/j.jinf.2015.04.015

Elmore, D., and Eberle, R. (2008). Monkey B virus (*Cercopithecine herpesvirus 1*). *Comp. Med.* 58, 11–21.

Felsenfeld, A. D., and Schmidt, N. J. (1979). *Varicella-zoster virus* immunizes patas monkeys against simian varicella-like disease. *J. Gen. Virol.* 42, 171–178. doi: 10.1099/0022-1317-42-1-171

Gan, L., Wang, M., Chen, J. J., Gershon, M. D., and Gershon, A. A. (2014). Infected peripheral blood mononuclear cells transmit latent *Varicella zoster virus* infection to the guinea pig enteric nervous system. *J. Neurovirol.* 20, 442–456. doi: 10.1007/s13365-014-0259-1

Gershon, A. A. (2017). Is chickenpox so bad, what do we know about immunity to *Varicella zoster virus*, and what does it tell us about the future? *J. Infect.* 74(Suppl. 1), S27–S33. doi: 10.1016/S0163-4453(17)30188-3

Gershon, A. A., Chen, J., and Gershon, M. D. (2008). A model of lytic, latent, and reactivating *Varicella-zoster virus* infections in isolated enteric neurons. *J. Infect. Dis.* 197(Suppl. 2), S61–S65. doi: 10.1086/522149

Gnann, J. W. Jr. (2002). *Varicella-zoster virus*: atypical presentations and unusual complications. *J. Infect. Dis.* 186(Suppl. 1), S91–S98. doi: 10.1086/342963

Gray, W. L. (2008). Simian varicella in old world monkeys. *Comp. Med.* 58, 22–30.

Gray, W. L. (2010). *Simian varicella virus*: molecular virology. *Curr. Top. Microbiol. Immunol.* 342, 291–308. doi: 10.1007/82_2010_27

Gray, W. L., Davis, K., Ou, Y., Ashburn, C., and Ward, T. M. (2007). *Simian varicella virus* gene 61 encodes a viral transactivator but is non-essential for in vitro replication. *Arch. Virol.* 152, 553–563. doi: 10.1007/s00705-006-0866-0

Gray, W. L., and Oakes, J. E. (1984). *Simian varicella virus* DNA shares homology with human *varicella-zoster virus* DNA. *Virology* 136, 241–246. doi: 10.1016/0042-6822(84)90263-0

Gray, W. L., Starnes, B., White, M. W., and Mahalingam, R. (2001). The DNA sequence of the *Simian varicella virus* genome. *Virology* 284, 123–130. doi: 10.1006/viro.2001.0912

Gray, W. L., Zhou, F., Noffke, J., and Tischer, B. K. (2011). Cloning the *Simian varicella virus* genome in *E. coli* as an infectious bacterial artificial chromosome. *Arch. Virol.* 156, 739–746. doi: 10.1007/s00705-010-0889-4

Haberthur, K., Engelmann, F., Park, B., Barron, A., Legasse, A., Dewane, J., et al. (2011). CD4 T cell immunity is critical for the control of *Simian varicella virus* infection in a nonhuman primate model of VZV infection. *PLoS Pathog.* 7:e1002367. doi: 10.1371/journal.ppat.1002367

Haberthur, K., Kraft, A., Arnold, N., Park, B., Meyer, C., Asquith, M., et al. (2013). Genome-wide analysis of T cell responses during acute and latent *Simian varicella virus* infections in rhesus macaques. *J. Virol.* 87, 11751–11761. doi: 10.1128/JVI.01809-13

Haberthur, K., and Messaoudi, I. (2013). Animal models of varicella zoster virus infection. *Pathogens* 2, 364–382. doi: 10.3390/pathogens2020364

Haberthur, K., Meyer, C., Arnold, N., Engelmann, F., Jeske, D. R., and Messaoudi, I. (2014). Intrabronchial infection of rhesus macaques with *Simian varicella virus* results in a robust immune response in the lungs. *J. Virol.* 88, 12777–12792. doi: 10.1128/JVI.01814-14

Heininger, U., and Seward, J. F. (2006). Varicella. *Lancet* 368, 1365–1376. doi: 10.1016/S0140-6736(06)69561-5

James, S. F., Chahine, E. B., Sucher, A. J., and Hanna, C. (2018). Shingrix: the new adjuvanted recombinant herpes zoster vaccine. *Ann. Pharmacother.* 52, 673–680. doi: 10.1177/1060028018758431

James, S. F., Traina-Dorge, V., Deharo, E., Wellish, M., Palmer, B. E., Gilden, D., et al. (2014). T cells increase before zoster and PD-1 expression increases at the time of zoster in immunosuppressed nonhuman primates latently infected with *Simian varicella virus*. *J. Neurovirol.* 20, 309–313. doi: 10.1007/s13365-014-0237-7

Jones, J. O., and Arvin, A. M. (2003). Microarray analysis of host cell gene transcription in response to *Varicella-zoster virus* infection of human T cells and fibroblasts in vitro and SCIDhu skin xenografts in vivo. *J. Virol.* 77, 1268–1280. doi: 10.1128/JVI.77.2.1268-1280.2003

Keating, G. M. (2016). Shingles (Herpes Zoster) Vaccine (Zostavax((R))): a review in the prevention of herpes zoster and postherpetic neuralgia. *BioDrugs* 30, 243–254. doi: 10.1007/s40259-016-0180-7

Ku, C.-C., Zerboni, L., Ito, H., Graham, B. S., Wallace, M., and Arvin, A. M. (2004). *Varicella-zoster virus* transfer to skin by t cells and modulation of viral replication by epidermal cell interferon-{alpha}. *J. Exp. Med.* 200, 917–925. doi: 10.1084/jem.20040634

Leclair, J. M., Zaia, J. A., Levin, M. J., Congdon, R. G., and Goldmann, D. A. (1980). Airborne transmission of chickenpox in a hospital. *N. Engl. J. Med.* 302, 450–453. doi: 10.1056/NEJM198002213020807

Levin, M. J., Kroehl, M. E., Johnson, M. J., Hammes, A., Reinhold, D., Lang, N., et al. (2018). Th1 memory differentiates recombinant from live herpes zoster vaccines. *J. Clin. Invest.* 128, 4429–4440. doi: 10.1172/JCI121484

Long, S. Y., Latimer, E. M., and Hayward, G. S. (2016). Review of elephant endotheliotropic herpesviruses and acute hemorrhagic disease. *ILAR J.* 56, 283–296. doi: 10.1093/ilar/ilv041

Mahalingam, R., and Gilden, D. H. (2007). "*Simian varicella virus*," in *Human Herpesviruses: Biology, Therapy, and Immunoprophylaxis*, eds A. Arvin, G. Campadelli-Fiume, E. Mocarski, P. S. Moore, B. Roizman, R. Whitley, et al. (Cambridge: Cambridge University Press), 2007.

Mahalingam, R., Traina-Dorge, V., Wellish, M., Deharo, E., Singletary, M. L., Ribka, E. P., et al. (2010). Latent *Simian varicella virus* reactivates in monkeys treated with tacrolimus with or without exposure to irradiation. *J. Neurovirol.* 16, 342–354. doi: 10.3109/13550284.2010.513031

Mahalingam, R., Traina-Dorge, V., Wellish, M., Lorino, R., Sanford, R., Ribka, E. P., et al. (2007). *Simian varicella virus* reactivation in cynomolgus monkeys. *Virology* 368, 50–59. doi: 10.1016/j.virol.2007.06.025

Messaoudi, I., Barron, A., Wellish, M., Engelmann, F., Legasse, A., Planer, S., et al. (2009). *Simian varicella virus* infection of rhesus macaques recapitulates essential features of *Varicella zoster virus* infection in humans. *PLoS Pathog.* 5:e1000657. doi: 10.1371/journal.ppat.1000657

Meyer, C., Dewane, J., Haberthur, K., Engelmann, F., Arnold, N., Gray, W., et al. (2013a). Bacterial artificial chromosome derived *Simian varicella virus* is pathogenic in vivo. *Virol. J.* 8:278. doi: 10.1186/1743-422X-10-278

Meyer, C., Dewane, J., Kerns, A., Haberthur, K., Barron, A., Park, B., et al. (2013b). Age and immune status of rhesus macaques impact *Simian varicella virus* gene expression in sensory ganglia. *J. Virol.* 87, 8294–8306.doi: 10.1128/JVI.01112-13

Meyer, C., Engelmann, F., Arnold, N., Krah, D. L., ter Meulen, J., Haberthur, K., et al. (2015a). Abortive intrabronchial infection of rhesus macaques with *Varicella-zoster virus* provides partial protection against *Simian varicella virus* challenge. *J. Virol.* 89, 1781–1793. doi: 10.1128/JVI.03124-14

Meyer, C., Kerns, A., Barron, A., Kreklywich, C., Streblow, D. N., and Messaoudi, I. (2011). *Simian varicella virus* gene expression during acute and latent infection of rhesus macaques. *J. Neurovirol.* 17, 600–612. doi: 10.1007/s13365-011-0057-y

Meyer, C., Kerns, A., Haberthur, K., Dewane, J., Walker, J., Gray, W., et al. (2013c). Attenuation of the adaptive immune response in rhesus macaques infected with *Simian varicella virus* lacking open reading frame 61. *J. Virol.* 87, 2151–2163. doi: 10.1128/JVI.02369-12

Meyer, C., Walker, J., Dewane, J., Engelmann, F., Laub, W., Pillai, S., et al. (2015b). Impact of irradiation and immunosuppressive agents on immune system homeostasis in rhesus macaques. *Clin. Exp. Immunol.* 181, 491–510. doi: 10.1111/cei.12646

Mo, C., Lee, J., Sommer, M., Grose, C., and Arvin, A. M. (2002). The requirement of *Varicella zoster virus* glycoprotein E (gE) for viral replication and effects of glycoprotein I on gE in melanoma cells. *Virology* 304, 176–186. doi: 10.1006/viro.2002.1556

Moffat, J., Mo, C., Cheng, J. J., Sommer, M., Zerboni, L., Stamatis, S., et al. (2004). Functions of the C-terminal domain of *varicella-zoster virus* glycoprotein E in viral replication in vitro and skin and T-cell tropism in vivo. *J. Virol.* 78, 12406–12415. doi: 10.1128/JVI.78.22.12406-12415.2004

Moffat, J. F., Stein, M. D., Kaneshima, H., and Arvin, A. M. (1995). Tropism of *varicella-zoster virus* for human CD4+ and CD8+ T lymphocytes and epidermal cells in SCID-hu mice. *J. Virol.* 69, 5236–5242.

Myers, M. G., Kramer, L. W., and Stanberry, L. R. (1987). Varicella in a gorilla. *J. Med. Virol.* 23, 317–322. doi: 10.1002/jmv.1890230403

Nader, S., Bergen, R., Sharp, M., and Arvin, A. M. (1995). Age-related differences in cell-mediated immunity to *Varicella-zoster virus* among children and adults immunized with live attenuated varicella vaccine. *J. Infect. Dis.* 171, 13–17. doi: 10.1093/infdis/171.1.13

Ou, Y., Davis, K. A., Traina-Dorge, V., and Gray, W. L. (2007). *Simian varicella virus* expresses a latency-associated transcript that is antisense to open reading frame 61 (ICP0) mRNA in neural ganglia of latently infected monkeys. *J. Virol.* 81, 8149–8156. doi: 10.1128/JVI.00407-07

Ouwendijk, W. J., Abendroth, A., Traina-Dorge, V., Getu, S., Steain, M., Wellish, M., et al. (2013a). T-Cell Infiltration Correlates with CXCL10 expression in ganglia of cynomolgus macaques with reactivated *Simian varicella virus*. *J. Virol.* 87, 2979–2982. doi: 10.1128/JVI.03181-12

Ouwendijk, W. J., Getu, S., Mahalingam, R., Gilden, D., Osterhaus, A. D., and Verjans, G. M. (2016). Characterization of the immune response in ganglia after primary *Simian varicella virus* infection. *J. Neurovirol.* 22, 376–388. doi: 10.1007/s13365-015-0408-1

Ouwendijk, W. J., Mahalingam, R., de Swart, R. L., Haagmans, B. L., van Amerongen, G., Getu, S., et al. (2013b). T-Cell tropism of *Simian varicella virus* during primary infection. *PLoS Pathog.* 9:e1003368. doi: 10.1371/journal.ppat.1003368

Ouwendijk, W. J. D., van Veen, S., Mehraban, T., Mahalingam, R., and Verjans, G. (2018). *Simian varicella virus* infects enteric neurons and alpha4beta7 integrin-expressing gut-tropic t-cells in nonhuman primates. *Viruses* 10:156. doi: 10.3390/v10040156

Provost, P. J., Keller, P. M., Banker, F. S., Keech, B. J., Klein, H. J., Lowe, R. S., et al. (1987). Successful infection of the common marmoset (*Callithrix jacchus*) with human *varicella-zoster virus*. *J. Virol.* 61, 2951–2955.

Redman, R. L., Nader, S., Zerboni, L., Liu, C., Wong, R. M., Brown, B. W., et al. (1997). Early reconstitution of immunity and decreased severity of herpes zoster in bone marrow transplant recipients immunized with inactivated varicella vaccine. *J. Infect. Dis.* 176, 578–585. doi: 10.1086/514077

Reichelt, M., Zerboni, L., and Arvin, A. M. (2008). Mechanisms of *Varicella-zoster virus* neuropathogenesis in human dorsal root ganglia. *J. Virol.* 82, 3971–3983. doi: 10.1128/JVI.02592-07

Sadzot-Delvaux, C., Merville-Louis, M. P., Delree, P., Marc, P., Piette, J., Moonen, G., et al. (1990). An in vivo model of *Varicella-zoster virus* latent infection of dorsal root ganglia. *J. Neurosci. Res.* 26, 83–89. doi: 10.1002/jnr.490260110

Sawyer, M. H., Chamberlin, C. J., Wu, Y. N., Aintablian, N., and Wallace, M. R. (1994). Detection of *Varicella-zoster virus* DNA in air samples from hospital rooms. *J Infect Dis.* 169, 91–94. doi: 10.1093/infdis/169.1.91

Sen, N., and Arvin, A. M. (2016). Dissecting the molecular mechanisms of the tropism of *Varicella-zoster virus* for human T Cells. *J. Virol.* 90, 3284–3287. doi: 10.1128/JVI.03375-14

Sen, N., Mukherjee, G., and Arvin, A. M. (2015). Single cell mass cytometry reveals remodeling of human T cell phenotypes by *Varicella zoster virus*. *Methods* 15, 85–94. doi: 10.1016/j.ymeth.2015.07.008

Sen, N., Mukherjee, G., Sen, A., Bendall, S. C., Sung, P., Nolan, G. P., et al. (2014). Single-cell mass cytometry analysis of human tonsil T cell remodeling by *Varicella zoster virus*. *Cell Rep.* 8, 633–645. doi: 10.1016/j.celrep.2014.06.024

Soike, K. F., Rangan, S. R., and Gerone, P. J. (1984). Viral disease models in primates. *Adv. Vet. Sci. Comp. Med.* 28, 151–199. doi: 10.1016/B978-0-12-039228-5.50011-5

Sorel, O., Chen, T., Myster, F., Javaux, J., Vanderplasschen, A., and Dewals, B. G. (2017). Macavirus latency-associated protein evades immune detection through regulation of protein synthesis in cis depending upon its glycin/glutamate-rich domain. *PLoS Pathog.* 13:e1006691. doi: 10.1371/journal.ppat.1006691

Steain, M., Gowrishankar, K., Rodriguez, M., Slobedman, B., and Abendroth, A. (2011). Upregulation of CXCL10 in human dorsal root ganglia during experimental and natural *Varicella-zoster virus* infection. *J. Virol.* 85, 626–631. doi: 10.1128/JVI.01816-10

Suzuki, K., Yoshikawa, T., Tomitaka, A., Matsunaga, K., and Asano, Y. (2004). Detection of aerosolized *Varicella-zoster virus* DNA in patients with localized herpes zoster. *J. Infect. Dis.* 189, 1009–1012. doi: 10.1086/382029

Syed, Y. Y. (2018). Recombinant Zoster Vaccine (Shingrix((R))): a review in herpes zoster. *Drugs Aging* 35, 1031–1040. doi: 10.1007/s40266-018-0603-x

Traina-Dorge, V., Doyle-Meyers, L. A., Sanford, R., Manfredo, J., Blackmon, A., Wellish, M., et al. (2015). *Simian varicella virus* is present in macrophages, dendritic cells, and T cells in lymph nodes of rhesus macaques after experimental reactivation. *J. Virol.* 89, 9817–9824. doi: 10.1128/JVI.01324-15

Traina-Dorge, V., Sanford, R., James, S., Doyle-Meyers, L. A., de Haro, E., Wellish, M., et al. (2014). Robust pro-inflammatory and lesser anti-inflammatory immune responses during primary *Simian varicella virus* infection and reactivation in rhesus macaques. *J. Neurovirol.* 20, 526–530. doi: 10.1007/s13365-014-0274-2

Vizoso Pinto, M. G., Pfrepper, K. I., Janke, T., Noelting, C., Sander, M., Lueking, A., et al. (2010). A systematic approach for the identification of novel, serologically reactive recombinant *Varicella-Zoster Virus* (VZV) antigens. *Virol. J.* 20:165. doi: 10.1186/1743-422X-7-165

Wang, W., Pan, D., Fu, W., Cai, L., Ye, J., Liu, J., et al. (2017). A SCID mouse-human lung xenograft model of *Varicella-zoster virus* infection. *Antiviral Res.* 146, 45–53. doi: 10.1016/j.antiviral.2017.08.012

Wareham, D. W., and Breuer, J. (2007). Herpes zoster. *BMJ* 334, 1211–1215. doi: 10.1136/bmj.39206.571042.AE

Weinberg, A., Kroehl, M. E., Johnson, M. J., Hammes, A., Reinhold, D., Lang, N., et al. (2018). Comparative immune responses to licensed herpes zoster vaccines. *J. Infect. Dis.* 218(Suppl._2), S81–S87.

White, T. M., Mahalingam, R., Traina-Dorge, V., and Gilden, D. H. (2002). Persistence of *Simian varicella virus* DNA in CD4(+) and CD8(+) blood mononuclear cells for years after intratracheal inoculation of African green monkeys. *Virology* 303, 192–198. doi: 10.1006/viro.2002.1664

Whitmer, T., Malouli, D., Uebelhoer, L. S., DeFilippis, V. R., Fruh, K., and Verweij, M. C. (2015). The ORF61 protein encoded by *Simian varicella virus* and *Varicella-zoster virus* inhibits NF-kappaB Signaling by Interfering with IkappaBalpha Degradation. *J. Virol.* 89, 8687–8700. doi: 10.1128/JVI.01149-15

Wiegering, V., Schick, J., Beer, M., Weissbrich, B., Gattenlohner, S., Girschick, H. J., et al. (2011). *Varicella-zoster virus* infections in immunocompromised patients - a single centre 6-years analysis. *BMC Pediatr.* 10:31. doi: 10.1186/1471-2431-11-31

Willer, D. O., Ambagala, A. P., Pilon, R., Chan, J. K., Fournier, J., Brooks, J., et al. (2012). Experimental infection of Cynomolgus Macaques (*Macaca fascicularis*) with human *Varicella-zoster virus*. *J. Virol.* 86, 3626–3634. doi: 10.1128/JVI.06264-11

Wilson, A., Sharp, M., Koropchak, C. M., Ting, S. F., and Arvin, A. M. (1992). Subclinical *Varicella-zoster virus* viremia, herpes zoster, and T lymphocyte immunity to *Varicella-zoster viral* antigens after bone marrow transplantation. *J. Infect. Dis.* 165, 119–126. doi: 10.1093/infdis/165.1.119

Yamanishi, K. (2008). Molecular analysis of the Oka vaccine strain of *Varicella-zoster virus*. *J. Infect. Dis.* 197(Suppl. 2), S45–S48. doi: 10.1086/522122

Zerboni, L., Berarducci, B., Rajamani, J., Jones, C. D., Zehnder, J. L., and Arvin, A. (2011). *Varicella-zoster virus* glycoprotein E is a critical determinant of virulence in the SCID mouse-human model of neuropathogenesis. *J. Virol.* 85, 98–111. doi: 10.1128/JVI.01902-10

Zerboni, L., Ku, C.-C., Jones, C. D., Zehnder, J. L., and Arvin, A. M. (2005). *Varicella-zoster virus* infection of human dorsal root ganglia in vivo. *Proc. Natl. Acad. Sci. U.S.A.* 102, 6490–6495. doi: 10.1073/pnas.0501045102

Zerboni, L., Nader, S., Aoki, K., and Arvin, A. M. (1998). Analysis of the persistence of humoral and cellular immunity in children and adults immunized with varicella vaccine. *J. Infect. Dis.* 177, 1701–1704. doi: 10.1086/517426

Zerboni, L., Sen, N., Oliver, S. L., and Arvin, A. M. (2014). Molecular mechanisms of *Varicella zoster virus* pathogenesis. *Nat. Rev. Microbiol.* 12, 197–210. doi: 10.1038/nrmicro3215

Conflict of Interest Statement: The authors declare that the research was conducted in the absence of any commercial or financial relationships that could be construed as a potential conflict of interest.

frontiers in Microbiology

OPINION
published: 07 January 2019
doi: 10.3389/fmicb.2018.03207

"Novel" Triggers of Herpesvirus Reactivation and Their Potential Health Relevance

Tobias Stoeger[1]* *and Heiko Adler*[2,3]*

[1] Institute of Lung Biology and Disease, Comprehensive Pneumology Center, Helmholtz Zentrum München - German Research Center for Environmental Health (GmbH), Neuherberg, Germany, [2] Research Unit Lung Repair and Regeneration, Comprehensive Pneumology Center, Helmholtz Zentrum München - German Research Center for Environmental Health (GmbH), and University Hospital Grosshadern, Ludwig-Maximilians-University, Munich, Germany, [3] German Center for Lung Research (DZL), Giessen, Germany

Keywords: herpesvirus, reactivation, nanoparticle, non-canonical triggers, health relevance

OPEN ACCESS

Edited by:
Benjamin G. Dewals, University of Liege, Belgium

Reviewed by:
Bénédicte Machiels, University of Liege, Belgium
Xiaozhen Liang, Institut Pasteur of Shanghai (CAS), China
Tiffany Reese, University of Texas Southwestern Medical Center, United States

***Correspondence:**
Tobias Stoeger
tobias.stoeger@helmholtz-muenchen.de
Heiko Adler
h.adler@helmholtz-muenchen.de

Specialty section:
This article was submitted to Virology, a section of the journal Frontiers in Microbiology

Received: *09 October 2018*
Accepted: *11 December 2018*
Published: *07 January 2019*

Citation:
Stoeger T and Adler H (2019) "Novel" Triggers of Herpesvirus Reactivation and Their Potential Health Relevance. Front. Microbiol. 9:3207. doi: 10.3389/fmicb.2018.03207

After primary infection, herpesviruses persist for life in their hosts in a latent stage (Adler et al., 2017). Different subfamilies of herpesviruses establish latency in specific and different sets of cells (Pellett and Roizman, 2013; Lieberman, 2016). The latent stage can be interrupted by periods of lytic replication, termed reactivation. Reactivation is important for viral spread to new hosts or for the maintenance of the viral reservoir in the host. Usually, reactivation is not associated with disease but under certain circumstances, it may be accompanied by clinical symptoms. The stimuli and the precise molecular mechanisms that lead to reactivation from the latent state are not fully understood and can differ from one herpesvirus to another.

HERPESVIRUS REACTIVATION IN THE HUMAN HOST BY "CLASSICAL" TRIGGERS

A number of stimuli that trigger reactivation in humans are known for a long time – we term them as "classical" triggers of herpesvirus reactivation (**Figure 1**): (i) Alphaherpesviruses, e.g., latent HSV-1 in neurons of various ganglia, are for example reactivated by local injury to tissues innervated by latently infected neurons or by systemic physical or emotional stress, fever and microbial co-infection as well as UV-exposure or hormonal imbalance (Roizman and Whitley, 2013; Roizman et al., 2013). (ii) Reactivation of betaherpesviruses, for example CMV, is observed commonly in the setting of immunosuppression, particularly where allogeneic stimulation and pro-inflammatory cytokines are present and stimulate cellular differentiation to macrophages or dendritic cells (Stinski and Meier, 2007; Liu et al., 2013; Dupont and Reeves, 2016; Lieberman, 2016). (iii) Stimuli that induce reactivation of gammaherpesviruses, for example EBV, are differentiation of B cells into plasma cells through antigen stimulation of the B-cell receptor. *In vitro*, and potentially likewise *in vivo*, also cytokines including TGF-beta can induce B-cell activation and thus result in lytic EBV infection. Additionally, host cell stress, induced for example by chemotherapy or body irradiation, can reactivate latent EBV. In cell culture, EBV reactivation can also be triggered by phorbol ester 12-0-tetradecanoyl phorbol-13-acetate (TPA), sodium butyrate or calcium ionophores (Kenney, 2007; Murata, 2014). Many of these reactivation triggers activate classical signal transduction pathways, including protein kinase C, p38 kinase, c-Jun N-terminal kinase (JNK), ERK kinase and PI3 kinase. In conclusion, there are many settings of a specific herpesvirus, a specific host cell and a specific stimulus, determining the transition from latency to lytic cycle (Kenney, 2007; Murata, 2014; Dupont and Reeves, 2016; Cliffe and Wilson, 2017).

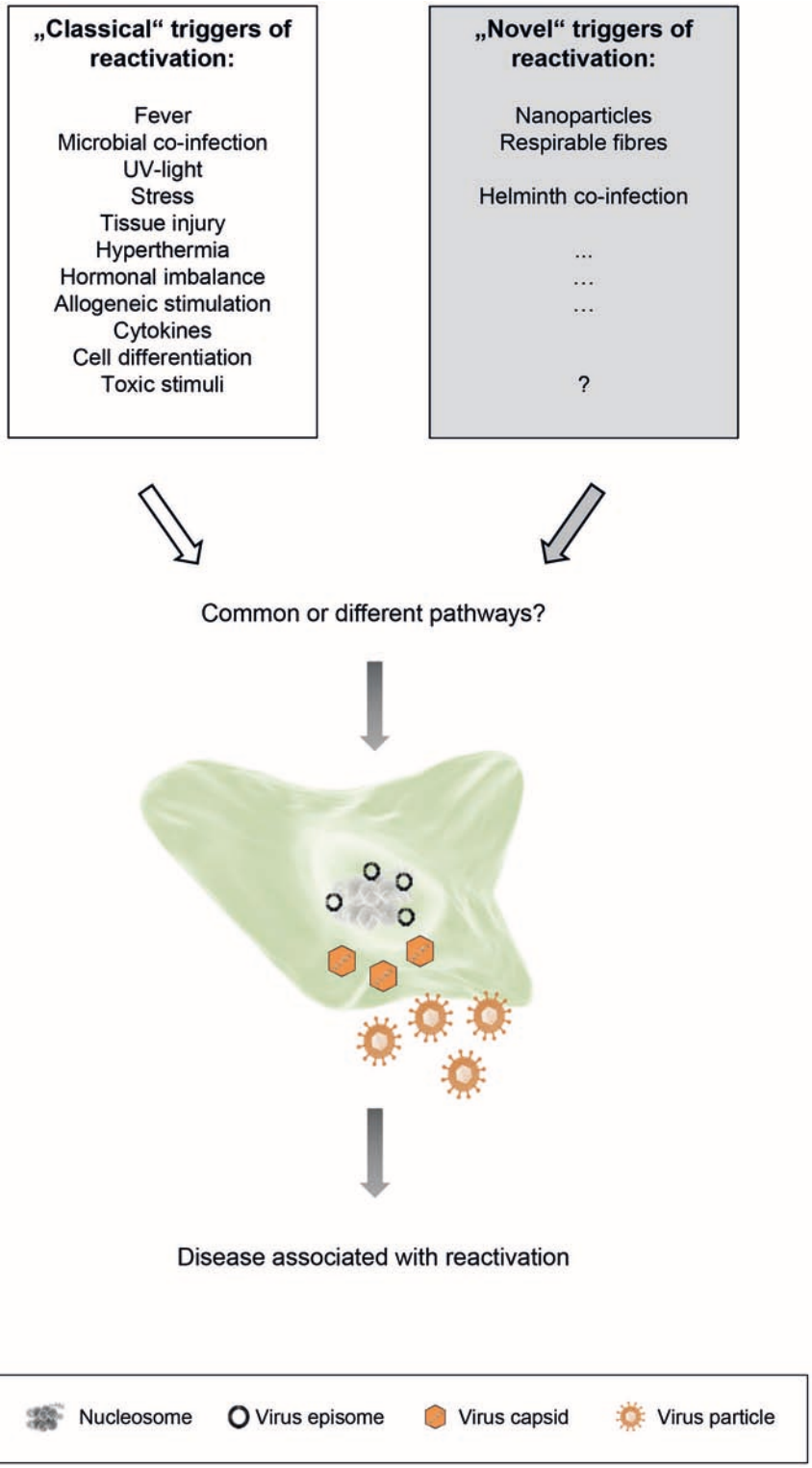

FIGURE 1 | "Classical" and "novel" triggers of herpesvirus reactivation. Both types of triggers are able to induce reactivation of latent herpesviruses. The respective signal transduction pathways that are activated may be shared, or may vary depending on the stimulus, the cell type and the virus. Although reactivation is usually not associated with disease, it may be accompanied by clinical symptoms under certain circumstances.

"NOVEL" TRIGGERS OF HERPESVIRUS REACTIVATION

Beside the above described "classical" triggers of herpesvirus reactivation, we propose the existence of additional, so far unappreciated "novel" triggers of herpesvirus reactivation (**Figure 1**). This proposal is based on recent findings by us and by others. Reese et al. found that helminth co-infection reactivated murine gammaherpesvirus 68 (MHV-68) *in vivo* in an IL-4/Stat6-dependent manner (Reese et al., 2014; Reese, 2016). We demonstrated that cells persistently infected with murine or human gammaherpesviruses responded to nanoparticle (NP) exposure by reactivation of latent virus and by restoring a molecular signature found during productive infection (Sattler et al., 2017). In our study, we exposed cells or mice latently infected with MHV-68 to different NP. *In vitro*, NP-exposure resulted in expression of lytic viral genes and virus production. *In vivo*, an increase in lytic viral proteins and gene expression was observed in lungs and cells from bronchoalveolar lavage. The patterns of gene and metabolite expression in whole lung tissue were strikingly similar to acute virus infection. In human cells latently infected with EBV, NP-exposure also induced virus production. The carbonaceous NPs used in our study were (i) carbon black like surrogates of environmental NPs, derived for example from combustion or mass production, as well as (ii) carbon nanotubes (CNTs) as examples for promising new materials in technology and biomedicine. Thus, it is well-conceivable that other types of NPs, derived from different materials, might also be able to induce herpesvirus reactivation. Furthermore, a variety of additional factors, present in the environment but so far not considered to be triggers of herpesvirus reactivation, might be relevant too.

POTENTIAL HEALTH RELEVANCE OF "NOVEL" INDUCERS OF HERPESVIRUS REACTIVATION

The finding, that helminth co-infection wakes up dormant gammaherpesviruses might have major implications for human health. This has already been discussed by Maizels and Gause (Maizels and Gause, 2014). Equally, our discovery that exposure to NP is able to activate gammaherpesviruses that are dormant in the lung may have consequences for human health in an environment with an increasing exposure to NP. Both innate and adaptive immune responses are modulated by NP, leading for example to immunosuppression or hypersensitivity (Pallardy et al., 2017). Exposure to ambient respirable particles such as man-made mineral fibers or vehicle exhaust emissions have been associated with various adverse health effects (Seaton et al., 2010). When inhaled, NP deposit efficiently and persistently in the alveolar region of the respiratory tract. Their pro-inflammatory properties shape chronic lung diseases like asthma, chronic obstructive pulmonary disease (COPD), pulmonary fibrosis or cancer (Byrne and Baugh, 2008; Morgenstern et al., 2008; Bonner, 2010; Sese et al., 2018; Siroux and Crestani, 2018). The rapid expansion of nanotechnology bears the risk of increasing the incidences of these diseases. Herpesvirus infections may also contribute to the development of chronic pulmonary diseases (Meneghin and Hogaboam, 2007; Vannella and Moore, 2008; Naik and Moore, 2010; Kropski et al., 2012). However, potentiation by a combined exposure to both triggers has not been investigated. We propose that repeated NP exposure and concomitant herpesvirus reactivation result in chronic inflammatory and remodeling processes in the lung, for example by permanently stimulating an aberrant immune response, finally leading to immunopathology and disease development. It is tempting to speculate that inhaled NP might also be among the unknown triggers suspected to enable propagation of additional resident viruses of the airway virome, thereby causing exacerbations of various lung diseases (Marsland and Gollwitzer, 2014).

Following exposure via various routes including inhalation, NP are not only found in the lung but also deposited in numerous organs including the central nervous system (Hong et al., 2017; You et al., 2018). Inhaled nanoparticles can translocate into the systemic circulation and have been shown to accumulate at sites of vascular inflammation and disease (Miller et al., 2017). There is a long term controversy with regard to the contribution of herpesviruses to other chronic diseases beyond the lung: For example, CMV has been associated with coronary heart disease (atherosclerosis) (Du et al., 2018), and EBV, HHV-6 and VZV with multiple sclerosis (Geginat et al., 2017). We propose that also in these disease entities, an interaction of NP with latent herpesviruses may result in reactivation with subsequent chronic inflammation and disease development.

Taken together, future studies on effects of NP-induced herpesvirus reactivation on human health, possible treatments and potential regulatory measures are warranted.

AUTHOR CONTRIBUTIONS

All authors listed have made a substantial, direct and intellectual contribution to the work, and approved it for publication.

FUNDING

The work in the laboratories of TS and HA was funded by intramural funding for Environmental Health Projects of the Helmholtz Zentrum München - German Research Center for Environmental Health (GmbH).

ACKNOWLEDGMENTS

We are grateful to Barbara Adler (Gene Center, Munich, Germany) and the members of our institutes for helpful discussions.

REFERENCES

Adler, B., Sattler, C., and Adler, H. (2017). Herpesviruses and their host cells: a successful liaison. *Trends Microbiol.* 25, 229–241. doi: 10.1016/j.tim.2016.11.009

Bonner, J. C. (2010). Nanoparticles as a potential cause of pleural and interstitial lung disease. *Proc. Am. Thorac. Soc.* 7, 138–141. doi: 10.1513/pats.200907-061RM

Byrne, J. D., and Baugh, J. A. (2008). The significance of nanoparticles in particle-induced pulmonary fibrosis. *Mcgill J. Med.* 11, 43–50.

Cliffe, A. R., and Wilson, A. C. (2017). Restarting lytic gene transcription at the onset of herpes simplex virus reactivation. *J. Virol.* 91, JVI—16. doi: 10.1128/JVI.01419-16

Du, Y., Zhang, G., and Liu, Z. (2018). Human cytomegalovirus infection and coronary heart disease: a systematic review. *Virol. J.* 15, 31–0937. doi: 10.1186/s12985-018-0937-3

Dupont, L., and Reeves, M. B. (2016). Cytomegalovirus latency and reactivation: recent insights into an age old problem. *Rev. Med. Virol.* 26, 75–89. doi: 10.1002/rmv.1862

Geginat, J., Paroni, M., Pagani, M., Galimberti, D., De, F. R., Scarpini, E., et al. (2017). The enigmatic role of viruses in multiple sclerosis: molecular mimicry or disturbed immune surveillance? *Trends Immunol.* 38, 498–512. doi: 10.1016/j.it.2017.04.006

Hong, F., Yu, X., Wu, N., and Zhang, Y. Q. (2017). Progress of *in vivo* studies on the systemic toxicities induced by titanium dioxide nanoparticles. *Toxicol Res.* 6, 115–133. doi: 10.1039/C6TX00338A

Kenney, S. C. (2007). "Reactivation and lytic replication of EBV," in *Human Herpesviruses: Biology, Therapy, and Immunoprophylaxis,* eds A. Arvin, G. Campadelli-Fiume, E. Mocarski, P. S. Moore, B. Roizman, R. Whitley, and K. Yamanishi (Cambridge: Cambridge University Press), 403–433.

Kropski, J. A., Lawson, W. E., and Blackwell, T. S. (2012). Right place, right time: the evolving role of herpesvirus infection as a "second hit" in idiopathic pulmonary fibrosis. *Am. J. Physiol. Lung Cell Mol. Physiol.* 302, L441–L444. doi: 10.1152/ajplung.00335.2011

Lieberman, P. M. (2016). Epigenetics and genetics of viral latency. *Cell Host Microbe* 19, 619–628. doi: 10.1016/j.chom.2016.04.008

Liu, X. F., Wang, X., Yan, S., Zhang, Z., Abecassis, M., and Hummel, M. (2013). Epigenetic control of cytomegalovirus latency and reactivation. *Viruses* 5, 1325–1345. doi: 10.3390/v5051325

Maizels, R. M., and Gause, W. C. (2014). Immunology. How helminths go viral. *Science* 345, 517–518. doi: 10.1126/science.1258443

Marsland, B. J., and Gollwitzer, E. S. (2014). Host-microorganism interactions in lung diseases. *Nat. Rev. Immunol.* 14, 827–835. doi: 10.1038/nri3769

Meneghin, A., and Hogaboam, C. M. (2007). Infectious disease, the innate immune response, and fibrosis. *J. Clin. Invest.* 117, 530–538. doi: 10.1172/JCI30595

Miller, M. R., Raftis, J. B., Langrish, J. P., McLean, S. G., Samutrtai, P., Connell, S. P., et al. (2017). Inhaled nanoparticles accumulate at sites of vascular disease. *ACS Nano* 11, 4542–4552. doi: 10.1021/acsnano.6b08551

Morgenstern, V., Zutavern, A., Cyrys, J., Brockow, I., Koletzko, S., Kramer, U., et al. (2008). Atopic diseases, allergic sensitization, and exposure to traffic-related air pollution in children. *Am. J Respir. Crit. Care Med.* 177, 1331–1337. doi: 10.1164/rccm.200701-036OC

Murata, T. (2014). Regulation of Epstein-Barr virus reactivation from latency. *Microbiol. Immunol.* 58, 307–317. doi: 10.1111/1348-0421.12155

Naik, P. K., and Moore, B. B. (2010). Viral infection and aging as cofactors for the development of pulmonary fibrosis. *Expert Rev. Respir. Med.* 4, 759–771. doi: 10.1586/ers.10.73

Pallardy, M. J., Turbica, I., and Biola-Vidamment, A. (2017). Why the immune system should be concerned by nanomaterials? *Front. Immunol.* 8:544. doi: 10.3389/fimmu.2017.00544

Pellett, P. E., and Roizman, B. (2013). "Herpesviridae, " in *Fields – Virology,* eds D. M. Knipe, P. M. Howley, D. E. Griffin, M. A. Martin, and R. A. Lamb, et al. (Philadelphia, PA: Lippincott Williams & Wilkins), 1802–1822.

Reese, T. A. (2016). Coinfections: another variable in the herpesvirus latency-reactivation dynamic. *J. Virol.* 90, 5534–5537. doi: 10.1128/JVI.01865-15

Reese, T. A., Wakeman, B. S., Choi, H. S., Hufford, M. M., Huang, S. C., Zhang, X., et al. (2014). Helminth infection reactivates latent gamma-herpesvirus via cytokine competition at a viral promoter. *Science* 345, 573–577. doi: 10.1126/science.1254517

Roizman, B., Knipe, D. M., and Whitley, R. J. (2013). "Herpes Simplex Viruses," in *Fields – Virology,* eds D. M. Knipe, P. M., Howley, D. E., Griffin, M. A., Martin, R. A., and Lamb, et al.(Philadelphia: Lippincott Williams & Wilkins), 1823–1897.

Roizman, B., and Whitley, R. J. (2013). An inquiry into the molecular basis of HSV latency and reactivation. *Annu. Rev. Microbiol.* 67, 355–374. doi: 10.1146/annurev-micro-092412-155654

Sattler, C., Moritz, F., Chen, S., Steer, B., Kutschke, D., Irmler, M., et al. (2017). Nanoparticle exposure reactivates latent herpesvirus and restores a signature of acute infection. *Part Fibre Toxicol.* 14, 2–0181. doi: 10.1186/s12989-016-0181-1

Seaton, A., Tran, L., Aitken, R., and Donaldson, K. (2010). Nanoparticles, human health hazard and regulation. *J. R. Soc. Interface* 7 (Suppl.1), S119–S129. doi: 10.1098/rsif.2009.0252.focus

Sese, L., Nunes, H., Cottin, V., Sanyal, S., Didier, M., Carton, Z., et al. (2018). Role of atmospheric pollution on the natural history of idiopathic pulmonary fibrosis. *Thorax* 73, 145–150. doi: 10.1136/thoraxjnl-2017-209967

Siroux, V., and Crestani, B. (2018). Is chronic exposure to air pollutants a risk factor for the development of idiopathic pulmonary fibrosis? *Eur. Respir. J.* 51, 13993003–13992017. doi: 10.1183/13993003.02663-2017

Stinski, M. F., and Meier, J. L. (2007). "Immediate-early viral gene regulation and function," in *Human Herpesviruses: Biology, Therapy, and Immunoprophylaxis,* eds A. Arvin, G. Campadelli-Fiume, E. Mocarski, P. S. Moore, B. Roizman, R. Whitley, and K. Yamanishi (Cambridge: Cambridge University Press), 241–263.

Vannella, K. M., and Moore, B. B. (2008). Viruses as co-factors for the initiation or exacerbation of lung fibrosis. *Fibrogenesis Tissue Repair.* 1, 2. doi: 10.1186/1755-1536-1-2

You, R., Ho, Y. S., Hung, C. H., Liu, Y., Huang, C. X., Chan, H. N., et al. (2018). Silica nanoparticles induce neurodegeneration-like changes in behavior, neuropathology, and affect synapse through MAPK activation. *Part Fibre Toxicol.* 15, 28–0263. doi: 10.1186/s12989-018-0263-3

Conflict of Interest Statement: The authors declare that the research was conducted in the absence of any commercial or financial relationships that could be construed as a potential conflict of interest.

frontiers in Microbiology

REVIEW
published: 09 January 2019
doi: 10.3389/fmicb.2018.03315

The Critical Role of Genome Maintenance Proteins in Immune Evasion During Gammaherpesvirus Latency

Océane Sorel[1,2] *and Benjamin G. Dewals*[1]*

[1] *Immunology-Vaccinology, Department of Infectious and Parasitic Diseases, Faculty of Veterinary Medicine-FARAH, University of Liège, Liège, Belgium,* [2] *Department of Molecular Biology and Biochemistry, University of California, Irvine, Irvine, CA, United States*

Gammaherpesviruses are important pathogens that establish latent infection in their natural host for lifelong persistence. During latency, the viral genome persists in the nucleus of infected cells as a circular episomal element while the viral gene expression program is restricted to non-coding RNAs and a few latency proteins. Among these, the genome maintenance protein (GMP) is part of the small subset of genes expressed in latently infected cells. Despite sharing little peptidic sequence similarity, gammaherpesvirus GMPs have conserved functions playing essential roles in latent infection. Among these functions, GMPs have acquired an intriguing capacity to evade the cytotoxic T cell response through self-limitation of MHC class I-restricted antigen presentation, further ensuring virus persistence in the infected host. In this review, we provide an updated overview of the main functions of gammaherpesvirus GMPs during latency with an emphasis on their immune evasion properties.

Keywords: herpesvirus, viral latency, genome maintenance protein, immune evasion, antigen presentation, viral proteins

OPEN ACCESS

Edited by:
Michael Nevels,
University of St Andrews,
United Kingdom

Reviewed by:
Neil Blake,
University of Liverpool,
United Kingdom
James Craig Forrest,
University of Arkansas for Medical Sciences, United States

***Correspondence:**
Benjamin G. Dewals
bgdewals@uliege.be

Specialty section:
This article was submitted to Virology, a section of the journal Frontiers in Microbiology

Received: *28 September 2018*
Accepted: *20 December 2018*
Published: *09 January 2019*

Citation:
Sorel O and Dewals BG (2019) The Critical Role of Genome Maintenance Proteins in Immune Evasion During Gammaherpesvirus Latency. Front. Microbiol. 9:3315. doi: 10.3389/fmicb.2018.03315

INTRODUCTION

Herpesviruses are enveloped double-stranded DNA viruses that are in general responsible for persistent infections in a large number of animal species. In 2008, the International Committee on Taxonomy of Viruses (ICTV) created the order *Herpesvirales* comprising three families: the family *Malacoherpesviridae* composed of viruses infecting molluscs such as oysters, the family *Alloherpesviridae* composed of viruses infecting fish species and amphibians, and the predominantly studied family *Herpesviridae* that includes viruses of mammals and birds, itself classified into the three subfamilies *Alpha*-, *Beta*-, and *Gammaherpesvirinae*. A hallmark of all herpesviruses is their unique capacity to induce lifelong infection through establishing and maintaining latent infection. The definition of herpesvirus latency involves: (i) the presence of the viral genome in the nucleus of the infected cell (either as an episome or integrated in cellular chromosomes), (ii) reduced viral gene expression together with the absence of virion production, and (iii) the ability of latently infected cells to reactivate lytic viral replication either *in vivo* and/or *in vitro* (Lieberman, 2016). In addition, latent lifelong infection requires evasion mechanisms from the host immune response. Most alphaherpesviruses such as herpes simplex virus (HSV-1 or *human alphaherpesvirus 1* – HHV-1) establish latency in non-dividing sensory

neurons through maintenance of a quiescent episomal genome and expression of viral transcripts, in the absence of viral protein detection (Roizman and Whitley, 2013). In betaherpesviruses, myeloid cells such as macrophages are the main target of latent infection but the latency mechanisms in this subfamily have yet to be fully deciphered (Goodrum, 2016; Collins-McMillen et al., 2018). Gammaherpesviruses essentially establish latency in either B or T lymphocytes, although some species such as *bovine gammaherpesvirus 4* (BoHV-4) seem to infect cells of the monocyte/macrophage lineage (Machiels et al., 2011, 2013). The mechanisms regulating latency establishment, maintenance of such a dormant infection in actively dividing cells, and how gammaherpesviruses escape the immune system of the infected host have been thoroughly studied (Stevenson and Efstathiou, 2005; Blake, 2010; Barton et al., 2011; White et al., 2012; Lieberman, 2013; Schuren et al., 2016; Dong et al., 2017; Ueda, 2018).

Most significant advances in the understanding of herpesvirus latency mechanisms have been identified in gammaherpesviruses, which can probably be explained by the fact that one major latency protein, named the "*genome maintenance protein*" (GMP): (i) is encoded by the genome of all described gammaherpesvirus species, (ii) is expressed during latent infection, (iii) regulates the maintenance of viral episomes in actively dividing lymphocytes through tethering the viral genome to cellular chromosomes, and (iv) evades immune detection (Verma et al., 2007; Frappier, 2015). The main objective of this review is to briefly summarize the importance of gammaherpesvirus infections and how GMPs maintain viral episomes in infected lymphocytes, before focusing on a more detailed description of the mechanisms mediated by GMPs to escape immune surveillance, in particular $CD8^+$ cytotoxic T cells (CTLs), during latent infection.

THE SUBFAMILY *Gammaherpesvirinae*

Based on genomic and biological characteristics, gammaherpesviruses have been classified into four genera: the *Lymphocryptovirus* genus, the *Rhadinovirus* genus, the *Percavirus* genus and the *Macavirus* genus (Davison et al., 2009). Lymphocryptoviruses mainly infect human and non-human primates, and include one of the two gammaherpesviruses infecting humans: Epstein-Barr virus (EBV or *human gammaherpesvirus 4* – HHV-4) (Jha et al., 2016). Rhadinoviruses also infect human and non-human primates, and include the second human gammaherpesvirus, Kaposi's sarcoma-associated herpesvirus (KSHV or *human gammaherpesvirus 8* – HHV-8) (Li et al., 2017). In addition to KSHV and viruses infecting Old World primates such as macaques, gorillas and chimpanzees, some rhadinoviruses also infect New World monkeys. Two examples are *saimiriine gammaherpesvirus 2* (or SaHV-2) also known as herpesvirus saimiri (HVS); and *ateline gammaherpesvirus 3*, which infects spider monkeys (Damania and Desrosiers, 2001). In addition to viruses infecting primates, rhadinoviruses also include a number of viral species infecting other mammalians (Davison et al., 2009). For instance, *murid gammaherpesvirus 4* (MuHV-4), also referred to as murine gammaherpesvirus 68 (MHV-68) is a natural pathogen of the yellow-necked field mouse (Ehlers et al., 2007) and is largely used in the laboratory mouse (*Mus musculus*). Furthermore, *Bovine herpesvirus 4* (BoHV-4) infection is prevalent in cows while this virus is thought to have originally evolved in another *Bovinae*, the African buffalo (*Syncerus caffer*) (Dewals et al., 2005). Macaviruses are viruses infecting ruminants and are mainly associated with a lymphoproliferative disease named malignant catarrhal fever (MCF). Among these, *alcelaphine gammaherpesvirus 1* (AlHV-1) and *ovine gammaherpesvirus 2 (*OvHV-2) naturally infect wildebeest (*Connochaetes taurinus*) and sheep (*Ovis aries*). They are responsible for wildebeest-derived and sheep-associated MCF in ruminants, respectively. The genus *Percavirus* is less well-defined and includes virus species infecting horses or mustelids.

The importance of latent infection by gammaherpesviruses is evident, both in term of lifelong persistence and related clinical diseases. The majority of epidemiological and clinical data comes from human gammaherpesviruses, although some veterinary viruses also induce latency-associated malignancies. EBV infects >90% of the human population, with seroconversion occurring early during childhood (Henle et al., 1969; Andersson, 2000). Whereas EBV latent infection is mostly asymptomatic, a number of clinical manifestations are associated with EBV infection. Beside infectious mononucleosis when primary infection occurs during adolescence (Callan et al., 1996), EBV is further associated with malignancies including Burkitt's and Hodgkin's lymphomas and other types of cancers (Rezk et al., 2018). In addition, EBV infection has been positively correlated with multiple sclerosis (MS). Nonetheless, the exact mechanisms and the causative role of EBV in MS induction remain open for investigation (Levin et al., 2010; Munger et al., 2011; Pender, 2011; Pakpoor et al., 2013; Moreno et al., 2018). The prevalence of KSHV is more variable and ranges from 5 to 50% depending on regions across the world. Like EBV, KSHV infection is in general asymptomatic but can be responsible for severe malignancies such as Kaposi's sarcoma in immunocompromised patients but also other cancers such as multicentric Castlemans's disease or primary effusion lymphoma (Li et al., 2017). Just like EBV and KSHV, animal gammaherpesviruses are also extensively studied, either for their veterinary importance or used as experimental models to study the biology of gammaherpesvirus infection *in vivo*. The former category includes MCF-inducing AlHV-1 that is responsible for the induction of a deadly peripheral T cell lymphoma-like disease in cattle caused by latently infected $CD8^+$ T lymphocytes (Dewals et al., 2008, 2011; Dewals and Vanderplasschen, 2011; Palmeira et al., 2013). MuHV-4 and SaHV-2 are two examples of animal gammaherpesviruses of the latter category. Whereas the functions of gammaherpesvirus GMPs have been extensively investigated for EBV and KSHV in cell culture *in vitro*, animal gammaherpesviruses have provided important insights on the role of GMPs during *in vivo* infection.

GENOME MAINTENANCE PROTEINS AND THEIR ROLES DURING GAMMAHERPESVIRUS INFECTION

After primary infection of target cells, gammaherpesviruses enter the lytic cycle that leads to production of viral particles and cell death. However, and depending on the infected cell type, the latent phase of the infection is in general rapidly established and is accompanied with the production of latency transcripts, including GMP. All sequenced gammaherpesviruses encode a predicted GMP (**Table 1**). In lymphocryptoviruses, GMPs are encoded by open reading frame (ORF) BKRF1 and are named according to Epstein-Barr virus (EBV) nuclear antigen 1 (EBNA-1). The GMPs in *Rhadinovirus*, *Percavirus,* and *Macavirus* genera are encoded by ORF73 and can be named after KSHV latency-associated nuclear antigen 1 (LANA-1). GMPs are DNA-binding proteins able to bind sequences within the viral genome while at the same time interacting with cell chromosome-associated proteins, to ensure partitioning to daughter cells during mitosis. Early studies have already demonstrated that

TABLE 1 | Gammaherpesvirus genome maintenance proteins based on functional evidence and/or sequence prediction.

Genus/species	Common name (common abbreviation)	GMP	Size (amino acids)	Central repeat (size)*	Central repeat content†	Accession number
Lymphocryptovirus						
Callitrichine gammaherpesvirus 3	Marmoset herpesvirus	ORF39	327	− (NA)	–	NP_733892
Human gammaherpesvirus 4	Epstein-Barr virus (EBV)	EBNA1	641	+ (239)	GA	YP_401677
Macacine gammaherpesvirus 4	Rhesus lymphocryptovirus (rhLCV)	rhEBNA1	511	+ (47)	GSA	YP_067973
Papiine gammaherpesvirus 1	Herpesvirus papio	baEBNA1	476	+ (49)	GSA	AAA66373
Rhadinovirus						
Ateline gammaherpesvirus 3	Herpesvirus ateles strain 73 (AtHV-3)	ORF73	447	+ (157)	DG(E)	NP_048045
Bovine gammaherpesvirus 4	Bovine herpesvirus 4, Movar virus, V. test virus	ORF73 (boLANA)	243	− (NA)	–	NP_076567, AEL29819
Cricetid gammaherpesvirus 2	Rodent herpesvirus Peru	RHP73	294	− (NA)	–	YP_004207909
Human gammaherpesvirus 8	Kaposi's sarcoma-associated herpesvirus (KSHV)	LANA1	1129	+ (585)	Acidic	YP_001129431
Macacine gammaherpesvirus 5‡	Rhesus rhadinovirus	ORF73 (rhLANA)	1071§	+/− (521)	Acidic	ABH07414
Murid gammaherpesvirus 4	Murine gammaherpesvirus 68 (MHV68)	ORF73 (mLANA)	314	− (NA)	–	NP_044913
Murid gammaherpesvirus 7¶	Wood mouse herpesvirus	ORF73	327	− (NA)	–	ACY41142
Saimiriine gammaherpesvirus 2	Herpesvirus saimiri (HVS)	ORF73 (sLANA)	501#	+ (265)	GE/EA	CAC84371
Percavirus						
Equid gammaherpesvirus 2	Equine herpesvirus 2 (EHV-2)	ORF73	985	+ (578)	Acidic	YP_009118179
Equid gammaherpesvirus 5	Equine herpesvirus 5 (EHV-5)	ORF73	996	+ (476)	Acidic	YP_009118462
Macavirus						
Alcelaphine gammaherpesvirus 1	Wildebeest-derived malignant catarrhal fever virus	ORF73 (aLANA)	1324	+ (986)	G(P)E	APB09566, ATI21957
Alcelaphine gammaherpesvirus 2	Topi herpesvirus	ORF73	1277	+ (913)	G(P)E	YP_009044454
Ovine gammaherpesvirus 2	Sheep-associated malignant catarrhal fever virus	ORF73 (oLANA)	495	+ (330)	G(P)E	YP_438196

**Presence of a central repeat (CR) domain is indicated. The size of the present CR domain is given for the prototypic sequence for which the genbank accession number is provided.*

†Information on the composition of most represented amino acid residues or the presence of an acidic domain without clear consensus repeat in the CR is given. D, aspartic acid; E, glutamate; G, glycine; P, proline; S, serine.

‡Macacine gammaherpesvirus 5 are a group of closely related viruses of Old and New World non-human primates that are classified in two lineages within the Rhadinovirus genus, RV1 and RV2 (Damania and Desrosiers, 2001).

§Only RV1 viruses possess a CR domain. The given accession number is from strain M78114.

¶Murid gammaherpesvirus 7 is phylogenetically related to MuHV-4 and Brest herpesvirus. No GMP sequence is available for the latter (Chastel et al., 1994; Hughes et al., 2010).

#The GMP of SaHV-2 is given for strain C488.

GMPs, such as EBNA-1 and LANA-1, are essential for episome persistence (Ballestas et al., 1999; Ballestas and Kaye, 2001; Sears et al., 2003). Similar data have been generated for SaHV-2 and MuHV-4 for which it has been demonstrated that the gene ORF73 is required for efficient establishment of latency (Fowler et al., 2003; Calderwood et al., 2005). Likewise, deletion from the BoHV-4 genome of ORF73 impaired viral persistence in a macrophage cell line *in vitro* and *in vivo* in the rabbit model (Thirion et al., 2010). In addition, the ORF73-encoded protein of strain H26-95 of *macacine gammaherpesvirus 5* was shown to bind to the viral episome and to be essential for establishment of latency (DeWire and Damania, 2005; Wen et al., 2009). The deletion of ORF73 from the genome of AlHV-1 also rendered AlHV-1 unable to persist and induce MCF *in vivo*, whereas impairment of its expression did not affect viral lytic replication (Palmeira et al., 2013). To enable partitioning in proliferating cells and avoid losing the episomal genomes in the cytoplasm, GMPs bind viral episomes to host chromosomes. Tethering of viral episomes to host DNA is accomplished by the ability of GMPs to simultaneously bind to several chromosome-associated proteins, other cellular components of the mitotic apparatus and specific viral DNA sequences (Yates et al., 1984; Cotter and Robertson, 1999; Shire et al., 1999; Cruickshank et al., 2000; Wu et al., 2000; Ballestas and Kaye, 2001; Cotter et al., 2001; Kapoor and Frappier, 2003; Verma and Robertson, 2003; Barbera et al., 2004, 2006; Calderwood et al., 2004; Waldmann et al., 2004; Kapoor et al., 2005; You et al., 2006; Kelley-Clarke et al., 2007; Habison et al., 2012; Verma et al., 2013; Gupta et al., 2016).

Genome maintenance proteins are nuclear proteins with very little sequence similarity among gammaherpesviruses, even though GMPs within one genus show higher sequence similarity. The C-terminal region shows the highest degree of sequence similarity and is involved in DNA-binding (Tellam et al., 2012). Regarding protein primary structure, most GMPs contain a central repeat (CR) domain composed of repeated amino acid motives that are divergent between gammaherpesvirus species. Interestingly, the size of the different GMPs greatly varies due to the presence of the CR domain (**Figure 1**). However, such variation in size does not seem to alter its role in maintaining the viral genome and the CR domain appears to be dispensable for genome maintenance properties with some gammaherpesviruses being devoid of a CR domain, such as MuHV-4 or BoHV-4 (Lomonte et al., 1995; Bennett et al., 2005). In addition to genome-maintenance functions, studies performed essentially on EBV EBNA-1 and KSHV LANA-1 have revealed additional roles for GMPs during latency and latency-associated diseases. GMPs are involved in initiating viral DNA replication during latency to generate sufficient copies of viral episomes prior to cell division (Wysokenski and Yates, 1989; Harrison et al., 1994; Yates et al., 2000; Ballestas and Kaye, 2001; Cotter et al., 2001; Stedman et al., 2004; Wong and Wilson, 2005; Verma et al., 2006; Lu et al., 2012), modulating viral gene expression to promote latency and repress reactivation (Gahn and Sugden, 1995; Evans et al., 1996; Schafer et al., 2003; Lu et al., 2006; Sivachandran et al., 2012), promoting tumorigenesis (Radkov et al., 2000; Humme et al., 2003; Altmann et al., 2006; Cai et al., 2006, 2012), and evading the immune system.

GENOME MAINTENANCE PROTEINS AND THEIR IMMUNE EVASION PROPERTIES

To ensure lifelong latency, gammaherpesviruses must maintain their genomes in dividing cells and remain undetected by virus-specific $CD8^+$ CTLs. Thus, the GMPs must overcome the dilemma of efficiently maintaining viral episomes within infected cells while, at the same time, evading immune surveillance. Viral proteins are expressed endogenously within cells and are thus degraded by the proteasome into antigenic peptides before being translocated from the cytosol to the endoplasmic reticulum (ER) and loaded on major histocompatibility class I (MHC class I) molecules to form MHC-I-peptide (MHCp) complexes. MHCp complexes are exported to the cell surface for recognition by $CD8^+$ cytotoxic T lymphocytes (CTLs) (Blum et al., 2013) (**Figure 2**).

The main source of viral antigens was previously thought to uniquely arise from the turnover of mature proteins. However, more recent studies highlighted an alternate hypothesis regarding the origin of MHC class I-restricted viral peptides, pointing to a major role of defective ribosomal products (DRiPs) as the main source of antigenic peptides during viral infection (Yewdell et al., 1996; Yewdell, 2011). DRiPs are translational products derived from prematurely terminated or misfolded polypeptides. Prioritizing DRiPs as the main source of antigenic peptides is believed to provide opportunities for the immune system to rapidly detect an active viral infection and thus optimize immune surveillance (Anton and Yewdell, 2014; Wei and Yewdell, 2018). Nevertheless, data supporting this hypothesis are still limited and further studies are necessary to exactly quantify whether MHC class I antigen presentation can be attributed to DRiPs of newly synthesized proteins. Indeed, the MHC class I-presented peptides seem to come from both short-lived and stable mature proteins depending on the origin of proteins and the biological status of the cell environment (Rock et al., 2014, 2016). Although autophagy is in some key aspects involved in the induction of adaptive immunity and control of some viral infections (Paludan et al., 2005), it appears that gammaherpesviruses have rather evolved to develop strategies to co-opt autophagy for viral benefit, during the lytic cycle but also during latency. However, GMPs do not seem to be directly involved in such mechanisms [see recent review (Lussignol and Esclatine, 2017)].

Gammaherpesviruses have evolved to acquire different strategies to escape the immune response. These mechanisms have been extensively reviewed in the past (Stevenson and Efstathiou, 2005; Means et al., 2007; Blake, 2010; Feng et al., 2013; Hu and Usherwood, 2014; Ressing et al., 2015; Sorel and Dewals, 2016; Zuo et al., 2017). The significant downregulation of viral gene expression during latent infection contributes to immune evasion, with viral gene expression being restricted to non-coding RNAs and latency proteins, including GMPs. GMPs must indeed be expressed in infected cells due to their

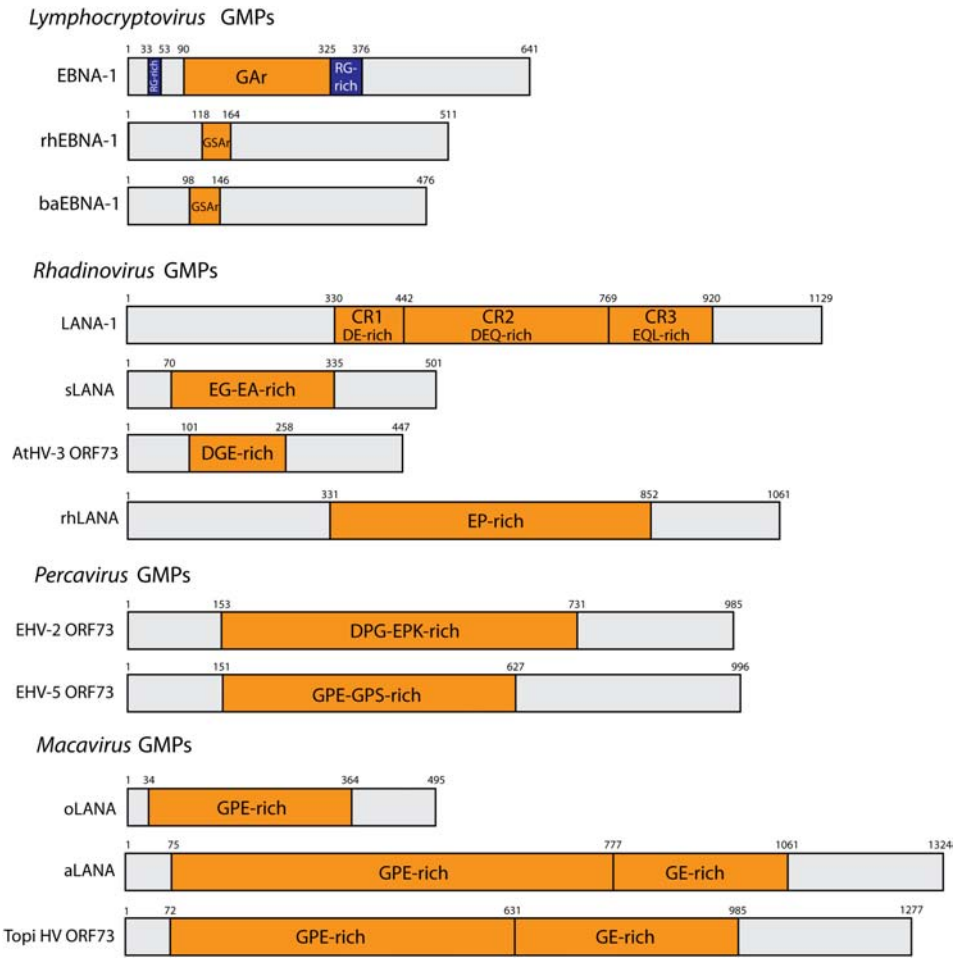

FIGURE 1 | Schematic representation of representative gammaherpesvirus GMPs. N- and C- terminal domains are separated by a central amino acid repeat domain (CR), highlighted in orange. Repeat residues are indicated. The RG-rich regions of EBNA-1 are depicted in blue. Genus *Lymphocryptovirus*: EBNA-1 (EBV, strain B95.8), rhEBNA1 (rhLCV, strain LCL8664) and baEBNA-1 (baLCV, strain S594). Genus *Rhadinovirus*: AtHV3 ORF73 (strain 73), LANA-1 (KSHV, strain JK-18), sLANA (SaHV-2, strain C488), rhLANA (M78114). Genus *Percavirus*: EHV-2 ORF73 (strain 86/87), EHV-5 (strain 2-141/67). Genus *Macavirus*: oLANA (OvHV-2, strain BJ1035), and aLANA (AlHV-1, strain C500).

key functions during long-term latency but at the same time need to remain hidden from the immune system. In order to evade CTL recognition of latently infected cells, all studied gammaherpesvirus GMPs have evolved to put into place immune evasion mechanisms consisting of the inhibition of their own presentation in the context of MHC class I on the cell surface, a mechanism that has been termed "*cis*-acting immune evasion" (**Figure 2**). Pioneer work came from studying EBV GMP where the CR domain could directly be involved in self-inhibition of antigen presentation (Levitskaya et al., 1995). Although most GMPs encoded by gammaherpesviruses contain a CR domain and are generally involved in the described *cis*-acting immune evasion mechanism, GMPs encoded by MuHV-4 (mLANA) or BoHV-4 (boLANA) do not have a CR domain (Lomonte et al., 1995; Bennett et al., 2005). While no data are available for immune evasion mechanism by boLANA, mLANA was able to inhibit self-presentation in MHC class I despite its lack of a CR domain (Bennett et al., 2005). Intriguingly, despite the conserved functions of gammaherpesviruses GMPs, the peptidic sequence in their repeat regions differs to a great extent from one ortholog to another. In contrast, comparative mRNA sequence analysis revealed that the internal repeat regions of GMP mRNAs displayed high nucleotide sequence similarities (Tellam et al., 2012). The results detailed in the next sections suggest that GMPs have evolved to adopt various strategies depending on the viral species, in order to achieve the ultimate goal consisting of the inhibition of their own presentation by MHC class I.

GENUS *Lymphocryptovirus*

Epstein-Barr Virus (EBV)

Epstein-Barr virus EBNA-1 is one of the most studied GMPs with regards to its different functional aspects, from genome maintenance (Yates et al., 1984, 1985), to *cis*-acting immune evasion. Early studies have demonstrated that EBNA-1 is able to

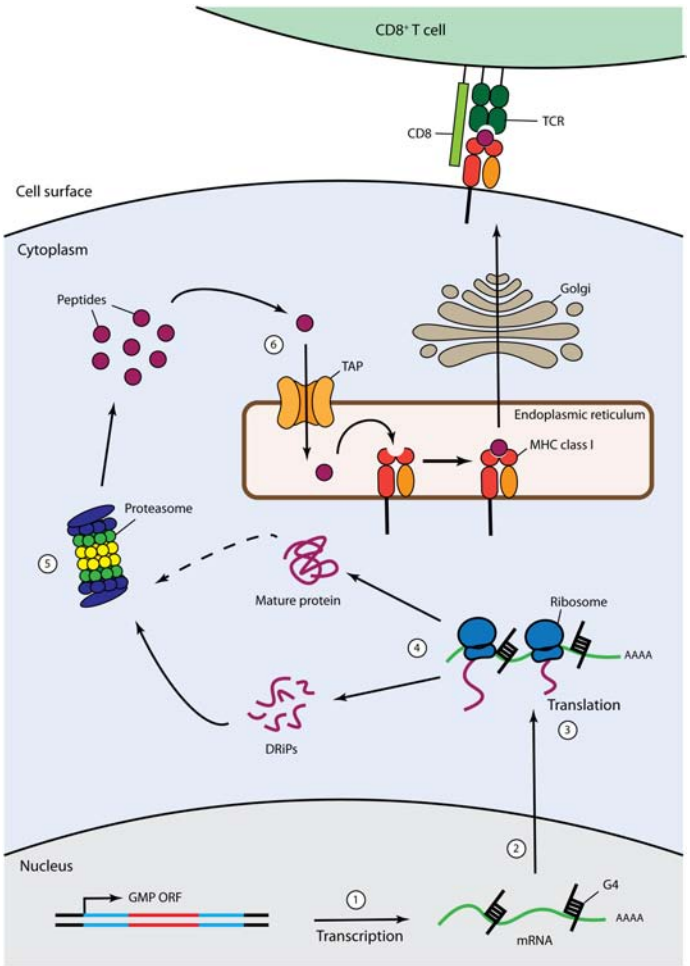

FIGURE 2 | *Cis*-acting immune evasion of MHC Class I antigen presentation of gammaherpesvirus GMPs. The MHC class I antigen presentation pathway is depicted with described GMP-mediated *cis*-acting immune evasion mechanisms. Cytoplasmic endogenously expressed viral proteins are degraded by the proteasome into antigenic peptides that are then translocated from the cytosol to the endoplasmic reticulum (ER) through the transporter for antigen processing (TAP). Then, antigenic peptides are loaded on MHC class I molecules to form MHC-I-peptides complexes that are subsequently exported to the cell surface through the Golgi apparatus for recognition by $CD8^+$ cytotoxic T lymphocytes. GMPs have been demonstrated to inhibit this process through various mechanisms: (1) sLANA and aLANA were shown to decrease their own steady-state RNA levels; (2) EBNA-1 can inhibit pre-mRNA processing of the primary EBNA-1 transcript; (3) structural constraints, such as G-quadruplexes (G4), contained in aLANA and EBNA-1 mRNA rather than protein sequences can regulate self-translation; (4) EBNA-1, aLANA, LANA-1, sLANA, and mLANA are able to induce retardation of self-translation; (5) EBNA-1, mLANA, and LANA-1 were shown to be protected from proteasomal degradation; (6) LANA-1 was reported to hold an inhibitory effect prior to translocation of its own cytoplasmic peptides into the ER.

prevent MHC class I-restricted self-peptide presentation in *cis* to CTLs through a mechanism involving its CR domain (GAr) (Levitskaya et al., 1995). The GAr domain is a region rich in glycine (G) and alanine (A) residues, which corresponds to 239 aa in strain B95.8 of EBV (Baer et al., 1984). Although its size can vary based on the strain, all isolates contain a GAr region (Falk et al., 1995). In order to decipher the immune evasion mechanism driving this effect, several studies have shown that the GAr domain provides increased stability to the EBNA-1 protein by inhibiting proteasome-mediated degradation (Levitskaya et al., 1997; Sharipo et al., 1998; Heessen et al., 2002, 2003; Hoyt et al., 2006; Coppotelli et al., 2011). In these studies, increased CTL responses could be induced with EBNA-1ΔGAr recombinant proteins, where the GAr was removed. Using conventional chromium-51 cytotoxicity assays, MHC-tetramer stains and/or peptide restimulation, it appeared that removal of the GAr domain resulted in increased presentation of a model T-cell epitope inserted into the GMP backbone but also increased presentation of T-cell epitopes of EBNA-1 itself, including the HLA-B*35:01-restricted CTL epitope (HPVGEADYFEY). Despite the potential self-protection of EBNA-1 from MHC class I antigen presentation, several studies found that EBNA-1-specific CTLs exist in EBV-seropositive patients (Blake et al., 1997, 2000; Subklewe et al., 1999; Sim et al., 2013). Whereas inhibition of proteasome degradation was initially suggested, other reports found that GAr would more likely self-inhibit protein translation efficiency to reduce presentation of CTL epitopes from EBNA-1. These latter observations led to the

conclusion that the GAr domain could inhibit the production of translation-dependent DRiPs. However, it remains unresolved whether control of the production of DRiPs during *de novo* translation is the only mechanism explaining EBNA-1 *cis*-acting immune evasion. Indeed, additional data contradicted the direct implication of the GAr domain in protecting EBNA-1 from proteasome degradation and increased protein stability (Yin et al., 2003; Lee et al., 2004; Tellam et al., 2004, 2007a; Voo et al., 2004; Daskalogianni et al., 2008).

What is clear from the studies investigating *cis*-acting immune evasion of EBNA-1 is that the GAr-mediated self-inhibition of antigen presentation to CTLs is not absolute. Indeed, although reduced in presence of GAr, EBNA-1 can be immunogenic and lead to the development of EBNA-1-specific CTLs in humans (Blake et al., 1997, 2000; Subklewe et al., 1999; Sim et al., 2013), but also in a mouse model where EBNA-1 was transduced using an adenovirus expression vector (Tellam et al., 2014). Recent advances have put forward a hypothesis to explain how the GAr domain is able to reduce self-translation efficiency. Studies which investigated mRNA translation of EBNA-1 suggested that the nascent GAr peptide alone was able to delay the assembly of the translation initiation complex mRNA, therefore reducing mRNA translation (Apcher et al., 2009, 2010). However, more recent reports suggested that EBNA-1 mRNA structure itself rather than the GAr peptidic sequence could regulate EBNA-1 protein translation (Tellam et al., 2008). Further findings supported this hypothesis by demonstrating that mRNA sequence could regulate the level of self-synthesis and antigen presentation of EBNA-1 *in vitro* through the GAr domain (Tellam et al., 2012). These authors highlighted the fact that the GAr domain, but also most GMP CR domains, display a nucleotidic sequence bias with enrichment of purines that is associated with reduced efficiency of protein translation. The role of purine-rich domains was demonstrated when replacement of the third base position of codons by pyrimidines led to increased translation of the protein and CTL activation (Tellam et al., 2008, 2014). Moreover, generating frameshifts in the EBNA-1 GAr internal repeat sequence to create alternate peptidic repeats had no effect on the *cis*-acting immune evasion (Tellam et al., 2012). Indeed, EBNA-1 frameshift mutants expressing GQE-rich or GRS-rich repeats could inhibit the presentation of a linked model epitope with an efficacy similar to native EBNA-1. Shortly after, the same group highlighted a key role played by clusters of unusual structural elements within the EBNA-1 mRNA sequence, named G-quadruplexes (G4), in the modulation of protein synthesis (Murat et al., 2014). G4 are secondary structures of nucleic acids that form within G-rich DNA or RNA sequences (Murat and Tellam, 2015). Four guanine bases can associate through hydrogen bonding to form a guanine tetrad and two or more guanine tetrads can stack on top of each other to constitute a G4 structure (Metifiot et al., 2014). Globally, these structures are present in telomeres, promoters, and gene bodies where they perform important regulatory roles in diverse biological processes including replication, transcription and translation (Rhodes and Lipps, 2015). Bioinformatics analysis of the EBNA-1 mRNA sequence revealed the presence of multiple putative G4 structures within the GAr domain (Murat et al., 2014). These authors further demonstrated that destabilization of G4 structures using antisense oligonucleotides led to an increase of EBNA-1 mRNA translation (Murat et al., 2014). To go further, as mentioned above, a modification of codon usage to reduce the purine bias in GAr resulted in reverted *in vivo* MHC class I epitope presentation and early priming of $CD8^+$ T cells (Tellam et al., 2014). The mechanism underlying this effect was suggested to be determined by a capacity of G4 structures present in GAr to alter the association of ribosomes with EBNA-1 mRNA by inducing premature termination and/or ribosome stalling, therefore impeding protein translation (Murat et al., 2014). Nonetheless, whether G4 structures are present in all gammaherpesvirus GMPs and involved in self-inhibition of protein translation for immune evasion, needs to be further elucidated. Interestingly, the generation of memory T cell response was not affected by the codon-modification within the GAr domain (Tellam et al., 2014). These results were of high interest as they reported that promoting CTL priming against EBNA-1 through impairment of the GAr-dependent *cis*-acting immune evasion mechanisms could result in a more rapid CTL response and the establishment of efficient immune memory. In addition to translation regulation, previous studies have also established that EBNA-1 could act at the transcriptional level through inhibition of pre-mRNA processing of the primary EBNA-1 transcript (Yoshioka et al., 2008).

Other Lymphocryptoviruses

Studies on the GMPs encoded by baboon lymphocryptovirus (baLCV) and rhesus lymphocryptovirus (rhLCV), namely baEBNA-1 and rhEBNA-1, respectively, provided conflicting data. Indeed, the first results suggested that both the ba- and rhGSAr domains were not able to prevent MHC class I restricted peptide presentation in *cis* (Blake et al., 1999), whereas a second study showed that rhEBNA-1-specific CTLs expanded *in vitro* from rhLCV-infected animals failed to recognize endogenously expressed rhEBNA-1 (Fogg et al., 2005). A more recent study provided data supporting the hypothesis whereby rhEBNA-1 and baEBNA-1 proteins do not possess *cis*-acting immune evasion properties (Tellam et al., 2007b). Both proteins were translated at a higher rate than EBV EBNA-1 with no effect of deletion of the GSAr domains on translation rates and the rhGSAr domain could not avoid *cis*-acting presentation of a model epitope. A potential explanation for the adversarial result regarding the lack of recognition of rhEBNA-1 by the rhEBNA-1-specific CTLs reported in a study by Fogg and collaborators, could be that the specific clones isolated were of low affinity against the GMP (Blake, 2010).

GENUS *Rhadinovirus*

Kaposi's Sarcoma-Associated Herpesvirus (KSHV)

LANA-1 is also able to act in *cis* to inhibit MHC class I-restricted epitope presentation to CTLs through involvement of the CR domain (Zaldumbide et al., 2007). LANA-1 is subdivided into three domains based on the peptidic sequence, with imperfect

repeats: CR1 (aa 330–442) is a DE-rich region, CR2 (aa 442–768) is a DEQ-rich region, and CR3 (aa 769–920) consists of an EQL-rich region (**Figure 1**). Interestingly, the size of the CR domain varies between different KSHV strains or isolates (Gao et al., 1999). While a junctional domain between LANA-1 CR2 and CR3 has been mapped to contribute to retardation of translation and inhibition of proteasomal degradation of LANA-1 (Kwun et al., 2007), neither the CR2 nor CR3 domains were found to be involved in the inhibition of peptide presentation (Kwun et al., 2011). These data suggested that, in contrast to EBNA-1, the mechanism combining protection of LANA-1 from proteasomal degradation and reduction in the DRiPs generation level is not sufficient to block peptide presentation on MHC class I. Another notifiable difference with EBNA-1 is that the retardation of LANA-1 translation seems to be due to CR amino acid sequence rather than to the nucleotide level. Indeed, the introduction of a stop codon between CR2 and CR3 resulted in increased translation (Kwun et al., 2007). This observation is of importance considering the high degree (about 50% for CR1 and CR2, and about 70% for CR3) of similarity between EBNA-1 and LANA-1 in terms of nucleotidic sequence (Tellam et al., 2012). Conversely, CR1 has been implicated in LANA-1 *cis*-acting immune evasion through an apparent inhibitory effect prior to translocation of cytoplasmic peptides into the ER (Kwun et al., 2011). Here, fusion of a signal peptide to LANA-1 led to efficient processing of the protein for MHC Class I presentation. However, the presence or absence of CR1 had no effect on protein translation or proteasomal degradation. Using interferon-dependent induction of proteasomal degradation and proteasome inhibitor MG132, Kwun and collaborators further highlighted that LANA-1 is processed for MHC I presentation through the canonical proteasome pathway with little contribution of autophagy (Kwun et al., 2007, 2011). Thus, LANA-1 seems to have evolved to adopt immune evasion mechanisms that differ from EBNA-1, despite having conserved nucleotide sequence similarities. Although G4 structures have been involved in KSHV DNA replication and episomal persistence (Madireddy et al., 2016), it remains unappreciated whether G4 structures are present in LANA-1 or not, as demonstrated for EBNA-1. EBNA-1-specific $CD8^+$ CTLs could be identified in patients (Blake et al., 1997, 2000; Subklewe et al., 1999; Sim et al., 2013). Likewise, several studies have identified LANA-1-specific $CD8^+$ T-cell responses in KSHV seropositive subjects, highlighting the premise that the self-protection of GMPs against MHC class I-restricted epitope presentation is not absolute (Brander et al., 2002; Woodberry et al., 2005; Bihl et al., 2007; Lepone et al., 2010). Nonetheless, to our knowledge, no LANA-1-specific T cell clone is available to be tested *in vitro*.

Other Rhadinoviruses

Infection of squirrel monkeys with SaHV-2 results in asymptomatic latency in T lymphocytes. However, co-species transmission to New World non-human primates can lead to the development of acute T-cell lymphomas (Fickenscher and Fleckenstein, 2001). Interestingly, SaHV-2 can induce transformation of human and rabbit T lymphocytes (Fleckenstein and Ensser, 2004). The transforming capability of SaHV-2 has been identified to be mainly driven by two viral proteins termed Stp and Tip (Fleckenstein and Ensser, 2007). SaHV-2 infection of T lymphocytes is associated with episomal maintenance in absence of production of viral particles and the GMP encoded by SaHV-2 (sLANA) has been demonstrated to be essential for episomal maintenance (Calderwood et al., 2005). The CR domain of sLANA varies between strains, with a EG-rich domain of 15 aa in strain A11 or of 111 aa in strain C488; and a EA-rich region of 147 and 132 aa in both strains, respectively. One study thoroughly investigated the role of sLANA in evading CTL recognition (Gao et al., 2009). In this study, Gao and collaborators demonstrated that sLANA could reduce the MHC class I presentation of the linked-OT1 epitope SIINFEKL (Gao et al., 2009). The authors further observed that the steady-state levels of sLANA protein were reduced due to the presence of the CR domain rich in EG and EA residues, an observation that could be explained by a decrease in the steady-state levels of sLANA mRNA. Unexpectedly, the CR domain was not responsible for an increased turnover of sLANA mRNA but for a better stability over time of sLANA mRNAs compared to constructs deleted of the EG-EA repeat. Moreover, the authors showed that neither protein stability nor the efficiency of protein translation were influenced by the CR region, which revealed significant differences compared to both EBNA-1 and LANA-1. Finally, a single copy of the motif EEAEEAEEE, which is present multiple times in the EA-rich domain of two strains of SaHV-2, was shown to be sufficient to inhibit MHC class I-restricted antigen presentation when fused in frame with the sequence of the heterologous ovalbumin protein (Gao et al., 2009). The mechanism underlying this effect was suggested to be due to both stabilization of mRNA and repression of self-transcription. Thus, the presence of the EA-rich region could potentially influence the total amount of translated sLANA and protein synthesis efficiency, which in turn could potentially reduce the generation of DRiPs although this aspect has not been directly addressed.

MuHV-4 infects and persists in the laboratory mouse. Following primary infection, usually experimental intranasal or intra-tracheal infection, MuHV-4 replicates in epithelial cells and macrophages before reaching secondary lymphoid organs where the virus is maintained as episomal genomes in memory B lymphocytes (Barton et al., 2011; Gillet et al., 2015). MuHV-4 GMP (mLANA) has been demonstrated to be essential for episome maintenance *in vitro* but also *in vivo* as shown using recombinant strains of MuHV-4 impaired for the expression of mLANA (Fowler et al., 2003; Forrest et al., 2007; Habison et al., 2012). Among gammaherpesvirus GMPs, mLANA is probably one of the most intriguing proteins. Indeed, despite a lack of CR domain, mLANA has retained the ability of its orthologs to act in *cis* to self-inhibit MHC class I antigen presentation through a region mapped to amino acids 170–220 of mLANA (Bennett et al., 2005). This region was shown to be able to decrease the steady-state levels of mLANA protein while at the same time contributing to enhancing protein stability and protection from proteasomal degradation (Bennett et al., 2005), similar to EBNA-1. However, the exact mechanisms of action have not been fully deciphered and it remains unclear how protein translation

efficiency and potential G4 structures could be involved. MuHV-4 provides an invaluable model to study gammaherpesvirus infection *in vivo*, including viral pathogenesis and latency (Barton et al., 2011). Using recombinant strains of MuHV-4 expressing model T-cell epitopes in tandem under the control of ORF73, Bennett and collaborators used an internal ribosome entry site following the ORF73 coding sequence to bypass the *cis*-acting evasion of ORF73 and to force expression of a tandem sequence of three T-cell epitopes *in vivo*. By doing so, latently-infected cells could express, in *trans*, CTL epitopes encoded by the ORF73 mRNA. Using this recombinant virus, infected mice showed a critical MHC class I-restricted and CTL-dependent reduction in viral latency, demonstrating that *trans*-acting immune evasion could not inhibit peptide presentation to CTLs during latency but rather indirectly suggests that *cis*-acting evasion by the GMP is critical for normal establishment of long-term latency *in vivo*. This study was the first to tackle the immune evasion mechanisms of GMPs *in vivo*. Interestingly, three recent studies used chimeric MuHV-4 recombinant viruses where mLANA was replaced by functional KSHV LANA-1 (Gupta et al., 2017; Habison et al., 2017; Pires de Miranda et al., 2018). These studies demonstrated the ability of LANA-1-expressing chimeric MuHV-4 to be maintained and establish latency *in vivo*, although at lower levels compared to wildtype MuHV-4. These studies are encouraging for future prospects to further investigate the role of immune evasion mechanisms *in vivo* that are directly mediated by LANA-1 or even other related GMPs.

GENUS *Percavirus*

Numerous clinical syndromes have been identified in equid species in association with EHV-2 or EHV-5 infection. However, true evidence for causal implication in the described diseases remain elusive (Marenzoni et al., 2015), with the exception of pulmonary fibrosis induced by EHV-5 infection (Williams et al., 2013). The full sequence of only two members of the *Percavirus* genus has been recently obtained. Although originally thought to not express a GMP (Telford et al., 1995), a recent report identified ORF73-encoding GMPs in two strains of *equid gammaherpesvirus 2* (EHV-2), including the initially sequenced strain, and one strain of *equid gammaherpesvirus 5* (EHV-5) (Wilkie et al., 2015). Whereas strain 86/67 of EHV-2 expresses a GMP of 985 amino acids, strain G9/92 expresses a 949-aa GMP. Strain 2-141/67 of EHV-5 encodes a GMP of 996 residues. Although GMPs of EHV-2 and EHV-5 contain a predicted CR domain, no data is currently available on a potential *cis*-acting immune evasion. More studies need be performed to uncover the role of EHV-2 and EHV-5 GMPs in infection of equids with these viruses.

GENUS *Macavirus*

All sequenced macaviruses encode a GMP but only the role of AlHV-1 GMP (aLANA) has recently been investigated experimentally (Palmeira et al., 2013; Sorel et al., 2017). AlHV-1 infects and persists in wildebeest asymptomatically and one can assume that the entire population of free-ranging wildebeest are infected. However, upon reactivation events, AlHV-1 can be transmitted to a range of phylogenetically related ruminant species, like cattle. In these susceptible species, AlHV-1 induces MCF that ultimately leads to the death of the infected animal. In both wildebeest and cattle, AlHV-1 establishes latency but results either in true quiescent/latent infection (in wildebeest) or latency-associated lymphoproliferation of $CD8^+$ T lymphocytes (in cattle). During AlHV-1-associated MCF, aLANA is highly expressed (Palmeira et al., 2013). Thus, an adaptive immune response is likely induced against the protein, potentially including $CD8^+$ CTLs that are specific to aLANA-derived antigenic peptides. However, if such a putative response exists, it fails to be protective as MCF-susceptible animals ultimately develop MCF and die upon infection. In our recent study, aLANA was shown to have acquired *cis*-acting immune evasion properties similarly to its orthologs (Sorel et al., 2017). In particular, this immune evasion mechanism was shown to be mediated through the CR domain of aLANA that is rich in G and E residues (termed GE). Importantly, the inhibitory properties of GE could be transferred to a heterologous protein such as enhanced green fluorescent protein, which is consistent with the data obtained with the EA-rich domain of sLANA (Gao et al., 2009). Mutant constructs expressing aLANA deleted for the GE-rich domain exhibited similar protein and mRNA turnover suggesting that GE inhibits proteasome-dependent antigen presentation through a mechanism that does not involve protein or mRNA degradation processes (Sorel et al., 2017). Although these data are consistent with the results obtained with sLANA (Gao et al., 2009), the internal region of several GMPs, including LANA-1 and EBNA-1, as well as the amino acid region 170–220 of mLANA were shown to mediate decreased protein turnover (Levitskaya et al., 1997; Bennett et al., 2005; Kwun et al., 2007). However, the CR2CR3 region of LANA-1 that was mapped to inhibit proteasomal degradation was, however, not found to be involved in the self-inhibition of antigen presentation (Kwun et al., 2011). Although the mechanisms involved in immune evasion are not necessarily shared by all gammaherpesvirus GMPs, these data are nonetheless strengthened by another study that revealed that the half-life of a polypeptide does not determine antigen presentation (Apcher et al., 2010). Thus, it can be suggested that protection of GMPs from proteasomal degradation might not be sufficient to block antigen presentation. The lack of aLANA GE resulted in increased protein expression levels due to a combination of enhanced translation efficiency and increased steady-state RNA levels (Sorel et al., 2017), which resulted in increased proteasome-dependent processing of aLANA for MHC-I presentation. This mechanism was, however, independent of autophagy, as treatments with the autophagy inducer rapamycin, or autophagy inhibitors chloroquine or 3-methyladenine, did not affect peptide presentation by MHC-I. Thus, these results suggested that the GE-rich domain could inhibit self-antigen presentation through regulation of both protein translation and RNA transcription levels, leading as a consequence to a decrease in DRiPs generation. Several related gammaherpesviruses were shown to have acquired mechanisms

that lead to reduced steady-state protein levels of their respective GMPs (Tellam et al., 2007a; Yoshioka et al., 2008; Gao et al., 2009), resulting in a potential reduction of DRiPs production. Thus, targeting pathways leading to DRiPs production seems to be a valuable mechanism to ensure episome persistence during latency while avoiding detection by the immune system. Furthermore, replacing the native GE-rich region of aLANA by a synthetic codon-modified sequence, in order to reduce the purine bias in the mRNA sequence without modifying the protein sequence, similar to EBNA-1 GAr (Tellam et al., 2014), led to significantly enhanced antigen presentation and increased activation of antigen-specific CTLs in a mouse model of DNA immunization (Sorel et al., 2017). These results were suggestive of potential constraints, such as G4 structures, within native GE mRNA structure that could limit antigen presentation in a similar manner as EBNA-1 (Tellam et al., 2008; Murat et al., 2014). Then, mRNA constraints contained in the GE-rich domain of aLANA, rather than peptidic sequence, is likely responsible for CTL immune evasion. However, the GE-mediated *cis*-limitation of MHC class I antigen presentation of aLANA was further shown to be dispensable for the induction of MCF in the experimental rabbit model (Sorel et al., 2017). Indeed, a recombinant virus expressing a GE-deleted form of aLANA could induce MCF in rabbits in a similar manner to a wild type virus expressing aLANA. Although the viral-specific CTL response could not be monitored to determine the role of the GE-rich domain in the efficient priming of CTLs by aLANA *in vivo*, it clearly appears that aLANA-mediated *cis*-acting immune evasion is not determinant during MCF. While the mechanisms explaining this finding in the context of MCF remain to be identified, these results suggest that the immune evasion functions of aLANA are more likely to play a role in the context of lifelong infection of the natural host of AlHV-1, the wildebeest.

CONCLUSION

All sequenced gammaherpesviruses encode a GMP that tethers viral genomes to the cellular chromosomes, ensuring even segregation of viral episomes in daughter cells during cell division (Blake, 2010). Besides their role in viral persistence, GMPs can also modify the cellular environment to promote cell immortalization and tumorigenesis in gammaherpesvirus-induced malignancies. Because of their essential roles in gammaherpesvirus latency, GMPs need to be expressed while remaining hidden from immune surveillance in the infected host. Evasion mechanisms of the cytotoxic T cell response through self-limitation of MHC class I antigen presentation constitute unique properties developed by GMPs to ensure gammaherpesvirus long-term persistence. Importantly, more questions need to be addressed for a complete understanding of how GMPs successfully achieve both viral persistence and escape of the CTL response. Such future understanding is of interest to develop potential treatments to target and efficiently disrupt latency. Among these questions, we could ask whether the presence of G4 structures does represent a major and common mechanism in gammaherpesviruses to control the production of DRiPs from nascent GMP proteins during latency? Moreover, how important is the *cis*-acting immune evasion during lymphoproliferation, a hallmark of gammaherpesvirus-associated malignancies? Indeed, a recombinant strain of AlHV-1 expressing a mutated aLANA unable to self-inhibit protein processing for presentation by MHC class I was, however, fully able to induce normal MCF. Whether this observation after AlHV-1 infection represents a general rule or just an exception is unknown. Thus, it makes no doubt that understanding the degree of involvement of GMP *cis*-acting immune evasion during gammaherpesvirus latency will be determined depending on our understanding of latency mechanisms themselves and, for instance, how distinct are silent latency in healthy individuals and latency-dependent lymphoproliferative diseases. In other words, would self-inhibition of antigen presentation by GMP represent the essential mechanism to avoid CTL recognition during gammaherpesvirus-induced lymphoproliferation? We are eager to uncover future investigations that will clarify these questions.

AUTHOR CONTRIBUTIONS

All authors listed have made a substantial, direct and intellectual contribution to the work, and approved it for publication.

FUNDING

This work was funded through F.R.S.-FNRS grant #MIS-F.4501.15.

ACKNOWLEDGMENTS

BD is a Research Associate of the F.R.S.-FNRS (Belgium). The authors are grateful to Léa Morvan for careful reading of the manuscript.

REFERENCES

Altmann, M., Pich, D., Ruiss, R., Wang, J., Sugden, B., and Hammerschmidt, W. (2006). Transcriptional activation by EBV nuclear antigen 1 is essential for the expression of EBV's transforming genes. *Proc. Natl. Acad. Sci. U.S.A.* 103, 14188–14193. doi: 10.1073/pnas.0605985103

Andersson, J. (2000). An overview of epstein-barr virus: from discovery to future directions for treatment and prevention. *Herpes* 7, 76–82.

Anton, L. C., and Yewdell, J. W. (2014). Translating DRiPs: MHC class I immunosurveillance of pathogens and tumors. *J. Leukoc. Biol.* 95, 551–562. doi: 10.1189/jlb.1113599

Apcher, S., Daskalogianni, C., Manoury, B., and Fahraeus, R. (2010). Epstein Barr virus-encoded EBNA1 interference with MHC class I antigen presentation reveals a close correlation between mRNA translation initiation and antigen presentation. *PLoS Pathog.* 6:e1001151. doi: 10.1371/journal.ppat.1001151

Apcher, S., Komarova, A., Daskalogianni, C., Yin, Y., Malbert-Colas, L., and Fåhraeus, R. (2009). mRNA translation regulation by the Gly-Ala repeat of Epstein-Barr virus nuclear antigen 1. *J. Virol.* 83, 1289–1298. doi: 10.1128/jvi.01369-08

Baer, R., Bankier, A. T., Biggin, M. D., Deininger, P. L., Farrell, P. J., Gibson, T. J., et al. (1984). DNA sequence and expression of the B95-8 Epstein-Barr virus genome. *Nature* 310, 207–211. doi: 10.1038/310207a0

Ballestas, M. E., Chatis, P. A., and Kaye, K. M. (1999). Efficient persistence of extrachromosomal KSHV DNA mediated by latency-associated nuclear antigen. *Science* 284, 641–644. doi: 10.1126/science.284.5414.641

Ballestas, M. E., and Kaye, K. M. (2001). Kaposi's sarcoma-associated herpesvirus latency-associated nuclear antigen 1 mediates episome persistence through cis-acting terminal repeat (TR) sequence and specifically binds TR DNA. *J. Virol.* 75, 3250–3258. doi: 10.1128/JVI.75.7.3250-3258.2001

Barbera, A. J., Ballestas, M. E., and Kaye, K. M. (2004). The Kaposi's sarcoma-associated herpesvirus latency-associated nuclear antigen 1 N terminus is essential for chromosome association, DNA replication, and episome persistence. *J. Virol.* 78, 294–301. doi: 10.1128/JVI.78.1.294-301.2004

Barbera, A. J., Chodaparambil, J. V., Kelley-Clarke, B., Joukov, V., Walter, J. C., Luger, K., et al. (2006). The nucleosomal surface as a docking station for Kaposi's sarcoma herpesvirus LANA. *Science* 311, 856–861. doi: 10.1126/science.1120541

Barton, E., Mandal, P., and Speck, S. H. (2011). Pathogenesis and host control of gammaherpesviruses: lessons from the mouse. *Annu. Rev. Immunol.* 29, 351–397. doi: 10.1146/annurev-immunol-072710-081639

Bennett, N. J., May, J. S., and Stevenson, P. G. (2005). Gamma-herpesvirus latency requires T cell evasion during episome maintenance. *PLoS Biol.* 3:e120. doi: 10.1371/journal.pbio.0030120

Bihl, F., Narayan, M., Chisholm, J. V. III, Henry, L. M., Suscovich, T. J., Brown, E. E., et al. (2007). Lytic and latent antigens of the human gammaherpesviruses Kaposi's sarcoma-associated herpesvirus and Epstein-Barr virus induce T-cell responses with similar functional properties and memory phenotypes. *J. Virol.* 81, 4904–4908. doi: 10.1128/jvi.02509-06

Blake, N. (2010). Immune evasion by gammaherpesvirus genome maintenance proteins. *J. Gen. Virol.* 91(Pt 4), 829–846. doi: 10.1099/vir.0.018242-0

Blake, N., Haigh, T., Shaka'a, G., Croom-Carter, D., and Rickinson, A. (2000). The importance of exogenous antigen in priming the human CD8+ T cell response: lessons from the EBV nuclear antigen EBNA1. *J. Immunol.* 165, 7078–7087. doi: 10.4049/jimmunol.165.12.7078

Blake, N., Lee, S., Redchenko, I., Thomas, W., Steven, N., Leese, A., et al. (1997). Human CD8+ T cell responses to EBV EBNA1: HLA class I presentation of the (Gly-Ala)-containing protein requires exogenous processing. *Immunity* 7, 791–802. doi: 10.1016/S1074-7613(00)80397-0

Blake, N. W., Moghaddam, A., Rao, P., Kaur, A., Glickman, R., Cho, Y. G., et al. (1999). Inhibition of antigen presentation by the glycine/alanine repeat domain is not conserved in simian homologues of Epstein-Barr virus nuclear antigen 1. *J. Virol.* 73, 7381–7389.

Blum, J. S., Wearsch, P. A., and Cresswell, P. (2013). Pathways of antigen processing. *Annu. Rev. Immunol.* 31, 443–473. doi: 10.1146/annurev-immunol-032712-095910

Brander, C., Raje, N., O'Connor, P. G., Davies, F., Davis, J., Chauhan, D., et al. (2002). Absence of biologically important Kaposi sarcoma-associated herpesvirus gene products and virus-specific cellular immune responses in multiple myeloma. *Blood* 100, 698–700. doi: 10.1182/blood.V100.2.698

Cai, Q., Xiao, B., Si, H., Cervini, A., Gao, J., Lu, J., et al. (2012). Kaposi's sarcoma herpesvirus upregulates Aurora A expression to promote p53 phosphorylation and ubiquitylation. *PLoS Pathog.* 8:e1002566. doi: 10.1371/journal.ppat.1002566

Cai, Q. L., Knight, J. S., Verma, S. C., Zald, P., and Robertson, E. S. (2006). EC5S ubiquitin complex is recruited by KSHV latent antigen LANA for degradation of the VHL and p53 tumor suppressors. *PLoS Pathog.* 2:e116. doi: 10.1371/journal.ppat.0020116

Calderwood, M., White, R. E., Griffiths, R. A., and Whitehouse, A. (2005). Open reading frame 73 is required for herpesvirus saimiri A11-S4 episomal persistence. *J. Gen. Virol.* 86(Pt 10), 2703–2708. doi: 10.1099/vir.0.81230-0

Calderwood, M. A., Hall, K. T., Matthews, D. A., and Whitehouse, A. (2004). The herpesvirus saimiri ORF73 gene product interacts with host-cell mitotic chromosomes and self-associates via its C terminus. *J. Gen. Virol.* 85(Pt 1), 147–153. doi: 10.1099/vir.0.19437-0

Callan, M. F., Steven, N., Krausa, P., Wilson, J. D., Moss, P. A., Gillespie, G. M., et al. (1996). Large clonal expansions of CD8+ T cells in acute infectious mononucleosis. *Nat. Med.* 2, 906–911. doi: 10.1038/nm0896-906

Chastel, C., Beaucournu, J. P., Chastel, O., Legrand, M. C., and Le Goff, F. (1994). A herpesvirus from an European shrew (*Crocidura russula*). *Acta Virol.* 38:309.

Collins-McMillen, D., Buehler, J., Peppenelli, M., and Goodrum, F. (2018). Molecular determinants and the regulation of human cytomegalovirus latency and reactivation. *Viruses* 10:E444. doi: 10.3390/v10080444

Coppotelli, G., Mughal, N., Marescotti, D., and Masucci, M. G. (2011). High avidity binding to DNA protects ubiquitylated substrates from proteasomal degradation. *J. Biol. Chem.* 286, 19565–19575. doi: 10.1074/jbc.M111.224782

Cotter, M. A. II, and Robertson, E. S. (1999). The latency-associated nuclear antigen tethers the Kaposi's sarcoma-associated herpesvirus genome to host chromosomes in body cavity-based lymphoma cells. *Virology* 264, 254–264. doi: 10.1006/viro.1999.9999

Cotter, M. A. II, Subramanian, C., and Robertson, E. S. (2001). The Kaposi's sarcoma-associated herpesvirus latency-associated nuclear antigen binds to specific sequences at the left end of the viral genome through its carboxy-terminus. *Virology* 291, 241–259. doi: 10.1006/viro.2001.1202

Cruickshank, J., Shire, K., Davidson, A. R., Edwards, A. M., and Frappier, L. (2000). Two domains of the epstein-barr virus origin DNA-binding protein, EBNA1, orchestrate sequence-specific DNA binding. *J. Biol. Chem.* 275, 22273–22277. doi: 10.1074/jbc.M001414200

Damania, B., and Desrosiers, R. C. (2001). Simian homologues of human herpesvirus 8. *Philos. Trans. R. Soc. Lond. B Biol. Sci.* 356, 535–543. doi: 10.1098/rstb.2000.0782

Daskalogianni, C., Apcher, S., Candeias, M. M., Naski, N., Calvo, F., and Fahraeus, R. (2008). Gly-Ala repeats induce position- and substrate-specific regulation of 26 S proteasome-dependent partial processing. *J. Biol. Chem.* 283, 30090–30100. doi: 10.1074/jbc.M803290200

Davison, A. J., Eberle, R., Ehlers, B., Hayward, G. S., McGeoch, D. J., Minson, A. C., et al. (2009). The order *Herpesvirales*. *Arch. Virol.* 154, 171–177. doi: 10.1007/s00705-008-0278-4

Dewals, B., Boudry, C., Farnir, F., Drion, P. V., and Vanderplasschen, A. (2008). Malignant catarrhal fever induced by alcelaphine herpesvirus 1 is associated with proliferation of CD8+ T cells supporting a latent infection. *PLoS One* 3:e1627. doi: 10.1371/journal.pone.0001627

Dewals, B., Gillet, L., Gerdes, T., Taracha, E. L., Thiry, E., and Vanderplasschen, A. (2005). Antibodies against bovine herpesvirus 4 are highly prevalent in wild African buffaloes throughout eastern and southern Africa. *Vet. Microbiol.* 110, 209–220. doi: 10.1016/j.vetmic.2005.08.006

Dewals, B., Myster, F., Palmeira, L., Gillet, L., Ackermann, M., and Vanderplasschen, A. (2011). Ex vivo bioluminescence detection of alcelaphine herpesvirus 1 infection during malignant catarrhal fever. *J. Virol.* 85, 6941–6954. doi: 10.1128/JVI.00286-11

Dewals, B. G., and Vanderplasschen, A. (2011). Malignant catarrhal fever induced by *Alcelaphine herpesvirus 1* is characterized by an expansion of activated CD3+CD8+CD4- T cells expressing a cytotoxic phenotype in both lymphoid and non-lymphoid tissues. *Vet. Res.* 42:95. doi: 10.1186/1297-9716-42-95

DeWire, S. M., and Damania, B. (2005). The latency-associated nuclear antigen of rhesus monkey rhadinovirus inhibits viral replication through repression of Orf50/Rta transcriptional activation. *J. Virol.* 79, 3127–3138. doi: 10.1128/JVI.79.5.3127-3138.2005

Dong, S., Forrest, J. C., and Liang, X. (2017). Murine gammaherpesvirus 68: a small animal model for gammaherpesvirus-associated diseases. *Adv. Exp. Med. Biol.* 1018, 225–236. doi: 10.1007/978-981-10-5765-6_14

Ehlers, B., Kuchler, J., Yasmum, N., Dural, G., Voigt, S., Schmidt-Chanasit, J., et al. (2007). Identification of novel rodent herpesviruses, including the first gammaherpesvirus of *Mus musculus*. *J. Virol.* 81, 8091–8100. doi: 10.1128/jvi.00255-07

Evans, T. J., Farrell, P. J., and Swaminathan, S. (1996). Molecular genetic analysis of Epstein-Barr virus Cp promoter function. *J. Virol.* 70, 1695–1705.

Falk, K., Gratama, J. W., Rowe, M., Zou, J. Z., Khanim, F., Young, L. S., et al. (1995). The role of repetitive DNA sequences in the size variation of Epstein-Barr virus (EBV) nuclear antigens, and the identification of different EBV isolates using RFLP and PCR analysis. *J. Gen. Virol.* 76(Pt 4), 779–790. doi: 10.1099/0022-1317-76-4-779

Feng, P., Moses, A., and Fruh, K. (2013). Evasion of adaptive and innate immune response mechanisms by gamma-herpesviruses. *Curr. Opin. Virol.* 3, 285–295. doi: 10.1016/j.coviro.2013.05.011

Fickenscher, H., and Fleckenstein, B. (2001). *Herpesvirus saimiri. Philos. Trans. R. Soc. Lond. B Biol. Sci.* 356, 545–567. doi: 10.1098/rstb.2000.0780

Fleckenstein, B., and Ensser, A. (2004). *Herpesvirus saimiri* transformation of human T lymphocytes. *Curr. Protoc. Immunol.* 63, 7.21.1–7.21.11. doi: 10.1002/0471142735.im0721s63

Fleckenstein, B., and Ensser, A. (2007). "Gammaherpesviruses of new world primates," in *Human Herpesviruses: Biology, Therapy, and Immunoprophylaxis*, eds A. Arvin, G. Campadelli-Fiume, E. Mocarski, P. S. Moore, B. Roizman, R. Whitley, et al. (Cambridge: Cambridge University Press).

Fogg, M. H., Kaur, A., Cho, Y. G., and Wang, F. (2005). The CD8+ T-cell response to an Epstein-Barr virus-related gammaherpesvirus infecting rhesus macaques provides evidence for immune evasion by the EBNA-1 homologue. *J. Virol.* 79, 12681–12691. doi: 10.1128/jvi.79.20.12681-12691.2005

Forrest, J. C., Paden, C. R., Allen, R. D. III, Collins, J., and Speck, S. H. (2007). ORF73-null murine gammaherpesvirus 68 reveals roles for mLANA and p53 in virus replication. *J. Virol.* 81, 11957–11971. doi: 10.1128/JVI.00111-07

Fowler, P., Marques, S., Simas, J. P., and Efstathiou, S. (2003). ORF73 of murine herpesvirus-68 is critical for the establishment and maintenance of latency. *J. Gen. Virol.* 84(Pt 12), 3405–3416. doi: 10.1099/vir.0.19594-0

Frappier, L. (2015). EBNA1. *Curr. Top. Microbiol. Immunol.* 391, 3–34. doi: 10.1007/978-3-319-22834-1_1

Gahn, T. A., and Sugden, B. (1995). An EBNA-1-dependent enhancer acts from a distance of 10 kilobase pairs to increase expression of the Epstein-Barr virus LMP gene. *J. Virol.* 69, 2633–2636.

Gao, J., Coulson, J. M., Whitehouse, A., and Blake, N. (2009). Reduction in RNA levels rather than retardation of translation is responsible for the inhibition of major histocompatibility complex class I antigen presentation by the glutamic acid-rich repeat of *Herpesvirus saimiri* open reading frame 73. *J. Virol.* 83, 273–282. doi: 10.1128/JVI.01532-08

Gao, S. J., Zhang, Y. J., Deng, J. H., Rabkin, C. S., Flore, O., and Jenson, H. B. (1999). Molecular polymorphism of Kaposi's sarcoma-associated herpesvirus (Human herpesvirus 8) latent nuclear antigen: evidence for a large repertoire of viral genotypes and dual infection with different viral genotypes. *J. Infect. Dis.* 180, 1466–1476. doi: 10.1086/315098

Gillet, L., Frederico, B., and Stevenson, P. G. (2015). Host entry by gamma-herpesviruses–lessons from animal viruses? *Curr. Opin. Virol.* 15, 34–40. doi: 10.1016/j.coviro.2015.07.007

Goodrum, F. (2016). Human cytomegalovirus latency: approaching the gordian knot. *Annu. Rev. Virol.* 3, 333–357. doi: 10.1146/annurev-virology-110615-042422

Gupta, A., Oldenburg, D. G., Salinas, E., White, D. W., and Forrest, J. C. (2017). Murine gammaherpesvirus 68 expressing kaposi sarcoma-associated herpesvirus latency-associated nuclear antigen (LANA) reveals both functional conservation and divergence in LANA homologs. *J. Virol.* 91:e00992-17. doi: 10.1128/JVI.00992-17

Gupta, N., Thakker, S., and Verma, S. C. (2016). KSHV encoded LANA recruits nucleosome assembly protein NAP1L1 for regulating viral DNA replication and transcription. *Sci. Rep.* 6:32633. doi: 10.1038/srep32633

Habison, A. C., Beauchemin, C., Simas, J. P., Usherwood, E. J., and Kaye, K. M. (2012). Murine gammaherpesvirus 68 LANA acts on terminal repeat DNA to mediate episome persistence. *J. Virol.* 86, 11863–11876. doi: 10.1128/JVI.01656-12

Habison, A. C., de Miranda, M. P., Beauchemin, C., Tan, M., Cerqueira, S. A., Correia, B., et al. (2017). Cross-species conservation of episome maintenance provides a basis for in vivo investigation of Kaposi's sarcoma herpesvirus LANA. *PLoS Pathog.* 13:e1006555. doi: 10.1371/journal.ppat.1006555

Harrison, S., Fisenne, K., and Hearing, J. (1994). Sequence requirements of the Epstein-Barr virus latent origin of DNA replication. *J. Virol.* 68, 1913–1925.

Heessen, S., Dantuma, N. P., Tessarz, P., Jellne, M., and Masucci, M. G. (2003). Inhibition of ubiquitin/proteasome-dependent proteolysis in *Saccharomyces cerevisiae* by a Gly-Ala repeat. *FEBS Lett.* 555, 397–404. doi: 10.1016/S0014-5793(03)01296-1

Heessen, S., Leonchiks, A., Issaeva, N., Sharipo, A., Selivanova, G., Masucci, M. G., et al. (2002). Functional p53 chimeras containing the Epstein-Barr virus Gly-Ala repeat are protected from Mdm2- and HPV-E6-induced proteolysis. *Proc. Natl. Acad. Sci. U.S.A.* 99, 1532–1537. doi: 10.1073/pnas.022306499

Henle, G., Henle, W., Clifford, P., Diehl, V., Kafuko, G. W., Kirya, B. G., et al. (1969). Antibodies to Epstein-Barr virus in Burkitt's lymphoma and control groups. *J. Natl. Cancer Inst.* 43, 1147–1157.

Hoyt, M. A., Zich, J., Takeuchi, J., Zhang, M., Govaerts, C., and Coffino, P. (2006). Glycine-alanine repeats impair proper substrate unfolding by the proteasome. *EMBO J.* 25, 1720–1729. doi: 10.1038/sj.emboj.7601058

Hu, Z., and Usherwood, E. J. (2014). Immune escape of gamma-herpesviruses from adaptive immunity. *Rev. Med. Virol.* 24, 365–378. doi: 10.1002/rmv.1791

Hughes, D. J., Kipar, A., Milligan, S. G., Cunningham, C., Sanders, M., Quail, M. A., et al. (2010). Characterization of a novel wood mouse virus related to murid herpesvirus 4. *J. Gen. Virol.* 91(Pt 4), 867–879. doi: 10.1099/vir.0.017327-0

Humme, S., Reisbach, G., Feederle, R., Delecluse, H. J., Bousset, K., Hammerschmidt, W., et al. (2003). The EBV nuclear antigen 1 (EBNA1) enhances B cell immortalization several thousandfold. *Proc. Natl. Acad. Sci. U.S.A.* 100, 10989–10994. doi: 10.1073/pnas.1832776100

Jha, H. C., Pei, Y., and Robertson, E. S. (2016). Epstein-Barr Virus: diseases linked to infection and transformation. *Front. Microbiol.* 7:1602. doi: 10.3389/fmicb.2016.01602

Kapoor, P., and Frappier, L. (2003). EBNA1 partitions Epstein-Barr virus plasmids in yeast cells by attaching to human EBNA1-binding protein 2 on mitotic chromosomes. *J. Virol.* 77, 6946–6956. doi: 10.1128/jvi.77.12.6946-6956.2003

Kapoor, P., Lavoie, B. D., and Frappier, L. (2005). EBP2 plays a key role in Epstein-Barr virus mitotic segregation and is regulated by aurora family kinases. *Mol. Cell. Biol.* 25, 4934–4945. doi: 10.1128/mcb.25.12.4934-4945.2005

Kelley-Clarke, B., Ballestas, M. E., Komatsu, T., and Kaye, K. M. (2007). Kaposi's sarcoma herpesvirus C-terminal LANA concentrates at pericentromeric and peri-telomeric regions of a subset of mitotic chromosomes. *Virology* 357, 149–157. doi: 10.1016/j.virol.2006.07.052

Kwun, H. J., da Silva, S. R., Qin, H., Ferris, R. L., Tan, R., Chang, Y., et al. (2011). The central repeat domain 1 of Kaposi's sarcoma-associated herpesvirus (KSHV) latency associated-nuclear antigen 1 (LANA1) prevents cis MHC class I peptide presentation. *Virology* 412, 357–365. doi: 10.1016/j.virol.2011.01.026

Kwun, H. J., da Silva, S. R., Shah, I. M., Blake, N., Moore, P. S., and Chang, Y. (2007). Kaposi's sarcoma-associated herpesvirus latency-associated nuclear antigen 1 mimics Epstein-Barr virus EBNA1 immune evasion through central repeat domain effects on protein processing. *J. Virol.* 81, 8225–8235. doi: 10.1128/JVI.00411-07

Lee, S. P., Brooks, J. M., Al-Jarrah, H., Thomas, W. A., Haigh, T. A., Taylor, G. S., et al. (2004). CD8 T cell recognition of endogenously expressed epstein-barr virus nuclear antigen 1. *J. Exp. Med.* 199, 1409–1420. doi: 10.1084/jem.20040121

Lepone, L., Rappocciolo, G., Knowlton, E., Jais, M., Piazza, P., Jenkins, F. J., et al. (2010). Monofunctional and polyfunctional CD8+ T cell responses to human herpesvirus 8 lytic and latency proteins. *Clin. Vaccine Immunol.* 17, 1507–1516. doi: 10.1128/CVI.00189-10

Levin, L. I., Munger, K. L., O'Reilly, E. J., Falk, K. I., and Ascherio, A. (2010). Primary infection with the Epstein-Barr virus and risk of multiple sclerosis. *Ann. Neurol.* 67, 824–830. doi: 10.1002/ana.21978

Levitskaya, J., Coram, M., Levitsky, V., Imreh, S., Steigerwald-Mullen, P. M., Klein, G., et al. (1995). Inhibition of antigen processing by the internal repeat region of the Epstein-Barr virus nuclear antigen-1. *Nature* 375, 685–688. doi: 10.1038/375685a0

Levitskaya, J., Sharipo, A., Leonchiks, A., Ciechanover, A., and Masucci, M. G. (1997). Inhibition of ubiquitin/proteasome-dependent protein degradation by the Gly-Ala repeat domain of the Epstein-Barr virus nuclear antigen 1. *Proc. Natl. Acad. Sci. U.S.A.* 94, 12616–12621. doi: 10.1073/pnas.94.23.12616

Li, S., Bai, L., Dong, J., Sun, R., and Lan, K. (2017). Kaposi's sarcoma-associated herpesvirus: epidemiology and molecular biology. *Adv. Exp. Med. Biol.* 1018, 91–127. doi: 10.1007/978-981-10-5765-6_7

Lieberman, P. M. (2013). Keeping it quiet: chromatin control of gammaherpesvirus latency. *Nat. Rev. Microbiol.* 11, 863–875. doi: 10.1038/nrmicro3135

Lieberman, P. M. (2016). Epigenetics and genetics of viral latency. *Cell Host Microbe* 19, 619–628. doi: 10.1016/j.chom.2016.04.008

Lomonte, P., Bublot, M., van Santen, V., Keil, G. M., Pastoret, P. P., and Thiry, E. (1995). Analysis of bovine herpesvirus 4 genomic regions located outside the conserved gammaherpesvirus gene blocks. *J. Gen. Virol.* 76(Pt 7), 1835–1841. doi: 10.1099/0022-1317-76-7-1835

Lu, F., Day, L., Gao, S. J., and Lieberman, P. M. (2006). Acetylation of the latency-associated nuclear antigen regulates repression of Kaposi's sarcoma-associated herpesvirus lytic transcription. *J. Virol.* 80, 5273–5282. doi: 10.1128/JVI.02541-05

Lu, F., Tsai, K., Chen, H. S., Wikramasinghe, P., Davuluri, R. V., Showe, L., et al. (2012). Identification of host-chromosome binding sites and candidate gene targets for Kaposi's sarcoma-associated herpesvirus LANA. *J. Virol.* 86, 5752–5762. doi: 10.1128/JVI.07216-11

Lussignol, M., and Esclatine, A. (2017). Herpesvirus and autophagy: "all right, everybody be cool, this is a robbery!" *Viruses* 9:E372. doi: 10.3390/v9120372

Machiels, B., Lete, C., de Fays, K., Mast, J., Dewals, B., Stevenson, P. G., et al. (2011). The bovine herpesvirus 4 Bo10 gene encodes a nonessential viral envelope protein that regulates viral tropism through both positive and negative effects. *J. Virol.* 85, 1011–1024. doi: 10.1128/JVI.01092-10

Machiels, B., Stevenson, P. G., Vanderplasschen, A., and Gillet, L. (2013). A gammaherpesvirus uses alternative splicing to regulate its tropism and its sensitivity to neutralization. *PLoS Pathog.* 9:e1003753. doi: 10.1371/journal.ppat.1003753

Madireddy, A., Purushothaman, P., Loosbroock, C. P., Robertson, E. S., Schildkraut, C. L., and Verma, S. C. (2016). G-quadruplex-interacting compounds alter latent DNA replication and episomal persistence of KSHV. *Nucleic Acids Res.* 44, 3675–3694. doi: 10.1093/nar/gkw038

Marenzoni, M. L., Stefanetti, V., Danzetta, M. L., and Timoney, P. J. (2015). Gammaherpesvirus infections in equids: a review. *Vet. Med.* 6, 91–101. doi: 10.2147/VMRR.S39473

Means, R. E., Lang, S. M., and Jung, J. U. (2007). "Human gammaherpesvirus immune evasion strategies," in *Human Herpesviruses: Biology, Therapy, and Immunoprophylaxis*, eds A. Arvin, G. Campadelli-Fiume, E. Mocarski, P. S. Moore, B. Roizman, R. Whitley, et al. (Cambridge: Cambridge University Press).

Metifiot, M., Amrane, S., Litvak, S., and Andreola, M. L. (2014). G-quadruplexes in viruses: function and potential therapeutic applications. *Nucleic Acids Res.* 42, 12352–12366. doi: 10.1093/nar/gku999

Moreno, M. A., Or-Geva, N., Aftab, B. T., Khanna, R., Croze, E., Steinman, L., et al. (2018). Molecular signature of Epstein-Barr virus infection in MS brain lesions. *Neurol. Neuroimmunol. Neuroinflamm.* 5:e466. doi: 10.1212/NXI.0000000000000466

Munger, K. L., Levin, L. I., O'Reilly, E. J., Falk, K. I., and Ascherio, A. (2011). Anti-Epstein-Barr virus antibodies as serological markers of multiple sclerosis: a prospective study among United States military personnel. *Mult. Scler.* 17, 1185–1193. doi: 10.1177/1352458511408991

Murat, P., and Tellam, J. (2015). Effects of messenger RNA structure and other translational control mechanisms on major histocompatibility complex-I mediated antigen presentation. *Wiley Interdiscip. Rev. RNA* 6, 157–171. doi: 10.1002/wrna.1262

Murat, P., Zhong, J., Lekieffre, L., Cowieson, N. P., Clancy, J. L., Preiss, T., et al. (2014). G-quadruplexes regulate Epstein-Barr virus-encoded nuclear antigen 1 mRNA translation. *Nat. Chem. Biol.* 10, 358–364. doi: 10.1038/nchembio.1479

Pakpoor, J., Disanto, G., Gerber, J. E., Dobson, R., Meier, U. C., Giovannoni, G., et al. (2013). The risk of developing multiple sclerosis in individuals seronegative for Epstein-Barr virus: a meta-analysis. *Mult. Scler.* 19, 162–166. doi: 10.1177/1352458512449682

Palmeira, L., Sorel, O., Van Campe, W., Boudry, C., Roels, S., Myster, F., et al. (2013). An essential role for gamma-herpesvirus latency-associated nuclear antigen homolog in an acute lymphoproliferative disease of cattle. *Proc. Natl. Acad. Sci. U.S.A.* 110, E1933–E1942. doi: 10.1073/pnas.1216531110

Paludan, C., Schmid, D., Landthaler, M., Vockerodt, M., Kube, D., Tuschl, T., et al. (2005). Endogenous MHC class II processing of a viral nuclear antigen after autophagy. *Science* 307, 593–596. doi: 10.1126/science.1104904

Pender, M. P. (2011). The essential role of Epstein-Barr virus in the pathogenesis of multiple sclerosis. *Neuroscientist* 17, 351–367. doi: 10.1177/1073858410381531

Pires de Miranda, M., Quendera, A. P., McVey, C. E., Kaye, K. M., and Simas, J. P. (2018). In vivo persistence of chimeric virus after substitution of the Kaposi's sarcoma-associated herpesvirus LANA DNA binding domain with that of murid herpesvirus 4. *J. Virol.* 92:e01251-18. doi: 10.1128/JVI.01251-18

Radkov, S. A., Kellam, P., and Boshoff, C. (2000). The latent nuclear antigen of Kaposi sarcoma-associated herpesvirus targets the retinoblastoma-E2F pathway and with the oncogene Hras transforms primary rat cells. *Nat. Med.* 6, 1121–1127. doi: 10.1038/80459

Ressing, M. E., van Gent, M., Gram, A. M., Hooykaas, M. J., Piersma, S. J., and Wiertz, E. J. (2015). Immune evasion by Epstein-Barr virus. *Curr. Top. Microbiol. Immunol.* 391, 355–381. doi: 10.1007/978-3-319-22834-1_12

Rezk, S. A., Zhao, X., and Weiss, L. M. (2018). Epstein-Barr virus (EBV)-associated lymphoid proliferations, a 2018 update. *Hum. Pathol.* 79, 18–41. doi: 10.1016/j.humpath.2018.05.020

Rhodes, D., and Lipps, H. J. (2015). G-quadruplexes and their regulatory roles in biology. *Nucleic Acids Res.* 43, 8627–8637. doi: 10.1093/nar/gkv862

Rock, K. L., Farfan-Arribas, D. J., Colbert, J. D., and Goldberg, A. L. (2014). Re-examining class-I presentation and the DRiP hypothesis. *Trends Immunol.* 35, 144–152. doi: 10.1016/j.it.2014.01.002

Rock, K. L., Reits, E., and Neefjes, J. (2016). Present yourself! By MHC Class I and MHC Class II molecules. *Trends Immunol.* 37, 724–737. doi: 10.1016/j.it.2016.08.010

Roizman, B., and Whitley, R. J. (2013). An inquiry into the molecular basis of HSV latency and reactivation. *Annu. Rev. Microbiol.* 67, 355–374. doi: 10.1146/annurev-micro-092412-155654

Schafer, A., Lengenfelder, D., Grillhosl, C., Wieser, C., Fleckenstein, B., and Ensser, A. (2003). The latency-associated nuclear antigen homolog of *Herpesvirus saimiri* inhibits lytic virus replication. *J. Virol.* 77, 5911–5925. doi: 10.1128/JVI.77.10.5911-5925.2003

Schuren, A. B., Costa, A. I., and Wiertz, E. J. (2016). Recent advances in viral evasion of the MHC Class I processing pathway. *Curr. Opin. Immunol.* 40, 43–50. doi: 10.1016/j.coi.2016.02.007

Sears, J., Kolman, J., Wahl, G. M., and Aiyar, A. (2003). Metaphase chromosome tethering is necessary for the DNA synthesis and maintenance of oriP plasmids but is insufficient for transcription activation by Epstein-Barr nuclear antigen 1. *J. Virol.* 77, 11767–11780. doi: 10.1128/JVI.77.21.11767-11780.2003

Sharipo, A., Imreh, M., Leonchiks, A., Imreh, S., and Masucci, M. G. (1998). A minimal glycine-alanine repeat prevents the interaction of ubiquitinated I kappaB alpha with the proteasome: a new mechanism for selective inhibition of proteolysis. *Nat. Med.* 4, 939–944. doi: 10.1038/nm0898-939

Shire, K., Ceccarelli, D. F., Avolio-Hunter, T. M., and Frappier, L. (1999). EBP2, a human protein that interacts with sequences of the Epstein-Barr virus nuclear antigen 1 important for plasmid maintenance. *J. Virol.* 73, 2587–2595.

Sim, A. C., Too, C. T., Oo, M. Z., Lai, J., Eio, M. Y., Song, Z., et al. (2013). Defining the expression hierarchy of latent T-cell epitopes in Epstein-Barr virus infection with TCR-like antibodies. *Sci. Rep.* 3:3232. doi: 10.1038/srep03232

Sivachandran, N., Wang, X., and Frappier, L. (2012). Functions of the Epstein-Barr virus EBNA1 protein in viral reactivation and lytic infection. *J. Virol.* 86, 6146–6158. doi: 10.1128/jvi.00013-12

Sorel, O., Chen, T., Myster, F., Javaux, J., Vanderplasschen, A., and Dewals, B. G. (2017). Macavirus latency-associated protein evades immune detection through regulation of protein synthesis in cis depending upon its glycin/glutamate-rich domain. *PLoS Pathog.* 13:e1006691. doi: 10.1371/journal.ppat.1006691

Sorel, O., and Dewals, B. G. (2016). MicroRNAs in large herpesvirus DNA genomes: recent advances. *Biomol. Concepts* 7, 229–239. doi: 10.1515/bmc-2016-0017

Stedman, W., Deng, Z., Lu, F., and Lieberman, P. M. (2004). ORC, MCM, and histone hyperacetylation at the Kaposi's sarcoma-associated herpesvirus latent replication origin. *J. Virol.* 78, 12566–12575. doi: 10.1128/JVI.78.22.12566-12575.2004

Stevenson, P. G., and Efstathiou, S. (2005). Immune mechanisms in murine gammaherpesvirus-68 infection. *Viral Immunol.* 18, 445–456. doi: 10.1089/vim.2005.18.445

Subklewe, M., Chahroudi, A., Bickham, K., Larsson, M., Kurilla, M. G., Bhardwaj, N., et al. (1999). Presentation of epstein-barr virus latency antigens to CD8(+), interferon-gamma-secreting, T lymphocytes. *Eur. J.*

Immunol. 29, 3995–4001. doi: 10.1002/(SICI)1521-4141(199912)29:12<3995::AID-IMMU3995>3.0.CO;2-E

Telford, E. A., Watson, M. S., Aird, H. C., Perry, J., and Davison, A. J. (1995). The DNA sequence of equine herpesvirus 2. *J. Mol. Biol.* 249, 520–528. doi: 10.1006/jmbi.1995.0314

Tellam, J., Connolly, G., Green, K. J., Miles, J. J., Moss, D. J., Burrows, S. R., et al. (2004). Endogenous presentation of CD8+ T cell epitopes from Epstein-Barr virus-encoded nuclear antigen 1. *J. Exp. Med.* 199, 1421–1431. doi: 10.1084/jem.20040191

Tellam, J., Fogg, M. H., Rist, M., Connolly, G., Tscharke, D., Webb, N., et al. (2007a). Influence of translation efficiency of homologous viral proteins on the endogenous presentation of CD8+ T cell epitopes. *J. Exp. Med.* 204, 525–532. doi: 10.1084/jem.20062508

Tellam, J., Rist, M., Connolly, G., Webb, N., Fazou, C., Wang, F., et al. (2007b). Translation efficiency of EBNA1 encoded by lymphocryptoviruses influences endogenous presentation of CD8+ T cell epitopes. *Eur. J. Immunol.* 37, 328–337. doi: 10.1002/eji.200636153

Tellam, J., Smith, C., Rist, M., Webb, N., Cooper, L., Vuocolo, T., et al. (2008). Regulation of protein translation through mRNA structure influences MHC class I loading and T cell recognition. *Proc. Natl. Acad. Sci. U.S.A.* 105, 9319–9324. doi: 10.1073/pnas.0801968105

Tellam, J. T., Lekieffre, L., Zhong, J., Lynn, D. J., and Khanna, R. (2012). Messenger RNA sequence rather than protein sequence determines the level of self-synthesis and antigen presentation of the EBV-encoded antigen, EBNA1. *PLoS Pathog.* 8:e1003112. doi: 10.1371/journal.ppat.1003112

Tellam, J. T., Zhong, J., Lekieffre, L., Bhat, P., Martinez, M., Croft, N. P., et al. (2014). mRNA structural constraints on EBNA1 synthesis impact on in vivo antigen presentation and early priming of CD8+ T cells. *PLoS Pathog.* 10:e1004423. doi: 10.1371/journal.ppat.1004423

Thirion, M., Machiels, B., Farnir, F., Donofrio, G., Gillet, L., Dewals, B., et al. (2010). Bovine herpesvirus 4 ORF73 is dispensable for virus growth in vitro, but is essential for virus persistence in vivo. *J. Gen. Virol.* 91(Pt 10), 2574–2584. doi: 10.1099/vir.0.023192-0

Ueda, K. (2018). KSHV genome replication and maintenance in latency. *Adv. Exp. Med. Biol.* 1045, 299–320. doi: 10.1007/978-981-10-7230-7_14

Verma, S. C., Cai, Q., Kreider, E., Lu, J., and Robertson, E. S. (2013). Comprehensive analysis of LANA interacting proteins essential for viral genome tethering and persistence. *PLoS One* 8:e74662. doi: 10.1371/journal.pone.0074662

Verma, S. C., Choudhuri, T., Kaul, R., and Robertson, E. S. (2006). Latency-associated nuclear antigen (LANA) of Kaposi's sarcoma-associated herpesvirus interacts with origin recognition complexes at the LANA binding sequence within the terminal repeats. *J. Virol.* 80, 2243–2256. doi: 10.1128/JVI.80.5.2243-2256.2006

Verma, S. C., Lan, K., and Robertson, E. (2007). Structure and function of latency-associated nuclear antigen. *Curr. Top. Microbiol. Immunol.* 312, 101–136. doi: 10.1007/978-3-540-34344-8_4

Verma, S. C., and Robertson, E. S. (2003). ORF73 of *Herpesvirus saimiri* strain C488 tethers the viral genome to metaphase chromosomes and binds to cis-acting DNA sequences in the terminal repeats. *J. Virol.* 77, 12494–12506. doi: 10.1128/JVI.77.23.12494-12506.2003

Voo, K. S., Fu, T., Wang, H. Y., Tellam, J., Heslop, H. E., Brenner, M. K., et al. (2004). Evidence for the presentation of major histocompatibility complex class I-restricted Epstein-Barr virus nuclear antigen 1 peptides to CD8+ T lymphocytes. *J. Exp. Med.* 199, 459–470. doi: 10.1084/jem.20031219

Waldmann, T., Scholten, I., Kappes, F., Hu, H. G., and Knippers, R. (2004). The DEK protein–an abundant and ubiquitous constituent of mammalian chromatin. *Gene* 343, 1–9. doi: 10.1016/j.gene.2004.08.029

Wei, J., and Yewdell, J. W. (2018). Flu DRiPs in MHC Class I immunosurveillance. *Virol. Sin.* doi: 10.1007/s12250-018-0061-y [Epub ahead of print].

Wen, K. W., Dittmer, D. P., and Damania, B. (2009). Disruption of LANA in rhesus rhadinovirus generates a highly lytic recombinant virus. *J. Virol.* 83, 9786–9802. doi: 10.1128/JVI.00704-09

White, D. W., Suzanne Beard, R., and Barton, E. S. (2012). Immune modulation during latent herpesvirus infection. *Immunol. Rev.* 245, 189–208. doi: 10.1111/j.1600-065X.2011.01074.x

Wilkie, G. S., Kerr, K., Stewart, J. P., Studdert, M. J., and Davison, A. J. (2015). Genome sequences of equid herpesviruses 2 and 5. *Genome Announc.* 3:e00119-15. doi: 10.1128/genomeA.00119-15

Williams, K. J., Robinson, N. E., Lim, A., Brandenberger, C., Maes, R., Behan, A., et al. (2013). Experimental induction of pulmonary fibrosis in horses with the gammaherpesvirus equine herpesvirus 5. *PLoS One* 8:e77754. doi: 10.1371/journal.pone.0077754

Wong, L. Y., and Wilson, A. C. (2005). Kaposi's sarcoma-associated herpesvirus latency-associated nuclear antigen induces a strong bend on binding to terminal repeat DNA. *J. Virol.* 79, 13829–13836. doi: 10.1128/JVI.79.21.13829-13836.2005

Woodberry, T., Suscovich, T. J., Henry, L. M., Martin, J. N., Dollard, S., O'Connor, P. G., et al. (2005). Impact of Kaposi sarcoma-associated herpesvirus (KSHV) burden and HIV coinfection on the detection of T cell responses to KSHV ORF73 and ORF65 proteins. *J. Infect. Dis.* 192, 622–629. doi: 10.1086/432103

Wu, H., Ceccarelli, D. F., and Frappier, L. (2000). The DNA segregation mechanism of Epstein-Barr virus nuclear antigen 1. *EMBO Rep.* 1, 140–144. doi: 10.1038/sj.embor.embor611

Wysokenski, D. A., and Yates, J. L. (1989). Multiple EBNA1-binding sites are required to form an EBNA1-dependent enhancer and to activate a minimal replicative origin within oriP of Epstein-Barr virus. *J. Virol.* 63, 2657–2666.

Yates, J., Warren, N., Reisman, D., and Sugden, B. (1984). A cis-acting element from the Epstein-Barr viral genome that permits stable replication of recombinant plasmids in latently infected cells. *Proc. Natl. Acad. Sci. U.S.A.* 81, 3806–3810. doi: 10.1073/pnas.81.12.3806

Yates, J. L., Camiolo, S. M., and Bashaw, J. M. (2000). The minimal replicator of Epstein-Barr virus oriP. *J. Virol.* 74, 4512–4522. doi: 10.1128/JVI.74.10.4512-4522.2000

Yates, J. L., Warren, N., and Sugden, B. (1985). Stable replication of plasmids derived from Epstein-Barr virus in various mammalian cells. *Nature* 313, 812–815. doi: 10.1038/313812a0

Yewdell, J. W. (2011). DRiPs solidify: progress in understanding endogenous MHC class I antigen processing. *Trends Immunol.* 32, 548–558. doi: 10.1016/j.it.2011.08.001

Yewdell, J. W., Anton, L. C., and Bennink, J. R. (1996). Defective ribosomal products (DRiPs): a major source of antigenic peptides for MHC class I molecules? *J. Immunol.* 157, 1823–1826.

Yin, Y., Manoury, B., and Fahraeus, R. (2003). Self-inhibition of synthesis and antigen presentation by Epstein-Barr virus-encoded EBNA1. *Science* 301, 1371–1374. doi: 10.1126/science.1088902

Yoshioka, M., Crum, M. M., and Sample, J. T. (2008). Autorepression of Epstein-Barr virus nuclear antigen 1 expression by inhibition of pre-mRNA processing. *J. Virol.* 82, 1679–1687. doi: 10.1128/jvi.02142-07

You, J., Srinivasan, V., Denis, G. V., Harrington, W. J. Jr., Ballestas, M. E., Kaye, K. M., et al. (2006). Kaposi's sarcoma-associated herpesvirus latency-associated nuclear antigen interacts with bromodomain protein Brd4 on host mitotic chromosomes. *J. Virol.* 80, 8909–8919. doi: 10.1128/JVI.00502-06

Zaldumbide, A., Ossevoort, M., Wiertz, E. J., and Hoeben, R. C. (2007). In cis inhibition of antigen processing by the latency-associated nuclear antigen I of Kaposi sarcoma herpes virus. *Mol. Immunol.* 44, 1352–1360. doi: 10.1016/j.molimm.2006.05.012

Zuo, L., Yue, W., Du, S., Xin, S., Zhang, J., Liu, L., et al. (2017). An update: Epstein-Barr virus and immune evasion via microRNA regulation. *Virol. Sin.* 32, 175–187. doi: 10.1007/s12250-017-3996-5

Conflict of Interest Statement: The authors declare that the research was conducted in the absence of any commercial or financial relationships that could be construed as a potential conflict of interest.

frontiers in Microbiology

REVIEW
published: 07 February 2019
doi: 10.3389/fmicb.2019.00016

Herpes Virus Reactivation in Astronauts During Spaceflight and Its Application on Earth

*Bridgette V. Rooney[1], Brian E. Crucian[2], Duane L. Pierson[2], Mark L. Laudenslager[3] and Satish K. Mehta[4]**

[1] GeoControl Systems, Inc., Houston, TX, United States, [2] NASA Johnson Space Center, Houston, TX, United States, [3] Anschutz Medical Campus, University of Colorado Denver, Aurora, CO, United States, [4] Jes Tech, KBR Wyle Laboratories Houston, Houston, TX, United States

Latent herpes virus reactivation has been demonstrated in astronauts during shuttle (10–16 days) and International Space Station (≥180 days) flights. Following reactivation, viruses are shed in the body fluids of astronauts. Typically, shedding of viral DNA is asymptomatic in astronauts regardless of mission duration; however, in some cases, live/infectious virus was recovered by tissue culture that was associated with atopic-dermatitis or skin lesions during and after spaceflight. Hypothalamic-pituitary-adrenal (HPA) and sympathetic-adrenal-medullary (SAM) axes activation during spaceflight occurs as indicated by increased levels of stress hormones including cortisol, dehydroepiandrosterone, epinephrine, and norepinephrine. These changes, along with a decreased cell mediated immunity, contribute to the reactivation of latent herpes viruses in astronauts. Currently, 47/89 (53%) astronauts from shuttle-flights and 14/23 (61%) astronauts from ISS missions shed one or more herpes viruses in saliva/urine samples. Astronauts shed Epstein–Barr virus (EBV), varicella-zoster virus (VZV), and herpes-simplex-1 (HSV-1) in saliva and cytomegalovirus (CMV) in urine. Larger quantities and increased frequencies for these viruses were found during spaceflight as compared to before or after flight samples and their matched healthy controls. The shedding did not abate during the longer ISS missions, but rather increased in frequency and amplitude. These findings coincided with the immune system dysregulation observed in astronauts from shuttle and ISS missions. VZV shedding increased from 41% in space shuttle to 65% in ISS missions, EBV increased 82 to 96%, and CMV increased 47 to 61%. In addition, VZV/CMV shed ≤30 days after ISS in contrast to shuttle where VZV/CMV shed up to 5 and 3 days after flight respectively. Continued shedding of infectious-virus post-flight may pose a potential risk for crew who may encounter newborn infants, sero-negative adults or any immunocompromised individuals on Earth. Therefore, developing spaceflight countermeasures to prevent viral reactivation is essential. Our spaceflight-developed technologies for saliva collection/rapid viral detection have been extended to include clinical applications including zoster patients, chicken pox, post-herpetic neuralgia, multiple sclerosis, and various neurological disorders. These protocols are employed in various clinics and hospitals including the CDC and Columbia University in New York, as well as overseas in Switzerland and Israel.

Keywords: herpes, latency, viral reactivation, spaceflight, immunity

OPEN ACCESS

Edited by:
Randall J. Cohrs, University of Colorado, United States

Reviewed by:
Peter Graham Edward Kennedy, University of Glasgow, United Kingdom
Nancy M. Sawtell, Cincinnati Children's Hospital Medical Center, United States

***Correspondence:**
Satish K. Mehta
satish.k.mehta@nasa.gov

Specialty section:
This article was submitted to Virology, a section of the journal Frontiers in Microbiology

Received: *26 October 2018*
Accepted: *09 January 2019*
Published: *07 February 2019*

Citation:
Rooney BV, Crucian BE, Pierson DL, Laudenslager ML and Mehta SK (2019) Herpes Virus Reactivation in Astronauts During Spaceflight and Its Application on Earth. Front. Microbiol. 10:16. doi: 10.3389/fmicb.2019.00016

INTRODUCTION

Herpes Virus

Herpes viruses have co-evolved with humans for millennia and subsequently employ sophisticated strategies to evade the host immune response. Consequently, after primary infection, they persist lifelong in a latent or dormant phase, and are generally asymptomatic in immunocompetent individuals. However, they may reactivate during periods of increased stress, isolation, and during times of immune challenge. Eight major herpes viruses parasitize humans with worldwide infection rates of 70–95%. Four of the eight are shed in the body fluids of NASA astronauts during both short and long duration spaceflight. Though viral load (virus detected in the body fluids) can be high, these astronauts often have no clinical symptoms associated with reactivation (Mehta et al., 2004). Post-reactivation, replication of the virus may also be enhanced which could account for the significant increase in viral shedding during spaceflight. Yet, there have been a few cases where the reactivation culminated in commensurate atopic dermatitis and/or viral lesions (Crucian B. E. et al., 2016).

Astronaut Stress/Exposures

Exposure of astronauts, during both short and long duration spaceflight, to non-terrestrial hazards such as variable gravitational forces including acceleration/deceleration, cosmic radiation, and microgravity result in a unique set of stressors that contribute to the dysregulation of the immune and endocrine systems (Crucian and Sams, 2009; Crucian et al., 2013). In addition, they also endure some common stressors including but not limited to social separation, confinement, sleep deprivation, circadian rhythm disruption, and anxiety. There is increasing evidence to suggest that these spaceflight-associated stressors chronically amplify the release of stress hormones, which negatively affects the immune system, especially the adaptive immune system facilitating latent herpes virus reactivation during and after spaceflight. Increased levels of salivary, plasma and urinary stress hormones such as cortisol and catecholamines commonly accompany spaceflight (Stowe et al., 2001a).

Altered Immunity

Maintenance of viral latency requires a vigorous and vigilant immune system, highly dependent upon competent cytotoxic T-cells, and any changes in immune status tend to promote viral reactivation. This is evident in both terrestrial space-analog studies (Crucian B. et al., 2014) and spaceflight studies (Stowe et al., 2001b, 2011; Mehta et al., 2014, 2017). The alterations in immune status for terrestrial analog studies are minor and coincide with mild viral reactivation. Spaceflight studies illustrate major immune dysregulation and functional changes in conjunction with significant viral reactivation, regardless of mission duration. In fact, substantial changes in cell-mediated immunity exist in most astronauts that reactivated one or more herpes viruses (Mehta et al., 2014; Crucian et al., 2015). This was also highlighted by Glaser et al. (1993), who previously showed an association of EBV reactivation and diminished cell-mediated immunity.

The hypothalamus-pituitary-adrenal (HPA) axis along with the sympathetic-adrenal-medullary (SAM) axis partially mediate the stress response where glucocorticoids and catecholamines are secreted in proportionate concentrations relative to the stress stimulus (**Figure 1**) (Padgett and Glaser, 2003; Webster and Glaser, 2008; Goldstein, 2010). Though acute responses to stress can be positive, long duration or chronically high levels of stress hormones can negatively affect the regulation of the immune system and its individual components (Crucian B. E. et al., 2014). Changes in a variety of immune cells, both in form (phenotype) and function (killing capacity), result in decreased cell-mediated immunity, which facilitates opportunistic reactivation of latent viruses (Crucian et al., 2015; Bigley et al., 2017).

Stress Hormones/Cytokines

Cortisol and dehydroepiandrosterone (DHEA) are glucocorticoid steroid hormones released by the adrenal glands in response to stress. Cortisol is anti-inflammatory and immunosuppressive, but DHEA is an important antagonist to cortisol. For that reason, the molar ratio of cortisol to DHEA [C]/[D] is an important indicator of immune regulation. In recent flight studies, the regular diurnal release of these hormones was tracked in saliva samples to evaluate any changes/trends occurring through the various phases of flight; launch/pre-flight, flight, and return (Mehta et al., 2014). Salivary cortisol was present in significantly higher concentrations in samples taken before and during flight. Salivary DHEA followed its normal daily decline kinetics in the samples taken before, during and after flight, but has been found to have significantly lower waking concentrations during the flight phase in comparison to samples taken before and after flight. Altogether, diurnal patterns of salivary cortisol were significantly higher during flight while DHEA was significantly lower. The cortisol area under the curve relative to ground (AUCg) did not change significantly during flight relative to baseline whereas DHEA AUCg significantly declined during flight relative to baseline. Ultimately, this results in an increased [C]/[D] molar ratio during spaceflight (**Figure 2**) which potentially indicates immune challenge, and has been linked to immune modulation (Christeff et al., 1997), including the increased inflammatory cytokine response and the TH2 shift observed in earlier spaceflight studies (Mehta et al., 2013a; Crucian B. E. et al., 2014).

Cytokines are small cell-signaling proteins that play a crucial role in the modulation of the human immune response. They can facilitate both pro- and anti-inflammatory immune states and are generally analyzed in the categories of inflammatory cytokines (IL-1α, IL-1β, TNFα, IL-6, IL-8), lymphoid growth factors (IL-2, IL-7, IL-15), Th1/17 cytokines (IFNγ, IL-12, IL-17), Th2 cytokines (IL-4, IL-5, IL-10, IL-13), myeloid growth factors (G-CSF, GM-CSF), and chemokines (eotaxin, MCP-1, M1P1α, IP-10). Recent flight studies (Mehta et al., 2013a; Crucian B. E. et al., 2014; Crucian et al., 2015) have shown that astronauts displayed significant increases in the pro-inflammatory plasma cytokines IL-1α, IL-6, IL-8, IFNγ, IL-4, eotaxin, and IP-10 in samples taken 10 days before launch (L-10), in comparison to their baseline samples taken 180 days before launch (L-180). The increase of IL-6, IL-8, IL-4, eotaxin, and IP-10 is also evident

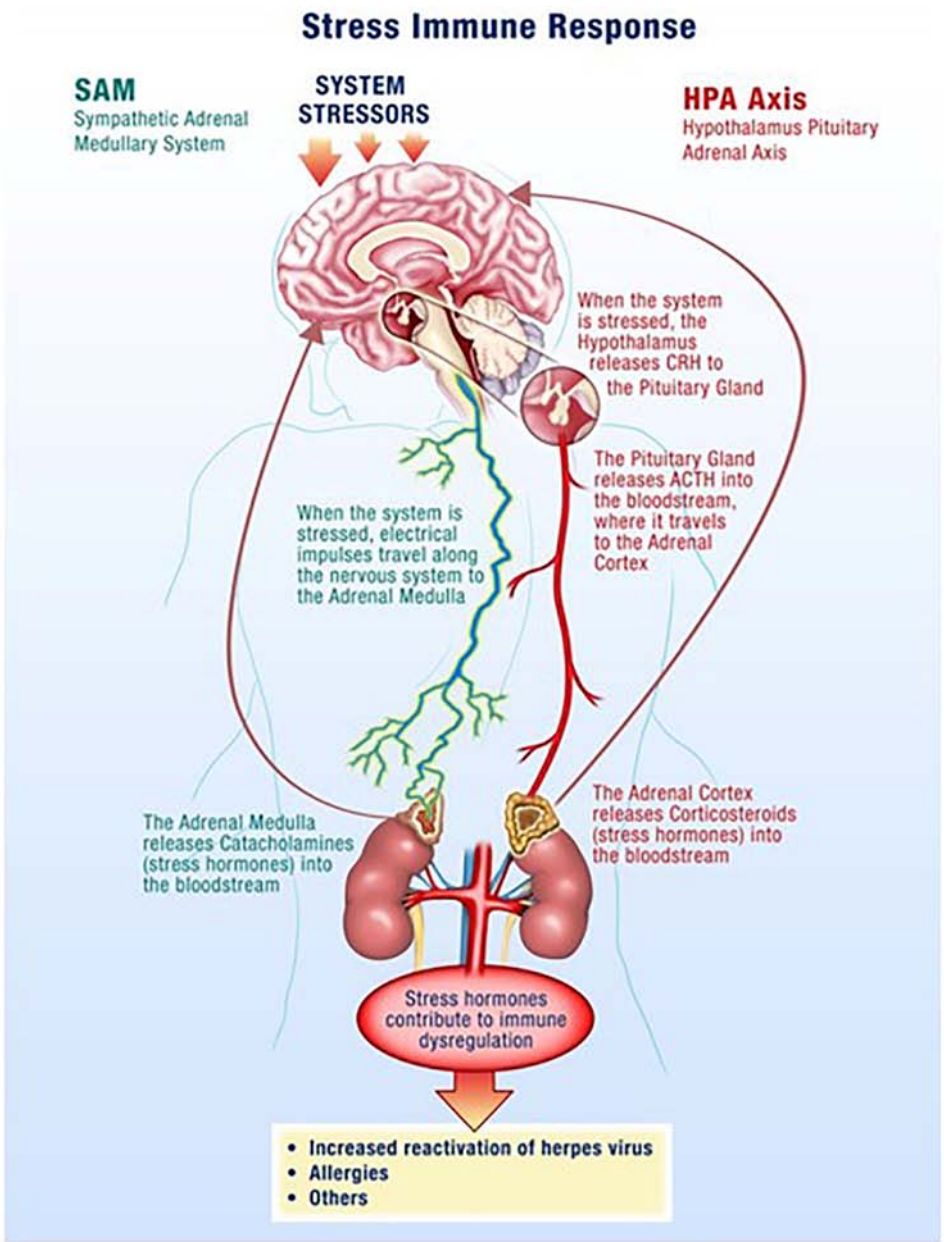

FIGURE 1 | Spaceflight is a stressful environment with various stressors acting through the hypothalamus-pituitary-adrenal (HPA)-axis and the sympathetic-adrenal-medullary (SAM)-axis. Increases in stress hormones, such as cortisol from the adrenal glands, result in reductions in cellular immunity which facilitates opportunistic viral reactivation.

immediately upon return to Earth at landing, designated as R+0. The Th2 cytokine IL-4 was the most sensitive/responsive to the phases of flight with 35- and 21-fold increases from baseline values at L-10 and R+0, respectively.

When analyzing plasma cytokine levels in the context of virus shedding, there seems to be a connection between astronauts who shed virus and significantly elevated levels of cytokines (IL-1α, IL-6, IL-8, IFNγ, IL-12p70, IL-4, IL-10, IL-13, eotaxin, and IP-10) (Mehta et al., 2013a). Lymphoid and myeloid growth factors are also elevated in virus shedding astronauts, by about twofold. As mentioned earlier, the Th2 cytokine IL-4 shows the largest fold increases through launch and return flight phases, and this is evident again when restricting the analysis to only viral-shedding astronauts at the return time point R+0. For these astronauts, the single largest plasma cytokine increases were IL-4 (21-fold increase) and IL- 6 (33-fold increase). This indicates a dynamic shift from a Th1 antiviral immune state to a Th2 antibacterial/antifungal immune state. Further emphasizing the Th1-Th2 shift is an analysis of the ratio of IFNγ: IL-4. The results from some of the most recent flight studies suggest

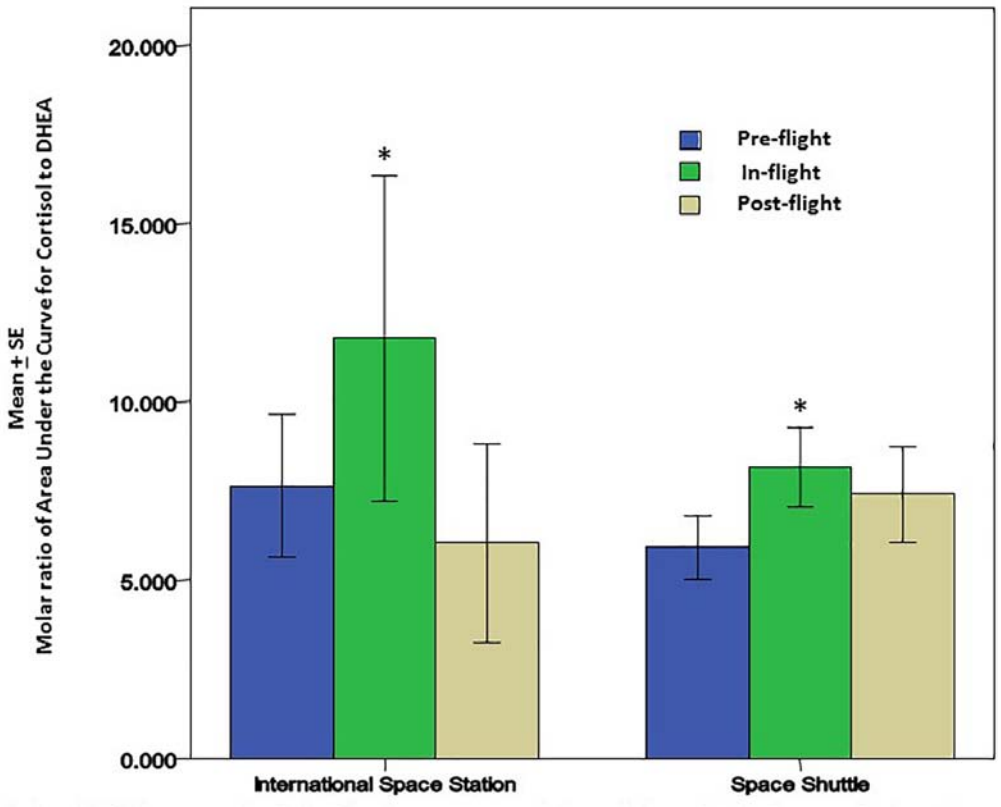

FIGURE 2 | Cortisol and DHEA were analyzed in saliva from astronauts before, during and after the space flights using a commercially available ELISA assays (Salimetrics, LLC, State College, PA, United States). There was a significant increase in the molar ratio of cortisol to DHEA during the flight phase for both Space Shuttle (N = 17) or ISS (N = 10). The increase in this ratio may be associated with lower cellular immunity and innate immunity; potentially contributing to greater inflammatory cytokines that may affect bone remodeling and bone growth. * Indicates significance when comparing flight against pre-flight and post-flight. $p < 0.01$.

a significant decrease in the IFNγ: IL-4 ratio for shedders compared to astronauts who did not shed any viruses during their duty rotation (Mehta et al., 2013a; Crucian B. E. et al., 2014).

Viral Specific T-Cell and NK-Cell Function

Alterations in the aforementioned cytokines play a critical role in the fate of many important leukocyte populations. The cytokine profile changes, acting either independently or in conjunction with microgravity, generate a variety of immune vulnerabilities by significantly changing the numbers, proportions, and functions of leukocytes. Monocyte (Kaur et al., 2005), granulocyte (Stowe et al., 1999), and lymphocyte functions (Crucian et al., 2015; Bigley et al., 2017) are diminished, critically reducing the effectiveness of the immune response to pathogens, as well as its capacity to prevent viral reactivation. T-Cells and NK-Cells in particular, which function to attack and destroy viruses/virally infected cells, are substantially debilitated during spaceflight. Flight studies focusing on T-Cell function have elucidated that both CD4+ and CD8+ T-Cells taken from astronauts during the flight phase respond ineffectively against a variety of stimuli. Under normal circumstances, these same stimuli would have elicited a more profound response by the T-Cells. The weakened response can last the duration of the flight phase (Crucian et al., 2015). Additional flight studies focusing on the function of NK-Cells have shown decrements in cytotoxicity due to decreased production of the enzymes perforin and granzyme B (Bigley et al., 2017). Without these enzymes, NK-Cells are rendered ineffective against the target cell/pathogen and this impairment may last up to 60 days post-flight. In both cases, reductions in T-Cell and NK-Cell function lead to the inability of the immune system to suppress/sequester/eliminate opportunistic viral reactivation.

Viral Latency

As stated earlier, herpes viruses share a long-term co-evolutionary history with humankind. This promotes a relatively benign life-long persistence of the virus within the host. In healthy individuals with robust immune surveillance, viral activity can occur in the absence of clinical symptoms (Grinde, 2013). Injury to the host is antithetical to viral survival. Viral persistence in the host is aided by viral strategies for latency. Latency is a well-orchestrated series of concomitant events that allow for viral genome maintenance, while actively repressing lytic (replicative) gene expression and promoting latent

gene expression. A hallmark of viral latency is that infectious viral progeny are not produced, so the surrounding cells remain uninfected or naïve. Viral latency is the culmination of a handful of factors; infection of cell types permissive to latency, viral promotion of infected cell survival, and the general evasion of the host immune response. Cellular tropism is dictated by cell surface receptor expression, as well as intracellular conditions permissive to viral activity, and is very specific to the individual herpes viruses. HSV and VZV infect neurons in ganglia, while EBV and CMV preferentially infect the cells of the immune system, B cells and myeloid progenitor cells, respectively. Other cell types can be infected by the viruses, but the aforementioned cell types serve as the greater viral latent reservoirs. The promotion of infected cell survival is the product of viral manipulation of host cell machinery. For example, the manipulation of Bcl-2 family proteins promotes survival of CMV infected monocytes (Collins-McMillen et al., 2015). Not only can herpes viruses manipulate the cells they infect, but they can also affect the host immune response. Interestingly, latent viruses are still very genetically active even in the absence of replication. There is emerging evidence of significant miRNA activity during latency that can act to override lytic transcription, as well as to alter the cell secretome. Though the role of miRNA are yet to be fully teased out, they seem to facilitate the transcription of proteins that mimic host cytokines and chemokines which ultimately inhibit host anti-viral activity. For the many nuances of viral latency, specific to each virus, the reader is directed to the following review articles (Eshleman et al., 2011; Nicoll et al., 2012; Kempkes and Robertson, 2015; Wills et al., 2015).

Viral Reactivation

Reactivation and shedding of latent herpes viruses has been reported in astronauts during space shuttle, Russian Soyuz and International Space Station missions (Pierson et al., 2005, 2007; Mehta and Pierson, 2007; Mehta et al., 2014, 2017). Virus reactivation has also been observed in ground-based models of spaceflight including Antarctica, undersea habitat, artificial gravity and bed rest studies, though not to the extent seen during spaceflight studies. So far, 47 out of 89 (53%) astronauts from short duration space shuttle flights, and 14 out of 23 (61%) from long duration ISS spaceflight missions shed at least one or more herpes viruses in their saliva or urine samples. Significant reactivations of EBV, CMV, and VZV occurred during flight phase and the magnitude and frequency of viral shedding during spaceflight directly correlates with duration of spaceflight. VZV shedding increased from 41% in space shuttle to 65% in ISS missions, EBV increased from 82 to 96%, and CMV increased from 47 to 61%. In addition, VZV and CMV shed up to a month post-long duration flight. Percent distribution of these viruses during shuttle and ISS missions is depicted in **Figure 3**. These viruses often reactivate in concert with one another, but they may also reactivate independently of the other viruses. Reactivation of latent viruses during long-duration spaceflight could increase risk for adverse medical events during exploration-class deep-space missions (Crucian and Sams, 2009). Taken altogether, and to our knowledge, there have been six incidences of astronauts with complaints of symptoms related to herpes viral reactivation (Crucian B. et al., 2016). VZV is an important health risk to crewmembers (several have experienced shingles during flight). Furthermore, CMV can be immuno-suppressive and may play

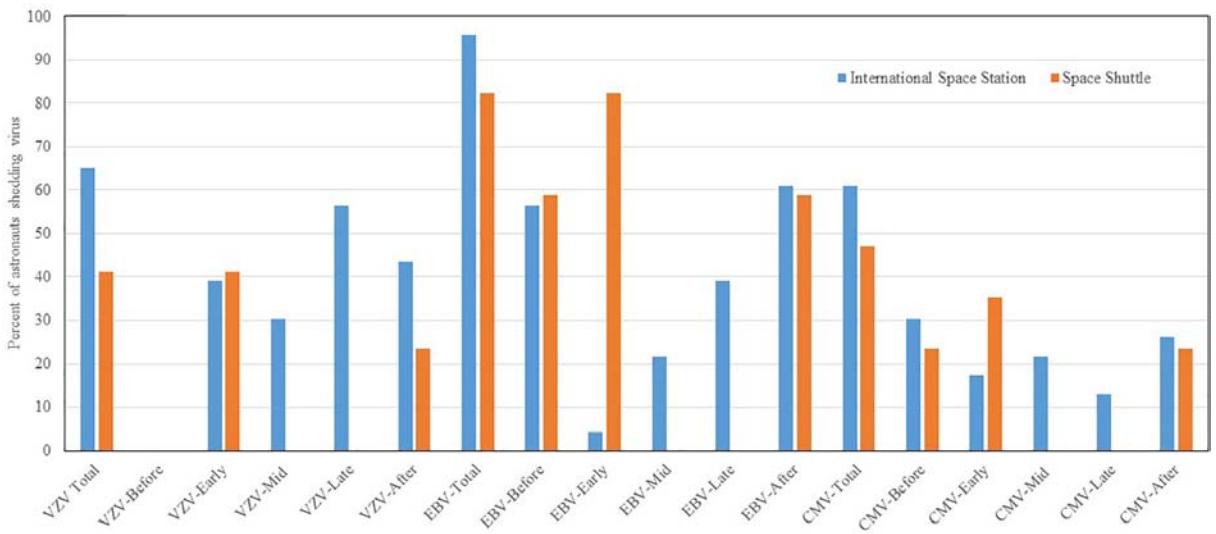

FIGURE 3 | Percent distribution of astronauts shedding VZV. EBV and CMV before, during the mission at time point early-mission, mid-mission, late-mission, and after either short and long duration space flights. Saliva and urine samples were collected from 112 astronauts (89 short duration and 23 long duration) before, during, and after the spaceflight. Saliva was analyzed for Epstein–Barr virus (EBV) and varicella-zoster virus (VZV), and urine was analyzed for Cytomegalovirus CMV by real time PCR assay using Taqman 7900 (Thermofisher, Inc.). The shedding of EBV. VZV and CMV DNA in body fluids is significantly higher during spaceflight as compared to pre-flight, post-flight, and the control $p < 0.01$ (Mehta et al., 2014, 2017). However, when comparing these shedding patterns between space shuttle and ISS missions, the differences were not significant.

a role in the well-documented immune dysfunction observed in crewmembers.

Epstein–Barr Virus

Epstein–Barr virus (EBV) is responsible for infectious mononucleosis and is associated with several malignancies (Niedobitek et al., 2001; Thompson and Kurzrock, 2004; Bravender, 2010). It is a highly infectious DNA virus transmitted by aerosolized micro-droplets and by direct contact with saliva. It has a 95% infection rate among adults worldwide, which makes it an ideal target for investigation among a limited and unique astronaut population. EBV preferentially infects B-lymphocytes and these cells serve as a latent virus reservoir. Early flight studies from the shuttle missions were the first to demonstrate that EBV DNA was shed in astronaut saliva samples taken before, during, and after space flight (Stowe et al., 2001b; Pierson et al., 2005; Mehta et al., 2014). These studies highlighted a 10-fold increase in viral load during the flight phase in comparison to samples taken before or after flight. Additionally, EBV copies shed during space flight seemed to increase as a function of time in space, and as a result of diminished cell immunity (Mehta et al., 2000a). These early findings have been repeatedly corroborated in longer duration ISS missions (Stowe et al., 2011; Mehta et al., 2017). Altogether, flight studies have illustrated that approximately 90% of astronauts, regardless of mission duration, shed EBV during spaceflight.

Varicella Zoster Virus

Varicella Zoster virus (VZV) is highly communicable and responsible for both chicken pox (primary infection) and shingles (secondary infection). The virus is transmitted via saliva and can be aerosolized by sneezing and coughing. After primary infection, VZV becomes latent in various nerve ganglia (Reichelt et al., 2008) (cranial, dorsal root, autonomic) along the entire length of the neuroaxis, and reactivation often results in characteristic skin lesions that range from aggravating to painful. Though reactivation of VZV is evident from flight studies where viral DNA was found in saliva of astronauts from both shuttle and ISS missions, astronauts do not often develop symptoms or rash (Mehta et al., 2004; Cohrs et al., 2008). Additionally, we have found that saliva samples taken 2–6 days following landing were infectious by culturing that saliva with human fetal lung (HFL) cells. Infectious VZV was present and confirmed by visual inspection of the culture where viral plaques were obvious, as well as by antibody staining and real-time PCR DNA analysis. This poses a risk to the welfare of both astronauts and their seronegative contacts back on Earth, as VZV viral load also increases with time in space and is present in saliva of about 60% of astronauts from combined shuttle and ISS missions.

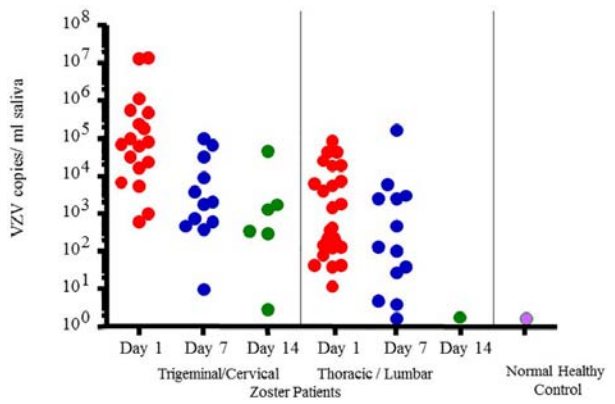

FIGURE 4 | Varicella-zoster virus (VZV) copy number per mL of saliva in Fifty-four zoster patients treated with valacyclovir and 14 healthy subjects. On treatment days 1, 7-, and 14 later, pain was scored (data not given here) and saliva examined for VZV-DNA by real time PCR. Patients were divided into two groups based upon the infected dermatome, Trigeminal Cervical and Thoracic/Lumbar. VZV-DNA was found in every patient the day treatment was started and disappeared in 82% with the treatment. Analysis of human saliva has potential usefulness in diagnosing neurological disease produced by VZV without rash. When comparing patient shedding against normal healthy controls, it was significantly higher, $p < 0.01$ (Mehta et al., 2008).

Herpes Simplex Virus-1

Herpes Simplex virus-1 is highly prevalent and communicable and persists as a latent virus lifelong. Generally referred to as oral herpes, reactivation can be either asymptomatic or lead to lesions/rash anywhere on the body. Incidences of HSV-1 reactivation are very low with only 8% of astronaut saliva samples test positive for viral DNA, though recently, an astronaut suffering persistent dermatitis during a long duration spaceflight, >180 day, was positive for HSV-1 viral DNA in saliva and lesion samples. The saliva containing virus was infectious, as evidenced by a culture of the saliva atop HFL cells, where visual disruption of HFL cells was apparent at 3 days post-infection with saliva, with viral load verified/quantified by real-time PCR.

Cytomegalovirus

Cytomegalovirus is the only beta-herpes virus known to reactivate in astronauts. It is typically acquired asymptomatically during childhood and has a worldwide prevalence of 75–90%. Though it remains asymptomatic in immunocompetent people, it may reactivate in individuals whose immune systems are either immature or immunocompromised causing multiple diseases such as encephalitis, gastroenteritis, pneumonia, and chorioretinitis (Seitz, 2010). Moreover, several studies have suggested that CMV infection is immunosuppressive because it directly infects leukocytes as well as hematopoietic cells (Varani and Landini, 2011; O'Connor and Murphy, 2012; Stevenson et al., 2014). Additionally, CMV has been uniquely linked to early immune senescence (Pawelec, 2014; Sansoni et al., 2014). However, a study was able to illustrate a benefit of CMV infection specifically to young adults (20–30 years old) regarding increased antibody response to the influenza vaccine (Furman et al., 2015). Spaceflight studies have shown that 27% of the astronauts from short-term space missions shed CMV DNA in either pre- or post-flight urine samples, and that anti-CMV IgG antibody titers increased significantly for all shedders from each time point compared to their baseline values (Mehta et al., 2000b). In long duration spaceflight, 61% of astronauts shed CMV

DNA in their urine during and after spaceflight in stark contrast to the absence of CMV DNA in urine samples taken 180 days before flight. These findings demonstrate that CMV reactivation occurs in astronauts regardless of mission duration, and this may pose additional threats to the health of crewmembers during longer-duration missions (Mehta et al., 2014, 2017).

Rapid Detection of Virus for Application in Patient Populations

The most obvious signs of VZV reactivation are the vesicular rash and the pain associated with zoster, however even in the absence of rash, the virus is active and can spread to the retina causing blindness, to the spinal cord causing paralysis and incontinence, and to cerebral arteries resulting in stroke (Kleinschmidt-DeMasters and Gilden, 2001; Orme et al., 2007). Associating VZV with a disease asymptomatically can be challenging. For example, when stroke occurs in the elderly, especially many months following zoster, the association with VZV reactivation requires cerebral spinal fluid (CSF) analysis for VZV antibodies (Nagel et al., 2007). Likewise, detection of asymptomatic VZV reactivation, which often is only seen as an increase in antibody titer against VZV (but may also result in virus transmission), is difficult to detect. In such instances, virological verification of VZV disease has relied on the detection of VZV DNA or anti-VZV IgG antibodies in CSF or, less often, the presence of VZV DNA in blood mononuclear cells or anti-VZV IgM antibodies in serum.

However, VZV DNA has been detected in the saliva samples from patients with acute zoster (Mehta et al., 2008), zoster sine herpete (Hato et al., 2000), chickenpox (Mehta et al., 2013b) and post-herpetic neuralgia (PHN) (Nagel et al., 2011) even before the rash appears, which now makes diagnosis less invasive and less time consuming. In fact, a rapid and sensitive virus detection method has been developed and used to detect virus in saliva samples taken from asymptomatic patients with neurologic and other VZV related disease (Mehta et al., 2013b). **Figure 4** illustrates VZV copy numbers in saliva from shingles patients before anti-viral treatment. For this method, the saliva is collected by passive drool or by way of a synthetic swab and then processed for DNA within an hour from sample collection. The results from a few studies using this technique have shown that VZV DNA is present in 100% of patients tested before antiviral treatment and is exclusively in the cell pelleted fraction of saliva. These studies further showed that VZV, isolated from zoster patient saliva, was primarily associated with the epithelial cell membrane but could also be inside the cell. Epithelial cells with VZV continued to be present in the saliva of a single zoster patient up to 10 months after recovery. These kinds of studies are ongoing and our spaceflight-developed technology for rapid viral detection continues to be used locally and around the world for patients with zoster (Mehta et al., 2013b), chicken pox (Mehta et al., 2008), PHN (Nagel et al., 2011), multiple sclerosis (Ricklin et al., 2013), and various other neurological disorders (Gilden et al., 2010; Pollak et al., 2015).

CONCLUSION

Reactivation of latent viruses is a powerful biomarker of immune status for astronauts deployed to space. There are multiple factors that influence reactivation including increases in glucocorticoid/catecholamine secretion, cytokine profile shifts, and decreased function in the major leukocyte and lymphocyte subsets designed to suppress and eliminate viruses/virally infected cells. Viral reactivation is evident through the shedding of viral DNA in the body fluids of astronauts, and the viral load only increases with more time in space. Additionally, more than one virus generally reactivates at a time, potentially compounding the physiological ramifications of uncontrolled viral reactivation to not only rashes, but also severe target organ failures, and permanent vision and hearing loss. The occupational hazards for astronauts are profound, but research into the causes and mechanics of viral reactivation not only benefit the astronaut but also the general patient population. As our understanding of viral reactivation widens, we are better able to develop and implement effective countermeasures for our astronaut professionals, as well as targeted treatment regimens for immunocompromised individuals suffering the consequences of viral reactivation. As a result, this research has tremendous clinical relevance.

Ultimately, the information gleaned from these space studies will shape the way we prepare for and design exploration-class missions, beyond the moon and mars, where reactivation of latent viruses could result in increased risk for wide-ranging adverse medical events. Partial-gravity environments, e.g., on Mars, might be sufficient to curtail serious viral reactivation, but this needs to be addressed in future research. In the interim, because astronaut saliva contains increasingly significant viral DNA, during and after spaceflight that can be infectious, we recommend prophylactics (vaccines), where available, to the astronauts before they go into space.

AUTHOR CONTRIBUTIONS

SM designed and executed the study, collected and processed the samples from astronauts, analyzed the data, and wrote the manuscript. DP designed the study and wrote the manuscript. BC executed the study and wrote the manuscript. BR wrote the manuscript. ML contributed to the measurement of salivary cortisol and DHEA processing and manuscript preparation.

FUNDING

This work was supported by NASA (Grant Nos. 111-30-10-03 and 111-30-10-06) to DP.

ACKNOWLEDGMENTS

We gratefully acknowledge the conscientious participation of the astronauts in the study.

REFERENCES

Bigley, A. B., Agha, N., Baker, F. L., Rezvani, K., Crucian, B. E., and Simpson, R. J. (2017). "Dysregulated NK-cell function during long-duration spaceflight," in *Proceedings of the 13th ISEI Symposium*, Coimbra.

Bravender, T. (2010). Epstein-Barr virus, cytomegalovirus, and infectious mononucleosis. *Adolesc. Med. State Art Rev.* 21, 251–264.

Christeff, N., Gherbi, N., Mammes, O., Dalle, M. T., Gharakhanian, S., Lortholary, O., et al. (1997). Serum cortisol and DHEA concentrations during HIV Infection. *Psychoneuroendocrinology* 22(Suppl. 1), S11–S18. doi: 10.1016/S0306-4530(97)00015-2

Cohrs, R. J., Mehta, S. K., Schmid, D. S., Gilden, D. H., and Pierson, D. L. (2008). Asymptomatic reactivation and shed of infectious varicella zoster virus in astronauts. *J. Med. Virol.* 80, 1116–1122. doi: 10.1002/jmv.21173

Collins-McMillen, D., Kim, J. H., Nogalski, M. T., Stevenson, E. V., Chan, G. C., Caskey, J., et al. (2015). HCMV promotes survival of infected monocytes via a distinct temporal regulation of cellular Bcl-2 family proteins. *J. Virol.* 90, 2356–2371. doi: 10.1128/JVI.01994-15

Crucian, B., Babiak-Vazquez, A., Johnston, S., Pierson, D. L., Ott, C. M., Sams, C., et al. (2016). Incidence of clinical symptoms during long-duration orbital spaceflight. *Int. J. Gen. Med.* 9, 383–391. doi: 10.2147/IJGM.S114188

Crucian, B., and Sams, C. (2009). Immune system dysregulation during spaceflight: clinical risk for exploration-class missions. *J. Leukoc. Biol.* 86, 1017–1018. doi: 10.1189/jlb.0709500

Crucian, B., Simpson, R. J., Mehta, S., Stowe, R., Chouker, A., Hwang, S. A., et al. (2014). Terrestrial stress analogs for spaceflight associated immune system dysregulation. *Brain Behav. Immun.* 39, 23–32. doi: 10.1016/j.bbi.2014.01.011

Crucian, B., Stowe, R., Mehta, S., Uchakin, P., Quiriarte, H., Pierson, D., et al. (2013). Immune system dysregulation occurs during short duration spaceflight on board the space shuttle. *J. Clin. Immunol.* 33, 456–465. doi: 10.1007/s10875-012-9824-7

Crucian, B., Stowe, R. P., Mehta, S., Quiriarte, H., Pierson, D., and Sams, C. (2015). Alterations in adaptive immunity persist during long-duration spaceflight. *NPJ Microgravity* 1:15013. doi: 10.1038/npjmgrav.2015.13

Crucian, B. E., Johnston, S., Mehta, S. K., Stowe, R., Uchakin, P., Quiriarte, H., et al. (2016). A case of persistent skin rash and rhinitis with immune system dysregulation onboard the international space station. *J. Allergy Clin. Immunol. Pract.* 4, 759–762.e8. doi: 10.1016/j.jaip.2015.12.021

Crucian, B. E., Zwart, S. R., Mehta, S. K., Uchakin, P., Quiriarte, H. D., Pierson, D. L., et al. (2014). Plasma cytokine concentrations indicate that in vivo hormonal regulation of immunity is altered during long-duration spaceflight. *J. Interferon Cytokine Res.* 34, 778–786. doi: 10.1089/jir.2013.0129

Eshleman, E., Shahzad, A., and Cohrs, R. J. (2011). Varicella zoster virus latency. *Future Virol.* 6, 341–355. doi: 10.2217/fvl.10.90

Furman, D., Jojic, V., Sharma, S., Shen-Orr, S. S., Angel, C. J. L., Onengut-Gumuscu, S., et al. (2015). Cytomegalovirus infection enhances the immune response to influenza. *Sci. Transl. Med.* 7:281ra43. doi: 10.1126/scitranslmed.aaa2293

Gilden, D., Cohrs, R. J., Mahalingam, R., and Nagel, M. A. (2010). Neurological disease produced by varicella zoster virus reactivation without rash. *Curr. Top. Microbiol. Immunol.* 342, 243–253. doi: 10.1007/82-2009-3

Glaser, R., Pearson, G. R., Bonneau, R. H., Esterling, B. A., Atkinson, C., and Kiecolt-Glaser, J. K. (1993). Stress and the memory T-cell response to the Epstein-Barr virus in healthy medical students. *Health Psychol.* 12, 435–442. doi: 10.1037/0278-6133.12.6.435

Goldstein, D. S. (2010). Adrenal responses to stress. *Cell. Mol. Neurobiol.* 30, 1433–1440. doi: 10.1007/s10571-010-9606-9

Grinde, B. (2013). Herpesviruses: latency and reactivation – viral strategies and host response. *J. Oral Microbiol.* 5, 1–9. doi: 10.3402/jom.v5i0.22766

Hato, N., Kisaki, H., Honda, N., Gyo, K., Murakami, S., and Yanagihara, N. (2000). Ramsay hunt syndrome in children. *Ann. Neurol.* 48, 254–256. doi: 10.1002/1531-8249(200008)48:2<254::AID-ANA17>3.0.CO;2-V

Kaur, I., Simons, E. R., Castro, V. A., Ott, C. M., and Pierson, D. L. (2005). Changes in monocyte functions of astronauts. *Brain Behav. Immun.* 19, 547–554. doi: 10.1016/j.bbi.2004.12.006

Kempkes, B., and Robertson, E. S. (2015). Epstein-Barr virus latency: current and future perspectives. *Curr. Opin. Virol.* 14, 138–144. doi: 10.1016/j.coviro.2015.09.007

Kleinschmidt-DeMasters, B. K., and Gilden, D. H. (2001). Varicella-zoster virus infections of the nervous system: clinical and pathologic correlates. *Arch. Pathol. Lab. Med.* 125, 770–780.

Mehta, S. K., Cohrs, R. J., Forghani, B., Zerbe, G., Gilden, D. H., and Pierson, D. L. (2004). Stress-induced subclinical reactivation of varicella zoster virus in astronauts. *J. Med. Virol.* 72, 174–179. doi: 10.1002/jmv.10555

Mehta, S. K., Crucian, B. E., Stowe, R. P., Simpson, R. J., Ott, C. M., Sams, C. F., et al. (2013a). Reactivation of latent viruses is associated with increased plasma cytokines in astronauts. *Cytokine* 61, 205–209. doi: 10.1016/j.cyto.2012.09.019

Mehta, S. K., Laudenslager, M. L., Stowe, R. P., Crucian, B. E., Sams, C. F., and Pierson, D. L. (2014). Multiple latent viruses reactivate in astronauts during space shuttle missions. *Brain Behav. Immun.* 41, 210–217. doi: 10.1016/j.bbi.2014.05.014

Mehta, S. K., Tyring, S. K., Cohrs, R. J., Gilden, D. H., Feiveson, A. H., Lechler, K. J., et al. (2013b). Rapid and sensitive detection of varicella zoster virus in saliva of patients with herpes zoster. *J. Virol. Methods* 193, 128–130. doi: 10.1016/j.jviromet.2013.05.019

Mehta, S. K., Laudenslager, M. L., Stowe, R. P., Crucian, B. E., Feiveson, A. H., Sams, C. F., et al. (2017). Latent virus reactivation in astronauts on the international space station. *NPJ Microgravity* 3:11. doi: 10.1038/s41526-017-0015-y

Mehta, S. K., and Pierson, D. L. (2007). Reactivation of latent herpes viruses in cosmonauts during a Soyuz taxi mission. *Microgravity Sci. Technol.* 19, 215–218. doi: 10.1007/BF02919485

Mehta, S. K., Pierson, D. L., Cooley, H., Dubow, R., and Lugg, D. (2000a). Epstein-Barr virus reactivation associated with diminished cell-mediated immunity in antarctic expeditioners. *J. Med. Virol.* 61, 235–240.

Mehta, S. K., Stowe, R. P., Feiveson, A. H., Tyring, S. K., and Pierson, D. L. (2000b). Reactivation and shedding of cytomegalovirus in astronauts during spaceflight. *J. Infect. Dis.* 182, 1761–1764. doi: 10.1086/317624

Mehta, S. K., Tyring, S. K., Gilden, D. H., Cohrs, R. J., Leal, M. J., Castro, V. A., et al. (2008). Varicella-zoster virus in the saliva of patients with herpes zoster. *J. Infect. Dis.* 197, 654–657. doi: 10.1086/527420

Nagel, M. A., Choe, A., Cohrs, R. J., Traktinskiy, I., Sorensen, K., Mehta, S. K., et al. (2011). Persistence of varicella zoster virus DNA in saliva after herpes zoster. *J. Infect. Dis.* 204, 820–824. doi: 10.1093/infdis/jir425

Nagel, M. A., Forghani, B., Mahalingam, R., Wellish, M. C., Cohrs, R. J., Russman, A. N., et al. (2007). The value of detecting anti-VZV IgG antibody in CSF to diagnose VZV vasculopathy. *Neurology* 68, 1069–1073. doi: 10.1212/01.wnl.0000258549.13334.16

Nicoll, M. P., Proença, J. T., and Efstathiou, S. (2012). The molecular basis of herpes simplex virus latency. *FEMS Microbiol. Rev.* 36, 684–705. doi: 10.1111/j.1574-6976.2011.00320.x

Niedobitek, G., Meru, N., and Delecluse, H. J. (2001). Epstein-Barr virus infection and human malignancies. *Int. J. Exp. Pathol.* 82, 149–170. doi: 10.1046/j.1365-2613.2001.00190.x

O'Connor, C. M., and Murphy, E. A. (2012). A myeloid progenitor cell line capable of supporting human cytomegalovirus latency and reactivation, resulting in infectious progeny. *J. Virol.* 86, 9854–9865. doi: 10.1128/JVI.01278-12

Orme, H. T., Smith, A. G., Nagel, M. A., Bert, R. J., Mickelson, T. S., and Gilden, D. H. (2007). VZV spinal cord infarction identified by diffusion-weighted MRI (DWI). *Neurology* 69, 398–400. doi: 10.1212/01.wnl.0000266390.27177.7b

Padgett, D. A., and Glaser, R. (2003). How stress influences the immune response. *Trends Immunol.* 24, 444–448. doi: 10.1016/S1471-4906(03)00173-X

Pawelec, G. (2014). Immunosenenescence: role of cytomegalovirus. *Exp. Gerontol.* 54, 1–5. doi: 10.1016/j.exger.2013.11.010

Pierson, D. L., Mehta, S. K., and Stowe, R. P. (2007). Reactivation of latent herpes viruses in astronauts. *Psychoneuroimmunology* II, 851–868 doi: 10.1016/B978-012088576-3/50047-2

Pierson, D. L., Stowe, R. P., Phillips, T. M., Lugg, D. J., and Mehta, S. K. (2005). Epstein-Barr virus shedding by astronauts during space flight. *Brain Behav. Immun.* 19, 235–242. doi: 10.1016/j.bbi.2004.08.001

Pollak, L., Mehta, S. K., Pierson, D. L., Sacagiu, T., Kalmanovich, S. A., and Cohrs, R. J. (2015). Varicella-zoster DNA in saliva of patients with meningoencephalitis: a preliminary study. *Acta Neurol. Scand.* 131, 417–421. doi: 10.1111/ane.12335

Reichelt, M., Zerboni, L., and Arvin, A. M. (2008). Mechanisms of varicella-zoster virus neuropathogenesis in human dorsal root ganglia. *J. Virol.* 82, 3971–3983. doi: 10.1128/JVI.02592-07

Ricklin, M. E., Lorscheider, J., Waschbisch, A., Paroz, C., Mehta, S. K., Pierson, D. L., et al. (2013). T-cell response against varicella-zoster virus in fingolimod-treated MS patients. *Neurology* 81, 174–181. doi: 10.1212/WNL.0b013e31829a3311

Sansoni, P., Vescovini, R., Fagnoni, F. F., Akbar, A., Arens, R., Chiu, Y. L., et al. (2014). New advances in CMV and immunosenescence. *Exp. Gerontol.* 55, 54–62. doi: 10.1016/j.exger.2014.03.020

Seitz, R. (2010). Human cytomegalovirus (HCMV)-revised. *Transfus. Med. Hemother.* 37, 365–375. doi: 10.1159/000322141

Stevenson, E. V., Collins-McMillen, D., Kim, J. H., Cieply, S. J., Bentz, G. L., and Yurochko, A. D. (2014). HCMV reprogramming of infected monocyte survival and differentiation: a goldilocks phenomenon. *Viruses* 6, 782–807. doi: 10.3390/v6020782

Stowe, R. P., Kozlova, E. V., Sams, C. F., Pierson, D. L., and Walling, D. M. (2011). Latent and lytic Epstein-Barr virus gene expression in the peripheral blood of astronauts. *J. Med. Virol.* 83, 1071–1077. doi: 10.1002/jmv.22079

Stowe, R. P., Pierson, D. L., and Barrett, A. D. T. (2001a). Elevated stress hormone levels relate to Epstein-Barr virus reactivation in astronauts. *Psychosom. Med.* 63, 891–895. doi: 10.1097/00006842-200111000-00007

Stowe, R. P., Pierson, D. L., and Barrett, A. D. T. (2001b). "Space flight-induced reactivation of latent Epstein-Barr virus," in *Proceedings of the Conference and Exhibit on International Space Station Utilization*, Cape Canaveral, FL.

Stowe, R. P., Sams, C. F., Mehta, S. K., Kaur, I., Jones, M. L., Feeback, D. L., et al. (1999). Leukocyte subsets and Neutrophil function after short-term spaceflight. *J. Leukoc. Biol.* 65, 179–186. doi: 10.1002/jlb.65.2.179

Thompson, M. P., and Kurzrock, R. (2004). Epstein-Barr virus and cancer. *Clin. Cancer Res.* doi: 10.1158/1078-0432.CCR-0670-3 [Epub ahead of print].

Varani, S., and Landini, M. (2011). Cytomegalovirus-induced immunopathology and its clinical consequences. *Herpesviridae* 2:6. doi: 10.1186/2042-4280-2-6

Webster, J. I., and Glaser, R. (2008). Stress hormones and immune Function. *Cell. Immunol.* 252, 16–26. doi: 10.1016/j.cellimm.2007.09.006

Wills, M. R., Poole, E., Lau, B., Krishna, B., and Sinclair, J. H. (2015). The immunology of human cytomegalovirus latency: could latent infection be cleared by novel immunotherapeutic strategies? *Cell. Mol. Immunol.* 12, 128–138. doi: 10.1038/cmi.2014.75

Conflict of Interest Statement: BR was employed by GeoControl Systems Incorporated and SM was employed by Jes Tech, KBR Wyle Laboratories.

The remaining authors declare that the research was conducted in the absence of any commercial or financial relationships that could be construed as a potential conflict of interest.

frontiers in Microbiology

REVIEW
published: 12 March 2019
doi: 10.3389/fmicb.2019.00358

Arachidonic Acid Derived Lipid Mediators Influence Kaposi's Sarcoma-Associated Herpesvirus Infection and Pathogenesis

Jayashree A. Chandrasekharan† *and Neelam Sharma-Walia**†

Department of Microbiology and Immunology, H.M. Bligh Cancer Research Laboratories, Chicago Medical School, Rosalind Franklin University of Medicine and Science, North Chicago, IL, United States

Kaposi's sarcoma-associated herpesvirus (KSHV) infection, particularly latent infection is often associated with inflammation. The arachidonic acid pathway, the home of several inflammation and resolution associated lipid mediators, is widely altered upon viral infections. Several *in vitro* studies show that these lipid mediators help in the progression of viral pathogenesis. This review summarizes the findings related to human herpesvirus KSHV infection and arachidonic acid pathway metabolites. KSHV infection has been shown to promote inflammation by upregulating cyclooxygenase-2 (COX-2), 5 lipoxygenase (5LO), and their respective metabolites prostaglandin E_2 (PGE_2) and leukotriene B4 (LTB_4) to promote latency and an inflammatory microenvironment. Interestingly, the anti-inflammatory lipid mediator lipoxin is downregulated during KSHV infection to facilitate infected cell survival. These studies aid in understanding the role of arachidonic acid pathway metabolites in the progression of viral infection, the host inflammatory response, and pathogenesis. With limited therapeutic options to treat KSHV infection, use of inhibitors to these inflammatory metabolites and their synthetic pathways or supplementing anti-inflammatory lipid mediators could be an effective alternative therapeutic.

Keywords: KSHV, latency, cyclooxegenase-2, lipoxygenase, lipoxin A4

OPEN ACCESS

Edited by:
Benoit Muylkens, University of Namur, Belgium

Reviewed by:
Masahiro Fujimuro, Kyoto Pharmaceutical University, Japan
Carlos Arterio Sorgi, Universidade de São Paulo Ribeirão Preto, Brazil

****Correspondence:***
Neelam Sharma-Walia
neelam.sharma-walia@rosalindfranklin.edu;
nsharmawalia@gmail.com

†These authors have contributed equally to this work

Specialty section:
This article was submitted to Virology, a section of the journal Frontiers in Microbiology

Received: *09 August 2018*
Accepted: *11 February 2019*
Published: *12 March 2019*

Citation:
Chandrasekharan JA and Sharma-Walia N (2019) Arachidonic Acid Derived Lipid Mediators Influence Kaposi's Sarcoma-Associated Herpesvirus Infection and Pathogenesis. Front. Microbiol. 10:358. doi: 10.3389/fmicb.2019.00358

INTRODUCTION

Kaposi's sarcoma-associated herpesvirus or human herpesvirus 8 (HHV8) is the causative agent of KS, PEL, MCD, and KICS (Cesarman and Knowles, 1999; Greene et al., 2007; Kalt et al., 2009; Ganem, 2010). KS lesions are characterized by proliferating spindle shaped endothelial cells while PEL is characterized by a null lymphocyte immunophenotype (CD45+, but neither T cells nor B cells) arising in body cavities (Chen et al., 2007; Saini et al., 2013). KS occurs in less than

Abbreviations: cAMP, cyclic AMP; COX, cyclooxygenase; EGF, epidermal growth factor; FAK, focal adhesion kinase; FLAP, 5-lipoxygenase activating protein; G-CSF, granulocyte colony-stimulating factor; GM-CSF, granulocyte-macrophage colony-stimulating factor; HFF, human foreskin fibroblasts; HMVEC-d, human microvascular endothelial cells; H-PGDS, hematopoietic PGD synthase; IRIS, immune reconstitution inflammatory syndrome; KICS, KSHV inflammatory cytokine syndrome; KS, Kaposi's sarcoma; KSHV, Kaposi's sarcoma-associated herpesvirus; LO, lipoxygenase; LTA4H, leukotriene A4 hydrolase; LTs, leukotrienes; MCD, multicentric Castleman's disease; MCP, macrophage chemoattractant protein; MEK, mitogen-activated protein kinase; MIP, macrophage inflammatory protein; mPGES, microsomal PGE synthase; PDGF-B, platelet-derived growth factor-B; PEL, primary effusion lymphoma; PGs, prostaglandins; PI3K, phosphoinositide-3-kinase; PKA, protein kinase A; PKC, protein kinase C; TIVE-LTC, long-term infected telomerase immortalized endothelial cells; TXS, thromboxane synthase; VEGF, vascular endothelial growth factor; VEGFR, vascular endothelial growth factor receptor.

1% of the population in the United States mostly found in HIV infected patients, while PEL, an aggressive AIDS-linked KSHV-associated non-Hodgkin's lymphoma (NHL) occurs in about 4% of the population in the United States (Chen et al., 2007; Saini et al., 2013). While the number of AIDS-KS and PEL cases has been dramatically reduced in the United States since the widespread use of combined antiretroviral therapy, KSHV still causes major mortality in the developing world (Mesri et al., 2010). PEL has complications such as extracavitary KSHV associated solid lymphoma (solid PEL) without serous effusions that involves mainly extranodal tissues (De Paoli and Carbone, 2016). KSHV is detected in all clinical forms of KS, including classical KS, endemic KS in Africa, epidemic AIDS-related KS, and iatrogenic/organ-transplant KS. KICS is a newly characterized condition caused by lytic KSHV infection (Uldrick et al., 2010; Tamburro et al., 2012).

Kaposi's sarcoma-associated herpesvirus was discovered using representational difference analysis of DNA extracted from an AIDS-KS specimen and DNA from healthy skin of the same patient in 1994 by Yuan Chang, Patrick S. Moore, and colleagues (Chang et al., 1994; Boshoff et al., 1995a,b; Cesarman et al., 1995; Schulz and Weiss, 1995; Soulier et al., 1995). KSHV has a double-stranded DNA genome of approximately 165k bases inside a capsid, which is then surrounded by a proteinaceous layer called the tegument (Sathish et al., 2012). Upon infection, KSHV can undergo two distinct types of life cycle (**Figure 1**), lytic where the genome replicates to produce more virions and a latent cycle where the viral genome remains as an episome (Ye et al., 2011). Recently, with structured illumination microscopy (SIM), it was shown that KSHV tethers its genomes not only to nucleosome bound chromosomal DNA but also to nucleosome-bound viral DNA to form clusters of genomes that partition as units and that is predicted to help in the rapid establishment of high viral copy numbers in infected cells (Chiu et al., 2017). During both cycles, KSHV transcribes several genes which can subvert a variety of host cell processes such as cell death and proliferation (Murtadak et al., 2015), glucose uptake and energy management, immunosuppression, and inflammation (Mesri, 1999; Morini et al., 1999).

Latency is characterized by the expression of the following gene open reading frames *OrfK12*/Kaposin, viral FLICE, FADD-like interferon converting enzyme-like inhibitory protein (*Orf71*/K13/vFLIP), *Orf72*/vCyclin, latency associated nuclear antigen-1 (*Orf73*/LANA1), and a cluster made up of 12 pre-miRNAs (Gottwein, 2012; Qin et al., 2017). The KSHV lytic cycle is characterized by expression of over 80 genes classified into immediate early, early, and late, which aid in infectious virus production (**Figure 1**; Jenner et al., 2001). Immediate early genes such as *OrfK8* (bZIP), *Orf45*, and *OrfK4.2* help in a transition from latency to the lytic phase. Early lytic genes including PAN/nut-1/T1.1 RNA (*OrfK7*) and *OrfK14* encode for proteins involved in DNA replication while late lytic genes code for various structural proteins. Late lytic genes include *Orf22*, *Orf25*, and *Orf64* (Wakeman et al., 2017). *Orf50*/RTA (replication and transcriptional activator), master latency/lytic switch, an important player as both an initiator and a controller of KSHV lytic DNA replication is an immediate-early protein that disrupts the latency and promotes lytic cycle (**Figure 1**; Wakeman et al., 2017). *Orf50*/RTA auto-activates its own promoter and transactivates the expression of several downstream lytic genes such as *K5*, *K8*, *K2*, *K12*, *ORF6*, *ORF57*, *ORF74*, *K9*, *ORF59*, *vIL6*, *PAN-RNA*, *vIRF1*, *K1*, and *ORF65*, either through an RTA-responsive element (RRE) or via other viral regulatory genes (Deng et al., 2000).

Arachidonic acid is an unsaturated (ω-6 fatty acid) fatty acid which is transformed into a variety of lipid mediators to modulate primarily inflammatory reactions (Samuelsson, 1991). Arachidonic acid is released from the membrane by the action of phospholipase A2 (PLA2; **Figure 2**). Arachidonic acid is metabolized by the COX and LO pathways, to produce eicosanoids, which include PGs and LTs and their derivatives (Fanning and Boyce, 2013; Chandrasekharan et al., 2016; **Figure 2**). PLA2 also result in the formation of lysoglycero-phospholipids, which are the precursors for lysophosphatidic acid (LPA) and sphingosine-1-phosphate (S1P; Fanning and Boyce, 2013; Chandrasekharan et al., 2016). The arachidonic acid pathway widely influences the process of inflammation through its lipid mediators (Bennett and Gilroy, 2016). These lipid mediators are known to play a pivotal role(s) in cancer and inflammation associated diseases like arthritis, allergy, and asthma (Greene et al., 2011). Viral infection also alters the lipid mediators of this pathway to establish infection and pathogenesis (Chandrasekharan et al., 2016; **Figure 2**).

Kaposi's sarcoma-associated herpesvirus is known to alter several host pathways for its survival and one such extensively studied is the arachidonic acid pathway (Sharma-Walia et al., 2006, 2010b, 2012, 2014; George Paul et al., 2010; Paul et al., 2011, 2013a,b; Chandrasekharan and Sharma-Walia, 2015; Marginean and Sharma-Walia, 2015; Chandrasekharan et al., 2016). KSHV triggers a pro-inflammatory microenvironment to promote its latency and pathogenesis (Chandrasekharan et al., 2016). Arachidonic acid pathway is a key connection between KSHV infection and its associated inflammatory responses (Mesri, 1999; Zhong et al., 2017). Having stated the importance of the arachidonic acid pathway in KSHV infection/pathogenesis one can envisage the role of lipid mediators in the treatment of KS and PEL. This review summarizes the key findings of the role of several enzymes and metabolites of the arachidonic acid pathway during KSHV infection.

ROLE OF ARACHIDONIC ACID METABOLISM IN KSHV INFECTION AND PATHOGENESIS

Cyclooxygenase-2, a Prominent Enzyme Upregulated During KSHV Infection

Cyclooxygenase, an enzyme involved in the synthesis of PGs, regulated by the popular non-steroidal anti-inflammatory drugs (NSAIDs; Sasaki et al., 2017). Aspirin inhibits the COX pathway by downregulating the levels of pro-inflammatory PGs, particularly PG E2 (PGE_2; Vane and Botting, 1997; Botting, 2010). COX-1 and COX-2 are the two isoforms of this enzyme (Williams

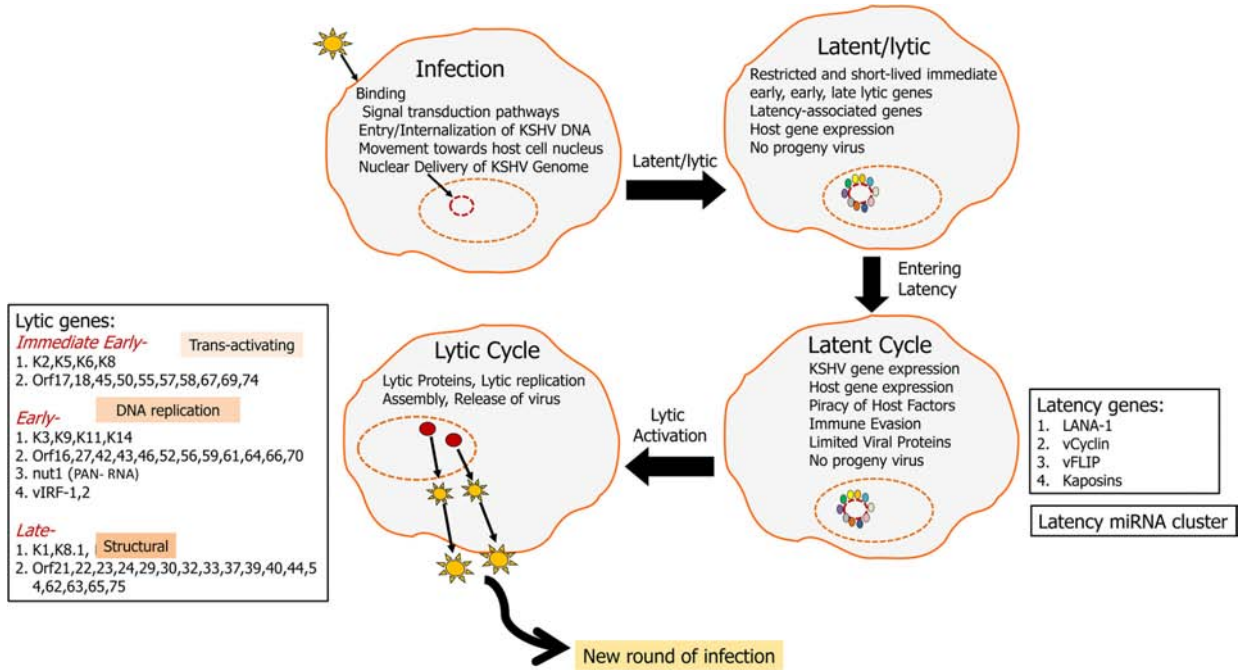

FIGURE 1 | KSHV life cycle: KSHV infects a variety of cells including endothelial, epilthelial, B cells, monocytes, and keratinocytes. Upon infection, KSHV aims at lifelong persistence by adopting two lifestyles including a long persistent latency cycle and a short reproductive lytic cycle. The KSHV genome (165–170 kbp) consists of dsDNA that is linear within the viral particle but circularizes after it traverses to the host nucleus. This circular form is known as the viral episome (Hu et al., 2002; Si et al., 2008). During latency, the virus replicates via the host DNA synthetic machinery, viral genome remains as an episome tethered to the host chromosome and is characterized by the expression of a limited repertoire of genes, including LANA1, vCyclin, vFLIP, and kaposin. LANA1 is a predominant latency gene that plays an important role in episome maintenance and it drives latency. KSHV can then enter lytic cycle, which is marked by the viral replication, virion assembly, and release of infectious virions from the infected cells. Lytic genes can be classified into immediate early, early, and late. RTA (ORF50) is a critical lytic gene that helps the transition of genome from latency to the lytic cycle. During the lytic cycle, KSHV expresses many other proteins including K1 and viral interleukin 6 (vIL6), which plays important roles in promoting oncogenesis by activating multiple signaling pathways driving cellular growth.

et al., 1999a,b,c; Rouzer and Marnett, 2009; Greene et al., 2011; Schneider et al., 2011; Yu et al., 2016; Grosch et al., 2017) with COX-1 produced constitutively while COX-2 is inducible (Dubois et al., 1998; **Figure 2**). COX-1 and COX-2 catalyze two sequential reactions to initiate the COX pathway and produce PGG2. An endoperoxidase then reduces PGG2 to PGH2. PGH2 then gets converted into bioactive prostanoids PGD_2, PGE_2, $PGF_{2\alpha}$, PGI_2, and TXA_2 by H-PGDS, mPGESs mPGES-1, mPGES-2/cytosolic PGES, PGF synthase (PGFS), PGI synthase (PGIS), and TXS, respectively (Fanning and Boyce, 2013; Chandrasekharan et al., 2016; **Figure 2**). Cycloxygenase is a clinically important enzyme and its inhibitors are widely used to treat inflammation (Fitzpatrick, 2004; Suleyman et al., 2007; Greene et al., 2011; Yu et al., 2016; Grosch et al., 2017; **Figure 2**).

De novo KSHV infection of primary HMVEC-d or HFF cells is a good *in vitro* model for KS and is characterized by the sustained expression of latency-associated *ORF73*/LANA1, *ORF72*/vCyclin, and *ORF71*/K13/vFLIP genes (Krishnan et al., 2004). However, a unique aspect of this *in vitro* infection is the concurrent transient expression of a limited number of lytic KSHV genes, such as the lytic cycle switch gene *ORF50*/RTA and the immediate early lytic *K5*, *K8*, and *vIRF2* genes (Krishnan et al., 2004). In the first step of identifying host molecules involved in KSHV pathogenesis, a variety of genes involved in cellular apoptosis, transcription, cell cycle, signaling, inflammatory response and angiogenesis were identified and COX-2 was one of the upregulated genes (Naranatt et al., 2004). Further studies performed on HMVEC-d cells infected with KSHV for various time points showed that COX-2 levels were induced as early as 30 min postinfection, reached a high level at 2 h and gradually started returning to basal level by 72 h (Sharma-Walia et al., 2006). No change in the level of COX-1 was observed in endothelial cells infected with KSHV (Sharma-Walia et al., 2006). COX-2 induction could be triggered by KSHV binding and entry while the augmented levels require KSHV genome (Sharma-Walia et al., 2006). This was identified by screening levels of COX-2 in HMVEC-d cells infected with UV inactivated KSHV. UV inactivated KSHV was generated by inactivating KSHV in UV (365 nm) for 20 min. UV inactivated KSHV efficiently binds and enters into host cells but it does not express viral genes (Sharma-Walia et al., 2004). UV inactivated KSHV infection could enhance COX-2 levels suggesting the role of KSHV binding and entry stages of infection involving the interplay of viral glycoprotein's (Sharma-Walia et al., 2006). Like COX-2, the level of its metabolite PGE_2 was elevated at 2 h post infection and gradually decreased to basal levels at 72 h (Sharma-Walia et al., 2006). Since COX-2 induction by UV-inactivated KSHV suggested stimulation during the binding and entry stages

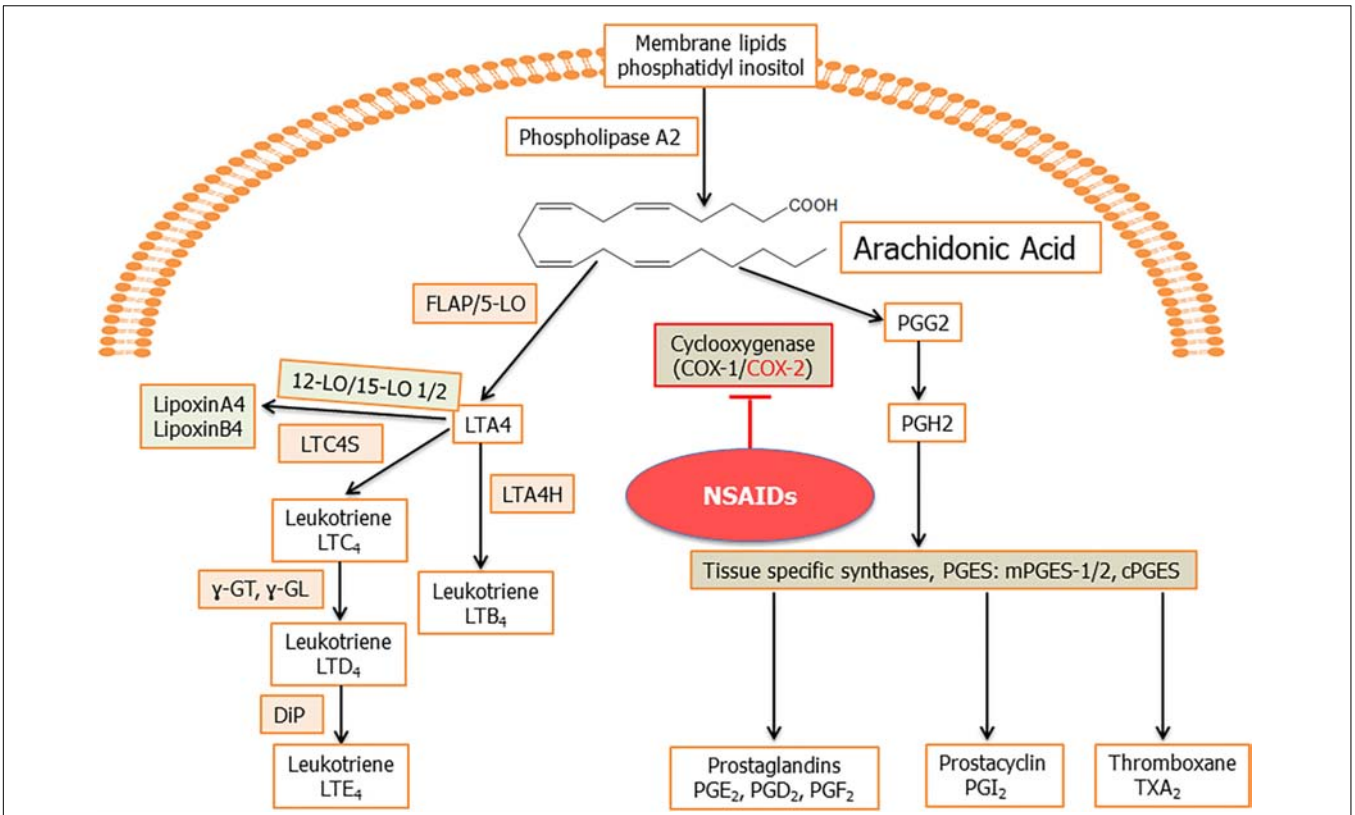

FIGURE 2 | Schematic for arachidonic acid (AA) pathway: phospholipids from the plasma membrane are mobilized and converted to AA by phospholipase A2 (PLA_2) enzyme activity. Cyclooxygenase 1 (constitutive) and cyclooxygenase 2 (inducible) enzymes catalyze the synthesis of prostaglandin H2 (PGH2) from AA through an unstable intermediate PGG2 (Vane et al., 1998; Smith et al., 2000). PGH2 is converted by microsomal prostaglandin E synthase (mPGES) to PGE_2, which is released in the microenvironment. Besides PGE_2, other prostanoids formed from PGH2 include PGI_2, TXA_2, PGD_2, and PGF2α (Hyde and Missailidis, 2009). In human cells, generally, four types of LOs, namely, 5-, 12-, and 15-LO-1 and -2 have been identified. 5LO in conjunction with its activating protein, FLAP, catalyze the dioxygenation of AA into give 5-hydroperoxy eicosapentaenoic acid (5-HpETE). 5LO, with FLAP, then catalyze a second step, the dehydration of 5-HpETE to the intermediate LTA_4, that leads to the formation of the leukotrienes and lipoxins (Hyde and Missailidis, 2009). Hydrolysis of LTA_4 is catalyzed by LTA_4 hydrolase (LTA4H) to produce LTB4. LTA_4 is also metabolized by the enzyme LTC_4 synthase to produce LTC_4, which is acted upon by γ-glutamyl-transpeptidases to yield LTD_4. LTD_4 is acted upon by a dipeptidase (DiP) to produce LTE_4. The combination of LO, -5, -12, or -15 on the same arachidonic acid molecule produces lipoxins.

of infection, the ability of KSHV envelope glycoproteins gB and gpK8.1A to induce COX-2 was examined (Sharma-Walia et al., 2006). Both glycoproteins induced COX-2 but to a lesser extent than KSHV live virus, suggesting that viral gene expression early during infection, and possibly together with viral gene-induced host genes are probably essential for the increased and sustained induction of COX-2 and PGE_2 (Sharma-Walia et al., 2006).

OUTCOMES OF ELEVATED COX-2

Since elevated levels of COX-2 were found in KS patient tissue sections, its role in pathogenesis events such as secretion of inflammatory cytokines, angiogenesis, cell survival, and invasion were explored (Sharma-Walia et al., 2010b). HMVEC-d cells infected with KSHV at various time points secreted a high level of inflammatory cytokines such as growth regulated oncogene (GRO), GROα, IL1α, IL1β, ILs-(2, 3, 6, 7, and 12-p40), TNFα, TNFβ, and SDF-1 [a ligand for the chemokine receptor CXCR4 or fusin or CD184 (cluster of differentiation 184)], and IFNγ in their spent culture supernatants (Sharma-Walia et al., 2010b). The levels of these inflammatory cytokines were constantly increased 2 h post infection and at 8 h post infection reached a high (3–3.5-fold increase) level. Chemokines such as RANTES (cytokine regulating T cell response), MCPs-2 and 3, thymus and activation-regulated chemokine, MIP, macrophage derived chemokine, monokine induced by IFN-γ, epithelial neutrophil-activating peptide and inflammatory cytokine were found upregulated in *de novo* KSHV infected HMVEC-d cells. Similarly, several growth and angiogenic factors such as EGF, insulin-like growth factor-1, platelet-derived growth factor-BB (PDGF-BB), macrophage colony stimulating factor, G-CSF, GM-CSF, angiogenin, oncostatin-M, thrombopoietin, VEGF, stromal cell derived factor-1, stem cell factor, TGFβ1, and leptin were elevated in KSHV infected HMVEC-d cells.

To validate the involvement of KSHV induced COX-2 on inflammatory cytokines and angiogenic factors, HMVEC-d cells were either pretreated with COX-2 inhibitors NS-398 or indomethacin or silenced for COX-2 gene expression (Sharma-Walia et al., 2010b). VEGF-A, VEGF-C (angiogenic

molecules), GRO (cytokine with inflammatory and growth-regulatory properties), RANTES, and SDF-1 were alleviated upon blocking COX-2 (Sharma-Walia et al., 2010b). IL-8 was not affected by COX-2 inhibition (Sharma-Walia et al., 2010b). Many of the observed upregulated molecules such as PGE_2, VEGF, and b-FGF play a vital role in endothelial cell migration and tube formation. KSHV-induced COX-2 enhanced the levels of these molecules and promoted endothelial cell tube formation, while this effect was reversed upon blocking COX-2 using chemical inhibitors (Sharma-Walia et al., 2010b). VEGF-A levels were reduced in latently infected TIVE-LTC cells treated with COX inhibitors, plus a significant reduction in capillary tube formation was observed (Sharma-Walia et al., 2010b). MMPs play an important role in maintaining tissue homeostasis and are often seen to be upregulated in several cancers. KSHV infection enhanced expression and secretion of MMPs including MMP-1, -2, -8, -9, and -13 (Sharma-Walia et al., 2010b). KSHV-induced COX-2 significantly induced MMP-2 and -9 in *de novo* infected HMVEC-d cells and blocking it drastically reduced their levels (Sharma-Walia et al., 2010b). This study demonstrated that COX-2 and its metabolite PGE_2 are upregulated during KSHV infection of primary endothelial cells; KSHV utilizes those to target several pathways that facilitate pathogenesis and angiogenesis (Sharma-Walia et al., 2010b).

UNDERSTANDING COX-2 REGULATION BY KSHV INFECTION

Since COX-2 and PGE_2 are upregulated during KSHV infection, understanding the mechanism of induction could help in designing therapeutic strategies for KS and PEL. To determine if regulation occurs at the transcriptional level, HMEVC-d cells were pretreated with transcriptional inhibitor actinomycin D prior to *de novo* KSHV infection (Sharma-Walia et al., 2010b). Pretreatment of HMVEC-d cells with actinomycin D drastically inhibited the effect of KSHV infection on both COX-2 mRNA levels and PGE_2 secretion. To determine if a KSHV-induced signal cascade and/or viral gene expression is required for COX-2 induction, COX-2 promoter activity in HMVEC-d cells were monitored. These HMVEC-d cells were transfected with the COX-2 promoter and then infected with 30 DNA copies of KSHV/cell (either live or UV inactivated and replication incompetent; Sharma-Walia et al., 2010b). Compared to live virus UV-KSHV could not induce sustained levels of COX-2, thus suggesting that virus entry and binding induces COX-2 but KSHV gene transcription is required to sustain COX-2 (Sharma-Walia et al., 2010a). It is well known that COX-2 promoter activity is regulated by several transcription factors, including NFkB, nuclear factor IL-6, activator protein AP-1, cAMP response element binding (CREB) protein, and nuclear factor of activated T cells (NFAT; Iniguez et al., 1999, 2000). The COX-2 promoter has distal NFAT (dNFAT) and proximal NFAT (pNFAT) *cis*-acting elements. Promoter assays show that dNFAT plays an important role in KSHV-induced COX-2 promoter activity (Sharma-Walia et al., 2010a). cAMP response element (CRE) recognition sequences in the human COX-2 promoter are also important for KSHV infection-induced transcriptional activity as promoter deletion experiments show that these regions are vital for transcriptional activation upon KSHV infection. CRE and NFAT together are important for KSHV infection-induced COX-2 regulation (Sharma-Walia et al., 2010b). To identify the role of KSHV-induced signal transduction pathways in COX-2 regulation, several signaling inhibitors were used to study COX-2 promoter activity and its gene expression. PI3K, PKC, FAK, MEK, P38, and JNK inhibition strongly reduced COX-2 promoter activity and its gene expression (Sharma-Walia et al., 2010a). PGE_2 being the end product its influence on COX-2 promoter and gene expression was studied by supplementing PGE_2 exogenously (Sharma-Walia et al., 2010a). It was found that PGE_2 could stimulate both COX-2 promoter activity and gene expression concluding that PGE_2 autoregulates COX-2 (Sharma-Walia et al., 2010a). PGE_2 amplifies COX-2 levels by cAMP/PKA signaling mediated inactivation of GSK3 (Sharma-Walia et al., 2010a).

In another study, the interplay between KSHV latency protein vFLIP and host protein COX-2 was demonstrated (Sharma-Walia et al., 2012; Paul et al., 2013b). Studies showed that vFLIP activates COX-2/PGE_2 in a NF-κB-dependent manner and conversely, COX-2/PGE_2 is required for vFLIP induced NF-κB activation, extracellular matrix (ECM) interaction, FAK/Src/AKT, Rac1-GTPase activation, mitochondrial antioxidant enzyme manganese superoxide dismutase (MnSOD) level, and anoikis resistance (Sharma-Walia et al., 2012; Paul et al., 2013b). vFLIP expression mediated the secretion of pro-inflammatory cytokines, and spindle cell differentiation activated the phosphorylation of p38, RSK, FAK, Src, Akt, and Rac1-GTPase (Sharma-Walia et al., 2012; Paul et al., 2013b). Celecoxib, a selective inhibitor of COX-2, has demonstrated its chemotherapeutic properties in a variety of cancers including colon, breast, skin, prostate, and pancreatic cancer cells, but was never tested in KSHV-associated malignancies (Jendrossek, 2013). Blocking COX-2 with celecoxib or NS398 [*N*-(2-cyclohexyloxy-4-nitrophenyl)-methanesulfonamide] decreased activation of signaling molecules including NFKB (reduced nuclear translocation of p65), FAK, Src, AKT, ERK, P-38, RSK, and Rac1-GTPase, and thereby decreased vFLIP-mediated protection of HMVECs from anoikis (Sharma-Walia et al., 2012). KSHV vGPCR (G-protein coupled receptor), vFLIP have been shown to induce expression of COX-2/PGE_2 but not COX-1, and its paracrine effects in KS pathogenesis (Matta et al., 2007; Shelby et al., 2007). Another elegant study linked STE20 kinase family member-MAP4K4 (MEK kinase kinase kinase) to COX-2, which contributed to KSHV lytic reactivation (Haas et al., 2013; Mariggio et al., 2017).

UTILIZING COX-2 AS A THERAPEUTIC TARGET

To determine the role of KSHV induced COX-2 on the secretion of PGE_2, indomethacin and NS 398 (inhibitors of COX-2) were used to pretreat KSHV infected HMVEC-d cells. A 93 and 88% reduction in levels of PGE_2 was observed thereby concluding that

KSHV infection associated COX-2 upregulation was the reason for enhanced PGE_2 levels. Pretreating HMVEC-d and HFF cells with COX-2 inhibitors did not interfere in KSHV binding, entry, and trafficking (Paul et al., 2011). However, viral latency gene *Orf73*/LANA1 was significantly reduced by 80% at 24 h post infection in HMVEC-d cells pretreated with indomethacin, an NSAID (Ghosh et al., 2015). The level of lytic gene *Orf50*/RTA was not affected by indomethacin or NS-398 pretreatment. NS-398 is a COX-2-specific inhibitor that has been shown to have chemotherapeutic potential against colon and pancreatic cancer cells (Paul et al., 2011). Exogenous PGE_2 supplementation could reverse this inhibitory effect of indomethacin and NS-398 (Sharma-Walia et al., 2006). Treating PEL cells with orally active COX-2 selective inhibitor Nimesulide (4-nitro-2-phenoxymethanesulfonanilide) to disrupt latency has shown to be beneficial (Paul et al., 2011). Effect of nimesulide treatment was tested on PEL (BCBL-1, BC-3, JSC-1), EBV-infected (Raji) and non-infected (Akata, Loukes, Ramos, BJAB) human Burkitt's lymphoma (BL), and EBV harboring lymphoblastoid (LCL), KSHV infected (TIVE-LTC), TIVE, and primary endothelial HMVEC-d cells (Paul et al., 2011). KSHV positive PEL cells (BCBL-1, BC-3) reduced cell proliferation, colony formation, and enhanced apoptosis when compared to KSHV negative B-lymphoma cells (BJAB; Paul et al., 2011). Nimesulide treatment of PEL cells blocked LANA1 and vFLIP latency genes. Targeting COX-2 is effective in downregulating latency in PEL cells; however, further studies are required using *in vivo* models as these inhibitors are associated with cardiovascular diseases (Pawlosky, 2013).

ROLE OF PROSTAGLANDIN E_2 (E-TYPE PROSTANOID RECEPTORS, EP) RECEPTORS IN KSHV INFECTION

Prostaglandin E_2, the most versatile prostanoid exerts its pleiotropic effects through a group of four G-protein-coupled receptors (GPCRs) designated subtypes EP1, EP2, EP3, and EP4 (Sugimoto and Narumiya, 2007; Yokoyama et al., 2014; **Figure 3**). These GPCRs have seven transmembrane helices (Funk, 2001). There are multiple splicing isoforms of the subtype EP3 (α, β, γ), which are generated by alternative splicing of the C-terminal tail (Sugimoto and Narumiya, 2007). Among all EP receptors, EP1 is known to regulate Ca2+ channel gating (Sugimoto and Narumiya, 2007) and increase intracellular calcium via receptor-activated Ca2+ channels (RACC; Katoh et al., 1995; Tabata et al., 2002; **Figure 3**). EPs, both EP2 and EP4 are coupled to induction of cAMP via adenylate cyclase (AC; Sugimoto and Narumiya, 2007; **Figure 3**). However, EP3 receptor inhibits AC and decreases cAMP concentrations (Sugimoto and Narumiya, 2007; **Figure 3**). EP4 is widely distributed in the body and it can activate PI3K and can be coupled to GPCR kinases (GRK), β-arrestin, and β-catenin signaling pathways during carcinogenesis (Yokoyama et al., 2013). Therapeutic potential of EP modulators has been shown in colorectal cancer, neurologic disease, glaucoma, ocular hypertension, bone formation, cardiovascular disease, ulcerative colitis, solid tumors, and B cell lymphoma (Markovic et al., 2017). Functional EP receptors EP1, EP2, EP3α, and EP4 have been reported to be present on perinuclear sites and nuclear membranes of a variety of cell types and tissues but the signaling pathways for these have not been investigated (Gobeil et al., 2003, 2006; Zhu et al., 2006).

Cyclooxygenase-2 has been shown as a major player of tumor progression in melanoma as COX-2 has strong relationship with the dynamic expression of programmed cell death protein ligand 1 (PD-L1) on tumor cells (Botti et al., 2017). The tumor-induced PGE_2 due to overexpression of PGE2 synthase 1 and reduction of PGE_2 degrading enzyme 15-hydroxyprostaglandin dehydrogenase induces PD-L1 expression in bone marrow-derived cells, macrophages, and myeloid-derived suppressor cells (MDSCs; Prima et al., 2017). COX2 inhibitors or PGE_2 receptors EP2 and EP4 antagonists combined with anti-PD-1 blockade have shown the therapeutic potential in improving eradication of tumors and augmenting the numbers of functional tumor-specific cytotoxic T lymphocytes (CTL) function in tumor-bearing hosts (Miao et al., 2017). Follicular dendritic cells (FDCs) of the lymphoid tissue produce PGE_2, and it plays an immunoregulatory function. Targeting PGE_2 receptors using EP2 and EP4 antagonists along with COX-2 inhibitors results in synergistic inhibition of PGE_2-mediated Akt phosphorylation/activation in FDC like (Harizi et al., 2003; Lee et al., 2008).

Prostaglandin E_2 suppresses effector functions of macrophages and neutrophils and the Th1-, CTL-, and NK cell-mediated immunity (Kalinski, 2012; Agard et al., 2013; Turcotte et al., 2017). PGE_2 promotes Th2, Th17, and regulatory T cell responses, impairs CD4+ T cell activation (Chemnitz et al., 2006; Kalinski, 2012; Sreeramkumar et al., 2012), and also tempers chemokine production (Kalinski, 2012). PGE_2 can promote the tissue influx of neutrophils (Yu and Chadee, 1998), macrophages (Nakayama et al., 2006), and mast cells (Weller et al., 2007). PGE_2 suppresses the cytolytic effector functions of NK cells (Bankhurst, 1982; Goto et al., 1983). PGE_2 inhibits NK cell production of IFN-γ, abolishes NK cell "helper" function in the DC-mediated induction of Th1 and CTL responses (Mailliard et al., 2005), and facilitates the establishment of metastases in experimental animals (Yakar et al., 2003). PGE_2 inhibits granulocyte functions (Smith, 1977) and underwrites to the defective innate host defense in patients after bone marrow transplantation (Ballinger et al., 2006). PGE_2 limits the phagocytosis by alveolar macrophages and their pathogen-killing function (Serezani et al., 2007) partly via EP2 (Aronoff et al., 2004). PGE_2 promotes mast cell induction, their local attraction, and degranulation via EP1 and EP3 (Hu et al., 1995; Gomi et al., 2000; Nakayama et al., 2006; Wang and Lau, 2006). Murine splenic NK cells express all EP1-4 receptors and inhibiting PGE_2 production or preventing signaling through the EP4 receptor could suppress NK cell functions including migration, cytotoxicity, and cytokine release (Holt et al., 2012; Park et al., 2018).

Prostaglandin E_2 disturbs early stages of DC differentiation and adds to systemic DC dysfunction in cancer (Kalinski et al., 1997; Sombroek et al., 2002; Sharma et al., 2003; Heusinkveld et al., 2011). PGE_2 subdues the differentiation

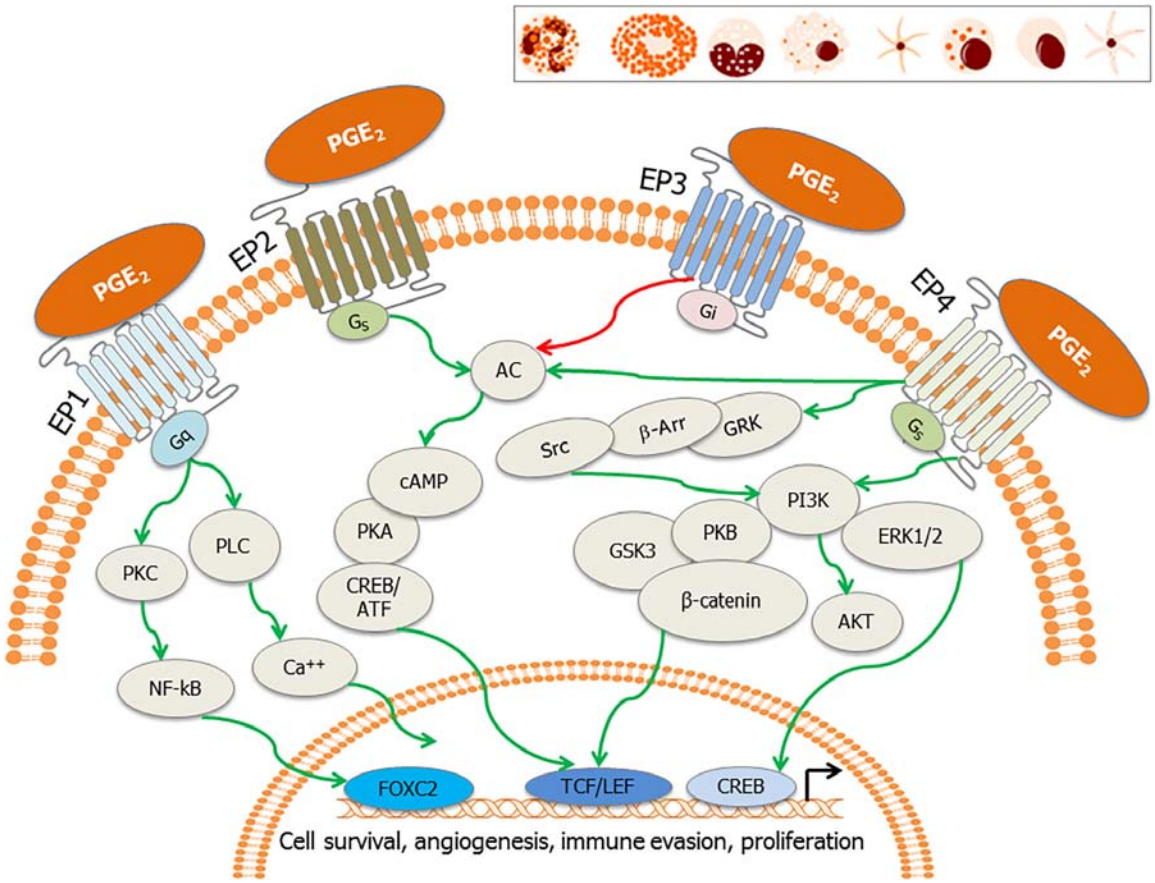

FIGURE 3 | EP receptors and their downstream signaling: PGE_2 binds to its cognate receptors, the E-series of prostaglandin receptors (EP1–EP4) on the plasma membrane and nuclear membrane. These receptors are also present on tumor cells, stromal cells and immune effector cells such as neutrophils, mast cells, monocytes, macrophages, myeloid dendritic cells, natural killer (NK) cells, plasma cells, and lymphoid dendritic cells (inset). Major signaling pathways involve activation of activation of phospholipase C (PLC) resulting in the increase in intracellular calcium (EP1), also the activation of PKC, NF-κB, adenylate cyclase; AC (EP2 and EP4) and subsequent surge in cAMP, and inhibition of adenylate cyclase (EP3). EP4 stimulates cAMP-independent signaling through activation of GRK/β-arrestin/Src/PI3K/GSK3 pathway, leading to the nuclear translocation of β-catenin. These signaling pathways subsequently induce the nuclear translocation/activation of transcription factors, which bind to the promoters of genes involved in cell cycle survival, anti-apoptosis, angiogenesis, immune evasion, and cell proliferation.

of functionally competent Th1-inducing DCs and the subsequent "PGE_2 DCs" characterize MDSCs, which can suppress CTL responses (Obermajer et al., 2011). Besides these functions, PGE2 acts as an inhibitory damage-associated molecular pattern (DAMP) and negatively regulates cell death-induced inflammatory responses, which may have translational magnitudes in therapeutic interventions for inflammation-associated diseases (Hangai et al., 2016).

Previous studies (Sharma-Walia et al., 2006, 2010a,b, 2012; George Paul et al., 2010; Paul et al., 2011, 2013a,b) revealed that COX-2 and its metabolite PGE_2 are two pivotal molecules controlling KSHV latency. PGE_2 binds to EP1-4 receptors (Buchanan and DuBois, 2006; Dubois, 2014). KS patient tissue section staining revealed higher levels of PGE_2 receptors EP1-4 and mPGES when compared to tissue sections obtained from healthy controls (George Paul et al., 2010). TIVE-LTC exhibited upregulated expression of EP1, 3, and 4 with downregulated EP2. Blocking EP1 in TIVE-LTC cells reduced KSHV latency protein LANA1 while blocking EP4 downregulated COX-2 gene expression and PGE_2 levels suggesting that KSHV utilizes EP receptors to maintain latency and COX-2/PGE_2 levels. Blocking EP receptors also downregulated several cell signaling molecules such as pPI3K, pPKCζ/λ, Ca2+, pNFκB, and pERK, which impact KSHV infection and pathogenesis (**Figure 4**). EP1 (8-chloro-2-[3-[(2-furalphanylmethyl)thio]-1-oxopropyl] hydralphazide, dibenze [b,f] oxalphazepine-10 (11H)-calpharboxylic acid) and 2 (6-isopropoxy-9-oxoxanthene-2-carboxylic acid) antagonists reduced levels of pSrc. EP1, 2, and 3 antagonists reduced levels of p-PI3K. In addition, EP2 and EP4 (4-(4,9-diethoxy-1, 3-dihydro-1-oxo-2H-benz[f]isoindol-2-yl)-N-(phenylsulfonylbenzenacetamide)) antagonists downregulated p-PKCζ/λ whereas EP1, EP2, and EP4 antagonists treatment abrogated p-NFκB activation (George Paul et al., 2010). The mechanism of EP receptor regulation of LANA1 was found to be linked to its Ca2+ inducing property (George Paul et al., 2010). KSHV induced PGE_2 induced Ca2+ levels, which sequentially

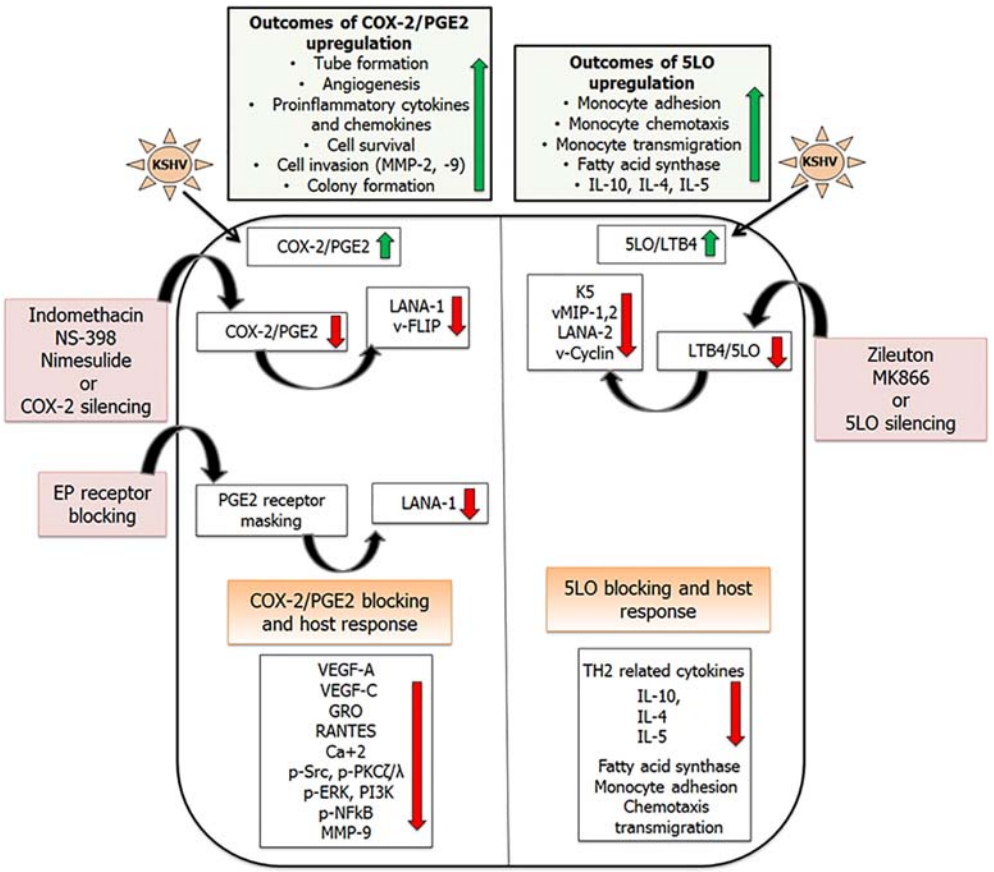

FIGURE 4 | Combating inflammation promoted by KSHV infection: KSHV infection promotes pro-inflammatory lipid mediators of arachidonic acid pathway and the enzymes involved in their synthesis. Inhibiting these lipid mediators and the enzymes involved in their synthesis has shown efficacy in downregulating KSHV latent gene expression. This schematic has been divided into two sections showing inflammatory COX-2 (Sharma-Walia et al., 2006, 2010a,b, 2012; George Paul et al., 2010; Paul et al., 2011, 2013a,b), and LO pathways induced upon KSHV infection (Sharma-Walia et al., 2014). Upregulation of COX-2/PGE_2 in KSHV infected cells promotes tube formation, angiogenesis, pro-inflammatory cytokine and chemokine release, cell survival, and cell invasion. 5LO/LTB_4 upregulation promotes monocyte adhesion, chemotaxis, and transmigration. Reducing the levels of these lipid mediators by using their specific inhibitors (indomethacin, nimesulide, NS-398, Zileuton, MK866), gene silencing, or blocking PGE_2 receptors (EP receptors) showed promise in downregulating KSHV gene expression (LANA1, vFLIP, vCyclin, LANA2, K5, vMIPs), angiogenesis (VEGFs), inflammatory cytokines (GRO, RANTES), and inflammation associated signaling cascades (pSrc, PI3K, and pNFκB; Sharma-Walia et al., 2006, 2010a,b, 2012, 2014; George Paul et al., 2010; Paul et al., 2011, 2013a,b).

enhanced signaling via EP1 receptor (George Paul et al., 2010). PGE_2 then alters the LANA promoter in the −262 and −159 region. Blocking Ca2+ abrogated the effect of PGE_2 induced LANA1 (George Paul et al., 2010). This study helped in understanding latency in a whole new breadth of calcium signaling via EP receptors in KSHV infected cells. This study advanced the role of COX-2 and PGE_2 in latency establishment (George Paul et al., 2010). Studies were performed to understand how blockade of both COX and EP receptors would work in combination to treat KSHV infection and pathogenesis (Paul et al., 2013a). A combination of COX-2 inhibitor celecoxib, EP1 antagonist SC-51322, and EP4 antagonist GW 627368X induced apoptosis and promoted expression of tumor suppressors such as ATM, FHIT, HIC1, MCL1, NCAM1, RASSF1, TIMP2, TIMP3, and TP53 in PEL cells. One of the major issues with this treatment is the risk of thrombotic and cardiovascular events due to the absence of aspirin-like platelet aggregation inhibiting properties (Paul et al., 2013a). Due to the abundance of EP2 and EP4 receptors in cancer, it is considered as an appropriate target for treating breast and colorectal cancer (Reader et al., 2011; Ma et al., 2015). The highly specific and potent EP4 antagonist BGC20-1531 was also under clinical trial for treating headaches caused by a PGE_2 outburst (Cai et al., 1999).

5-Lipoxygenase (5LO), an Enzyme of the Leukotriene Pathway, Upregulated During KSHV Infection

Yet another pro-inflammatory metabolite of the arachidonic acid pathway is leukotriene B4 (LTB_4). Enzyme arachidonate 5-oxidoreductase [EC1.13.11.34] (5LO), its activating protein FLAP (5LO activating protein), and LTA4H are responsible for the synthesis of potent chemotactic LTB_4 (Haeggstrom, 2004). LTB_4 has been shown to impact the immune response

and spread of viral infections, including those caused by HIV, respiratory syncytial virus (RSV), and Epstein-Barr virus (EBV). 5LO, LTA4H, and LTB_4 are found at high levels in most of the inflammation and oxidative stress-associated cancers, such as breast, lung, prostate, pancreatic, colon, bladder, esophageal, and testicular cancers; glioma; chronic myelogenous leukemia; Mantle cell lymphoma (MCL); and NHLs. 5LO pathway inhibitors have been tested as chemoprevention agents in many cancers. Since LTB_4 is linked to inflammation and immune modulation and KS, PEL, and MCD are chronic inflammation-associated malignancies, the regulation of 5LO/LTB_4 cascade was tested as one of the virus's triggered host factors involved in KSHV pathogenesis. It was demonstrated that KSHV infection induces the 5LO/LTB_4 cascade to support its latent infection and in the induction of the inflammatory milieu (Sharma-Walia et al., 2014). Targeting of 5LO/LTB_4 provides a new avenue of treatment against KSHV associated malignancies (Sharma-Walia et al., 2014).

To study the role of 5LO and LTA4H in KS, the skin tissue sections of healthy subjects and KS patients for the presence of 5LO and LTA4H were analyzed. KS patient tissue sections showed higher levels of 5LO and LTA4H when compared to healthy patient tissue sections (Sharma-Walia et al., 2014). 5LO is generally found in the cytoplasm but on activation it moves to the nuclear membrane with the help of FLAP to actively synthesize LTB_4. 5LO also requires Ca2+ or NF-κB for its nuclear translocation. Latently infected TIVE-LTC cells showed a dense staining for 5LO in the nucleus when compared to uninfected TIVE cells (Sharma-Walia et al., 2014). The presence of 5LO in the nucleus determines its active state. This indicated that TIVE-LTC cells have a higher capacity to synthesize LTB_4 when compared to TIVE cells (Sharma-Walia et al., 2014). TIVE-LTC cells also express high levels of LTA4H and FLAP enzymes when compared to TIVE cells (Sharma-Walia et al., 2014). HMVEC-d cells were *de novo* latently infected with KSHV and the status of 5LO pathway genes was examined. When compared to uninfected control HMVEC-d cells, latently infected HMVEC-d cells expressed higher levels of 5LO, LTA4H, and FLAP. Similar upregulation of 5LO pathway enzymes was seen in KSHV infected BCBL-1 than KSHV negative BJAB cells (Sharma-Walia et al., 2014). The induction of 5LO was dependent on the presence of the KSHV transcriptome, as UV-KSHV was unsuccessful in upregulating 5LO levels (Sharma-Walia et al., 2014). As KSHV infection has been shown to enhance levels of enzymes that synthesize LTB_4, the level of this metabolite was measured in latently infected HMVEC-d cells. When compared to uninfected cells, latently infected HMVEC-d cells secreted high levels of LTB_4. Cytoplasmic and nuclear fractions were isolated from KSHV infected HMVEC-d cells and TIVE LTC cells then the levels of 5LO, FLAP, and LTA4H were evaluated against respective controls. When compared to uninfected HMVEC-d cells, KSHV infected HMVEC-d cells showed high levels of 5LO, FLAP, and LTA4H in the nuclear fractions. A similar enrichment of 5LO pathway enzymes was seen in the nuclear fractions of TIVE-LTC when compared to TIVE cells (Sharma-Walia et al., 2014).

INHIBITING 5LO PATHWAY

5 Lipoxygenase is localized in the nucleus as well as the cytosol, but on cellular activation, 5LO undergoes Ca+2 or NF-κB-dependent translocation to the nuclear envelope (Balcarek et al., 1988; Dixon et al., 1988; Funk, 2001; Peters-Golden and Brock, 2001). The mechanism of nuclear translocation involves the necessary association of 5LO with a novel 18-kDa membrane protein known as 5LO-activating protein, or FLAP (Miller et al., 1990). KSHV infection has already been shown to upregulate NF-κB (Cannon et al., 2003; Sadagopan et al., 2007). Treating BCBL-1 cells with NF-κB inhibitor Bay11-7082 has shown to drastically reduce the levels of 5LO (**Figure 4**). 5LO activation also requires Ca2+ for its nuclear translocation. Using Ca2+ inhibitors BAPTA-AM and TMB-8 showed no change in levels of 5LO suggesting that KSHV-induced NF-κB plays an important role in 5LO activation (Sharma-Walia et al., 2014). KSHV infection promoted 5LO and FLAP interaction (Sharma-Walia et al., 2014). Blocking 5LO either by silencing (5LO short hairpin RNA (h) lentiviral particle (5LO)-transduction) or by using inhibitors (MK866 and zileuton) reduced the levels of LTB_4 secreted (Sharma-Walia et al., 2014). MK866 is an orally active anticancer drug that blocks binding of 5LO to the membrane by specifically interacting with the membrane-bound activating protein FLAP, which is necessary for cellular LT biosynthesis (Rouzer et al., 1990). Zileuton is a FDA-approved orally active inhibitor of 5LO and thus inhibits LTB_4 formation. Zileuton is used to prevent difficulty in breathing, chest tightness, wheezing, and coughing due to asthma and has also been tested for its antineoplastic properties in colon, lung, and prostate cancers (Chen et al., 2004; Li et al., 2005). Inhibiting 5LO affected a lot of viral gene expression, including the lytic gene K5, which is involved in the downregulation of major histocompatibility complex class I (MHC1), intercellular adhesion molecule 1 (ICAM-1), and B7.2 (Russo et al., 1996; Neipel et al., 1997). 5LO inhibition also had a significant impact on reducing vMIP-1 and vMIP-2 gene expression as well as downregulates KSHV latent vCyclin and LANA2 gene expression (Sharma-Walia et al., 2014; **Figure 4**). KS lesions are prominent sites for leukocyte infiltration consisting of monocytes, lymphocytes, and mast cells (Ensoli and Sturzl, 1998; Ensoli et al., 2000; Remenyik et al., 2005). KSHV infection has been shown to shift the immune response from a TH1 to a TH2 microenvironment (Stine et al., 2000). 5LO inhibition on the other hand could reverse this by promoting TH1-related cytokines such as interferon gamma (IFNγ) and IL-2 (**Figure 4**). KSHV infection promotes lipogenesis (Bhatt and Damania, 2012) to aid in latency establishment (Delgado et al., 2012). Blocking 5LO reduces lipogenesis and is a target in treating obesity and its related disorders (Neels, 2013). KSHV infection promotes lipogenesis by stimulating fatty acid synthase (FASN) transcription via enhancing the levels of 5LO. Silencing 5LO reversed lipogenesis by lowering FASN promoter activity and its expression (Sharma-Walia et al., 2014). Since FASN, a key enzyme required in lipogenesis, is important in KSHV latency, study (Sharma-Walia et al., 2014) suggested that 5LO/LTB_4 play important roles in KSHV biology and that effective inhibition

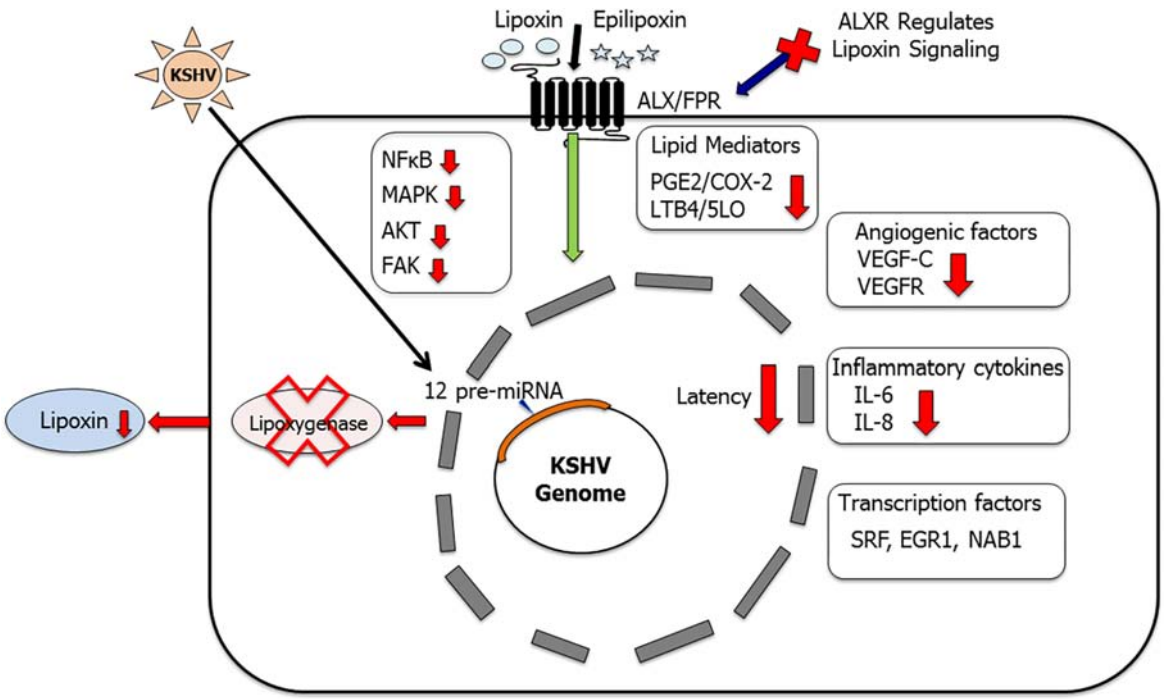

FIGURE 5 | Lipoxins as anti-inflammatory lipid mediators in KSHV infection and pathogenesis: this schematic summarizes our findings (Sharma-Walia et al., 2010b; Marginean and Sharma-Walia, 2015; Chandrasekharan et al., 2016) that KSHV utilizes its miRNA cluster to target enzyme 15 lipoxygenase (15LO) to downregulate anti-inflammatory lipoxin secretion. Treating KSHV infected cells with lipoxins has been shown to provide a more resolving anti-inflammatory microenvironment (Sharma-Walia et al., 2010b; Marginean and Sharma-Walia, 2015; Chandrasekharan et al., 2016). Key inflammatory cytokines IL-6 and IL-8 were downregulated, levels of PGE_2 and LTB_4 were reduced, and several cellular signaling molecules such as NF-κB, AKT, FAK, and ERK levels were also lowered. Lipoxin treatment reduced angiogenic VEGF-C secretion and downregulated the phosphorylation of VEGFR (Marginean and Sharma-Walia, 2015). Lipoxin receptor ALX is a vital component of lipoxin signaling (Chandrasekharan et al., 2016). ALX silencing enhanced KSHV infection-induced NF-κB and ERK activation (Chandrasekharan et al., 2016). Lipoxin treatment also regulates KSHV infection-induced multiple transcription factors such as SRF, EGR1, and NAB1 (Marginean and Sharma-Walia, 2015).

of the 5LO/LTB_4 pathway could potentially be used to control KS/PEL (**Figure 4**).

LIPOXINS AS ANTI-INFLAMMATORY PATHWAYS OF ARACHIDONIC ACID

Kaposi's sarcoma-associated herpesvirus infection apart from triggering a lot of pro-inflammatory molecules of the arachidonic acid pathway also influences anti-inflammatory molecules such as lipoxins (Chandrasekharan et al., 2016). KS-IMM is a human Kaposi's sarcoma tumor-derived cell line (AIDS-KS spindle cells), which was chosen as a model to study the influence of lipoxins on KSHV pathogenesis (Albini et al., 2001). KS-IMM (human Kaposi's sarcoma tumor-derived cell line), which represents KSHV reprogrammed and transformed cells, is a spontaneously immortalized cell line obtained from a KS biopsy (Albini et al., 2001). KS-IMM cells no longer carry the KSHV genome and lack viral latency gene expression but form highly vascularized, rapidly growing tumors when injected into immunocompromised mice. In nude mice, subcutaneously injected KS-IMM cells mixed with matrigel develop palpable tumors. KS cells have been used to test the antiangiogenic, antioxidant, and anti-inflammatory potential of many clinical compounds *in vivo* (Albini et al., 1994, 2001, 2010; De Flora et al., 1996; D'Agostini et al., 1998; Cai et al., 1999; Aluigi et al., 2000; Tosetti et al., 2002; Vannini et al., 2007). It was reported that KS-IMM cells express abundant levels of enzymes COX-2 and 5LO along with their respective metabolites PGE2 and LTB_4 (Marginean and Sharma-Walia, 2015). Similar to the previously published reports (Albini et al., 1994, 1995, 2001; Morini et al., 1999), recent study found that KS-IMM cells have a rich angiogenic and inflammatory microenvironment comprised of cytokines such as IL-6, IL-8, and VEGF-A and VEGF-C (Marginean and Sharma-Walia, 2015). Treating these cells with lipoxins decreased the levels of enzymes COX-2, 5LO, and their metabolites PGE_2 and LTB_4 (Marginean and Sharma-Walia, 2015; **Figure 5**). PGE_2 receptors/EPs, as previously shown to influence KSHV latency, were also affected by lipoxin treatment (Marginean and Sharma-Walia, 2015). The level of EP1 receptor was reduced while EP2 and EP4 did not change on lipoxin treatment of KS-IMM cells (Marginean and Sharma-Walia, 2015). The levels of pro-inflammatory cytokines IL-6 and IL-8 secretion were markedly reduced upon lipoxin treatment of KS-IMM cells (Marginean and Sharma-Walia, 2015; **Figure 5**). A significant decrease in the phosphorylation status of FAK, AKT, NF-κB, and ERK1/2

upon lipoxin treatment was observed (Marginean and Sharma-Walia, 2015). These signaling pathway molecules are generally upregulated during KSHV infection. In addition to influencing signaling molecules, lipoxin treatment also altered the levels of transcription factors to control gene expression of various pro-inflammatory molecules such as interferons, and cytokines (Marginean and Sharma-Walia, 2015). Angiogenic factor VEGF-C secretion was lowered on lipoxin treatment while VEGF-A levels were not affected (Marginean and Sharma-Walia, 2015). VEGFs are primarily involved in endothelial cell tube formation, which was abrogated in cells treated with lipoxins. VEGFs interact with VEGFRs, which consist of three types VEGF-R1, -R2, and -R3 (Neufeld et al., 1996, 1999; Poltorak et al., 1997, 2000). This interaction between VEGF and its receptor promoted KSHV pathogenesis (Montaner et al., 2001; Bais et al., 2003; Zhang et al., 2005; Sivakumar et al., 2008; Dai et al., 2012). When compared to HMVEC-d cells, KS-IMM cells express higher levels of VEGFR2 (Marginean and Sharma-Walia, 2015). Lipoxin treatment of KS-IMM cells markedly reduced the activity (phosphorylation) of VEGFR2 by translocating it from lipid raft to non-lipid raft domains (Marginean and Sharma-Walia, 2015). Lipoxins exert their anti-inflammatory activity by binding to a GPCR called lipoxin A4 receptor/formyl peptidyl receptor (ALX/FPR) (Serhan et al., 1984; Maderna and Godson, 2009). The status of ALXR/FPR was examined on KS-IMM cells. When compared to HMVEC-d cells, KS-IMM cells express reduced numbers of ALXRs (Marginean and Sharma-Walia, 2015).

This study was further expanded to a more relevant model of KSHV infection using HMVEC-d cells. *De novo* KSHV infection in HMVEC-d cells shows a time of infection dependent decrease in lipoxin secretion. Similarly, KSHV positive PEL cell lines including BCBL-1, BC-3 have a reduced level of lipoxin secretion when compared to KSHV negative BJAB cells and healthy B cells (Chandrasekharan et al., 2016). This observation shows that KSHV infection downregulates lipoxin secretion. The role of lipoxin receptor in this process was then studied. Immunohistochemistry of an array of KS patient tissue sections shows that ALXR is widely present in infected cells and the levels of ALXR/FPR in KS cells are like those in healthy cells (Chandrasekharan et al., 2016). Treating latently infected HMVEC-d cells with lipoxin/epilipoxin reduced levels of signaling molecules (NF-κB, AKT, and ERK1/2) as well as pro-inflammatory enzymes and their metabolites (COX-2/PGE_2 and 5LO/LTB_4; Chandrasekharan et al., 2016; **Figure 5**). The ALXR receptor is vital for lipoxin to exert its anti-inflammatory activity. Knocking down ALXR/FPR in Osteosarcoma U2OS cells using CRISPR/CAS9 technology affected lipoxin signaling as high levels of NFKB, AKT, ERK1/2, and inflammatory proteins (COX-2, 5LO) were still persistent in lipoxin treated cells (Chandrasekharan et al., 2016). This observation of increased levels of pro-inflammatory proteins despite lipoxin/epilipoxin treatment could be attributed to the absence of the ALX/FPR receptor.

Since both KS and PEL are associated with latency, the influence of latency genes on lipoxin secretion was studied. Lipoxin secretion was measured in HMVEC-d cells transduced with various viral latency genes such as vCyclin, vFLIP, and LANA1. No significant change in lipoxin secretion was observed when latency genes were expressed in HMVEC-d cells (Chandrasekharan et al., 2016). The latency cluster also contains a group of KSHV 12 pre-miRNAs. To evaluate the effect of KSHV miRNA on lipoxin secretion, EA.hy 926 endothelial cells were modified lentivirally to express KSHV miRNA. As a control, EA.hy cells were lentivirally transduced with GFP. On comparing the lipoxin levels in these lentivirally modified cells, the KSHV miRNA cluster was identified as a potential cause for the observed decrease in lipoxin levels in EA.hy cells carrying KSHV miRNA (Chandrasekharan et al., 2016). miRNAs function by targeting the 3′ end of mRNA for degradation. The KSHV-miRNA cluster was found to lower levels of the enzyme 15LO, which is involved in the synthesis of lipoxins (**Figure 5**). This study identified that KSHV utilizes lipoxin pathway for its own advantage and treating infected cells with lipoxins could be an alternative therapeutic approach (Chandrasekharan et al., 2016). Further studies are required to understand the mechanism of lipoxins action on the KSHV life cycle. Understanding the mechanism of action of lipoxins could help to develop novel therapeutic options for KSHV infection. Our studies on KSHV and lipoxins could be extended to other viral mediated pathogenesis. Lipoxins could possibly be used in conjunction with existing therapeutics to enhance a resolving environment in PEL cells.

CONCLUSION AND PERSPECTIVES

Studies so far have shown that KSHV alters the lipid mediators of the arachidonic acid pathway for its own advantage. Several herpesviruses induce COX-2 expression and PGE_2 production to enhance and establish efficient infection (Shelby et al., 2005). Like KSHV, EBV has also been shown to induce COX-2 (Gandhi et al., 2017). High levels of COX-2 were reported in Hodgkin's lymphoma patients (Al-Salam et al., 2013). This enhanced COX-2 helps in establishing angiogenesis by upregulating VEGF. COX-2 inhibition by NS 398 has been shown to decrease VEGF levels suggesting that COX-2 plays a vital role in angiogenesis (Murono et al., 2001).

With the newly identified clinical manifestations of KSHV infection, KICS, and the IRIS, controlling inflammation could be a key strategy for treating KSHV infected patients (Gasperini et al., 2012; Polizzotto et al., 2012; Ray et al., 2012; Uldrick et al., 2012). KS and IRIS patients show high morbidity (Chandrasekharan et al., 2016). KICS is expected to be an unknown cause of mortality in HIV patients. KICS patients show extremely high levels of IL-6 and IL-10 along with other inflammatory cytokines (Polizzotto et al., 2012; Ray et al., 2012). Arachidonic acid, being a key pathway in inflammation and resolution, is a potential solution to combat KSHV associated pathogenesis. Although KSHV utilizes the pro-inflammatory arm of the arachidonic acid pathway to promote inflammation but anti-inflammatory metabolites from this pathway could be beneficial to treat/resolve inflammation induced by KSHV infection. Hence, understanding how every molecule of this pathway interacts with KSHV is essential to design therapeutic strategies. The arachidonic acid pathway provides multiple

ways of targeting the virus. On one hand, using inhibitors for the inflammatory metabolites/enzymes and on the other hand promoting anti-inflammatory lipid mediators can provide benefits. Further studies are required to understand the other lipid mediators of this pathway and its relation to KSHV. With limitations in the current treatment options for KS and PEL, there is an urge to develop safer, more powerful therapeutics. Although the introduction of HAART therapy significantly reduced death due to KSHV infection, and KSHV is therefore no longer a threat to human health but treating advanced cases of KS, which do not respond to any treatment, is still challenging. Additionally, understanding viral interaction with the host is essential as similar pathways are involved in other pathogenic infections. Current treatment strategies for KS and PEL involve the use of conventional chemotherapeutics such as anthracyclines, antimitotic agents, and microtubule stabilizers, and CHOP (cyclophosphamide, doxorubicin, vincristine, and prednisone) which provide no specific cure for PEL (Okada et al., 2014). Many studies describing specific anti-PEL therapies are underway, which include development of pro-apoptotic agents (proteasome inhibitor bortezomib and azidothymidine), anti-proliferative antibiotic rapamycin, anti-proliferative (PI3K/AKT, NFkB inhibitors), p53 activator nutlin-3a, antiviral compounds cidofovir and interferon-α, and KSHV latency gene blocking agents such as glycyrrhizic acid (GA), and G-quadruplex stabilizers (Hocqueloux et al., 2001; Toomey et al., 2001; An et al., 2004; Curreli et al., 2005; Klass and Offermann, 2005; Luppi et al., 2005; Halfdanarson et al., 2006; Sarek and Ojala, 2007; Sarek et al., 2007; Sin et al., 2007; Carbone et al., 2009; Bhatt et al., 2010; Madireddy et al., 2016). Antiviral drugs such as acyclovir, adefovir, foscarnet, and cidofovir are in clinical use and have shown moderate benefits in reducing viral load (Hocqueloux et al., 2001; Luppi et al., 2005; Halfdanarson et al., 2006). KSHV is commonly co-infected with HIV and effective control of the latter by HAART therapy has been shown to be effective; however, treating advanced KS remains a problem (Casper, 2008).

AUTHOR CONTRIBUTIONS

Both authors equally contributed to review organization, concept, interpretation of studies, and drafting the figures.

FUNDING

We are grateful to funding from H.M. Bligh Cancer Research Laboratories and NIH-funded grant R01CA 192970 to NS-W. The funders had no role in design, decision to publish, or preparation of the manuscript.

ACKNOWLEDGMENTS

NS-W gratefully acknowledges all the valuable scientific contributions made by Prof. Bala Chandran, Dr. Arun George Paul, Dr. Mohanan Valiya Veettil, Dr. Kinjan Patel, Dr. Karthic Chandran, Dr. Alexandru Marginean, Dr. Virginie Bottero, Dr. Nagaraj Kerur, Dr. Sathish Sadagopan, Dr. Waseem Ahmad, Dr. Xiao M. Huang, Dr. Alexander C. Hwang, Dr. Kumari Asha, Ms. Miroslava Repak, Ms. Sabrina Najibi and Ms. Olivia Powrozek. NS-W apologizes to all the colleagues whose work could not be cited in this manuscript.

REFERENCES

Agard, M., Asakrah, S., and Morici, L. A. (2013). PGE(2) suppression of innate immunity during mucosal bacterial infection. *Front. Cell. Infect. Microbiol.* 3:45. doi: 10.3389/fcimb.2013.00045

Albini, A., D'Agostini, F., Giunciuglio, D., Paglieri, I., Balansky, R., and De Flora, S. (1995). Inhibition of invasion, gelatinase activity, tumor take and metastasis of malignant cells by N-acetylcysteine. *Int. J. Cancer* 61, 121–129. doi: 10.1002/ijc.2910610121

Albini, A., Fontanini, G., Masiello, L., Tacchetti, C., Bigini, D., Luzzi, P., et al. (1994). Angiogenic potential in vivo by Kaposi's sarcoma cell-free supernatants and HIV-1 tat product: inhibition of KS-like lesions by tissue inhibitor of metalloproteinase-2. *Aids* 8, 1237–1244. doi: 10.1097/00002030-199409000-00004

Albini, A., Morini, M., D'Agostini, F., Ferrari, N., Campelli, F., Arena, G., et al. (2001). Inhibition of angiogenesis-driven Kaposi's sarcoma tumor growth in nude mice by oral N-acetylcysteine. *Cancer Res.* 61, 8171–8178.

Albini, A., Pennesi, G., Donatelli, F., Cammarota, R., De Flora, S., and Noonan, D. M. (2010). Cardiotoxicity of anticancer drugs: the need for cardio-oncology and cardio-oncological prevention. *J. Natl. Cancer Inst.* 102, 14–25. doi: 10.1093/jnci/djp440

Al-Salam, S., Awwad, A., Sudhadevi, M., Daoud, S., Nagelkerke, N. J., Castella, A., et al. (2013). Epstein-Barr virus infection correlates with the expression of COX-2, p16(INK4A) and p53 in classic Hodgkin lymphoma. *Int. J. Clin. Exp. Pathol.* 6, 2765–2777.

Aluigi, M. G., De Flora, S., D'Agostini, F., Albini, A., and Fassina, G. (2000). Antiapoptotic and antigenotoxic effects of N-acetylcysteine in human cells of endothelial origin. *Anticancer Res.* 20, 3183–3187.

An, J., Sun, Y., Fisher, M., and Rettig, M. B. (2004). Antitumor effects of bortezomib (PS-341) on primary effusion lymphomas. *Leukemia* 18, 1699–1704. doi: 10.1038/sj.leu.2403460

Aronoff, D. M., Canetti, C., and Peters-Golden, M. (2004). Prostaglandin E2 inhibits alveolar macrophage phagocytosis through an E-prostanoid 2 receptor-mediated increase in intracellular cyclic AMP. *J. Immunol.* 173, 559–565. doi: 10.4049/jimmunol.173.1.559

Bais, C., Van Geelen, A., Eroles, P., Mutlu, A., Chiozzini, C., Dias, S., et al. (2003). Kaposi's sarcoma associated herpesvirus G protein-coupled receptor immortalizes human endothelial cells by activation of the VEGF receptor-2/KDR. *Cancer Cell* 3, 131–143. doi: 10.1016/S1535-6108(03)00024-2

Balcarek, J. M., Theisen, T. W., Cook, M. N., Varrichio, A., Hwang, S. M., Strohsacker, M. W., et al. (1988). Isolation and characterization of a cDNA clone encoding rat 5-lipoxygenase. *J. Biol. Chem.* 263, 13937–13941.

Ballinger, M. N., Aronoff, D. M., McMillan, T. R., Cooke, K. R., Olkiewicz, K., Toews, G. B., et al. (2006). Critical role of prostaglandin E2 overproduction in impaired pulmonary host response following bone marrow transplantation. *J. Immunol.* 177, 5499–5508. doi: 10.4049/jimmunol.177.8.5499

Bankhurst, A. D. (1982). The modulation of human natural killer cell activity by prostaglandins. *J. Clin. Lab. Immunol.* 7, 85–91.

Bennett, M., and Gilroy, D. W. (2016). Lipid mediators in inflammation. *Microbiol. Spectr.* 4: MCHD-0035-2016.

Bhatt, A. P., Bhende, P. M., Sin, S. H., Roy, D., Dittmer, D. P., and Damania, B. (2010). Dual inhibition of PI3K and mTOR inhibits autocrine and paracrine proliferative loops in PI3K/Akt/mTOR-addicted lymphomas. *Blood* 115, 4455–4463. doi: 10.1182/blood-2009-10-251082

Bhatt, A. P., and Damania, B. (2012). AKTivation of PI3K/AKT/mTOR signaling pathway by KSHV. *Front. Immunol.* 3:401. doi: 10.3389/fimmu.2012.00401

Boshoff, C., Schulz, T. F., Kennedy, M. M., Graham, A. K., Fisher, C., Thomas, A., et al. (1995a). Kaposi's sarcoma-associated herpesvirus infects endothelial and spindle cells. *Nat. Med.* 1, 1274–1278. doi: 10.1038/nm1295-1274

Boshoff, C., Whitby, D., Hatziioannou, T., Fisher, C., van der Walt, J., Hatzakis, A., et al. (1995b). Kaposi's-sarcoma-associated herpesvirus in HIV-negative Kaposi's sarcoma. *Lancet* 345, 1043–1044. doi: 10.1016/S0140-6736(95)90780-7

Botti, G., Fratangelo, F., Cerrone, M., Liguori, G., Cantile, M., Anniciello, A. M., et al. (2017). COX-2 expression positively correlates with PD-L1 expression in human melanoma cells. *J. Transl. Med.* 15:46. doi: 10.1186/s12967-017-1150-7

Botting, R. M. (2010). Vane's discovery of the mechanism of action of aspirin changed our understanding of its clinical pharmacology. *Pharmacol. Rep.* 62, 518–525. doi: 10.1016/S1734-1140(10)70308-X

Buchanan, F. G., and DuBois, R. N. (2006). Connecting COX-2 and Wnt in cancer. *Cancer Cell* 9, 6–8. doi: 10.1016/j.ccr.2005.12.029

Cai, T., Fassina, G., Morini, M., Aluigi, M. G., Masiello, L., Fontanini, G., et al. (1999). N-acetylcysteine inhibits endothelial cell invasion and angiogenesis. *Lab. Invest.* 79, 1151–1159.

Cannon, M., Philpott, N. J., and Cesarman, E. (2003). The Kaposi's sarcoma-associated herpesvirus G protein-coupled receptor has broad signaling effects in primary effusion lymphoma cells. *J. Virol.* 77, 57–67. doi: 10.1128/JVI.77.1.57-67.2003

Carbone, A., Cesarman, E., Spina, M., Gloghini, A., and Schulz, T. F. (2009). HIV-associated lymphomas and gamma-herpesviruses. *Blood* 113, 1213–1224. doi: 10.1182/blood-2008-09-180315

Casper, C. (2008). New approaches to the treatment of human herpesvirus 8-associated disease. *Rev. Med. Virol.* 18, 321–329. doi: 10.1002/rmv.583

Cesarman, E., Chang, Y., Moore, P. S., Said, J. W., and Knowles, D. M. (1995). Kaposi's sarcoma-associated herpesvirus-like DNA sequences in AIDS-related body-cavity-based lymphomas. *N. Engl. J. Med.* 332, 1186–1191. doi: 10.1056/NEJM199505043321802

Cesarman, E., and Knowles, D. M. (1999). The role of Kaposi's sarcoma-associated herpesvirus (KSHV/HHV-8) in lymphoproliferative diseases. *Semin. Cancer Biol.* 9, 165–174. doi: 10.1006/scbi.1998.0118

Chandrasekharan, J. A., Huang, X. M., Hwang, A. C., and Sharma-Walia, N. (2016). Altering the anti-inflammatory lipoxin microenvironment: a new insight into Kaposi's sarcoma-associated herpesvirus pathogenesis. *J. Virol.* 90, 11020–11031. doi: 10.1128/JVI.01491-16

Chandrasekharan, J. A., and Sharma-Walia, N. (2015). Lipoxins: nature's way to resolve inflammation. *J. Inflamm. Res.* 8, 181–192. doi: 10.2147/JIR.S90380

Chang, Y., Cesarman, E., Pessin, M. S., Lee, F., Culpepper, J., Knowles, D. M., et al. (1994). Identification of herpesvirus-like DNA sequences in AIDS-associated Kaposi's sarcoma. *Science* 266, 1865–1869. doi: 10.1126/science.7997879

Chemnitz, J. M., Driesen, J., Classen, S., Riley, J. L., Debey, S., Beyer, M., et al. (2006). Prostaglandin E2 impairs CD4+ T cell activation by inhibition of lck: implications in Hodgkin's lymphoma. *Cancer Res.* 66, 1114–1122. doi: 10.1158/0008-5472.CAN-05-3252

Chen, X., Wang, S., Wu, N., Sood, S., Wang, P., Jin, Z., et al. (2004). Overexpression of 5-lipoxygenase in rat and human esophageal adenocarcinoma and inhibitory effects of zileuton and celecoxib on carcinogenesis. *Clin. Cancer Res.* 10, 6703–6709. doi: 10.1158/1078-0432.CCR-04-0838

Chen, Y. B., Rahemtullah, A., and Hochberg, E. (2007). Primary effusion lymphoma. *Oncologist* 12, 569–576. doi: 10.1634/theoncologist.12-5-569

Chiu, Y. F., Sugden, A. U., Fox, K., Hayes, M., and Sugden, B. (2017). Kaposi's sarcoma-associated herpesvirus stably clusters its genomes across generations to maintain itself extrachromosomally. *J. Cell Biol.* 216, 2745–2758. doi: 10.1083/jcb.201702013

Curreli, F., Friedman-Kien, A. E., and Flore, O. (2005). Glycyrrhizic acid alters Kaposi sarcoma-associated herpesvirus latency, triggering p53-mediated apoptosis in transformed B lymphocytes. *J. Clin. Invest.* 115, 642–652. doi: 10.1172/JCI200523334

D'Agostini, F., Bagnasco, M., Giunciuglio, D., Albini, A., and De Flora, S. (1998). Inhibition by oral N-acetylcysteine of doxorubicin-induced clastogenicity and alopecia, and prevention of primary tumors and lung micrometastases in mice. *Int. J. Oncol.* 13, 217–224. doi: 10.3892/ijo.13.2.217

Dai, L., Bratoeva, M., Toole, B. P., Qin, Z., and Parsons, C. (2012). KSHV activation of VEGF secretion and invasion for endothelial cells is mediated through viral upregulation of emmprin-induced signal transduction. *Int. J. Cancer* 131, 834–843. doi: 10.1002/ijc.26428

De Flora, S., D'Agostini, F., Masiello, L., Giunciuglio, D., and Albini, A. (1996). Synergism between N-acetylcysteine and doxorubicin in the prevention of tumorigenicity and metastasis in murine models. *Int. J. Cancer* 67, 842–848. doi: 10.1002/(SICI)1097-0215(19960917)67:6<842::AID-IJC14>3.0.CO;2-3

De Paoli, P., and Carbone, A. (2016). Kaposi's Sarcoma Herpesvirus: twenty years after its discovery. *Eur. Rev. Med. Pharmacol. Sci.* 20, 1288–1294.

Delgado, T., Sanchez, E. L., Camarda, R., and Lagunoff, M. (2012). Global metabolic profiling of infection by an oncogenic virus: KSHV induces and requires lipogenesis for survival of latent infection. *PLoS Pathog.* 8:e1002866. doi: 10.1371/journal.ppat.1002866

Deng, H., Young, A., and Sun, R. (2000). Auto-activation of the rta gene of human herpesvirus-8/Kaposi's sarcoma-associated herpesvirus. *J. Gen. Virol.* 81, 3043–3048. doi: 10.1099/0022-1317-81-12-3043

Dixon, R. A., Jones, R. E., Diehl, R. E., Bennett, C. D., Kargman, S., and Rouzer, C. A. (1988). Cloning of the cDNA for human 5-lipoxygenase. *Proc. Natl. Acad. Sci. U.S.A.* 85, 416–420. doi: 10.1073/pnas.85.2.416

Dubois, R. N. (2014). Role of inflammation and inflammatory mediators in colorectal cancer. *Trans. Am. Clin. Climatol. Assoc.* 125, 358–372. discussion 372–353,

Dubois, R. N., Abramson, S. B., Crofford, L., Gupta, R. A., Simon, L. S., Van De Putte, L. B., et al. (1998). Cyclooxygenase in biology and disease. *FASEB J.* 12, 1063–1073. doi: 10.1096/fasebj.12.12.1063

Ensoli, B., and Sturzl, M. (1998). Kaposi's sarcoma: a result of the interplay among inflammatory cytokines, angiogenic factors and viral agents. *Cytokine Growth Factor Rev.* 9, 63–83. doi: 10.1016/S1359-6101(97)00037-3

Ensoli, B., Sturzl, M., and Monini, P. (2000). Cytokine-mediated growth promotion of Kaposi's sarcoma and primary effusion lymphoma. *Semin. Cancer Biol.* 10, 367–381. doi: 10.1006/scbi.2000.0329

Fanning, L. B., and Boyce, J. A. (2013). Lipid mediators and allergic diseases. *Ann. Allergy Asthma Immunol.* 111, 155–162. doi: 10.1016/j.anai.2013.06.031

Fitzpatrick, F. A. (2004). Cyclooxygenase enzymes: regulation and function. *Curr. Pharm. Des.* 10, 577–588. doi: 10.2174/1381612043453144

Funk, C. D. (2001). Prostaglandins and leukotrienes: advances in eicosanoid biology. *Science* 294, 1871–1875. doi: 10.1126/science.294.5548.1871

Gandhi, J., Khera, L., Gaur, N., Paul, C., and Kaul, R. (2017). Role of modulator of inflammation cyclooxygenase-2 in Gammaherpesvirus mediated Tumorigenesis. *Front. Microbiol.* 8:538. doi: 10.3389/fmicb.2017.00538

Ganem, D. (2010). KSHV and the pathogenesis of Kaposi sarcoma: listening to human biology and medicine. *J. Clin. Invest.* 120, 939–949. doi: 10.1172/JCI40567

Gasperini, P., Espigol-Frigole, G., McCormick, P. J., Salvucci, O., Maric, D., Uldrick, T. S., et al. (2012). Kaposi sarcoma herpesvirus promotes endothelial-to-mesenchymal transition through Notch-dependent signaling. *Cancer Res.* 72, 1157–1169. doi: 10.1158/0008-5472.CAN-11-3067

George Paul, A., Sharma-Walia, N., Kerur, N., White, C., and Chandran, B. (2010). Piracy of prostaglandin E2/EP receptor-mediated signaling by Kaposi's sarcoma-associated herpes virus (HHV-8) for latency gene expression: strategy of a successful pathogen. *Cancer Res.* 70, 3697–3708. doi: 10.1158/0008-5472.CAN-09-3934

Ghosh, R., Alajbegovic, A., and Gomes, A. V. (2015). NSAIDs and cardiovascular diseases: role of reactive oxygen species. *Oxid. Med. Cell. Longev.* 2015:536962. doi: 10.1155/2015/536962

Gobeil, F. Jr., Vazquez-Tello, A., Marrache, A. M., Bhattacharya, M., Checchin, D., Bkaily, G., et al. (2003). Nuclear prostaglandin signaling system: biogenesis and actions via heptahelical receptors. *Can. J. Physiol. Pharmacol.* 81, 196–204. doi: 10.1139/y02-163

Gobeil, F., Fortier, A., Zhu, T., Bossolasco, M., Leduc, M., Grandbois, M., et al. (2006). G-protein-coupled receptors signalling at the cell nucleus: an emerging paradigm. *Can. J. Physiol. Pharmacol.* 84, 287–297. doi: 10.1139/y05-127

Gomi, K., Zhu, F. G., and Marshall, J. S. (2000). Prostaglandin E2 selectively enhances the IgE-mediated production of IL-6 and granulocyte-macrophage colony-stimulating factor by mast cells through an EP1/EP3-dependent mechanism. *J. Immunol.* 165, 6545–6552. doi: 10.4049/jimmunol.165.11.6545

Goto, T., Herberman, R. B., Maluish, A., and Strong, D. M. (1983). Cyclic AMP as a mediator of prostaglandin E-induced suppression of human natural killer cell activity. *J. Immunol.* 130, 1350–1355.

Gottwein, E. (2012). Kaposi's Sarcoma-associated herpesvirus microRNAs. *Front. Microbiol.* 3:165. doi: 10.3389/fmicb.2012.00165

Greene, E. R., Huang, S., Serhan, C. N., and Panigrahy, D. (2011). Regulation of inflammation in cancer by eicosanoids. *Prostaglandins Other Lipid Mediat.* 96, 27–36. doi: 10.1016/j.prostaglandins.2011.08.004

Greene, W., Kuhne, K., Ye, F., Chen, J., Zhou, F., Lei, X., et al. (2007). Molecular biology of KSHV in relation to AIDS-associated oncogenesis. *Cancer Treat. Res.* 133, 69–127. doi: 10.1007/978-0-387-46816-7_3

Grosch, S., Niederberger, E., and Geisslinger, G. (2017). Investigational drugs targeting the prostaglandin E2 signaling pathway for the treatment of inflammatory pain. *Expert Opin. Investig. Drugs* 26, 51–61. doi: 10.1080/13543784.2017.1260544

Haas, D. A., Bala, K., Busche, G., Weidner-Glunde, M., Santag, S., Kati, S., et al. (2013). The inflammatory kinase MAP4K4 promotes reactivation of Kaposi's sarcoma herpesvirus and enhances the invasiveness of infected endothelial cells. *PLoS Pathog.* 9:e1003737. doi: 10.1371/journal.ppat.1003737

Haeggstrom, J. Z. (2004). Leukotriene A4 hydrolase/aminopeptidase, the gatekeeper of chemotactic leukotriene B4 biosynthesis. *J. Biol. Chem.* 279, 50639–50642. doi: 10.1074/jbc.R400027200

Halfdanarson, T. R., Markovic, S. N., Kalokhe, U., and Luppi, M. (2006). A non-chemotherapy treatment of a primary effusion lymphoma: durable remission after intracavitary cidofovir in HIV negative PEL refractory to chemotherapy. *Ann. Oncol.* 17, 1849–1850. doi: 10.1093/annonc/mdl139

Hangai, S., Ao, T., Kimura, Y., Matsuki, K., Kawamura, T., Negishi, H., et al. (2016). PGE2 induced in and released by dying cells functions as an inhibitory DAMP. *Proc. Natl. Acad. Sci. U.S.A.* 113, 3844–3849. doi: 10.1073/pnas.1602023113

Harizi, H., Grosset, C., and Gualde, N. (2003). Prostaglandin E2 modulates dendritic cell function via EP2 and EP4 receptor subtypes. *J. Leukoc. Biol.* 73, 756–763. doi: 10.1189/jlb.1002483

Heusinkveld, M., de Vos van Steenwijk, P. J., Goedemans, R., Ramwadhdoebe, T. H., Gorter, A., Welters, M. J., et al. (2011). M2 macrophages induced by prostaglandin E2 and IL-6 from cervical carcinoma are switched to activated M1 macrophages by CD4+ Th1 cells. *J. Immunol.* 187, 1157–1165. doi: 10.4049/jimmunol.1100889

Hocqueloux, L., Agbalika, F., Oksenhendler, E., and Molina, J. M. (2001). Long-term remission of an AIDS-related primary effusion lymphoma with antiviral therapy. *Aids* 15, 280–282. doi: 10.1097/00002030-200101260-00023

Holt, D. M., Ma, X., Kundu, N., Collin, P. D., and Fulton, A. M. (2012). Modulation of host natural killer cell functions in breast cancer via prostaglandin E2 receptors EP2 and EP4. *J. Immunother.* 35, 179–188. doi: 10.1097/CJI.0b013e318247a5e9

Hu, J., Garber, A. C., and Renne, R. (2002). The latency-associated nuclear antigen of Kaposi's sarcoma-associated herpesvirus supports latent DNA replication in dividing cells. *J. Virol.* 76, 11677–11687. doi: 10.1128/JVI.76.22.11677-11687.2002

Hu, Z. Q., Asano, K., Seki, H., and Shimamura, T. (1995). An essential role of prostaglandin E on mouse mast cell induction. *J. Immunol.* 155, 2134–2142.

Hyde, C. A., and Missailidis, S. (2009). Inhibition of arachidonic acid metabolism and its implication on cell proliferation and tumour-angiogenesis. *Int. Immunopharmacol.* 9, 701–715. doi: 10.1016/j.intimp.2009.02.003

Iniguez, M. A., Martinez-Martinez, S., Punzon, C., Redondo, J. M., and Fresno, M. (2000). An essential role of the nuclear factor of activated T cells in the regulation of the expression of the cyclooxygenase-2 gene in human T lymphocytes. *J. Biol. Chem.* 275, 23627–23635. doi: 10.1074/jbc.M001381200

Iniguez, M. A., Punzon, C., and Fresno, M. (1999). Induction of cyclooxygenase-2 on activated T lymphocytes: regulation of T cell activation by cyclooxygenase-2 inhibitors. *J. Immunol.* 163, 111–119.

Jendrossek, V. (2013). Targeting apoptosis pathways by Celecoxib in cancer. *Cancer Lett.* 332, 313–324. doi: 10.1016/j.canlet.2011.01.012

Jenner, R. G., Alba, M. M., Boshoff, C., and Kellam, P. (2001). Kaposi's sarcoma-associated herpesvirus latent and lytic gene expression as revealed by DNA arrays. *J. Virol.* 75, 891–902. doi: 10.1128/JVI.75.2.891-902.2001

Kalinski, P. (2012). Regulation of immune responses by prostaglandin E2. *J. Immunol.* 188, 21–28. doi: 10.4049/jimmunol.1101029

Kalinski, P., Hilkens, C. M., Snijders, A., Snijdewint, F. G., and Kapsenberg, M. L. (1997). IL-12-deficient dendritic cells, generated in the presence of prostaglandin E2, promote type 2 cytokine production in maturing human naive T helper cells. *J. Immunol.* 159, 28–35.

Kalt, I., Masa, S. R., and Sarid, R. (2009). Linking the Kaposi's sarcoma-associated herpesvirus (KSHV/HHV-8) to human malignancies. *Methods Mol. Biol.* 471, 387–407. doi: 10.1007/978-1-59745-416-2_19

Katoh, H., Watabe, A., Sugimoto, Y., Ichikawa, A., and Negishi, M. (1995). Characterization of the signal transduction of prostaglandin E receptor EP1 subtype in cDNA-transfected Chinese hamster ovary cells. *Biochim. Biophys. Acta* 1244, 41–48. doi: 10.1016/0304-4165(94)00182-W

Klass, C. M., and Offermann, M. K. (2005). Targeting human herpesvirus-8 for treatment of Kaposi's sarcoma and primary effusion lymphoma. *Curr. Opin. Oncol.* 17, 447–455. doi: 10.1097/01.cco.0000172823.01190.6c

Krishnan, H. H., Naranatt, P. P., Smith, M. S., Zeng, L., Bloomer, C., and Chandran, B. (2004). Concurrent expression of latent and a limited number of lytic genes with immune modulation and antiapoptotic function by Kaposi's sarcoma-associated herpesvirus early during infection of primary endothelial and fibroblast cells and subsequent decline of lytic gene expression. *J. Virol.* 78, 3601–3620. doi: 10.1128/JVI.78.7.3601-3620.2004

Lee, I. Y., Cho, W., Kim, J., Park, C. S., and Choe, J. (2008). Human follicular dendritic cells interact with T cells via expression and regulation of cyclooxygenases and prostaglandin E and I synthases. *J. Immunol.* 180, 1390–1397. doi: 10.4049/jimmunol.180.3.1390

Li, N., Sood, S., Wang, S., Fang, M., Wang, P., Sun, Z., et al. (2005). Overexpression of 5-lipoxygenase and cyclooxygenase 2 in hamster and human oral cancer and chemopreventive effects of zileuton and celecoxib. *Clin. Cancer Res.* 11, 2089–2096. doi: 10.1158/1078-0432.CCR-04-1684

Luppi, M., Trovato, R., Barozzi, P., Vallisa, D., Rossi, G., Re, A., et al. (2005). Treatment of herpesvirus associated primary effusion lymphoma with intracavity cidofovir. *Leukemia* 19, 473–476. doi: 10.1038/sj.leu.2403646

Ma, X., Aoki, T., Tsuruyama, T., and Narumiya, S. (2015). Definition of prostaglandin E2-EP2 signals in the colon tumor microenvironment that amplify inflammation and tumor growth. *Cancer Res.* 75, 2822–2832. doi: 10.1158/0008-5472.CAN-15-0125

Maderna, P., and Godson, C. (2009). Lipoxins: resolutionary road. *Br. J. Pharmacol.* 158, 947–959. doi: 10.1111/j.1476-5381.2009.00386.x

Madireddy, A., Purushothaman, P., Loosbroock, C. P., Robertson, E. S., Schildkraut, C. L., and Verma, S. C. (2016). G-quadruplex-interacting compounds alter latent DNA replication and episomal persistence of KSHV. *Nucleic Acids Res.* 44, 3675–3694. doi: 10.1093/nar/gkw038

Mailliard, R. B., Alber, S. M., Shen, H., Watkins, S. C., Kirkwood, J. M., Herberman, R. B., et al. (2005). IL-18-induced CD83+CCR7+ NK helper cells. *J. Exp. Med.* 202, 941–953. doi: 10.1084/jem.20050128

Marginean, A., and Sharma-Walia, N. (2015). Lipoxins exert antiangiogenic and anti-inflammatory effects on Kaposi's sarcoma cells. *Transl. Res.* 166, 111–133. doi: 10.1016/j.trsl.2015.02.009

Mariggio, G., Koch, S., and Schulz, T. F. (2017). Kaposi sarcoma herpesvirus pathogenesis. *Philos. Trans. R. Soc. Lond. B Biol. Sci.* 372:20160275. doi: 10.1098/rstb.2016.0275

Markovic, T., Jakopin, Z., Dolenc, M. S., and Mlinaric-Rascan, I. (2017). Structural features of subtype-selective EP receptor modulators. *Drug Discov. Today* 22, 57–71. doi: 10.1016/j.drudis.2016.08.003

Matta, H., Surabhi, R. M., Zhao, J., Punj, V., Sun, Q., Schamus, S., et al. (2007). Induction of spindle cell morphology in human vascular endothelial cells by human herpesvirus 8-encoded viral FLICE inhibitory protein K13. *Oncogene* 26, 1656–1660. doi: 10.1038/sj.onc.1209931

Mesri, E. A. (1999). Inflammatory reactivation and angiogenicity of Kaposi's sarcoma-associated herpesvirus/HHV8: a missing link in the pathogenesis of acquired immunodeficiency syndrome-associated Kaposi's sarcoma. *Blood* 93, 4031–4033.

Mesri, E. A., Cesarman, E., and Boshoff, C. (2010). Kaposi's sarcoma and its associated herpesvirus. *Nat. Rev. Cancer* 10, 707–719. doi: 10.1038/nrc2888

Miao, J., Lu, X., Hu, Y., Piao, C., Wu, X., Liu, X., et al. (2017). Prostaglandin E2 and PD-1 mediated inhibition of antitumor CTL responses in the human tumor microenvironment. *Oncotarget* 8, 89802–89810. doi: 10.18632/oncotarget.21155

Miller, D. K., Gillard, J. W., Vickers, P. J., Sadowski, S., Leveille, C., Mancini, J. A., et al. (1990). Identification and isolation of a membrane protein necessary for leukotriene production. *Nature* 343, 278–281. doi: 10.1038/343278a0

Montaner, S., Sodhi, A., Pece, S., Mesri, E. A., and Gutkind, J. S. (2001). The Kaposi's sarcoma-associated herpesvirus G protein-coupled receptor promotes endothelial cell survival through the activation of Akt/protein kinase B. *Cancer Res.* 61, 2641–2648.

Morini, M., Cai, T., Aluigi, M. G., Noonan, D. M., Masiello, L., De Flora, S., et al. (1999). The role of the thiol N-acetylcysteine in the prevention of tumor invasion and angiogenesis. *Int. J. Biol. Markers* 14, 268–271. doi: 10.1177/172460089901400413

Murono, S., Inoue, H., Tanabe, T., Joab, I., Yoshizaki, T., Furukawa, M., et al. (2001). Induction of cyclooxygenase-2 by Epstein-Barr virus latent membrane protein 1 is involved in vascular endothelial growth factor production in nasopharyngeal carcinoma cells. *Proc. Natl. Acad. Sci. U.S.A.* 98, 6905–6910. doi: 10.1073/pnas.121016998

Murtadak, V., Becker, C., and Sturzl, M. (2015). Cell death inhibition by KSHV. *Aging* 7, 750–751. doi: 10.18632/aging.100829

Nakayama, T., Mutsuga, N., Yao, L., and Tosato, G. (2006). Prostaglandin E2 promotes degranulation-independent release of MCP-1 from mast cells. *J. Leukoc. Biol.* 79, 95–104. doi: 10.1189/jlb.0405226

Naranatt, P. P., Krishnan, H. H., Svojanovsky, S. R., Bloomer, C., Mathur, S., and Chandran, B. (2004). Host gene induction and transcriptional reprogramming in Kaposi's sarcoma-associated herpesvirus (KSHV/HHV-8)-infected endothelial, fibroblast, and B cells: insights into modulation events early during infection. *Cancer Res.* 64, 72–84. doi: 10.1158/0008-5472.CAN-03-2767

Neels, J. G. (2013). A role for 5-lipoxygenase products in obesity-associated inflammation and insulin resistance. *Adipocyte* 2, 262–265. doi: 10.4161/adip.24835

Neipel, F., Albrecht, J. C., and Fleckenstein, B. (1997). Cell-homologous genes in the Kaposi's sarcoma-associated rhadinovirus human herpesvirus 8: determinants of its pathogenicity? *J. Virol.* 71, 4187–4192.

Neufeld, G., Cohen, T., Gengrinovitch, S., and Poltorak, Z. (1999). Vascular endothelial growth factor (VEGF) and its receptors. *FASEB J.* 13, 9–22. doi: 10.1096/fasebj.13.1.9

Neufeld, G., Cohen, T., Gitay-Goren, H., Poltorak, Z., Tessler, S., Sharon, R., et al. (1996). Similarities and differences between the vascular endothelial growth factor (VEGF) splice variants. *Cancer Metastasis Rev.* 15, 153–158. doi: 10.1007/BF00437467

Obermajer, N., Muthuswamy, R., Lesnock, J., Edwards, R. P., and Kalinski, P. (2011). Positive feedback between PGE2 and COX2 redirects the differentiation of human dendritic cells toward stable myeloid-derived suppressor cells. *Blood* 118, 5498–5505. doi: 10.1182/blood-2011-07-365825

Okada, S., Goto, H., and Yotsumoto, M. (2014). Current status of treatment for primary effusion lymphoma. *Intractable Rare Dis. Res.* 3, 65–74. doi: 10.5582/irdr.2014.01010

Park, A., Lee, Y., Kim, M. S., Kang, Y. J., Park, Y. J., Jung, H., et al. (2018). Prostaglandin E2 secreted by thyroid cancer cells contributes to immune escape through the suppression of natural killer (NK) cell cytotoxicity and NK cell differentiation. *Front. Immunol.* 9:1859. doi: 10.3389/fimmu.2018.01859

Paul, A. G., Chandran, B., and Sharma-Walia, N. (2013a). Concurrent targeting of eicosanoid receptor 1/eicosanoid receptor 4 receptors and COX-2 induces synergistic apoptosis in Kaposi's sarcoma-associated herpesvirus and Epstein-Barr virus associated non-Hodgkin lymphoma cell lines. *Transl. Res.* 161, 447–468. doi: 10.1016/j.trsl.2013.02.008

Paul, A. G., Chandran, B., and Sharma-Walia, N. (2013b). Cyclooxygenase-2-prostaglandin E2-eicosanoid receptor inflammatory axis: a key player in Kaposi's sarcoma-associated herpes virus associated malignancies. *Transl. Res.* 162, 77–92. doi: 10.1016/j.trsl.2013.03.004

Paul, A. G., Sharma-Walia, N., and Chandran, B. (2011). Targeting KSHV/HHV-8 latency with COX-2 selective inhibitor nimesulide: a potential chemotherapeutic modality for primary effusion lymphoma. *PLoS One* 6:e24379. doi: 10.1371/journal.pone.0024379

Pawlosky, N. (2013). Cardiovascular risk: Are all NSAIDs alike? *Can. Pharm. J.* 146, 80–83. doi: 10.1177/1715163513481569

Peters-Golden, M., and Brock, T. G. (2001). Intracellular compartmentalization of leukotriene synthesis: unexpected nuclear secrets. *FEBS Lett.* 487, 323–326. doi: 10.1016/S0014-5793(00)02374-7

Polizzotto, M. N., Uldrick, T. S., Hu, D., and Yarchoan, R. (2012). Clinical manifestations of kaposi sarcoma herpesvirus lytic activation: multicentric Castleman disease (KSHV-MCD) and the KSHV inflammatory cytokine syndrome. *Front. Microbiol.* 3:73. doi: 10.3389/fmicb.2012.00073

Poltorak, Z., Cohen, T., and Neufeld, G. (2000). The VEGF splice variants: properties, receptors, and usage for the treatment of ischemic diseases. *Herz* 25, 126–129. doi: 10.1007/PL00001950

Poltorak, Z., Cohen, T., Sivan, R., Kandelis, Y., Spira, G., Vlodavsky, I., et al. (1997). VEGF145, a secreted vascular endothelial growth factor isoform that binds to extracellular matrix. *J. Biol. Chem.* 272, 7151–7158. doi: 10.1074/jbc.272.11.7151

Prima, V., Kaliberova, L. N., Kaliberov, S., Curiel, D. T., and Kusmartsev, S. (2017). COX2/mPGES1/PGE2 pathway regulates PD-L1 expression in tumor-associated macrophages and myeloid-derived suppressor cells. *Proc. Natl. Acad. Sci. U.S.A.* 114, 1117–1122. doi: 10.1073/pnas.1612920114

Qin, J., Li, W., Gao, S. J., and Lu, C. (2017). KSHV microRNAs: tricks of the Devil. *Trends Microbiol.* 25, 648–661. doi: 10.1016/j.tim.2017.02.002

Ray, A., Marshall, V., Uldrick, T., Leighty, R., Labo, N., Wyvill, K., et al. (2012). Sequence analysis of Kaposi sarcoma-associated herpesvirus (KSHV) microRNAs in patients with multicentric Castleman disease and KSHV-associated inflammatory cytokine syndrome. *J. Infect. Dis.* 205, 1665–1676. doi: 10.1093/infdis/jis249

Reader, J., Holt, D., and Fulton, A. (2011). Prostaglandin E2 EP receptors as therapeutic targets in breast cancer. *Cancer Metastasis Rev.* 30, 449–463. doi: 10.1007/s10555-011-9303-2

Remenyik, E., Juhasz, A., and Hunyadi, J. (2005). [Kaposi's sarcoma]. *Orv. Hetil.* 146, 2047–2055.

Rouzer, C. A., Ford-Hutchinson, A. W., Morton, H. E., and Gillard, J. W. (1990). MK886, a potent and specific leukotriene biosynthesis inhibitor blocks and reverses the membrane association of 5-lipoxygenase in ionophore-challenged leukocytes. *J. Biol. Chem.* 265, 1436–1442.

Rouzer, C. A., and Marnett, L. J. (2009). Cyclooxygenases: structural and functional insights. *J. Lipid Res.* 50(Suppl.), S29–S34. doi: 10.1194/jlr.R800042-JLR200

Russo, J. J., Bohenzky, R. A., Chien, M. C., Chen, J., Yan, M., Maddalena, D., et al. (1996). Nucleotide sequence of the Kaposi sarcoma-associated herpesvirus (HHV8). *Proc. Natl. Acad. Sci. U.S.A.* 93, 14862–14867. doi: 10.1073/pnas.93.25.14862

Sadagopan, S., Sharma-Walia, N., Veettil, M. V., Raghu, H., Sivakumar, R., Bottero, V., et al. (2007). Kaposi's sarcoma-associated herpesvirus induces sustained NF-kappaB activation during de novo infection of primary human dermal microvascular endothelial cells that is essential for viral gene expression. *J. Virol.* 81, 3949–3968. doi: 10.1128/JVI.02333-06

Saini, N., Hochberg, E. P., Linden, E. A., Jha, S., Grohs, H. K., and Sohani, A. R. (2013). HHV8-negative primary effusion lymphoma of B-cell lineage: two cases and a comprehensive review of the literature. *Case Rep. Oncol. Med.* 2013:292301. doi: 10.1155/2013/292301

Samuelsson, B. (1991). Arachidonic acid metabolism: role in inflammation. *Z. Rheumatol.* 50(Suppl. 1), 3–6.

Sarek, G., Kurki, S., Enback, J., Iotzova, G., Haas, J., Laakkonen, P., et al. (2007). Reactivation of the p53 pathway as a treatment modality for KSHV-induced lymphomas. *J. Clin. Invest.* 117, 1019–1028. doi: 10.1172/JCI30945

Sarek, G., and Ojala, P. M. (2007). p53 reactivation kills KSHV lymphomas efficiently in vitro and in vivo: new hope for treating aggressive viral lymphomas. *Cell Cycle* 6, 2205–2209. doi: 10.4161/cc.6.18.4730

Sasaki, Y., Ochiai, T., Takamura, M., Kondo, Y., Yokoyama, C., and Hara, S. (2017). Role of prostacyclin synthase in carcinogenesis. *Prostaglandins Other Lipid Mediat.* 133, 49–52. doi: 10.1016/j.prostaglandins.2017.05.001

Sathish, N., Wang, X., and Yuan, Y. (2012). Tegument proteins of Kaposi's sarcoma-associated herpesvirus and related gamma-herpesviruses. *Front. Microbiol.* 3:98. doi: 10.3389/fmicb.2012.00098

Schneider, E. M., Du, W., Fiedler, J., Hogel, J., Gunther, K. P., Brenner, H., et al. (2011). The (-765 G– > C) promoter variant of the COX-2/PTGS2 gene is associated with a lower risk for end-stage hip and knee osteoarthritis. *Ann. Rheum. Dis.* 70, 1458–1460. doi: 10.1136/ard.2009.124040

Schulz, T. F., and Weiss, R. A. (1995). Kaposi's sarcoma. A finger on the culprit. *Nature* 373, 17–18. doi: 10.1038/373017a0

Serezani, C. H., Chung, J., Ballinger, M. N., Moore, B. B., Aronoff, D. M., and Peters-Golden, M. (2007). Prostaglandin E2 suppresses bacterial killing in alveolar macrophages by inhibiting NADPH oxidase. *Am. J. Respir. Cell Mol. Biol.* 37, 562–570. doi: 10.1165/rcmb.2007-0153OC

Serhan, C. N., Hamberg, M., and Samuelsson, B. (1984). Lipoxins: novel series of biologically active compounds formed from arachidonic acid in human leukocytes. *Proc. Natl. Acad. Sci. U.S.A.* 81, 5335–5339. doi: 10.1073/pnas.81.17.5335

Sharma, S., Stolina, M., Yang, S. C., Baratelli, F., Lin, J. F., Atianzar, K., et al. (2003). Tumor cyclooxygenase 2-dependent suppression of dendritic cell function. *Clin. Cancer Res.* 9, 961–968.

Sharma-Walia, N., Chandran, K., Patel, K., Veettil, M. V., and Marginean, A. (2014). The Kaposi's sarcoma-associated herpesvirus (KSHV)-induced 5-lipoxygenase-leukotriene B4 cascade plays key roles in KSHV latency, monocyte recruitment, and lipogenesis. *J. Virol.* 88, 2131–2156. doi: 10.1128/JVI.02786-13

Sharma-Walia, N., George Paul, A., Patel, K., Chandran, K., Ahmad, W., and Chandran, B. (2010a). NFAT and CREB regulate Kaposi's sarcoma-associated herpesvirus-induced cyclooxygenase 2 (COX-2). *J. Virol.* 84, 12733–12753. doi: 10.1128/JVI.01065-10

Sharma-Walia, N., Paul, A. G., Bottero, V., Sadagopan, S., Veettil, M. V., Kerur, N., et al. (2010b). Kaposi's sarcoma associated herpes virus (KSHV) induced COX-2: a key factor in latency, inflammation, angiogenesis, cell survival and invasion. *PLoS Pathog.* 6:e1000777. doi: 10.1371/journal.ppat.1000777

Sharma-Walia, N., Naranatt, P. P., Krishnan, H. H., Zeng, L., and Chandran, B. (2004). Kaposi's sarcoma-associated herpesvirus/human herpesvirus 8 envelope glycoprotein gB induces the integrin-dependent focal adhesion kinase-Src-phosphatidylinositol 3-kinase-rho GTPase signal pathways and cytoskeletal rearrangements. *J. Virol.* 78, 4207–4223. doi: 10.1128/JVI.78.8.4207-4223.2004

Sharma-Walia, N., Patel, K., Chandran, K., Marginean, A., Bottero, V., Kerur, N., et al. (2012). COX-2/PGE2: molecular ambassadors of Kaposi's sarcoma-associated herpes virus oncoprotein-v-FLIP. *Oncogenesis* 1:e5. doi: 10.1038/oncsis.2012.5

Sharma-Walia, N., Raghu, H., Sadagopan, S., Sivakumar, R., Veettil, M. V., Naranatt, P. P., et al. (2006). Cyclooxygenase 2 induced by Kaposi's sarcoma-associated herpesvirus early during in vitro infection of target cells plays a role in the maintenance of latent viral gene expression. *J. Virol.* 80, 6534–6552. doi: 10.1128/JVI.00231-06

Shelby, B. D., LaMarca, H. L., McFerrin, H. E., Nelson, A. B., Lasky, J. A., Sun, G., et al. (2007). Kaposi's sarcoma associated herpesvirus G-protein coupled receptor activation of cyclooxygenase-2 in vascular endothelial cells. *Virol. J.* 4:87. doi: 10.1186/1743-422X-4-87

Shelby, B. D., Nelson, A., and Morris, C. (2005). Gamma-herpesvirus neoplasia: a growing role for COX-2. *Microsc. Res. Tech.* 68, 120–129. doi: 10.1002/jemt.20226

Si, H., Verma, S. C., Lampson, M. A., Cai, Q., and Robertson, E. S. (2008). Kaposi's sarcoma-associated herpesvirus-encoded LANA can interact with the nuclear mitotic apparatus protein to regulate genome maintenance and segregation. *J. Virol.* 82, 6734–6746. doi: 10.1128/JVI.00342-08

Sin, S. H., Roy, D., Wang, L., Staudt, M. R., Fakhari, F. D., Patel, D. D., et al. (2007). Rapamycin is efficacious against primary effusion lymphoma (PEL) cell lines in vivo by inhibiting autocrine signaling. *Blood* 109, 2165–2173. doi: 10.1182/blood-2006-06-028092

Sivakumar, R., Sharma-Walia, N., Raghu, H., Veettil, M. V., Sadagopan, S., Bottero, V., et al. (2008). Kaposi's sarcoma-associated herpesvirus induces sustained levels of vascular endothelial growth factors A and C early during in vitro infection of human microvascular dermal endothelial cells: biological implications. *J. Virol.* 82, 1759–1776. doi: 10.1128/JVI.00873-07

Smith, R. J. (1977). Modulation of phagocytosis by and lysosomal enzyme secretion from guinea-pig neutrophils: effect of nonsteroid anti-inflammatory agents and prostaglindins. *J. Pharmacol. Exp. Ther.* 200, 647–657.

Smith, W. L., DeWitt, D. L., and Garavito, R. M. (2000). Cyclooxygenases: structural, cellular, and molecular biology. *Annu. Rev. Biochem.* 69, 145–182. doi: 10.1146/annurev.biochem.69.1.145

Sombroek, C. C., Stam, A. G., Masterson, A. J., Lougheed, S. M., Schakel, M. J., Meijer, C. J., et al. (2002). Prostanoids play a major role in the primary tumor-induced inhibition of dendritic cell differentiation. *J. Immunol.* 168, 4333–4343. doi: 10.4049/jimmunol.168.9.4333

Soulier, J., Grollet, L., Oksenhendler, E., Cacoub, P., Cazals-Hatem, D., Babinet, P., et al. (1995). Kaposi's sarcoma-associated herpesvirus-like DNA sequences in multicentric Castleman's disease. *Blood* 86, 1276–1280.

Sreeramkumar, V., Fresno, M., and Cuesta, N. (2012). Prostaglandin E2 and T cells: friends or foes? *Immunol. Cell Biol.* 90, 579–586. doi: 10.1038/icb.2011.75

Stine, J. T., Wood, C., Hill, M., Epp, A., Raport, C. J., Schweickart, V. L., et al. (2000). KSHV-encoded CC chemokine vMIP-III is a CCR4 agonist, stimulates angiogenesis, and selectively chemoattracts TH2 cells. *Blood* 95, 1151–1157.

Sugimoto, Y., and Narumiya, S. (2007). Prostaglandin E receptors. *J. Biol. Chem.* 282, 11613–11617. doi: 10.1074/jbc.R600038200

Suleyman, H., Demircan, B., and Karagoz, Y. (2007). Anti-inflammatory and side effects of cyclooxygenase inhibitors. *Pharmacol. Rep.* 59, 247–258.

Tabata, H., Tanaka, S., Sugimoto, Y., Kanki, H., Kaneko, S., and Ichikawa, A. (2002). Possible coupling of prostaglandin E receptor EP(1) to TRP5 expressed in *Xenopus laevis* oocytes. *Biochem. Biophys. Res. Commun.* 298, 398–402. doi: 10.1016/S0006-291X(02)02455-5

Tamburro, K. M., Yang, D., Poisson, J., Fedoriw, Y., Roy, D., Lucas, A., et al. (2012). Vironome of Kaposi sarcoma associated herpesvirus-inflammatory cytokine syndrome in an AIDS patient reveals co-infection of human herpesvirus 8 and human herpesvirus 6A. *Virology* 433, 220–225. doi: 10.1016/j.virol.2012.08.014

Toomey, N. L., Deyev, V. V., Wood, C., Boise, L. H., Scott, D., Liu, L. H., et al. (2001). Induction of a TRAIL-mediated suicide program by interferon alpha in primary effusion lymphoma. *Oncogene* 20, 7029–7040. doi: 10.1038/sj.onc.1204895

Tosetti, F., Ferrari, N., De Flora, S., and Albini, A. (2002). Angioprevention': angiogenesis is a common and key target for cancer chemopreventive agents. *FASEB J.* 16, 2–14. doi: 10.1096/fj.01-0300rev

Turcotte, C., Zarini, S., Jean, S., Martin, C., Murphy, R. C., Marsolais, D., et al. (2017). The Endocannabinoid metabolite prostaglandin E2 (PGE2)-glycerol inhibits human neutrophil functions: involvement of its hydrolysis into PGE2 and EP receptors. *J. Immunol.* 198, 3255–3263. doi: 10.4049/jimmunol.1601767

Uldrick, T. S., Polizzotto, M. N., and Yarchoan, R. (2012). Recent advances in Kaposi sarcoma herpesvirus-associated multicentric Castleman disease. *Curr. Opin. Oncol.* 24, 495–505. doi: 10.1097/CCO.0b013e328355e0f3

Uldrick, T. S., Wang, V., O'Mahony, D., Aleman, K., Wyvill, K. M., Marshall, V., et al. (2010). An interleukin-6-related systemic inflammatory syndrome in patients co-infected with Kaposi sarcoma-associated herpesvirus and HIV but without Multicentric Castleman disease. *Clin. Infect. Dis.* 51, 350–358. doi: 10.1086/654798

Vane, J. R., Bakhle, Y. S., and Botting, R. M. (1998). Cyclooxygenases 1 and 2. *Annu. Rev. Pharmacol. Toxicol.* 38, 97–120. doi: 10.1146/annurev.pharmtox.38.1.97

Vane, J. R., and Botting, R. M. (1997). Mechanism of action of aspirin-like drugs. *Semin. Arthritis Rheum.* 26, 2–10. doi: 10.1016/S0049-0172(97)80046-7

Vannini, N., Lorusso, G., Cammarota, R., Barberis, M., Noonan, D. M., Sporn, M. B., et al. (2007). The synthetic oleanane triterpenoid, CDDO-methyl ester, is a potent antiangiogenic agent. *Mol. Cancer Ther.* 6, 3139–3146. doi: 10.1158/1535-7163.MCT-07-0451

Wakeman, B. S., Izumiya, Y., and Speck, S. H. (2017). Identification of novel Kaposi's sarcoma-associated herpesvirus Orf50 transcripts: discovery of new RTA isoforms with variable transactivation potential. *J. Virol.* 91:e01434-16. doi: 10.1128/JVI.01434-16

Wang, X. S., and Lau, H. Y. (2006). Prostaglandin E potentiates the immunologically stimulated histamine release from human peripheral blood-derived mast cells through EP1/EP3 receptors. *Allergy* 61, 503–506. doi: 10.1111/j.1398-9995.2006.01043.x

Weller, C. L., Collington, S. J., Hartnell, A., Conroy, D. M., Kaise, T., Barker, J. E., et al. (2007). Chemotactic action of prostaglandin E2 on mouse mast cells acting via the PGE2 receptor 3. *Proc. Natl. Acad. Sci. U.S.A.* 104, 11712–11717. doi: 10.1073/pnas.0701700104

Williams, C. S., Shattuck-Brandt, R. L., and DuBois, R. N. (1999a). The role of COX-2 in intestinal cancer. *Ann. N. Y. Acad. Sci.* 889, 72–83. doi: 10.1111/j.1749-6632.1999.tb08725.x

Williams, C. S., Mann, M., and DuBois, R. N. (1999b). The role of cyclooxygenases in inflammation, cancer, and development. *Oncogene* 18,7908–7916.

Williams, C. S., Shattuck-Brandt, R. L., and DuBois, R. N. (1999c). The role of COX-2 in intestinal cancer. *Expert Opin. Investig. Drugs* 8, 1–12. doi: 10.1517/13543784.8.1.1

Yakar, I., Melamed, R., Shakhar, G., Shakhar, K., Rosenne, E., Abudarham, N., et al. (2003). Prostaglandin e(2) suppresses NK activity in vivo and promotes postoperative tumor metastasis in rats. *Ann. Surg. Oncol.* 10, 469–479. doi: 10.1245/ASO.2003.08.017

Ye, F., Lei, X., and Gao, S. J. (2011). Mechanisms of Kaposi's sarcoma-associated herpesvirus latency and reactivation. *Adv. Virol.* 2011:193860. doi: 10.1155/2011/193860

Yokoyama, U., Iwatsubo, K., Umemura, M., Fujita, T., and Ishikawa, Y. (2013). The prostanoid EP4 receptor and its signaling pathway. *Pharmacol. Rev.* 65, 1010–1052. doi: 10.1124/pr.112.007195

Yokoyama, U., Minamisawa, S., Shioda, A., Ishiwata, R., Jin, M. H., Masuda, M., et al. (2014). Prostaglandin E2 inhibits elastogenesis in the ductus arteriosus via EP4 signaling. *Circulation* 129, 487–496. doi: 10.1161/CIRCULATIONAHA.113.004726

Yu, T., Lao, X., and Zheng, H. (2016). Influencing COX-2 Activity by COX Related Pathways in Inflammation and Cancer. *Mini Rev. Med. Chem.* 16, 1230–1243. doi: 10.2174/1389557516666160505115743

Yu, Y., and Chadee, K. (1998). Prostaglandin E2 stimulates IL-8 gene expression in human colonic epithelial cells by a posttranscriptional mechanism. *J. Immunol.* 161, 3746–3752.

Zhang, X., Wang, J. F., Chandran, B., Persaud, K., Pytowski, B., Fingeroth, J., et al. (2005). Kaposi's sarcoma-associated herpesvirus activation of vascular endothelial growth factor receptor 3 alters endothelial function and enhances infection. *J. Biol. Chem.* 280, 26216–26224. doi: 10.1074/jbc.M411392200

Zhong, C., Xu, M., Wang, Y., Xu, J., and Yuan, Y. (2017). An APE1 inhibitor reveals critical roles of the redox function of APE1 in KSHV replication and pathogenic phenotypes. *PLoS Pathog.* 13:e1006289. doi: 10.1371/journal.ppat.1006289

Zhu, T., Gobeil, F., Vazquez-Tello, A., Leduc, M., Rihakova, L., Bossolasco, M., et al. (2006). Intracrine signaling through lipid mediators and their cognate nuclear G-protein-coupled receptors: a paradigm based on PGE2, PAF, and LPA1 receptors. *Can. J. Physiol. Pharmacol.* 84, 377–391. doi: 10.1139/y05-147

Conflict of Interest Statement: The authors declare that the research was conducted in the absence of any commercial or financial relationships that could be construed as a potential conflict of interest.

frontiers in Microbiology

ORIGINAL RESEARCH
published: 08 May 2019
doi: 10.3389/fmicb.2019.00998

Comparison of HEp-2 and Vero Cell Responses Reveal Unique Proapoptotic Activities of the Herpes Simplex Virus Type 1 α0 Gene Transcript and Product

*Marie L. Nguyen[1], Elisabeth Gennis[2], Kristen C. Pena[2] and John A. Blaho[3]**

[1] Department of Microbiology and Immunology, Des Moines University, Des Moines, IA, United States, [2] Department of Microbiology, Mount Sinai School of Medicine, New York, NY, United States, [3] NYC Regional Innovation Node, The City University of New York, New York, NY, United States

Previous studies have provided evidence suggesting a role for apoptosis in the control of Herpes Simplex Virus 1 (HSV-1) latency. HSV-1 induces and then later blocks apoptosis in infected cells. The immediate early viral gene α0, which synthesizes the ICP0 protein, is necessary and sufficient for HSV-1-induced apoptosis in human epithelial (HEp-2) cells. While previous research showed that ICP0 protein synthesis is not necessary for HSV-1-induced apoptosis in infected HEp-2 cells, circumstantial evidence suggested that it might be needed in infected African green monkey kidney (Vero) cells. In this study, we determined the specific aspects of α0 needed to trigger apoptosis in these two cell types. HEp-2 cells transfected with α0 expressing plasmids that generated either full-length, truncated, or no detectable (multiple stop codons) ICP0 protein died through apoptosis. This indicates that ICP0 protein is not necessary for α0-induced apoptosis and that α0 mRNA alone has apoptotic induction properties in HEp-2 cells. We next investigated the primary structure of α0's mRNA to better define its proapoptotic ability. Since α0 is one of the few HSV-1 genes that are spliced, we transfected cells with a plasmid expressing ICP0 from cDNA copy, pcDNAICP0. The cells transfected with pcDNAICP0 underwent apoptosis at a level equivalent to those transfected with the genomic copy of α0, which indicates that neither splicing events nor introns are required for the apoptotic function of α0 in HEp-2 cells. Next, we studied the ability of α0 to cause apoptosis in Vero cells. Since HSV-1-induced apoptosis in Vero cells requires protein synthesis early in infection, proteins synthesized with immediate early kinetics may facilitate apoptosis. Vero cells were transfected with plasmids producing either full-length ICP0 or ICP0 truncated at codon 212. Full-length ICP0, but not truncated ICP0, induced apoptosis in Vero cells. Together, these results suggest that α0 gene expression triggers apoptosis, but ICP0 protein is needed to facilitate apoptosis in Vero cells. In addition, ICP0's facilitation activity may lie in its carboxyl-terminated domain. Thus, our results demonstrate that α0's mRNA and protein possess proapoptotic properties. The requirement for ICP0 protein during HSV-dependent apoptosis appears to be cell type specific.

Keywords: apoptosis induction, α0 gene, ICP0 protein, HEp-2, Vero cells

OPEN ACCESS

Edited by:
Randall J. Cohrs, University of Colorado Denver, United States

Reviewed by:
James R. Smiley, University of Alberta, Canada
Igor Jurak, University of Rijeka, Croatia
Chiharu Graybill, University of Colorado Denver, United States

***Correspondence:**
John A. Blaho
jblaho@cuny.edu

Specialty section:
This article was submitted to Virology, a section of the journal Frontiers in Microbiology

Received: *28 September 2018*
Accepted: *18 April 2019*
Published: *08 May 2019*

Citation:
Nguyen ML, Gennis E, Pena KC and Blaho JA (2019) Comparison of HEp-2 and Vero Cell Responses Reveal Unique Proapoptotic Activities of the Herpes Simplex Virus Type 1 α0 Gene Transcript and Product. Front. Microbiol. 10:998. doi: 10.3389/fmicb.2019.00998

INTRODUCTION

Herpes simplex virus 1 (HSV-1) is a large, enveloped DNA virus belonging to the *Herpesviridae* family. The most common clinical manifestation of HSV-1 infections is herpes labialis, commonly referred to as a cold sore. However, when the virus enters tissues outside of the oral epithelium, more serious disease outcomes occur. For example, HSV-1 infections of the cornea cause herpes simplex keratitis, which is the leading cause of infectious blindness in the United States (Liesegang et al., 1989). Furthermore, neonatal HSV infections often spread to the brain, causing life threatening encephalitis. The majority of neonate infections are the result of HSV transmission from maternal genital infections to newborn infects during childbirth. There has been an increase in genital HSV-1 infections in young women in the United States (Peña et al., 2010). Therefore, insights in the HSV replication cycle have the potential to significantly impact human disease.

One of the defining features of the *Herpesviridae* family is the ability to form a latent state, from which reactivation events lead to subsequent virus replication and often clinical symptoms. HSV establishes a latent infection in the sensory neurons located at the sites of initial infection, e.g., trigeminal ganglia for oral HSV infections. Reactivation events throughout the lifespan of infected individuals lead to new rounds of lytic virus replication in adjacent epithelial tissues and recurrent herpetic lesions. There is evidence for cellular apoptotic events playing a role in controlling the latent and lytic states of the HSV life cycle (reviewed in Nguyen and Blaho, 2007).

Apoptosis is a form of programmed cell death that has been shown to be important for proper tissue development, prevention of tumors, and cellular responses to pathogens (reviewed in Koyama et al., 2003). Apoptotic cell death is distinguished from other forms of cell death by defined morphological and biochemical features displayed by the dying cells. These features include blebbing and alterations in the chemical makeup of the plasma membrane, condensation and eventual fragmentation of the chromosomal DNA, and loss of mitochondrial membrane potential (Kerr et al., 1972; Wyllie et al., 1980; Takano et al., 1991). One class of enzymes required for most forms of apoptotic cell death are the caspases (reviewed in Salvesen and Dixit, 1997; Villa et al., 1997). Caspases are synthesized as large inactive precursors, which are cleaved and form active tetramers during apoptosis. The caspases cleave their targets at specific peptide motifs containing aspartate residues. Caspase targets include caspases themselves and a variety of other cellular proteins, many which are involved in maintaining the structural or chemical integrity of the cell, e.g., lamin B, DFF/ICAD, and poly(ADP)ribose polymerase (PARP) (reviewed in Sanfilippo and Blaho, 2003).

There are two types of gene products abundantly produced during HSV latency. Both are transcripts from the R_L and surrounding regions of the genome. The long transcripts have been the most well-studied and are called the latency associated transcripts (LATs) (Stevens et al., 1987; Spivack and Fraser, 1988). More recently, microRNAs have also been found to be produced during latent infection (reviewed in Phelan et al., 2017). Infections with recombinant viruses harboring LAT deletions have been reported to yield reduced numbers of latently infected neurons compared to wild-type (Sawtell and Thompson, 1992; Thompson and Sawtell, 1997). Other studies reported a reduced ability for LAT mutants to reactivate from latently infected explants (Leib et al., 1989a). LATs have been shown to possess anti-apoptotic activities (Perng et al., 2000; Inman et al., 2001a; Ahmed et al., 2002; Jin et al., 2003). The anti-apoptotic regions of LATs have been correlated with the domains needed for latency (Perng et al., 2000; Inman et al., 2001a; Ahmed et al., 2002). Furthermore, replacement of LAT domains with other anti-apoptotic genes, such as the bovine herpesvirus 1 LR and Baculovirus cpIAP, restore LAT latency functions in rabbit and mouse HSV infection models (Perng et al., 2002; Jin et al., 2005, 2008). Finally, inducting apoptosis in latently infected trigeminal ganglia with dexamethasone accelerated their reactivation (Du et al., 2012). Thus, investigations into apoptosis in HSV-1 infected cells may provide insight into the establishment, maintenance, and/or reactivation from latency.

Previous studies have provided evidence that an intricate balance between apoptotic agonists and antagonists exists within herpes simplex virus-infected cells in both tissue culture and animal models (Nguyen and Blaho, 2009). Seven viral genes have been reported to possess apoptotic antagonistic properties. When these antagonists are not efficiently produced, such as infections in the presence of protein synthesis inhibitors or in the absence of key immediate early genes (vBSΔ27 infection) the apoptotic balance is upset, and the infected cells die through the intrinsic apoptotic pathway (Aubert et al., 2007).

The trigger of this HSV-dependent apoptosis has been mapped to the HSV-1 α0 gene (Sanfilippo and Blaho, 2006). Initial studies into the viral factors triggering apoptosis in HEp-2 cells utilized the protein synthesis inhibitor, cycloheximide (CHX) (Aubert and Blaho, 1999). The human carcinoma HEp-2 cells infected in the presence of CHX underwent apoptosis, suggesting that at least in these cells, triggering of HSV-dependent apoptosis does not require *de novo* protein synthesis. Further studies using actinomycin D or a recombinant virus lacking all immediate early genes (IE), *d*109, demonstrated that IE gene transcription was required to trigger apoptosis during infection (Sanfilippo et al., 2004a). HSV encodes four immediate early genes, α4, α27, α22, α0. Infections with recombinant viruses containing mutations in the α4 (CgalΔ3), α27 (vBSΔ27), or α22 (R7802) gene maintained the ability to trigger HSV-dependent apoptosis. In contrast, infection with a recombinant virus lacking expression of the α0 gene (7134) failed to induce apoptosis (Sanfilippo and Blaho, 2006). Furthermore, a virus lacking expression of all immediate early genes except for α0, *d*106, maintained the ability to trigger apoptosis. The α0 gene encodes a multifunctional protein of 110 kDa in size, ICP0 (reviewed in Everett, 2000; Hagglund and Roizman, 2004). In HEp-2 cells, infection with a virus containing a nonsense mutation at amino acid 212 of ICP0 (n212), which was therefore, unable to produce full length ICP0 protein, was still capable of inducing apoptosis. Finally, one series of experiments determined that expression of ICP0 from a plasmid outside of an HSV infection induced apoptosis in a dose dependent manner in HEp-2 cells (Sanfilippo and Blaho, 2006). Together, these studies demonstrated that the ability of HSV to trigger apoptosis within

infected cells maps to the α0 gene, and that translation of the full-length protein was not required for induction of HSV-dependent apoptosis in HEp-2 cells. The α0 gene is located in the long repeat regions of the HSV-1 genome and is unique compared to other HSV-1 genes in that it contains three exons and two introns (**Figure 1**, line 2). α0 is also unique because the spliced introns remain stable in the cytoplasm and accumulate in a cell-type-dependent manner (Carter and Roizman, 1996). In this study, we go on to further investigate the nature of α0's pro-apoptotic activities in HEp-2 cells.

We also expanded our analysis to investigate the role of α0 and ICP0 in apoptosis in primate kidney Vero cells, which have been previously been shown to possess different requirements for HSV-dependent apoptosis compared to HEp-2 cells (Nguyen et al., 2005). Vero cells undergo HSV-dependent apoptosis when infected with the vBSΔ27-mutant virus, but, unlike HEp-2 cells, fail to undergo apoptosis when infected with wild-type HSV in the presence of cycloheximide. In fact, cycloheximide treatment at or before 3 hpi suppressed the apoptosis induced by vBSΔ27 infection. This data led to the conclusion that as opposed to HEp-2 cells, Vero cells require *de novo* synthesis of a protein produced by 3 hpi in order to undergo HSV dependent apoptosis. This protein was named the facilitator of apoptosis (FAP), due to its key role in viral apoptosis (Nguyen et al., 2005). FAP could be either a cellular protein produced prior to 3 hpi, or one of the immediate early proteins. In this study we explore whether the ICP0 protein itself can facilitate viral apoptosis during HSV infection in Vero cells.

MATERIALS AND METHODS

Cell Lines and Viruses

Human epithelial (HEp-2) and African green monkey kidney (Vero) cells were obtained from the American Type Culture Collection (Rockville, MD, United States). It has been shown that the HEp-2 strain, which was previously described to be derived from laryngeal carcinoma, is a HeLa contaminant; we have referred to this HeLa-derived strain as HEp-2 (Nguyen et al., 2005). Vero and HEp-2 cells were cultured in Dulbecco's modified Eagle's medium (DMEM) and supplemented with 5% fetal bovine serum (FBS). FO6 cells are a Vero derivative, which express the ICP0, ICP4, and ICP27 genes from their respective viral promoters (Samaniego et al., 1998). FO6 cells were grown in DMEM supplemented with 5% FBS containing 400 μg/ml G418 and 300 μg/ml hygromycin. The Vero-derived cell line expressing ICP0 from its viral promotor, L7 (Samaniego et al., 1998), was grown in DMEM supplemented with 5% FBS containing 400 μg/ml G418. HSV-1 strain KOS1.1 (KOS) and HSV-1 strain 17+ (17) are the wild-type strains of HSV-1 used in this study. The HSV-1 mutant, vCPc0, was generously provided by Dr. Saul Silverstein (Columbia University) and has both ICP0 genomic coding regions of 17 replaced by cDNA copies of the ICP0 transcript (Panagiotidis et al., 1997). Vero cells were used for growth and tittering of wild-type HSV-1 strains and of vCPc0. 7134 and n212 viruses were generously provided by Dr. Pricilla Schaffer (Harvard Medical School). 7134 is an ICP0-null virus, which has both copies of ICP0 in KOS replaced by the *E. coli lacZ* gene (Cai and Schaffer, 1989). This virus was propagated and tittered on FO6 cells. The KOS-derived HSV-1 n212 (n212) contains a stop codon in all three reading frames at amino acid 212 of ICP0 (Cai and Schaffer, 1989). This virus was propagated and tittered on L7 cells. All virus titers were determined at 48 h post-infection by standard dilution techniques.

Viral Infection and Protein Synthesis Inhibition by CHX

HEp-2 cells were seeded in DMEM supplemented with 5% new born calf serum (NBCS) 24 h prior to infection. Cells were infected at a multiplicity of infection (MOI) of 10 and incubated at 37°C for 1 h. Media was aspirated and replaced with 5% NBCS and incubated at 37°C and 5% CO_2 for 24 h. In experiments designed to inhibit *de novo* protein synthesis, cycloheximide (CHX) was added directly to the medium of monolayers at a final concentration of 10 μg/ml, which has been previously shown to sufficiently block viral protein synthesis in KOS-infected cells (Aubert and Blaho, 1999). One hour prior to infection, CHX is added at 37°C and was maintained in the medium until 24 h post-infection when morphological and biochemical analyses were performed (described below).

Plasmids

The pSH, pn212, pn12/106, and pn12/212 plasmids were generously provided by Pricilla Schaffer (Harvard Medical School) and were previously described (Cai and Schaffer, 1989). Briefly, pSH includes the entire ICP0 coding region (3.2 kB) as well as the flanking sequences (0.81 kB 5′ and 0.4 kB 3′) in a pUC8 backbone and for clarity in this study is hereafter referred to as pICP0 (**Figure 1**, line 6). The plasmid expressing ICP0 from a cDNA copy of ICP0 in pUC19, pDS-16 (Panagiotidis et al., 1997), was generously provided by Saul Silverstein (Columbia University) and hereafter is referred to as pcDNAICP0 (**Figure 1**, line 7). pn212 is a derivative of pICP0 (Cai and Schaffer, 1989) containing a stop codon in all three reading frames at amino acid 212 and therefore generates full-length α0 transcript and a truncated ICP0 protein, referred to as pTruncICP0 (**Figure 1**, line 8). pα0RNAn12/106 (**Figure 1**, line 9) and pα0RNAn12/212 (**Figure 1**, line 10) are related to pTruncICP0 and contain additional stop codons at a.a. 12 and 106 or 212 respectively. In pICP0, pcDNAICP0, pTuncICP0, pα0RNAn12/106, and pα0RNAn12/212, ICP0 synthesis is regulated by the viral α0 promotor, which is contained in the 5′ flanking region.

pICP0GFP simultaneously expresses ICP0 and the efficient green fluorescent protein (GFP) from the same transcript. To create it, an internal ribosome entry site (IRES) and the GFP gene from the pHR′-CMV MCS IRES GFP delta B plasmid (generously obtained from Mary Klotman, Mount Sinai School of Medicine), were cloned directly after the ICP0 3′ flanking region of the pICP0 plasmid (**Figure 1**, line 11). pcDNAICP0GFP (**Figure 1**, line 12) and pα0RNAn12/106GFP (**Figure 1**, line 13) were created by replacing the ICP0 in pICP0GFP with the cDNA and α0RNAn12/106 versions. The BAK plasmid (pBAK) was obtained from Peter Palese (Mount Sinai School of Medicine) and

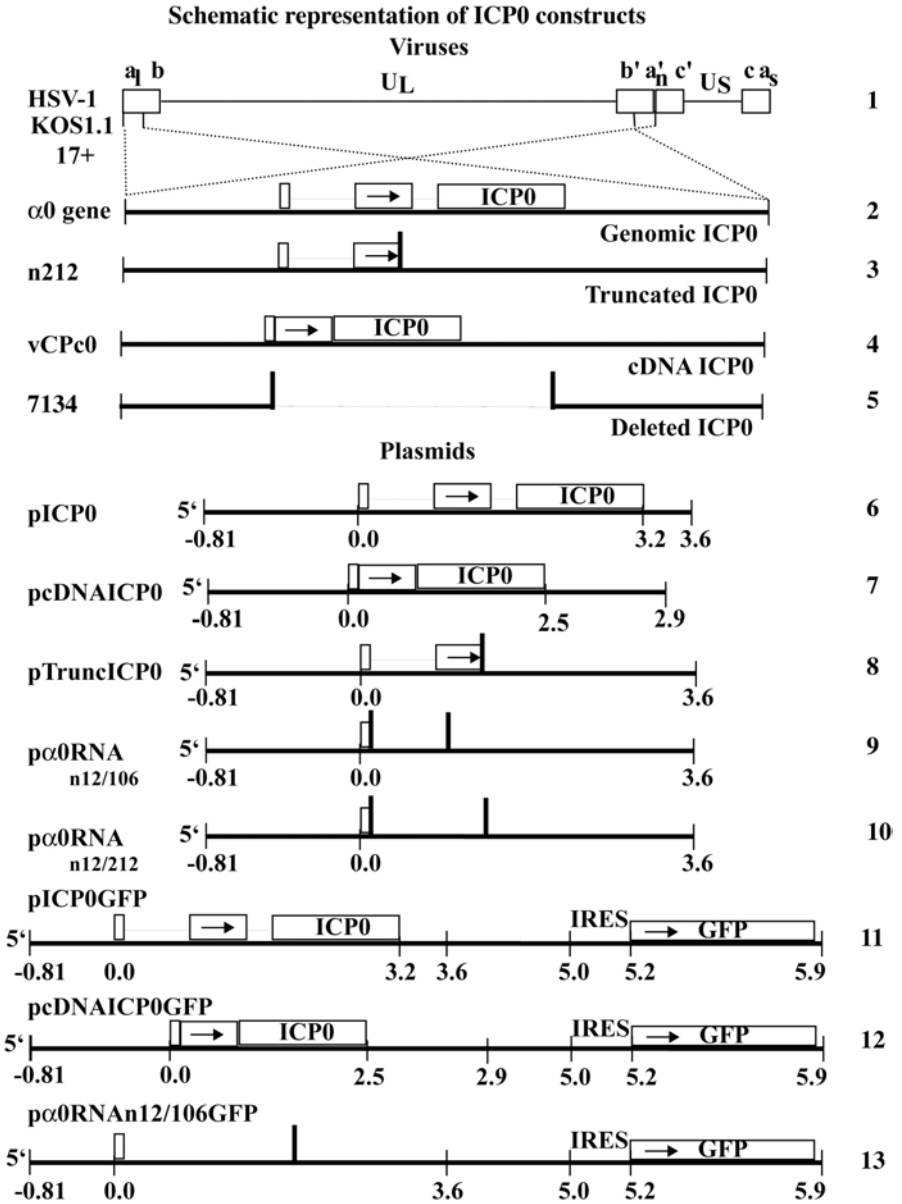

FIGURE 1 | Schematic representation of HSV-1 viral constructs and ICP0 plasmids. HSV-1 (line 1) contains two copies of the α0 gene (line 2), encoding ICP0, in the inverted repeated regions (abc a′b′c′) that flank the unique long region (U_L) in the HSV-1 genome. The α0 introns and exons are represented by lines and boxes, respectively. The n212 virus generates full-length α0 mRNA but a truncated ICP0 protein. It contains the same α0 sequences as wild-type HSV-1 but there are nonsense mutations in all three reading frames inserted after codon 212 in both copies of ICP0 (line 3). The vCPc0 virus generates cDNA-expressed ICP0 protein from both copies of α0 (line 4). The 7134 virus contains deletions of both copies of α0 and does not produce ICP0 (line 5). The pICP0 plasmid contains the entire genomic ICP0 coding region and flanking sequences (810 bases and 0.4 kB at the 5′ and 3′ ends, respectively) within the pUC8 vector (line 6). The pcDNAICP0 plasmid includes the cDNA copies of ICP0 and flanking sequences from ICP0 coding region (810 bases and 1.1 kB at the 5′ and 3′ ends, respectively) within the pUC19 vector (line 7). pTrunclCP0 generates full-length ICP0 mRNA and a truncated protein due to a nonsense mutation after codon 212 (line 8). pα0RNAn12/106 contain nonsense codons at a.a. 12 and 106 (line 9). pα0RNAn12/212 contain nonsense codons at a.a. 12 and 212 (line 10). pICP0GFP contains an internal ribosome entry site (IRES) and the efficient green fluorescent protein (GFP) immediately following the ICP0 gene of pICP0 (line 11). Similarly, pcDNAICP0GFP and pα0RNAn12/106GFP contain the IRES-GFP inserted into pcDNAICP0 and pα0RNAn12/106, respectively (lines 12 and 13).

expresses an HA-tagged BAK protein from the CMV promotor. pUC19 was obtained from New England Biolabs. In several previous studies, the amount of apoptosis in DNA-negative, control transfected cells is undetectable (Goodkin et al., 2003; Sanfilippo et al., 2004a,b; Sanfilippo and Blaho, 2006).

Transfections

HEp-2 and Vero cells were seeded at 2.5×10^5 cells/2 cm^2-surface area dish in DMEM containing 5% FBS and transfected 24 h later (approximately 80% confluence) using Lipofectamine 2000 (Invitrogen) according to the manufacturer's protocol. Briefly,

purified plasmid DNA (0.4 and 1.0 μg, respectively) was diluted in 25 μl DMEM. Lipofectamine 2000 reagent (1.0 and 1.5 μl, respectively) was diluted in 25 μl DMEM. After 5 min, the diluted Lipofectamine was added to the DNA solution, and complexes formed at room temperature for 20 min. The media was aspirated off cell monolayers and replaced with 200 μl DMEM, and 50 μl of the DNA-Lipofectamine complex solution was added to each well. Cells were incubated at 37°C and 5% CO_2 for 4 to 6 h when the media was aspirated and replaced with DMEM supplemented with 10% FBS and incubated until the time of harvest, as denoted in the text.

Microscopic Analyses and Quantification of Chromatin Condensation

Infected and transfected cell phenotypes were documented using phase-contrast light microscopy with an inverted fluorescence microscope. Images were obtained using QCapture software. For analysis of chromatin condensation in live cells, the DNA dye, Hoechst 33258 (Sigma), was added to media at a final concentration of 5 μg/ml for at least 1 h at 37°C. Phase-contrast (phase) and fluorescent (Hoechst and/or GFP) images were taken for each well. Merged (overlay) images were generated using Adobe Photoshop CS software. The percentage of nuclei containing condensed chromatin to total cells was determined for triplicate wells and the mean (M) and standard deviation (SD) of apoptotic cells were determined for each treatment. Typically, 100–300 cells were counted for each well. For HEp-2 experiments, raw data from five experiments with identical conditions was pooled and overall M and SD were determined:

i = Treatment, j = Well

$$M_i^{HEp-2} = \left(\frac{\sum CondensedChromatin_i}{\sum TotalCells_i}\right)$$

$$SD_i^{HEp-2} = \sqrt{\frac{\sum\left(\frac{CondendedChromatin_{ij}}{TotalCells_{ij}} - M_i\right)^2}{TotalCells_i}}$$

Since Vero experiments were done in a time course, data from each time-point was standardized by dividing the percentage of apoptotic cells for each treatment by the percentage of apoptotic cells in pUC19-transfected cells. The M and SD was calculated from three independent experiments using the following formula:

i = Treatment, j = Well, k = Time Point

$$M_i^{Vero} = \frac{\sum\left(\frac{[CondensedChromatin_{ijk}/TotalCells_{ijk}]}{[M_k^{pUC19}]}\right)}{TotalWells_i}$$

$$SD_i^{Vero} = \sqrt{\frac{\sum\left(\frac{[CondensedChromatin_{ijk}/TotalCells_{ijk}]}{[M_k^{pUC19}]} - M_i\right)}{TotalWells_i}}$$

Cellular Extractions, Denaturing Gel Electrophoresis, and Immunoblotting

Whole cell extracts were obtained as previously described (Nguyen et al., 2007). Briefly, cells were scraped into the media, combined and collected by centrifugation for 5 min at 4°C and 1000 × *g*. For transfection experiments, cells from three identically treated wells were combined for protein analysis. Pellets were washed in cold phosphate buffered saline (PBS) containing the inhibitors: 2 mM phenylmethylsulfonyl fluoride (PMSF), 1% Transylol, 0.1 mM L-1-chloro-3-(4-tosulamido)-4-phenyl-2butanone (TPCK), and 0.01 mM L-1-chloro-3-(4-tosylanmido)-7-aminoheptanonhydrochloride (TLCK). Cells were lysed in RIPA buffer (50 mM Tris-HCl, pH 7.5, 150 mM NaCl, 1% Triton X-100, 1% deoxycholate, 0.1% SDS) containing the inhibitors described above and vortexed for 30 s. Lysates were cleared by centrifugation for 10 m at 4°C and 16,000 × *g*. Protein concentrations were determined using a modified Bradford assay (BioRad) as recommended by the vendor. Equal amounts of cell proteins were separated in denaturing 12% *N,N′*-diallyltartardiamide (DATD)-acrylamide gels and electrically transferred to nitrocellulose membranes in a tank apparatus (BioRad). Membranes were blocked for at least 1 h at room temperature in PBS containing 5% non-fat dry milk (blocking buffer), washed with Tris-buffered saline containing 0.1% Tween-20 (TBS-T), and incubated overnight in primary antibody at 4°C. The mouse monoclonal antibodies anti-PARP (PharMingin), -procaspase-7 (BD Transduction), -ICP0 (Goodwin Institute for Cancer Research, Plantation, FL, United States), -VP22 (Blaho et al., 1994), -ICP27 (Goodwin) and -actin (Sigma) were used at a 1:1000 dilution in Tris-buffered saline containing 0.1% Tween 20 and 0.1% BSA. Mouse anti-HA monoclonal antibody (Southern Biotech) (to screen for HA-tagged BAK protein) was used at a 1:5000 dilution. After washing with TBS-T, membranes were treated with secondary anti-mouse antibodies conjugated with alkaline phosphatase (AP) (Southern Biotech) or with horseradish peroxidase (HRP) (GE Healthcare) at a 1:1000 dilution in blocking buffer. Membranes treated with AP secondary were developed using AP buffer containing 5-bromo-4-chloro-3-indolyl phosphate and 4-nitrobluetetrazolium chloride. Membranes treated with HRP antibodies were immersed in western blotting substrates (Roche) and exposed to Biomax XAR film (Kodak). Complete blots were cut with razor blades and sections were probed using specific, relevant antibodies. Blots were reassembled and scanned in a single run. The resulting digital images were cropped as necessary to create figures.

Densitometric Analysis

To quantify PARP and procaspase-7 cleavage densitometry of images was performed and analyzed using NIH image software. For PARP cleavage, the mean density (MD) of the cleaved PARP band was divided by the sum of MD cleaved and MD uncleaved PARP bands and expressed in a percentage: i = Treatment

$$\%\ \text{PARP cleavage}_i = 100 \times \left(\frac{MD_{cleaved_i}}{[MD_{uncleaved_i} + MD_{cleaved_i}]}\right).$$

Procaspase-7 cleavage was determined by dividing MD procaspase-7 band by the MD of the respective band in the actin loading control. Values were normalized to the pUC19 procaspase-7 to actin ratio to determine percentage of

procaspase-7 compared to pUC19 as follows. i = Treatment

$$\text{Normalized \% procaspase-7 Cleavage} = 100 \times \frac{[MD_{casp7_i}/MD_{actin_i}]}{[MD_{casp7pUC19}/MD_{actinpUC19}]}.$$

Statistical Analysis

To determine statistical significance, Microsoft Excel was used to perform the Student's t-test on apoptotic morphology data (**Figures 3**, **5**, **6**, **8**). p-Values of 0.05 or lower were considered statistically significant.

RESULTS

Introns Are Not Required for ICP0's Proapoptotic Activity in HEp-2 Cells

Because α0 appeared able to confer its pro-apoptotic activity through an RNA-mediated mechanism (Sanfilippo and Blaho, 2006), we asked whether the two ICP0 introns are necessary for inducing apoptosis in HEp-2 cells. We tested whether cDNA-expressed α0 induced apoptosis upon HSV-1 infection in the presence of CHX. HEp-2 cells were treated with CHX and infected with vCPc0, which is a virus derived from the wild-type HSV-1 strain 17 that generates both copies of ICP0 using the viral promotor and cDNA copies of α0. Infection of HEp-2 cells with both wild-type strains of HSV-1, 17 and KOS, in the presence of CHX were used as positive controls. Infection with wild-type HSV-1 strains and vCPc0 in the absence of CHX and infection with the ICP0-null virus, 7134, in the absence and presence of CHX were used as negative controls. At 24 h post-infection, Hoechst DNA dye was added to the media to allow for visualization of chromatin and cellular and nuclear morphologies were assessed. Following imaging, whole-cell extracts were prepared, separated on a denaturing gel, and probed with anti-PARP, -ICP27, -ICP0 and -VP22 antibodies as described in Section "Materials and Methods." VP22 detection is a marker for late phase viral replication (Blaho et al., 1994).

This experiment was repeated twice and the results from a representative experiment are shown in **Figure 2**. Phase contrast, Hoechst images, and apoptotic cell percentages are displayed in **Figure 2A**. The morphological results show that cells infected with wild-type HSV-1 strains, vCPc0 and 7134 in the absence of CHX show enlarged cell size and diffuse cytoplasmic DNA patterns indicative of infectious cytopathic effect (CPE). This morphology results when the HSV-1 virus is regulating cellular machinery and generating HSV-1 virions. Eventually, cells are lysed and viral progeny are released. These treatments show very low levels of apoptosis, since HSV-1 generates anti-apoptotic proteins to prevent programmed cell death to result in infected cells. Cells treated with CHX in the absence of infection show a baseline level of chromatin condensation and membrane blebbing (13%) due to CHX treatment. Cells infected with ICP0-null HSV-1 in the presence of CHX show a baseline level of apoptosis that is slightly increased from CHX treatment alone (26%). This is consistent with previous results (Sanfilippo and Blaho, 2006). KOS and 17 infection in the presence of CHX shows marked increase in apoptotic morphologies (52 and 62%, respectively). Infection with vCPc0 in the presence of CHX shows chromatin condensation and membrane blebbing morphologies at levels (51%) similar to that of KOS.

Additionally, we assessed biochemical markers for apoptosis. When CHX is not present, all wild-type and mutant HSV-1 infections show the presence of VP22, indicating late viral replication and verifying the morphological results (**Figure 2B**, lanes 2–5). All HSV-1- cells infected in the absence of CHX also generated ICP27 and, with the exception of 7134, ICP0. 7134-infected cells do not generate ICP0 since this is an ICP0-null virus. Conversely, wild-type and mutant infections in the presence of CHX did not synthesize VP22, ICP0, and ICP27 (**Figure 2B**, lanes 7–10). In the presence of CHX, all HSV-1-infected cells generate low levels of modified ICP27 compared to infection in the absence of CHX. The production of these ICP27 immune reactive triplet forms was previously reported and is likely due to a unique feature of the ICP27 transcript that allows for translation in the presence of CHX (Sanfilippo et al., 2004b). When the apoptotic marker, PARP, was analyzed in this experiment, all wild-type and mutant HSV-1-infected cells without CHX had low levels of PARP cleavage (lanes 2–5). This indicates that little to no apoptosis occurring in these wells, which confirms the morphological results (**Figure 2A**). CHX-treated cells show baseline PARP cleavage for this treatment (lane 6). 7134-infected cells in the presence of CHX had PARP cleavage similar to CHX-treated cells (compare lane 10 with 6), which indicates that HSV-1 infection without α0 does not induce apoptosis. Whole-cell extracts from KOS- and 17-infected cells in the presence of CHX resulted in nearly complete PARP cleavage (lanes 7–9), indicating high rates of apoptosis and verifying morphological results (**Figure 2A**). Importantly, vCPc0-infection in the presence of CHX caused PARP cleavage at rates equivalent to KOS-infected cells plus CHX. Together, these morphological and biochemical results indicate that in the absence of protein synthesis intron-less, cDNA-expressed α0 induces apoptosis in infected cells at similar rates to wild-type-infected cells.

Previous studies have indicated that transfection with a plasmid expressing ICP0 induces apoptosis in cells (Inman et al., 2001b; Sanfilippo and Blaho, 2006). To test whether α0 introns are needed for induction of apoptosis in this setting, we transfected cells with a plasmid expressing ICP0 from a cDNA copy of the α0 gene (pcDNAICP0) and compared the response to cells transfected with a plasmid expressing ICP0 from the intron-containing, genomic copy of the gene (pICP0). The pUC19 plasmid was used as a negative control. In addition, a plasmid (pBAK) expressing the proapoptotic BCl-2 family member, BAK, which induces the intrinsic apoptotic pathway, was used as a positive control. This experiment was repeated five times in triplicate. At 24 h post-transfection, cellular and nuclear morphologies were assessed and the results from a representative experiment are displayed in **Figure 3A**. The overall means and standard deviations of chromatin condensation from all five experiments are graphed in **Figure 3B**.

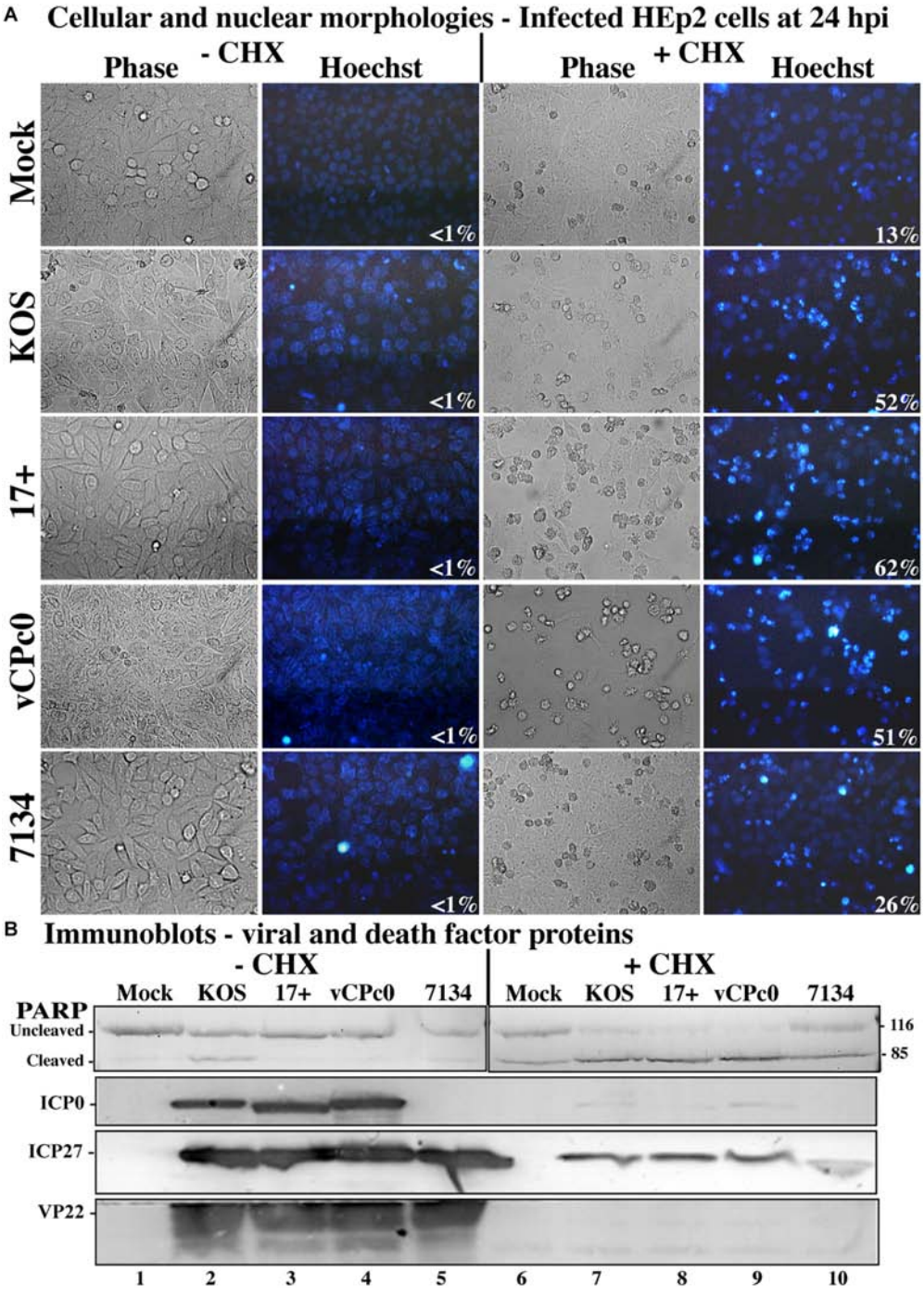

FIGURE 2 | Morphological and biochemical assessment of infected HEp-2 cells at 24 h post-infection. **(A)** HEp-2 cells were infected at MOI of 10 with wild-type HSV-1 (KOS), HSV-1 (17+), and recombinant ICP0 viruses vCPc0 and 7134. Twenty-four hours following post-infection Hoechst DNA dye was added to the media at a concentration of 5 μg/ml to visualize chromatin condensation. Phase contrast and Hoechst-stained images were obtained at 24 h post-infection (40X magnification). Numbers in the lower right corner of Hoechst panels represent the percentage of nuclei displaying chromatin condensation in that treatment. **(B)** Whole-cell extracts were obtained from these cells. Subsequently, the extracted proteins were immunoblotted for PARP, ICP0, ICP27, and VP22. Cropped images of blots were prepared as described in Section "Materials and Methods."

Cells transfected with pcDNAICP0 showed more chromatin condensation (52.8 ± 10.3%) compared to pUC19 transfected cells (18 ± 11.4%). This difference was deemed to be statistically significant ($p < 0.05$) using Student's *t*-test. Cells transfected with positive control plasmids, pICP0 and pBAK, showed levels near and above that for pcDNAICP0, respectively.

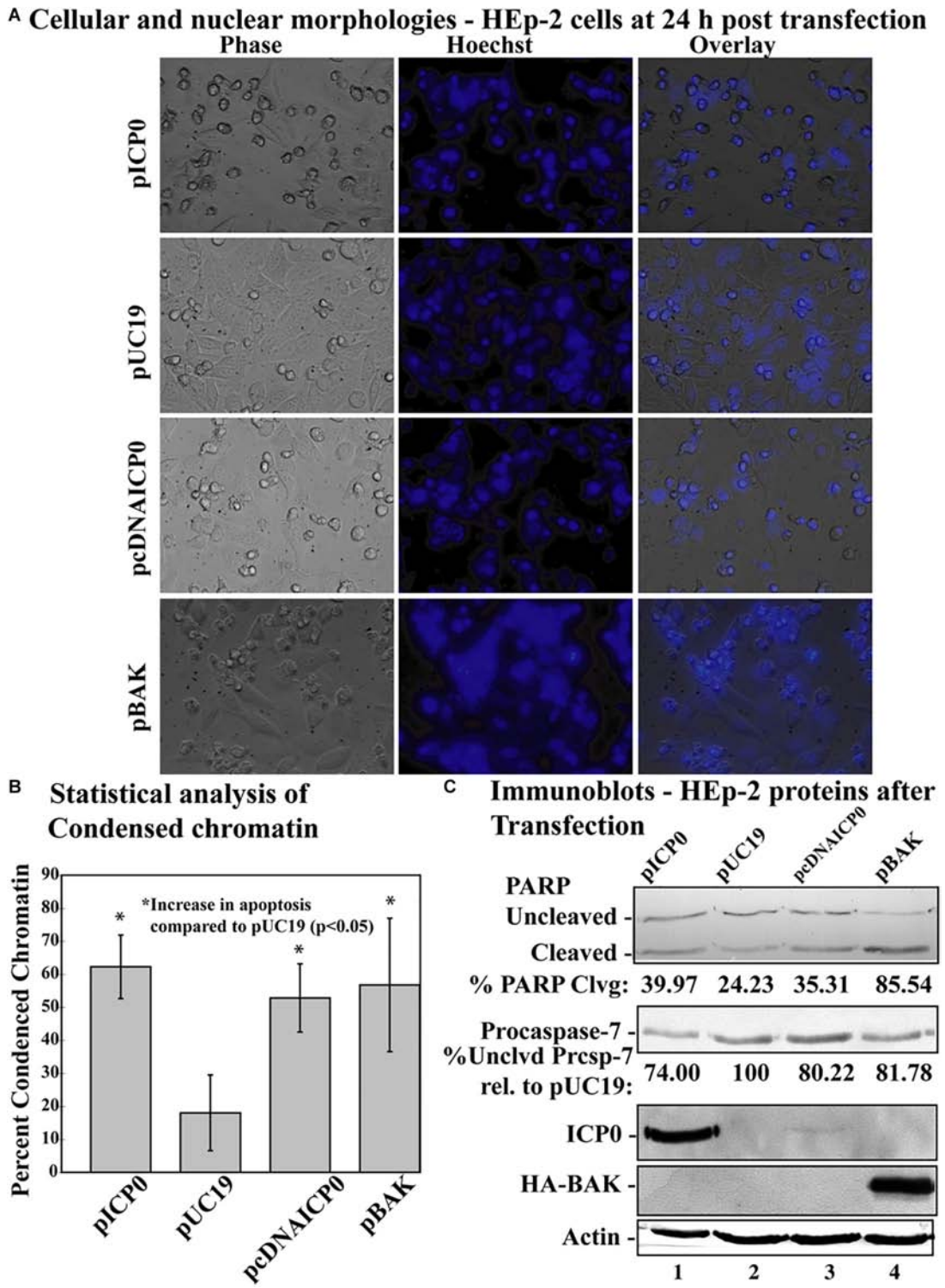

FIGURE 3 | Apoptosis in HEp-2 cells following transfection with pICP0 and pcDNA. **(A)** Cell morphologies of HEp-2 cells transfected with 0.4 μg of pICP0, pcDNAICP0, and pBAK. Twenty-four hours following transfection Hoechst DNA dye was added to the media at a concentration of 5 μg/ml to visualize chromatin condensation. Phase contrast, Hoechst-stained, and overlayed images were captured with a digital camera (40X magnification). Images are representative of a single experiment. **(B)** Statistical analysis of percentages of condensed chromatin for each treatment was conducted using Student's *t*-test ($p < 0.05$). The results represented in the bar graphs are from five independent experiments performed in triplicate. The mean of the percentage of cells exhibiting chromatin condensation following transfection is graphed. Error bars represent standard deviation for each treatment group. **(C)** Immune reactivities of transfected cells from triplicate wells

(Continued)

FIGURE 3 | Continued
that were combined, harvested, separated in a denaturing gel, transferred to nitrocellulose, probed with anti-PARP, -ICP0, -actin, -procaspase-7 and -HA primary antibodies. PARP and procaspase-7 band intensities were quantified using NIH image software, as described in Section "Materials and Methods." Percent PARP cleavage was calculated as a ratio of the band intensity of cleaved PARP relative to the sum of uncleaved and cleaved bands. For procaspase-7 protein, the band intensity for cells transfected with pUC19 was set to 100% and all other groups are displayed relative to this number. Cropped images of blots were prepared as described in Section "Materials and Methods."

Previously, we have demonstrated that procaspase-7 is cleaved and activated during HSV-dependent apoptosis (Kraft et al., 2006); we used immunoblots for this and PARP as markers for apoptosis (**Figure 3C**). Immunoblotting was also used to detect ICP0 and BAK produced in transfected cells. Transfection with pcDNAICP0 led to an increase in PARP cleavage (35.31%) and a decrease in procaspase-7 protein (80.22%) from pUC19 (24.23% PARP cleavage and 100% procaspase-7 protein). It is of note that the magnitude of biochemical markers for apoptosis in these groups was less than the magnitude of the difference in apoptotic morphologies (**Figure 3B**). Because we are looking at whole cell lysates from both transfected and non-transfected cells, some of the differences in protein levels can be more difficult to detect, than distinctions in morphologies that are quantitated on a per cell basis. Although pcDNAICP0 produces less ICP0 protein than pICP0 as seen in the ICP0 blot (**Figure 3B**, compare lane 3 with 1), pcDNAICP0-transfected cells show increased levels of apoptosis from the pUC19 baseline. Based on the results presented in **Figures 2**, **3**, we conclude that the α0 introns are not required for the apoptotic activity of ICP0.

Apoptosis Is Cell-Autonomous in ICP0-Transfected HEp-2 Cells

The apoptosis induction by α0 transfection could either be explained by ICP0 expression directly causing apoptosis in transfected cells or indirectly causing apoptosis in nearby non-expressing cells via the secretion of a pro-apoptotic factor. To distinguish between these possibilities, we constructed plasmids expressing either the full-length ICP0 open reading frame or the cDNA version, containing GFP driven from an adjacent IRES, termed pICP0GFP and pcDNAICP0GFP, respectively (**Figure 1**, lines 11 and 12). Transfecting HEp-2 cells with these GFP-expressing constructs allowed us to identify the cells expressing ICP0 and assess their morphologies. HEp-2 cells were transfected with control GFP-expressing plasmid (pGFP), pcDNAICP0GFP, or pICP0GFP. At 24 h following transfection, GFP fluorescence, stained chromatin, and morphological changes were assessed using phase contrast and fluorescence microscopy (**Figure 4A**). Green fluorescence indicative of GFP expression was evident in pGFP-, pcDNAICP0GFP-, and pICP0GFP-transfected cells. The majority of the GFP positive cells from the pGFP transfection displayed a cobblestone morphology and their chromatin was evenly distributed throughout the nuclei, indicative of a healthy cell monolayer, and similar to the morphologies of the surrounding non-transfected cells. In contrast, the majority of the GFP-positive cells from the pcDNAICP0GFP- and pICP0GFP-transfected wells were smaller, exhibited membrane blebbing, and displayed smaller, more brightly stained nuclei than pGFP-transfected cells. These phenotypes are indicative of cells undergoing apoptosis. We quantitated the percentage of GFP-positive cells displaying apoptotic morphologies to surrounding non-expressing cells in 12 individual wells. 82.11 ± 1.54% of the cells transfected with pICP0GFP and 79.37 ± 4.92% of pcDNAICP0GFP-transfected cells were apoptotic, while only 6.23 ± 2.33% of the cells transfected with pGFP were apoptotic. Cell lysates from transfected cells were assessed for the biochemical features of apoptosis via immunoblotting. pICP0GFP- and pcDNAICP0GFP-tranfected cells showed more PARP and caspase-7 cleavage than control pGFP (**Figure 4B**, compare lanes 1 and 2 with 3). These results indicate ICP0 expression leads to apoptosis in a cell autonomous manner in the HEp-2 cells.

Full-Length ICP0 Protein Is Not Required for Apoptosis Induction in HEp-2 Cells

Previous studies showed that HSV-1 infected cells undergo HSV-dependent apoptosis when protein synthesis is inhibited and when both copies of genomic ICP0 contain a stop codon (Sanfilippo and Blaho, 2006). This finding suggests that the ICP0 RNA is a proapoptotic stimulus in infected HEp-2 cells. The next investigation was to determine whether partial ICP0 protein synthesis could facilitate α0's proapoptotic activity in HEp-2 cells. HEp-2 cells were transfected with a plasmid expressing a mutant of ICP0 with a nonsense mutation after codon 212, pTruncICP0 (**Figure 1**, line 8). The vector pUC19 was transfected as a negative control. The pBAK and pUC19 plasmids were used as positive and negative controls, respectively. At 24 h post-transfection, cellular and nuclear morphologies were assessed. This experiment was repeated in five times in triplicate. Phase contrast and Hoechst images from a representative experiment are displayed in **Figure 5A**. The overall means and standard deviations of chromatin condensation from all five experiments are graphed in **Figure 5B**. The cumulative results (**Figure 5**) were as follows. 14.07 ± 10.7% of the pUC19-transfected cells showed chromatin condensation, which indicates a baseline level of apoptosis due to transfection. 61.7 ± 22% of the pBAK-transfected cells exhibited chromatin condensation. Transfection of HEp-2 cells with pICP0 showed a statistically significant increased in chromatin condensation (34.8 ± 19.4%) compared to pUC19-transfected cells. Cells transfected with pTruncICP0 showed comparable amounts of chromatin condensation (36.9 ± 19.4%) to pICP0-transfected cells.

Additionally, we assessed the biochemical markers of apoptosis by immunoblotting (**Figure 5C**). Procaspase-7 and the downstream caspase substrate PARP were used as markers for apoptosis. pUC19 transfection led to 30.53% PARP cleavage, showing background levels of apoptosis due to transfection

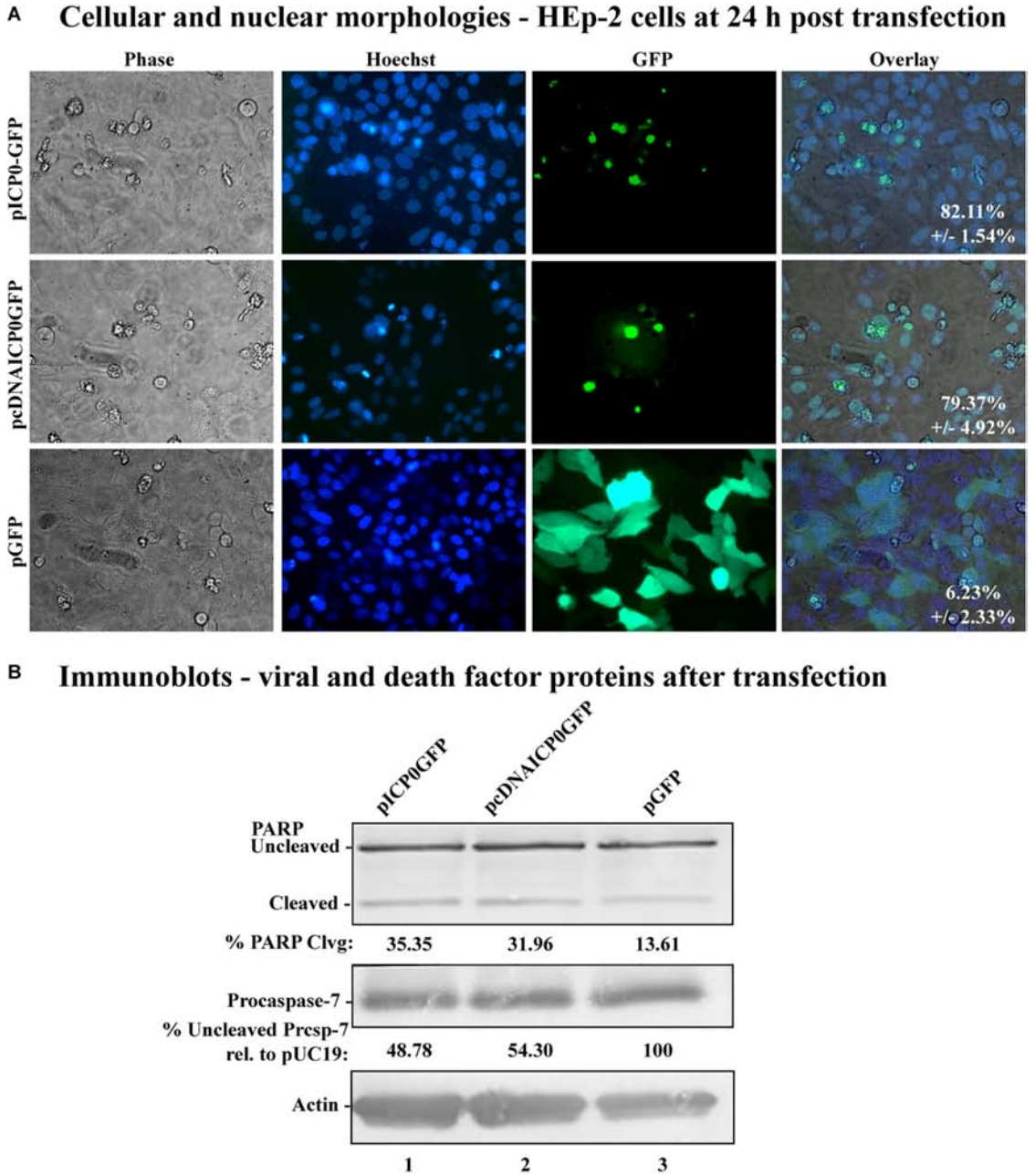

FIGURE 4 | Morphological and biochemical assessment of transfected HEp-2 cells at 24 h post-transfection. **(A)** Cell morphologies of HEp-2 cells transfected with 0.4 μg of pICP0GFP, pcDNAICP0GFP, or pGFP. Fluorescence images were obtained to identify Hoechst DNA staining (Hoechst) and the presence of the GFP. Phase contrast, Hoechst-stained, and GFP images were layered to obtain a merged image (overlay). The numbers inside each frame refers to the percentage of GFP positive cells exhibiting condensed chromatin. **(B)** Whole-cell extracts of HEp-2 cells transfected with pICP0GFP, pcDNAICP0GFP, and a GFP expressing control plasmid (pGFP) were obtained from triplicate wells, separated in a denaturing gel, transferred to nitrocellulose, and probed with anti-PARP, -procaspase-7 and -actin antibodies. PARP and procaspase-7 band intensities were quantified using NIH image software, as described in Section "Materials and Methods." Percent PARP cleavage was calculated as a ratio of the band intensity of cleaved PARP relative to the sum of uncleaved and cleaved bands. For procaspase-7 protein, the band intensity for cells transfected with pUC19 was set to 100% and all other groups are displayed relative to this number. Cropped images of blots were prepared as described in Section "Materials and Methods."

protocols. We set the levels of procaspase-7 protein present in this group to 100%. pBAK-transfected cells displayed 49.7% PARP cleavage and 64.45% procaspase-7 protein relative to pUC19. This is consistent with the majority of cells undergoing apoptosis as based on the morphological assessment above. pICP0- and pTruncICP0-transfected cells displayed similar levels of PARP cleavage (36.64 and 36.82%, respectively) and procaspase-7 protein (57.11 and 41.33%, respectively). The above

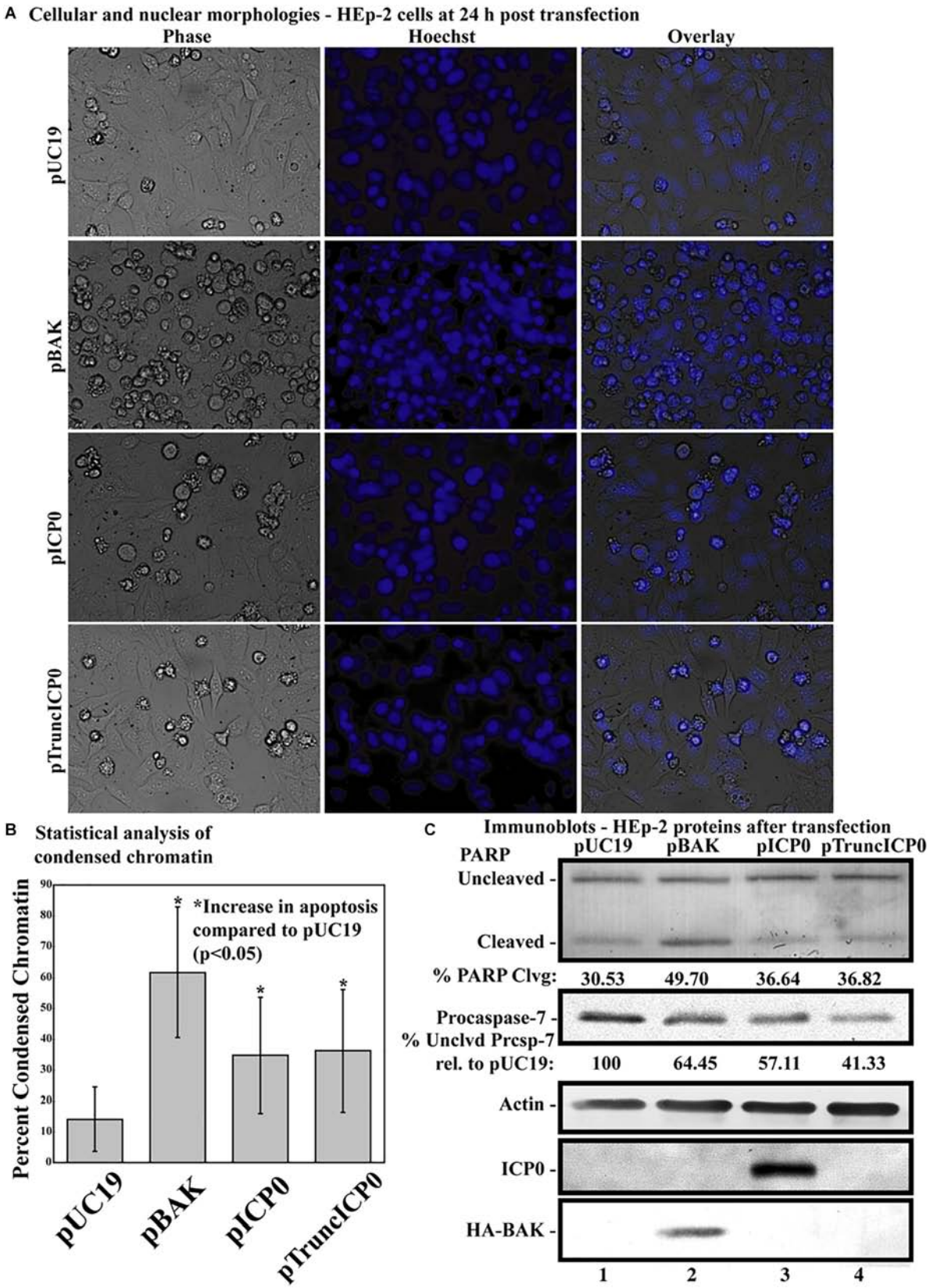

FIGURE 5 | Continued

FIGURE 5 | Apoptosis in HEp-2 cells following transfection with pICP0 and pTruncICP0. **(A)** Cell morphologies of HEp-2 cells transfected with 0.4 μg of pUC19, pBAK, pICP0, or pTruncICP0. Phase contrast, Hoechst and overlay images were captured with a digital camera (40X magnification). Images are representative of a single experiment. **(B)** Statistical analysis of percentages of condensed chromatin for each treatment was conducted using Student's *t*-test ($p < 0.05$). The results represented in the bar graphs are from five independent experiments performed in triplicate. The mean of the percentage of cells exhibiting chromatin condensation following transfection is graphed. Error bars represent the standard deviation for each treatment group. **(C)** Immune reactivities of transfected cells from triplicate wells that were combined, harvested, separated in a denaturing gel, transferred to nitrocellulose, probed with anti-PARP, -procaspase-7, -ICP0, -actin, and -HA (to recognize HA-tagged BAK protein) primary antibodies. PARP and procaspase-7 band intensities were quantified using NIH image software, as described in Section "Materials and Methods." Percent PARP cleavage was calculated as a ratio of the band intensity of cleaved PARP relative to the sum of uncleaved and cleaved bands. For procaspase-7 protein, the band intensity for cells transfected with pUC19 was set to 100% and all other groups are displayed relative to this number. Cropped images of blots were prepared as described in Section "Materials and Methods."

morphological and biochemical results show that full-length ICP0 protein is not necessary for ICP0-induced apoptosis in transfected cells. These findings suggest other properties of the α0 gene may affect apoptosis induction in HEp-2 cells.

ICP0 RNA Is Sufficient to Induce Apoptosis in HEp-2 Cells

We next investigated the ability of ICP0 gene expression to induce apoptosis in the absence of ICP0 protein production in transfected cells HEp-2 cells. HEp-2 cells were transfected either with a plasmid expressing genomic α0 with two stop mutations after codons 12 and 106, pα0RNA12/106, or after codons 12 and 212, pα0RNAn12/212 (**Figure 1**, lines 9 and 10). The vector pUC19 was transfected as a negative control, and pICP0 and pBAK were used as positive controls. At 24 h post-transfection, cellular and nuclear morphologies were assessed. This experiment was repeated in triplicate wells two times. Phase contrast and Hoechst images from a representative experiment are displayed in **Figure 6A**. The cumulative means and standard deviations of chromatin condensation from both experiments are graphed in **Figure 6B**. 5.1 ± 2.2% of the pUC19-transfected cells showed chromatin condensation. 37.5 ± 8.5% of the pBAK-transfected cells exhibited chromatin condensation. Transfection of HEp-2 cells with pICP0 showed a statistically significant increased in chromatin condensation (22.9 ± 5.4%) compared to pUC19-transfected cells. Cells transfected with pα0RNAn12/106 and pα0RNAn12/212 showed comparable amounts of chromatin condensation to pICP0-transfected cells (22.1 ± 7.0 and 20.6 ± 6.2%, respectively).

PARP and procaspase-7 cleavage were assessed for biochemical indication of apoptosis using immunoblotting (**Figure 6C**). pUC19 transfection leads to 18.01% PARP cleavage, showing background levels of apoptosis due to transfection protocols, and again we set the levels of procaspase-7 protein in this group to 100%. pBAK-transfected cells displayed 35.34% PARP cleavage and 73.63% procaspase-7 protein relative to pUC19, which is consistent with a significant portion of cells undergoing apoptosis as based on the morphological assessment above. pICP0-, pα0RNAn12/106- and pα0RNAn12/212-transfected cells displayed similar levels of PARP cleavage (27.78, 27.95, and 27.96, respectively) and procaspase-7 protein (88.15, 85.84, and 88.75, respectively).

Together, the above morphological and biochemical findings show that ICP0 protein is not necessary for ICP0-induced apoptosis in transfected cells. These results support previous findings which suggest that ICP0 RNA is responsible for HSV-1-induced apoptosis in HEp-2 cells.

ICP0 Protein Is Not Required for Autonomous Proapoptotic Activity in HEp-2 Cells

Results above (**Figure 4**) indicate that transfection of the wild-type ICP0 gene causes apoptosis in a cell autonomous manner. To determine whether this was also true for α0 RNA expression alone the ICP0 open reading frame of pICP0GFP was replaced with α0 with two stop mutations after codons 12 and 106, pα0RNA12/106, termed pα0RNAn12/106GFP. This plasmid was transfected into HEp-2 cells; pcDNAICP0GFP, pICP0, and pGFP were transfected into cells as controls. At 24 h following transfection, GFP fluorescence, chromatin condensation, and morphological changes were assessed using phase and fluorescence microscopy (**Figure 7**). Green fluorescence indicative of GFP expression was evident in all transfected cells. The majority of the GFP positive cells from the pGFP transfection displayed cobblestone morphology and their chromatin was evenly distributed throughout the nuclei, indicative of a healthy cell monolayer, and similar to the morphologies of the surrounding non-transfected cells. In contrast, the majority of the GFP-positive cells from the pICP0GFP-, pcDNAICP0GFP-, and pα0RNAn12/106GFP-transfected wells were smaller, exhibited membrane blebbing, and displayed smaller, more brightly stained nuclei than surrounding non-transfected cells. These phenotypes are indicative of cells undergoing apoptosis. We quantified the percentage of GFP-positive cells displaying apoptotic morphologies to surrounding non-GFP-expressing cells in 12 individual wells. 80.01 ± 5.67, 97.53 ± 2.50, and 99.52 ± 1.26% of the cells transfected with pcDNAICP0GFP, pICP0GFP, pα0RNAn12/106GFP were apoptotic, while only 11.67 ± 2.06% of the cells transfected with pGFP were apoptotic. Together, these results indicate that ICP0 protein is not required for the autonomous proapoptotic activity of α0 in HEp-2 cells.

A Nonsense Mutation at Amino Acid 212 Abrogates Apoptosis in Vero Cells

Previously, we determined while infected HEp-2 cells can undergo HSV-dependent apoptosis in the absence of protein expression, infected Vero cells require expression of a protein facilitator for HSV-dependent apoptosis (Nguyen et al., 2005). Given that some form of infected cell protein synthesis was needed for apoptosis in infected Vero cells, it was possible that

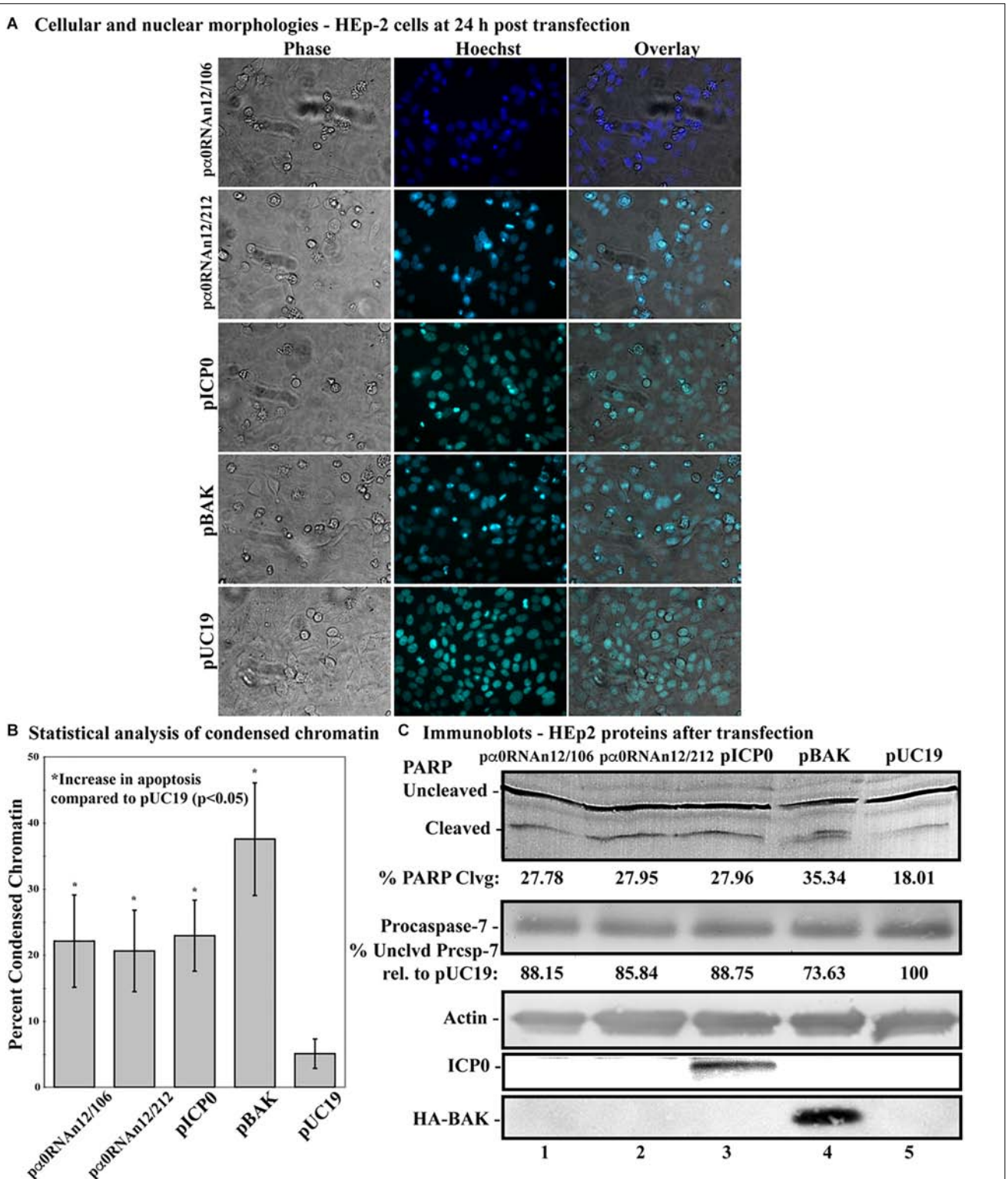

FIGURE 6 | Apoptosis in HEp-2 cells following transfection with pα0RNAn12/106, and pα0RNAn12/212. **(A)** Cell morphologies of HEp-2 cells transfected with 0.4 μg of pα0RNAn12/106, pα0RNAn12/212, pICP0, pBAK, or pUC19. Phase contrast, Hoechst-stained, and overlayed images were captured with a digital camera (40X magnification). Images are representative of a single triplicate experiment. **(B)** Statistical analysis of percentages of condensed chromatin for each treatment was conducted using Student's *t*-test ($p < 0.05$). The results represented in the bar graphs are from five independent experiments performed in triplicate. The mean of the percentage of cells exhibiting chromatin condensation following transfection is graphed. Error bars represent standard deviation for each treatment group.

(Continued)

FIGURE 6 | Continued

(C) Immune reactivities of transfected cells from triplicate wells that were combined, harvested, separated in a denaturing gel, transferred to nitrocellulose, probed with anti-PARP, -procaspase-7, -ICP0, -actin, and -HA primary antibodies. PARP and procaspase-7 band intensities were quantified using NIH image software, as described in Section "Materials and Methods." Percent PARP cleavage was calculated as a ratio of the band intensity of cleaved PARP relative to the sum of uncleaved and cleaved bands. For procaspase-7 protein, the band intensity for cells transfected with pUC19 was set to 100% and all other groups are displayed relative to this number. Cropped images of blots were prepared as described in Section "Materials and Methods."

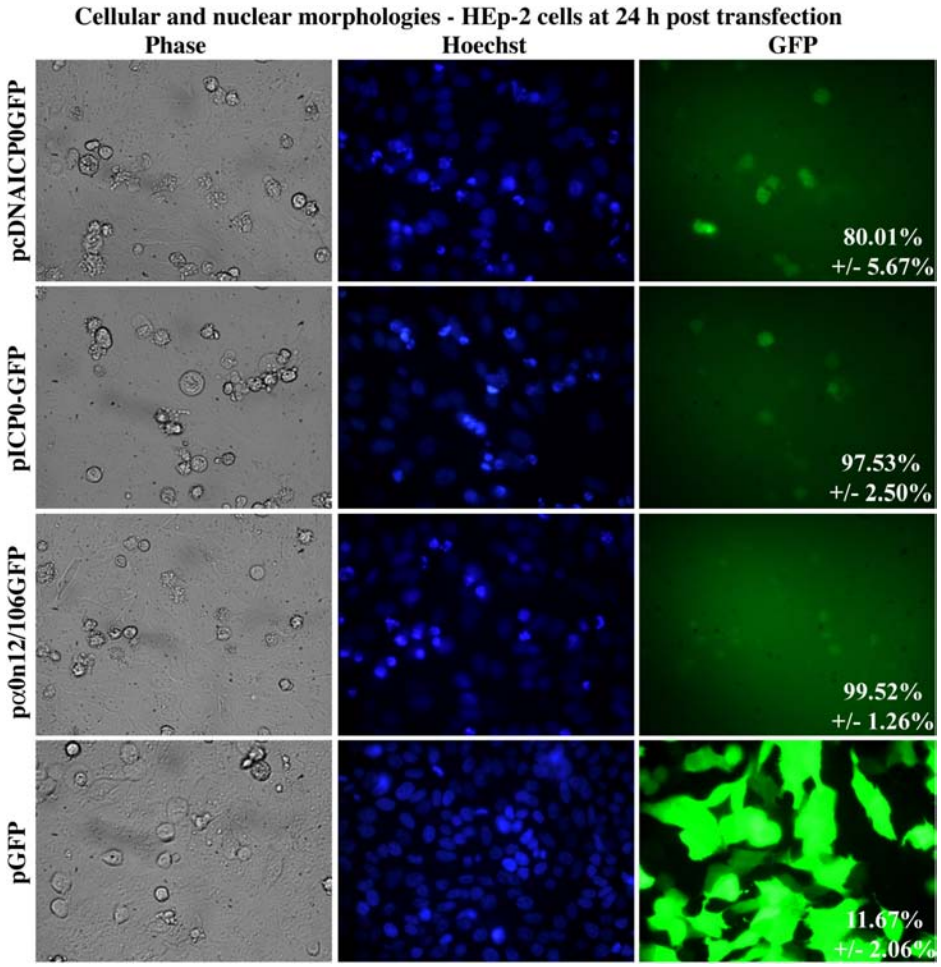

FIGURE 7 | Apoptosis in HEp-2 cells following transfection with pα0RNAn12/106GFP. Cell morphologies of HEp-2 cells transfected with 0.4 μg of pcDNAICP0GFP, pICP0GFP, pα0RNAn12/106GFP, or pGFP. Phase contrast, Hoechst-stained, and overlayed images were captured with a digital camera (40X magnification). Images are representative of a single experiment and numbers inside the overlay represent the mean and standard deviation of the percentage of GFP positive cells displaying condensed chromatin in the given triplicate experiment.

it was the ICP0 protein itself that facilitates this viral apoptosis. To determine if full-length ICP0 protein was necessary for the α0 induced apoptosis, Vero cells were transfected with pTruncICP0. The pUC19 plasmid was used as a negative control and pICP0 and pBAK were used as positive controls. At 24, 36, 48, and 72 h post-transfection, cellular, and nuclear morphologies were assessed and the results from a representative experiment at 48 h post-transfection are shown in **Figure 8A**. Apoptotic percentages were determined by dividing the number of apoptotic cells by the total number of cells per image. To account for any minor variations in background levels of apoptosis throughout the timecourse, each treatment was divided by the apoptotic percentage of the pUC19 well for the given time point to calculate the fold increase in apoptosis from pUC19. The means and standard deviations for each timepoint were determined and displayed graphically in **Figure 8B**. pUC19-transfected cells showed little chromatin condensation (1.66 ± 0.92%). This indicates that the baseline level of apoptosis due to transfection for Vero cells is very low. The pBAK-transfected cells displayed chromatin condensation that was 6–12 fold higher than that of pUC19. Transfection of Vero cells with pICP0 showed a statistically significant increase in chromatin condensation

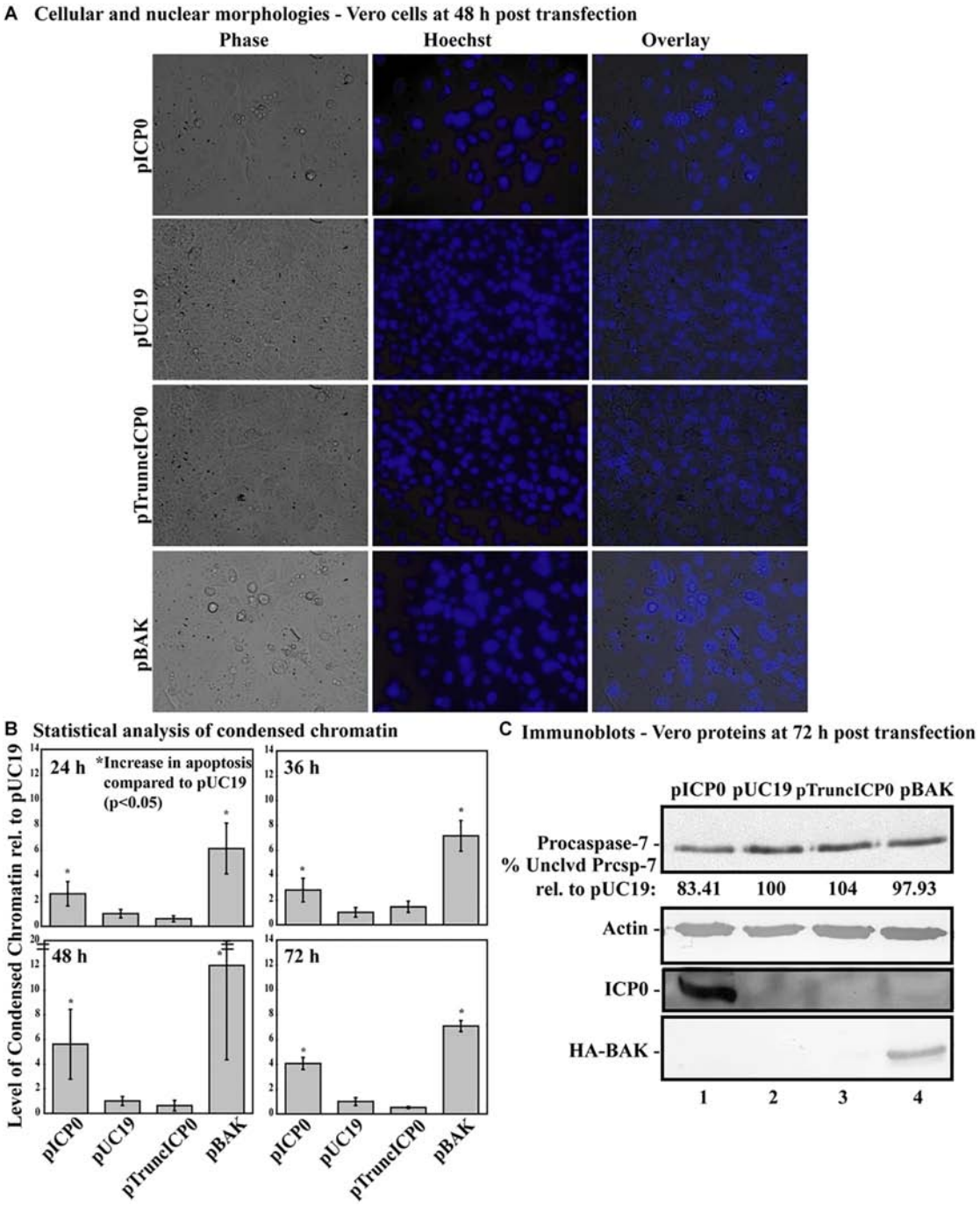

FIGURE 8 | Vero cells do not undergo apoptosis following transfection with pTruncICP0. Vero cells were transfected with 1.0 μg of pICP0, pUC19, pTruncICP0, or pBAK and Hoechst DNA dye was added to the media at 23 h post-transfection. At 24, 36, 48, and 72 h post-transfection, phase contrast and fluorescence microscopy was used to visualize cellular and nuclear morphologies. **(A)** Phase contrast, Hoechst-stained, and overlay images were obtained at 48 h post-transfection (40X magnification). **(B)** The percentage of chromatin condensation at 24, 36, 48, and 72 h in triplicate wells was calculated for four independent experiments. The mean chromatin condensation percentage was calculated for each time point. The percentage of condensed chromatin in pUC19 treated cells was set to 1 for each time point and other groups are presented as a relative value compared to pUC19. The mean relative chromatin condensation is graphed. Error bars represent the standard deviation. Statistical analysis of percentages of condensed chromatin for each treatment and time point was conducted using Student's *t*-test. **(C)** Triplicate wells were combined at 72 h post-transfection and whole-cell extracts were obtained, separated in a denaturing gel, transferred to nitrocellulose, probed with anti-procaspase-7, -actin, -ICP0, -HA primary antibodies. The intensities of procaspase-7 bands were quantified using NIH image, as described in Section "Materials and Methods." For procaspase-7 protein, the band intensity for cells transfected with pUC19 was set to 100% and all other groups are displayed relative to this number. Cropped images of blots were prepared as described in Section "Materials and Methods."

(2.6–5.6 times) compared to pUC19. Cells transfected with pTruncICP0 showed low levels of chromatin condensation (0.6–1.4) relative to pUC19.

At 72 h post-transfection, whole-cell extracts from transfected cells were analyzed for apoptotic proteins, ICP0 and BAK using immunoblotting (**Figure 8C**). Lysates from pBAK-transfected cells exhibited detectable decreases in procaspase-7 protein (97.93%) compared to pUC19. These findings show that Vero cells are more resistant to BAK-induced apoptosis than HEp-2 cells. Transfection with pICP0 led to decreased levels of procaspase-7 (83.41%) compared to pUC19 (100%). pTruncICP0 transfection displayed little to no reduction of procaspase-7 levels (104%) compared to pUC19. These results demonstrate that full-length ICP0 protein is necessary for ICP0-induced apoptosis in transfected Vero cells. Based on these findings, we conclude that the facilitator protein must be either full-length ICP0 or a cellular protein that is dependent on ICP0.

Apoptosis Is Cell-Autonomous in ICP0-Transfected Vero Cells

In this final study, we assessed whether Vero cells expressing ICP0 were undergoing apoptosis themselves or if they were releasing proapoptotic factors causing death in surrounding non-transfected cells. To differentiate between these possibilities, Vero cells were transfected with pICP0GFP so we could identify the cells expressing ICP0 and assess their morphologies. Transfection with pGFP was used as a negative control. At 48 h post-transfection, Hoechst DNA dye was added to the media to allow for visualization of chromatin. Subsequent GFP fluorescence, chromatin condensation and morphological changes were assessed using phase and fluorescence microscopy (**Figure 9**). The GFP positive cells from the pGFP transfection were flat and well spread out, similar to surrounding non-transfected cells. Additionally, they displayed an evenly distributed nuclear Hoechst staining pattern, which is typical of healthy cells. The GFP-positive cells from the pICP0GFP-transfected wells displayed phenotypes indicative of cells undergoing apoptosis. We quantified the percentage of GFP-positive cells displaying apoptotic morphologies compared to surrounding non-expressing cells. 78.44 ± 12.13% of the cells transfected with pICP0GFP were apoptotic. This result indicates that the cells are undergoing ICP0-dependent apoptosis do it in a cell autonomous manner. Thus, if a cellular protein is also involved in the apoptotic process in Vero cells, it does not likely migrate to surrounding cells.

DISCUSSION

A link between apoptosis and the latency of HSV is supported by many studies from multiple research groups. Therefore, studies of apoptosis in HSV infected cells is likely to provide insight into the establishment, maintenance, and reactivation from latency. Our previous studies have identified the α0 gene as the viral trigger of apoptosis during HSV infections. In this study, we set out to address several key unknowns. The first was focused on the structure of the α0 gene in apoptosis induction in HEp-2 cells. The second involved whether this process occurred in a cell autonomous manner. Finally, we investigated the role of ICP0 protein in apoptosis in Vero cells. Our key findings may be summarized as follows.

ICP0 is sufficient to serve as the herpes apoptosis facilitator (HDAP) in Vero cells. This does not exclude the possibility that other cellular proteins may also be involved. This finding is consistent with previous studies (Inman et al., 2001b) and may be related to the noted ICP0 toxicity in viral gene therapy vectors (Samaniego et al., 1998). The key question remains about the basis of the difference between HEp-2 and Vero cells

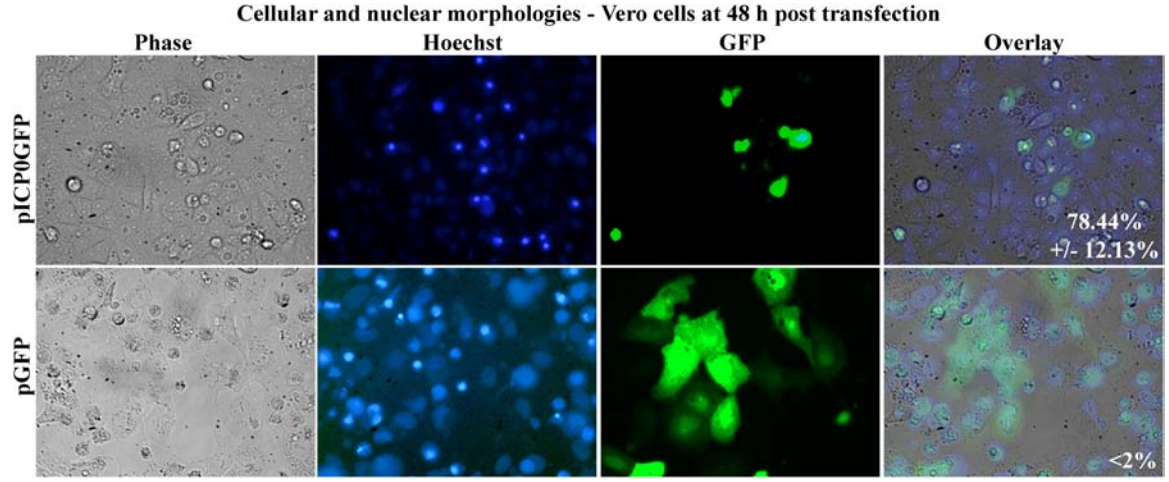

FIGURE 9 | Apoptosis in Vero cells following transfection with pICP0GFP. Cell morphologies of Vero cells transfected with 0.4 μg of pICP0GFP or pGFP. Phase contrast, Hoechst-stained, and overlayed images were captured with a digital camera (40X magnification). Images are representative of a single experiment and numbers inside the overlay represent the mean and standard deviation of the percentage of GFP positive cells displaying condensed chromatin quantified in the given triplicate experiment.

in the requirements for apoptosis induction. HEp-2 cells are transformed cells and fail to express p53, due to the presence of the human papillomavirus E6 protein (Ogura et al., 1993), which has been previously shown to influence HSV-dependent apoptosis (Nguyen et al., 2007). Vero cells are immortalized, but not transformed; this distinction appears to imply that the pro-apoptotic activity of ICP0 may be affected by p53 status. Previous reports have shown that ICP0 can mediate the ubiquitination of p53 by acting as a RING finger ubiquitin E3 ligase (Boutell and Everett, 2003). Interestingly, a recent study described a reduced replication of HSV-1 in p53 deficient cells. They also reported that the ICP0 protein itself could be degraded in a p53-dependent manner in cells and that this was inhibited during a wild-type infection by ICP22 (Maruzuru et al., 2013), suggesting that a complex interplay between ICP0 and p53 may exist during HSV-1 infection.

α0-Dependent apoptosis likely plays a role during HSV reactivation from latency. ICP0 is essential for viral replication upon reactivation from HSV latency (Leib et al., 1989b). It is now recognized that VP16 is key to reactivation (Kim et al., 2012; Sawtell and Thompson, 2016). α0 is the first viral gene transcribed by VP16 (Harris-Hamilton and Bachenheimer, 1985). That both α0 RNA and ICP0 protein are proapoptotic in certain cells, raises the possibility that neuronal apoptosis occurs during reactivation. This might explain previous observations of apoptosis in herpes encephalitis (DeBiasi et al., 2002).

Although the LATs and miRNA of HSV are the only HSV gene products found to be abundantly expressed during latency, previous studies have detected low levels of α0 transcripts during HSV latency (Chen et al., 2002; Pesola et al., 2005; Maillet et al., 2006). A recent study by Raja and colleagues indicated that interruption of ICP0 expression led to reduced association of viral genomes with histones and lower levels of LAT transcripts in a murine latency model (Raja et al., 2016). The authors of this study propose a model in which low levels of ICP0 protein expression contribute to the establishment and/or maintenance of latency by facilitating genome association with heterochromatin and enhancing LAT expression. It is possible that ICP0's pro-apoptotic functions may also contribute to this newly identified role for ICP0 in establishment and maintenance of latency.

Together, this study has determined that the α0 gene produces two pro-apoptotic gene products during HSV infection. The α0 transcript is sufficient for apoptosis induction in at least one cell line, HEp-2 cells. On the other hand, other cell types, e.g., Vero cells, require both the transcript and protein of the ICP0 open reading frame to trigger HSV-dependent apoptosis. It is important to note that primary human keratinocytes, the first cells that the virus usually interacts with, are susceptible to HSV-dependent apoptosis (Pradhan and Nguyen, 2013). Further investigation into α0-dependent apoptosis may allow for an improved understanding of the control of both latent and lytic HSV-1 infections. The ICP0 protein is necessary for viral replication upon reactivation (Leib et al., 1989b). Additionally, a recent study has reported that disruption of ICP0 expression led to reduced LAT transcript levels (Raja et al., 2016). Thus, both apoptosis regulation and α0 gene expression have been implicated in latency regulation. Investigators seeking to understanding the role of ICP0 in HSV latency most now consider the potential that both α0 RNA and protein may trigger apoptosis as part of the reactivation process.

AUTHOR CONTRIBUTIONS

MN and JB designed, supervised, and interpreted the experiments and finalized the figures and manuscript. EG and KP performed the experiments as research coordinators. EG organized the original figures and wrote an initial version of the manuscript.

FUNDING

These studies were supported in part by a grant from the USPHS (AI48582 to JB). MN was supported in part by USPHS Institutional Research Training Awards (AI07647 and CA088796). KP was supported in part by an Undergraduate Research Fellowship from the Howard Hughes Medical Institute to Manhattan College, Riverdale, NY, United States. JB acknowledges the NYCRIN and CUNY I-Corps support of the National Science Foundation (Award Nos. OIA-1305023, IPP-1644664, and IIP-1740622).

ACKNOWLEDGMENTS

We thank Elise Morton and Leah Kang (MSSM) for expert technical cell culture assistance and Saul Silverstein, Priscilla Schaffer, Mary Klotman, and Peter Palese for providing reagents. We wish to dedicate this paper to the memory of Priscilla Schaffer who was always so helpful and supportive of our work.

REFERENCES

Ahmed, M., Lock, M., Miller, C. G., and Fraser, N. W. (2002). Regions of the herpes simplex virus type 1 latency-associated transcript that protect cells from apoptosis in vitro and protect neuronal cells in vivo. *J. Virol.* 76, 717–729. doi: 10.1128/jvi.76.2.717-729.2002

Aubert, M., and Blaho, J. A. (1999). The herpes simplex virus type 1 regulatory protein ICP27 is required for the prevention of apoptosis in infected human cells. *J. Virol.* 73, 2803–2813.

Aubert, M., Pomeranz, L. E., and Blaho, J. A. (2007). Herpes simplex virus blocks apoptosis by precluding mitochondrial cytochrome c release independent of caspase activation in infected human epithelial cells. *Apoptosis* 12, 19–35. doi: 10.1007/s10495-006-0330-3

Blaho, J. A., Mitchell, C., and Roizman, B. (1994). An amino acid sequence shared by the herpes simplex virus 1 alpha regulatory proteins 0, 4, 22, and 27 predicts the nucleotidylylation of the UL21, UL31, UL47, and UL49 gene products. *J. Biol. Chem.* 269, 17401–17410.

Boutell, C., and Everett, R. D. (2003). The herpes simplex virus type 1 (HSV-1) regulatory protein ICP0 interacts with and Ubiquitinates p53. *J. Biol. Chem.* 278, 36596–36602. doi: 10.1074/jbc.m300776200

Cai, W. Z., and Schaffer, P. A. (1989). Herpes simplex virus type 1 ICP0 plays a critical role in the de novo synthesis of infectious virus following transfection of viral DNA. *J. Virol.* 63, 4579–4589.

Carter, K. L., and Roizman, B. (1996). Alternatively spliced mRNAs predicted to yield frame-shift proteins and stable intron 1 RNAs of the herpes simplex virus 1 regulatory gene alpha 0 accumulate in the cytoplasm of infected cells. *Proc. Natl. Acad. Sci. U.S.A.* 93, 12535–12540. doi: 10.1073/pnas.93.22.12535

Chen, S. H., Lee, L. Y., Garber, D. A., Schaffer, P. A., Knipe, D. M., and Coen, D. M. (2002). Neither LAT nor open reading frame P mutations increase expression of spliced or intron-containing ICP0 transcripts in mouse ganglia latently infected with herpes simplex virus. *J. Virol.* 76, 4764–4772. doi: 10.1128/jvi.76.10.4764-4772.2002

DeBiasi, R. L., Kleinschmidt-DeMasters, B. K., Richardson-Burns, S., and Tyler, K. L. (2002). Central nervous system apoptosis in human herpes simplex virus and cytomegalovirus encephalitis. *J. Infect. Dis.* 186, 1547–1557. doi: 10.1086/345375

Du, T., Zhou, G., and Roizman, G. (2012). Induction of apoptosis accelerates reactivation of latent HSV-1 in ganglionic organ cultures and replication in cell cultures. *Proc. Natl. Acad. Sci. U.S.A.* 109, 14616–14621. doi: 10.1073/pnas.1212661109

Everett, R. D. (2000). ICP0, a regulator of herpes simplex virus during lytic and latent infection. *Bioessays* 22, 761–770. doi: 10.1002/1521-1878(200008)22:8<761::aid-bies10>3.0.co;2-a

Goodkin, M. L., Ting, A. T., and Blaho, J. A. (2003). NF-kappaB is required for apoptosis prevention during herpes simplex virus type 1 infection. *J. Virol.* 77, 7261–7280. doi: 10.1128/jvi.77.13.7261-7280.2003

Hagglund, R., and Roizman, B. (2004). Role of ICP0 in the strategy of conquest of the host cell by herpes simplex virus 1. *J. Virol.* 78, 2169–2178. doi: 10.1128/jvi.78.5.2169-2178.2004

Harris-Hamilton, E., and Bachenheimer, S. L. (1985). Accumulation of herpes simplex virus type 1 RNAs of different kinetic classes in the cytoplasm of infected cells. *J. Virol.* 53, 144–151.

Inman, M., Perng, G. C., Henderson, G., Ghiasi, H., Nesburn, A. B., Wechsler, S. L., et al. (2001a). Region of herpes simplex virus type 1 latency-associated transcript sufficient for wild-type spontaneous reactivation promotes cell survival in tissue culture. *J. Virol.* 75, 3636–3646. doi: 10.1128/jvi.75.8.3636-3646.2001

Inman, M., Zhang, Y., Geiser, V., and Jones, C. (2001b). The zinc ring finger in the bICP0 protein encoded by bovine herpesvirus-1 mediates toxicity and activates productive infection. *J. Gen. Virol.* 82(Pt 3), 483–492. doi: 10.1099/0022-1317-82-3-483

Jin, L., Carpenter, D., Moerdyk-Schauwecker, M., Vanarsdall, A. L., Osorio, N., Hsiang, C., et al. (2008). Cellular FLIP can substitute for the herpes simplex virus type 1 latency-associated transcript gene to support a wild-type virus reactivation phenotype in mice. *J. Neurovirol.* 14, 389–400. doi: 10.1080/13550280802216510

Jin, L., Peng, W., Perng, G. C., Brick, D. J., Nesburn, A. B., Jones, C., et al. (2003). Identification of herpes simplex virus type 1 latency-associated transcript sequences that both inhibit apoptosis and enhance the spontaneous reactivation phenotype. *J. Virol.* 77, 6556–6561. doi: 10.1128/jvi.77.11.6556-6561.2003

Jin, L., Perng, G. C., Mott, K. R., Osorio, N., Naito, J., Brick, D. J., et al. (2005). A herpes simplex virus type 1 mutant expressing a baculovirus inhibitor of apoptosis gene in place of latency-associated transcript has a wild-type reactivation phenotype in the mouse. *J. Virol.* 79, 12286–12295. doi: 10.1128/jvi.79.19.12286-12295.2005

Kerr, J. F., Wyllie, A. H., and Currie, A. R. (1972). Apoptosis: a basic biological phenomenon with wide-ranging implications in tissue kinetics. *Br. J. Cancer* 26, 239–257. doi: 10.1038/bjc.1972.33

Kim, J. Y., Mandarino, A., Chao, M. V., Mohr, I., and Wilson, A. C. (2012). Transient reversal of episome silencing precedes VP16-dependent transcription during reactivation of latent HSV-1 in neurons. *PLoS Pathog.* 8:e1002540. doi: 10.1371/journal.ppat.1002540

Koyama, A. H., Adachi, A., and Irie, H. (2003). Physiological significance of apoptosis during animal virus infection. *Int. Rev. Immunol.* 22, 341–359. doi: 10.1080/08830180305210

Kraft, R. M., Nguyen, M. L., Yang, X. H., Thor, A. D., and Blaho, J. A. (2006). Caspase 3 activation during herpes simplex virus 1 infection. *Virus Res.* 120, 163–175. doi: 10.1016/j.virusres.2006.03.003

Leib, D. A., Bogard, C. L., Kosz-Vnenchak, M., Hicks, K. A., Coen, D. M., Knipe, D. M., et al. (1989a). A deletion mutant of the latency-associated transcript of herpes simplex virus type 1 reactivates from the latent state with reduced frequency. *J. Virol.* 63, 2893–2900.

Leib, D. A., Coen, D. M., Bogard, C. L., Hicks, K. A., Yager, D. R., Knipe, D. M., et al. (1989b). Immediate-early regulatory gene mutants define different stages in the establishment and reactivation of herpes simplex virus latency. *J. Virol.* 63, 759–768.

Liesegang, T. J., Melton, L. J., Daly, P. J., and Ilstrup, D. M. (1989). Epidemiology of ocular herpes simplex. Incidence in Rochester, Minn, 1950 through 1982. *Arch. Ophthalmol.* 107, 1155–1159.

Maillet, S., Naas, T., Crepin, S., Roque-Afonso, A. M., Lafay, F., Efstathiou, S., et al. (2006). Herpes simplex virus type 1 latently infected neurons differentially express latency-associated and ICP0 transcripts. *J. Virol.* 80, 9310–9321. doi: 10.1128/jvi.02615-05

Maruzuru, Y., Fujii, H., Oyama, M., Kozuka-Hata, H., Kato, A., and Kawaguchi, Y. (2013). Roles of p53 in herpes simplex virus 1 replication. *J. Virol.* 87, 9323–9332. doi: 10.1128/JVI.01581-13

Nguyen, M. L., and Blaho, J. A. (2007). Apoptosis during herpes simplex virus infection. *Adv. Virus Res.* 69, 67–97. doi: 10.1016/s0065-3527(06)69002-7

Nguyen, M. L., and Blaho, J. A. (2009). Cellular players in the herpes simplex virus dependent apoptosis balancing act. *Viruses* 1, 965–978. doi: 10.3390/v1030965

Nguyen, M. L., Kraft, R. M., Aubert, M., Goodwin, E., DiMaio, D., and Blaho, J. A. (2007). p53 and hTERT determine sensitivity to viral apoptosis. *J. Virol.* 81, 12985–12995. doi: 10.1128/jvi.01485-07

Nguyen, M. L., Kraft, R. M., and Blaho, J. A. (2005). African green monkey kidney Vero cells require de novo protein synthesis for efficient herpes simplex virus 1-dependent apoptosis. *Virology* 336, 274–290. doi: 10.1016/j.virol.2005.03.026

Ogura, H., Yoshinouchi, M., Kudo, T., Imura, M., Fujiwara, T., and Yabe, Y. (1993). Human papillomavirus type 18 DNA in so-called HEP-2, KB and FL cells–further evidence that these cells are HeLa cell derivatives. *Cell. Mol. Biol.* 39, 463–467.

Panagiotidis, C. A., Lium, E. K., and Silverstein, S. J. (1997). Physical and functional interactions between herpes simplex virus immediate-early proteins ICP4 and ICP27. *J. Virol.* 71, 1547–1557.

Peña, K. C., Adelson, M. E., Mordechai, E., and Blaho, J. A. (2010). Genital herpes simplex virus type 1 in women: detection in cervicovaginal specimens from gynecological practices in the United States. *J. Clin. Microbiol.* 48, 150–153. doi: 10.1128/JCM.01336-09

Perng, G. C., Jones, C., Ciacci-Zanella, J., Stone, M., Henderson, G., Yukht, A., et al. (2000). Virus-induced neuronal apoptosis blocked by the herpes simplex virus latency-associated transcript. *Science* 287, 1500–1503. doi: 10.1126/science.287.5457.1500

Perng, G. C., Maguen, B., Jin, L., Mott, K. R., Osorio, N., Slanina, S. M., et al. (2002). A gene capable of blocking apoptosis can substitute for the herpes simplex virus type 1 latency-associated transcript gene and restore wild-type reactivation levels. *J. Virol.* 76, 1224–1235. doi: 10.1128/jvi.76.3.1224-1235.2002

Pesola, J. M., Zhu, J., Knipe, D. M., and Coen, D. M. (2005). Herpes simplex virus 1 immediate-early and early gene expression during reactivation from latency under conditions that prevent infectious virus production. *J. Virol.* 79, 14516–14525. doi: 10.1128/jvi.79.23.14516-14525.2005

Phelan, D., Barrozo, E. R., and Bloom, D. C. (2017). HSV1 latent transcription and non-coding RNA: a critical retrospective. *J. Neuroimmunol.* 308, 65–101. doi: 10.1016/j.jneuroim.2017.03.002

Pradhan, P., and Nguyen, M. L. (2013). Early passage neonatal and adult keratinocytes are sensitive to apoptosis induced by infection with an ICP27-null mutant of herpes simplex virus 1. *Apoptosis* 18, 160–170. doi: 10.1007/s10495-012-0773-7

Raja, P., Lee, J. S., Pan, D., Pesola, J. M., Coen, D. M., and Knipe, D. M. (2016). A herpesviral lytic protein regulates the structure of latent viral chromatin. *mBio* 7:e633-16. doi: 10.1128/mBio.00633-16

Salvesen, G. S., and Dixit, V. M. (1997). Caspases: intracellular signaling by proteolysis. *Cell* 91, 443–446. doi: 10.1016/s0092-8674(00)80430-4

Samaniego, L. A., Neiderhiser, L., and DeLuca, N. A. (1998). Persistence and expression of the herpes simplex virus genome in the absence of immediate-early proteins. *J. Virol.* 72, 3307–3320.

Sanfilippo, C. M., and Blaho, J. A. (2003). The facts of death. *Int. Rev. Immunol.* 22, 327–340.

Sanfilippo, C. M., and Blaho, J. A. (2006). ICP0 gene expression is a herpes simplex virus type 1 apoptotic trigger. *J. Virol.* 80, 6810–6821. doi: 10.1128/jvi.00334-06

Sanfilippo, C. M., Chirimuuta, F. N., and Blaho, J. A. (2004a). Herpes simplex virus type 1 immediate-early gene expression is required for the induction of apoptosis in human epithelial HEp-2 cells. *J. Virol.* 78, 224–239. doi: 10.1128/jvi.78.1.224-239.2004

Sanfilippo, C. M., Lombardozzi, R. C., Chirimuuta, F. N., and Blaho, J. A. (2004b). Herpes simplex virus 1 infection is required to produce ICP27 immunoreactive triplet forms when ribosomal aminoacyl-tRNA translocation is blocked by cycloheximide. *Virology* 324, 554–566. doi: 10.1016/j.virol.2004.04.011

Sawtell, N. M., and Thompson, R. L. (1992). Rapid in vivo reactivation of herpes simplex virus in latently infected murine ganglionic neurons after transient hyperthermia. *J. Virol.* 66, 2150–2156.

Sawtell, N. M., and Thompson, R. L. (2016). De novo herpes simplex virus VP16 expression gates a dynamic programmatic transition and sets the latent/lytic balance during acute infection in trigeminal Ganglia. *PLoS Pathog.* 12:e1005877. doi: 10.1371/journal.ppat.1005877

Spivack, J. G., and Fraser, N. W. (1988). Expression of herpes simplex virus type 1 latency-associated transcripts in the trigeminal ganglia of mice during acute infection and reactivation of latent infection. *J. Virol.* 62, 1479–1485.

Stevens, J. G., Wagner, E. K., Devi-Rao, G. B., Cook, M. L., and Feldman, L. T. (1987). RNA complementary to a herpesvirus alpha gene mRNA is prominent in latently infected neurons. *Science* 235, 1056–1059. doi: 10.1126/science.2434993

Takano, Y. S., Harmon, B. V., and Kerr, J. F. (1991). Apoptosis induced by mild hyperthermia in human and murine tumour cell lines: a study using electron microscopy and DNA gel electrophoresis. *J. Pathol.* 163, 329–336. doi: 10.1002/path.1711630410

Thompson, R. L., and Sawtell, N. M. (1997). The herpes simplex virus type 1 latency-associated transcript gene regulates the establishment of latency. *J. Virol.* 71, 5432–5440.

Villa, P., Kaufmann, S. H., and Earnshaw, W. C. (1997). Caspases and caspase inhibitors. *Trends Biochem. Sci.* 22, 388–393. doi: 10.1016/s0968-0004(97)01107-9

Wyllie, A. H., Kerr, J. F., and Currie, A. R. (1980). Cell death: the significance of apoptosis. *Int. Rev. Cytol.* 68, 251–306. doi: 10.1016/s0074-7696(08)62312-8

Conflict of Interest Statement: The authors declare that the research was conducted in the absence of any commercial or financial relationships that could be construed as a potential conflict of interest.

frontiers in Microbiology

ORIGINAL RESEARCH
published: 09 May 2019
doi: 10.3389/fmicb.2019.01009

Simian Varicella Virus DNA in Saliva and Buccal Cells After Experimental Acute Infection in Rhesus Macaques

Vicki Traina-Dorge[1], Satish Mehta[2,3], Bridgette Rooney[4], Brian Crucian[5], Lara Doyle-Meyers[6], Arpita Das[1], Colin Coleman[7], Maria Nagel[7,8] and Ravi Mahalingam[7]*

[1]Division of Microbiology, Tulane National Primate Research Center, Tulane University, Covington, LA, United States, [2]Jes Tech, Houston, TX, United States, [3]KBR wyle Laboratories, Houston, TX, United States, [4]GeoControl Systems, Inc., Houston, TX, United States, [5]Johnson Space Center, NASA, Houston, TX, United States, [6]Division of Veterinary Medicine, Tulane National Primate Research Center, Tulane University, Covington, LA, United States, [7]Department of Neurology, University of Colorado Anschutz Medical Campus, Aurora, CO, United States, [8]Department of Ophthalmology, University of Colorado Anschutz Medical Campus, Aurora, CO, United States

OPEN ACCESS

Edited by:
Benedikt B. Kaufer, Freie Universität Berlin, Germany

Reviewed by:
Anne Gershon, Columbia University, United States
Bernard A. P. Lafont, National Institute of Allergy and Infectious Diseases (NIAID), United States
Paul R. Kinchington, University of Pittsburgh, United States

***Correspondence:**
Vicki Traina-Dorge
vtraina@tulane.edu

Specialty section:
This article was submitted to Virology, a section of the journal Frontiers in Microbiology

Received: *19 February 2019*
Accepted: *23 April 2019*
Published: *09 May 2019*

Citation:
Traina-Dorge V, Mehta S, Rooney B, Crucian B, Doyle-Meyers L, Das A, Coleman C, Nagel M and Mahalingam R (2019) Simian Varicella Virus DNA in Saliva and Buccal Cells After Experimental Acute Infection in Rhesus Macaques. Front. Microbiol. 10:1009. doi: 10.3389/fmicb.2019.01009

Simian varicella virus (SVV) infection of non-human primates is the counterpart of varicella zoster virus (VZV) infection in humans. To develop non-invasive methods of assessing SVV infection, we tested for the presence of SVV DNA in saliva, as has been documented in human VZV infection, and in buccal cells to determine whether epithelial cells might provide a more reliable source of material for analysis. Five rhesus macaques intratracheally inoculated with SVV all developed varicella with viremia and macular-papular skin rash in 1–2 weeks, which resolved followed by establishment of latency. DNA extracted from longitudinal blood peripheral blood mononuclear cells (PBMCs), saliva and buccal samples collected during acute infection and establishment of latency were analyzed by real-time qPCR. After intratracheal inoculation, viremia was observed, with peak levels of 10^1–10^2 copies of SVV DNA in 100 ng of PBMC DNA at 4 and 7 days post inoculation (dpi), which then decreased at 9–56 dpi. In saliva and buccal cells at 7 dpi, 10^1–10^4 copies and 10^1–10^5 copies of SVV DNA in 100 ng of cellular DNA, respectively, were detected in all the five monkeys. At 9 dpi, saliva samples from only two of the five monkeys contained SVV DNA at 10^2–10^3 copies/100 ng of saliva DNA, while buccal cells from all five monkeys showed 10^0–10^3 copies of SVV DNA/100 ng of buccal cell DNA. Similar to viremia, SVV DNA in saliva and buccal cells at 11–56 dpi was lower, suggesting clearance of viral shedding. SVV DNA levels were generally higher in buccal cells than in saliva. Our findings indicate that SVV shedding into the oral cavity parallels acute SVV infection and underscore the relevance of both saliva and buccal cell samples to monitor acute varicella virus infection.

Keywords: simian varicella virus, rhesus macaque, acute infection, saliva, buccal cells

INTRODUCTION

Simian varicella virus (SVV) infection of non-human primates (NHP) is the simian counterpart of varicella zoster virus (VZV) infection in humans. Similar to primary VZV infection in humans, NHPs experimentally infected with SVV, develop acute varicella with malaise, fever, viremia, and generalized vesicular rash (Messaoudi et al., 2009; Ouwendijk et al., 2013). Following acute

SVV infection, the virus establishes latency and later reactivates to produce zoster (Mahalingam et al., 2007, 2010; James et al., 2014; Traina-Dorge et al., 2014). As such, the SVV infection in NHP has been an extremely valuable animal model to further study the pathobiology and neurotropism of VZV showing virus entering ganglia before the appearance of primary rash; viral transport is *via* both hematogenous and non-hematogenous routes, critical gene expression, and cell signaling changes associated with disease; tropism of ganglionic, epithelial, and T lymphocytes (Mahalingam et al., 2001; Ouwendijk et al., 2013; Traina-Dorge et al., 2015, 2019; Arnold et al., 2016).

Our goal here was the development of a non-invasive method to analyze SVV infection and viremia after acute infection in non-human primates. We attempted to detect SVV DNA in saliva, as has been performed in VZV infection in adult humans (Mehta et al., 2012), in patients with zoster (Mehta et al., 2008, 2013, 2017; Depledge et al., 2011; Nagel et al., 2011; Gershon et al., 2015), and in patients with zoster sine herpete (Furuta et al., 2001; Gershon et al., 2015). We also analyzed buccal cells for SVV DNA to determine whether buccal epithelial cells from anesthetized animals could provide a more reliable source of material.

MATERIALS AND METHODS

Animals

Five male rhesus macaques (KB95, KG58, KI87, KI92, and KT89), *Macaca mulatta*, (4–5 kg) were prescreened for SVV-seronegativity using plaque reduction antibody neutralization assays. All animals were housed at the Tulane National Primate Research Center in Covington, LA. On day 0, baseline physical examinations were performed, and blood, saliva, and buccal samples were obtained, while the ventrum and appendages of the animals were shaved. All the five animals were then intratracheally inoculated with 5×10^5 pfu (plaque forming units) wild type SVV (wtSVV) in 1 ml using a sterile #10 French feeding tube. SVV was grown in Rhesus fibroblast monolayers and cell-associated virus harvested for inoculation. After SVV inoculation, all monkeys were monitored by physical examination and collection of blood, saliva, and buccal samples, 2–3 times for the first 2 weeks, weekly for 8 weeks, and monthly thereafter. Animals were evaluated for respiratory, cardiac, lymphatic, or dermal involvement, and any adverse findings were documented. Typical varicella lesions (macules, papules, and vesicles) were scored as follows: +/− 1–2; 1+: 3–10; 2+: 11–50; 3+: 51–100; 4+: >101 lesions. All examinations and procedures were performed following anesthesia of the animals with 10 mg/kg intramuscular ketamine hydrochloride or 6–8 mg/kg intramuscular Tiletamine/zolazepam (Telazol) in accordance with the recommendations of the US Department of Agriculture Animal Welfare Act regulations, the *Guide for the Care and Use of Laboratory Animals* and regulations of the Association for Assessment and Accreditation of Laboratory Animal Care (AAALAC). All experiments were reviewed and approved by the Tulane National Primate Research Center (TNPRC) Institutional Animal Care and Use Committee (IACUC), prior to the start of the study.

Saliva and Buccal Swab Collection

Saliva—Synthetic polymer saliva swabs, SalivaBio (Salimetrics, State College, PA), were placed for 3 min each in the left and right cheek pouches of each anesthetized monkey to saturate with saliva. The swabs were removed, transferred to the compartmentalized collection tube, and placed on ice. Swabs and tubes were centrifuged at 5,000 × g at 4°C for 20 min and saliva was recovered in the bottom chamber. The volume of saliva (50–1,200 µl) was recorded and transferred to 1.5 ml microcentrifuge tubes. Saliva was again spun at 18,407 × g at 4°C for 20 min. Supernatant and pellets from saliva were tested for SVV by qPCR and no SVV was found in the supernatant. As such, for all study samples following centrifugation, all but 200 µl of the supernatant was decanted, the cell pellet was resuspended, and then placed on ice for DNA extraction.

Buccal cells—A Cytobrush Plus brush (Cooper Surgical, Trumball, CT) was inserted into both the left and right cheek pouches of anesthetized monkeys, rotated 10 times at each site, removed, and inserted into a sterile tube and kept at 4°C until DNA extraction.

DNA Extraction and qPCR Assays

Saliva—DNA was extracted from saliva using the QIA-Amp DNA kit (Qiagen; Germantown, MD) (Mehta et al., 2017).

Buccal cells—Brushes containing buccal cells were placed directly in the DNA extraction buffer for lysis and DNA extraction, using a Gentra Puregene Buccal Cell Kit (Qiagen, Germantown, MD), following the manufacturer's instructions.

PBMCs—DNA was extracted from PBMCs using a Qiagen DNA extraction kit (Qiagen), as described (White et al., 2002a,b; Mahalingam et al., 2007). DNA concentrations were determined using a NanoDrop ND-1000 Spectrophotometer (NanoDrop Technologies, Inc. Wilmington, DE).

Quantitative real-time polymerase chain reaction (qPCR)—SVV copy number was measured by real-time qPCR performed on the salivary and buccal DNA (3.5 µl per reaction) and PBMC DNA (100 ng per reaction) with TaqMan® 7900, using fluorescence-based amplification (Applied Biosystems, Inc, Life Technologies, Grand Island, NY). Primers and Taqman probes specific for the SVV open reading frame (ORF) 61 were used for real-time qPCR as described (Cohrs et al., 2008) and have been our lab standard for all SVV diagnostics (Mahalingam et al., 2007, 2010; Traina-Dorge et al., 2015, 2019). Briefly, final concentrations of primers and probes in PCR were 500 and 250 nM, respectively. SVV ORF-61 sequences (forward primer 5′-ACACAGCGCTAATGAGAAGCC-3′; reverse primer 5′-GAAAGACGCTGCTGTTGTCG-3′; probe 5′-FAM/CAACCCCGCGTGTTGGCCC/3BHQ-3′). The presence of DNA in samples was confirmed by amplification of the cell gene, glyceraldehyde 6-phosphate dehydrogenase (GAPDH) using primers specific for GAPDH DNA (forward primer 5′-CAAGGTCATCCATGACAACT TTG-3′; reverse primer 5'GGCCATCCACAGTCTTCTGG-3′; probe 5′-ACCACAGTCCATGCCATCACTGCCA-3′). A standard

curve was generated for GAPDH amplification using 0.1, 1.0, and 10 μg uninfected Vero cell DNA as substrate (**Supplementary Figure 1**). PCR conditions were as follows: 95°C for 20 s followed by 40 cycles of 95°C for 1 s and 60°C for 20 s.

Each animal sample was analyzed in a clean PCR room in triplicate and the copy numbers were averaged. Samples were only confirmed positive if two or three of the triplicate assays were positive. To generate standard curves for amplification with SVV ORF61 primers and probes, serial dilutions of wtSVV bacmid DNA (Gray et al., 2011) ranging from 1 to 10^8 copies were prepared in a background of 20 μg/ml of herring sperm DNA and included a no DNA control. Any possible contamination showing previously amplified fragments are eliminated. Based on this SVV DNA standard curve, the sensitivity of our assay is 1–10 copies of SVV DNA. All PCR assays were carried out blinded with respect to identification of clinical specimens and positive controls.

PBMC SVV copy numbers were calculated as SVV DNA copies per 100 ng PBMC DNA. The saliva and buccal sample materials were more limited and contained lower quantities of extractable DNA than found in PBMC samples. GAPDH DNA amplification in these samples was used to quantify cellular DNA. Saliva and buccal cell samples yielded 0.4–3,693 ng/ul of cellular DNA based on GAPDH detection. Further, SVV qPCR was performed on these same samples to calculate SVV copies per ng cellular DNA. Results were multiplied by 100 and reported as SVV DNA copies per 100 ng of saliva or buccal cell DNA.

FIGURE 1 | Primary varicella in experimentally inoculated rhesus macaque KG58. All monkeys developed typical varicella rash at 7–14 days post inoculation (dpi). Wide-spread generalized varicella rash of monkey KG58 on 9 dpi is shown on the neck, shoulders, torso, arms and abdomen (right panel) and compared with the pre-inoculation baseline skin from the same animal (left panel).

RESULTS

All five monkeys inoculated with wtSVV developed typical acute varicella with viremia and macular/papular/vesicular skin rash in 1–2 weeks, **Figure 1**, shows skin in animal KG58 from d0 (left panel) and 9 dpi (right panel) showing typical acute varicella generalized rash. **Figure 2** summarizes the extent of rash in all five animals. Monkeys KB95, KI92, and KT89 developed minimal 1+ skin lesions at 7 dpi, while all five monkeys developed moderate to severe, 2+ to 4+ peak rash at 9 dpi, with reduction to 1+ to 3+ at 11 dpi. Animals KB95, KI92, and KG58 still had minimal 1+ rash at 14 dpi. Varicella rash in all five animals was resolved by 21 dpi.

At multiple timepoints after intratracheal SVV inoculation, PBMC were isolated and DNA was extracted and analyzed by real-time qPCR for the presence of SVV DNA. Four of five animals at 4 dpi and all five animals at 7 dpi, demonstrated peak viremia with 10–78 (mean = 35.5) and 4–161 (mean = 45.0) copies of SVV DNA per 100 ng of PBMC DNA, respectively. At days 9 and 11 dpi, only four of five animals had reduced levels of virus, with 0–20 (mean = 8.8 and 8.7, respectively) copies/100 ng PBMC DNA, while analysis at 14–56 dpi showed only sporadic 0–3 copies of SVV DNA/100 ng PBMC DNA (**Figure 3**).

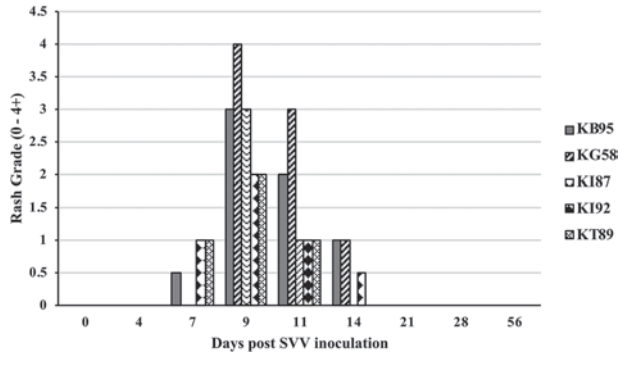

FIGURE 2 | Rash after SVV inoculation. Monkeys were monitored for 56 days for varicella rash after SVV inoculation. All animals developed varicella with typical macular-papular-vesicular skin rash, graded (0 to 4+) during 0–14 dpi. Rash was first observed at 7 dpi, peaked at 9–11 dpi and resolved by 21 dpi.

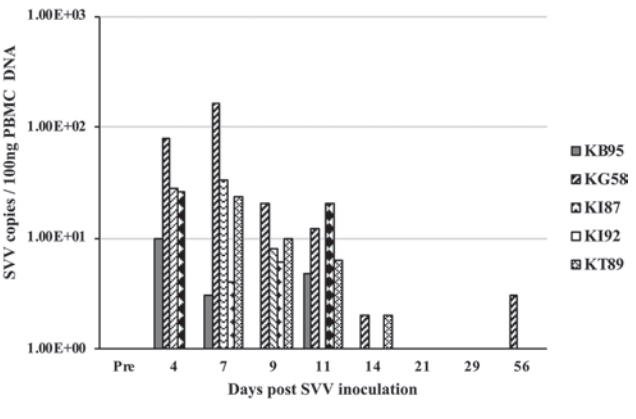

FIGURE 3 | Viremia after SVV inoculation. Blood samples from the five intratracheally inoculated monkeys, were collected longitudinally at multiple times post inoculation. Peripheral blood mononuclear cells (PBMC) were isolated, DNA extracted, and SVV qPCR performed in triplicate on 100 ng DNA. Average SVV copy numbers/100 ng of PBMC DNA are shown.

DNA from longitudinal samples of saliva and buccal cells were also analyzed by real-time qPCR for the presence of SVV DNA. At 7 dpi, SVV DNA was detected in all five animals, with 10^1–10^4 copies of SVV/ 100 ng of saliva DNA (mean = 4.6×10^3, **Figure 4A**) and 10^1–10^5 copies SVV/100 ng of buccal cell DNA (mean = 3.8×10^4, **Figure 4B**). At 9 dpi, saliva samples from two of the five monkeys contained 10^2–10^3 SVV copies/100 ng of saliva DNA (mean = 2.9×10^2) while buccal samples from all five animals contained 10^1–10^4 SVV copies/100 ng of buccal cell DNA (mean = 2.5×10^3). Similar to viremia, the SVV DNA present in saliva and buccal cells at 11–56 dpi was less frequent, with fewer animals positive for SVV DNA and in those monkeys, SVV copy numbers decreased from the earlier peak levels.

SVV DNA-positive samples as well as DNA copy number were higher in the majority of buccal samples than in saliva samples. On both 7 and 9 dpi, 9 of 10 buccal samples from monkeys: KB95, KG58, KI87, and KT89 had more copies of SVV DNA than did saliva samples (**Figures 4A,B**). Higher SVV DNA copy numbers in buccal samples than in saliva samples were also observed in monkey KT89 at: 4,11,14, and 21 dpi, showing SVV DNA-positive buccal cells with 1, 37, 250, and 1,030 copies of SVV DNA/100 ng buccal cell DNA, respectively, while their corresponding saliva samples were negative. Buccal samples from monkey KB95 obtained at 11 dpi had 256 copies SVV DNA/100 ng saliva DNA, while the matching saliva sample was negative. Saliva samples showing higher SVV copy numbers than in buccal samples were also seen, but less frequently. For example, the saliva sample from monkey KG58 obtained at 11 dpi contained 2.1×10^4 copies of SVV DNA/100 ng saliva DNA compared to only 143 copies of SVV DNA/ 100 ng buccal cell DNA in the buccal sample obtained at that time. Monkey KI92 had SVV DNA-positive saliva at 7 and 11 dpi, with 119 and 37 copies of SVV DNA/100 ng saliva DNA, respectively, while the matching buccal samples had 11 and 0 copies of SVV DNA/100 ng buccal cell DNA, respectively. At 29 dpi, saliva from monkey KT89 also showed high levels (2.6×10^5 copies of SVV DNA/100 ng saliva DNA), while the matching buccal sample was negative.

DISCUSSION

After SVV experimental inoculation of rhesus macaques, all monkeys became viremic (PBMC) and developed typical varicella rash within the first 2 weeks, as previously shown (Messaoudi et al., 2009; Ouwendijk et al., 2013). In our study, viremia reached peak levels at 4–7 dpi while rash presented later, with peak levels at 9-11 dpi. Despite viremia in four of five animals on 4 dpi, the saliva from only one of the five animals was SVV

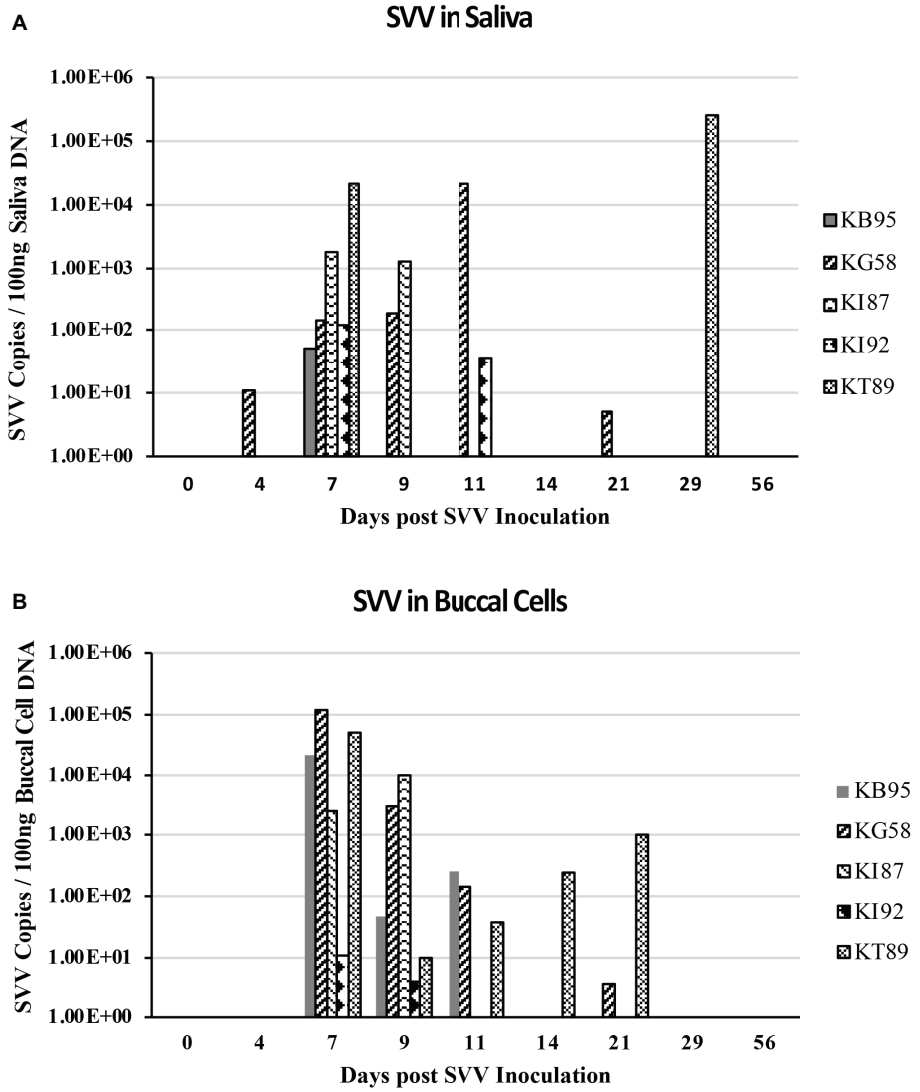

FIGURE 4 | SVV DNA in saliva and buccal samples during acute infection. DNA was extracted from longitudinal saliva **(A)** and buccal **(B)** samples collected during acute SVV infection and analyzed by real-time qPCR for virus (SVV) and cellular (GAPDH) DNA. SVV qPCR was performed in triplicate on a standard 3.5 µl volume. Average SVV copy numbers/100 ng saliva DNA or buccal cell DNA for each sample are shown.

DNA positive while all buccal samples were negative, suggesting a possible non-hematogenous route for dissemination into the oral mucosa or delay in replication within epithelial cells. Our study demonstrated positive shedding of SVV into the oral cavity of non-human primates, as is also shown in human VZV acute infection of adults (Mehta et al., 2012), patients with zoster (Cohrs et al., 2008, Mehta et al., 2008, 2013, 2017, Depledge et al., 2011, Nagel et al., 2011, Gershon et al., 2015), and patients with zoster sine herpete (Furuta et al., 2001; Gershon et al., 2015).

We tested both saliva and buccal cells for SVV DNA to assess whether epithelial cells would provide a more reliable source of material for analysis from anesthetized animals. Epithelial cells are susceptible target cells of SVV infection and likely the source of virus in saliva. Volumes of saliva >1 ml are more difficult to reproducibly obtain from anesthetized animals compared with 2–3 ml saliva yields from human subjects (Mehta et al., 2013, 2017). Peak SVV DNA copies were present in both 7 and 9 dpi saliva and buccal samples. Although some discordances were observed, numbers of SVV DNA-positive samples and SVV copy numbers were generally greater for buccal cells than saliva samples, possibly due to the larger cellular yield of buccal samples than that obtained from saliva samples.

Our results clearly demonstrate SVV shedding in the oral cavity during acute SVV infection. Peak SVV copy numbers at 7 dpi, in both saliva and buccal samples parallels viremia, indicating that both sample types are relevant for diagnosis of SVV infection after experimental inoculation. Overall, the SVV DNA yield from buccal samples was higher than that obtained with saliva samples from anesthetized animals.

DATA AVAILABILITY

All datasets generated for this study are included in the manuscript and/or the **Supplementary Files**.

ETHICS STATEMENT

All animal housing and procedures were in accordance with the recommendations of the US Department of Agriculture Animal Welfare Act regulations, the *Guide for the Care and Use of Laboratory Animals,* and regulations of the Association for Assessment and Accreditation of Laboratory Animal Care (AAALAC). All experiments were reviewed and approved by the Tulane National Primate Research Center (TNPRC) Institutional Animal Care and Use Committee (IACUC), prior to the start of the study.

AUTHOR CONTRIBUTIONS

All authors contributed to the research as well as the writing of the manuscript.

FUNDING

This work was supported in part by Public Health Service grants AG032958 (to RM, VT-D, AD, LD-M, MN) from the National Institutes of Health and NASA Grants 111-30-10-03 and 111-3010-06 (SM, BR, BC), and in part, with federal funds from the National Center for Research Resources and the Office of Research Infrastructure Programs (ORIP) of the NIH through grant P51 OD011104 to the Tulane National Primate Research Center (VT-D, AD, LD-M).

ACKNOWLEDGMENTS

We thank the Tulane National Primate Research Center Veterinary Medicine staff for excellent animal care. We are grateful to Theresa Glissman for preparing the manuscript and Marina Hoffman for editorial assistance.

SUPPLEMENTARY MATERIAL

The Supplementary Material for this article can be found online at: https://www.frontiersin.org/articles/10.3389/fmicb.2019.01009/full#supplementary-material

SUPPLEMENTARY FIGURE 1 | Efficiency of GAPDH DNA amplification in real-time qPCR. Primers and TaqMan probes specific for GAPDH were used for real-time qPCR using 0.1, 1.0 and 10 μg of uninfected Vero cell DNA as substrate, as detailed in Material and Methods. The threshold cycle (C_T) values for each concentration from triplicate samples were plotted against the copy numbers. The slope of the curve and the efficiency of amplification (R^2 value and percent efficiency) were calculated.

REFERENCES

Arnold, N., Girke, T., Sureshchandra, S., and Messaoudi, I. (2016). Acute Simian Varicella virus infection causes robust and sustained changes in gene expression in the sensory ganglia. *J. Virol.* 90, 10823–10843. doi: 10.1128/JVI.01272-16

Cohrs, R. J., Mehta, S. K., Schmid, D. S., Gilden, D. H., and Pierson, D. L. (2008). Asymptomatic reactivation and shed of infectious varicella zoster virus in astronauts. *J. Med. Virol.* 80, 1116–1122. doi: 10.1002/jmv.21173

Depledge, D. P., Palser, A. L., Watson, S. J., Lai, I. Y., Gray, E. R., Grant, P., et al. (2011). Specific capture and whole-genome sequencing of viruses from clinical samples. *PLoS One* 6:e27805. doi: 10.1371/journal.pone.0027805

Furuta, Y., Ohtani, F., Sawa, H., Fukuda, S., and Injyama, Y. (2001). Quantitation of varicella-zoster virus dna in patients with ramsay hunt syndrome and zoster sine herpete. *J. Clin. Microbiol.* 39, 2856–2859. doi: 10.1128/JCM.39.8.2856-2859.2001

Gershon, A., Chen, J., and Gershon, M. D. (2015). Use of saliva to identify varicella zoster virus infection of the gut. *Clin. Infect. Dis.* 61, 536–544. doi: 10.1093/cid/civ320

Gray, W. L., Zhou, R., Noffke, J., and Tischer, B. K. (2011). Cloning the simian varicella virus genome in E. coli as an infectious bacterial artificial chromosome. *Arch. Virol.* 156, 739–746. doi: 10.1007/s00705-010-0889-4

James, S. F., Traina-Dorge, V., Deharo, E., Wellish, M., Palmer, B. E., Gilden, D., et al. (2014). T cells increase before zoster and PD-1 expression increases at the time of zoster in immunosuppressed nonhuman primates latently infected with simian varicella virus. *J. Neurovirol.* 20, 309–313. doi: 10.1007/s13365-014-0237-7

Mahalingam, R., Traina-Dorge, V., Wellish, M., Deharo, E., Singletary, M. L., Ribka, E. P., et al. (2010). Latent simian varicella virus reactivates in monkeys treated with tacrolimus with or without exposure to irradiation. *J. Neurovirol.* 16, 342–354. doi: 10.3109/13550284.2010.513031

Mahalingam, R., Traina-Dorge, V., Wellish, M., Lorino, R., Sanford, R., Ribka, E. P., et al. (2007). Simian varicella virus reactivation in cynomolgus monkeys. *Virology* 368, 50–59. doi: 10.1016/j.virol.2007.06.025

Mahalingam, R., Wellish, M., Soike, K., White, T., Kleinschmidt-DeMasters, B. K., and Gilden, D. H. (2001). Simian varicella virus infects ganglia before rash in experimentally infected monkeys. *Virology* 279, 339–342. doi: 10.1006/viro.2000.0700

Mehta, S. K., Gilden, D., Crucian, B. E., Sams, C. F., Cohrs, R., and Pierson, D. L. (2012). A case report: Pcr-assisted diagnosis of varicella in an adult. *Open J. Med. Microbiol.* 2:23019. doi: 10.4236/ojmm.2012.23019

Mehta, S. K., Nelman-Dogzalez, M., Tyring, S. K., Tong, Y., Beitman, A., Crucian, B. E., et al. (2017). Localization of VZV in saliva of zoster patients. *J. Med. Virol.* 89, 1686–1689. doi: 10.1002/jmv.24807

Mehta, S. K., Trying, S. K., Gilden, D. H., Cohrs, R. J., Leal, M. J., Castro, V. A., et al. (2008). Varicella-zoster virus in the saliva of patients with herpes zoster. *J. Infect. Dis.* 197, 654–657. doi: 10.1086/527420

Mehta, S. K., Tyring, S. K., Cohrs, R. J., Gilden, D., Feiverson, A. H., Lechler, K. J., et al. (2013). Rapid and sensitive detection of varicella zoster virus in saliva of patients with herpes zoster. *J. Virol. Methods* 193, 128–130. doi: 10.1016/j.jviromet.2013.05.019

Messaoudi, I., Barron, A., Wellish, M., Engelmann, F., Legasse, A., Planer, S., et al. (2009). Simian varicella virus infection of rhesus macaques recapitulates essential features of varicella zoster virus infection in humans. *PLoS Pathog.* 5:e1000657. doi: 10.1371/journal.ppat.1000657

Nagel, M. A., Choe, A., Cohrs, R. J., Traktinskiy, I., Sorensen, K., Mehta, S. K., et al. (2011). Persistence of varicella zoster virus DNA in saliva after herpes zoster. *J. Infect. Dis.* 204, 820–824. doi: 10.1093/infdis/jir425

Ouwendijk, W. J., Mahalingam, R., de Swart, R. L., Haagmans, B. L., van Amerongen, G., Getu, S., et al. (2013). T-cell tropism of simian varicella virus during primary infection. *PLoS Pathog.* 9:e1003368. doi: 10.1371/journal.ppat.1003368

Traina-Dorge, V., Doyle-Meyers, L. A., Sanford, R., Manfredo, J., Blackmon, A., Wellish, M., et al. (2015). Simian varicella virus is present in macrophages, dendritic cells, and T cells in lymph nodes of rhesus macaques after experimental reactivation. *J. Virol.* 89, 9817–9824. doi: 10.1128/JVI.01324-15

Traina-Dorge, V., Palmer, B. E., Coleman, C., Hunter, M., Frieman, A., Gilmore, A., et al. (2019). Reactivation of Simian Varicella Virus in rhesus macaques after CD4 T cell depletion. *J. Virol.* 93, e01375–e01318. doi: 10.1128/JVI.01375-18

Traina-Dorge, V., Sanford, R., James, S., Doyle-Meyers, L. A., de Haro, E., Wellish, M., et al. (2014). Robust pro-inflammatory and lesser anti-inflammatory immune responses during primary simian varicella virus infection and reactivation in rhesus macaques. *J. Neuro-Oncol.* 20, 526–530. doi: 10.1007/s13365-014-0274-2

White, T. M., Mahalingam, R., Traina-Dorge, V., and Gilden, D. H. (2002a). Simian varicella virus DNA is present and transcribed months after experimental infection of adult African green monkeys. *J Neurovirol.* 8, 191–203. doi: 10.1080/13550280290049705

White, T. M., Mahalingam, R., Traina-Dorge, V., and Gilden, D. H. (2002b). Persistence of simian varicella virus DNA in CD4(+) and CD8(+) blood mononuclear cells for years after intratracheal inoculation of African green monkeys. *Virol.* 303, 192–198. doi: 10.1006/viro.2002.1664

Conflict of Interest Statement: The authors declare that the research was conducted in the absence of any commercial or financial relationships that could be construed as a potential conflict of interest.

The handling editor declared a past co-authorship with one of the authors RM.

frontiers in Microbiology

MINI REVIEW
published: 28 May 2019
doi: 10.3389/fmicb.2019.01186

Human Cytomegalovirus Latency and Reactivation in Allogeneic Hematopoietic Stem Cell Transplant Recipients

Lauren Stern[1], Barbara Withers[2†], Selmir Avdic[3,4†], David Gottlieb[3,4,5†], Allison Abendroth[1†], Emily Blyth[3,4,5†] and Barry Slobedman[1†]*

[1] Discipline of Infectious Diseases and Immunology, Sydney Medical School, Charles Perkins Centre, University of Sydney, Sydney, NSW, Australia, [2] Department of Haematology, St Vincent's Hospital, Darlinghurst, NSW, Australia, [3] Westmead Institute of Medical Research, University of Sydney, Sydney, NSW, Australia, [4] Sydney Cellular Therapies Laboratory, Westmead, NSW, Australia, [5] Blood and Marrow Transplant Unit, Westmead Hospital, Sydney, NSW, Australia

Human cytomegalovirus (HCMV) reactivation is a major infectious cause of morbidity and mortality after allogeneic hematopoietic stem cell transplantation (HSCT). HCMV is a ubiquitous beta-herpesvirus which asymptomatically infects immunocompetent individuals but establishes lifelong latency, with the potential to reactivate to a life-threatening productive infection when the host immune system is suppressed or compromised. Opportunistic HCMV reactivation is the most common viral complication following engraftment after HSCT and is associated with a marked increase in non-relapse mortality, which appears to be linked to complex effects on post-transplant immune recovery. This minireview explores the cellular sites of HCMV latency and reactivation in HSCT recipients and provides an overview of the risk factors for HCMV reactivation post-HSCT. The impact of HCMV in shaping post-transplant immune reconstitution and its relationship with patient outcomes such as relapse and graft-versus-host disease will be discussed. Finally, we survey current and emerging strategies to prevent and control HCMV reactivation in HSCT recipients, with recent developments including adoptive T cell therapies to accelerate HCMV-specific T cell reconstitution and new anti-HCMV drug therapy for HCMV reactivation after HSCT.

Keywords: human cytomegalovirus, HCMV, CMV, latency, reactivation, hematopoietic stem cell transplant, HSCT

OPEN ACCESS

Edited by:
Benedikt B. Kaufer, Freie Universität Berlin, Germany

Reviewed by:
Mark R. Wills, University of Cambridge, United Kingdom
Sebastian Voigt, Charité Medical University of Berlin, Germany

****Correspondence:***
Barry Slobedman
barry.slobedman@sydney.edu.au

† These authors have contributed equally to this work

Specialty section:
This article was submitted to Virology, a section of the journal Frontiers in Microbiology

Received: *31 March 2019*
Accepted: *09 May 2019*
Published: *28 May 2019*

Citation:
Stern L, Withers B, Avdic S, Gottlieb D, Abendroth A, Blyth E and Slobedman B (2019) Human Cytomegalovirus Latency and Reactivation in Allogeneic Hematopoietic Stem Cell Transplant Recipients. Front. Microbiol. 10:1186. doi: 10.3389/fmicb.2019.01186

INTRODUCTION

Human cytomegalovirus (HCMV) is a beta-herpesvirus carried by a majority of the global population (Cannon et al., 2010; Zuhair et al., 2019). The seroprevalence of HCMV increases with age and has an estimated global mean of 83% (Zuhair et al., 2019). While primary infection is usually asymptomatic in immunocompetent individuals, the virus establishes a lifelong latent infection that is never eliminated by the host immune system. Intermittent subclinical viral reactivation events are thought to be controlled by effective immune surveillance and may drive the high frequencies of HCMV-specific T-cells found in the peripheral blood of healthy seropositive individuals (Sester et al., 2002; Sylwester et al., 2005). By contrast, reactivation from latency is responsible for significant morbidity and mortality in immunocompromised and immunosuppressed populations,

including solid-organ transplant and allogeneic hematopoietic stem cell transplant (HSCT) recipients, HIV/AIDS patients and the developing fetus.

HCMV reactivation is the major viral infectious complication after allogeneic HSCT and is associated with an increased risk of non-relapse mortality (Takenaka et al., 2015; Green et al., 2016; Teira et al., 2016), which is not principally attributable to direct HCMV disease (Green et al., 2016). Uncontrolled HCMV replication following reactivation can lead to life-threatening end-organ disease, commonly manifesting as pneumonia and gastrointestinal disease, and less frequently as retinitis, hepatitis and encephalitis. Reactivation may also indirectly contribute to detrimental patient outcomes through antiviral drug toxicities and complex impacts on post-transplant immune reconstitution, including links with graft-versus-host disease (GvHD) (Cantoni et al., 2010) and microbial superinfections (Nichols et al., 2002; Yong et al., 2017a). There is no licensed HCMV vaccine and current antiviral agents are limited by their toxic side-effects and the risk of antiviral drug resistance.

The cellular sites and mechanisms associated with HCMV latency and reactivation are incompletely understood, in part due to the high human-specificity of HCMV which precludes the use of animal models to directly study HCMV infection. Clinical evidence indicates that the risk of reactivation post-HSCT is strongly connected to the pre-transplant HCMV serostatus of the donor and recipient (Boeckh and Nichols, 2004; George et al., 2010) and the pace of post-transplant HCMV-specific T-cell recovery. However, the lack of well-validated biomarkers for reactivation makes it challenging to predict the incidence and outcome of infection in individual patients, and greater knowledge of the influence of HCMV on post-transplant immune reconstitution is required.

HCMV REACTIVATION IN ALLOGENEIC HEMATOPOIETIC STEM CELL TRANSPLANTATION (HSCT)

Allogeneic HSCT is the only curative option for many hematological malignancies and diseases (Copelan, 2006). GvHD, opportunistic infections and relapse are the leading causes of mortality in the first 2 years post-transplant (Gratwohl et al., 2005; D'Souza and Fretham, 2018). The reactivation of latent double-stranded DNA viruses is common in the early post-engraftment period (Hill et al., 2017) and HCMV reactivation is the most frequent opportunistic viral infection after HSCT. Virological surveillance for HCMV replication is routinely performed in the first 100 days post-transplant through quantitative PCR monitoring for HCMV genomes in blood plasma (Emery et al., 2000), with HCMV DNAemia being an independent risk factor for disease (Zaia et al., 1997) and non-relapse mortality (Hiwarkar et al., 2013; Green et al., 2016; Ramanathan et al., 2016; Teira et al., 2016).

Reactivation develops in over 60% of HCMV seropositive recipients (R+), and in approximately 10% of seronegative recipients (R−) transplanted from seropositive donors (D+) (George et al., 2010). In R+/D+ patients, reactivation may derive from endogenous latent HCMV in the seropositive recipient (Winston et al., 1985; Kawasaki et al., 1999) and/or from latently infected cells transferred within the seropositive donor stem cell allograft. Recipient seropositivity alone is an adverse prognostic factor for overall survival (Broers et al., 2000; Craddock et al., 2001). Seropositive recipients who receive grafts from HCMV-naïve donors (R+/D−) experience the highest incidence of HCMV reactivation and disease (Ljungman et al., 2006; Webb et al., 2018), a likely consequence of delayed HCMV-specific immune recovery owing to the lack of pre-existing HCMV-specific memory lymphocytes in the graft (Cwynarski et al., 2001; Zhou et al., 2009). As the recipient's existing cellular immune system is eradicated by transplant conditioning regimens, R+/D− patients rely on *de novo* T-cell reconstitution via the thymus from donated pluripotent hematopoietic stem cells to generate a primary T-cell response to HCMV reactivation. By contrast, HCMV-specific memory T-cells contained in D+ grafts can undergo more rapid antigen-driven expansion within the recipient in the early post-transplant period and contribute to early control of reactivation (Cwynarski et al., 2001; Gandhi et al., 2003; Scheinberg et al., 2009). For a seropositive recipient, the choice of a seropositive over seronegative donor offers a survival advantage in the setting of myeloablative unrelated donor transplantation, but the effect on survival with matched sibling donors is less strong (Ljungman et al., 2003, 2014). Nonetheless, due to the high incidence of HCMV-related complications in R+/D− patients, where possible, attempts are made to match serostatus in donors and recipients.

Advances in transplant and antiviral treatment practices over the last 25 years have reduced the incidence of HCMV disease to ∼10% in the first year post-transplant (Boeckh and Ljungman, 2009; Green et al., 2016). However, the use of prophylactic or pre-emptive antiviral therapy delays HCMV-specific T-cell recovery (Li et al., 1994) and has led to increasing rates of late HCMV reactivation and disease (Einsele et al., 2000). Additionally, HCMV pneumonia remains associated with high (up to 70%) mortality (Erard et al., 2015). Gastrointestinal HCMV disease often develops without detection of HCMV DNAemia (Cho et al., 2013; Gabanti et al., 2015) and can be difficult to distinguish from gastrointestinal GvHD, often occurring in the same patients (Cho et al., 2013; Bhutani et al., 2015).

CELLULAR SITES OF HCMV LATENCY AND REACTIVATION

The transition from viral latency to reactivation underpins the pathogenesis of HCMV in HSCT. HCMV latency is characterized by maintenance of the viral genome as an intranuclear episome (Bolovan-Fritts et al., 1999) without replication, but with the potential to reactivate to a productive infection. A wide range of cell types support productive infection (Ibanez et al., 1991; Sinzger et al., 2008), but latency appears to be restricted to primitive bone-marrow-resident $CD34^+$ cells and $CD33^+$ myeloid progenitor cells (Mendelson et al., 1996; Hahn et al., 1998; Reeves et al., 2005b), which retain the latent viral genome as they differentiate into peripheral blood $CD14^+$ monocytes and

myeloid dendritic cells (mDCs) (Taylor-Wiedeman et al., 1991, 1994; Hahn et al., 1998; Khaiboullina et al., 2004; Reeves et al., 2005b). A recent study found that $CD14^+$ monocytes expressing the surface marker B7-H4 were a predominant site of latency in peripheral blood of healthy donors (Zhu et al., 2018). It may be that HCMV preferentially infects early myeloid progenitors or promotes the differentiation of infected pluripotent $CD34^+$ cells to myeloid-lineage subsets that support latency (Zhu et al., 2018).

Latently infected cells contain HCMV DNA (Minton et al., 1994) but do not support infectious virus production. The terminal differentiation to mature mDCs and macrophages is accompanied by chromatin remodeling of the HCMV major immediate-early promoter (Reeves et al., 2005a,b), which facilitates reactivation of the lytic gene cascade and the production of infectious virus (Taylor-Wiedeman et al., 1994; Reeves et al., 2005b; Reeves and Sinclair, 2013; Poole et al., 2015). Allogeneic stimulation (Soderberg-Naucler et al., 1997) and pro-inflammatory cytokines such as IFN-γ, TNF, and IL-6 are implicated in driving myeloid cell maturation and reactivation (Fietze et al., 1994; Söderberg-Nauclér et al., 2001; Hargett and Shenk, 2010; Reeves and Compton, 2011; Huang et al., 2012; Reeves and Sinclair, 2013; Forte et al., 2018).

Latently infected cells are present at very low frequencies (0.004–0.01% of mononuclear cells) in GCSF-mobilized peripheral blood or bone-marrow from healthy seropositive donors (Slobedman and Mocarski, 1999), but underlie the capacity for iatrogenic transmission of latent HCMV through D+ HSCT allografts. Additionally, the high risk of reactivation in R+/D− patients suggests that pre-transplant conditioning regimens incompletely eradicate latent HCMV reservoirs in the recipient (Wills et al., 2015). It also remains possible there are additional sites of HCMV latency, with conflicting evidence regarding possible latency in aortic endothelial cells (Fish et al., 1998; Pampou et al., 2000; Reeves et al., 2004). Whether HCMV establishes a low-level productive infection in bone-marrow stromal cells (Taichman et al., 1997; Smirnov et al., 2007; Soland et al., 2014) or in a self-renewing $CD34^+$ cell subset (Goodrum et al., 2004) also remains unclear, yet HCMV DNA has been detected in diverse tissue sites (Hendrix et al., 1997; Chen and Hudnall, 2006; Gordon et al., 2017) and recent RNA-seq uncovered HCMV transcripts at multiple locations, including the ovaries, blood, adipose tissue, and lung (Shnayder et al., 2018). The specific cell types harboring HCMV in these studies and whether they represent productive, abortive, or latent infection is unknown. The widespread prevalence of HCMV within asymptomatic individuals nonetheless highlights the importance of host immune control in preventing unchecked HCMV replication leading to life-threatening disease.

RISK FACTORS FOR HCMV REACTIVATION AFTER HSCT

In addition to recipient and donor HCMV serostatus, independent risk factors for reactivation include increasing recipient age (Tong et al., 2013; Takenaka et al., 2015), use of unrelated or HLA-mismatched donors (Qayed et al., 2014; Takenaka et al., 2015), T-cell depletion (Walker et al., 2007; Yoon et al., 2009), GvHD (Walker et al., 2007; George et al., 2010; Qayed et al., 2014; Cohen et al., 2015), and high-dose corticosteroids for GvHD (Yanada et al., 2003; Tong et al., 2013; Melendez-Munoz et al., 2019). T-cell depletion and prolonged steroid therapy mitigate GvHD but delay antiviral T-cell reconstitution (Aubert et al., 2001; Craddock et al., 2001; Wagner et al., 2005; Lilleri et al., 2009; Tormo et al., 2011). A high incidence of HCMV reactivation is also observed after T-cell replete haploidentical HSCT with post-transplant cyclophosphamide (Di Stasi et al., 2014; Crocchiolo et al., 2015; Goldsmith et al., 2016; Slade et al., 2017).

The reconstitution kinetics of HCMV-specific T-cells post-HSCT have a close relationship with the risk and prognosis of reactivation (Lilleri et al., 2006; Gratama et al., 2010; Espigado et al., 2014). HCMV-specific $CD4^+$ and $CD8^+$ T-cells expand with reactivation and are likely both required for control and/or protection (Foster et al., 2002; Sacre et al., 2008; Widmann et al., 2008; Pourgheysari et al., 2009; Lilleri et al., 2012; Gabanti et al., 2015; Raeiszadeh et al., 2015; Ciaurriz et al., 2017). Quantitative thresholds of $CD8^+$ and $CD4^+$ HCMV-specific T-cells associated with protection from, or control of, reactivation or disease post-HSCT have been defined using HLA tetramers or *ex vivo* viral stimulation assays (Aubert et al., 2001; Cwynarski et al., 2001; Gratama et al., 2001, 2010; Lilleri et al., 2008; Moins-Teisserenc et al., 2008; Borchers et al., 2011, 2012; Tormo et al., 2011; Lilleri et al., 2012; Liu et al., 2016). Threshold numbers have not been well-validated for routine clinical use and are less informative of protection from reactivation and disease in patients under steroid therapy or with prior GvHD (Lilleri et al., 2012; Gabanti et al., 2015).

Control of reactivation may depend more heavily on the functional recovery of HCMV-specific T-cell immunity (Quinnan et al., 1982; Reusser et al., 1991; Ozdemir et al., 2002; Nakamura et al., 2004; Gratama et al., 2008; Zhou et al., 2009; Tormo et al., 2010; Krol et al., 2011; Tey et al., 2013; Espigado et al., 2014; Ciaurriz et al., 2017). Polyfunctional HCMV-specific T-cell responses post-HSCT are associated with lower viral loads, protection from subsequent episodes of reactivation and lower antiviral therapy requirements (Zhou et al., 2009; Munoz-Cobo et al., 2012; Gimenez et al., 2015; Pelak et al., 2017). Delayed or undetectable HCMV-specific cytotoxic T-cell responses are prominent risk factors for HCMV disease (Reusser et al., 1991; Gratama et al., 2001; Ganepola et al., 2007). Camargo et al. (2019) recently described a composite biomarker comprising a protective (IL-2+IFN-γ+TNF-α+MIP-1β+) and non-protective (IL-2-IFN-γ+TNF-α-MIP-1β+) $CD8^+$ T-cell cytokine signature in response to *in vitro* HCMV pp65 peptide stimulation that independently predicted the risk of clinically significant reactivation. Assessment of HCMV-specific immunity through measurement of whole blood *ex vivo* IFN-γ secretion responses to HCMV peptides has also emerged as a promising prognostic approach for HCMV reactivation post-HSCT (Tey et al., 2013; Yong et al., 2017b). However, it is argued that the selective recovery of HCMV-specific T-cell immunity ahead of global T-cell reconstitution carries a higher risk of subsequent reactivation (Tey et al., 2014).

The detection of reactivation prior to 100 days post-transplant (Boeckh et al., 2003; Kim et al., 2004; Liu et al., 2015), plasma viral load (Zaia et al., 1997), leukopenia (Jang et al., 2012), lymphopenia (Einsele et al., 1993), and GvHD (Boeckh et al., 2003; Ljungman et al., 2006; Green et al., 2012) represent additional risk factors for HCMV disease. Donor grafts with ≥5 activating killer-cell immunoglobulin-like receptor (KIR) genes or with both KIR2DS2 and KIR2DS4 predict a lower risk of reactivation (Zaia et al., 2009), and the use of donors with multiple or additional activating KIRs is associated with a lower incidence of reactivation (Chen et al., 2006; Cook et al., 2006).

IMPACT OF HCMV REACTIVATION ON POST-HSCT IMMUNE RECOVERY, RELAPSE AND GvHD

The immune system crucially regulates the risk of HCMV reactivation and disease, but HCMV itself also has a profound influence in shaping immune profiles in healthy seropositive individuals (Chidrawar et al., 2009; Brodin et al., 2015; Patin et al., 2018) and HSCT patients (Itzykson et al., 2015; Lakshmikanth et al., 2017), although the functional implications of this immune modulation are not yet clear. In some HSCT recipients, reactivation might be an epiphenomenon of poor immune reconstitution, but it is also possible that the immunomodulatory effects of HCMV infection may contribute to poor post-transplant outcomes (Nichols et al., 2002). Indeed, while HCMV DNAemia-guided pre-emptive antiviral therapy has reduced the incidence of HCMV disease post-HSCT, the survival disadvantage associated with HCMV infection has not been eliminated (Broers et al., 2000; Schmidt-Hieber et al., 2013; Green et al., 2016). HCMV encodes a range of immunomodulatory gene products that are expressed during both productive infection and latency, including a homolog of the immunosuppressive cytokine IL-10 (Jenkins et al., 2004; McSharry et al., 2012; Avdic et al., 2014; Young et al., 2017). HCMV infection in HSCT recipients increases the risk of bacterial and fungal superinfections (Nichols et al., 2002; Yong et al., 2017a) and GvHD (Lonnqvist et al., 1984; Broers et al., 2000; Cantoni et al., 2010), which might be connected to complex impacts of HCMV reactivation and/or its treatment on post-transplant immune recovery.

T Cell Reconstitution

Reactivation stimulates the recovery of HCMV-specific T-cells after HSCT (see section "Risk Factors for HCMV Reactivation After HSCT") (Hakki et al., 2003; Tormo et al., 2010; Ciaurriz et al., 2017), but is also accompanied by broader changes in the T-cell compartment. Patients with reactivation display accelerated $CD8^+$ T-cell reconstitution in the first year post-transplant (Lugthart et al., 2014; Drylewicz et al., 2016), which is likely to be driven by clonal expansions of HCMV-specific effector-memory αβ $CD8^+$ T-cells (Suessmuth et al., 2015; Link et al., 2016), leading to an inverted CD4:CD8 ratio. Deep sequencing of the TCR-β repertoire at 1 year post-HSCT uncovered a contraction in effector-memory $CD8^+$ TCR diversity and holes in the underlying effector-memory $CD8^+$ T-cell repertoire in patients who had experienced reactivation (Suessmuth et al., 2015). The selective expansion of HCMV-reactive $V\delta2^{neg}$ γδ T-cells (Knight et al., 2010; Scheper et al., 2013), and clonal ($V\gamma9^{neg}$ and $V\delta2^{neg}$) γδ T-cell proliferations suggestive of adaptive responses (Ravens et al., 2017), are also observed following reactivation. Reactivation also triggers the expansion of large granular lymphocytes (Nann-Rütti et al., 2012). Lugthart et al. (2014) found the reconstitution of naïve and central memory T-cells up to 2 years post-transplant was not compromised by reactivation, but Suessmuth et al. (2015) observed lower numbers of naïve T-cells in the first year post-HSCT in patients with reactivation. Many of the immunological features associated with HCMV reactivation after HSCT, including oligoclonal expansions of terminally differentiated HCMV-specific T-cells, are also found with aging in seropositive individuals (Khan et al., 2002; Hadrup et al., 2006), although recently it was reported that these HCMV-induced clonal T-cell expansions may not compromise $CD8^+$ T-cell repertoire diversity in the elderly (Lindau et al., 2019). The prominent influence of HCMV seropositivity and reactivation in shaping global immune reconstitution signatures after HSCT is apparent (Itzykson et al., 2015), but the impact of reactivation on immune recovery beyond 2 years post-transplant is not well-characterized.

NK Cell Reconstitution

HCMV reactivation drives a rapid expansion of IFN-γ-producing $NKG2C^+$ NK cells (Foley et al., 2012b), which likely contribute to early control of reactivation (Kheav et al., 2014; Davis et al., 2015; Muccio et al., 2016). Expanded proportions of mature ($CD56^{dim}CD57^+NKG2A^-CD158b^+$) $NKG2C^+$ NK cells persist after viral clearance (Foley et al., 2012b) and memory-like expansions of $NKG2C^+CD57^+$ NK cells are also observed in R+/D+ patients with subclinical HCMV infection (Foley et al., 2012a). Specific recognition by $NKG2C^+$ NK cells of HCMV UL40 peptides presented in the context of HLA-E was recently identified to be the mechanism that drives the expansion and differentiation of $NKG2C^+$ NK cells during HCMV infection (Hammer et al., 2018).

Relapse

An association between early HCMV reactivation and reduced myeloid leukemia relapse has been reported (Lonnqvist et al., 1986; Elmaagacli et al., 2011; Green et al., 2013; Ito et al., 2013; Takenaka et al., 2015; Peric et al., 2018). This putative protective effect might be mediated through the anti-leukemic activities of $CD56^{dim}CD57^+NKG2C^+$ NK cell and $V\delta2^{neg}$ γδ T-cell subsets which expand with reactivation (Scheper et al., 2013; Cichocki et al., 2016), or via enhancement of donor alloimmune responses in the presence of infection and HCMV-specific $CD8^+$ T-cells (Ogonek et al., 2017; Varanasi et al., 2019). However, the role of reactivation in protection from malignancy relapse post-HSCT is controversial, as others have not found evidence of this association in patients with acute myeloid leukemia, chronic myeloid leukemia, acute lymphoid leukemia, lymphoma, or myelodysplastic syndrome (Nakamura et al., 2004; Green et al., 2013; Jeljeli et al., 2014; Mariotti et al., 2014; Takenaka et al., 2015;

Teira et al., 2016; Ramanathan et al., 2016; Admiraal et al., 2017). Further studies are thus required to better define the patient subgroups and immunological features associated with possible relapse protection in HSCT patients with HCMV reactivation.

Graft-Versus-Host Disease

Graft-versus-host disease and its steroid therapy increase the risk of reactivation after HSCT (Miller et al., 1986; Yanada et al., 2003; Ljungman et al., 2006; George et al., 2012; Liu et al., 2015; Valadkhani et al., 2016). The alloimmune responses mediating GvHD impair thymopoiesis (Weinberg et al., 2001; Castermans et al., 2011) and delay HCMV-specific T-cell reconstitution, and high-dose steroids impair the recovery of HCMV-specific T-cells in a dose-dependent manner (Hakki et al., 2003; Widmann et al., 2008). Further, it has been speculated that the proinflammatory immune environment associated with GvHD may promote reactivation, as has been demonstrated following allogeneic stimulation of latently infected cells *ex vivo* (Soderberg-Naucler et al., 1997). Conversely, patients with reactivation more frequently develop GvHD (Lonnqvist et al., 1984; Janeczko et al., 2016) and the risk of extensive chronic GvHD was reduced with the use of HCMV DNAemia-guided pre-emptive antiviral therapy (Larsson et al., 2004). An increased risk of acute GvHD was observed during episodes of active HCMV replication after HSCT, supporting a bidirectional relationship between reactivation and GvHD (Cantoni et al., 2010). Further research is required to delineate the mechanisms underlying this phenomenon, but an inflammatory response to reactivation or the potential cross-reactivity of HCMV-specific T-cells with human alloantigens (Hall et al., 2017) might play a role.

PREVENTION AND TREATMENT STRATEGIES

Standard antiviral drugs for reactivation after HSCT are ganciclovir, valganciclovir and foscarnet. Prophylactic use is reserved for high-risk patients due to their significant toxic side effects. Ganciclovir causes neutropenia which increases the risk of bacterial and fungal superinfections (Goodrich et al., 1993; Boeckh et al., 1996; Broers et al., 2000; Einsele et al., 2000; Yanada et al., 2003), while foscarnet and cidofovir (used as a second- or third- line therapy) (Ljungman et al., 2008) are nephrotoxic (Ljungman et al., 2001; Reusser et al., 2002). Additional concerns relate to the development of antiviral drug resistance (Campos et al., 2016; Servais et al., 2016; Chemaly et al., 2018) and breakthrough reactivation or disease (Green et al., 2012). HCMV drug resistance has been reported in up to 14.5% of HSCT recipients receiving pre-emptive therapy (Shmueli et al., 2014). Prolonged antiviral exposure (Boeckh and Ljungman, 2009), suboptimal prophylactic dosing (Lischka et al., 2016), corticosteroid therapy (Frietsch et al., 2019) and delayed immune reconstitution foster the selection of drug resistant HCMV mutants. Mutations in the HCMV UL97 (viral protein kinase) gene confer resistance to (val)ganciclovir and maribavir (Marfori et al., 2007; Piret and Boivin, 2019), while HCMV UL54 (viral DNA polymerase) gene mutations are associated with resistance to foscarnet, cidofovir and (val)ganciclovir (El Chaer et al., 2016). Infection with multiple HCMV genotypes is associated with reduced efficacy of antiviral treatment (Zawilinska et al., 2016; Vinuesa et al., 2017). Importantly, current drugs do not target HCMV during latency, as these drugs target the viral replication machinery, and latency is typified by maintenance of the viral genome without replication. This highlights the potential for clinically relevant recurrence of reactivation following therapy cessation.

Prophylactic administration of Letermovir, a new anti-HCMV agent which inhibits the viral terminase complex, recently demonstrated the capacity to reduce the risk of HCMV disease and all-cause mortality at 24 weeks post-transplant, in a Phase 3 trial (Marty et al., 2017). There are, however, reports emerging of breakthrough viraemia and disease associated with HCMV UL56 terminase mutations conferring Letermovir resistance in HSCT recipients (Lischka et al., 2016; Knoll et al., 2018; Frietsch et al., 2019). Letermovir has now been licensed for HCMV prophylaxis after HSCT and its efficacy in treating refractory or resistant HCMV infection and disease will be evaluated in an upcoming Phase 2 trial (NCT03728426). Given its unique mechanism of action, combination therapy of Letermovir with other currently licensed antivirals (Wildum et al., 2015) may represent a means to more effectively control HCMV and limit the emergence of antiviral drug resistance in HSCT patients, although this area remains to be explored.

Pre-emptive treatment based on viral DNAemia surveillance (Emery et al., 2000) minimizes toxic drug exposure and reduces rates of HCMV disease and mortality (Einsele et al., 1995; Ljungman et al., 1998; Reusser et al., 2002), but there is no consensus on the appropriate plasma viral load threshold for initiating such therapy (Green et al., 2012; Tan et al., 2015; Green et al., 2016; Hanna et al., 2017). Inter-laboratory assays for HCMV DNA quantitation vary and the WHO reference standard for HCMV DNA lacks commutability in many assays (Hayden et al., 2015). Lower viral load thresholds may be required in settings of corticosteroid treatment and T-cell depletion (Green et al., 2012; Melendez-Munoz et al., 2019). Monitoring both HCMV-specific T-cell immunity and viral load has recently been successfully applied to guide the withholding or early discontinuation of antiviral treatment (Avetisyan et al., 2007; Navarro et al., 2016; Kumar et al., 2017). Further to characterizing immune reconstitution profiles in patients who spontaneously resolve reactivation without antiviral treatment (Camargo et al., 2019), more detailed investigation of the immune environment prior to the detection of HCMV DNAemia should be a focus of future studies to optimize the identification of high-risk patients and timing of pre-emptive therapy.

Pooled HCMV-specific or polyclonal intravenous immunoglobulin is not effective at preventing reactivation or reducing mortality when used in the treatment of HCMV pneumonia post-HSCT (Raanani et al., 2009; Erard et al., 2015), although strain-specific antibody therapy was recently shown to potently inhibit murine cytomegalovirus (MCMV) reactivation after bone-marrow transplantation in a preclinical murine model (Martins et al., 2019). Adoptive HCMV-specific T-cell therapies to prevent and treat reactivation after HSCT have been developed

since the early 1990s (Riddell et al., 1992; Walter et al., 1995; Mackinnon et al., 2008). Third-party- or stem cell donor-derived HCMV-specific T-cells expanded *ex vivo* or isolated directly with HCMV-specific tetramers and infused in the post-transplant period can accelerate HCMV-specific immune recovery and contribute to long-term control of reactivation and protection from HCMV disease (Peggs et al., 2009; Peggs et al., 2011; Neuenhahn et al., 2017; Withers et al., 2017). The post-transplant infusion of donor-derived HCMV-specific cytotoxic T-cells was shown to reduce the requirement for antiviral drug therapy in a Phase 2 trial (Blyth et al., 2013). Further studies are needed to determine the optimal timing of adoptive cell infusion and understand its impact on post-transplant immune reconstitution.

CONCLUSION

HCMV is a highly prevalent, opportunistic pathogen that continues to cause substantial morbidity and mortality after HSCT. Improved knowledge of the cellular sites of HCMV latency and the conditions which enable its reactivation to clinically significant infection will be needed to better predict, prevent and control reactivation post-HSCT. Future strategies might involve the selective depletion of latently infected cells from the graft (Krishna et al., 2016, 2017), plasma metabolomics profiling to predict the emergence of reactivation (Monleon et al., 2018), the vaccination of transplant recipients and donors to enhance HCMV-specific immune reconstitution (Kharfan-Dabaja et al., 2012; Ma et al., 2018), or the engineering of corticosteroid-resistant HCMV-specific T-cells to improve adoptive cell therapies (Menger et al., 2015). The marked impact of HCMV on post-transplant immune reconstitution warrants continued research to understand its relationship with patient outcomes. New therapeutic approaches for reactivation are actively being pursued and it is hoped these will lessen the clinical impact of reactivation after HSCT in the near future.

AUTHOR CONTRIBUTIONS

LS and BW generated the initial draft of the manuscript. All authors contributed to the subsequent writing and review of the manuscript.

FUNDING

This work was funded by a Biomed Connect Grant (University of Sydney) awarded to BS and EB and an Australian Government Research Training Program Scholarship awarded to LS. EB is a NSW Cancer Institute Research Fellow.

ACKNOWLEDGMENTS

The authors wish to acknowledge the many research groups who have contributed to a better understanding of HCMV latency and reactivation in HSCT patients, and apologize to those whose work has not been cited due to space constraints.

REFERENCES

Admiraal, R., de Koning, C. C. H., Lindemans, C. A., Bierings, M. B., Wensing, A. M. J., Versluys, A. B., et al. (2017). Viral reactivations and associated outcomes in the context of immune reconstitution after pediatric hematopoietic cell transplantation. *J. Allergy Clin. Immunol.* 140, 1643–1650.e9. doi: 10.1016/j.jaci.2016.12.992

Aubert, G., Hassan-Walker, A. F., Madrigal, J. A., Emery, V. C., Morte, C., Grace, S., et al. (2001). Cytomegalovirus-specific cellular immune responses and viremia in recipients of allogeneic stem cell transplants. *J. Infect. Dis.* 184, 955–963. doi: 10.1086/323354

Avdic, S., McSharry, B. P., and Slobedman, B. (2014). Modulation of dendritic cell functions by viral IL-10 encoded by human cytomegalovirus. *Front. Microbiol.* 5:337. doi: 10.3389/fmicb.2014.00337

Avetisyan, G., Aschan, J., Hägglund, H., Ringdén, O., and Ljungman, P. (2007). Evaluation of intervention strategy based on CMV-specific immune responses after allogeneic SCT. *Bone Marrow Transplant.* 40, 865–869. doi: 10.1038/sj.bmt.1705825

Bhutani, D., Dyson, G., Manasa, R., Deol, A., Ratanatharathorn, V., Ayash, L., et al. (2015). Incidence, risk factors, and outcome of cytomegalovirus viremia and gastroenteritis in patients with gastrointestinal graft-versus-host disease. *Biol. Blood Marrow Transplant.* 21, 159–164. doi: 10.1016/j.bbmt.2014.10.004

Blyth, E., Clancy, L., Simms, R., Ma, C. K. K., Burgess, J., Deo, S., et al. (2013). Donor-derived CMV-specific T cells reduce the requirement for CMV-directed pharmacotherapy after allogeneic stem cell transplantation. *Blood* 121, 3745–3758. doi: 10.1182/blood-2012-08-448977

Boeckh, M., Gooley, T. A., Myerson, D., Cunningham, T., Schoch, G., and Bowden, R. A. (1996). Cytomegalovirus pp65 antigenemia-guided early treatment with ganciclovir versus ganciclovir at engraftment after allogeneic marrow transplantation: a randomized double-blind study. *Blood* 88, 4063–4071.

Boeckh, M., Leisenring, W., Riddell, S. R., Bowden, R. A., Huang, M. L., Myerson, D., et al. (2003). Late cytomegalovirus disease and mortality in recipients of allogeneic hematopoietic stem cell transplants: importance of viral load and T-cell immunity. *Blood* 101, 407–414. doi: 10.1182/blood-2002-03-0993

Boeckh, M., and Ljungman, P. (2009). How we treat cytomegalovirus in hematopoietic cell transplant recipients. *Blood* 113, 5711–5719. doi: 10.1182/blood-2008-10-143560

Boeckh, M., and Nichols, W. G. (2004). The impact of cytomegalovirus serostatus of donor and recipient before hematopoietic stem cell transplantation in the era of antiviral prophylaxis and preemptive therapy. *Blood* 103, 2003–2008. doi: 10.1182/blood-2003-10-3616

Bolovan-Fritts, C. A., Mocarski, E. S., and Wiedeman, J. A. (1999). Peripheral blood CD14(+) cells from healthy subjects carry a circular conformation of latent cytomegalovirus genome. *Blood* 93, 394–398.

Borchers, S., Bremm, M., Lehrnbecher, T., Dammann, E., Pabst, B., Wölk, B., et al. (2012). Sequential anti-cytomegalovirus response monitoring may allow prediction of cytomegalovirus reactivation after allogeneic stem cell transplantation. *PLoS One* 7:e50248. doi: 10.1371/journal.pone.0050248

Borchers, S., Luther, S., Lips, U., Hahn, N., Kontsendorn, J., Stadler, M., et al. (2011). Tetramer monitoring to assess risk factors for recurrent cytomegalovirus reactivation and reconstitution of antiviral immunity post allogeneic hematopoietic stem cell transplantation. *Transpl. Infect. Dis.* 13, 222–236. doi: 10.1111/j.1399-3062.2011.00626.x

Brodin, P., Jojic, V., Gao, T., Bhattacharya, S., Angel, C. J., Furman, D., et al. (2015). Variation in the human immune system is largely driven by non-heritable influences. *Cell* 160, 37–47. doi: 10.1016/j.cell.2014.12.020

Broers, A. E., van Der Holt, R., van Esser, J. W., Gratama, J. W., Henzen-Logmans, S., Kuenen-Boumeester, V., et al. (2000). Increased transplant-related morbidity and mortality in CMV-seropositive patients despite highly effective prevention

of CMV disease after allogeneic T-cell-depleted stem cell transplantation. *Blood* 95, 2240–2245.

Camargo, J. F., Wieder, E. D., Kimble, E., Benjamin, C. L., Kolonias, D. S., Kwon, D., et al. (2019). Deep functional immunophenotyping predicts risk of cytomegalovirus reactivation after hematopoietic cell transplantation. *Blood* 133, 867–877. doi: 10.1182/blood-2018-10-878918

Campos, A. B., Ribeiro, J., Boutolleau, D., and Sousa, H. (2016). Human cytomegalovirus antiviral drug resistance in hematopoietic stem cell transplantation: current state of the art. *Rev. Med. Virol.* 26, 161–182. doi: 10.1002/rmv.1873

Cannon, M. J., Schmid, D. S., and Hyde, T. B. (2010). Review of cytomegalovirus seroprevalence and demographic characteristics associated with infection. *Rev. Med. Virol.* 20, 202–213. doi: 10.1002/rmv.655

Cantoni, N., Hirsch, H. H., Khanna, N., Gerull, S., Buser, A., Bucher, C., et al. (2010). Evidence for a bidirectional relationship between cytomegalovirus replication and acute graft-versus-host disease. *Biol. Blood Marrow Transplant.* 16, 1309–1314. doi: 10.1016/j.bbmt.2010.03.020

Castermans, E., Hannon, M., Dutrieux, J., Humblet-Baron, S., Seidel, L., Cheynier, R., et al. (2011). Thymic recovery after allogeneic hematopoietic cell transplantation with non-myeloablative conditioning is limited to patients younger than 60 years of age. *Haematologica* 96, 298–306. doi: 10.3324/haematol.2010.029702

Chemaly, R. F., Chou, S., Einsele, H., Griffiths, P., Avery, R., Razonable, R. R., et al. (2018). Definitions of resistant and refractory cytomegalovirus infection and disease in transplant recipients for use in clinical trials. *Clin. Infect. Dis.* 68, 1420–1426. doi: 10.1093/cid/ciy696

Chen, C., Busson, M., Rocha, V., Appert, M. L., Lepage, V., Dulphy, N., et al. (2006). Activating KIR genes are associated with CMV reactivation and survival after non-T-cell depleted HLA-identical sibling bone marrow transplantation for malignant disorders. *Bone Marrow Transplant.* 38, 437–444. doi: 10.1038/sj.bmt.1705468

Chen, T., and Hudnall, S. D. (2006). Anatomical mapping of human herpesvirus reservoirs of infection. *Mod. Pathol.* 19, 726–737. doi: 10.1038/modpathol.3800584

Chidrawar, S., Khan, N., Wei, W., McLarnon, A., Smith, N., Nayak, L., et al. (2009). Cytomegalovirus-seropositivity has a profound influence on the magnitude of major lymphoid subsets within healthy individuals. *Clin. Exp. Immunol.* 155, 423–432. doi: 10.1111/j.1365-2249.2008.03785.x

Cho, B. S., Yahng, S. A., Kim, J. H., Yoon, J. H., Shin, S. H., Lee, S. E., et al. (2013). Impact of cytomegalovirus gastrointestinal disease on the clinical outcomes in patients with gastrointestinal graft-versus-host disease in the era of preemptive therapy. *Ann. Hematol.* 92, 497–504. doi: 10.1007/s00277-012-1632-x doi: 10.1007/s00277-012-1632-x

Ciaurriz, M., Beloki, L., Zabalza, A., Bandres, E., Mansilla, C., Perez-Valderrama, E., et al. (2017). Functional specific-T-cell expansion after first cytomegalovirus reactivation predicts viremia control in allogeneic hematopoietic stem cell transplant recipients. *Transpl. Infect. Dis.* 19:e12778. doi: 10.1111/tid.12778

Cichocki, F., Cooley, S., Davis, Z., DeFor, T. E., Schlums, H., Zhang, B., et al. (2016). CD56dimCD57+NKG2C+ NK cell expansion is associated with reduced leukemia relapse after reduced intensity HCT. *Leukemia* 30, 456–463. doi: 10.1038/leu.2015.260

Cohen, L., Yeshurun, M., Shpilberg, O., and Ram, R. (2015). Risk factors and prognostic scale for cytomegalovirus (CMV) infection in CMV-seropositive patients after allogeneic hematopoietic cell transplantation. *Transpl. Infect. Dis.* 17, 510–517. doi: 10.1111/tid.12398

Cook, M., Briggs, D., Craddock, C., Mahendra, P., Milligan, D., Fegan, C., et al. (2006). Donor KIR genotype has a major influence on the rate of cytomegalovirus reactivation following T-cell replete stem cell transplantation. *Blood* 107, 1230–1232. doi: 10.1182/blood-2005-03-1039

Copelan, E. A. (2006). Hematopoietic stem-cell transplantation. *N. Engl. J. Med.* 354, 1813–1826.

Craddock, C., Szydlo, R. M., Dazzi, F., Olavarria, E., Cwynarski, K., Yong, A., et al. (2001). Cytomegalovirus seropositivity adversely influences outcome after T-depleted unrelated donor transplant in patients with chronic myeloid leukaemia: the case for tailored graft-versus-host disease prophylaxis. *Br. J. Haematol.* 112, 228–236. doi: 10.1046/j.1365-2141.2001.02519.x

Crocchiolo, R., Bramanti, S., Vai, A., Sarina, B., Mineri, R., Casari, E., et al. (2015). Infections after T-replete haploidentical transplantation and high-dose cyclophosphamide as graft-versus-host disease prophylaxis. *Transpl. Infect. Dis.* 17, 242–249. doi: 10.1111/tid.12365

Cwynarski, K., Ainsworth, J., Cobbold, M., Wagner, S., Mahendra, P., Apperley, J., et al. (2001). Direct visualization of cytomegalovirus-specific T-cell reconstitution after allogeneic stem cell transplantation. *Blood* 97, 1232–1240. doi: 10.1182/blood.v97.5.1232

Davis, Z. B., Cooley, S. A., Cichocki, F., Felices, M., Wangen, R., Luo, X., et al. (2015). Adaptive natural killer cell and killer cell immunoglobulin-like receptor-expressing T cell responses are induced by cytomegalovirus and are associated with protection against cytomegalovirus reactivation after allogeneic donor hematopoietic cell transplantation. *Biol. Blood Marrow Transplant.* 21, 1653–1662. doi: 10.1016/j.bbmt.2015.05.025

Di Stasi, A., Milton, D. R., Poon, L. M., Hamdi, A., Rondon, G., Chen, J., et al. (2014). Similar transplantation outcomes for acute myeloid leukemia and myelodysplastic syndrome patients with haploidentical versus 10/10 human leukocyte antigen-matched unrelated and related donors. *Biol. Blood Marrow Transplant.* 20, 1975–1981. doi: 10.1016/j.bbmt.2014.08.013

Drylewicz, J., Schellens, I. M., Gaiser, R., Nanlohy, N. M., Quakkelaar, E. D., Otten, H., et al. (2016). Rapid reconstitution of CD4 T cells and NK cells protects against CMV-reactivation after allogeneic stem cell transplantation. *J. Transl. Med.* 14:230. doi: 10.1186/s12967-016-0988-4

D'Souza, A., and Fretham, C. (2018). *Current Uses and Outcomes of Hematopoietic Cell Transplantation (HCT): CIBMTR Summary Slides, 2018*. Available at: https://www.cibmtr.org (accessed March 30, 2019).

Einsele, H., Ehninger, G., Hebart, H., Wittkowski, K. M., Schuler, U., Jahn, G., et al. (1995). Polymerase chain reaction monitoring reduces the incidence of cytomegalovirus disease and the duration and side effects of antiviral therapy after bone marrow transplantation. *Blood* 86, 2815–2820.

Einsele, H., Ehninger, G., Steidle, M., Fischer, I., Bihler, S., Gerneth, F., et al. (1993). Lymphocytopenia as an unfavorable prognostic factor in patients with cytomegalovirus infection after bone marrow transplantation. *Blood* 82, 1672–1678.

Einsele, H., Hebart, H., Kauffmann-Schneider, C., Sinzger, C., Jahn, G., Bader, P., et al. (2000). Risk factors for treatment failures in patients receiving PCR-based preemptive therapy for CMV infection. *Bone Marrow Transplant.* 25, 757–763. doi: 10.1038/sj.bmt.1702226

El Chaer, F., Shah, D. P., and Chemaly, R. F. (2016). How I treat resistant cytomegalovirus infection in hematopoietic cell transplantation recipients. *Blood* 128, 2624–2636. doi: 10.1182/blood-2016-06-688432

Elmaagacli, A. H., Steckel, N. K., Koldehoff, M., Hegerfeldt, Y., Trenschel, R., Ditschkowski, M., et al. (2011). Early human cytomegalovirus replication after transplantation is associated with a decreased relapse risk: evidence for a putative virus-versus-leukemia effect in acute myeloid leukemia patients. *Blood* 118, 1402–1412. doi: 10.1182/blood-2010-08-304121

Emery, V. C., Sabin, C. A., Cope, A. V., Gor, D., Hassan-Walker, A. F., and Griffiths, P. D. (2000). Application of viral-load kinetics to identify patients who develop cytomegalovirus disease after transplantation. *Lancet* 355, 2032–2036. doi: 10.1016/s0140-6736(00)02350-3

Erard, V., Guthrie, K. A., Seo, S., Smith, J., Huang, M., Chien, J., et al. (2015). Reduced mortality of cytomegalovirus pneumonia after hematopoietic cell transplantation due to antiviral therapy and changes in transplantation practices. *Clin. Infect. Dis.* 61, 31–39. doi: 10.1093/cid/civ215

Espigado, I., de la Cruz-Vicente, F., BenMarzouk-Hidalgo, O. J., Gracia-Ahufinger, I., Garcia-Lozano, J. R., Aguilar-Guisado, M., et al. (2014). Timing of CMV-specific effector memory T cells predicts viral replication and survival after allogeneic hematopoietic stem cell transplantation. *Transpl. Int.* 27, 1253–1262. doi: 10.1111/tri.12406

Fietze, E., Prosch, S., Reinke, P., Stein, J., Docke, W. D., Staffa, G., et al. (1994). Cytomegalovirus infection in transplant recipients. The role of tumor necrosis factor. *Transplantation* 58, 675–680. doi: 10.1097/00007890-199409270-00007

Fish, K. N., Soderberg-Naucler, C., Mills, L. K., Stenglein, S., and Nelson, J. A. (1998). Human cytomegalovirus persistently infects aortic endothelial cells. *J. Virol.* 72, 5661–5668.

Foley, B., Cooley, S., Verneris, M. R., Curtsinger, J., Luo, X., Waller, E. K., et al. (2012a). Human cytomegalovirus (CMV)-induced memory-like NKG2C(+) NK cells are transplantable and expand in vivo in response to recipient CMV antigen. *J. Immunol.* 189, 5082–5088. doi: 10.4049/jimmunol.1201964

Foley, B., Cooley, S., Verneris, M. R., Pitt, M., Curtsinger, J., Luo, X., et al. (2012b). Cytomegalovirus reactivation after allogeneic transplantation promotes a lasting increase in educated NKG2C+ natural killer cells with potent function. *Blood* 119, 2665–2674. doi: 10.1182/blood-2011-10-386995

Forte, E., Swaminathan, S., Schroeder, M. W., Kim, J. Y., Terhune, S. S., and Hummel, M. (2018). Tumor necrosis factor alpha induces reactivation of human cytomegalovirus independently of myeloid cell differentiation following posttranscriptional establishment of latency. *mBio* 9:e01560-18. doi: 10.1128/mBio.01560-18

Foster, A. E., Gottlieb, D. J., Sartor, M., Hertzberg, M. S., and Bradstock, K. F. (2002). Cytomegalovirus-specific CD4+ and CD8+ T-cells follow a similar reconstitution pattern after allogeneic stem cell transplantation. *Biol. Blood Marrow Transplant.* 8, 501–511. doi: 10.1053/bbmt.2002.v8.pm12374455

Frietsch, J. J., Michel, D., Stamminger, T., Hunstig, F., Birndt, S., Schnetzke, U., et al. (2019). In vivo emergence of UL56 C325Y cytomegalovirus resistance to letermovir in a patient with acute myeloid leukemia after hematopoietic cell transplantation. *Mediterr. J. Hematol. Infect. Dis.* 11:e2019001. doi: 10.4084/MJHID.2019.001

Gabanti, E., Lilleri, D., Ripamonti, F., Bruno, F., Zelini, P., Furione, M., et al. (2015). Reconstitution of human cytomegalovirus-specific CD4+ T cells is critical for control of virus reactivation in hematopoietic stem cell transplant recipients but does not prevent organ infection. *Biol. Blood Marrow Transplant.* 21, 2192–2202. doi: 10.1016/j.bbmt.2015.08.002

Gandhi, M. K., Wills, M. R., Okecha, G., Day, E. K., Hicks, R., Marcus, R. E., et al. (2003). Late diversification in the clonal composition of human cytomegalovirus-specific CD8+ T cells following allogeneic hemopoietic stem cell transplantation. *Blood* 102, 3427–3438. doi: 10.1182/blood-2002-12-3689

Ganepola, S., Gentilini, C., Hilbers, U., Lange, T., Rieger, K., Hofmann, J., et al. (2007). Patients at high risk for CMV infection and disease show delayed CD8+ T-cell immune recovery after allogeneic stem cell transplantation. *Bone Marrow Transplant.* 39, 293–299. doi: 10.1038/sj.bmt.1705585

George, B., Kerridge, I. H., Gilroy, N., Huang, G., Hertzberg, M. S., Bradstock, K. F., et al. (2012). A risk score for early cytomegalovirus reactivation after allogeneic stem cell transplantation identifies low-, intermediate-, and high-risk groups: reactivation risk is increased by graft-versus-host disease only in the intermediate-risk group. *Transpl. Infect. Dis.* 14, 141–148. doi: 10.1111/j.1399-3062.2011.00706.x

George, B., Pati, N., Gilroy, N., Ratnamohan, M., Huang, G., Kerridge, I., et al. (2010). Pre-transplant cytomegalovirus (CMV) serostatus remains the most important determinant of CMV reactivation after allogeneic hematopoietic stem cell transplantation in the era of surveillance and preemptive therapy. *Transpl. Infect. Dis.* 12, 322–329. doi: 10.1111/j.1399-3062.2010.00504.x

Gimenez, E., Blanco-Lobo, P., Munoz-Cobo, B., Solano, C., Amat, P., Perez-Romero, P., et al. (2015). Role of cytomegalovirus (CMV)-specific polyfunctional CD8+ T-cells and antibodies neutralizing virus epithelial infection in the control of CMV infection in an allogeneic stem-cell transplantation setting. *J. Gen. Virol.* 96, 2822–2831. doi: 10.1099/vir.0.000203

Goldsmith, S. R., Slade, M., DiPersio, J. F., Westervelt, P., Lawrence, S. J., Uy, G. L., et al. (2016). Cytomegalovirus viremia, disease, and impact on relapse in T-cell replete peripheral blood haploidentical hematopoietic cell transplantation with post-transplant cyclophosphamide. *Haematologica* 101, e465–e468. doi: 10.3324/haematol.2016.149880

Goodrich, J. M., Bowden, R. A., Fisher, L., Keller, C., Schoch, G., and Meyers, J. D. (1993). Ganciclovir prophylaxis to prevent cytomegalovirus disease after allogeneic marrow transplant. *Ann. Intern. Med.* 118, 173–178.

Goodrum, F., Jordan, C. T., Terhune, S. S., High, K., and Shenk, T. (2004). Differential outcomes of human cytomegalovirus infection in primitive hematopoietic cell subpopulations. *Blood* 104, 687–695. doi: 10.1182/blood-2003-12-4344

Gordon, C. L., Miron, M., Thome, J. J., Matsuoka, N., Weiner, J., Rak, M. A., et al. (2017). Tissue reservoirs of antiviral T cell immunity in persistent human CMV infection. *J. Exp. Med.* 214, 651–667. doi: 10.1084/jem.20160758

Gratama, J. W., Boeckh, M., Nakamura, R., Cornelissen, J. J., Brooimans, R. A., Zaia, J. A., et al. (2010). Immune monitoring with iTAg MHC Tetramers for prediction of recurrent or persistent cytomegalovirus infection or disease in allogeneic hematopoietic stem cell transplant recipients: a prospective multicenter study. *Blood* 116, 1655–1662. doi: 10.1182/blood-2010-03-273508 doi: 10.1182/blood-2010-03-273508

Gratama, J. W., Brooimans, R. A., van der Holt, B., Sintnicolaas, K., van Doornum, G., Niesters, H. G., et al. (2008). Monitoring cytomegalovirus IE-1 and pp65-specific CD4+ and CD8+ T-cell responses after allogeneic stem cell transplantation may identify patients at risk for recurrent CMV reactivations. *Cytometry B Clin. Cytom.* 74B, 211–220. doi: 10.1002/cyto.b.20420 doi: 10.1002/cyto.b.20420

Gratama, J. W., van Esser, J. W., Lamers, C. H., Tournay, C., Lowenberg, B., Bolhuis, R. L., et al. (2001). Tetramer-based quantification of cytomegalovirus (CMV)-specific CD8+ T lymphocytes in T-cell-depleted stem cell grafts and after transplantation may identify patients at risk for progressive CMV infection. *Blood* 98, 1358–1364. doi: 10.1182/blood.v98.5.1358

Gratwohl, A., Brand, R., Frassoni, F., Rocha, V., Niederwieser, D., Reusser, P., et al. (2005). Cause of death after allogeneic haematopoietic stem cell transplantation (HSCT) in early leukaemias: an EBMT analysis of lethal infectious complications and changes over calendar time. *Bone Marrow Transplant.* 36, 757–769. doi: 10.1038/sj.bmt.1705140

Green, M. L., Leisenring, W., Stachel, D., Pergam, S. A., Sandmaier, B. M., Wald, A., et al. (2012). Efficacy of a viral load-based, risk-adapted, preemptive treatment strategy for prevention of cytomegalovirus disease after hematopoietic cell transplantation. *Biol. Blood Marrow Transplant.* 18, 1687–1699. doi: 10.1016/j.bbmt.2012.05.015

Green, M. L., Leisenring, W., Xie, H., Mast, T. C., Cui, Y., Sandmaier, B. M., et al. (2016). Cytomegalovirus viral load and mortality after haemopoietic stem cell transplantation in the era of pre-emptive therapy: a retrospective cohort study. *Lancet Haematol.* 3, e119–e127. doi: 10.1016/S2352-3026(15)00289-6

Green, M. L., Leisenring, W. M., Xie, H., Walter, R. B., Mielcarek, M., Sandmaier, B. M., et al. (2013). CMV reactivation after allogeneic HCT and relapse risk: evidence for early protection in acute myeloid leukemia. *Blood* 122, 1316–1324. doi: 10.1182/blood-2013-02-487074

Hadrup, S. R., Strindhall, J., Kollgaard, T., Seremet, T., Johansson, B., Pawelec, G., et al. (2006). Longitudinal studies of clonally expanded CD8 T cells reveal a repertoire shrinkage predicting mortality and an increased number of dysfunctional cytomegalovirus-specific T cells in the very elderly. *J. Immunol.* 176, 2645–2653. doi: 10.4049/jimmunol.176.4.2645

Hahn, G., Jores, R., and Mocarski, E. S. (1998). Cytomegalovirus remains latent in a common precursor of dendritic and myeloid cells. *Proc. Natl. Acad. Sci. U.S.A.* 95, 3937–3942. doi: 10.1073/pnas.95.7.3937

Hakki, M., Riddell, S. R., Storek, J., Carter, R. A., Stevens-Ayers, T., Sudour, P., et al. (2003). Immune reconstitution to cytomegalovirus after allogeneic hematopoietic stem cell transplantation: impact of host factors, drug therapy, and subclinical reactivation. *Blood* 102, 3060–3067. doi: 10.1182/blood-2002-11-3472

Hall, C. E., Koparde, V. N., Jameson-Lee, M., Elnasseh, A. G., Scalora, A. F., Kobulnicky, D. J., et al. (2017). Sequence homology between HLA-bound cytomegalovirus and human peptides: a potential trigger for alloreactivity. *PLoS One* 12:e0178763. doi: 10.1371/journal.pone.0178763

Hammer, Q., Ruckert, T., Borst, E. M., Dunst, J., Haubner, A., Durek, P., et al. (2018). Peptide-specific recognition of human cytomegalovirus strains controls adaptive natural killer cells. *Nat. Immunol.* 19, 453–463. doi: 10.1038/s41590-018-0082-6

Hanna, Z., Karrick, M., Jayaprakash, R., Morgan, W., Lutfi, S., Gunasekaran, K., et al. (2017). Establishing the optimal viral load threshold for initiation of therapy for cytomegalovirus infection in hematopoietic stem cell transplant recipients: a prospective derivation cohort study using the international standardized CMV quantitative nucleic acid testing. *Open Forum Infect. Dis.* 4(Suppl._1), S713–S714.

Hargett, D., and Shenk, T. E. (2010). Experimental human cytomegalovirus latency in CD14+ monocytes. *Proc. Natl. Acad. Sci. U.S.A.* 107, 20039–20044. doi: 10.1073/pnas.1014509107

Hayden, R. T., Preiksaitis, J., Tong, Y., Pang, X., Sun, Y., Tang, L., et al. (2015). Commutability of the first world health organization international standard for human cytomegalovirus. *J. Clin. Microbiol.* 53, 3325–3333. doi: 10.1128/JCM.01495-15

Hendrix, R. M., Wagenaar, M., Slobbe, R. L., and Bruggeman, C. A. (1997). Widespread presence of cytomegalovirus DNA in tissues of healthy trauma victims. *J. Clin. Pathol.* 50, 59–63. doi: 10.1136/jcp.50.1.59

Hill, J. A., Mayer, B. T., Xie, H., Leisenring, W. M., Huang, M. L., Stevens-Ayers, T., et al. (2017). The cumulative burden of double-stranded DNA virus detection after allogeneic HCT is associated with increased mortality. *Blood* 129, 2316–2325. doi: 10.1182/blood-2016-10-748426

Hiwarkar, P., Gaspar, H. B., Gilmour, K., Jagani, M., Chiesa, R., Bennett-Rees, N., et al. (2013). Impact of viral reactivations in the era of pre-emptive antiviral drug therapy following allogeneic haematopoietic SCT in paediatric recipients. *Bone Marrow Transplant.* 48, 803–808. doi: 10.1038/bmt.2012.221

Huang, M. M., Kew, V. G., Jestice, K., Wills, M. R., and Reeves, M. B. (2012). Efficient human cytomegalovirus reactivation is maturation dependent in the Langerhans dendritic cell lineage and can be studied using a CD14+ experimental latency model. *J. Virol.* 86, 8507–8515. doi: 10.1128/JVI.00598-12

Ibanez, C. E., Schrier, R., Ghazal, P., Wiley, C., and Nelson, J. A. (1991). Human cytomegalovirus productively infects primary differentiated macrophages. *J. Virol.* 65, 6581–6588.

Ito, S., Pophali, P., Co, W., Koklanaris, E. K., Superata, J., Fahle, G. A., et al. (2013). CMV reactivation is associated with a lower incidence of relapse after allo-SCT for CML. *Bone Marrow Transplant.* 48, 1313–1316. doi: 10.1038/bmt.2013.49

Itzykson, R., Robin, M., Moins-Teisserenc, H., Delord, M., Busson, M., Xhaard, A., et al. (2015). Cytomegalovirus shapes long-term immune reconstitution after allogeneic stem cell transplantation. *Haematologica* 100, 114–123. doi: 10.3324/haematol.2014.113415

Janeczko, M., Mielcarek, M., Rybka, B., Ryczan-Krawczyk, R., Noworolska-Sauren, D., and Kalwak, K. (2016). Immune recovery and the risk of CMV/ EBV reactivation in children post allogeneic haematopoietic stem cell transplantation. *Cent. Eur. J. Immunol.* 41, 287–296. doi: 10.5114/ceji.2016.63129

Jang, J. E., Hyun, S. Y., Kim, Y. D., Yoon, S. H., Hwang, D. Y., Kim, S. J., et al. (2012). Risk factors for progression from cytomegalovirus viremia to cytomegalovirus disease after allogeneic hematopoietic stem cell transplantation. *Biol. Blood Marrow Transplant.* 18, 881–886. doi: 10.1016/j.bbmt.2011.10.037

Jeljeli, M., Guerin-El Khourouj, V., Porcher, R., Fahd, M., Leveille, S., Yakouben, K., et al. (2014). Relationship between cytomegalovirus (CMV) reactivation, CMV-driven immunity, overall immune recovery and graft-versus-leukaemia effect in children. *Br. J. Haematol.* 166, 229–239. doi: 10.1111/bjh.12875

Jenkins, C., Abendroth, A., and Slobedman, B. (2004). A novel viral transcript with homology to human interleukin-10 is expressed during latent human cytomegalovirus infection. *J. Virol.* 78, 1440–1447. doi: 10.1128/jvi.78.3.1440-1447.2004

Kawasaki, S., Oshitani, H., Suzuki, H., Arakawa, M., Mizuta, K., Imaizumi, M., et al. (1999). PCR-RFLP analysis of cytomegalovirus infections associated with bone marrow transplantation in Japanese children. *Microbiol. Immunol.* 43, 359–364. doi: 10.1111/j.1348-0421.1999.tb02416.x

Khaiboullina, S. F., Maciejewski, J. P., Crapnell, K., Spallone, P. A., Dean Stock, A., Pari, G. S., et al. (2004). Human cytomegalovirus persists in myeloid progenitors and is passed to the myeloid progeny in a latent form. *Br. J. Haematol.* 126, 410–417. doi: 10.1111/j.1365-2141.2004.05056.x

Khan, N., Shariff, N., Cobbold, M., Bruton, R., Ainsworth, J. A., Sinclair, A. J., et al. (2002). Cytomegalovirus seropositivity drives the CD8 T cell repertoire toward greater clonality in healthy elderly individuals. *J. Immunol.* 169, 1984–1992. doi: 10.4049/jimmunol.169.4.1984

Kharfan-Dabaja, M. A., Boeckh, M., Wilck, M. B., Langston, A. A., Chu, A. H., Wloch, M. K., et al. (2012). A novel therapeutic cytomegalovirus DNA vaccine in allogeneic haemopoietic stem-cell transplantation: a randomised, double-blind, placebo-controlled, phase 2 trial. *Lancet Infect. Dis.* 12, 290–299. doi: 10.1016/S1473-3099(11)70344-9

Kheav, V. D., Busson, M., Scieux, C., Peffault de Latour, R., Maki, G., Haas, P., et al. (2014). Favorable impact of natural killer cell reconstitution on chronic graft-versus-host disease and cytomegalovirus reactivation after allogeneic hematopoietic stem cell transplantation. *Haematologica* 99, 1860–1867. doi: 10.3324/haematol.2014.108407

Kim, D. H., Kim, J. G., Lee, N. Y., Sung, W. J., Sohn, S. K., Suh, J. S., et al. (2004). Risk factors for late cytomegalovirus infection after allogeneic stem cell transplantation using HLA-matched sibling donor: donor lymphocyte infusion and previous history of early CMV infection. *Bone Marrow Transplant.* 34, 21–27. doi: 10.1038/sj.bmt.1704528

Knight, A., Madrigal, A. J., Grace, S., Sivakumaran, J., Kottaridis, P., Mackinnon, S., et al. (2010). The role of Vdelta2-negative gamma delta T cells during cytomegalovirus reactivation in recipients of allogeneic stem cell transplantation. *Blood* 116, 2164–2172. doi: 10.1182/blood-2010-01-255166

Knoll, B. M., Seiter, K., Phillips, A., and Soave, R. (2018). Breakthrough cytomegalovirus pneumonia in hematopoietic stem cell transplant recipient on letermovir prophylaxis. *Bone Marrow Transplant.* .

Krishna, B. A., Lau, B., Jackson, S. E., Wills, M. R., Sinclair, J. H., and Poole, E. (2016). Transient activation of human cytomegalovirus lytic gene expression during latency allows cytotoxic T cell killing of latently infected cells. *Sci. Rep.* 6:24674. doi: 10.1038/srep24674

Krishna, B. A., Spiess, K., Poole, E. L., Lau, B., Voigt, S., Kledal, T. N., et al. (2017). Targeting the latent cytomegalovirus reservoir with an antiviral fusion toxin protein. *Nat. Commun.* 8:14321. doi: 10.1038/ncomms14321

Krol, L., Stuchly, J., Hubacek, P., Keslova, P., Sedlacek, P., Stary, J., et al. (2011). Signature profiles of CMV-specific T-cells in patients with CMV reactivation after hematopoietic SCT. *Bone Marrow Transplant.* 46, 1089–1098. doi: 10.1038/bmt.2010.261

Kumar, D., Mian, M., Singer, L., and Humar, A. (2017). An interventional study using cell-mediated immunity to personalize therapy for cytomegalovirus infection after transplantation. *Am. J. Transplant.* 17, 2468–2473. doi: 10.1111/ajt.14347

Lakshmikanth, T., Olin, A., Chen, Y., Mikes, J., Fredlund, E., Remberger, M., et al. (2017). Mass cytometry and topological data analysis reveal immune parameters associated with complications after allogeneic stem cell transplantation. *Cell Rep.* 20, 2238–2250. doi: 10.1016/j.celrep.2017.08.021

Larsson, K., Aschan, J., Remberger, M., Ringden, O., Winiarski, J., and Ljungman, P. (2004). Reduced risk for extensive chronic graft-versus-host disease in patients receiving transplants with human leukocyte antigen-identical sibling donors given polymerase chain reaction-based preemptive therapy against cytomegalovirus. *Transplantation* 77, 526–531. doi: 10.1097/01.tp.0000109778.39235.f4

Li, C. R., Greenberg, P. D., Gilbert, M. J., Goodrich, J. M., and Riddell, S. R. (1994). Recovery of HLA-restricted cytomegalovirus (CMV)-specific T-cell responses after allogeneic bone marrow transplant: correlation with CMV disease and effect of ganciclovir prophylaxis. *Blood* 83, 1971–1979.

Lilleri, D., Fornara, C., Chiesa, A., Caldera, D., Alessandrino, E. P., and Gerna, G. (2008). Human cytomegalovirus-specific CD4+ and CD8+ T-cell reconstitution in adult allogeneic hematopoietic stem cell transplant recipients and immune control of viral infection. *Haematologica* 93, 248–256. doi: 10.3324/haematol.11912

Lilleri, D., Gerna, G., Fornara, C., Chiesa, A., Comolli, G., Zecca, M., et al. (2009). Human cytomegalovirus-specific T cell reconstitution in young patients receiving T cell-depleted, allogeneic hematopoietic stem cell transplantation. *J. Infect. Dis.* 199, 829–836. doi: 10.1086/597123

Lilleri, D., Gerna, G., Fornara, C., Lozza, L., Maccario, R., and Locatelli, F. (2006). Prospective simultaneous quantification of human cytomegalovirus-specific CD4+ and CD8+ T-cell reconstitution in young recipients of allogeneic hematopoietic stem cell transplants. *Blood* 108, 1406–1412. doi: 10.1182/blood-2005-11-012864

Lilleri, D., Gerna, G., Zelini, P., Chiesa, A., Rognoni, V., Mastronuzzi, A., et al. (2012). Monitoring of human cytomegalovirus and virus-specific T-cell response in young patients receiving allogeneic hematopoietic stem cell transplantation. *PLoS One* 7:e41648. doi: 10.1371/journal.pone.0041648

Lindau, P., Mukherjee, R., Gutschow, M. V., Vignali, M., Warren, E. H., Riddell, S. R., et al. (2019). Cytomegalovirus exposure in the elderly does not reduce CD8 T cell repertoire diversity. *J. Immunol.* 202, 476–483. doi: 10.4049/jimmunol.1800217

Link, C. S., Eugster, A., Heidenreich, F., Rucker-Braun, E., Schmiedgen, M., Oelschlagel, U., et al. (2016). Abundant cytomegalovirus (CMV) reactive clonotypes in the CD8(+) T cell receptor alpha repertoire following allogeneic transplantation. *Clin. Exp. Immunol.* 184, 389–402. doi: 10.1111/cei.12770

Lischka, P., Michel, D., and Zimmermann, H. (2016). Characterization of cytomegalovirus breakthrough events in a phase 2 prophylaxis trial of letermovir (AIC246, MK 8228). *J. Infect. Dis.* 213, 23–30. doi: 10.1093/infdis/jiv352

Liu, J., Chang, Y. J., Yan, C. H., Xu, L. P., Jiang, Z. F., Zhang, X. H., et al. (2016). Poor CMV-specific CD8+ T central memory subset recovery at early stage post-HSCT associates with refractory and recurrent CMV reactivation. *J. Infect.* 73, 261–270. doi: 10.1016/j.jinf.2016.04.033

Liu, J., Kong, J., Chang, Y. J., Chen, H., Chen, Y. H., Han, W., et al. (2015). Patients with refractory cytomegalovirus (CMV) infection following allogeneic haematopoietic stem cell transplantation are at high risk for CMV disease and non-relapse mortality. *Clin. Microbiol. Infect.* 21, 1121.e9–1121.e15. doi: 10.1016/j.cmi.2015.06.009

Ljungman, P., Aschan, J., Lewensohn-Fuchs, I., Carlens, S., Larsson, K., Lonnqvist, B., et al. (1998). Results of different strategies for reducing: cytomegalovirus-associated mortality in allogeneic stem cell transplant recipients. *Transplantation* 66, 1330–1334. doi: 10.1097/00007890-199811270-00012

Ljungman, P., Brand, R., Einsele, H., Frassoni, F., Niederwieser, D., and Cordonnier, C. (2003). Donor CMV serologic status and outcome of CMV-seropositive recipients after unrelated donor stem cell transplantation: an EBMT megafile analysis. *Blood* 102, 4255–4260. doi: 10.1182/blood-2002-10-3263

Ljungman, P., Brand, R., Hoek, J., de la Camara, R., Cordonnier, C., Einsele, H., et al. (2014). Donor cytomegalovirus status influences the outcome of allogeneic stem cell transplant: a study by the European group for blood and marrow transplantation. *Clin. Infect. Dis.* 59, 473–481. doi: 10.1093/cid/ciu364

Ljungman, P., de la Camara, R., Cordonnier, C., Einsele, H., Engelhard, D., Reusser, P., et al. (2008). Management of CMV, HHV-6, HHV-7 and Kaposi-sarcoma herpesvirus (HHV-8) infections in patients with hematological malignancies and after SCT. *Bone Marrow Transplant.* 42, 227–240. doi: 10.1038/bmt.2008.162

Ljungman, P., Deliliers, G. L., Platzbecker, U., Matthes-Martin, S., Bacigalupo, A., Einsele, H., et al. (2001). Cidofovir for cytomegalovirus infection and disease in allogeneic stem cell transplant recipients. The infectious diseases working party of the European group for blood and marrow transplantation. *Blood* 97, 388–392. doi: 10.1182/blood.v97.2.388

Ljungman, P., Perez-Bercoff, L., Jonsson, J., Avetisyan, G., Sparrelid, E., Aschan, J., et al. (2006). Risk factors for the development of cytomegalovirus disease after allogeneic stem cell transplantation. *Haematologica* 91, 78–83.

Lonnqvist, B., Ringden, O., Ljungman, P., Wahren, B., and Gahrton, G. (1986). Reduced risk of recurrent leukaemia in bone marrow transplant recipients after cytomegalovirus infection. *Br. J. Haematol.* 63, 671–679. doi: 10.1111/j.1365-2141.1986.tb07551.x

Lonnqvist, B., Ringden, O., Wahren, B., Gahrton, G., and Lundgren, G. (1984). Cytomegalovirus infection associated with and preceding chronic graft-versus-host disease. *Transplantation* 38, 465–468. doi: 10.1097/00007890-198411000-00004

Lugthart, G., van Ostaijen-Ten Dam, M. M., Jol-van der Zijde, C. M., van Holten, T. C., Kester, M. G., Heemskerk, M. H., et al. (2014). Early cytomegalovirus reactivation leaves a specific and dynamic imprint on the reconstituting T cell compartment long-term after hematopoietic stem cell transplantation. *Biol. Blood Marrow Transplant.* 20, 655–661. doi: 10.1016/j.bbmt.2014.01.018

Ma, C. K. K., Clancy, L., Simms, R., Burgess, J., Deo, S., Blyth, E., et al. (2018). Adjuvant peptide pulsed dendritic cell vaccination in addition to T cell adoptive immunotherapy for cytomegalovirus infection in allogeneic hematopoietic stem cell transplantation recipients. *Biol. Blood Marrow Transplant.* 24, 71–77. doi: 10.1016/j.bbmt.2017.08.028

Mackinnon, S., Thomson, K., Verfuerth, S., Peggs, K., and Lowdell, M. (2008). Adoptive cellular therapy for cytomegalovirus infection following allogeneic stem cell transplantation using virus-specific T cells. *Blood Cells Mol. Dis.* 40, 63–67. doi: 10.1016/j.bcmd.2007.07.003

Marfori, J. E., Exner, M. M., Marousek, G. I., Chou, S., and Drew, W. L. (2007). Development of new cytomegalovirus UL97 and DNA polymerase mutations conferring drug resistance after valganciclovir therapy in allogeneic stem cell recipients. *J. Clin. Virol.* 38, 120–125. doi: 10.1016/j.jcv.2006.11.005

Mariotti, J., Maura, F., Spina, F., Roncari, L., Dodero, A., Farina, L., et al. (2014). Impact of cytomegalovirus replication and cytomegalovirus serostatus on the outcome of patients with B cell lymphoma after allogeneic stem cell transplantation. *Biol. Blood Marrow Transplantat.* 20, 885–890. doi: 10.1016/j.bbmt.2014.02.015

Martins, J. P., Andoniou, C. E., Fleming, P., Kuns, R. D., Schuster, I. S., Voigt, V., et al. (2019). Strain-specific antibody therapy prevents cytomegalovirus reactivation after transplantation. *Science* 363, 288–293. doi: 10.1126/science.aat0066

Marty, F. M., Ljungman, P., Chemaly, R. F., Maertens, J., Dadwal, S. S., Duarte, R. F., et al. (2017). Letermovir prophylaxis for cytomegalovirus in hematopoietic-cell transplantation. *N. Engl. J. Med.* 377, 2433–2444. doi: 10.1056/NEJMoa1706640

McSharry, B. P., Avdic, S., and Slobedman, B. (2012). Human cytomegalovirus encoded homologs of cytokines, chemokines and their receptors: roles in immunomodulation. *Viruses* 4, 2448–2470. doi: 10.3390/v411|2448 doi: 10.3390/v4112448

Melendez-Munoz, R., Marchalik, R., Jerussi, T., Dimitrova, D., Nussenblatt, V., Beri, A., et al. (2019). Cytomegalovirus infection incidence and risk factors across diverse hematopoietic cell transplantation platforms using a standardized monitoring and treatment approach: a comprehensive evaluation from a single institution. *Biol. Blood Marrow Transplant.* 25, 577–586. doi: 10.1016/j.bbmt.2018.10.011

Mendelson, M., Monard, S., Sissons, P., and Sinclair, J. (1996). Detection of endogenous human cytomegalovirus in CD34+ bone marrow progenitors. *J. Gen. Virol.* 77(Pt 12), 3099–3102. doi: 10.1099/0022-1317-77-12-3099

Menger, L., Gouble, A., Marzolini, M. A., Pachnio, A., Bergerhoff, K., Henry, J. Y., et al. (2015). TALEN-mediated genetic inactivation of the glucocorticoid receptor in cytomegalovirus-specific T cells. *Blood* 126, 2781–2789. doi: 10.1182/blood-2015-08-664755

Miller, W., Flynn, P., McCullough, J., Balfour, H. J., Goldman, A., Haake, R., et al. (1986). Cytomegalovirus infection after bone marrow transplantation: an association with acute graft-v-host disease. *Blood* 67, 1162–1167.

Minton, E. J., Tysoe, C., Sinclair, J. H., and Sissons, J. G. (1994). Human cytomegalovirus infection of the monocyte/macrophage lineage in bone marrow. *J. Virol.* 68, 4017–4021.

Moins-Teisserenc, H., Busson, M., Scieux, C., Bajzik, V., Cayuela, J. M., Clave, E., et al. (2008). Patterns of cytomegalovirus reactivation are associated with distinct evolutive profiles of immune reconstitution after allogeneic hematopoietic stem cell transplantation. *J. Infect. Dis.* 198, 818–826. doi: 10.1086/591185

Monleon, D., Talaya, A., Gimenez, E., Vinuesa, V., Morales, J. M., Hernandez-Boluda, J. C., et al. (2018). Validation of a plasma metabolomics model that allows anticipation of the occurrence of cytomegalovirus DNAaemia in allogeneic stem cell transplant recipients. *J. Med. Microbiol.* .

Muccio, L., Bertaina, A., Falco, M., Pende, D., Meazza, R., Lopez-Botet, M., et al. (2016). Analysis of memory-like natural killer cells in human cytomegalovirus-infected children undergoing αβ+T and B cell-depleted hematopoietic stem cell transplantation for hematological malignancies. *Haematologica* 101, 371–381. doi: 10.3324/haematol.2015.134155

Munoz-Cobo, B., Solano, C., Benet, I., Costa, E., Remigia, M. J., de la Camara, R., et al. (2012). Functional profile of cytomegalovirus (CMV)-specific CD8+ T cells and kinetics of NKG2C+ NK cells associated with the resolution of CMV DNAemia in allogeneic stem cell transplant recipients. *J. Med. Virol.* 84, 259–267. doi: 10.1002/jmv.22254

Nakamura, R., Battiwalla, M., Solomon, S., Follmann, D., Chakrabarti, S., Cortez, K., et al. (2004). Persisting posttransplantation cytomegalovirus antigenemia correlates with poor lymphocyte proliferation to cytomegalovirus antigen and predicts for increased late relapse and treatment failure. *Biol. Blood Marrow Transplantat.* 10, 49–57. doi: 10.1016/j.bbmt.2003.08.011

Nann-Rütti, S., Tzankov, A., Cantoni, N., Halter, J., Heim, D., Tsakiris, D., et al. (2012). Large granular lymphocyte expansion after allogeneic hematopoietic stem cell transplant is associated with a cytomegalovirus reactivation and shows an indolent outcome. *Biol. Blood Marrow Transplant.* 18, 1765–1770. doi: 10.1016/j.bbmt.2012.07.007

Navarro, D., Amat, P., de la Camara, R., Lopez, J., Vazquez, L., Serrano, D., et al. (2016). Efficacy and safety of a preemptive antiviral therapy strategy based on combined virological and immunological monitoring for active cytomegalovirus infection in allogeneic stem cell transplant recipients. *Open Forum Infect. Dis.* 3:ofw107. doi: 10.1093/ofid/ofw107

Neuenhahn, M., Albrecht, J., Odendahl, M., Schlott, F., Dossinger, G., Schiemann, M., et al. (2017). Transfer of minimally manipulated CMV-specific T cells from stem cell or third-party donors to treat CMV infection after allo-HSCT. *Leukemia* 31, 2161–2171. doi: 10.1038/leu.2017.16

Nichols, W. G., Corey, L., Gooley, T., Davis, C., and Boeckh, M. (2002). High risk of death due to bacterial and fungal infection among cytomegalovirus (CMV)-seronegative recipients of stem cell transplants from seropositive donors:

evidence for indirect effects of primary CMV infection. *J. Infect. Dis.* 185, 273–282. doi: 10.1086/338624

Ogonek, J., Varanasi, P., Luther, S., Schweier, P., Kuhnau, W., Gohring, G., et al. (2017). Possible impact of cytomegalovirus-specific CD8(+) T cells on immune reconstitution and conversion to complete donor chimerism after allogeneic stem cell transplantation. *Biol. Blood Marrow Transplant.* 23, 1046–1053. doi: 10.1016/j.bbmt.2017.03.027

Ozdemir, E., St John, L. S., Gillespie, G., Rowland-Jones, S., Champlin, R. E., Molldrem, J. J., et al. (2002). Cytomegalovirus reactivation following allogeneic stem cell transplantation is associated with the presence of dysfunctional antigen-specific CD8+ T cells. *Blood* 100, 3690–3697. doi: 10.1182/blood-2002-05-1387

Pampou, S., Gnedoy, S. N., Bystrevskaya, V. B., Smirnov, V. N., Chazov, E. I., Melnick, J. L., et al. (2000). Cytomegalovirus genome and the immediate-early antigen in cells of different layers of human aorta. *Virchows Arch.* 436, 539–552. doi: 10.1007/s004289900173

Patin, E., Hasan, M., Bergstedt, J., Rouilly, V., Libri, V., Urrutia, A., et al. (2018). Natural variation in the parameters of innate immune cells is preferentially driven by genetic factors. *Nat. Immunol.* 19, 302–314. doi: 10.1038/s41590-018-0049-7

Peggs, K. S., Thomson, K., Samuel, E., Dyer, G., Armoogum, J., Chakraverty, R., et al. (2011). Directly selected cytomegalovirus-reactive donor T cells confer rapid and safe systemic reconstitution of virus-specific immunity following stem cell transplantation. *Clin. Infect. Dis.* 52, 49–57. doi: 10.1093/cid/ciq042

Peggs, K. S., Verfuerth, S., Pizzey, A., Chow, S. L., Thomson, K., and Mackinnon, S. (2009). Cytomegalovirus-specific T cell immunotherapy promotes restoration of durable functional antiviral immunity following allogeneic stem cell transplantation. *Clin. Infect. Dis.* 49, 1851–1860. doi: 10.1086/648422

Pelak, O., Stuchly, J., Krol, L., Hubacek, P., Keslova, P., Sedlacek, P., et al. (2017). Appearance of cytomegalovirus-specific T-cells predicts fast resolution of viremia post hematopoietic stem cell transplantation. *Cytometry B Clin. Cytom.* 92, 380–388. doi: 10.1002/cyto.b.21348

Peric, Z., Wilson, J., Durakovic, N., Ostojic, A., Desnica, L., Vranjes, V. R., et al. (2018). Early human cytomegalovirus reactivation is associated with lower incidence of relapse of myeloproliferative disorders after allogeneic hematopoietic stem cell transplantation. *Bone Marrow Transplant.* 53, 1450–1456. doi: 10.1038/s41409-018-0172-y

Piret, J., and Boivin, G. (2019). Clinical development of letermovir and maribavir: overview of human cytomegalovirus drug resistance. *Antiviral Res.* 163, 91–105. doi: 10.1016/j.antiviral.2019.01.011

Poole, E., Juss, J. K., Krishna, B., Herre, J., Chilvers, E. R., and Sinclair, J. (2015). Alveolar macrophages isolated directly from human cytomegalovirus (HCMV)-seropositive individuals are sites of HCMV reactivation in vivo. *J. Infect. Dis.* 211, 1936–1942. doi: 10.1093/infdis/jiu837

Pourgheysari, B., Piper, K. P., McLarnon, A., Arrazi, J., Bruton, R., Clark, F., et al. (2009). Early reconstitution of effector memory CD4+ CMV-specific T cells protects against CMV reactivation following allogeneic SCT. *Bone Marrow Transplant.* 43, 853–861. doi: 10.1038/bmt.2008.403

Qayed, M., Khurana, M., Hilinski, J., Gillespie, S., McCracken, C., Applegate, K., et al. (2014). Risk for CMV reactivation in children undergoing allogeneic hematopoietic stem cell transplantation. *Pediatr. Blood Cancer* 62, 364–366. doi: 10.1002/pbc.25237

Quinnan, G. V., Kirmani, N., Rook, A. H., Manischewitz, J. F., Jackson, L., Moreschi, G., et al. (1982). Cytotoxic t cells in cytomegalovirus infection: HLA-restricted T-lymphocyte and non-T-lymphocyte cytotoxic responses correlate with recovery from cytomegalovirus infection in bone-marrow-transplant recipients. *N. Engl. J. Med.* 307, 7–13. doi: 10.1056/nejm198207013070102

Raanani, P., Gafter-Gvili, A., Paul, M., Ben-Bassat, I., Leibovici, L., and Shpilberg, O. (2009). Immunoglobulin prophylaxis in hematopoietic stem cell transplantation: systematic review and meta-analysis. *J. Clin. Oncol.* 27, 770–781. doi: 10.1200/jco.2008.16.8450

Raeiszadeh, M., Pachnio, A., Begum, J., Craddock, C., Moss, P., and Chen, F. E. (2015). Characterization of CMV-specific CD4+ T-cell reconstitution following stem cell transplantation through the use of HLA Class II-peptide tetramers identifies patients at high risk of recurrent CMV reactivation. *Haematologica* 100, e318–e322.

Ramanathan, M., Teira, P., Battiwalla, M., Barrett, J., Ahn, K. W., Chen, M., et al. (2016). Impact of early CMV reactivation in cord blood stem cell recipients in the current era. *Bone Marrow Transplant.* 51, 1113–1120. doi: 10.1038/bmt.2016.89

Ravens, S., Schultze-Florey, C., Raha, S., Sandrock, I., Drenker, M., Oberdorfer, L., et al. (2017). Human gammadelta T cells are quickly reconstituted after stem-cell transplantation and show adaptive clonal expansion in response to viral infection. *Nat. Immunol.* 18, 393–401. doi: 10.1038/ni.3686

Reeves, M. B., Coleman, H., Chadderton, J., Goddard, M., Sissons, J. G. P., and Sinclair, J. H. (2004). Vascular endothelial and smooth muscle cells are unlikely to be major sites of latency of human cytomegalovirus in vivo. *J. Gen. Virol.* 85, 3337–3341. doi: 10.1099/vir.0.80285-0

Reeves, M. B., and Compton, T. (2011). Inhibition of inflammatory interleukin-6 activity via extracellular signal-regulated kinase-mitogen-activated protein kinase signaling antagonizes human cytomegalovirus reactivation from dendritic cells. *J. Virol.* 85, 12750–12758. doi: 10.1128/JVI.05878-11

Reeves, M. B., Lehner, P. J., Sissons, J. G., and Sinclair, J. H. (2005a). An in vitro model for the regulation of human cytomegalovirus latency and reactivation in dendritic cells by chromatin remodelling. *J. Gen. Virol.* 86(Pt 11), 2949–2954. doi: 10.1099/vir.0.81161-0

Reeves, M. B., MacAry, P. A., Lehner, P. J., Sissons, J. G., and Sinclair, J. H. (2005b). Latency, chromatin remodeling, and reactivation of human cytomegalovirus in the dendritic cells of healthy carriers. *Proc. Natl. Acad. Sci. U.S.A.* 102, 4140–4145. doi: 10.1073/pnas.0408994102

Reeves, M. B., and Sinclair, J. H. (2013). Circulating dendritic cells isolated from healthy seropositive donors are sites of human cytomegalovirus reactivation in vivo. *J. Virol.* 87, 10660–10667. doi: 10.1128/JVI.01539-13

Reusser, P., Einsele, H., Lee, J., Volin, L., Rovira, M., Engelhard, D., et al. (2002). Randomized multicenter trial of foscarnet versus ganciclovir for preemptive therapy of cytomegalovirus infection after allogeneic stem cell transplantation. *Blood* 99, 1159–1164. doi: 10.1182/blood.v99.4.1159

Reusser, P., Riddell, S. R., Meyers, J. D., and Greenberg, P. D. (1991). Cytotoxic T-lymphocyte response to cytomegalovirus after human allogeneic bone marrow transplantation: pattern of recovery and correlation with cytomegalovirus infection and disease. *Blood* 78, 1373–1380.

Riddell, S. R., Watanabe, K. S., Goodrich, J. M., Li, C. R., Agha, M. E., and Greenberg, P. D. (1992). Restoration of viral immunity in immunodeficient humans by the adoptive transfer of T cell clones. *Science* 257, 238–241. doi: 10.1126/science.1352912

Sacre, K., Nguyen, S., Deback, C., Carcelain, G., Vernant, J. P., Leblond, V., et al. (2008). Expansion of human cytomegalovirus (HCMV) immediate-early 1-specific CD8+ T cells and control of HCMV replication after allogeneic stem cell transplantation. *J. Virol.* 82, 10143–10152. doi: 10.1128/JVI.00688-08

Scheinberg, P., Melenhorst, J. J., Brenchley, J. M., Hill, B. J., Hensel, N. F., Chattopadhyay, P. K., et al. (2009). The transfer of adaptive immunity to CMV during hematopoietic stem cell transplantation is dependent on the specificity and phenotype of CMV-specific T cells in the donor. *Blood* 114, 5071–5080. doi: 10.1182/blood-2009-04-214684

Scheper, W., van Dorp, S., Kersting, S., Pietersma, F., Lindemans, C., Hol, S., et al. (2013). γδT cells elicited by CMV reactivation after allo-SCT cross-recognize CMV and leukemia. *Leukemia* 27, 1328–1338. doi: 10.1038/leu.2012.374

Schmidt-Hieber, M., Labopin, M., Beelen, D., Volin, L., Ehninger, G., Finke, J., et al. (2013). CMV serostatus still has an important prognostic impact in de novo acute leukemia patients after allogeneic stem cell transplantation: a report from the Acute Leukemia Working Party of EBMT. *Blood* 122, 3359–3364. doi: 10.1182/blood-2013-05-499830

Servais, S., Dumontier, N., Biard, L., Schnepf, N., Resche-Rigon, M., Peffault de Latour, R., et al. (2016). Response to antiviral therapy in haematopoietic stem cell transplant recipients with cytomegalovirus (CMV) reactivation according to the donor CMV serological status. *Clin. Microbiol. Infect.* 22, 289.e1–289.e7. doi: 10.1016/j.cmi.2015.11.006

Sester, M., Sester, U., Gartner, B., Kubuschok, B., Girndt, M., Meyerhans, A., et al. (2002). Sustained high frequencies of specific CD4 T cells restricted to a single persistent virus. *J. Virol.* 76, 3748–3755. doi: 10.1128/jvi.76.8.3748-3755.2002

Shmueli, E., Or, R., Shapira, M. Y., Resnick, I. B., Caplan, O., Bdolah-Abram, T., et al. (2014). High rate of cytomegalovirus drug resistance among patients receiving preemptive antiviral treatment after haploidentical

stem cell transplantation. *J. Infect. Dis.* 209, 557–561. doi: 10.1093/infdis/jit475 doi: 10.1093/infdis/jit475

Shnayder, M., Nachshon, A., Krishna, B., Poole, E., Boshkov, A., Binyamin, A., et al. (2018). Defining the transcriptional landscape during cytomegalovirus latency with single-cell RNA sequencing. *mBio* 9:e00013-18. doi: 10.1128/mBio.00013-18

Sinzger, C., Digel, M., and Jahn, G. (2008). Cytomegalovirus cell tropism. *Curr. Top. Microbiol. Immunol.* 325, 63–83. doi: 10.1007/978-3-540-77349-8_4

Slade, M., Goldsmith, S., Romee, R., DiPersio, J. F., Dubberke, E. R., Westervelt, P., et al. (2017). Epidemiology of infections following haploidentical peripheral blood hematopoietic cell transplantation. *Transpl. Infect. Dis.* 19:e12629.

Slobedman, B., and Mocarski, E. S. (1999). Quantitative analysis of latent human cytomegalovirus. *J. Virol.* 73, 4806–4812.

Smirnov, S. V., Harbacheuski, R., Lewis-Antes, A., Zhu, H., Rameshwar, P., and Kotenko, S. V. (2007). Bone-marrow-derived mesenchymal stem cells as a target for cytomegalovirus infection: implications for hematopoiesis, self-renewal and differentiation potential. *Virology* 360, 6–16. doi: 10.1016/j.virol.2006.09.017

Soderberg-Naucler, C., Fish, K. N., and Nelson, J. A. (1997). Reactivation of latent human cytomegalovirus by allogeneic stimulation of blood cells from healthy donors. *Cell* 91, 119–126. doi: 10.1016/s0092-8674(01)80014-3

Söderberg-Nauclér, C., Streblow, D. N., Fish, K. N., Allan-Yorke, J., Smith, P. P., and Nelson, J. A. (2001). Reactivation of latent human cytomegalovirus in CD14(+) monocytes is differentiation dependent. *J. Virol.* 75, 7543–7554. doi: 10.1128/jvi.75.16.7543-7554.2001

Soland, M. A., Keyes, L. R., Bayne, R., Moon, J., Porada, C. D., St Jeor, S., et al. (2014). Perivascular stromal cells as a potential reservoir of human cytomegalovirus. *Am. J. Transplant.* 14, 820–830. doi: 10.1111/ajt.12642

Suessmuth, Y., Mukherjee, R., Watkins, B., Koura, D. T., Finstermeier, K., Desmarais, C., et al. (2015). CMV reactivation drives posttransplant T-cell reconstitution and results in defects in the underlying TCRbeta repertoire. *Blood* 125, 3835–3850. doi: 10.1182/blood-2015-03-631853

Sylwester, A. W., Mitchell, B. L., Edgar, J. B., Taormina, C., Pelte, C., Ruchti, F., et al. (2005). Broadly targeted human cytomegalovirus-specific CD4+ and CD8+ T cells dominate the memory compartments of exposed subjects. *J. Exp. Med.* 202, 673–685. doi: 10.1084/jem.20050882

Taichman, R. S., Nassiri, M. R., Reilly, M. J., Ptak, R. G., Emerson, S. G., and Drach, J. C. (1997). Infection and replication of human cytomegalovirus in bone marrow stromal cells: effects on the production of IL-6, MIP-1alpha, and TGF-beta1. *Bone Marrow Transplant.* 19, 471–480. doi: 10.1038/sj.bmt.1700685

Takenaka, K., Nishida, T., Asano-Mori, Y., Oshima, K., Ohashi, K., Mori, T., et al. (2015). Cytomegalovirus reactivation after allogeneic hematopoietic stem cell transplantation is associated with a reduced risk of relapse in patients with acute myeloid leukemia who survived to day 100 after transplantation: the Japan society for hematopoietic cell transplantation transplantation-related complication working group. *Biol. Blood Marrow Transplant.* 21, 2008–2016. doi: 10.1016/j.bbmt.2015.07.019

Tan, S. K., Waggoner, J. J., and Pinsky, B. A. (2015). Cytomegalovirus load at treatment initiation is predictive of time to resolution of viremia and duration of therapy in hematopoietic cell transplant recipients. *J. Clin. Virol.* 69, 179–183. doi: 10.1016/j.jcv.2015.06.006

Taylor-Wiedeman, J., Sissons, J. G., Borysiewicz, L. K., and Sinclair, J. H. (1991). Monocytes are a major site of persistence of human cytomegalovirus in peripheral blood mononuclear cells. *J. Gen. Virol.* 72(Pt 9), 2059–2064. doi: 10.1099/0022-1317-72-9-2059

Taylor-Wiedeman, J., Sissons, P., and Sinclair, J. (1994). Induction of endogenous human cytomegalovirus gene expression after differentiation of monocytes from healthy carriers. *J. Virol.* 68, 1597–1604.

Teira, P., Battiwalla, M., Ramanathan, M., Barrett, A. J., Ahn, K. W., Chen, M., et al. (2016). Early cytomegalovirus reactivation remains associated with increased transplant-related mortality in the current era: a CIBMTR analysis. *Blood* 127, 2427–2438. doi: 10.1182/blood-2015-11-679639

Tey, S. K., Davenport, M. P., Hill, G. R., Kennedy, G. A., Durrant, S. T., Khanna, R., et al. (2014). Post transplant CMV-specific T-cell immune reconstitution in the absence of global T-cell immunity is associated with a high risk of subsequent virus reactivation. *Bone Marrow Transplant.* 50, 315–316. doi: 10.1038/bmt.2014.265

Tey, S. K., Kennedy, G. A., Cromer, D., Davenport, M. P., Walker, S., Jones, L. I., et al. (2013). Clinical assessment of anti-viral CD8+ T cell immune monitoring using QuantiFERON-CMV(R) assay to identify high risk allogeneic hematopoietic stem cell transplant patients with CMV infection complications. *PLoS One* 8:e74744. doi: 10.1371/journal.pone.0074744

Tong, J., Sun, Z., Liu, H., Geng, L., Zheng, C., Tang, B., et al. (2013). Risk factors of CMV infection in patients after umbilical cord blood transplantation: a multicenter study in China. *Chin. J. Cancer Res.* 25, 695–703. doi: 10.3978/j.issn.1000-9604.2013.11.08

Tormo, N., Solano, C., Benet, I., Clari, M. A., Nieto, J., de la Camara, R., et al. (2010). Lack of prompt expansion of cytomegalovirus pp65 and IE-1-specific IFNgamma CD8+ and CD4+ T cells is associated with rising levels of pp65 antigenemia and DNAemia during pre-emptive therapy in allogeneic hematopoietic stem cell transplant recipients. *Bone Marrow Transplant.* 45, 543–549. doi: 10.1038/bmt.2009.172

Tormo, N., Solano, C., Benet, I., Nieto, J., de la Camara, R., Lopez, J., et al. (2011). Reconstitution of CMV pp65 and IE-1-specific IFN-gamma CD8(+) and CD4(+) T-cell responses affording protection from CMV DNAemia following allogeneic hematopoietic SCT. *Bone Marrow Transplant.* 46, 1437–1443. doi: 10.1038/bmt.2010.330

Valadkhani, B., Kargar, M., Ashouri, A., Hadjibabaie, M., Gholami, K., and Ghavamzadeh, A. (2016). The risk factors for cytomegalovirus reactivation following stem cell transplantation. *J. Res. Pharm. Pract.* 5, 63–69. doi: 10.4103/2279-042X.176554

Varanasi, P. R., Ogonek, J., Luther, S., Dammann, E., Stadler, M., Ganser, A., et al. (2019). Cytomegalovirus-specific CD8+ T-cells are associated with a reduced incidence of early relapse after allogeneic stem cell transplantation. *PLoS One* 14:e0213739. doi: 10.1371/journal.pone.0213739

Vinuesa, V., Bracho, M. A., Albert, E., Solano, C., Torres-Puente, M., Gimenez, E., et al. (2017). The impact of virus population diversity on the dynamics of cytomegalovirus DNAemia in allogeneic stem cell transplant recipients. *J. Gen. Virol.* 98, 2530–2542. doi: 10.1099/jgv.0.000916

Wagner, J. E., Thompson, J. S., Carter, S. L., Kernan, N. A., and Unrelated Donor Marrow Transplantation Trial. (2005). Effect of graft-versus-host disease prophylaxis on 3-year disease-free survival in recipients of unrelated donor bone marrow (T-cell Depletion Trial): a multi-centre, randomised phase II-III trial. *Lancet* 366, 733–741. doi: 10.1016/s0140-6736(05)66996-6

Walker, C. M., van Burik, J. A., De For, T. E., and Weisdorf, D. J. (2007). Cytomegalovirus infection after allogeneic transplantation: comparison of cord blood with peripheral blood and marrow graft sources. *Biol. Blood Marrow Transplant.* 13, 1106–1115. doi: 10.1016/j.bbmt.2007.06.006

Walter, E. A., Greenberg, P. D., Gilbert, M. J., Finch, R. J., Watanabe, K. S., Thomas, E. D., et al. (1995). Reconstitution of cellular immunity against cytomegalovirus in recipients of allogeneic bone marrow by transfer of T-cell clones from the donor. *N. Engl. J. Med.* 333, 1038–1044. doi: 10.1056/nejm199510193331603

Webb, B. J., Harrington, R., Schwartz, J., Kammerer, J., Spalding, J., Lee, E., et al. (2018). The clinical and economic impact of cytomegalovirus infection in recipients of hematopoietic stem cell transplantation. *Transpl. Infect. Dis.* 20:e12961. doi: 10.1111/tid.12961

Weinberg, K., Blazar, B. R., Wagner, J. E., Agura, E., Hill, B. J., Smogorzewska, M., et al. (2001). Factors affecting thymic function after allogeneic hematopoietic stem cell transplantation. *Blood* 97, 1458–1466. doi: 10.1182/blood.v97.5.1458

Widmann, T., Sester, U., Gartner, B. C., Schubert, J., Pfreundschuh, M., Kohler, H., et al. (2008). Levels of CMV specific CD4 T cells are dynamic and correlate with CMV viremia after allogeneic stem cell transplantation. *PLoS One* 3:e3634. doi: 10.1371/journal.pone.0003634

Wildum, S., Zimmermann, H., and Lischka, P. (2015). In vitro drug combination studies of Letermovir (AIC246, MK-8228) with approved anti-human cytomegalovirus (HCMV) and anti-HIV compounds in inhibition of HCMV and HIV replication. *Antimicrob. Agents Chemother.* 59, 3140–3148. doi: 10.1128/AAC.00114-15

Wills, M. R., Poole, E., Lau, B., Krishna, B., and Sinclair, J. H. (2015). The immunology of human cytomegalovirus latency: could latent infection be cleared by novel immunotherapeutic strategies? *Cell. Mol. Immunol.* 12, 128–138. doi: 10.1038/cmi.2014.75

Winston, D. J., Huang, E. S., Miller, M. J., Lin, C. H., Ho, W. G., Gale, R. P., et al. (1985). Molecular epidemiology of cytomegalovirus infections associated with bone marrow transplantation. *Ann. Intern. Med.* 102, 16–20.

Withers, B., Blyth, E., Clancy, L. E., Yong, A., Fraser, C., Burgess, J., et al. (2017). Long-term control of recurrent or refractory viral infections after allogeneic HSCT with third-party virus-specific T cells. *Blood Adv.* 1, 2193–2205. doi: 10.1182/bloodadvances.2017010223

Yanada, M., Yamamoto, K., Emi, N., Naoe, T., Suzuki, R., Taji, H., et al. (2003). Cytomegalovirus antigenemia and outcome of patients treated with pre-emptive ganciclovir: retrospective analysis of 241 consecutive patients undergoing allogeneic hematopoietic stem cell transplantation. *Bone Marrow Transplant.* 32, 801–807. doi: 10.1038/sj.bmt.1704232

Yong, M. K., Ananda-Rajah, M., Cameron, P. U., Morrissey, C. O., Spencer, A., Ritchie, D., et al. (2017a). Cytomegalovirus reactivation is associated with increased risk of late-onset invasive fungal disease after allogeneic hematopoietic stem cell transplantation: a multicenter study in the current era of viral load monitoring. *Biol. Blood Marrow Transplant.* 23, 1961–1967. doi: 10.1016/j.bbmt.2017.07.025

Yong, M. K., Cameron, P. U., Slavin, M., Morrissey, C. O., Bergin, K., Spencer, A., et al. (2017b). Identifying cytomegalovirus complications using the quantiferon-CMV assay after allogeneic hematopoietic stem cell transplantation. *J. Infect. Dis.* 215, 1684–1694. doi: 10.1093/infdis/jix192

Yoon, H. S., Lee, J. H., Choi, E. S., Seo, J. J., Moon, H. N., Kim, M. N., et al. (2009). Cytomegalovirus infection in children who underwent hematopoietic stem cell transplantation at a single center: a retrospective study of the risk factors. *Pediatr. Transplant.* 13, 898–905. doi: 10.1111/j.1399-3046.2008.01084.x

Young, V. P., Mariano, M. C., Tu, C. C., Allaire, K. M., Avdic, S., Slobedman, B., et al. (2017). Modulation of the host environment by human cytomegalovirus with viral interleukin 10 in peripheral blood. *J. Infect. Dis.* 215, 874–882. doi: 10.1093/infdis/jix043

Zaia, J. A., Gallez-Hawkins, G. M., Tegtmeier, B. R., ter Veer, A., Li, X., Niland, J. C., et al. (1997). Late cytomegalovirus disease in marrow transplantation is predicted by virus load in plasma. *J. Infect. Dis.* 176, 782–785. doi: 10.1086/517301

Zaia, J. A., Sun, J. Y., Gallez-Hawkins, G. M., Thao, L., Oki, A., Lacey, S. F., et al. (2009). The effect of single and combined activating killer immunoglobulin-like receptor genotypes on cytomegalovirus infection and immunity after hematopoietic cell transplantation. *Biol. Blood Marrow Transplant.* 15, 315–325. doi: 10.1016/j.bbmt.2008.11.030

Zawilinska, B., Szostek, S., Kopec, J., Piatkowska-Jakubas, B., and Kosz-Vnenchak, M. (2016). Multiplex real-time PCR to identify a possible reinfection with different strains of human cytomegalovirus in allogeneic hematopoietic stem cell transplant recipients. *Acta Biochim. Pol.* 63, 161–166. doi: 10.18388/abp.2015_1162

Zhou, W., Longmate, J., Lacey, S. F., Palmer, J. M., Gallez-Hawkins, G., Thao, L., et al. (2009). Impact of donor CMV status on viral infection and reconstitution of multifunction CMV-specific T cells in CMV-positive transplant recipients. *Blood* 113, 6465–6476. doi: 10.1182/blood-2009-02-203307

Zhu, D., Pan, C., Sheng, J., Liang, H., Bian, Z., Liu, Y., et al. (2018). Human cytomegalovirus reprogrammes haematopoietic progenitor cells into immunosuppressive monocytes to achieve latency. *Nat. Microbiol.* 3, 503–513. doi: 10.1038/s41564-018-0131-9

Zuhair, M., Smit, G. S. A., Wallis, G., Jabbar, F., Smith, C., Devleesschauwer, B., et al. (2019). Estimation of the worldwide seroprevalence of cytomegalovirus: a systematic review and meta-analysis. *Rev. Med. Virol.* 29:e2034. doi: 10.1002/rmv.2034

Conflict of Interest Statement: The authors declare that the research was conducted in the absence of any commercial or financial relationships that could be construed as a potential conflict of interest.

frontiers in Microbiology

ORIGINAL RESEARCH
published: 26 June 2019
doi: 10.3389/fmicb.2019.01408

Chromatin Profiles of Chromosomally Integrated Human Herpesvirus-6A

Anthony J. Saviola[1†‡], Cosima Zimmermann[2†], Michael P. Mariani[1], Sylvia A. Signorelli[1], Diana L. Gerrard[1], Joseph R. Boyd[3], Darren J. Wight[2], Guillaume Morissette[4], Annie Gravel[4], Isabelle Dubuc[4], Louis Flamand[4], Benedikt B. Kaufer[2] and Seth Frietze[1*]*

[1]Department of Biomedical and Health Sciences, University of Vermont, Burlington, VT, United States, [2]Institute of Virology, Department of Veterinary Medicine, Freie Universität Berlin, Berlin, Germany, [3]Department of Biochemistry and University of Vermont Cancer Center, University of Vermont College of Medicine, Burlington, VT, United States, [4]Department of Microbiology, Infectious Disease and Immunology, Université Laval and CHU de Quebec Research Center-Université Laval, Quebec, QC, Canada

Human herpesvirus-6A (HHV-6A) and 6B (HHV-6B) are two closely related betaherpesviruses that are associated with various diseases including seizures and encephalitis. The HHV-6A/B genomes have been shown to be present in an integrated state in the telomeres of latently infected cells. In addition, integration of HHV-6A/B in germ cells has resulted in individuals harboring this inherited chromosomally integrated HHV-6A/B (iciHHV-6) in every cell of their body. Until now, the viral transcriptome and the epigenetic modifications that contribute to the silencing of the integrated virus genome remain elusive. In the current study, we used a patient-derived iciHHV-6A cell line to assess the global viral gene expression profile by RNA-seq, and the chromatin profiles by MNase-seq and ChIP-seq analyses. In addition, we investigated an *in vitro* generated cell line (293-HHV-6A) that expresses GFP upon the addition of agents commonly used to induce herpesvirus reactivation such as TPA. No viral gene expression including miRNAs was detected from the HHV-6A genomes, indicating that the integrated virus is transcriptionally silent. Intriguingly, upon stimulation of the 293-HHV-6A cell line with TPA, only foreign promoters in the virus genome were activated, while all HHV-6A promoters remained completely silenced. The transcriptional silencing of latent HHV-6A was further supported by MNase-seq results, which demonstrate that the latent viral genome resides in a highly condensed nucleosome-associated state. We further explored the enrichment profiles of histone modifications *via* ChIP-seq analysis. Our results indicated that the HHV-6 genome is modestly enriched with the repressive histone marks H3K9me3/H3K27me3 and does not possess the active histone modifications H3K27ac/H3K4me3. Overall, these results indicate that HHV-6 genomes reside in a condensed chromatin state, providing insight into the epigenetic mechanisms associated with the silencing of the integrated HHV-6A genome.

Keywords: ChIP-seq, HHV-6A, iciHHV-6A, latency, MNase-seq, nucleosomes, RNA-seq

OPEN ACCESS

Edited by:
Slobodan Paessler,
The University of Texas Medical Branch at Galveston, United States

Reviewed by:
Paul M. Lieberman,
Wistar Institute, United States
Bhupesh K. Prusty,
University of Wuerzburg, Germany

****Correspondence:***
Benedikt B. Kaufer
b.kaufer@fu-berlin.de
Seth Frietze
seth.frietze@med.uvm.edu

[†]These authors have contributed equally to this work

[‡]Present address:
Anthony J. Saviola, Department of Molecular Medicine and Neurobiology, The Scripps Research Institute, La Jolla, CA, United States

Specialty section:
This article was submitted to Virology, a section of the journal Frontiers in Microbiology

Received: *25 February 2019*
Accepted: *04 June 2019*
Published: *26 June 2019*

Citation:
Saviola AJ, Zimmermann C, Mariani MP, Signorelli SA, Gerrard DL, Boyd JR, Wight DJ, Morissette G, Gravel A, Dubuc I, Flamand L, Kaufer BB and Frietze S (2019) Chromatin Profiles of Chromosomally Integrated Human Herpesvirus-6A. Front. Microbiol. 10:1408. doi: 10.3389/fmicb.2019.01408

INTRODUCTION

Human herpesvirus 6 (HHV-6) was first discovered in patients with lymphoproliferative disorders (Salahuddin et al., 1986) and has a seroprevalence of more than 90% (Zerr et al., 2005). Since then, two variants were identified termed HHV-6A and HHV-6B, which have been classified as two distinct species based on their biological, immunological, and molecular properties (Adams and Carstens, 2012; Ablashi et al., 2014). Infection with HHV-6B occurs within the first 2 years of life and is the primary cause of *Roseola infantum*, a febrile illness with a skin rash that can be accompanied by seizures, meningoencephalitis, and encephalopathy (Yamanishi et al., 1988; De Bolle et al., 2005). The pathologies associated with HHV-6A remain poorly characterized, although a recent report has suggested an association between HHV-6A and Alzheimer's disease (Readhead et al., 2018).

Upon primary infection, HHV-6A/B establishes a lifelong persistent infection in the host, termed latency (Takahashi et al., 1989; Lusso et al., 1991). In latently infected cells, both viruses integrate their genome into the telomere region of host chromosomes (Arbuckle et al., 2010, 2013). This integration is facilitated by telomeric repeats $(TTAGGG)_n$ at the ends of the virus genome (Kaufer et al., 2011; Kaufer and Flamand, 2014; Wallaschek et al., 2016); however, the viral and/or cellular proteins that mediate integration remain elusive. Aside from latently infected cells, both viruses can also integrate their genomes into germ cells. This allows vertical transmission of HHV-6A/B and consequently individuals harbor the integrated virus in every cell of their body (Pellett et al., 2012). Approximately 1% of the human population has this condition termed inherited chromosomally integrated HHV-6A/B (iciHHV-6) (Pellett et al., 2012). The clinical consequences for iciHHV-6 patients remain poorly understood. An analysis of a large cohort revealed that iciHHV-6 patients have an increased risk of developing angina pectoris and other diseases (Gravel et al., 2015), but more research is needed to provide a better understanding of these disease associations. Reactivation of HHV-6A/B is associated with a number of diseases including encephalitis, multiple sclerosis, and graft rejection following transplantation (De Bolle et al., 2005; Caselli and Di Luca, 2007). For example, reactivation occurs in 30–70% of hematopoietic stem cell transplantation (HSCT) recipients and is linked to graft rejections and higher mortality (Vinnard et al., 2009; Hill and Zerr, 2014; Winestone et al., 2018). In addition, a higher frequency and severity of both graft-versus-host disease (GvHD) and cytomegalovirus (CMV) viremia were observed in HSCT patients when either the recipient or donor were iciHHV-6 positive (Hill et al., 2017).

Analysis of iciHHV-6 cell lines by RT-qPCR revealed that few or none of the assessed genes are expressed from the integrated virus genome (Strenger et al., 2014), suggesting that the integrated genome is efficiently silenced. Epigenetic modifications likely contribute to this silencing and will be the focus of this manuscript. Chromatin dynamics are largely mediated by a variety of post-translational modifications of the N-terminal tail of histone proteins, which promotes either an active or repressive transcriptional state. Modifications such as trimethylation (me3) of lysine 4 (K4) of histone 3 (H3K4me3), and acetylation (ac) of lysine 27 (K27) of histone 3 (H3K27ac), are often associated with less condensed chromatin referred to as the transcriptionally active euchromatin. On the other hand, modifications such as H3K27me3 and H3K9me3 are often associated with highly condensed chromatin and a repressive transcriptional state referred to as heterochromatin (Berger, 2007; Li et al., 2007). Heterochromatin formation and nucleosomal occupancy have been linked to viral latency for herpes simplex virus 1 (HSV-1) (Deshmane and Fraser, 1989; Kubat et al., 2004; Wang et al., 2005; Knipe and Cliffe, 2008; Cliffe et al., 2009; Bloom et al., 2010), Epstein-Barr virus (Dyson and Farrell, 1985; Shaw, 1985; Moquin et al., 2018), and human immunodeficiency virus (HIV) (Jordan et al., 2003; du Chéné et al., 2007; Friedman et al., 2011). However, the epigenetic modifications that contribute to the silencing of integrated (latent) HHV-6A/B remain unknown.

In the current study, we employed unbiased genomic approaches using RNA-, MNase-, and ChIP-sequencing to explore the state of the viral genome in patient-derived iciHHV-6 and experimentally infected 293-HHV-6A cells. Our data reveal that integrated HHV-6A is entirely transcriptionally silent and exists in a highly condensed, nucleosome-associated state. Further, the repressive histone modifications H3K9me3 and H3K27me3 were detected across the HHV-6A genome, although both histone modifications were not significantly enriched. Additionally, the latent genome lacks the active histone modifications H3K27ac and H3K4me3. These results provide the first chromatin landscape of the integrated HHV-6A genome in experimentally infected and iciHHV-6 patient-derived cells.

MATERIALS AND METHODS

Cell Lines and Virus

Following approval by the CHU de Quebec-Université Laval ethics review board and patients consent, umbilical cords of women undergoing C-section were tested for the presence of iciHHV-6A as described previously (Gravel et al., 2015). Smooth muscle cells (SMCs) were obtained from the arteries of iciHHV-6A+ umbilical cords as described (Moreau et al., 2007) and immortalized by transduction with a lentiviral vector expressing SV40 T antigens (Addene #22298). Human SMCs (iciHHV-6A) were cultured in Dulbecco's modified Eagle's medium (DMEM) supplemented with 20% fetal bovine serum (FBS), 1% penicillin–streptomycin (Pen/Strep), and 1% L-Glutamine. Human epithelial kidney 293 T (293 T, ATCC CRL-11268) cells were cultured in the same medium but supplemented with 10% FBS. All cells were maintained in 10 cm^2 flasks as a monolayer culture in a humidified 5% CO_2 air incubator at 37°C. Bacterial artificial chromosome (BAC)-derived HHV-6A (strain U1102) expressing green fluorescent protein (GFP) under the control of the HCMV major immediate early (IE) promoter (HHV-6-GFP) was propagated in JJHan cells as described previously (Tang et al., 2010). 293 T cells were infected with HHV-6-GFP and GFP positive cells were isolated using a FACS AriaIII cell sorter (BD Biosciences). Clones harboring the integrated HHV-6A genome (293-HHV-6A) were identified by quantitative PCR (qPCR) and confirmed by fluorescent *in situ*

hybridization (FISH). To investigate whether expression of genes from the integrated virus can be induced, clonal 293-HHV-6A cells were treated with either phorbol 12-myristate 13 acetate (TPA, Sigma) (10 ng/ml), Trichostatin A (TSA, Sigma) (0.25 μM), sodium butyrate (NaBy, Sigma) (3 mM), Etoposide (ETP, Sigma) (0.5 μM), suberoylanilide hydroxamic acid (SAHA; also known as vorinostat, Sigma) (1 μM), Forskolin (FSK, Sigma) (10 μM), or hydrocortisone (Dexamethasone, Dexa) (10 μM) for 24 h. Reactivation of HHV-6A was monitored using FACS Calibur (BD Biosciences) to determine the percent of GFP positive (GFP+) cells.

Fluorescent *in situ* Hybridization

To prove that HHV-6A genome is present at the ends of metaphase chromosomes, FISH was performed as described previously (Rens et al., 2006; Kaufer et al., 2011; Kaufer, 2013). Briefly, cell cultures were treated with 0.05 μg/ml colcemid (Gibco) overnight to arrest the cells in metaphase. Cells were collected by centrifugation, resuspended in hypotonic solution (0.075 M KCl) followed by methanol/acetic acid fixation and stored at −20°C until further use. Metaphase spreads were generated as described previously (Kaufer et al., 2011). The virus genome was detected using a HHV-6A-specific digoxigenin-labeled probe and detected using different antibodies as described by Wight et al. (2018). Slides were mounted using DAPI Vectashield (Vector Laboratories) and images taken with an Axio Imager M1 (Zeiss).

Quantitative PCR

HHV-6 genome copies were determined by qPCR using specific primers and TaqMan probes for U94 as described previously (Wallaschek et al., 2016). Briefly, DNA was isolated using the RTP® DNA/RNA Virus Mini Kit (Stratec) according to manufacturer's instructions. U94 gene copy numbers were normalized against the genome copies of the cellular ß$_2$M gene and compared to a control cell line (AP3) harboring one copy of the HHV-6A genome per cell (Gravel et al., 2017).

RT-qPCR

For HHV-6A transcriptome quantification, cells were treated with TPA during 6 days and RNA was isolated using the RNeasy Plus Mini Kit (Qiagen) according to manufacturer's instructions. Total RNA was reverse transcribed to single-stranded cDNA using High-Capacity cDNA Reverse Transcription Kit (Applied Biosystems) according to manufacturer's instructions. qPCR was performed using TaqMan probes for immediate-early (U86, U90) and early genes (U41, U70) as described previously (Wight et al., 2018). Gene copy numbers were normalized against the genome copies of the cellular ß$_2$M gene.

RNA-seq

RNA was extracted from patient-derived iciHHV-6 cells using Trizol Reagent (Life Technologies) and purified using Direct-zol RNA MicroPrep Kit (Zymo Research #R2060) following the manufacturer's instructions. In addition, RNA was isolated and purified from *in vitro* generated HHV6-GFP cells treated with either DMSO or 10 ng/ml phorbol 12-myristate 13 acetate (TPA, Sigma) for 24 h at 37°C in duplicate. One microgram of total RNA was depleted of ribosomal RNA (rRNA) using the KAPA RiboErase Kit (#KR1142) and libraries were prepared using the KAPA Stranded RNA-seq Library Preparation Kit (#KR0934). Libraries were quantified using Qubit (Life Technologies), and quality was assessed using the Agilent Bioanalyzer High-Sensitivity DNA kit (Agilent Technologies). Barcoded libraries were pooled and sequenced on an Illumina HiSeq 2,500 at the Genomics Core Facility (University of Texas Health Science Center, San Antonio, TX) to obtain 50-bp single-end reads. RNA-seq data were processed using TopHat as described previously (Trapnell et al., 2009) using human (hg38), HHV-6A (NC_001664.2) and the custom HHV-6A-GFP BAC genome. BAM files were sorted and converted to SAM files using SAMtools (Li et al., 2009) and reads were counted with HTSeq against the corresponding Gencode GTF files (Anders et al., 2015). Differential analysis of RNA-seq count data between TPA- and DMSO-treated cells was performed using DESeq2 (Love et al., 2014) with a gene false discovery rate of <0.5% (FDR < 0.005) and a fold change >2 considered as significantly different. RNA-seq datasets were visualized using the Integrated Genome Browser (Nicol et al., 2009).

MicroRNA-seq

RNA was extracted and purified from iciHHV-6A, and TPA or DMSO treated 293-HHV-6A cells as described above. MicroRNA (miRNA) libraries were prepared using NEBNext Multiplex Small RNA Sample Prep for Illumina (#E7300) following the manufacturer's protocol. Library quantification and quality were assessed as described above, and pooled libraries were sequenced on an Illumina HiSeq 2,500 at the Genomics Core Facility (University of Texas Health Science Center, San Antonio, TX) to obtain 50-bp single-end reads. miRNA data were processed using the Oasis2 package (Rahman et al., 2018).

Micrococcal Nuclease-seq

Micrococcal nuclease (MNase)-seq was performed using the EZ Nucleosomal DNA Prep Kit (Zymo Research #D5220) following the manufacturer's protocol. Briefly, nuclei isolated from 1 million iciHHV-6A and 293-HHV-6A cells were treated with varying concentrations of MNase (final concentrations of 0.07, 0.1, 0.2, 0.3 U/100 μl reaction) and incubated at room temperature for 5 min. The reaction was terminated with MNase stop buffer, and following nucleosomal DNA purification, libraries for each individual titration were prepared with the NEB Ultra II Library Prep Kit (#E7645S) following the manufacturer's protocol. Libraries were purified using 0.8X AMPure beads and quantified using Qubit (Life Technologies). Library quality and presence of mono-, di-, and tri-nucloesomes were observed using the Agilent 2,100 Bioanalyzer High-Sensitivity DNA kit. Barcoded libraries were pooled and sequenced on an Illumina HiSeq 2,500 instrument lane at the Genomics Core Facility (University of Texas Health Science Center, San Antonio, TX) to obtain 80-bp paired-end reads. Sequences were aligned to the human (hg38), HHV-6A (NC_001664.2), and custom HHV-6A-GFP genome using Bowtie2 (Langmead and Salzberg, 2012), and the bamCoverage command

in deepTools was used to filter out reads with insert sizes <50 bp and >500 bp and to generate bigwigs (Ramírez et al., 2016). Profiles were generated for individual titration points, and as it has been previously reported that nucleosome occupancy can change across the genome in response to MNase treatment (Maehara and Ohkawa, 2016; Mieczkowski et al., 2016; Mueller et al., 2017), data for each titration were merged based on the cell line. Data were processed using DANPOS as described previously (Chen et al., 2013).

Chromatin Immunoprecipitation

The antibodies used for ChIP-seq experiments were: histone H3 [#2650 (Cell Signaling Technologies)], H3K4me3 [#8580 (Abcam, lot GR273043)], H3K27ac [#4729 (Abcam, lot GR288020)], H3K27me3 [#6002 (Abcam, lot GR275911-4)], H3K9me3 [#8898 (Abcam, lot GR21638-1)], and control IgG [#171870 (Abcam)]. ChIP sequencing was performed as described previously (O'Geen et al., 2010) on the iciHHV-6A cell lines. For all antibodies, 20 µg of chromatin was incubated with 4 µl of antibody overnight at 4°C. The complexes were precipitated with 20 µl of Pierce™ Protein A/G Magnetic Beads, followed by extensive washing, and final elution of the immunoprecipitated chromatin complexes in 100 µl of ChIP elution buffer for subsequent DNA purification and library construction. Libraries were prepared using the NEBNext ChIP-Seq Library Prep Master Mix Set for Illumina (#E6240) following the manufacturer's instructions. Library concentration and quality were assessed on a Qubit (Life Technologies) and an Agilent 2,100 Bioanalyzer, respectively. Pooled libraries were sequenced on an Illumina HiSeq 2,500 instrument lane at the Genomics Core Facility (University of Texas Health Science Center, San Antonio, TX) to obtain 50-bp single-end reads. Sequence reads were aligned to the human (hg38) and HHV-6A (NC_001664.2) genomes using Bowtie2 (Langmead and Salzberg, 2012). The resulting SAM alignment files were used for peak calling using MACS2 against the control (no antibody) inputs (Zhang et al., 2008) and using default parameters. ChIP DNA assayed by quantitative PCR is expressed as fold enrichment over an internal control (GAPDH) and is normalized to input. Primers for ChIP-qPCR are listed in **Table 3**.

RESULTS

Gene Expression Profiling of Integrated HHV-6A Genomes

To determine the gene expression of integrated HHV-6A genomes, we employed a global RNA-seq approach using clonal iciHHV-6A patient cells (iciHHV-6A) and an *in vitro* generated cell line (293-HHV-6A). The latter cell model was obtained by infecting 293 T cells with HHV-6A expressing GFP under the control of the major immediate-early (IE) HCMV promoter. Presence of the HHV-6A genome in both cell lines was confirmed by qPCR and FISH analyses (**Figures 1A,B**). To assess gene expression, we collected total RNA from latent cell cultures, constructed stranded rRNA-depleted Illumina RNA-seq libraries and mapped the reads to the human and the HHV-6A reference genomes. Characteristic of a typical RNA-seq profile, we detected a range of host cellular transcripts with RPKM (reads per kb per million mapped) values ranging from 1 to >1,000 RPKM in both iciHHV-6A (**Supplementary Figure S1A**) and 293-HHV-6A cell lines (**Supplementary Figure S1B**, DMSO treatment). Surprisingly, when our data were mapped to the HHV-6A reference genomes, we failed to detect any previously determined viral latency-associated transcripts in both HHV-6A cell lines with all RPKM

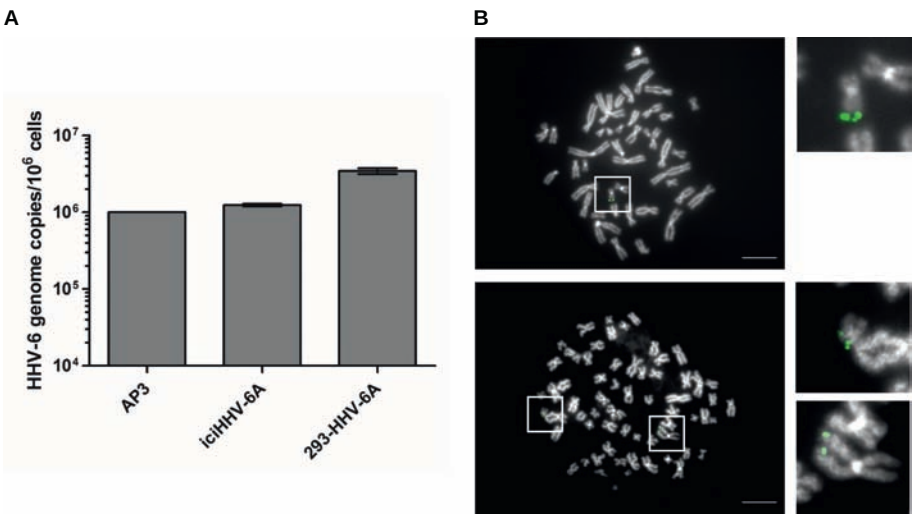

FIGURE 1 | Detection of HHV-6A genome at the end of methaphase chromosomes of iciHHV-6 and 293-HHV-6A cell lines. **(A)** HHV-6A (U94) genome copy numbers were detected by qPCR. Copy numbers per million cells are shown as means of three independent experiments with standard deviation. AP3 (HHV-6A) cells were used as a control. Copy numbers were normalized to AP3 cells carrying one HHV-6A copy per cell. **(B)** HHV-6A genome visualized by FISH. Representative metaphase images of iciHHV-6A (upper panel) and 293-HHV-6A (lower panel) cell lines. The HHV-6A genome was detected using a specific DIG-labeled probe (green) and chromosomes were visualized using DAPI (gray). Scale bar corresponds to 10 µm.

values <1.0. To confirm that the absence of transcripts was not due to major changes in the virus genome, we performed whole genome sequencing and genome-guided assembly. No deletion or mutations were observed that would explain the complete absence of viral transcripts. These results demonstrate a tight silencing of the entire HHV-6A genome in both patient-derived and an *in vitro* generated cell line.

Upon treatment of the 293-HHV-6A cell line with common reagents that induce reactivation (**Supplementary Figure S2**), greater than 90% of the TPA-treated cells express GFP while fewer than 1% express GFP in the DMSO-treated control (**Figure 2A**). Therefore, we set to determine how TPA treatment affects the global expression profile of the virus genome in 293-HHV-6A cells as described above. As expected, TPA induced global changes on human gene expression compared to the control (**Supplementary Figures S1B–D**). However, only the foreign HCMV IE and HSV-1 TK promoters driving GFP and EcoGPT respectively were induced in the HHV-6A genome, while all HHV-6A promoters remained silent (**Figure 2B**). To confirm this observation, we assessed the expression of selected viral genes following TPA induction for an extended period of time by RT-qPCR (**Supplementary Figure S2B**). Our data show that foreign but not HHV-6A promoters are efficiently induced by TPA, suggesting a selective activation by this activation stimulus.

Since viral encoded miRNAs play a pivotal role in the viral life cycle and latency of other herpesviruses, we also investigated the miRNA expression of these cells by small RNA-seq analysis. We performed small RNA-seq analysis using the patient-derived and experimental infected models (treated with TPA or DMSO control). Following adapter removal, we obtained a high number of reads that uniquely align to the human reference genome, the majority of these reads being identified as miRNAs (**Supplementary Figure S3**). No HHV-6A-derived miRNAs were identified in any of the libraries, indicating that HHV-6A does not express miRNAs in the cell lines we have tested. Taken together, our results suggest that both *in vitro* generated and patient-derived iciHHV-6A cells are transcriptionally silent. Moreover, this demonstrates that TPA stimulation fails to efficiently activate the HHV-6A promoters while foreign promoters in the viral genome are activated.

Chromosomally Integrated HHV-6A Is Associated With Nucleosomes

To better understand the transcriptional silencing observed from integrated HHV-6A, we examined the association of the virus genome with nucleosomes. Nucleosome positioning and occupancy profoundly influence gene expression (Li et al., 2007; Jiang and Pugh, 2009). Therefore, mapping the genomic location of nucleosomes is critical for understanding the mechanisms of chromatin-mediated transcriptional regulation. A commonly used approach is MNase-seq, in which nucleosome-free regions of chromatin are digested with MNase leaving nucleosome-associated DNA intact (Cui and Zhao, 2012; Mieczkowski et al., 2016; Pajoro et al., 2018). Mapping these data to a reference genome allows for a genome-wide profiling of nucleosome occupancy.

To profile the nucleosomal landscape of latent HHV-6A, we performed MNase-seq on non-TPA-treated ciHHV-6 samples with four different MNase concentrations (0.07, 0.1, 0.2, and 0.3 U). MNase-seq reads were aligned to both the human (hg38) and HHV-6A reference genomes (**Table 1**) and we determined the distribution of nucleosome occupancy around the transcription start sites (TSSs), which are nucleosome-free regions of the genome (Buenrostro et al., 2013; Mieczkowski et al., 2016). As previously demonstrated, there is decreased nucleosome signal at all active TSSs across

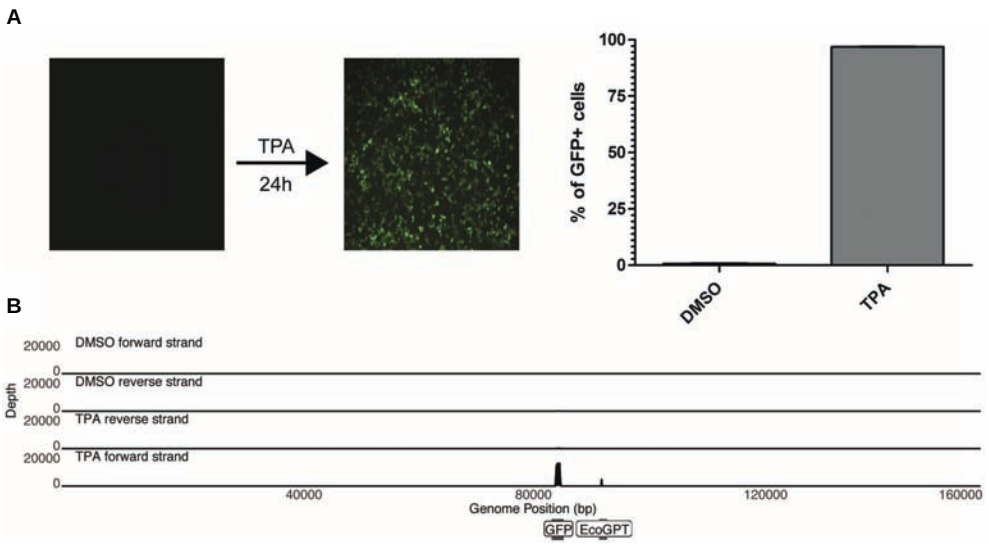

FIGURE 2 | TPA stimulation fails to reactivate *in vitro* chromosomally integrated HHV-6A. **(A)** 293-HHV-6A cells were treated with TPA or DMSO for 24 h. GFP expression was measured by flow cytometry. Mean of the % of GFP+ cells from two independent experiments is shown. **(B)** RNA was extracted from DMSO- or TPA-treated 293-HHV-6A cells and strand-specific RNA-seq libraries were generated. Alignment to the HHV-6A-GFP genome revealed that only transcripts associated with the GFP and the EcoGPT regions of the recombinant genome are detectable following TPA stimulation.

TABLE 1 | MNase-seq alignment statistics for both iciHHV-6A and 293-HHV-6A cell lines.

iciHHV-6A	Total reads	Mapped to hg38	Mapped to HHV-6A
0.07 U	108,672,380	104,671,364	3,119
0.1 U	129,284,350	123,825,376	3,842
0.2 U	115,427,930	107,820,045	3,030
0.3 U	139,973,048	130,960,010	3,905
293-HHV-6A			
0.07 U	115,412,822	110,409,085	5,635
0.1 U	117,406,422	109,932,492	5,777
0.2 U	110,616,804	100,882,910	5,766
0.3 U	91,897,360	74,527,515	3,957

iciHHV-6A sequences were mapped to the HHV-6A (NC_001664.2) genome, whereas 293-HHV-6A sequences were aligned to a custom HHV-6A genome.

the human genome for each of the four MNase titrations, and for the merged datasets (**Figures 3A,B**; Maehara and Ohkawa, 2016; Mieczkowski et al., 2016). In contrast, the MNase-seq data revealed that the HHV-6A genome has limited MNase accessibility (**Figures 3C,D**), indicating that in both HHV-6A cell lines, the majority of the viral genome is in a highly compacted heterochromatin state. Further, the GFP and EcoGPT regions of the 293-HHV-6A cell lines also exhibit a nucleosome-dense, heterochromatic formation (**Figure 3E**), which correlates with the lack of observable GFP in the untreated cells (**Figure 2A**). Overall, our results suggest that all major regions reside in a highly condensed nucleosome-associated state that likely contributes to the transcriptionally silent state of the virus genome.

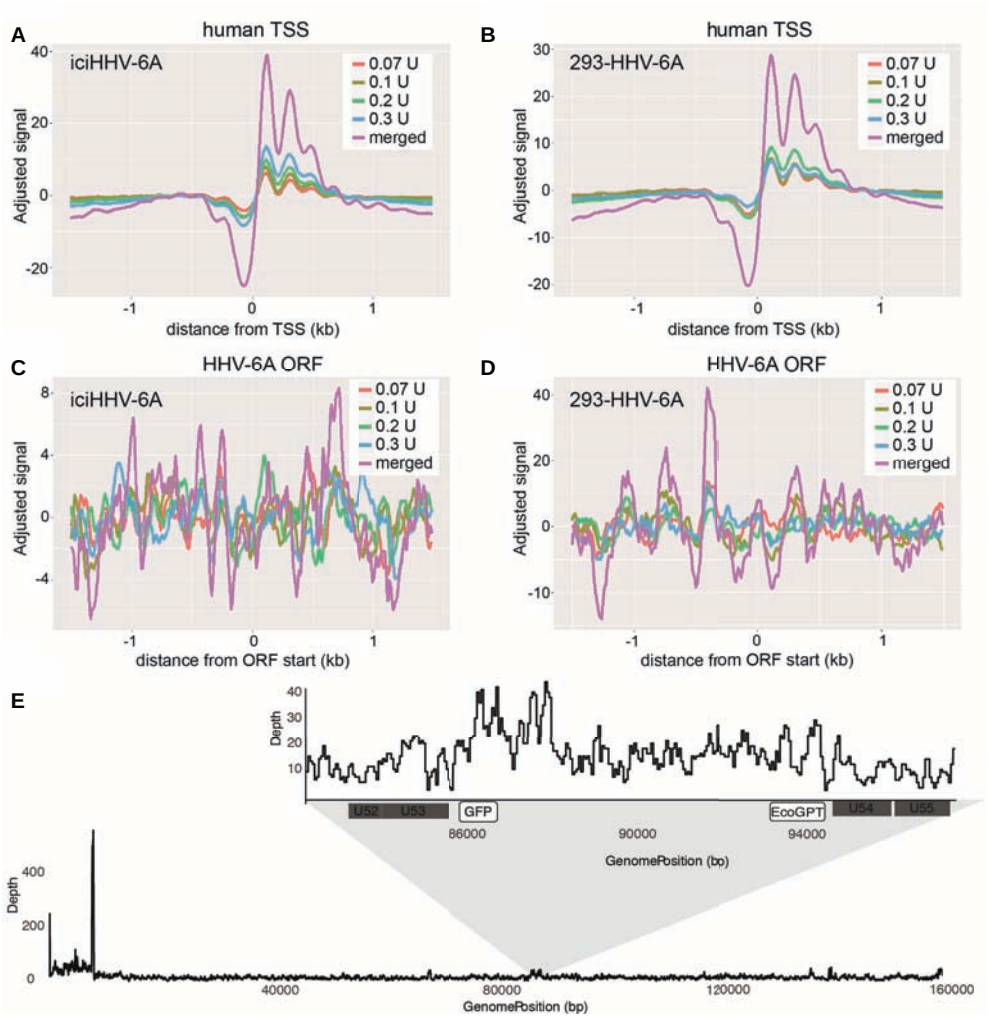

FIGURE 3 | Latent chromosomally integrated HHV-6A is associated with nucleosomes. The genome-wide distribution of the average nucleosomal occupancy in patient-derived iciHHV-6A and *in vitro* infected 293-HHV-6A cell lines. **(A,B)** Alignment to all transcription start sites (TSSs) for the human genome (hg38). For both cell lines, there is decreased nucleosome signal at all active TSSs across the hg38 genome for the four MNase titrations (0.07, 0.1, 0.2, 0.3 U), and for the merged datasets, validating our MNase-seq experiments. **(C,D)** Alignment to all open reading frame (ORF) start sites of the **(C)** iciHHV-6A (NC_001664.2) and 293-HHV-6A **(D)** genomes, respectively. Both cell lines demonstrate enriched nucleosome signal downstream and upstream from all ORF start sites found throughout the HHV-6A genome. **(E)** A zoomed-in snapshot showing nucleosomal enrichment across the 293-HHV-6A GFP and EcoGPT regions.

Repressive Histone Modifications Are Detected Across the Latent iciHHV-6A Genome

Mounting evidence indicates that regulatory histone modifications play central roles in viral latency and chromatin structure, including for both HSV-1 and HIV (Kubat et al., 2004; du Chéné et al., 2007). The density of nucleosome seeding of the integrated HHV-6A genome suggests that the virus may be associated with repressive histone modifications. Therefore, to identify potential epigenetic modifications that may regulate gene expression of the HHV-6A genome, we assayed the distribution of representative active (H3K27ac and H3K4me3) and repressive (H3K9me3 and H3K27me3) histone marks by a genome-wide ChIP-seq analysis in the patient-derived iciHHV-6 cell line. ChIP-seq reads were mapped to the HHV-6A genome and significantly enriched peaks were called against input controls.

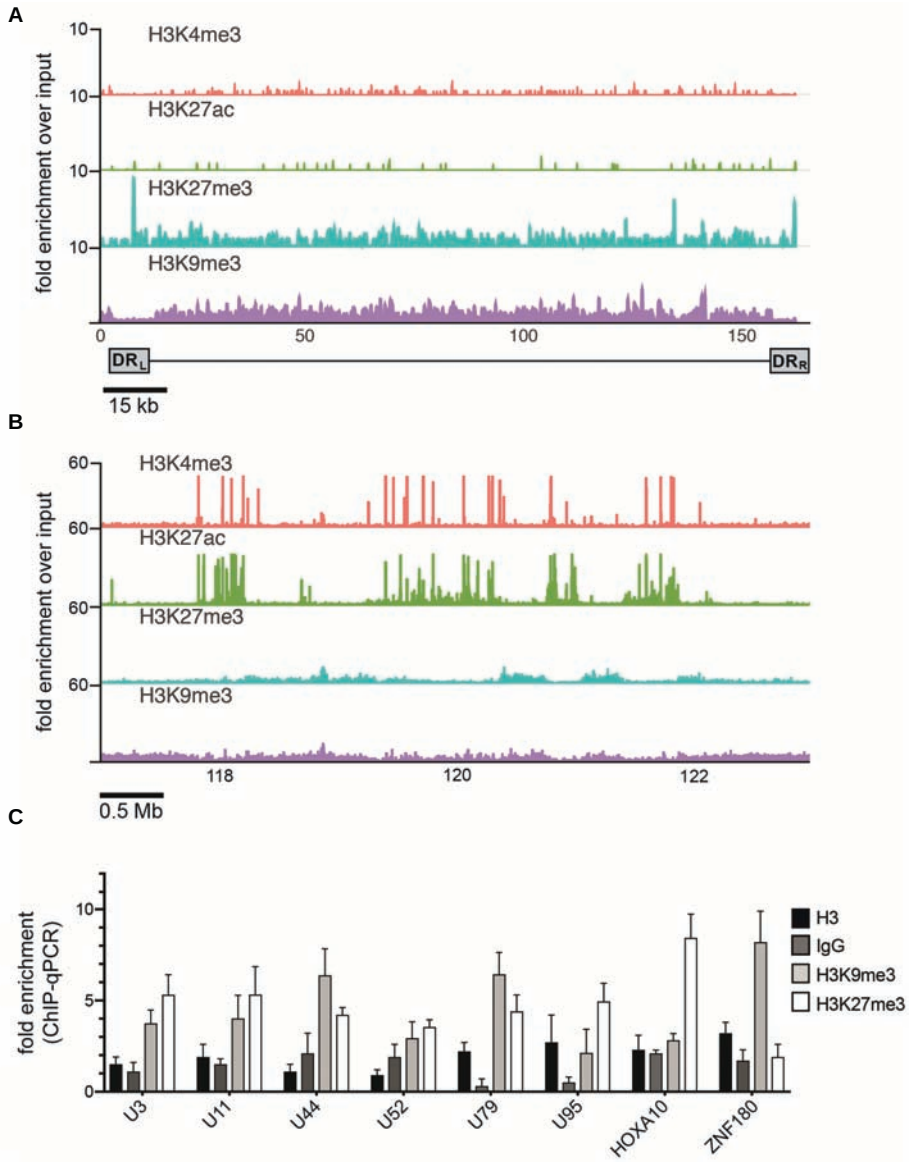

FIGURE 4 | ChIP enrichment profiles of histone modifications across the iciHHV-6A and human genomes. **(A)** The ChIP-seq enrichment patterns of two active (H3K27ac and H3K4me3) and two repressive modifications (H3K9me3 and H3K27me3) aligned to the HHV-6A (NC_001664.2) genome. The scale represents the fold enrichment of ChIP over input. **(B)** The ChIP-seq enrichment patterns of histone modification ChIP-seq datasets aligned to the human (hg38) genome. The ChIP-seq binding patterns demonstrate a typical profile of broad enrichment patterns of H3K27me3 and H3K9me3 in regions devoid of the active histone marks H3K27ac and H3K4me3. The locus at the indicated region of chromosome 2 of the hg38 human genome in mega base pairs is shown (Mb). **(C)** ChIP-qPCR assays using primers targeting HHV-6 gene regions U3, U11, U44, U52, U79, U95 and the cellular gene regions HOXA10 and ZNF180. Chromatin was immunoprecipitated with nonspecific IgG, total histone H3, H3K9me3, or H3K27me3 antibodies. Data are shown as the fold-enrichment over GAPDH normalized by input from three independent ChIP assays (mean ± SD).

TABLE 2 | ChIP-seq alignment statistics for the iciHHV-6A cell line.

iciHHV-6A	Total reads	Mapped to hg38	Mapped to HHV-6A
H3K4me3	16,934,452	15,997,762	342
H3K27ac	26,765,754	24,673,031	2,379
H3K9me3	9,538,766	8,845,283	1,443
H3K27me3	22,923,694	22,382,904	492

Sequences were mapped to the HHV-6A (NC_001664.2) genome using Bowtie2.

TABLE 3 | ChIP-qPCR primers.

Target	F primer	R primer
ZNF180	TGATGCACAATAAGTCGAGCA	TGCAGTCAATGTGGGAAGTC
GAPDH	CACCGTCAAGGCTGAGAACG	ATACCCAAGGGAGCCACACC
U3	ACAAACTGCAGCGATGACAC	TATGCGCACACGTGGTTATT
U11	TCCACACCGTTCGTATTCAA	AATCTGGATCTGCCGTTGTC
U44	GAGTTGGATCCGATTCTCCA	TTCAGACTCAACGCGTATCG
U52	GGGACACGGTTCAAAAAGAA	GCCCATGCTCTAAATCGAAA
U79	GCATATGGGTCATTTGACGA	TCACACGTTCCAGAGTCACC
U95	GTCGGATACAGACAGCGACA	TCTCTTGGCTTGGCGATACT

No enrichment of the active H3K27ac and H3K4me3 histone marks was detected across the HHV-6A genome (**Figure 4A**) as compared to the human genome (**Figure 4B**). In addition, the two repressive histone modifications H3K9me3 and H3K27me3 appeared to be present, but not significantly enriched compared to the input controls following peak calling using different peak calling algorithms with a range of parameters. This result may be due to the low number of overall reads mapped to the viral genome (**Table 2**). To further validate these findings, we performed ChIP-qPCR using primers specific to several HHV-6A genomic regions (**Table 3**). The repressive marks H3K9me3 or H3K27me3 are enriched over nonspecific IgG or pan-histone H3 antibodies, albeit at lower levels than cellular regions (**Figure 4C**). Taken together, these results suggest that the repressive histone modifications H3K9me3 and H3K27me3 are present on the latent virus genome and may be involved in chromatin-mediated repression of integrated HHV-6A gene expression.

DISCUSSION

HHV-6A/B has been shown to integrate its genomes into the telomere region of latently infected cells, while most other human herpesviruses maintain their genomes as extrachromosomal circular episomes during latency (Grinde, 2013). Latent episomal herpesvirus genomes are usually epigenetically silenced during latency; however, the transcriptional activity and epigenetic state of the telomere-integrated HHV-6A/B genome remain poorly characterized. In the current study, we used unbiased genomic methodologies to analyze viral gene expression and the epigenetic state of the latent HHV-6A genome in patient-derived and *in vitro* infected cell lines. Our work provides several lines of evidence that the latent HHV-6A genome is maintained in a transcriptionally silent and highly compacted state, associated with the repressive histone modifications H3K9me3 and H3K27me3. Overall, these findings further advance our understanding of the chromatin-based mechanisms regulating HHV-6A gene expression and latency.

Although previous studies have linked low levels of viral transcripts to herpesvirus latency (Collins-McMillen and Goodrum, 2017), our RNA-seq analysis demonstrates that viral associated transcripts were not detected from the integrated HHV-6A genome in both iciHHV-6A and 293-HHV-6A cells. A previous study described four HHV-6B latency-associated transcripts (LATs) in latently infected cells (Kondo et al., 2002); however, these LATs were barely detectable in a more sensitive assay and showed maximal expression during the establishment of latency, and just before the onset of reactivation both *in vivo* and *in vitro* (Kondo et al., 2003). Therefore, the detection of HHV-6A LATs may be dependent on specific time points assayed, as we were unable to detect any HHV-6A-associated transcripts in both *in vitro* generated and iciHHV-6 patient cell lines. Furthermore, only the U94 gene was transcribed in freshly isolated peripheral blood mononuclear cells from HHV-6A-infected adults and *in vitro* infected cells, whereas other viral transcripts were not detected (Rotola et al., 1998). For alphaherpesviruses, HSV latency is associated with the expression of LATs in some latently infected neurons; however, LAT equivalent transcripts are not expressed in varicella zoster virus (VZV) latency (Kinchington et al., 2012), although a recently discovered latency transcript antisense of ORF61 has been reported (Depledge et al., 2018). Varying degrees of evidence on LATs in both natural HCMV infection and experimental latency models have been reported (Cheng et al., 2017; Shnayder et al., 2018), suggesting that herpesvirus latency may be more complex and dynamic than previously assumed (Goodrum, 2016; Collins-McMillen and Goodrum, 2017).

The lack of viral associated miRNAs for both iciHHV-6A and 293-HHV-6A cells was a somewhat surprising result as viral miRNAs have been associated with herpesvirus latency, and have been shown to regulate the switch between latency and lytic replication (Skalsky and Cullen, 2010; Cullen, 2011; Piedade and Azevedo-Pereira, 2016). Latency-expressed miRNAs from HSV-1, EBV, and KSHV have been shown to target IE genes and thereby suppress lytic replication to maintain latency (Murphy et al., 2008; Skalsky and Cullen, 2010). Latency-specific viral miRNAs were also identified after deep sequencing of trigeminal ganglia latently infected with HSV-1; however, and similar to the results reported here, miRNAs have not been detected during VZV latency (Umbach et al., 2009). For HHV-6A and HHV-6B, virus-encoded miRNAs have been characterized in lytically infected cells (Tuddenham et al., 2012; Nukui et al., 2015). In a recent study, Prusty et al. (2018) was able to detect various viral sncRNAs in TSA-treated cells by Northern blotting, however, in the absence of detectable viral protein production or replication. Therefore, we hypothesized that viral associated transcripts, including LATs and miRNAs, would be detected upon reactivation of HHV-6A in 293-HHV-6A cells. RNA- and miRNA-seq following TPA stimulation, however, revealed that only transcripts associated with the GFP and EcoGPT regions were detected in our *in vitro* infected cells. Viral genes remained

below the detection limit of RNA-seq. The increased GFP expression suggests that TPA does not stimulate transcription of HHV-6A genes, and only the foreign viral promoters in the BAC sequence are expressed in the HHV-6-GFP genome. Along with this, Liu et al. (2010) showed that TPA reverses HCMV MIE gene silencing *via* a PKC-delta-dependent mechanism in human NT2 cells. HHV-6 reactivation and associations with diseases have previously been observed in patients (Gravel et al., 2013; Endo et al., 2014; Politikos et al., 2018). Reactivation of the virus genome using various compounds *in vitro* can result in viral gene expression; however, these stimuli were not sufficient to induce the production of infectious particles in several *in vitro* infected cells (Arbuckle et al., 2010; Gravel et al., 2017; Prusty et al., 2018). Through co-cultivation studies, Arbuckle et al. (2010) demonstrated that the integrated genome in TPA- and Dexamethason-treated PBMCs from different iciHHV-6 individuals can be transmitted to Molt-3 cells. This observation may support the hypothesis that, in contrast to cells directly *ex vivo*, the HHV-6A genome in immortalized cell lines might be harder to reactivate. Taken together, the ability and efficiency of reactivation appear to be dependent on the cell type, cell line, and drug used to stimulate reactivation.

The lack of viral gene expression in our iciHHV-6A and 293-HHV-6A models suggests that a chromatin-mediated mechanism could be involved in transcriptional silencing of integrated HHV-6A. Using MNase-seq, we profiled the nucleosomal positioning across the HHV-6A genome. Results presented here demonstrate a significant decrease in MNase accessibility, which is attributed to increased nucleosomal occupancy across the majority of the viral genome. These results strongly suggest that the latent virus resides in a highly compacted state, which would exclude the necessary transcriptional machinery required for gene expression. Furthermore, ChIP assays (ChIP-seq and ChIP-qPCR) indicate that active chromatin marks (H3K4me3 and H3K27ac) were not detected above background levels in these experiments (**Figure 4A**), despite H3K27ac having the highest amount of total mapped reads (**Table 2**). Human telomeres are enriched for H3K27ac (Cubiles et al., 2018); therefore, the high number of mapped reads to HHV-6A, in the absence of H3K27ac enrichment, is likely due to non-unique reads mapping to the viral telomeric repeats. In contrast, H3K9me3 and H3K27me3 levels are relatively low in human telomeres (O'Sullivan et al., 2010; Ichikawa et al., 2015; Cubiles et al., 2018), and these repressive histone modifications show modest enrichment across the HHV-6A genome. As opposed to H3K4me3 and H3K27ac, H3K9me3 and H3K27me3 are characterized by broad low-level enrichment patterns rather than sharp, clearly enriched peaks. On viruses, peak calling is often difficult to achieve with these marks, making it difficult to distinguish enriched regions from noisy and possibly under sampled data. While the quality of repressive histone ChIP-seq experiments is affected by several experimental parameters including sonication efficiency and sequencing depth, reaching ideal experimental parameters and comparable data quality across experiments is often difficult, costly, or even impossible, resulting in low sensitivity and specificity of measurements (Jung et al., 2014). Importantly, conducting ChIP-qPCR with primers specific to several HHV-6A genomic regions confirms H3K9me3 and H3K27me3 enrichment, albeit at lower levels than cellular regions, further suggesting that these repressive histone modifications are a mechanism regulating HHV-6A latency. Interestingly, HSV or VZV infection also results in the deposition of nucleosomes carrying H3K9me3 along the viral genome (Silva et al., 2008; Kwiatkowski et al., 2009; Liang et al., 2009), and HSV-1 reactivation from latency was blocked by inhibiting the H3K9me3 histone demethylase LSD1 (Liang et al., 2009). H3K9me3 was also enriched on the latent gammaherpesvirus EBV genome, whereas relatively low levels of H3K27me3 were found (Day et al., 2007; Tempera and Lieberman, 2010). In contrast, Cliffe et al. (2009) identified H3K27me3 as the most enriched histone mark on the latent HSV-1 genome. For the HHV-6A genome, both H3K27me3 and H3K9me3 exhibit similar patterns of enrichment, with the exception of the increased H3K27me3 signal in the viral direct repeat regions. Although this is an interesting outcome, the biological relevance of this observation currently remains unknown.

CONCLUSIONS

This study provides an unbiased integrative genomics approach toward uncovering the chromatin profile in patient-derived iciHHV-6 and experimentally infected 293-HHV-6A cell lines. Our results demonstrate that chromosomally integrated HHV-6A is completely transcriptionally silent, resides in a heterochromatic state, and is associated with H3K9me3 and H3K27me3 repressive histone modifications. Although we were unable to reactivate HHV-6A in the current study, it can be speculated that HHV-6A reactivation would alter the transcriptional state and that nucleosome occupancy would decrease across active regions of the viral genome. The lack of detectable viral associated transcripts and miRNAs in our analysis suggests that the mechanism underlying HHV-6A latency may differ significantly from those observed with other herpesviruses, e.g., HSV-1. Taken together, our data highlight how histone modifications and chromatin condensation play an important role in the control of the integrated HHV-6A genome and represent the baseline for further analysis to uncover epigenetic state during integration and reactivation.

DATA AVAILABILITY

The datasets generated and analyzed for this study can be found in the NCBI short read archive under reference number SRA#GSE121987.

AUTHOR CONTRIBUTIONS

BK and SF designed and supervised the study and acquired funding. AS, SS, and DG performed ChIP-seq experiments.

AS performed RNA-seq and MNase-seq experiments. CZ performed cell culture, qPCR, FISH, and flow cytometry experiments. AS, MM, JB, and SF performed the analysis of the sequencing data. DW, CZ, GM, AG, ID, and LF generated and provided cells. AS and CZ wrote the manuscript. AS, CZ, BK, SF, LF, and DW revised the manuscript.

FUNDING

This research was supported by the NIH R21AI121528 and European Research Council (ERC) grant number Stg 677673.

ACKNOWLEDGMENTS

We are grateful to Dr. Zhao Lai from the Genome Sequencing Facility at the University of Texas Health Science Center, San Antonio, TX, and Scott Tighe from the Vermont Integrative Genomics Resource for excellent technical services.

SUPPLEMENTARY MATERIAL

The Supplementary Material for this article can be found online at: https://www.frontiersin.org/articles/10.3389/fmicb.2019.01408/full#supplementary-material

REFERENCES

Ablashi, D., Agut, H., Alvarez-Lafuente, R., Clark, D. A., Dewhurst, S., DiLuca, D., et al. (2014). Classification of HHV-6A and HHV-6B as distinct viruses. *Arch. Virol.* 159, 863–870. doi: 10.1007/s00705-013-1902-5

Adams, M. J., and Carstens, E. B. (2012). Ratification vote on taxonomic proposals to the International Committee on Taxonomy of Viruses. *Arch. Virol.* 157, 1411–1422. doi: 10.1007/s00705-012-1299-6

Anders, S., Pyl, P. T., and Huber, W. (2015). HTSeq—a Python framework to work with high-throughput sequencing data. *Bioinformatics* 31, 166–169. doi: 10.1093/bioinformatics/btu638

Arbuckle, J. H., Medveczky, M. M., Luka, J., Hadley, S. H., Luegmayr, A., Ablashi, D., et al. (2010). The latent human herpesvirus-6A genome specifically integrates in telomeres of human chromosomes in vivo and in vitro. *Proc. Natl. Acad. Sci. USA* 107, 5563–5568. doi: 10.1073/pnas.0913586107

Arbuckle, J. H., Pantry, S. N., Medveczky, M. M., Prichett, J., Loomis, K. S., Ablashi, D., et al. (2013). Mapping the telomere integrated genome of human herpesvirus 6A and 6B. *Virology* 442, 3–11. doi: 10.1016/j.virol.2013.03.030

Berger, S. L. (2007). The complex language of chromatin regulation during transcription. *Nature* 447, 407–412. doi: 10.1038/nature05915

Bloom, D. C., Giordani, N. V., and Kwiatkowski, D. L. (2010). Epigenetic regulation of latent HSV-1 gene expression. *Biochim. Biophys. Acta* 1799, 246–256. doi: 10.1016/j.bbagrm.2009.12.001

Buenrostro, J. D., Giresi, P. G., Zaba, L. C., Chang, H. Y., and Greenleaf, W. J. (2013). Transposition of native chromatin for fast and sensitive epigenomic profiling of open chromatin, DNA-binding proteins and nucleosome position. *Nat. Methods* 10, 1213–1218. doi: 10.1038/nmeth.2688

Caselli, E., and Di Luca, D. (2007). Molecular biology and clinical associations of Roseoloviruses human herpesvirus 6 and human herpesvirus 7. *New Microbiol.* 30, 173–187. https://www.ncbi.nlm.nih.gov/pubmed/17802896

Chen, K., Xi, Y., Pan, X., Li, Z., Kaestner, K., Tyler, J., et al. (2013). DANPOS: dynamic analysis of nucleosome position and occupancy by sequencing. *Genome Res.* 23, 341–351. doi: 10.1101/gr.142067.112

Cheng, S., Caviness, K., Buehler, J., Smithey, M., Nikolich-Žugich, J., and Goodrum, F. (2017). Transcriptome-wide characterization of human cytomegalovirus in natural infection and experimental latency. *Proc. Natl. Acad. Sci. USA* 114, E10586–E10595. doi: 10.1073/pnas.1710522114

Cliffe, A. R., Garber, D. A., and Knipe, D. M. (2009). Transcription of the herpes simplex virus latency-associated transcript promotes the formation of facultative heterochromatin on lytic promoters. *J. Virol.* 83, 8182–8190. doi: 10.1128/JVI.00712-09

Collins-McMillen, D., and Goodrum, F. D. (2017). The loss of binary: pushing the herpesvirus latency paradigm. *Curr. Clin. Microbiol. Rep.* 4, 124–131. doi: 10.1007/s40588-017-0072-8

Cubiles, M. D., Barroso, S., Vaquero-Sedas, M. I., Enguix, A., Aguilera, A., and Vega-Palas, M. A. (2018). Epigenetic features of human telomeres. *Nucleic Acids Res.* 46, 2347–2355. doi: 10.1093/nar/gky006

Cui, K., and Zhao, K. (2012). "Genome-wide approaches to determining nucleosome occupancy in metazoans using MNase-Seq" in *Chromatin remodeling*. ed. R. Morse (Totowa, NJ: Humana Press), 413–419.

Cullen, B. R. (2011). Herpesvirus microRNAs: phenotypes and functions. *Curr. Opin. Virol.* 1, 211–215. doi: 10.1016/j.coviro.2011.04.003

Day, L., Chau, C. M., Nebozhyn, M., Rennekamp, A. J., Showe, M., and Lieberman, P. M. (2007). Chromatin profiling of Epstein-Barr virus latency control region. *J. Virol.* 81, 6389–6401. doi: 10.1128/JVI.02172-06

De Bolle, L., Naesens, L., and De Clercq, E. (2005). Update on human herpesvirus 6 biology, clinical features, and therapy. *Clin. Microbiol. Rev.* 18, 217–245. doi: 10.1128/CMR.18.1.217-245.2005

Depledge, D. P., Ouwendijk, W. J., Sadaoka, T., Braspenning, S. E., Mori, Y., Cohrs, R. J., et al. (2018). A spliced latency-associated VZV transcript maps antisense to the viral transactivator gene 61. *Nat. Commun.* 9:1167. doi: 10.1038/s41467-018-03569-2

Deshmane, S. L., and Fraser, N. W. (1989). During latency, herpes simplex virus type 1 DNA is associated with nucleosomes in a chromatin structure. *J. Virol.* 63, 943–947

du Chéné, I., Basyuk, E., Lin, Y. L., Triboulet, R., Knezevich, A., Chable-Bessia, C., et al. (2007). Suv39H1 and HP1γ are responsible for chromatin-mediated HIV-1 transcriptional silencing and post-integration latency. *EMBO J.* 26, 424–435. doi: 10.1038/sj.emboj.7601517

Dyson, P. J., and Farrell, P. J. (1985). Chromatin structure of Epstein-Barr virus. *J. Gen. Virol.* 66, 1931–1940. doi: 10.1099/0022-1317-66-9-1931

Endo, A., Watanabe, K., Ohye, T., Suzuki, K., Matsubara, T., Shimizu, N., et al. (2014). Molecular and virological evidence of viral activation from chromosomally integrated human herpesvirus 6A in a patient with X-linked severe combined immunodeficiency. *Clin. Infect. Dis.* 59, 545–548. doi: 10.1093/cid/ciu323

Friedman, J., Cho, W. K., Chu, C. K., Keedy, K. S., Archin, N. M., Margolis, D. M., et al. (2011). Epigenetic silencing of HIV-1 by the histone H3 lysine 27 methyltransferase enhancer of Zeste 2. *J. Virol.* 85, 9078–9089. doi: 10.1128/JVI.00836-11

Goodrum, F. (2016). Human cytomegalovirus latency: approaching the Gordian Knot. *Annu. Rev. Virol.* 3, 333–357. doi: 10.1146/annurev-virology-110615-042422

Gravel, A., Dubuc, I., Morissette, G., Sedlak, R. H., Jerome, K. R., and Flamand, L. (2015). Inherited chromosomally integrated human herpesvirus 6 as a predisposing risk factor for the development of angina pectoris. *Proc. Natl. Acad. Sci. USA* 112, 8058–8063. doi: 10.1073/pnas.1502741112

Gravel, A., Dubuc, I., Wallaschek, N., Gilbert-Girard, S., Collin, V., Hall-Sedlak, R., et al. (2017). Cell culture systems to study Human herpesvirus 6A/B chromosomal integration. *J. Virol.* 91, e00437–e00417. doi: 10.1128/JVI.00437-17

Gravel, A., Hall, C. B., and Flamand, L. (2013). Sequence analysis of transplacentally acquired human herpesvirus 6 DNA is consistent with transmission of a chromosomally integrated reactivated virus. *J. Infect. Dis.* 207, 1585–1589. doi: 10.1093/infdis/jit060

Grinde, B. (2013). Herpesviruses: latency and reactivation - viral strategies and host response. *J. Oral Microbiol.* 5:22766. doi: 10.3402/jom.v5i0.22766

Hill, J. A., Magaret, A. S., Hall-Sedlak, R., Mikhaylova, A., Huang, M. L., Sandmaier, B. M., et al. (2017). Outcomes of hematopoietic cell transplantation using donors or recipients with inherited chromosomally integrated HHV-6. *Blood* 130, 1062–1069. doi: 10.1182/blood-2017-03-775759

Hill, J. A., and Zerr, D. M. (2014). Roseoloviruses in transplant recipients: clinical consequences and prospects for treatment and prevention trials. *Curr. Opin. Virol.* 9, 53–60. doi: 10.1016/j.coviro.2014.09.006

Ichikawa, Y., Nishimura, Y., Kurumizaka, H., and Shimizu, M. (2015). Nucleosome organization and chromatin dynamics in telomeres. *Biomol. Concepts* 6, 67–75. doi: 10.1515/bmc-2014-0035

Jiang, C., and Pugh, B. F. (2009). Nucleosome positioning and gene regulation: advances through genomics. *Nat. Rev. Genet.* 10, 161–172. doi: 10.1038/nrg2522

Jordan, A., Bisgrove, D., and Verdin, E. (2003). HIV reproducibly establishes a latent infection after acute infection of T cells in vitro. *EMBO J.* 22, 1868–1877. doi: 10.1093/emboj/cdg188

Jung, Y. L., Luquette, L. J., Ho, J. W., Ferrari, F., Tolstorukov, M., Minoda, A., et al. (2014). Impact of sequencing depth in ChIP-seq experiments. *Nucleic Acids Res.* 42:e74. doi: 10.1093/nar/gku178

Kaufer, B. B. (2013). "Detection of integrated herpesvirus genomes by fluorescence in situ hybridization (FISH)" in *Virus-host interactions*. eds. S. Bailer, and D. Lieber (Totowa, NJ: Humana Press), 141–152.

Kaufer, B. B., and Flamand, L. (2014). Chromosomally integrated HHV-6: impact on virus, cell and organismal biology. *Curr. Opin. Virol.* 9, 111–118. doi: 10.1016/j.coviro.2014.09.010

Kaufer, B. B., Jarosinski, K. W., and Osterrieder, N. (2011). Herpesvirus telomeric repeats facilitate genomic integration into host telomeres and mobilization of viral DNA during reactivation. *J. Exp. Med.* 208, 605–615. doi: 10.1084/jem.20101402

Kinchington, P. R., St Leger, A. J., Guedon, J. M. G., and Hendricks, R. L. (2012). Herpes simplex virus and varicella zoster virus, the house guests who never leave. *Herpesviridae* 3:5. doi: 10.1186/2042-4280-3-5

Knipe, D. M., and Cliffe, A. (2008). Chromatin control of herpes simplex virus lytic and latent infection. *Nat. Rev. Microbiol.* 6, 211–221. doi: 10.1038/nrmicro1794

Kondo, K., Sashihara, J., Shimada, K., Takemoto, M., Amo, K., Miyagawa, H., et al. (2003). Recognition of a novel stage of betaherpesvirus latency in human herpesvirus 6. *J. Virol.* 77, 2258–2264. doi: 10.1128/JVI.77.3.2258-2264.2003

Kondo, K., Shimada, K., Sashihara, J., Tanaka-Taya, K., and Yamanishi, K. (2002). Identification of human herpesvirus 6 latency-associated transcripts. *J. Virol.* 76, 4145–4151. doi: 10.1128/JVI.76.8.4145-4151.2002

Kubat, N. J., Tran, R. K., McAnany, P., and Bloom, D. C. (2004). Specific histone tail modification and not DNA methylation is a determinant of herpes simplex virus type 1 latent gene expression. *J. Virol.* 78, 1139–1149. doi: 10.1128/JVI.78.3.1139-1149.2004

Kwiatkowski, D. L., Thompson, H. W., and Bloom, D. C. (2009). The polycomb group protein Bmi1 binds to the herpes simplex virus 1 latent genome and maintains repressive histone marks during latency. *J. Virol.* 83, 8173–8181. doi: 10.1128/JVI.00686-09

Langmead, B., and Salzberg, S. L. (2012). Fast gapped-read alignment with Bowtie 2. *Nat. Methods* 9, 357–359. doi: 10.1038/nmeth.1923

Li, B., Carey, M., and Workman, J. L. (2007). The role of chromatin during transcription. *Cell* 128, 707–719. doi: 10.1016/j.cell.2007.01.015

Li, H., Handsaker, B., Wysoker, A., Fennell, T., Ruan, J., Homer, N., et al. (2009). The sequence alignment/map format and SAMtools. *Bioinformatics* 25, 2078–2079. doi: 10.1093/bioinformatics/btp352

Liang, Y., Vogel, J. L., Narayanan, A., Peng, H., and Kristie, T. M. (2009). Inhibition of the histone demethylase LSD1 blocks alpha-herpesvirus lytic replication and reactivation from latency. *Nat. Med.* 15, 1312–1317. doi: 10.1038/nm.2051

Liu, X., Yuan, J., Wu, A. W., McGonagill, P. W., Galle, C. S., and Meier, J. L. (2010). Phorbol ester-induced human cytomegalovirus major immediate-early (MIE) enhancer activation through PKC-delta, CREB, and NF-kappaB desilences MIE gene expression in quiescently infected human pluripotent NTera2 cells. *J. Virol.* 84, 8495–8508. doi: 10.1128/JVI.00416-10

Love, M. I., Huber, W., and Anders, S. (2014). Moderated estimation of fold change and dispersion for RNA-seq data with DESeq2. *Genome Biol.* 15:550. doi: 10.1186/s13059-014-0550-8

Lusso, P., Malnati, M., De Maria, A., Balotta, C., Derocco, S. E., Markham, P. D., et al. (1991). Productive infection of CD4+ and CD8+ mature human T cell populations and clones by human herpesvirus 6. Transcriptional down-regulation of CD3. *J. Immunol.* 147, 685–691.

Maehara, K., and Ohkawa, Y. (2016). Exploration of nucleosome positioning patterns in transcription factor function. *Sci. Rep.* 6:19620. doi: 10.1038/srep19620

Mieczkowski, J., Cook, A., Bowman, S. K., Mueller, B., Alver, B. H., Kundu, S., et al. (2016). MNase titration reveals differences between nucleosome occupancy and chromatin accessibility. *Nat. Commun.* 7:11485. doi: 10.1038/ncomms11485

Moquin, S. A., Thomas, S., Whalen, S., Warburton, A., Fernandez, S. G., McBride, A. A., et al. (2018). The Epstein-Barr virus episome maneuvers between nuclear chromatin compartments during reactivation. *J. Virol.* 92, e01413–e01417. doi: 10.1128/JVI.01413-17

Moreau, M. E., Bawolak, M. T., Morissette, G., Adam, A., and Marceau, F. (2007). Role of nuclear factor-κB and protein kinase C signaling in the expression of the kinin B1 receptor in human vascular smooth muscle cells. *Mol. Pharmacol.* 71, 949–956. doi: 10.1124/mol.106.030684

Mueller, B., Mieczkowski, J., Kundu, S., Wang, P., Sadreyev, R., Tolstorukov, M. Y., et al. (2017). Widespread changes in nucleosome accessibility without changes in nucleosome occupancy during a rapid transcriptional induction. *Genes Dev.* 31, 451–462. doi: 10.1101/gad.293118.116

Murphy, E., Vaníček, J., Robins, H., Shenk, T., and Levine, A. J. (2008). Suppression of immediate-early viral gene expression by herpesvirus-coded microRNAs: implications for latency. *Proc. Natl. Acad. Sci. USA* 105, 5453–5458. doi: 10.1073/pnas.0711910105

Nicol, J. W., Helt, G. A., Blanchard, Jr., S. G., Raja, A., and Loraine, A. E. (2009). The Integrated Genome Browser: free software for distribution and exploration of genome-scale datasets. *Bioinformatics* 25, 2730–2731. doi: 10.1093/bioinformatics/btp472

Nukui, M., Mori, Y., and Murphy, E. A. (2015). A human herpesvirus 6A-encoded microRNA: role in viral lytic replication. *J. Virol.* 89, 2615–2627. doi: 10.1128/JVI.02007-14

O'Geen, H., Frietze, S., and Farnham, P. J. (2010). "Using ChIP-seq technology to identify targets of zinc finger transcription factors" in *Engineered zinc finger proteins: methods and protocols*. eds. J. Mackay, and D. Segal (Totowa, NJ: Humana Press), 437–455.

O'Sullivan, R. J., Kubicek, S., Schreiber, S. L., and Karlseder, J. (2010). Reduced histone biosynthesis and chromatin changes arising from a damage signal at telomeres. *Nat. Struct. Mol. Biol.* 17, 1218–1225. doi: 10.1038/nsmb.1897

Pajoro, A., Muiño, J. M., Angenent, G. C., and Kaufmann, K. (2018). "Profiling nucleosome occupancy by MNase-seq: experimental protocol and computational analysis" in *Plant chromatin dynamics*. Methods in Molecular Biology. eds. M. Bemer, and C. Baroux, Vol. 1675 (New York, NY: Humana Press).

Pellett, P. E., Ablashi, D. V., Ambros, P. F., Agut, H., Caserta, M. T., Descamps, V., et al. (2012). Chromosomally integrated human herpesvirus 6: questions and answers. *Rev. Med. Virol.* 22, 144–155. doi: 10.1002/rmv.715

Piedade, D., and Azevedo-Pereira, J. M. (2016). The role of microRNAs in the pathogenesis of herpesvirus infection. *Viruses* 8:156. doi: 10.3390/v8060156

Politikos, I., McMasters, M., Bryke, C., Avigan, D., and Boussiotis, V. A. (2018). Possible reactivation of chromosomally integrated human herpesvirus 6 after treatment with histone deacetylase inhibitor. *Blood Adv.* 2, 1367–1370. doi: 10.1182/bloodadvances.2018015982

Prusty, B. K., Gulve, N., Chowdhury, S. R., Schuster, M., Strempel, S., Descamps, V., et al. (2018). HHV-6 encoded small non-coding RNAs define an intermediate and early stage in viral reactivation. *NPJ Genom. Med.* 3:25. doi: 10.1038/s41525-018-0064-5

Rahman, R., Gautam, A., Bethune, J., Sattar, A., Fiosins, M., Magruder, D. S., et al. (2018). Oasis 2: improved online analysis of small RNA-seq data. *BMC Bioinform.* 19:54. doi: 10.1186/s12859-018-2047-z

Ramírez, F., Ryan, D. P., Grüning, B., Bhardwaj, V., Kilpert, F., Richter, A. S., et al. (2016). deepTools2: a next generation web server for deep-sequencing data analysis. *Nucleic Acids Res.* 44, W160–W165. doi: 10.1093/nar/gkw257

Readhead, B., Haure-Mirande, J. V., Funk, C. C., Richards, M. A., Shannon, P., Haroutunian, V., et al. (2018). Multiscale analysis of independent alzheimer's cohorts finds disruption of molecular, genetic, and clinical networks by human herpesvirus. *Neuron* 99, 64–82.e7. doi: 10.1016/j.neuron.2018.05.023

Rens, W., Fu, B., O'Brien, P. C., and Ferguson-Smith, M. (2006). Cross-species chromosome painting. *Nat. Protoc.* 1, 783–790. doi: 10.1038/nprot.2006.91

Rotola, A., Ravaioli, T., Gonelli, A., Dewhurst, S., Cassai, E., and Di Luca, D. (1998). U94 of human herpesvirus 6 is expressed in latently infected peripheral

blood mononuclear cells and blocks viral gene expression in transformed lymphocytes in culture. *Proc. Natl. Acad. Sci. USA* 95, 13911–13916. doi: 10.1073/pnas.95.23.13911

Salahuddin, S. Z., Ablashi, D. V., Markham, P. D., Josephs, S. F., Sturzenegger, S., Kaplan, M., et al. (1986). Isolation of a new virus, HBLV, in patients with lymphoproliferative disorders. *Science* 234, 596–601. doi: 10.1126/science.2876520

Shaw, J. E. (1985). The circular intracellular form of Epstein-Barr virus DNA is amplified by the virus-associated DNA polymerase. *J. Virol.* 53, 1012–1015.

Shnayder, M., Nachshon, A., Krishna, B., Poole, E., Boshkov, A., Binyamin, A., et al. (2018). Defining the transcriptional landscape during cytomegalovirus latency with single-cell RNA sequencing. *MBio* 9, e00013–e00018. doi: 10.1128/mBio.00013-18

Silva, L., Cliffe, A., Chang, L., and Knipe, D. M. (2008). Role for A-type lamins in herpesviral DNA targeting and heterochromatin modulation. *PLoS Pathog.* 4:e1000071. doi: 10.1371/journal.ppat.1000071

Skalsky, R. L., and Cullen, B. R. (2010). Viruses, microRNAs, and host interactions. *Annu. Rev. Microbiol.* 64, 123–141. doi: 10.1146/annurev.micro.112408.134243

Strenger, V., Caselli, E., Lautenschlager, I., Schwinger, W., Aberle, S. W., Loginov, R., et al. (2014). Detection of HHV-6-specific mRNA and antigens in PBMCs of individuals with chromosomally integrated HHV-6 (ciHHV-6). *Clin. Microbiol. Infect.* 20, 1027–1032. doi: 10.1111/1469-0691.12639

Takahashi, K., Sonoda, S., Higashi, K., Kondo, T., Takahashi, H., Takahashi, M., et al. (1989). Predominant CD4 T-lymphocyte tropism of human herpesvirus 6-related virus. *J. Virol.* 63, 3161–3163.

Tang, H., Kawabata, A., Yoshida, M., Oyaizu, H., Maeki, T., Yamanishi, K., et al. (2010). Human herpesvirus 6 encoded glycoprotein Q1 gene is essential for virus growth. *Virology* 407, 360–367. doi: 10.1016/j.virol.2010.08.018

Tempera, I., and Lieberman, P. M. (2010). Chromatin organization of gammaherpesvirus latent genomes. *Biochim. Biophys. Acta* 1799, 236–245. doi: 10.1016/j.bbagrm.2009.10.004

Trapnell, C., Pachter, L., and Salzberg, S. L. (2009). TopHat: discovering splice junctions with RNA-Seq. *Bioinformatics* 25, 1105–1111. doi: 10.1093/bioinformatics/btp120

Tuddenham, L., Jung, J. S., Chane-Woon-Ming, B., Dölken, L., and Pfeffer, S. (2012). Small RNA deep sequencing identifies microRNAs and other small noncoding RNAs from human herpesvirus 6B. *J. Virol.* 86, 1638–1649. doi: 10.1128/JVI.05911-11

Umbach, J. L., Nagel, M. A., Cohrs, R. J., Gilden, D. H., and Cullen, B. R. (2009). Analysis of human alphaherpesvirus microRNA expression in latently infected human trigeminal ganglia. *J. Virol.* 83, 10677–10683. doi: 10.1128/JVI.01185-09

Vinnard, C., Barton, T., Jerud, E., and Blumberg, E. (2009). A report of human herpesvirus 6-associated encephalitis in a solid organ transplant recipient and a review of previously published cases. *Liver Transpl.* 15, 1242–1246. doi: 10.1002/lt.21816

Wallaschek, N., Sanyal, A., Pirzer, F., Gravel, A., Mori, Y., Flamand, L., et al. (2016). The telomeric repeats of human herpesvirus 6A (HHV-6A) are required for efficient virus integration. *PLoS Pathog.* 12:e1005666. doi: 10.1371/journal.ppat.1005666

Wang, Q. Y., Zhou, C., Johnson, K. E., Colgrove, R. C., Coen, D. M., and Knipe, D. M. (2005). Herpesviral latency-associated transcript gene promotes assembly of heterochromatin on viral lytic-gene promoters in latent infection. *Proc. Natl. Acad. Sci. USA* 102, 16055–16059. doi: 10.1073/pnas.0505850102

Wight, D. J., Wallaschek, N., Sanyal, A., Weller, S. K., Flamand, L., and Kaufer, B. B. (2018). Viral Proteins U41 and U70 of human herpesvirus 6A are dispensable for telomere integration. *Viruses* 10:656. doi: 10.3390/v10110656

Winestone, L. E., Punn, R., Tamaresis, J. S., Buckingham, J., Pinsky, B. A., Waggoner, J. J., et al. (2018). High human herpesvirus 6 viral load in pediatric allogeneic hematopoietic stem cell transplant patients is associated with detection in end organs and high mortality. *Pediatr. Transplant.* 22:e13084. doi: 10.1111/petr.13084

Yamanishi, K., Okuno, T., Shiraki, K., Takahashi, M., Kondo, T., Asano, Y., et al. (1988). Identification of human herpesvirus-6 as a causal agent for exanthem subitum. *Lancet* 1, 1065–1067. doi: 10.1016/S0140-6736(88)91893-4

Zerr, D. M., Meier, A. S., Selke, S. S., Frenkel, L. M., Huang, M.-L., Wald, A., et al. (2005). A population-based study of primary human herpesvirus 6 infection. *N. Engl. J. Med.* 352, 768–776. doi: 10.1056/NEJMoa042207

Zhang, Y., Liu, T., Meyer, C. A., Eeckhoute, J., Johnson, D. S., Bernstein, B. E., et al. (2008). Model-based analysis of ChIP-Seq (MACS). *Genome Biol.* 9:R137. doi: 10.1186/gb-2008-9-9-r137

Conflict of Interest Statement: The authors declare that the research was conducted in the absence of any commercial or financial relationships that could be construed as a potential conflict of interest.

frontiers in Microbiology

ORIGINAL RESEARCH
published: 24 July 2019
doi: 10.3389/fmicb.2019.01624

Targeted Promoter Replacement Reveals That Herpes Simplex Virus Type-1 and 2 Specific VP16 Promoters Direct Distinct Rates of Entry Into the Lytic Program in Sensory Neurons *in vivo*

Richard L. Thompson[1]* *and Nancy M. Sawtell*[2]*

[1]Department of Molecular Genetics, Biochemistry, and Microbiology, University of Cincinnati, Cincinnati, OH, United States,
[2]Department of Pediatrics, Division of Infectious Diseases, Cincinnati Children's Hospital Medical Center, Cincinnati, OH, United States

OPEN ACCESS

Edited by:
Randall J. Cohrs,
University of Colorado Denver,
United States

Reviewed by:
David Bloom,
University of Florida, United States
Phil Krause,
United States Food and
Drug Administration,
United States

***Correspondence:**
Richard L. Thompson
richard.thompson@uc.edu
Nancy M. Sawtell
nancy.sawtell@cchmc.org

Specialty section:
This article was submitted to
Virology,
a section of the journal
Frontiers in Microbiology

Received: 11 February 2019
Accepted: 01 July 2019
Published: 24 July 2019

Citation:
Thompson RL and Sawtell NM (2019)
Targeted Promoter Replacement
Reveals That Herpes Simplex Virus
Type-1 and 2 Specific VP16
Promoters Direct Distinct Rates of
Entry Into the Lytic Program in
Sensory Neurons in vivo.
Front. Microbiol. 10:1624.
doi: 10.3389/fmicb.2019.01624

Infection and life-long residence in the human nervous system is central to herpes simplex virus (HSV) pathogenesis. Access is gained through innervating axonal projections of sensory neurons. This distinct mode of entry separates the viral genome from tegument proteins, including the potent transactivator of viral IE genes, VP16. This, in turn, promotes a balance between lytic and latent infection which underlies the ability of the virus to invade, disseminate, and set up a large reservoir of latent infections. In the mouse ocular model, TG neurons marked as either "latent" or "lytic" at 48 h postinfection indicated that these programs were selected early and were considered distinct and mutually exclusive. More recently, a temporal analysis of viral program selection revealed a default latent-like state that begins at ~18 h postinfection and in individual neurons, precedes entry into the viral lytic cycle. Studies using refined viral mutants demonstrated that transition out of this latent program depended upon the transactivation function of VP16. Pursuit of the apparent incongruity between the established leaky-late kinetics of VP16 expression with a "preimmediate-early" function led to the discovery of an unrecognized regulatory feature of the HSV-1 VP16 promoter near/downstream of its TATA box. Among three potential sites identified was a putative Egr-1/Sp1 site. Here, we report that a refined mutation of this site, while having no impact on replication in cultured cells or cornea, resulted in ~100-fold reduction in lytic infection in TG *in vivo*. Notably, the HSV-2 VP16 promoter has 13 direct tandem-repeats *upstream* of its TATA box forming multiple potential overlapping Egr-1/Sp1 sites. Thus, despite different structures, these promoters might share function in directing the preimmediate-early VP16 protein expression. To test this, the HSV-1 VP16 promoter/5′UTR was replaced by the HSV-2 VP16 promoter/5′UTR in the HSV-1 backbone. Compared to the genomically repaired isolate, the HSV-2 VP16 promoter/5′UTR (1) accelerated the transition into the lytic cycle, and enhanced (2) virulence, and (3) entry into the lytic cycle following a reactivation stressor. These gain-of-function phenotypes support the hypothesis that the VP16 promoter regulates the latent/lytic boundary in neurons and that the HSV-1 and HSV-2 promoter/5′UTRs encode distinct thresholds for this transition.

Keywords: herpes simplex virus, latent program, sensory neuron, HSV-1 and HSV-2 VP16 promoter, regulation, corneal infection model, trigeminal ganglion, serotype

INTRODUCTION

The US and global disease burden resulting from herpes simplex virus (HSV-1 and -2) infection includes life threatening encephalitis, blindness, devastating neonatal infection, increased risk of HIV infection, neurological disease, and a list of other disease outcomes. Life-long latent infections in sensory neurons and periodic reactivation of latent virus are central to the maintenance and propagation of these viruses, currently a worldwide endemic infection. Practical treatments to prevent transmission or eliminate the latent reservoir remain unmet goals. Greater insights into the regulatory mechanisms controlling latent and lytic program selection in the nervous system are needed to facilitate progress. Virion protein 16 (VP16) is a multifunctional viral protein expressed with leaky late kinetics and essential for virion morphogenesis. VP16, in complex with host proteins, is also a potent transactivator of the 5 HSV Immediate Early genes. In cultured cells, efficient infection by a single HSV-1 virion requires the VP16 transactivation function which is transported into the cell as part of the virion tegument (Campbell et al., 1984; Kristie and Roizman, 1987; Ace et al., 1988; Stern et al., 1989).

Most often, infection of the host with HSV starts at an external epithelial cell surface where viral replication leads to access and uptake into the nervous system *via* axons projecting from the neuronal cell body in the sensory ganglion. In the case of the sensory neuron, this single axon bifurcates in the ganglion near the cell body and projects to the CNS. Early studies in cultured neurons infected *via* axons did offer strong support for the idea that latency might be favored in neurons because the tegument protein VP16 is not efficiently transported to neuronal nuclei to initiate lytic infection (Miranda-Saksena et al., 2000; Diefenbach et al., 2008). This important finding was supported and extended by Hafezi et al. (2012) who showed that infection of cultured neurons *via* axons led to quiescent infection whereas infection on the cell body led to lytic infection, supporting early *in vivo* studies (Ecob-Prince et al., 1993). More recently, the addition of light particles containing pseudorabies virus tegument proteins disrupted quiescent infection of cultured neurons infected *via* axons, again implicating the presence or absence of tegument proteins in the switch between quiescent and lytic infection of neurons (Koyuncu et al., 2017).

In vivo, evidence that TG neurons marked as either "latent" or "lytic" as soon as 48 h post infection indicated that the latent or lytic program decision was being made during the acute stage of infection (Margolis et al., 1992; Sawtell and Thompson, 1992a,b; Lachmann and Efstathiou, 1997). This led to the hypothesis that the choice between latent or lytic infection occurred early during infection and was mutually exclusive and correlated with neuronal subsets (Margolis et al., 1992, 2007; Sawtell and Thompson, 1992a,b; Lachmann and Efstathiou, 1997).

More recently, a temporal analysis of program selection in TG neurons revealed that a characteristic feature of infection of the TG neuron from the periphery is an unexpected default latent state that occurs early in individual TG neurons. This default latency begins as early as 18 h post infection and precedes all lytic gene transcription by 12–14 h. Importantly, studies using a series of refined viral mutants demonstrated that the transition out of this latent program is dependent on VP16 transactivation function (Thompson et al., 2009; Sawtell and Thompson, 2016a,b). Further examination of the apparent incongruity between the established leaky late kinetics of VP16 expression with a pre-immediate early (preIE) function led to the discovery of previously unrecognized regulatory features of the VP16 promoter mapping near and downstream of the VP16 gene TATA box which directs *de novo* expression of VP16 (Sawtell and Thompson, 2016a,b). Thus *in vivo*, evidence is building that VP16 can function as a potent transactivator of viral IE genes in the sensory neuron and the regulation of this protein, either by limiting its transport into the neuron, or through its promoter regulating its expression as a pre-immediate early gene, is central in controlling the latent to lytic transition in neurons (Miranda-Saksena et al., 2000; Diefenbach et al., 2008; Thompson et al., 2009; Antinone and Smith, 2010; Thompson and Sawtell, 2010; Roizman et al., 2011; Sawtell et al., 2011; Aggarwal et al., 2012; Hafezi et al., 2012; Kim et al., 2012; Smith, 2012; Sawtell and Thompson, 2016a,b). Significantly, the regulation of expression of preIE VP16 transactivation function early during acute infection of TG is linked to downstream pathogenic outcomes, emphasizing the biological significance of this regulatory strategy.

How this context dependent expression strategy of VP16 is designed is not yet completely understood. Mutation of three putative transcription factor (TF) binding sequences near and downstream of the VP16 gene TATA box greatly decreases lytic cycle entry in TG neurons infected from the eye (Sawtell and Thompson, 2016a,b). Among these is a canonical overlapping Egr-1/Sp1 site. It is likely that the regulation of this gene in neurons *in vivo* is quite complex as has been seen in other systems. We refer to this as an "Egr-1/Sp1" site, but it should be recognized that many TFs could potentially bind to this region. In addition, interpretation of mutations in the 5′UTR is complicated because this region can influence transcriptional regulation and also protein production through additional mechanisms (Leppek et al., 2018). Indeed, analysis of how gene promoters function in the context of a living animal has proven to be one of the more intractable problems in molecular genetics. Of interest, the sequence of the HSV-2 VP16 promoter/5′UTR has a strikingly different architecture compared to that of HSV-1 and the 5′UTR Egr-1/Sp1 site is not apparent. There are, however, 13 direct tandem repeats of a sequence that can form multiple strong putative Egr-1/Sp1 sites upstream of the HSV-2 TATA box. The presence of these similar direct tandem repeats suggested that despite their very different structure, these divergent promoters may function similarly in directing *de novo* VP16 protein expression in neurons. If the 13 tandem sites do increase the transition from default latent to lytic infection in sensory neurons *in vivo*, replacing the HSV-1 VP16 promoter with the HSV-2 VP16 promoter would be expected to alter the pathobiological

properties of HSV-1 in the absence of all other HSV-2 adaptations and should be measurable. Importantly, *in vivo* phenotypic differences between the promoters could then be exploited to provide insight into key features of structure function relationship encoded in this regulatory region.

To begin to test this hypothesis, we first mutated the HSV-1 VP16 promoter disrupting only the putative Egr-1/Sp1 site within the 5′UTR. The *in vivo* phenotype of this mutant paralleled that of the triple site mutant described previously (Sawtell and Thompson, 2016a,b), establishing the importance of this sequence to the regulation of *de novo* VP16 expression. We next generated HSV-1 mutants in which the HSV-1 VP16 promoter and 5′UTR is replaced by the HSV-2 VP16 promoter and 5′UTR. All other viral promoters and all viral ORFs remain HSV type-1 in this targeted VP16 promoter replacement mutant. Compared to the genomically repaired mutant, in the context of the HSV-1 genome, the HSV-2 VP16 promoter/5′UTR (1) accelerates the transition from default latency into the lytic cycle, and enhances (2) virulence, and (3) entry into the lytic cycle following a reactivation inducing stressor by fourfold. These unusual gain of function phenotypes further support the hypothesis that the VP16 promoter regulates the latent/lytic boundary in neurons and that the HSV-1 and HSV-2 promoter/5′UTRs encode distinct thresholds for this transition.

MATERIALS AND METHODS

Ethics Statement

All procedures in mice were performed as approved by the Children's Hospital Institutional Animal Care and Use Committee (protocol# IACUC2017-0081 and were in compliance with the *Guide for the Care and Use of Laboratory Animals*. Animals were housed in American Association for Laboratory Animal Care-approved quarters.

Viral Strains/Mutants and Stock Production

An elite stock of HSV-1 strain 17syn+ (originally obtained from John H. Subak-Sharpe at the MRC Virology Unit in Glasgow, Scotland) was generated in 1980 and employed to make early passage working stocks. The wt and mutant viruses employed in this study were generated in rabbit skin cell (RSC) monolayers (RSC originally obtained from Bernard Roizman, University of Chicago) and the viral titers were determined by serial-dilution plaque assay (Thompson et al., 1983; Sawtell and Thompson, 1992a,b).

Construction of Mutated VP16 Promoters and Viral Mutants

Mutation of the Putative HSV-1 Overlapping Egr-1/Sp1 Site

Four bases in the core matrix of the canonical overlapping Egr-1/Sp1 site in the region of the 5′ UTR of the VP16 mRNA (BP 105,134 to 105,137 on the 17syn+ genome were mutated to "T" residues (the construct was purchased from Blue heron Biotec) (see **Figure 1B**). All restriction enzyme sites and base pair numbering are referred to as the corresponding positions in the published HSV-1 sequence of strain 17syn+ (McGeoch et al., 1988; Perry and McGeoch, 1988) as currently present in Genbank (JN555585). This mutation is predicted to inhibit binding of both Egr-1 and Sp1 to the site as determined with the analysis suite Cis-BP (Weirauch et al., 2014). The construct was employed to drive the firefly luciferase gene (Clontech) and was also cloned in place of the native VP16 promoter in front of the VP16 ORF, 3′UTR, and polyA+ sequences and flanked by ~500 bp of homologous sequences to facilitate recombination into the viral genome as previously detailed (Thompson et al., 2009; Sawtell and Thompson, 2016a,b). The mutation construct was recombined into a previously published mutant of strain 17syn+ modified with an insertion of a GFP gene driven by the beta actin promoter and terminated with the SV40 poly adenylation sequences (SVA+) (Thompson et al., 2009), which was employed for color selection of plaques as previously described (Thompson et al., 2009; Sawtell and Thompson, 2016a,b). Six independently derived mutants were selected, plaque purified by three rounds of limiting dilution and sequences of the insertion were confirmed by PCR followed by Sanger sequencing (Genewiz). General genomic structures were examined by RFLP analysis as previously described in detail (Sawtell and Thompson, 2014). Three mutants (named 17VP16pEgr-1/Sp1-1, 3, or 5) were characterized *in vitro* and *in vivo* as described in the text. One isolate was genomically restored to wt sequence (using the wt HSV-1 VP16 promoter +5′UTRsequences) to generate the control virus named 17VP16pEgr-1/Sp1-R. Virus plaque purification and characterization were as described above.

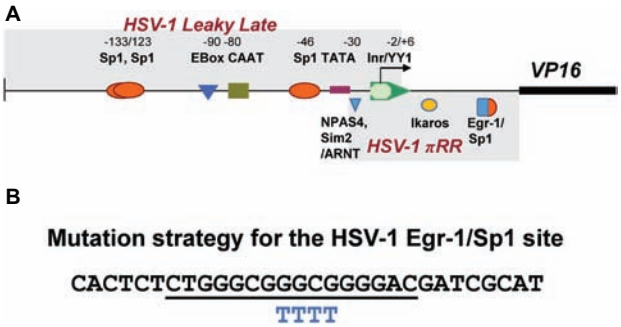

FIGURE 1 | Schematic representation of transcription factor (TF)-binding sites in HSV-1 VP16 promoter. **(A)** Shown above the line are the names of TF-binding sites identified as important for VP16 promoter strength Wagner and colleagues in transient assays (Lieu and Wagner, 2000). Below the line are high-scoring TF sites identified as potentially important for *de novo* VP16 expression (boxed and labeled as HSV-1πRR) that were simultaneously mutated resulting in failure to initiate lytic gene expression in sensory neurons *in vivo* (Sawtell and Thompson, 2016a,b). **(B)** Shown is the sequence of a 30mer oligonucleotide that contains a canonical overlapping Egr-1/Sp1 site (underlined) in the HSV-1 VP16 gene 5′UTR. Below this are shown the four bases that were changed to "T" residues to mutate the TF sites (BP 105,134–105,137).

Targeted Replacement of the HSV-1 VP16 Promoter and 5′UTR Sequences With Those of HSV-2

The HSV-1 VP16 promoter and 5′ UTR sequences (BP 105,440 to 105,110) were replaced with the HSV-2 VP16 promoter/5′UTR (BP 106,210 to 105,793) as found in Genbank Accession NC_001798 (**Figure 2A**). To help insure that all important HSV-2 VP16 regulatory sequences were included, the fragment extends 63 bp 5′ of the HSV-2 UL49 polyadenylation site (UL49 is upstream of UL48, the VP16 gene) through the HSV-2 VP16 promoter and includes all but 28 bp of the HSV-2 VP16 5′UTR, followed by the corresponding 27 bp of the HSV-1 VP16 5′UTR to preserve the HSV-1 gene Kozak consensus translation start site (Kozak, 1987). This short sequence has 67% identity in the two simplex viruses. These sequences were employed to drive firefly luciferase as above so that the relative strengths of the HSV-1 and HSV-2 regulatory regions could be compared in transient assays (see **Figure 2A**). Targeted replacement mutant viruses in which the HSV-1 VP16 regulatory sequences were replaced with these type-2 sequences were made as follows. The GFP cassette described above was place in front of the type-2 sequences and in the same orientation as the VP16 gene to provide color selection for plaques and flanked by ~500 bp of relevant HSV-1 sequences on the 5′ and 3′ ends of the construct to permit efficient recombination with viral genomic sequences. The mutagenesis construct was recombined into the mutant 17LATpLacZ [which marks the latent transcription program (Thompson et al., 2009; Sawtell and Thompson, 2016a,b)] to generate mutants 17LpLz/VP16p^2. Note that all HSV-1 viral genes including all ORFs remain intact in these mutants with the exception of exchanging the HSV-1 VP16 promoter and most of its 5′UTR with that of the HSV-2 VP16 promoter and most of its 5′UTR.

As above, all recombination crossover sites were confirmed by PCR and sequencing. The presence of the 13 tandem direct repeats of the canonical Egr-1/Sp1 site present in the type-2 promoter was confirmed by sequence and by high-resolution RFLP analysis as previously detailed (Sawtell and Thompson, 2014). Six independent derived promoter mutants were isolated and two of these (named 17LpLz/VP16p^2-5 and 6) were further characterized *in vitro* and *in vivo* as described in the text. The genome of 17LpLz/VP16p^2-5 was rescued back to wildtype (wt) to generate the control virus 17LpLz/VP16p^2-R in which the HSV-1 VP16 regulatory sequences were restored.

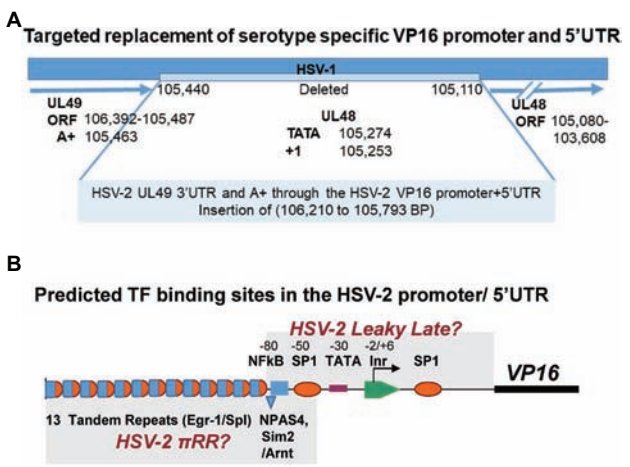

FIGURE 2 | Design of the targeted replacement of the HSV-1 VP16 promoter and 5′UTR with that of HSV-2, mutant 17LpLz/VP16p^2. **(A)** Note that the VP16 (UL48) gene runs in the opposite direction of the base pair numbers of the HSV genome in the prototypical genome arrangement. The HSV-1 promoter and UTR sequences (105,440 to 104,110 bp) were deleted and replaced with leaving the HSV-2 VP16 promoter and 5′UTR (106,210 to 105,793 bp) as detailed in Section "Materials and Methods." The VP16 ORF and 3′UTR remained entirely HSV-1 sequences. This mutant is designated 17LpLz/VP16p^2. **(B)** A schematic representation of the HSV-2 VP16 promoter and 5′UTR is shown. Putative binding sites for TFs that are thought to regulate HSV leaky late promoters (Lieu and Wagner, 2000) were identified *in silico* (see Section "Materials and Methods") and are indicated above the line. Two regions containing TF-binding sites similar to those implicated in the *de novo* synthesis of HSV-1 VP16 (Sawtell and Thompson, 2016a,b) are indicated below the line including tandem repeats of putative overlapping Egr-1/Sp1 sites and a potential NPAS4 (positive TF) or Sim2 (negative TF)/Arnt heterodimer binding site.

Luciferase Assays

Dual-Glo luciferase assays (Promega) were employed in co-transfection assays according to the manufacturers' protocols. To assay for promoter strengths, the constructs in which firefly luciferase was driven by wt or mutant VP16 promoters as well as a cytomegalovirus immediate early gene promoter (CMVIE) driven luciferase construct (Promega) as a positive control, were co-transfected with the pRL-TK renilla expression plasmid (Promega) or no promoter vector. The HSV-2 regulatory sequences were slightly stronger in this assay (≤2-fold higher). To assay for VP16 function, the VP16 constructs employed to make the mutants described above were co-transfected with an ICP0 promoter (124,818 to 124,109 BP) firefly luciferase construct (Sawtell and Thompson, 2016a,b). Transfection efficiency was determined and normalized by including the relevant renilla or firefly luciferase expression plasmids (**Figure 3A**).

Electrophoretic Mobility Shift Assays

Kits for the detection of Sp1 and Egr-1 were purchased from Signosis. The commercial oligonucleotide target for Egr-1 and Sp1 are shown along with their position weighted matrix PWM LogOdds scores determined with cis-BP (Weirauch et al., 2014) Egr-1 ATCCAGCGGGGGCAGCGGGGGCGA 15.6; Sp1 ATTCGATCGGGGCGGGGCGACTGAT 16.5. The 30mer HSV-1 oligonucleotide shown in **Figure 1B** (Invitrogen) scored 11.1 and 12.9 for Egr-1 and Sp1, respectively. The oligonucleotides were end labeled with T4 polynucleotide kinase (NEB) and γ-32p-ATP (Perkin Elmer) and hybridized to commercial recombinant Sp1, Egr-1, or HeLa cell nuclear extract and electrophoresed according to the manufacturers' protocols (Signosis and Sigma Aldrich). Blots were developed and analyzed on a Storm phosphoimager and quantified with GelQuantNet software. The repetitive elements in the HSV-2 sequence are

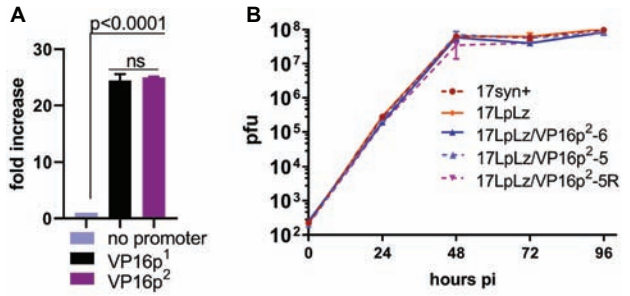

FIGURE 3 | Promoter function and *in vitro* multi-step viral replication kinetics. **(A)** A plasmid containing the wt HSV-1 VP16 gene (designated here as VP16p[1]), the same plasmid with the VP16 promoter deleted (designated as no promoter), and the plasmid generated to produce the HSV-2 VP16 regulatory sequence targeted replacement (designated here as VP16p[2], see **Figure 4A**) were employed in transient dual luciferase assays with a previously reported ICP0 promoter/Luciferase target plasmid (Sawtell and Thompson, 2016a,b) to test their ability to express VP16 and activate the ICP0 promoter as detailed in Section "Materials and Methods." The "no promoter" level of luciferase detected was set to one. Each bar represents the results of six transfection experiments. **(B)** Multi-step replication kinetics was performed in RSC. Each point is the average ± S.D. of three independently infected cultures harvested and titrated at the indicated times pi. Wild-type HSV-1 strain 17syn+ is the parent strain of 17LATpLacZ (here indicated as 17LpLz) which expresses beta-galactosidase from the LAT promoter as previously described (Sawtell and Thompson, 2016a,b). 17LATLpLacZ is the parent strain of the mutants generated for this study (17LpLzVP16p[2]-5 and 6) and the genomically restored isolate 17LpLzVP16p[2]-5R.

GGGGCGGGAGGGGCGGGAGGGGCGGGAGGGGCGGGA GGGGCGGGAGGGGCGGGAGGGGCGGGAGGGGCGGGA GGGGCGGGAGGGGCGGGAGGGGCGGGAGGGGCGGGA GGGGCGGG, and their PWM LogOdds scores are 11.1 (Egr-1) and 23.1 (Sp-1) at multiple sites.

Antibodies and Immunohistochemistry

Following removal, TG was placed in 0.5% formaldehyde (prepared from paraformaldehyde) for 2 h, rinsed in phosphate buffered saline, and incubated in x-gal buffer containing x-gal for 6 h as detailed previously (Sawtell and Thompson, 2014). Following rinsing, ganglia were post fixed in methanol containing 5% DMSO for 12 h. Hydrogen peroxide was then added to a final concentration of 10% and incubated for 1 h. Ganglia were rinsed twice in methanol and stored at −80°C for a minimum of 24 h. Viral proteins were detected in whole ganglia as described previously (Sawtell, 2003). Primary antibodies used included rabbit anti-HSV (Accurate, AXL237) at 1:3,000, or rabbit anti-VP16 antibody, 1:1,000 (Clonetech) followed by the secondary antibody, HRP-labeled goat anti-rabbit (Vector) at 1:500. Color development was achieved by incubating ganglia in a 0.1 M Tris (pH 8.2) solution containing 250 µg of diaminobenzidine (Aldrich)/ml and 0.004% H_2O_2 for approximately 5 min. Ganglia were rinsed in distilled water and cleared in glycerol to aid in visualization of the HSV protein positive neurons. These methods and the dilutions and characterizations of antibodies utilized have been detailed extensively in previous reports (Sawtell, 2003; Thompson et al., 2003, 2009; Thompson and Sawtell, 2006; Sawtell et al., 2011).

Animals

Male, outbred, Swiss Webster mice (22–25 g in weight) were obtained from Envigo and used throughout this study. Age-matched Swiss Webster female mice (Envigo) were used in a subset of experiments as indicated.

Inoculation of Mice

Prior to inoculation, mice were anesthetized by intraperitoneal injection of sodium pentobarbital (50 mg/kg of body weight). A 10 µl drop containing ~1–2 × 10^5 pfu of virus was placed onto each scarified cornea.

Pathobiological Characterization of Viral Mutants

Replication *in vivo*

Mice infected as above were euthanized at the indicated times post infection and tissues from a minimum three mice from each inoculation group were individually assayed for virus using a standard plaque assay. Tissue homogenates were plated in serial 10-fold dilutions on RSC monolayers, incubated for 2 h, and subsequently rinsed and overlaid with 1% carboxymethyl cellulose in minimal essential media as previously detailed (Sawtell and Thompson, 1992a,b).

Quantification of Viral Genomes by Real-Time PCR Assay

Isolation and quantification of total DNA from TG, using the PicoGreen double-stranded DNA quantification kit according to the manufacturer's instructions and with provided DNA standards (Molecular Probes), and quantification of total viral genomes was performed essentially as detailed previously except that the PicoGreen based real time PCR assay (Roche) was performed in a Roche 480 II instrument in a 96-well format and analyzed with the Roche 480 II LightCycler software (Sawtell et al., 2006).

In vivo Stress

Transition into the lytic cycle in the ganglia of mice *in vivo* was induced using hyperthermic stress (HS) (Sawtell and Thompson, 1992a,b). At 20 h post-induction, TG was harvested and assayed for viral protein expression as detailed previously (Sawtell, 2003).

Photomicrographs

Photomicrographs were obtained using an Olympus BX40 microscope outfitted with a Zeiss axiocam HRc camera and axiovision software. Cleared TG was viewed and marked cells populations were counted by two independent investigators.

Statistical Analysis

Statistical analyses were performed using GraphPad Prism software (GraphPad Software, San Diego, CA). $p < 0.05$ is considered significant.

RESULTS

The Egr-1/Sp1 Site in the 5′UTR of the HSV-1 VP16 Regulatory Region Can Bind Both Egr-1 and Sp1

Figure 1A depicts the region proposed by Lieu and Wagner to regulate leaky late expression of VP16 determined using mutated promoter analyses in transient assays (Lieu and Wagner, 2000). Mutations in these sites do not affect pre-immediate early *de novo* expression in neurons. However, simultaneous mutation of three potential TF sites identified *in silico* (labeled HSV-1πRR, **Figure 1A**) greatly reduced the capacity of HSV-1 to enter lytic infection in sensory neurons *in vivo*, which requires *de novo* pre-immediate early (πRR) VP16 expression (Sawtell and Thompson, 2016a,b). The sequence of the HSV-1 canonical Egr-1/Sp1 site present in the VP16 promoter 5′UTR region is shown in **Figure 1B**. The overlapping TF binding sites are underlined. To test whether Egr-1 and/or Sp1 could bind to this site, the HSV-1 30mer sequence shown (**Figure 1B**) was employed in electrophoretic mobility shift assays with recombinant Egr-1 and Sp1 proteins and HeLa cell nuclear extracts as described in Section "Materials and Methods." Both recombinant Egr-1 and Sp1 proteins bound to the fragment with affinities similar to those found with commercial oligonucleotides for individual Egr-1 and Sp1 sites, and the HSV-1 30mer effectively competed with the canonical commercial oligos. Likewise, Sp1 present in the HeLa cell nuclear extract bound to the HSV-1 sequence efficiently and both the commercial oligonucleotide and the HSV-1 30mer competed for binding with similar efficiencies. Egr-1 was not detected in the commercial HeLa extract (**Figure 4**). We conclude that the 30mer sequence from the HSV-1 VP16πRR regulatory region is capable of binding these TFs with efficiencies similar to the binding of the TFs to the commercial oligonucleotides. We note that other TFs (for example diverse Krupple-like factors, etc.) would also be expected to bind to these oligonucleotides.

Generation and Characterization of HSV-1 VP16 Promoter Mutant Constructs and Mutant Viruses

In order to test the ability of the wt promoter and the mutant promoter in which the four bases were mutated to "T" residues (**Figure 1B**) [predicted to eliminate binding of both Egr-1 and Sp1 (Weirauch et al., 2014)] to function as promoters in RSC in transient assays, two experiments with eight transfections each were performed using dual luciferase assays as described in Section "Materials and Methods." Both the wt and mutant promoters functioned equivalently. The second experiment included the CMV immediate early (IE) promoter for comparison, which was about eight-fold more efficient than the VP16 promoters. No differences were detected between the wt HSV-1 VP16 and mutated putative Egr-1/Sp1 site promoters.

We next tested the role of the putative Egr-1/Sp1 site in the regulation of VP16 in the context of the viral genome.

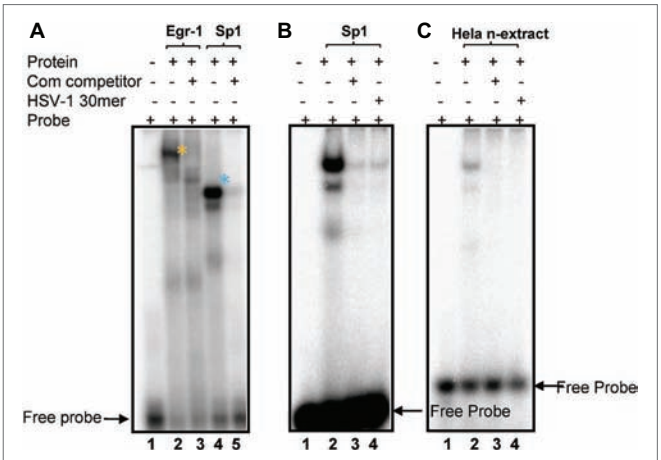

FIGURE 4 | Recombinant Sp1 and Egr-1 can bind to the putative Egr-1/Sp1 site. **(A)** The HSV-1 30 bp oligonucleotide shown in **Figure 1A** was end labeled, incubated with recombinant Egr-1 or Sp1 protein, electrophoresed and developed on a PhospholImager as detailed in Methods. Lanes: (1) no protein; (2) rEgr-1; (3) rEgr-1 + 40× cold probe; (4) rSp1; (5) rEgr-1 + 40× cold probe. Arrows indicated free probe (FP). Shifted probe bands are denoted with *. **(B)**. Labeled commercial probes were incubated rSp1 probe Lanes: (1) no protein; (2) rSp1 + probe. (3) +40× cold HSV-1 30mer; (4) + 40× cold probe. **(C)** Labeled HSV-1 30mer was incubated with HeLa nuclear extract as described in Section "Materials and Methods." Lanes: (1) no nuclear extract; (2) + extract; (3) + extract +40× cold HSV-1 30mer; (4) +extract +40× commercial Sp1 probe.

Three independently derived viral mutants named 17VP16pEgr-1/Sp1- 1, -3, and -5, were generated, as was a genomically restored variant of one isolate (17VP16pEgr-1/Sp1-R). Procedures for plaque color selection, plaque purification, confirmation of genomic structures, and DNA sequences across the sites of insertion are detailed in Section "Materials and Methods." No differences in replication were detected between either the independent mutant isolates, wt, or restored mutant under multi-step replication kinetic conditions in RSC (**Figure 5A**). Thus the mutations did not alter viral replication competency in RSC cultures (**Figure 5A**). Note that we previously reported that 17VP16πRR, a mutant in which three TF sites are mutated (**Figure 1A**; Sawtell and Thompson, 2016a,b) also replicates like wt in this assay.

Isolates 17VP16pEgr-1/Sp1-1 and -3, as well as the parental strain and the genomically restored mutant (17VP16pEgr-1/Sp1-R) were compared to the previously published 17VP16πRR mutant and its rescuant for their ability to replicate *in vivo* in the mouse cornea model. On day 4 pi, replication in the eyes was not different between any of the viruses tested, including the wt, rescuant viruses, 17VP16pEgr-1/Sp1, and the 17VP16πRR mutant viruses (**Figure 5B**). By contrast, while the genomically restored isolates replicated like the parental wt strain 17syn+ in the TG, the promoter mutants were severely replication impaired at this site (**Figure 5C**). The impaired replication in the TG is not a result of a transport deficiency, as the number of viral genomes detected in the TG at 20 hpi was not different among the groups, $p = 0.77$, ANOVA (**Table 1**). Combined with previous published analyses (Thompson et al., 2009; Sawtell and Thompson, 2016a,b), these findings support

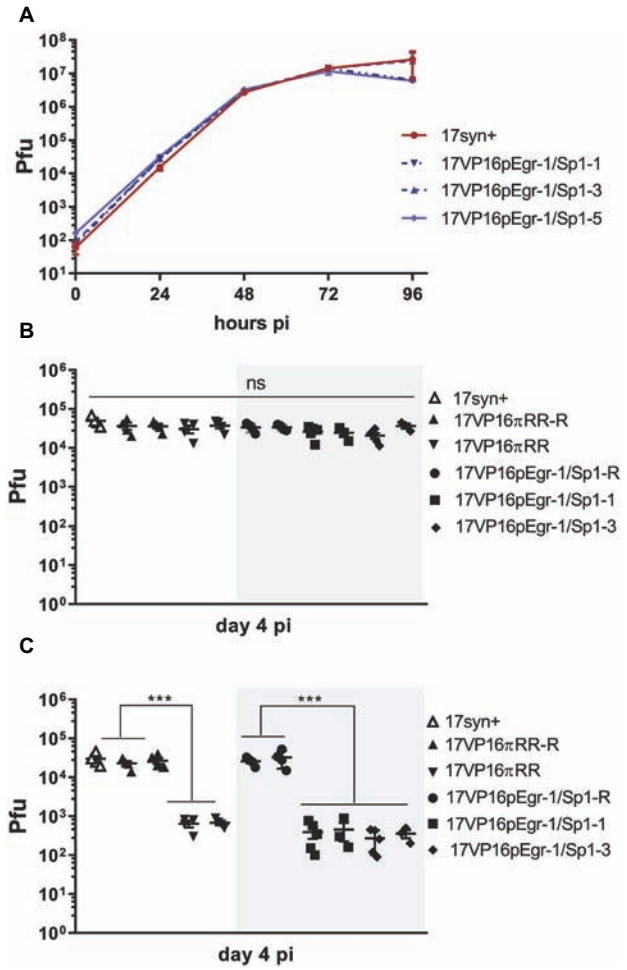

FIGURE 5 | *In vitro* **(A)** and *in vivo* **(B,C)** replication of 17VP16pEgr1/Sp1, its rescue, and wild-type parental strain 17syn+. **(A)**. Multistep *in vitro* replication kinetics of parental strain 17syn+ and three independent isolates of mutant 17VP16pEgr1/Sp1. Shown is one of two biological replicates. These mutants contain a refined 4-bp mutation in the putative Egr-1/Sp1 site at position 105,134 to 105,137 in the HSV-1 VP16 promoter/5′UTR sequence (see **Figure 1B**). **(B)** *In vivo* replication in eyes. Groups of 4–5 mice were inoculated on scarified corneas with 2×10^5 pfu of each of the 17VP16pEgr1/Sp1 and rescued viruses as indicated. In addition, groups of mice were infected with 2×10^5 pfu 17VP16πRR or its rescue 17VP16πRR-R. On day 4 pi, eyes and TG were harvested and infectious viral titers quantified by standard plaque assay. Replication on the eye **(B)** is not influenced by this mutation in the Egr-1/Sp1 site in the 5′UTR. By contrast, this Egr-1/Sp1 mutation results in a significant reduction in viral titers in the TG. This effect was also observed for the triple TF 5′UTR mutant, 17VP16πRR which was reported previously (Sawtell and Thompson, 2016a,b) **(C)** Shown are results from two independent biological replicates. ***$p \leq 0.001$.

the hypothesis that the mutated sequence (referred to as a mutated putative Egr-1/Sp1 site) in the HSV-1 VP16 5′UTR plays a role in initiating the transition into the lytic cycle in TG neurons infected *via* axons. However, the recognized complexities of interpreting mutations in the 5′UTR region (Leppek et al., 2018) prompted an additional approach to strengthen and extend this analysis.

Targeted Replacement of VP16p^1/5′UTR^1 With VP16p^2/5′UTR^2 in HSV-1 Strain 17LATpLacZ

Generation of 17LpLz/VP16p^2 and Rescuant, 17LpLz/VP16p^2-R

The HSV-1 VP16 promoter is hereafter referred to as VP16p^1, and the HSV-2 VP16 promoter is designated VP16p^2. Unless otherwise stated, these abbreviations refer to the promoter and 5′UTR sequences. Our strategy was to exploit the HSV-2 VP16 promoter as a second natural regulator of VP16 and generate an HSV-1 mutant in which the VP16p^1/5′UTR^1 (105,531–105,060 bp) was replaced with that of VP16p^2/5′UTR^2 (106,222–105,793 bp) in the background of 17LATpLacZ (Sawtell and Thompson, 2016a,b). The parental mutant 17LATpLacZ is wt in all regards except for the insertion of the *E. coli* LacZ gene driven by the basal latency associated transcript promoter (LATp) in the intergenic region between gJ (US5) and gD (US6). As reported (Thompson et al., 2009; Sawtell and Thompson, 2016a,b), an active LATp drives expression of the bacterial beta galactosidase enzyme (B-gal) which can be detected histochemically, thus marking neurons expressing the latent transcriptional program. This feature allows analysis of viral transcriptional program utilization (latent vs. lytic) in individual TG neurons over time following corneal infection. During long term latency, this promoter marks a subset of latently infected neurons. At the early times pi we examine here, this may also be the case, however, further studies are required to determine this.

To help ensure that all relevant upstream UL48 gene regulatory sequences were captured, part of the 3′UTR of the HSV-2 UL49 gene was included, as were sequences extending through most of the 5′UTR of the HSV-2 UL48 gene (**Figure 2A**). A short 27 bp region immediately preceding the VP16 ORF AUG codon (Lieu and Wagner, 2000) was left intact to preserve the HSV-1 UL48 Kozak consensus sequences (Kozak, 1987) to minimize effects on translation initiation efficiency. Read through transcription would be inhibited by the three separate poly A+ signals located upstream of the 5′ end of the HSV-2 VP16 promoter sequences (detailed in Methods) (**Figure 2A**) The position of predicted TF-binding sites in the HSV-2 VP16 regulatory region is

TABLE 1 | Analysis of viral genome copies in TG at 20 h pi.

17VP16pEgr-1/Sp1	17VP16pEgr-1/Sp1-R	17VP16πRR	17VP16πRR-R	ANOVA
8,337 ± 3,412	7,333 ± 1,528	10,367 ± 5,771	7,877 ± 2,846	$p = 0.77$

Viral genome copies/TG pair at 20 hpi n = 3 mice/group.

shown in **Figure 2B**. The architecture of the HSV-2 promoter is markedly different than that of HSV-1. Notably there are 13 direct tandem repeats of a sequence that forms multiple high scoring overlapping Egr-1/Sp1 sites located upstream of the VP16 gene TATA box, but a high scoring overlapping site located downstream in the 5′UTR as seen in HSV-1 is not evident. Similarly, an NPAS4 or Sim2/Arnt heterodimer site similar to a site known to confer rapid reciprocal regulation to the neuronal Drebrin gene (Woods and Whitelaw, 2002; Ooe et al., 2004) is found upstream of the HSV-2 TATA box, whereas a similar site previously implicated in the *de novo* expression of HSV-1 is located downstream of the TATA box (Sawtell and Thompson, 2016a,b). This suggests the HSV-2 pre-immediate early regulatory sequences might reside in the more distal region of the HSV-2 promoter (**Figure 2A**), but this remains to be determined.

Prior to construction of the HSV-2 targeted replacement VP16 promoter mutants, the mutagenesis and genomically wt HSV-1 constructs were tested in transient assays for their ability to express VP16 and to transactivate the immediate early ICP0 promoter driving luciferase as previously described (Sawtell and Thompson, 2016a,b) and detailed in Section "Materials and Methods." No difference was seen between the HSV-1 and HSV-2 VP16 promoters in this assay (**Figure 3A**). Two independently derived mutants (named 17LpLz/VP16p^2-5 and -6) were generated by homologous recombination, plaque purified, and characterized as detailed in Section "Materials and Methods," including sequencing of crossover sites and *in vitro* replication kinetics in RSC (**Figure 3B**). 17LpLz/VP16p^2-5 was restored to the wt HSV-1 genomic sequence and named 17LpLz/VP16p^2-R, which was plaque purified and analyzed as above.

In vivo Replication Kinetics

Analysis of replication *in vivo* in both male and female mice revealed slightly higher titers in the eyes at later times in mice infected with the 17LpLz/VP16p^2 promoter mutant (**Figure 6A**), but these differences did not reach significance. In TG, only differences at later times, days 6 and 8 pi, achieved significance with 17LpLz/VP16p^2 yielding higher titers compared to the restored isolate (**Figure 6B**). In the central nervous system (CNS), 17LpLz/VP16p^2 consistently replicated to higher titers and for prolonged periods of time compared to 17LpLz/VP16p^2-R. The absolute titers were low in the mid to front areas of the brain, but viral replication in these parts of the CNS continued past day 8 pi, when HSV-1 is typically cleared from the brain (**Figure 6C**; Thompson and Sawtell, 2000; Thompson et al., 2009; Sawtell and Thompson, 2016a,b). The increased neuroinvasiveness and replication in the CNS were reflected in the increased virulence of the isolates. In groups of male Swiss Webster mice infected with a total of 2×10^5 pfu of 17LpLz/VP16p^2 or 17LpLz/VP16p^2-R, significantly more deaths occurred in the 17LpLz/VP16p^2 group, $p = 0.039$ Log-rank Mantel-Cox test (**Figure 7**). However, as also shown (**Figure 7**), virulence was well below that of HSV-1 strain Mckrae so these viruses fall within the normal range of virulence displayed by HSV-1 strains.

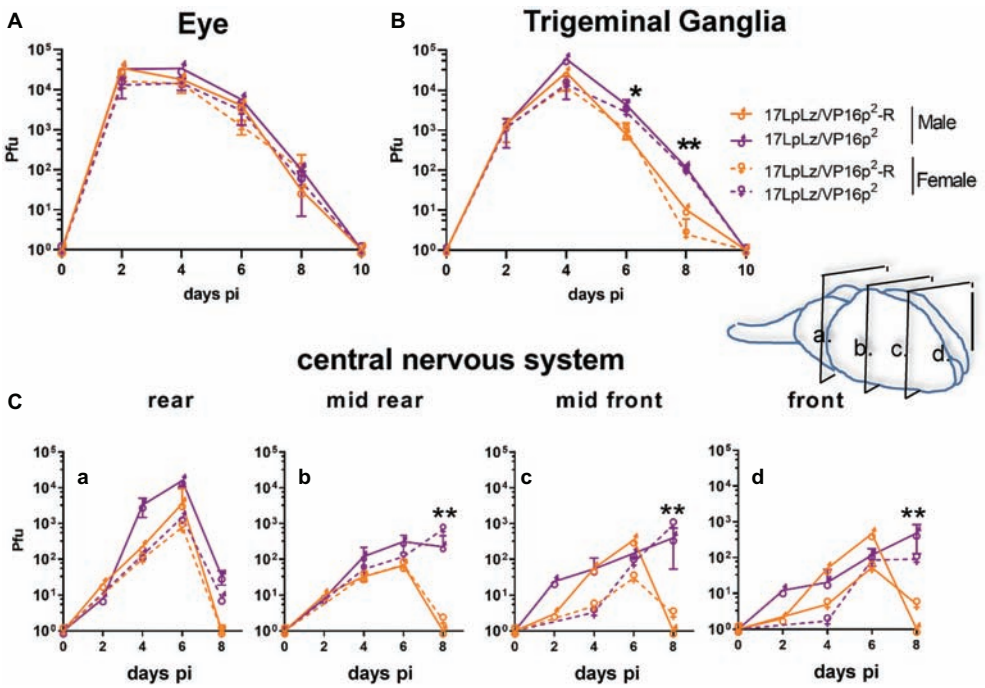

FIGURE 6 | *In vivo* replication kinetics. Shown are infectious viral titers in eyes **(A)**, trigeminal ganglia **(B)**, and brains **(C)** harvested from male and female mice infected with 17LpLz/VP16p^2 and the rescue of this mutant, 17LpLz/VP16p^2-R. Three mice from each group were harvested at each time point indicated and infectious viral titers were quantified in tissue homogenates (see Section "Materials and Methods"). Brains were divided coronally into four pieces, labeled a–d from brainstem to front of brain as indicated in the diagram. * and ** indicate $p = 0.01 < 0.05$ and $p = 0.001 < 0.01$, respectively (unpaired, two-tailed *t* test).

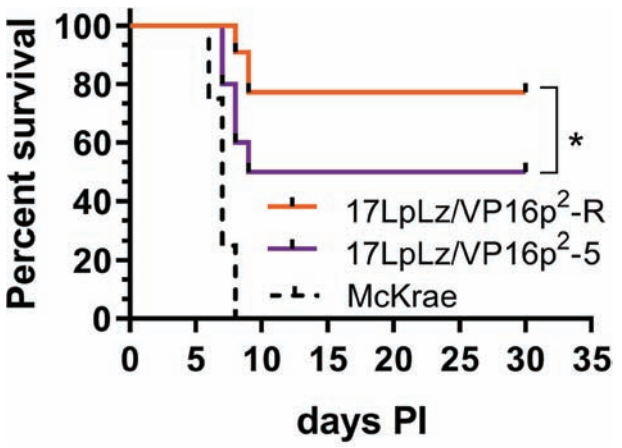

FIGURE 7 | Survival curve. Shown is percent survival following infection with 2×10^5 pfu of either 17LpLz/VP16p^2 or 17LpLz/VP16p^2-R in male Swiss Webster mice. Survival of mice infected with HSV-1 strain McKrae is shown for comparison, emphasizing that the modest increase in virulence of VP16p^2 is well below the virulence of this naturally occurring HSV-1 strain. Data shown are compiled from two independent experiments $n = 10$ mice per group infected with either 17LpLz/VP16p^2 or 17LpLz/VP16p^2-R ($p = 0.039$ Log-rank Mantel-Cox test). HSV-1 strain McKrae was evaluated at the same inoculation titer in a single experiment of four mice. *$p \leq 0.05$.

Characterization of Early Infection in TG Neurons Following Corneal Inoculation With 17LpLz/VP16p^2: Comparison With the Rescue, 17LpLz/VP16p^2-R

The measurable increases in replication in the TG and virulence are consistent with an HSV-2 VP16 promoter-driven shift in the early balance in the TG neuron between the latent and lytic programs (Sawtell and Thompson, 2016a,b). In order to examine this directly, we utilized the dual marker *in situ* approach with these mutants, determining the timing and number of neurons expressing LATp activity and viral protein expression to address the following questions: does the VP16p^2/5′UTR^2 (1) support early default latency, (2) alter its timing or stability (i.e., transition into the lytic cycle), and/or (3) alter stress induced lytic cycle entry?

HSV-2 VP16 Promoter Mutant Enhances the Transition From the Early Default Latent State

Groups of mice were infected on scarified corneas with 2×10^5 pfu of either 17LpLz/VP16p^2 or 17LpLz/VP16p^2-R (genomically restored to VP16p^1/5′UTR^1). Eyes and TG were harvested from each group at either 20 or 28 h pi. Shown in **Figures 8A–D** are data from each time point representing results compiled from two independent experiments (no significant differences between the replicate experiments were observed).

Eye titers were not different between 17LpLz/VP16p^2 and 17LpLz/VP16p^2-R infected mice at either 20 or 28 hpi ($p \geq 0.9$, unpaired, two-tailed *t* test) (**Figure 8A**). The number of blue neurons in the TG at 20 hpi was not different among the groups ($p = 0.74$, unpaired, two-tailed *t* test) (**Figure 8B**), and no evidence of transition into the lytic program was detected at this time in TG neurons infected with either 17LpLz/VP16p^2 (0/20) or the genomic rescue of this mutant (VP16p^1) (0/20) (**Figures 8C,D**). At 28 hpi, the number of neurons evidencing LATp activity in the absence of viral protein was not different between the mutant and rescue viruses ($p = 0.30$, unpaired, two-tailed *t* test) (**Figure 6B**). However, there were significantly more neurons expressing combined blue (LATp activity) and viral proteins (transitioning phenotype) in the TG from mice infected with the 17LpLz/VP16p^2 mutant ($p = 0.009$, unpaired, two-tailed *t* test) (**Figure 8C**). The number of neurons in which only viral proteins were detected was also significantly more in TG infected with the 17LpLz/VP16p^2 mutant ($p = 0.027$, unpaired, two-tailed *t* test) (**Figure 8D**). These data demonstrate that although the initial early default into the latent transcriptional program at 20 hpi is not different between the mutant and its rescue, within 8 h, (i.e., at 28 hpi), 26% of neurons were transitioning into the lytic cycle with the mutant compared to 7.5% with the rescue.

Transition Into the Lytic Program by HSV-2 VP16 Promoter Targeted Replacement Is Enhanced in Both Male and Female Mice

The preceding transition experiment was performed in male mice. An important question is whether a similar early expression from the LAT promoter followed by a transition into the lytic cycle would also occur in TG neurons during infection in female mice. To test this, age-matched male and female Swiss Webster mice were infected on scarified corneas as above. Eyes and TG were harvested, in this case at 24 and 38 hpi. There were no differences between 17LpLz/VP16p^2- or 17LpLz/VP16p^2-R-infected male or female eye titers at either 24 or 38 hpi (**Figure 8E**). Again at 24 hpi, there were no significant differences in the number of LATp-positive only neurons among the groups (compare **Figures 8B,F**). While neurons undergoing transition were not observed in either male or female mice infected with the rescue virus at 24 hpi, 4 and 5% of LATp-marked neurons were transitioning into lytic program in males and females infected with 17LpLz/VP16p^2. By 38 hpi, three-fold more neurons were transitioning in TG infected with 17LpLz/VP16p^2 compared to the rescue, 29 and 9%, respectively.

Effect of the Type-1- and -2-Specific VP16 Promoters on Early Spread of Infection in the TG

As infection *in vivo* proceeds past ~36 hpi, the viral expression landscape becomes more complex in the TG. Low levels of infectious virus become detectable and virus begins to spread within the TG (Kramer et al., 1998; Sawtell et al., 2006). At 44 hpi, cell to cell spread of infection in the TG is apparent and can be seen in "plaque-like" clusters of viral protein expressing neurons (**Figure 9B**).

Our hypothesis would predict that once a neuron has transitioned into the lytic cycle and progressed to infectious virus production, that VP16 within the tegument of these virions would be delivered into neighboring cells, be transported

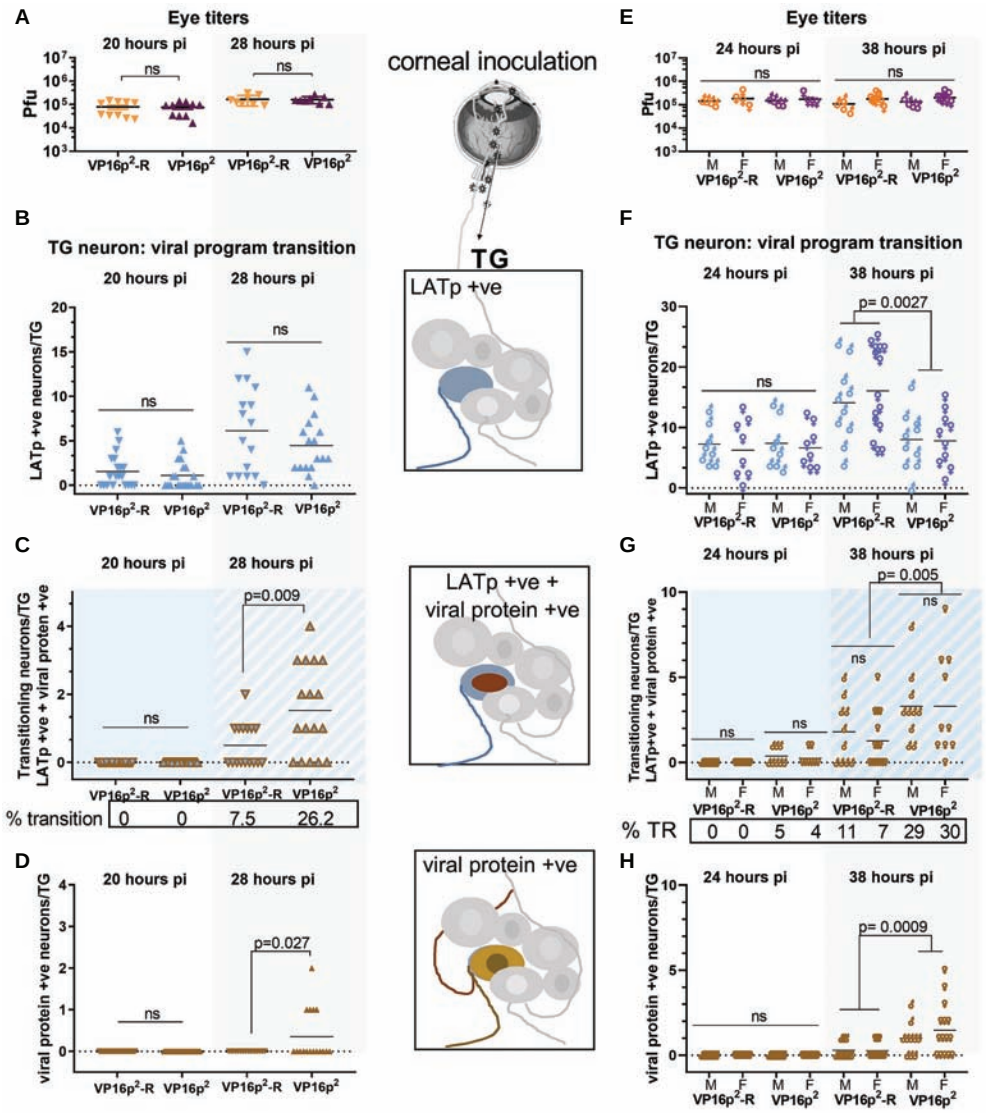

FIGURE 8 | Comparison of default latent state entry and transition into the lytic program regulated by VP16p^2/5′UTR^2 or VP16p^1/5′UTR^1. Groups of mice were inoculated on scarified corneas with 2 × 10^5 pfu of 17LpLz/VP16p^2 or 17LpLzVP16p^2-R. Eyes were processed (as pairs) for infectious virus titers as detailed in Section "Materials and Methods." TG was processed for detection of b-gal activity and viral protein expression *in situ* as detailed in Section "Materials and Methods." The number of marked neurons was enumerated on cleared and pressed whole mounted TG. Panels **(A–D)** include data from male mice. Panels **(E–H)** include data directly comparing male and female mice. The viral titers in eyes at 20 and 28 hpi **(A)** or at 24 and 38 hpi **(E)** were not different among the groups. **(B–D,F,G)** Quantification of viral expression program phenotype in individual neurons within each TG (n = 20 at 20 hpi, n = 16 at 28 hpi, n = 8 at 24 hpi, and n = 10–15 at 38 hpi). **(B,F)** Solid blue symbols indicate neurons expressing LATp in the absence of viral proteins. **(C,G)** Blue symbols with brown outline and/or blue background indicate neurons in which expression from both the LATp and viral protein is detected. **(D,H)** Brown symbols indicate neurons in which viral protein alone is detected. Data shown in **(A–D)** are compiled from two biological replicates for each viral mutant at each time point. n = 5 for each experiment at 20 hpi and n = 4–5 for each experiment at 28 hpi.

into the nucleus and initiate the lytic cycle (paralleling cell to cell spread in tissue culture or corneal infection). The accelerated transition into the lytic cycle from the default latent program linked to the HSV-2 VP16 promoter would be predicted to result in greater numbers of infected multi-cellular foci in the TG. In order to test this, three independent experiments were performed at 44 hpi. Groups of mice were infected as above, and at 44 hpi, eyes and TG were harvested from each group and processed as above. Infectious viral titers in the eyes harvested from 17LpLz/VP16p^2 and 17LpLz/VP16p^2-R were not different (**Figure 9A**). There were no significant differences between the individual biological replicates of the same group with respect to the number of LATp marked neurons or "plaques". However, the number of "plaques" in 17LpLz/VP16p^2 compared to its genomic rescue 17LpLzVP16p^2-R was greater in all three experiments (**Figure 7**; p = 0.0044,

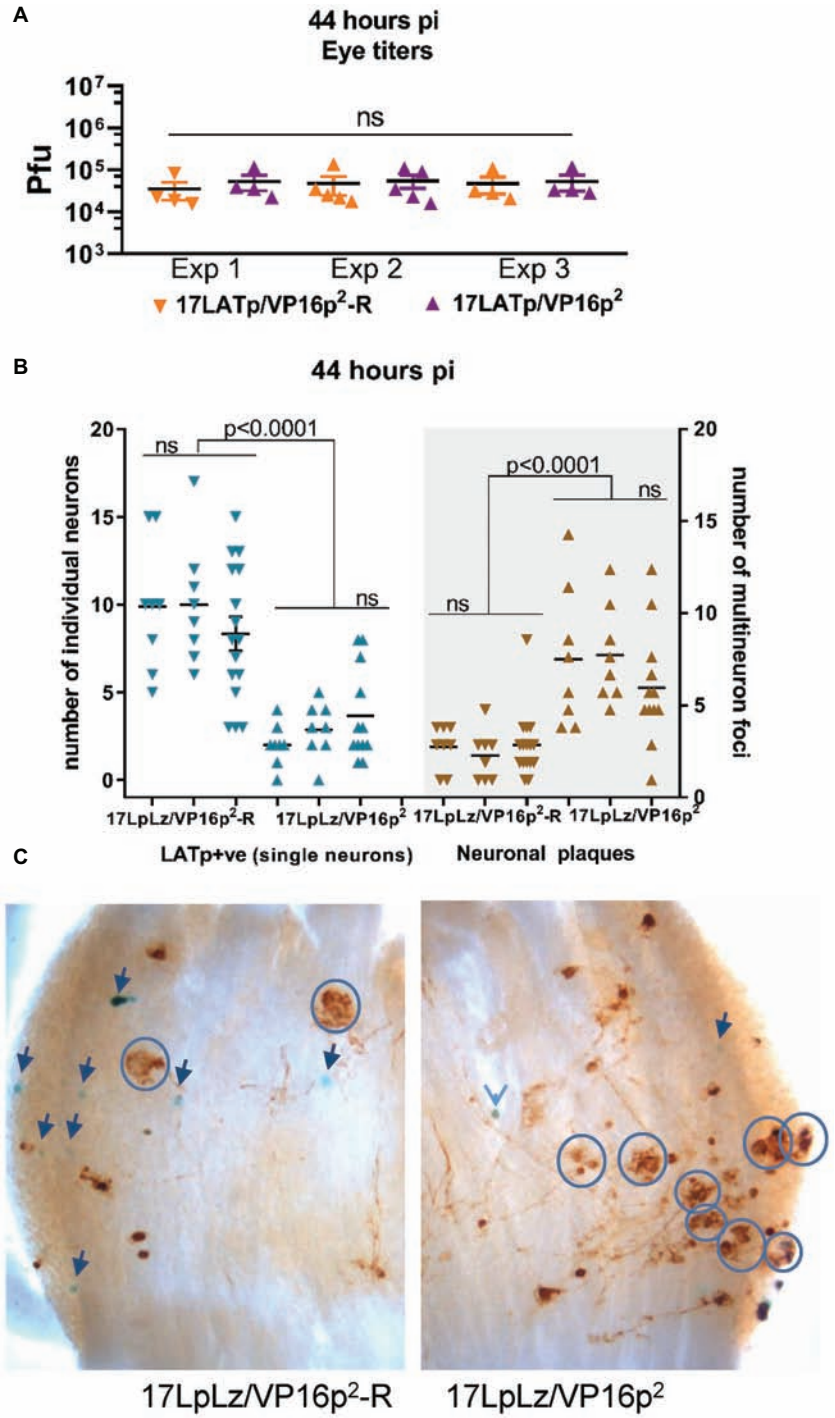

FIGURE 9 | Progression from isolated marked single neurons to multi-neuron (plaque-like) viral protein-positive foci at 44 hpi. Groups of mice were infected with 2 × 10^5pfu of 17LpLz/VP16p^2 or 17LpLz/VP16p^2-R on scarified corneas. At 44 hpi, eyes and TG were harvested. Eyes were processed for infectious virus titers. TG was processed for *in situ* detection of b-gal activity and viral protein expression (see Section "Materials and Methods"). Three independent experiments are shown, Exp 1 and 2, n = 8 TG for each group, Exp 3, n = 16 and 12 TG for the rescue and mutant, respectively. **(A)** Infectious viral titers in eyes were not different between experiments or between 17LpLz/VP16p^2- or 17LpLz/VP16p^2-R-infected mice (ANOVA p = 0.97). **(B)** The number of LATp expressing neurons (blue symbols) detected in individual TG are indicated in the left panel. Brown symbols indicate protein expressing multi-neuron foci in each of these same TG (right panel). **(C)** Photomicrographs of representative TG infected with either17LpLz/VP16p^2-R (left) or 17LpLz/VP16p^2 (right). Blue circles mark multi-neuron foci, and individual blue neurons are indicated by arrows. The numbers were compared using an ordinary one-way ANOVA with Tukey's multiple comparison test.

$p = 0.0001$, $p = 0.0025$, unpaired, two-tailed t test, experiments 1, 2, and 3, respectively). 17LpLz/VP16p^2-infected TG had nearly four times the number of "plaques" found in 17LpLz/VP16p^2-R-infected TG at this time pi. Interestingly, there was a reciprocal difference in the number of LATp-positive neurons and the number of plaque-like clusters within TG (**Figure 9B**). Significantly, as observed at the 38 h time point, fewer LATp-marked neurons were detected in 17LpLz/VP16p^2 mutant-infected ganglia compared to the VP16p^1 promoter rescue at this time ($p < 0.0001$ in all three experiments). Photomicrographs of representative ganglia from 17LpLz/VP16p^2-R (left panel) and 17LpLz/VP16p^2 (right panel) stained for b-gal activity and viral protein are shown in **Figure 9C**. Single blue + brown neurons were often surrounded by neurons that appeared to express only viral proteins. This suggested that in contrast to entry into the neuron through the axon, default entry into the latent program is not a feature of infection arising from cell to cell spread directly within the TG.

Mutation in the Egr1/Sp1 Site in the VP16p^1/5′UTR^1 Promoter Influences the Number of Plaque-Like Foci

17VP16πRR was shown previously to exhibit a reduced latent to lytic transition phenotype. In addition, 17VP16p^{1}Egr1/Sp1 would be anticipated to display phenotypes similar to those displayed by mutant 17VP16πRR. Groups of mice were infected with 2×10^5 pfu on scarified corneas with 17VP16πRR ($n = 8$), its rescue 17VP16πRR-R ($n = 8$), 17VP16p^{1}Egr1/Sp1 ($n = 8$), or its rescue 17VP16p^1 Egr1/Sp1-R ($n = 8$). At 44 hpi, tissues were harvested, processed, and analyzed as indicated above. TG infected with 17VP16πRR and 17VP16p^{1}Egr1/Sp1 contained nearly 10-fold fewer clusters of infected neurons than their corresponding genomic rescues (1.75 ± 1.25 vs. 0.19 ± 0.40, $p = 0.009$) and (2.0 ± 1.86 vs. 0.13 ± 0.34, $p = 0.0003$) for 17VP16πRR and 17VP16pEgr1/Sp1, respectively, and nearly 40-fold fewer than observed with 17LpLz/VP16p^2 infection.

VP16p^2/5′UTR^2 Promotes Enhanced Response to Reactivation Stress

The disposition of the latent viral genome in the TG neuron changes during the course of acute infection (Knipe, 2015; Kristie, 2015; Sloan et al., 2015; Maroui et al., 2016; Nicoll et al., 2016; Cohen et al., 2018). We previously demonstrated that as early as day 9 pi, reactivation stressors promote the transition into the lytic cycle in TG neurons, and we now asked whether the VP16p^2/5′UTR^2 is more responsive than VP16p^1/5UTR^1. Groups of 30 mice were infected with 1×10^5 pfu of 17LpLz/VP16p^2 or 17LpLz/VP16p^2-R (wt HSV-1 genotype) on scarified corneas. On day 11 pi, surviving mice were randomized into two groups for each virus and half were subjected to stress. TG was excised and whole ganglia were stained for viral proteins, cleared, mounted and examined as described in Section "Materials and Methods." Few neurons were positive for viral proteins in TG from the untreated groups regardless of whether VP16 was expressed from type-1 or type-2 regulatory sequences and the number found was not different between groups ($p = 0.98$, ordinary one-way ANOVA with Tukey's *post hoc* analysis, **Figure 10**). The numbers of positive neurons in TG from animals at 20 h post stress increased in both groups. This increase was not significant in mice infected with the wt genomically restored virus ($p = 0.46$), but a significant increase in positive neurons was observed in TG of mice infected with the mutant expressing VP16 from the HSV-2 promoter/5′UTR^2 ($p < 0.0001$) (**Figure 10**). We conclude that the VP16p^2/5′UTR^2 regulatory sequences were significantly more responsive to a stress that induces reactivation from the "early" latent state than the HSV-1 sequences.

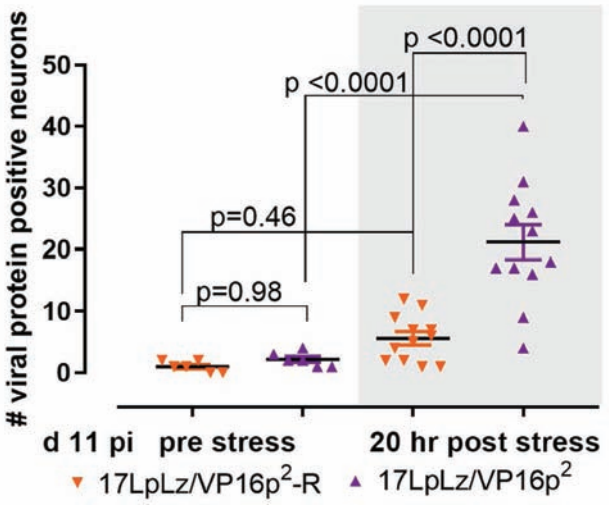

FIGURE 10 | Stress induced transition into the lytic cycle. Mice were infected on scarified corneas with 1×10^5 pfu of either 17LpLz/VP16p^2 or its rescue17LpLzVP16p^2-R. At 11 day pi, mice from each infection group were untreated or stressed (see Section "Materials and Methods"). At 20 h post stress, TG from both unstressed and stressed groups from each infection group were dissected and processed for the detection of viral proteins as detailed in Section "Materials and Methods." The number of neurons expressing viral proteins (evidence of entry into the lytic program) in each TG was counted. Data were analyzed using ordinary one-sided ANOVA with Tukey's multiple comparison test.

DISCUSSION

A schematic summary is shown in **Figure 11**. Evidence from diverse studies support the idea that the tegument protein VP16, which initiates lytic infection at low moi by transactivating the viral immediate early genes (Campbell et al., 1984; Bzik and Preston, 1986; Ace et al., 1988; Wysocka and Herr, 2003; Thompson et al., 2009; Sawtell and Thompson, 2016a,b), is not transported through axons efficiently favoring latency (Thompson et al., 2009; Antinone and Smith, 2010; Aggarwal et al., 2012; Hafezi et al., 2012; Smith, 2012; Koyuncu et al., 2015, 2017; Sawtell and Thompson, 2016a,b). It is noted that this acute stage "default" latent transcription program is

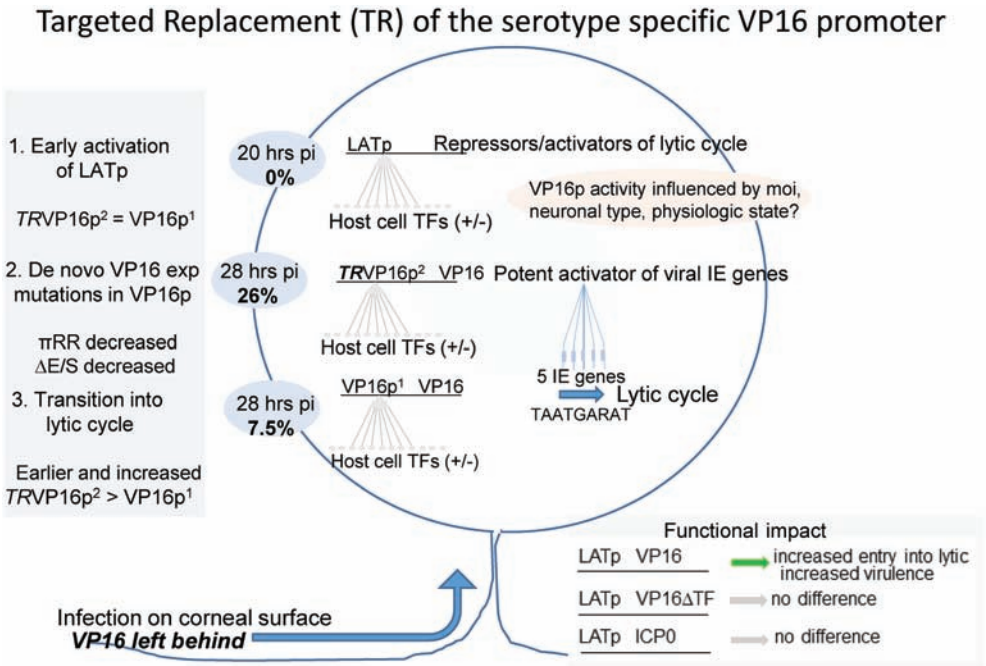

FIGURE 11 | Summary of the role of VP16 and its regulation in the earliest stages of HSV infection of sensory neurons *in vivo*. Sensory neurons residing in the trigeminal ganglion become infected with HSV through their axonal endings distributed at the body surface site of infection. This unique mode of entry into the neuron has long been thought to play a central role in the outcome of infection in the infected neuron. Early studies supported the concept that the outcome was binary-entering either latency in which only the LAT gene is abundantly transcribed, or lytic infection resulting in virus production and neuronal death (Margolis et al., 1992, 2007; Sawtell and Thompson, 1992a,b; Lachmann and Efstathiou, 1997). However, approaches that allow visualization and quantification of very rare events in the TG have revealed that individual neurons enter the latent program first, and a portion of these transition into the lytic cycle. This transition requires the *de novo* expression of VP16 (Thompson et al., 2009; Sawtell and Thompson, 2016a,b). This is important because it identifies a regulatory nexus residing in the VP16 gene, with the potential for multiple neuronal context dependent inputs feeding into the VP16 regulatory machinery. We propose that the VP16 promoter region functions as a host cell micro-environment sensor, which in turn is modified by systemic inputs. This regulation of VP16 expression serves to maximize the establishment of latency while minimizing severe morbidity or mortality in diverse hosts infected under differing conditions (age, immune system status etc.) with HSV-1 strains that vary in their pathobiologic properties. The near ubiquity of the virus in the human population at large and relative rarity of serious sequelae of infection is testimony to the success of this evolutionary strategy. (1) Latency is favored in neurons because tegument proteins including VP16 are not transported through axons to neuronal nuclei along with the viral genome. Because the IE genes are not transactivated and ICP4 protein (a repressor of the LAT promoter, LATp) is absent, the LATp interacts with a variety of host TFs, is turned on, and expresses RNAs that repress and/or possibly enhance lytic infection (Watson et al., 2018). (2) Embedded in both the HSV-1 and HSV-2 VP16 regulatory regions are sequences that promote its *de novo* expression in some of these neurons that are already expressing the LATp. (3) *De novo* VP16 expression initiates the lytic cascade in these neurons. By 28 hpi, 26% of the LATp+ neurons show evidence of viral protein expression when VP16 is driven by the type 2 promoter in the context of HSV-1, whereas about 7.5% are positive in wt HSV-1. This initiation of lytic gene expression requires functional VP16 transactivation and does not occur if ICP0 instead of VP16 is expressed during the default latent state (Thompson et al., 2009).

unlikely to share all features of a fully consolidated latent infection. The latter requires extensive changes to the chromatin structure on the viral genome which occurs over a prolonged period of time and involves interactions with subnuclear structures (Knipe and Cliffe, 2008; Cliffe et al., 2009, 2015; Kwiatkowski et al., 2009; Bloom et al., 2010; Lu and Triezenberg, 2010; Roizman et al., 2011; Knipe, 2015; Kristie, 2015; Sloan et al., 2015; Maroui et al., 2016; Nicoll et al., 2016; Cohen et al., 2018). Importantly, productive infection in TG neurons also occurs in animal models and humans, and this acute stage viral replication in the peripheral nervous system is important to maximize the latent burden and optimize reactivation potential in experimental models (Thompson and Sawtell, 2000). We and others are investigating how this viral replication is initiated in TG neurons. There is evidence for several mechanisms that might initiate HSV replication in neurons including alternate transport mechanisms for VP16 through axons (Antinone and Smith, 2010), high moi neuronal infections that obviate the requirement for VP16 (Koyuncu et al., 2015) as is well documented in cultured cells (Ace et al., 1989), a binary choice made based on neuronal subtype (Yang et al., 2000; Margolis et al., 2007; Bertke et al., 2013) and an unexpected neuronally directed expression program embedded in the HSV-1 VP16 promoter/5′ UTR that appears to induce the synthesis of VP16 protein *de novo* (Thompson et al., 2009; Sawtell and Thompson, 2016a,b).

This latter hypothesis is supported by several related observations. Infection of mice *via* the cornea results in detectable expression of only the latency associated transcript promoter (LATp) at very early times (18–32 hpi). Expression of lytic phase promoters of the immediate early and leaky late kinetic classes and their cognate proteins occurs about 12–14 h after the LATp is expressed, and only in cells already "marked" by LATp-driven *E. coli* beta-galactosidase (b-gal)

expression (Thompson et al., 2009; Sawtell and Thompson, 2016a,b and see also **Figures 8, 9**). The LAT promoter is strongly repressed by the immediate early protein ICP4 in cells including neurons during acute infection (Batchelor and O'Hare, 1990; Margolis et al., 1992; Sawtell and Thompson, 1992a,b; Farrell et al., 1994); we can therefore conclude that this transition out of the default latent transcription program requires *de novo* lytic protein expression that occurs after the LATp is activated. That the transition out of the latent state is driven by *de novo* VP16 expression is supported by several additional observations. (1) Analysis of a VP16 promoter/b-gal reporter mutant in the background of the VP16 transactivation-deficient mutant in1814 (Ace et al., 1989) demonstrated that the VP16 promoter can be activated in infected neurons in the absence of other viral proteins (Thompson et al., 2009). (2) Expression of an extra copy of VP16, but not of ICP0, *de novo* from the LATp eliminates the default latent state. With this mutant, virus replication in TG occurs within 20 hpi, is more extensive in TG and brain, and virulence is significantly enhanced (Sawtell and Thompson, 2016a,b). Mutation of TF binding sites downstream of the VP16 TATA resulted in replication reduced about 100-fold in TG and the exit from the default latent pathway into the lytic pathway was significantly reduced, as was virulence (Sawtell and Thompson, 2016a,b). Yet these mutations had no effect on the kinetics of VP16 expression or viral replication in cells in culture or on replication on the mouse eye *in vivo* (Sawtell and Thompson, 2016a,b). This is consistent with early studies mapping TF sites important for normal leaky late VP16 expression to regions upstream of the TATA box (Lieu and Wagner, 2000).

In this study, we first refined the analysis of sequences required for the *de novo* expression of HSV-1 in neurons. Introducing a four base change in the core matrix of a canonical Egr-1/Sp1 site located in the HSV-1 VP16 5′UTR resulted in mutants that replicated like wt in cultured cells and mouse eyes (**Figures 2A, 5B**). This later finding is important because the viral load entering the TG from the eye at early times was therefore equivalent as confirmed by QPCR for the viral genome in TG. Despite this, viral replication in TG was reduced by two orders of magnitude (**Figure 4C**), and virulence was abrogated. We emphasize that we do not yet know how these sequences function, but favor the hypothesis that this region represents a combinatorial TF-binding site that can confer both positive and negative regulation to VP16 transcription in neurons because (1) both Egr-1 and Sp1 can bind to the site with wt affinities (**Figure 4**); (2) many host genes including stress responsive neuronal genes are reciprocally regulated by these factors in response to stress (Carrasco-Serrano et al., 1998; Nitsch et al., 1998; Contestabile, 2008; Liu et al., 2014; Wu et al., 2017); and (3) the stress induced factor Egr-1, which can displace the ubiquitous positive factor Sp1, induces its corepressor NAB2 that rapidly induces a silenced chromatin state (Houston et al., 2001; Kumbrink et al., 2005). This latter feature is compatible with the fact that the vast majority of latent viral genomes do not respond to systemic stressors by exiting latency (Sawtell and Thompson, 1992a,b, 2016a,b; Sawtell, 2005; Thompson and Sawtell, 2006; Thompson et al., 2009). We note, however, this site can bind other TFs and is also located in the 5′UTR of the VP16 mRNA. 5′UTR sequences can influence protein production in many ways exclusive of transcriptional regulation. Unfortunately, it is currently not possible to computationally predict these functional aspects of 5′UTRs in eukaryotes (reviewed in Leppek et al., 2018), but most experimentally determined sequences act to inhibit protein expression (reviewed in Rhodes and Lipps, 2015). For example, the region containing the HSV-1 overlapping Egr-1/Sp1 site is predicted to have the capacity to form a single DNA as well as an RNA G-Quadruplex structure (Kikin et al., 2006). This structure is known to inhibit ribosome scanning on mRNA and reduce protein expression (Rhodes and Lipps, 2015). The 4-bp mutations would be expected to eliminate the predicted G-Quadruplex structure (Kikin et al., 2006), and if this was a functional 5′UTR RNA G-Quadruplex, the mutations would be expected to increase, rather than decrease VP16 protein production.

In order to extend our analyses of VP16 regulation and potentially avoid the problem of mutation of 5′ UTR sequences, we took advantage of the existence of a second natural human HSV VP16 promoter, that of HSV-2. We asked whether the HSV-2 promoter/5′UTR, which has a very different structure, could also direct the *de novo* VP16 synthesis *in vivo* in the context of the HSV-1 genome. HSV-1 mutants in which the HSV-1 VP16 promoter and 5′UTR were replaced with those of HSV-2 leaving all other genes and all ORFs as HSV-1 were produced in the background of 17LATpLacZ (which labels neurons expressing the latent transcription program with b-gal). In this way, the effects of the HSV-2 VP16 regulatory region on latent/lytic transition were isolated from all other HSV type-specific differences. If the hypothesis is correct, despite its very different architecture we would expect to see that the HSV-2 promoter would induce the transition of HSV-1 from the default latent program into the lytic program. This may be a unique feature of the VP16 promoters, as another leaky late promoter/5′UTR employed to drive VP16 (that of VP5) fully supports viral replication in culture and mouse eyes, but fails to efficiently transition out of the default latent state (Thompson et al., 2009). Furthermore, we anticipated that due to the presence of 13 tandem direct repeats that contain multiple putative overlapping canonical Egr-1/Sp1 sites in the HSV-2 promoter, this promoter might exhibit altered kinetics for the transition into lytic infection from default latency.

The targeted replacement mutant displayed phenotypes consistent with these hypotheses. The type-2 sequences efficiently directed the exit from the default latent state and initiated productive viral replication in TG neurons. Indeed, earlier and more extensive disruption of the latent transcription program and entry into the lytic program was evident by 28 hpi (**Figure 8**), this increase in transition continued through time (**Figure 9**), increased and prolonged viral replication was observed in the CNS (**Figure 6**), and a significant increase in virulence resulted in reduced mouse survival (**Figure 7**). The

type-2 promoter mutants also displayed increased responsiveness to systemic stresses that induce reactivation *in vivo* (**Figure 10**).

The phenotypes displayed by the type-2 promoter mutants are robust, and our transition index and pathobiological assays are sensitive enough to permit us to determine the relative roles played by the 13 tandem Erg-1/Sp1 sites and/or other regulatory regions in *de novo* VP16 expression in both the HSV-1 and HSV-2 backgrounds. One advantage is that the putative Egr-1/Sp1 sites in HSV-2 are in the distal promoter and mutations will not affect mRNA structures. Such studies may help illuminate the signaling pathways that lead to acute viral replication in the PNS, as well as reactivation. This knowledge may help direct the design of safer live vaccine candidates or reveal potential targets for pharmacological interventions.

DATA AVAILABILITY

All datasets generated for this study are included in the manuscript.

ETHICS STATEMENT

This study was carried out in accordance with the recommendations of the Guide for the Care and Use of Laboratory Animals. The protocol was approved by the Children's Hospital Institutional Animal Care and Use Committee (protocol# IACUC2017-0081).

AUTHOR CONTRIBUTIONS

Both authors contributed equally to the ideas underlying the investigation, the experimental design, execution, interpretation of the data, and preparation of the manuscript.

FUNDING

This study was supported by National Institutes of Health, Allergy and Infectious Diseases (R01AI1093614).

REFERENCES

Ace, C. I., Dalrymple, M. A., Ramsay, F. H., Preston, V. G., and Preston, C. M. (1988). Mutational analysis of the herpes simplex virus type 1 trans-inducing factor Vmw65. *J. Gen. Virol.* 69, 2595–2605. doi: 10.1099/0022-1317-69-10-2595

Ace, C. I., McKee, T. A., Ryan, J. M., Cameron, J. M., and Preston, C. M. (1989). Construction and characterization of a herpes simplex virus type 1 mutant unable to transinduce immediate-early gene expression. *J. Virol.* 63, 2260–2269.

Aggarwal, A., Miranda-Saksena, M., Boadle, R. A., Kelly, B. J., Diefenbach, R. J., Alam, W., et al. (2012). Ultrastructural visualization of individual tegument protein dissociation during entry of herpes simplex virus 1 into human and rat dorsal root ganglion neurons. *J. Virol.* 86, 6123–6137. doi: 10.1128/JVI.07016-11

Antinone, S. E., and Smith, G. A. (2010). Retrograde axon transport of herpes simplex virus and pseudorabies virus: a live-cell comparative analysis. *J. Virol.* 84, 1504–1512. doi: 10.1128/JVI.02029-09

Batchelor, A. H., and O'Hare, P. (1990). Regulation and cell-type-specific activity of a promoter located upstream of the latency-associated transcript of herpes simplex virus type 1. *J. Virol.* 64, 3269–3279.

Bertke, A. S., Ma, A., Margolis, M. S., and Margolis, T. P. (2013). Different mechanisms regulate productive herpes simplex virus 1 (HSV-1) and HSV-2 infections in adult trigeminal neurons. *J. Virol.* 87, 6512–6516. doi: 10.1128/JVI.00383-13

Bloom, D. C., Giordani, N. V., and Kwiatkowski, D. L. (2010). Epigenetic regulation of latent HSV-1 gene expression. *Biochim. Biophys. Acta* 1799, 246–256. doi: 10.1016/j.bbagrm.2009.12.001

Bzik, D. J., and Preston, C. M. (1986). Analysis of DNA sequences which regulate the transcription of herpes simplex virus immediate early gene 3: DNA sequences required for enhancer-like activity and response to trans-activation by a virion polypeptide. *Nucleic Acids Res.* 14, 929–943. doi: 10.1093/nar/14.2.929

Campbell, M. E., Palfreyman, J. W., and Preston, C. M. (1984). Identification of herpes simplex virus DNA sequences which encode a trans-acting polypeptide responsible for stimulation of immediate early transcription. *J. Mol. Biol.* 180, 1–19. doi: 10.1016/0022-2836(84)90427-3

Carrasco-Serrano, C., Campos-Caro, A., Viniegra, S., Ballesta, J. J., and Criado, M. (1998). GC- and E-box motifs as regulatory elements in the proximal promoter region of the neuronal nicotinic receptor alpha7 subunit gene. *J. Biol. Chem.* 273, 20021–20028. doi: 10.1074/jbc.273.32.20021

Cliffe, A. R., Arbuckle, J. H., Vogel, J. L., Geden, M. J., Rothbart, S. B., Cusack, C. L., et al. (2015). Neuronal stress pathway mediating a histone methyl/phospho switch is required for herpes simplex virus reactivation. *Cell Host Microbe* 18, 649–658. doi: 10.1016/j.chom.2015.11.007

Cliffe, A. R., Garber, D. A., and Knipe, D. M. (2009). Transcription of the herpes simplex virus latency-associated transcript promotes the formation of facultative heterochromatin on lytic promoters. *J. Virol.* 83, 8182–8190. doi: 10.1128/JVI.00712-09

Cohen, C., Corpet, A., Roubille, S., Maroui, M. A., Poccardi, N., Rousseau, A., et al. (2018). Promyelocytic leukemia (PML) nuclear bodies (NBs) induce latent/quiescent HSV-1 genomes chromatinization through a PML NB/histone H3.3/H3.3 chaperone axis. *PLoS Pathog.* 14:e1007313. doi: 10.1371/journal.ppat.1007313

Contestabile, A. (2008). Regulation of transcription factors by nitric oxide in neurons and in neural-derived tumor cells. *Prog. Neurobiol.* 84, 317–328. doi: 10.1016/j.pneurobio.2008.01.002

Diefenbach, R. J., Miranda-Saksena, M., Douglas, M. W., and Cunningham, A. L. (2008). Transport and egress of herpes simplex virus in neurons. *Rev. Med. Virol.* 18, 35–51. doi: 10.1002/rmv.560

Ecob-Prince, M. S., Preston, C. M., Rixon, F. J., Hassan, K., and Kennedy, P. G. (1993). Neurons containing latency-associated transcripts are numerous and widespread in dorsal root ganglia following footpad inoculation of mice with herpes simplex virus type 1 mutant in1814. *J. Gen. Virol.* 74, 985–994. doi: 10.1099/0022-1317-74-6-985

Farrell, M. J., Margolis, T. P., Gomes, W. A., and Feldman, L. T. (1994). Effect of the transcription start region of the herpes simplex virus type 1 latency-associated transcript promoter on expression of productively infected neurons in vivo. *J. Virol.* 68, 5337–5343.

Hafezi, W., Lorentzen, E. U., Eing, B. R., Muller, M., King, N. J., Klupp, B., et al. (2012). Entry of herpes simplex virus type 1 (HSV-1) into the distal axons of trigeminal neurons favors the onset of nonproductive, silent infection. *PLoS Pathog.* 8:e1002679. doi: 10.1371/journal.ppat.1002679

Houston, P., Campbell, C. J., Svaren, J., Milbrandt, J., and Braddock, M. (2001). The transcriptional corepressor NAB2 blocks Egr-1-mediated growth factor activation and angiogenesis. *Biochem. Biophys. Res. Commun.* 283, 480–486. doi: 10.1006/bbrc.2001.4810

Kikin, O., D'Antonio, L., and Bagga, P. S. (2006). QGRS mapper: a web-based server for predicting G-quadruplexes in nucleotide sequences. *Nucleic Acids Res.* 34, W676–W682. doi: 10.1093/nar/gkl253

Kim, J. Y., Mandarino, A., Chao, M. V., Mohr, I., and Wilson, A. C. (2012). Transient reversal of episome silencing precedes VP16-dependent transcription during reactivation of latent HSV-1 in neurons. *PLoS Pathog.* 8:e1002540. doi: 10.1371/journal.ppat.1002540

Knipe, D. M. (2015). Nuclear sensing of viral DNA, epigenetic regulation of herpes simplex virus infection, and innate immunity. *Virology* 479–480, 153–159. doi: 10.1016/j.virol.2015.02.009

Knipe, D. M., and Cliffe, A. (2008). Chromatin control of herpes simplex virus lytic and latent infection. *Nat. Rev. Microbiol.* 6, 211–221. doi: 10.1038/nrmicro1794

Koyuncu, O. O., MacGibeny, M. A., Hogue, I. B., and Enquist, L. W. (2017). Compartmented neuronal cultures reveal two distinct mechanisms for alpha herpesvirus escape from genome silencing. *PLoS Pathog.* 13:e1006608. doi: 10.1371/journal.ppat.1006608

Koyuncu, O. O., Song, R., Greco, T. M., Cristea, I. M., and Enquist, L. W. (2015). The number of alphaherpesvirus particles infecting axons and the axonal protein repertoire determines the outcome of neuronal infection. *MBio* 6:e00276-15. doi: 10.1128/mBio.00276-15

Kozak, M. (1987). An analysis of 5′-noncoding sequences from 699 vertebrate messenger RNAs. *Nucleic Acids Res.* 15, 8125–8148. doi: 10.1093/nar/15.20.8125

Kramer, M. F., Chen, S. H., Knipe, D. M., and Coen, D. M. (1998). Accumulation of viral transcripts and DNA during establishment of latency by herpes simplex virus. *J. Virol.* 72, 1177–1185.

Kristie, T. M. (2015). Dynamic modulation of HSV chromatin drives initiation of infection and provides targets for epigenetic therapies. *Virology* 479–480, 555–561. doi: 10.1016/j.virol.2015.01.026

Kristie, T. M., and Roizman, B. (1987). Host cell proteins bind to the cis-acting site required for virion-mediated induction of herpes simplex virus 1 alpha genes. *Proc. Natl. Acad. Sci. USA* 84, 71–75.

Kumbrink, J., Gerlinger, M., and Johnson, J. P. (2005). Egr-1 induces the expression of its corepressor nab2 by activation of the nab2 promoter thereby establishing a negative feedback loop. *J. Biol. Chem.* 280, 42785–42793. doi: 10.1074/jbc.M511079200

Kwiatkowski, D. L., Thompson, H. W., and Bloom, D. C. (2009). The polycomb group protein Bmi1 binds to the herpes simplex virus 1 latent genome and maintains repressive histone marks during latency. *J. Virol.* 83, 8173–8181. doi: 10.1128/JVI.00686-09

Lachmann, R. H., and Efstathiou, S. (1997). Utilization of the herpes simplex virus type 1 latency-associated regulatory region to drive stable reporter gene expression in the nervous system. *J. Virol.* 71, 3197–3207.

Leppek, K., Das, R., and Barna, M. (2018). Functional 5′ UTR mRNA structures in eukaryotic translation regulation and how to find them. *Nat. Rev. Mol. Cell Biol.* 19, 158–174. doi: 10.1038/nrm.2017.103

Lieu, P. T., and Wagner, E. K. (2000). Two leaky-late HSV-1 promoters differ significantly in structural architecture. *Virology* 272, 191–203. doi: 10.1006/viro.2000.0365

Liu, M., Wang, X., Peng, Y., Shen, S., and Li, G. (2014). Egr-1 regulates the transcription of NGX6 gene through a Sp1/Egr-1 overlapping site in the promoter. *BMC Mol. Biol.* 15:14. doi: 10.1186/1471-2199-15-14

Lu, X., and Triezenberg, S. J. (2010). Chromatin assembly on herpes simplex virus genomes during lytic infection. *Biochim. Biophys. Acta* 1799, 217–222. doi: 10.1016/j.bbagrm.2009.08.004

Margolis, T. P., Imai, Y., Yang, L., Vallas, V., and Krause, P. R. (2007). Herpes simplex virus type 2 (HSV-2) establishes latent infection in a different population of ganglionic neurons than HSV-1: role of latency-associated transcripts. *J. Virol.* 81, 1872–1878. doi: 10.1128/JVI.02110-06

Margolis, T. P., Sedarati, F., Dobson, A. T., Feldman, L. T., and Stevens, J. G. (1992). Pathways of viral gene expression during acute neuronal infection with HSV-1. *Virology* 189, 150–160. doi: 10.1016/0042-6822(92)90690-Q

Maroui, M. A., Calle, A., Cohen, C., Streichenberger, N., Texier, P., Takissian, J., et al. (2016). Latency entry of herpes simplex virus 1 is determined by the interaction of its genome with the nuclear environment. *PLoS Pathog.* 12:e1005834. doi: 10.1371/journal.ppat.1005834

McGeoch, D. J., Dalrymple, M. A., Davison, A. J., Dolan, A., Frame, M. C., McNab, D., et al. (1988). The complete DNA sequence of the long unique region in the genome of herpes simplex virus type 1. *J. Gen. Virol.* 69, 1531–1574. doi: 10.1099/0022-1317-69-7-1531

Miranda-Saksena, M., Armati, P., Boadle, R. A., Holland, D. J., and Cunningham, A. L. (2000). Anterograde transport of herpes simplex virus type 1 in cultured, dissociated human and rat dorsal root ganglion neurons. *J. Virol.* 74, 1827–1839. doi: 10.1128/JVI.74.4.1827-1839.2000

Nicoll, M. P., Hann, W., Shivkumar, M., Harman, L. E., Connor, V., Coleman, H. M., et al. (2016). The HSV-1 latency-associated transcript functions to repress latent phase lytic gene expression and suppress virus reactivation from latently infected neurons. *PLoS Pathog.* 12:e1005539. doi: 10.1371/journal.ppat.1005539

Nitsch, R. M., Rossner, S., Albrecht, C., Mayhaus, M., Enderich, J., Schliebs, R., et al. (1998). Muscarinic acetylcholine receptors activate the acetylcholinesterase gene promoter. *J. Physiol. Paris* 92, 257–264. doi: 10.1016/S0928-4257(98)80029-6

Ooe, N., Saito, K., Mikami, N., Nakatuka, I., and Kaneko, H. (2004). Identification of a novel basic helix-loop-helix-PAS factor, NXF, reveals a Sim2 competitive, positive regulatory role in dendritic-cytoskeleton modulator drebrin gene expression. *Mol. Cell. Biol.* 24, 608–616. doi: 10.1128/mcb.24.2.608-616.2004

Perry, L. J., and McGeoch, D. J. (1988). The DNA sequences of the long repeat region and adjoining parts of the long unique region in the genome of herpes simplex virus type 1. *J. Gen. Virol.* 69, 2831–2846. doi: 10.1099/0022-1317-69-11-2831

Rhodes, D., and Lipps, H. J. (2015). G-quadruplexes and their regulatory roles in biology. *Nucleic Acids Res.* 43, 8627–8637. doi: 10.1093/nar/gkv862

Roizman, B., Zhou, G., and Du, T. (2011). Checkpoints in productive and latent infections with herpes simplex virus 1: conceptualization of the issues. *J. Neurovirol.* 17, 512–517. doi: 10.1007/s13365-011-0058-x

Sawtell, N. M. (2003). Quantitative analysis of herpes simplex virus reactivation in vivo demonstrates that reactivation in the nervous system is not inhibited at early times postinoculation. *J. Virol.* 77, 4127–4138. doi: 10.1128/JVI.77.7.4127-4138.2003

Sawtell, N. M. (2005). Detection and quantification of the rare latently infected cell undergoing herpes simplex virus transcriptional activation in the nervous system in vivo. *Methods Mol. Biol.* 292, 57–72. doi: 10.1385/1-59259-848-X:057

Sawtell, N. M., and Thompson, R. L. (1992a). Herpes simplex virus type 1 latency-associated transcription unit promotes anatomical site-dependent establishment and reactivation from latency. *J. Virol.* 66, 2157–2169.

Sawtell, N. M., and Thompson, R. L. (1992b). Rapid in vivo reactivation of herpes simplex virus in latently infected murine ganglionic neurons after transient hyperthermia. *J. Virol.* 66, 2150–2156.

Sawtell, N. M., and Thompson, R. L. (2014). Herpes simplex virus mutant generation and dual-detection methods for gaining insight into latent/lytic cycles in vivo. *Methods Mol. Biol.* 1144, 129–147. doi: 10.1007/978-1-4939-0428-0_9

Sawtell, N. M., and Thompson, R. L. (2016a). De novo herpes simplex virus VP16 expression gates a dynamic programmatic transition and sets the latent/lytic balance during acute infection in trigeminal ganglia. *PLoS Pathog.* 12:e1005877. doi: 10.1371/journal.ppat.1005877

Sawtell, N. M., and Thompson, R. L. (2016b). Herpes simplex virus and the lexicon of latency and reactivation: a call for defining terms and building an integrated collective framework. *F1000Res* 5, F1000 Faculty Rev-2038. doi: 10.12688/f1000research.8886.1

Sawtell, N. M., Thompson, R. L., and Haas, R. L. (2006). Herpes simplex virus DNA synthesis is not a decisive regulatory event in the initiation of lytic viral protein expression in neurons in vivo during primary infection or reactivation from latency. *J. Virol.* 80, 38–50. doi: 10.1128/jvi.80.1.38-50.2006

Sawtell, N. M., Triezenberg, S. J., and Thompson, R. L. (2011). VP16 serine 375 is a critical determinant of herpes simplex virus exit from latency in vivo. *J. Neurovirol.* 17, 546–551. doi: 10.1007/s13365-011-0065-y

Sloan, E., Tatham, M. H., Groslambert, M., Glass, M., Orr, A., Hay, R. T., et al. (2015). Analysis of the SUMO2 proteome during HSV-1 infection. *PLoS Pathog.* 11:e1005059. doi: 10.1371/journal.ppat.1005059

Smith, G. (2012). Herpesvirus transport to the nervous system and back again. *Annu. Rev. Microbiol.* 66, 153–176. doi: 10.1146/annurev-micro-092611-150051

Stern, S., Tanaka, M., and Herr, W. (1989). The Oct-1 homoeodomain directs formation of a multiprotein-DNA complex with the HSV transactivator VP16. *Nature* 341, 624–630. doi: 10.1038/341624a0

Thompson, R. L., Preston, C. M., and Sawtell, N. M. (2009). De novo synthesis of VP16 coordinates the exit from HSV latency in vivo. *PLoS Pathog.* 5:e1000352. doi: 10.1371/journal.ppat.1000352

Thompson, R. L., and Sawtell, N. M. (2000). Replication of herpes simplex virus type 1 within trigeminal ganglia is required for high frequency but not high viral genome copy number latency. *J. Virol.* 74, 965–974. doi: 10.1128/JVI.74.2.965-974.2000

Thompson, R. L., and Sawtell, N. M. (2006). Evidence that the herpes simplex virus type 1 ICP0 protein does not initiate reactivation from latency in vivo. *J. Virol.* 80, 10919–10930. doi: 10.1128/JVI.01253-06

Thompson, R. L., and Sawtell, N. M. (2010). Therapeutic implications of new insights into the critical role of VP16 in initiating the earliest stages of HSV reactivation from latency. *Future Med. Chem.* 2, 1099–1105. doi: 10.4155/fmc.10.197

Thompson, R. L., Shieh, M. T., and Sawtell, N. M. (2003). Analysis of herpes simplex virus ICP0 promoter function in sensory neurons during acute infection, establishment of latency, and reactivation in vivo. *J. Virol.* 77, 12319–12330. doi: 10.1128/JVI.77.22.12319-12330.2003

Thompson, R. L., Wagner, E. K., and Stevens, J. G. (1983). Physical location of a herpes simplex virus type-1 gene function(s) specifically associated with a 10 million-fold increase in HSV neurovirulence. *Virology* 131, 180–192. doi: 10.1016/0042-6822(83)90544-5

Watson, Z. L., Washington, S. D., Phelan, D. M., Lewin, A. S., Tuli, S. S., Schultz, G. S., et al. (2018). In vivo knockdown of the herpes simplex virus 1 latency-associated transcript reduces reactivation from latency. *J. Virol.* 92:e00812-18. doi: 10.1128/JVI.00812-18

Weirauch, M. T., Yang, A., Albu, M., Cote, A. G., Montenegro-Montero, A., Drewe, P., et al. (2014). Determination and inference of eukaryotic transcription factor sequence specificity. *Cell* 158, 1431–1443. doi: 10.1016/j.cell.2014.08.009

Woods, S. L., and Whitelaw, M. L. (2002). Differential activities of murine single minded 1 (SIM1) and SIM2 on a hypoxic response element. Cross-talk between basic helix-loop-helix/per-Arnt-Sim homology transcription factors. *J. Biol. Chem.* 277, 10236–10243. doi: 10.1074/jbc.M110752200

Wu, W. S., You, R. I., Cheng, C. C., Lee, M. C., Lin, T. Y., and Hu, C. T. (2017). Snail collaborates with EGR-1 and SP-1 to directly activate transcription of MMP 9 and ZEB1. *Sci. Rep.* 7:17753. doi: 10.1038/s41598-017-18101-7

Wysocka, J., and Herr, W. (2003). The herpes simplex virus VP16-induced complex: the makings of a regulatory switch. *Trends Biochem. Sci.* 28, 294–304. doi: 10.1016/S0968-0004(03)00088-4

Yang, L., Voytek, C. C., and Margolis, T. P. (2000). Immunohistochemical analysis of primary sensory neurons latently infected with herpes simplex virus type 1. *J. Virol.* 74, 209–217. doi: 10.1128/JVI.74.1.209-217.2000

Conflict of Interest Statement: The authors declare that the research was conducted in the absence of any commercial or financial relationships that could be construed as a potential conflict of interest.

frontiers in Microbiology

REVIEW
published: 24 July 2019
doi: 10.3389/fmicb.2019.01634

Modeling Varicella Zoster Virus Persistence and Reactivation – Closer to Resolving a Perplexing Persistent State

*Lillian Laemmle[1], Ronald S. Goldstein[2] and Paul R. Kinchington[1,3]**

[1] Department of Ophthalmology, University of Pittsburgh, Pittsburgh, PA, United States, [2] Faculty of Life Sciences, Bar Ilan University, Ramat Gan, Israel, [3] Department of Molecular Microbiology and Genetics, University of Pittsburgh, Pittsburgh, PA, United States

The latent state of the human herpesvirus varicella zoster virus (VZV) has remained enigmatic and controversial. While it is well substantiated that VZV persistence is established in neurons after the primary infection (varicella or chickenpox), we know little of the types of neurons harboring latent virus genomes, if all can potentially reactivate, what exactly drives the reactivation process, and the role of immunity in the control of latency. Viral gene expression during latency has been particularly difficult to resolve, although very recent advances indicate that it is more restrictive than was once thought. We do not yet understand how genes expressed in latency function in the maintenance and reactivation processes. Model systems of latency are needed to pursue these questions. This has been especially challenging for VZV because the development of *in vivo* models of VZV infection has proven difficult. Given that up to one third of the population will clinically reactivate VZV to develop herpes zoster (shingles) and suffer from its common long term problematic sequelae, there is still a need for both *in vivo* and *in vitro* model systems. This review will summarize the evolution of models of VZV persistence and address insights that have arisen from the establishment of new *in vitro* human neuron culture systems that not only harbor a latent state, but permit experimental reactivation and renewed virus production. These models will be discussed in light of the recent data gleaned from the study of VZV latency in human cadaver ganglia.

Keywords: varicella zoster virus, latency, reactivation, animal models, human neuron culture models

OPEN ACCESS

Edited by:
Randall J. Cohrs, University of Colorado Denver, United States

Reviewed by:
Ilhem Messaoudi, University of California, Irvine, United States
Andrew Bubak, University of Colorado Anschutz Medical Campus, United States
Allison Abendroth, University of Sydney, Australia

****Correspondence:***
Paul R. Kinchington
kinchingtonp@upmc.edu

Specialty section:
This article was submitted to Microbial Physiology and Metabolism, a section of the journal Frontiers in Microbiology

Received: *20 March 2019*
Accepted: *02 July 2019*
Published: *24 July 2019*

Citation:
Laemmle L, Goldstein RS and Kinchington PR (2019) Modeling Varicella Zoster Virus Persistence and Reactivation – Closer to Resolving a Perplexing Persistent State. Front. Microbiol. 10:1634. doi: 10.3389/fmicb.2019.01634

INTRODUCTION

Varicella zoster virus (VZV) is a common and ubiquitous human-restricted neurotropic alphaherpesvirus of the *Herpesviridae* family that persists for life in the host after a primary infection (varicella or chickenpox). The site of latency is within neurons in ganglia of the peripheral somatic, autonomic, and enteric (Gershon and Gershon, 2018) nervous systems. Up to one third of infected individuals will clinically reactivate VZV in their lifetimes, usually in their elderly years when immunity is naturally senescing, or when immunity is suppressed by disease or iatrogenic cause. The most common clinical sign of reactivation is herpes zoster (HZ), manifested as a dermatome-limited, painful vesicular skin rash that causes greater morbidity than varicella with frequent complications. VZV reactivation may also underlie a variety of neurological

(Gilden et al., 2015), vascular (Nagel et al., 2017), and gastrointestinal diseases (Gershon and Gershon, 2018) that may occur with or without rash.

A greater understanding of the events occurring during VZV latency and early reactivation may reveal targets and strategies for novel therapeutics that treat or prevent HZ. However, VZV shows a high degree of host specificity, which has precluded most small animal modeling of VZV disease. There is arguably still no *in vivo* model of reactivated disease. A possible exception for the growth restriction of VZV in small animals is the guinea pig, discussed below. Many insights have come from study of the VZV-related Simian Varicella Virus (SVV), which replicates in several macaque species and African green monkeys, but SVV is a distinct virus that may not completely model all aspects of VZV. There are also significant financial and ethical issues associated with primate research. The relevance of the SVV model to VZV was recently reviewed (Sorel and Messaoudi, 2018).

A second issue that has made VZV persistence difficult to understand is the difficulty in interpreting studies of VZV-infected human cadaveric ganglia. We are now more cognizant that a partial viral gene expression program occurs throughout the post mortem interval (PMI) (Cohrs and Gilden, 2003; Ouwendijk et al., 2012). Early reports suggesting that VZV proteins were made during latency were subsequently complicated by staining artifacts or antibody cross-reactivity to blood group A1 antigens (Zerboni et al., 2012). Very recent work indicates VZV latent transcription is highly restricted in ganglia obtained with short PMI (Depledge et al., 2018a). Even with short PMI, cadaver ganglia rapidly undergo hypoxia that may induce death-induced spurious transcription. Importantly, we are not aware of any report of VZV virus production obtained from latently infected cadaveric ganglia explants. This contrasts to HSV-1, which readily produces virus from human axotomized ganglia (Lewis et al., 1982).

A third block to study of VZV latency is that, despite the efforts of many virologists, VZV remains a difficult virus to work with. Virus replicates inefficiently in a limited number of human cell lines, produces virus with high particle to infectivity ratios, and releases little to no infectious virus from cultured cells. Titers of cell-free virus released from infected cell sonicates are on the order of five magnitudes lower than that which can be obtained for HSV-1. As such, most experimental infections are initiated with infected cells. As detailed below, this is an important issue in the new stem cell-derived neuronal models of reactivatable latency, because persistence has not yet been obtained with cell-associated infection, but rather requires cell-free virus. Intriguingly, recent work suggests that cultured human neurons do release some infectious virus (Markus et al., 2011; Sadaoka et al., 2018).

This review complements other recent reviews of the current state of understanding of VZV latency from studies of cadaver ganglia (Depledge et al., 2018b) and *in vitro* models (Baird et al., 2019). We restrict this review to human VZV and discuss the potential of models that may be revisited in the near future, particularly in light of recent discoveries.

HUMAN VZV DISEASE

Primary varicella (chicken pox) is easily spread in unvaccinated Westernized populations, usually during childhood, by the inhalation of aerosolized droplets from individuals with varicella or active zoster. This exposure establishes primary replication sites in the upper respiratory mucosa and respiratory lymphoid tissues such as the tonsils, where lymphocytes become infected (Ku et al., 2005). VZV infected $CD4^+$ T cells are considered to be a predominant vehicle for systemic spread (Ku et al., 2005), but other circulating cells have been implicated in the viremia, including dendritic cells, monocytes and macrophages (Kennedy et al., 2019). Immune cells carrying VZV home to the skin and extravasate, seeding sites of virus infection at the deep dermal skin layers and hair follicles (Ku et al., 2002). Virus accesses peripheral innervating ganglia by infecting axons in the skin, followed by retrograde transport down axons to neuronal soma. Evidence from the SVV model suggests that ganglia are also directly infected by ganglion-infiltrating VZV-infected T cells at the viremic stage (Sorel and Messaoudi, 2018), allowing infection of ganglia that do not necessarily innervate the periphery, such as those of the enteric nervous system (Ku et al., 2002; Chen et al., 2003, 2011; Gershon et al., 2008). In the 14–21 days incubation period, VZV replication in the skin is partly controlled by innate immune mechanisms, including type 1 IFNs (Zerboni et al., 2014). Lesions then develop in the epidermis, concurrent with the onset of adaptive immunity that not only clears virus and infected tissues, but also protects against further varicella disease.

Reactivation leading to HZ occurs in about one third of those harboring latent VZV in their lifetimes. While the molecular triggers of VZV reactivation are not well understood, there are clear contributing factors that predispose to HZ development, including host genetics (Crosslin et al., 2015). The role of immunity in reactivation was established by the classic studies of Hope-Simpson (Hope-Simpson, 1967), and is evidenced by the fact that HZ rates are higher in those with immune modifying diseases such as HIV infection, or undergoing treatments that reduce cellular immune function. HZ incidence rises rapidly after age 60 years, and this may partially reflect a naturally senescing cellular immunity (Donahue et al., 1995). Clinical zoster probably requires both intracellular events in the host neuron that influence viral chromatin, as well as a failure in surveillance/protection by VZV-specific cellular immunity. The large lesions of HZ are clinically distinct from varicella in that they are usually topographically restricted to a skin region innervated by a single ganglion, termed a dermatome. The extensive lesions reflect the intra-ganglionic spread of virus after reactivation and the delivery to the skin by multiple neurons in a reactivating ganglion. It is not yet clear if reactivation originates from a single neuron or from multiple neurons triggered in parallel, nor is it clear if intra-ganglionic spread triggers sequential reactivation from other latently infected neurons in the same ganglia.

Zoster is frequently complicated by scarring and bacterial superinfection, but the most common complication is pain. Most individuals with zoster seek medication for pain, but a significant fraction progress to debilitating chronic pain states termed post

herpetic neuralgia (PHN). PHN may last months to years after the skin lesions have resolved and is often refractory to therapy. This is consistent with PHN reflecting neuronal events downstream of VZV replication and clearance after reactivation (Gershon, 1996). Reactivation causes massive inflammatory responses in the ganglia that may change neuron function, pain signaling and neuronal activity, but these transitions are poorly understood. A review of neurobiological models of PHN was recently published (Devor, 2018).

VACCINATION

The observation that adaptive immunity protects individuals from further varicella stimulated the development of successful vaccines. The FDA-approved live attenuated varicella vaccine (Varivax in the United States) has been in widespread use in the United States since the mid-1990s as a two-dose regimen. It is based on a VZV strain (vOka) that was attenuated by sequential passage in embryonic guinea pig fibroblasts. The vaccine strain is genetically heterogeneous, containing some fixed mutations and variable levels of other mutations and combinations thereof (Depledge et al., 2014; Quinlivan and Breuer, 2014). Varivax is administered to most United States preschool children and has dramatically reduced the number of varicella cases in the United States, as well as hospitalizations and deaths from it. However, many countries do not widely use the varicella vaccine, and even in the United States, most adults still harbor wild-type VZV with the potential to reactivate. The first individuals who received Varivax will not turn 60 years, the age when HZ incidence rises, until around 2050. The live vaccine retains the ability to establish latency and reactivate, albeit at very low levels (Hardy et al., 1991; Quinlivan et al., 2012).

Two FDA-approved HZ vaccines are available to boost VZV-specific adaptive immunity in those at risk for HZ. Zostavax is a 14 times larger infectious dose of the attenuated varicella vaccine that was licensed in 2006, and reduces HZ incidence by about half, and the burden of illness by two thirds (Oxman et al., 2005). The more recent Shingrix vaccine was FDA licensed in 2018 and is a subunit vaccine based on the VZV gE glycoprotein. It has higher efficacy than Zostavax in preventing HZ using a two-dose regimen (Cunningham et al., 2016). Both vaccines are under-utilized in the target population due to perceived lack of efficacy, cost, ignorance of the target population to HZ severity, and vaccine shortages (Harpaz and Leung, 2017).

DEFINITION OF THE VZV LATENT STATE

We consider it important to define "latency." Herpesvirus lytic infections involve the organized and regulated expression of most viral genes and proteins, the replication of the DNA genome, and the assembly and egress of progeny virus for spread and transmission. VZV latency is often defined as the persistence of viral genomes without virus production, in an endless or episomal form (Clarke et al., 1995) as seen for the latent state of all other herpesviruses. However, this definition may be inadequate: it does not separate reactivatable latency from an abortive infection in which genomes are maintained (perhaps due to a feature of the host cell, the neuron) that cannot complete a lytic cycle due to absence of factors required for full lytic growth. Human VZV latency is perhaps a mixture of both states as the vast majority of maintained genomes will never undergo a reactivation event. This scenario was highlighted in studies on the murine neuronal model of HSV-1 latency, where hundreds to thousands of genomes are maintained in multiple types of neurons, including some subtypes that do not appear to be capable of supporting productive infection (Bertke et al., 2011). We highlight this issue because most small animal models do not appear to support full VZV replication. Are the genomes present in such models stalled by the non-permissive state, and is this different from that in humans? We propose latency should be defined as the *reversible* persistence of non-productive viral genomes, since reactivation demonstrates maintained genome functionality.

A second issue is the silencing of genome expression during latency. Are viral RNAs or proteins made during the latent state? This question is of considerable interest, because any viral product made during latency could be potentially targeted by therapeutic strategies. Again, we turn to the more extensively studied HSV-1 as a guide. In HSV latency, expression is predominantly silenced by chromatin on the genome (Bloom et al., 2010). The exception is the non-coding transcripts termed Latency-Associated Transcripts or LAT (see below). However, HSV-1 latency is not necessarily antigenically silent, because latently infected ganglia in animal models (Knickelbein et al., 2008) and in humans (van Velzen et al., 2013) are associated with recently activated virus-specific $CD8^+$ T cells. In the well characterized HSV-1 murine model, accumulated work suggests that ganglionic T cells may control reactivation events after viral antigen recognition, acting through non-cytolytic mechanisms (Decman et al., 2005; Knickelbein et al., 2008). Such antigens arise through a dynamic state of repression during latency. An attractive model has proposed that HSV-1 reactivation involves a two-stage de-repression process, with the first stage being reversible to the silent latent state (Kim et al., 2012). The initial de-repression is driven by reactivation stimuli that alter chromatin states and drive a transient expression of viral proteins outside the typical lytic cascade. This state may or may not progress to a typical lytic-regulated cascade and virus production, or may reverse to quiescence, depending on the functional expression and cellular localization of viral factors initiating the lytic cascade. This two-step model of de-repression fits with the proposed role of ganglion-resident T cells in monitoring gene expression in the ganglia. Resident T-cells would be rapidly activated in response to renewed viral protein expression, and act using non-cytotoxic mechanisms that favor re-entry into latency (St Leger and Hendricks, 2011).

For VZV, a new picture is emerging that suggests that VZV gene expression during human latency is more limited than was once thought (Cohrs and Gilden, 2003; Ouwendijk et al., 2012; Zerboni et al., 2012). Using unbiased Illumina next generation sequencing methods coupled with Agilent's SureSelect template enrichment of VZV RNA from human ganglia obtained with

short PMI times, only two VZV transcripts were detected (Depledge et al., 2018a). Low levels of mRNA from ORF63 were observed confirming previous reports, but a more abundant transcript termed VZV Latency-associated Transcript (VLT) was mapped to the VZV region encoding ORF61, but from the antisense strand. This extensively spliced transcript extends into and past ORF61, a gene that encodes a key transcriptional regulator with E3 ubiquitin ligase activities (Wang et al., 2011; Zhu et al., 2011). The authors proposed that VLT works in an antisense manner to regulate ORF61, but it is not clear if this occurs in the context of VZV infection or latency. However, the VLT genomic position and direction are conserved with the latency-associated transcripts made by SVV, HSV-1, bovine herpesvirus type 1, and indeed, perhaps all neuronal alphaherpesviruses, raising the interesting concept of conserved functionality as these viruses have diverged. VZV VLT spliced RNA potentially encodes a short protein, a feature that is not fully conserved in these viruses; for example, while the vLAT of bovine herpesvirus encodes a protein, HSV-1 LAT does not. However, HSV LAT does encode miRNAs (Umbach et al., 2008). Intriguingly, two small non-coding RNAs found in VZV-infected cells, snc13 and snc14, map to the unspliced VLT RNA (Markus et al., 2017). It has been suggested that VZV ORF63 protein regulates apoptosis in neurons (Hood et al., 2006), an activity attributed to both the HSV LAT RNA and the BHV LAT protein (Jones, 2013). While these are exciting findings, we argue that some caution is still needed. Even a short term post mortem event cannot be avoided in human studies, and we do not know if all persisting VZV genomes express these transcripts. A similar transcript found in macaques latently infected with SVV with no PMI suggests VLT is authentic (Sorel and Messaoudi, 2018). Many questions still remain. Are VZV VLT and/or ORF63 RNA functionally involved in the establishment and/or maintenance of VZV latency? If so, how do they function? Is VLT made in animal models harboring VZV genomes? Are these RNAs made in all neurons hosting a VZV genome? We argue that a solid model of latency and reactivation is needed to address these issues.

IN VIVO MODELS OF VZV LATENCY

No small animal model recapitulates human disease, even after administration of high levels of VZV infectious units. Animals often seroconvert, but this is not surprising given the antigen in the cell-associated inoculates. Here, we discuss attempts at developing a model of VZV persistence and discuss those that may be re-evaluated in light of the new picture of human VZV latency transcription (summarized in **Table 1**).

Mice and Rats

Immunocompetent mice have not been widely used to study VZV latency and evidence indicates they do not support VZV replication. VZV introduced to the cornea by intrastromal placement of infected cells resulted in virus DNA reaching the TG (Wroblewska et al., 1993) but no clinical sign of infection was seen. VZV DNA in nervous tissues was seen by PCR at 33 days post infection. The refractory nature of the mouse to VZV suggests an abortive infection, where VZV enters axons at the site of inoculation and undergoes retrograde transport to the ganglia but is unable to complete the full lytic cycle. Restriction of VZV replication was also seen in Chinese hamster cell lines (Finnen et al., 2006) and rat primary cultures (Guedon et al., 2015). Severely compromised immune deficient mice show no evidence of VZV replication except in implanted human tissue (Moffat et al., 1998).

A similar situation appears to occur in rats. Multiple subcutaneous inoculations of VZV-infected human cells along the rat spine (Sadzot-Delvaux et al., 1990, 1995) did not lead to any clinical signs out to 9 months, but VZV DNA was detected in ganglia. No infectious virus was recovered from dissociated DRG cultures, although they did report live virus recovery after multiple rounds of ganglionic co-culture with VZV permissive MRC5 cells. Other groups have seen VZV DNA and, in some cases, RNA in rat ganglia corresponding to infected sites (Annunziato et al., 1998; Kennedy et al., 2001). The Sadzot-Delvaux group were the first to suggest ORF63 as a "latency associated gene" (Debrus et al., 1995). Brunell et al. (1999) studied VZV inoculated neonatal rats and detected RNA for the once-proposed "latency associated gene" from ORF21. It appears that these models have not been further developed.

Some attention was given to the outbred cotton rat, since it is more permissive for several human-specific viruses (Faith et al., 1997; Niewiesk et al., 1997; Langley et al., 1998). VZV was reported to replicate in cotton rat fibroblast cultures, but it has never been clear if VZV replicates *in vivo*. Cell-associated VZV inoculated by intramuscular or subcutaneous routes along the spine does lead to detectable levels of VZV DNA at ganglia and expression of ORF63 RNA. The model was extensively developed to assess the genetic requirements and ganglionic delivery of viral DNA, including several genes that are considered essential or near critical for lytic replication of VZV (Sato et al., 2002a). VZV genes deemed not to be required for DNA delivery to the ganglia included ORF61 (Sato et al., 2002b) and ORF17 (Sato et al., 2002a), both of which severely impair VZV growth when deleted. Surprisingly, DNA from VZV deleted for the essential ORF21 (Xia et al., 2003) was still delivered to ganglia. However, in these studies, the virus was inoculated in the complementing cells, so that functional virus was produced and able to infect axons for ganglionic delivery. In contrast, VZV mutants lacking the essential genes ORF63, ORF4 and ORF29 genes were considered deficient for ganglionic delivery of viral DNA in this model (Cohen et al., 2005a,b, 2007), but viruses were passaged once in non-complementing cells before inoculation. The mechanisms underlying these results are not clear, but fit with a model that as long as VZV is produced in the cell-associated inoculum, it can infect axons and reach the ganglia. The single pass of VZV in non-complementing cells before inoculation for the ORF63, 4 and 29 mutant studies would have resulted in a stalled infection and no virus production. Only one study did not fit this model, and reported that several recombinant VZV with alterations of portions of the ORF62 and ORF63 genes and the 3′ genome region could replicate in culture, but were deficient in ganglionic delivery of genomes (Ambagala et al., 2010).

TABLE 1 | Permissivity of currently available *in vivo* and *in vitro* systems for modeling VZV infection, latency, and reactivation.

Model	DNA in infected tissue	DNA in neurons/ ganglia	RNA	Protein	Replication	Spread	Latency/ Quiescence	Reactivation
In vivo								
Mice	✓	✓						
Rat	✓	✓	✓					
Cotton rat	✓	✓	✓					
Guinea pig*	✓	✓	✓	✓	✓	✓	✓	?
SCID-hu mouse/human xenograft†	✓	✓	✓	✓	✓	✓	✓	
In vitro								
Rat primary/progenitor cells	✓	✓	✓					
Immortalized human neuron-like cells	✓	✓	✓	✓	✓	✓		
Differentiated human neural progenitor lines	✓	✓	✓	✓	✓	✓		
hiPSC-derived neurons	✓	✓	✓	✓	✓	✓		
hESC-derived neurons	✓	✓	✓	✓	✓	✓	✓	✓

*While many models support VZV infection and limited viral RNA and protein expression programs, VZV replication and spread are limited to guinea pigs and human cells that are permissive for the full lytic virus life cycle. hESC-derived neurons are the only model in which experimental reactivation of a quiescent VZV infection has been reliably achieved. It has been claimed that the guinea pig model supports experimental reactivation. *Most studies use guinea pig adapted VZV. †In human tissue graft.*

We highlight that neither *in vivo* replication nor reactivation in the cotton rat has been demonstrated. The maintenance of viral DNA in rat ganglia is consistent with VZV entry into rat cells (and neuronal axons) without need for complete replication (Guedon et al., 2015). It will be interesting to determine if VLT is made in rat models, particularly since Wistar and Sprague Dawley rats develop prolonged behavioral signs of VZV-induced mechanical hypersensitivity (Fleetwood-Walker et al., 1999; Dalziel et al., 2004; Garry et al., 2005; Hasnie et al., 2007; Guedon et al., 2014, 2015; Kramer et al., 2017; Stinson et al., 2017).

Guinea Pig

The guinea pig appears different from rats and mice because it can support a productive VZV infection, particularly with VZV adapted by passage in primary guinea pig embryo or kidney fibroblast cultures. Guinea pig cells are known to be one of the few non-primate lines to support VZV replication, and the vaccine (vOka) was attenuated by serial passaging in guinea pig embryonic fibroblasts. The genetic changes in vOka that are associated with adaption are many, including several in the gene encoding IE62, the key *trans*-activator of gene expression (Wu et al., 2019). Early work reported VZV infection of both adult and weanling guinea pigs (Myers et al., 1980, 1985, 1991; Lowry et al., 1993), resulting in a viremia and seroconversion after nasal inoculation (Matsunaga et al., 1982). Viral transmission to cohoused animals based on seroconversion was also indicated, but animals did not exhibit observable clinical symptoms (Myers et al., 1980, 1985). The guinea pig model was used extensively in the early characterization of the cellular immune response to VZV (Jenski and Myers, 1987) and the predominant viral antigenic targets (Lowry et al., 1992, 1993, 1997; Sabella et al., 1993). After infection, VZV DNA is detected in ganglionic tissues, but evidence of *in vivo* reactivation was lacking, even after treatment with immunosuppression regimens. One report indicates that VZV in newborn hairless guinea pigs induced a short-term skin exanthem (Myers et al., 1991). The guinea pig was also developed as an ocular infection model. Following intrastromal inoculation, VZV could be recovered from TG, midbrain, and cerebellum by co-culture with permissive cells (Pavan-Langston and Dunkel, 1989). Others have found no signs of disease or infection after corneal inoculation (Matsunaga et al., 1982).

There is renewed interest in the guinea pig for modeling VZV infection and persistence in the enteric nervous system. Enteric forms of zoster in humans have now been observed (Pui et al., 2001; Chen et al., 2003, 2011; Edelman et al., 2010; Masood et al., 2015; Gershon and Gershon, 2018). Cultures comprised mostly of enteric primary afferent neurons derived from adult hosts can support a lytic VZV infection after cell-associated inoculation, yet retained VZV DNA long term after cell-free virus infection. However, a rather wide gene expression pattern was reported, with expression of multiple viral genes during persistence, including from ORFs 4, 21, 29, 40, 62, and 63. This gene expression is more extensive than seen in human cadaver ganglia, and occurs presumably with no PMI. Some protein expression was reported as "mislocated" in the cytoplasm (Chen et al., 2003; Gershon et al., 2008). However, long term VZV DNA-positive *in vitro* neuron cultures could produce infectious virus when infected with replication defective adenoviruses expressing VZV ORF61 or the HSV ortholog ICP0. This establishes functionality of the persisting genome, albeit using a non-physiological stimulus. The model has developed in parallel with data indicating VZV persistence in the human enteric nervous system (Gershon and Gershon, 2018). Resected intestinal tissues from VZV seropositive and negative children, or of vaccine recipients, contained VZV DNA and expressed VZV transcripts (Chen et al., 2011). In the guinea pig model, intravenously injected T-lymphocytes infected *in vitro* with VZV were found to transmit viral DNA to multiple neurological tissues, including the DRG and enteric nervous system (Gan et al., 2014). VZV was reported to be experimentally reactivated by administration of tacrolimus in combination with corticotrophin-releasing 4 hormone to mimic stress, but important experimental data was not shown (Gershon and Gershon, 2018). Taken together, the

recent work suggests the guinea pig is the strongest of the *in vivo* small animal models for study of VZV latency *in vivo,* and may be experimentally reactivatable. More work is needed to optimize reactivation strategies and establish similarities to human VZV persistence.

Human Tissues in SCID Mice

SCID mice are unable to reject implanted human tissues (the SCID-hu model) and have proven to be a powerful tool for *in vivo* studies of human specific viruses, albeit in the absence of any adaptive immunity. Implanted tissues retain many characteristics and structural organization for long periods in these mice, despite an unnatural ectopic location (McCune et al., 1988; Mosier et al., 1988). The application of the SCID-hu mice for VZV was pioneered by Moffat et al. (1995), using skin tissue from fetuses and, more recently, adults (Zerboni et al., 2018). Immune cells from grafted human fetal thymus and liver tissue are placed beneath the mouse kidney capsule, as are fetal ganglia. A wealth of important information on VZV pathogenesis patterns has been gleaned from these models, and the roles of many viral genes in specific tissue infections have been elucidated (Zerboni et al., 2014). Since we are addressing models of latency, we will restrict our review to the use of human fetal DRGs in the SCID-hu system.

Fetal implants of intact ganglia in SCID-hu mice maintain much of the structural organization seen in ganglia *in situ*, despite axotomy during acquisition. Neurons are surrounded by ganglionic glia and satellite cells, in a physiological state that permits glial cell–neuron interactions in VZV pathogenesis to be followed (Hanani, 2005; Zerboni et al., 2005). DRG neurons express many of the expected markers, synaptophysin and neural cell adhesion molecule (NCAM), and by 4 weeks post implantation contain differentiated subsets of nociceptive and mechanoreceptive neurons marked by peripherin and RT97 antibodies respectively. VZV infection can be tracked by tissue extraction and subsequent processing of the graft for presence of virus and IHC, or in real time by using VZV expressing firefly luciferase from viral promoters coupled with IVIS bioluminescent imaging (Jones et al., 2006; Oliver et al., 2008). VZV inoculated directly into grafts showed increasing replication during the first 2 weeks, followed by a decline to control levels by 4–6 weeks post infection. DRG xenografts could also be infected by tail vein injection of VZV-infected human T-lymphocytes, supporting the direct viremia infection of ganglia that is speculated to occur in human varicella. Acute infection is accompanied by extensive cytopathology that is similar to that seen in human ganglia of patients dying with active zoster in that there is loss of cellular integrity, fusion events between multiple cell types including neurons and support cells, the production of virus, and changes in the inflammatory state and cytokine milieu of the ganglia. The diminishment of the acute ganglionic replication and its resolution suggests there is no need for adaptive immunity for the establishment of persistence and the cessation of ganglionic lytic replication (Schaap et al., 2005). VZV genomes persisted at low levels for months in the xenograft and were interpreted as a transition to a latent infection. A recent correlation of infection with neuronal markers suggest that mechanoreceptor neurons marked by RT97 antibodies are more resistent to VZV replication (Zerboni and Arvin, 2011). It is not clear if these give rise to reactivatable latent infections or are more reflective of a cell restricted or abortive infection. Ganglia contained low levels of transcripts of ORF63 but showed little VZV protein expression (Pevenstein et al., 1999; Zerboni et al., 2007; Zerboni and Arvin, 2011). Intriguingly, it was demonstrated that the vaccine Oka strain retained the ability to establish a persistent state in SCID-hu DRG (Zerboni et al., 2005), supporting that the vaccine retains the ability to efficiently establish latency. A second intriguing observation was that persistence was not established if the interactions of the gI and gE glycoproteins were genetically interrupted. Rather VZV entered into a chronic low replication phase maintained over time, suggesting that this critical interaction somehow influences lytic/latent decisions of the virus (Zerboni and Arvin, 2011).

To date, spontaneous or experimentally induced reactivation from the persistent state has not been reported in the SCID-hu DRG model so it is not yet clear whether the persistent infection is latent, abortive or a mixture of both. While clearly this is a solid model for study of VZV neurotropism, additional work is required to establish if maintained VZV genomes are reactivatable.

IN VITRO MODELS OF VZV LATENCY AND REACTIVATION

Non-stem Cell Derived Neuron Cultures

There have been several attempts to develop *in vitro* systems for study of the VZV latent state (summarized in **Table 1**), and most have focused on human cultured neuron systems that should overcome the species restriction of VZV. Attempts using cultures derived from rat primary ganglia, rat embryonic ganglia and rat neuron progenitor lines resulted in the expression of a limited viral gene program, which nevertheless could alter host expression patterns (Kennedy et al., 2001, 2013; Hamza et al., 2007) and apoptosis (Hood et al., 2006). The lack of full viral replication is consistent with the observations of Guedon et al. (2015) that the rat does not support full VZV replication.

In vitro systems using cultured neurons from human adult cadaver ganglia are largely unsuitable for experimental infections leading to persistence because most are likely to harbor latent VZV and/or HSV. The latter has the potential to initiate a full productive reactivation (Bastian et al., 1972; Baringer and Swoveland, 1973; Lewis et al., 1982; Warren et al., 1982). However, analyses of cadaver ganglia were critical in establishing the presence of VLT and ORF63 transcripts during latency in humans (Depledge et al., 2018a). Reactivation of endogenous VZV from intact or dissociated ganglionic cultures leading to virus production has not been achieved (Azarkh et al., 2012), but axotomized cadaver ganglia show increased VZV DNA production upon the interruption of NGF signaling (Cohrs et al., 2017). NGF signaling is required to maintain HSV latency in murine and rat experimental neuron systems (Wilcox and Johnson, 1987; Camarena et al., 2010). Axotomized ganglia obtained from aborted fetuses offer an alternative as they are

unlikely to contain pre-existing herpesvirus latent genomes. However, their use raises ethical issues and presents logistical difficulties in obtaining fresh neuronal tissue that survives propagation in culture. The inherent genetic variability between donors is also potentially problematic. In addition to the studies of VZV infection of fetal ganglionic xenografts in SCID mice just described, intact and dissociated cultured human fetal ganglia *in vitro* has been shown to host a productive experimental VZV infection (Hood et al., 2006; Gowrishankar et al., 2007; Steain et al., 2011). The use of fetal tissues in modeling VZV latency and reactivation *in vitro* has not yet been reported.

Several attempts have been made to exploit neuron-like cells differentiated from cancer or immortalized lines for study of VZV, particularly the human neuroblastoma cell line SH-SY5Y. Both SH-SY5Y cells and their differentiated neuron-like derivatives can host full VZV replication and intracellular virus spread (Christensen et al., 2011). While they offer the advantage of expandability, they suffer the disadvantage of generating terminally differentiated cells from transformed lines that do not have all the characteristics of adult human ganglionic neurons. SH-SY5Y have been widely used with HSV and drug-induced genome persistence (Shipley et al., 2017), but a reactivatable VZV latent state has not been reported. The repertoire of other expandable cell lines continues to grow and awaits evaluation for modeling VZV latency.

Human neurons can be also differentiated from commercially available neural progenitor cells. Pugazhenthi et al. (2011) exploited commercially obtained neurospheres derived from human fetal brain to generate neuron cultures to host a VZV infection. The cultures were 90% positive for the early neuronal markers MAP2a and βIII tubulin, and expressed multiple VZV transcripts and proteins after infection, intriguingly without cytopathic effect. It was not established whether a full productive VZV infection was supported, and homogenates of infected cultures could not initiate infection of VZV-permissive fibroblasts, suggesting that this may not be a sufficiently robust model for exploring VZV latency.

Goodwin et al. (2013) detailed the use of stem cell-derived neuroprogenitors from the brain to derive long term cultured 3D assemblies containing neurons surviving for up to 6 months. The 3D systems could host a spreading VZV infection and maintain viral genomes long-term, with sporadic virus production and limited gene expression. It was not clear if the state of VZV persistence was experimentally reversible and reactivatable. We are not aware of additional publications using this system beyond the first report.

Human Pluripotent Stem Cell-Derived Neuron Culture Models

Recent advances in generating differentiated human neurons from pluripotent stem cells have widened the choice of systems for modeling VZV neuronal latency. Stem cell models are genetically consistent and expandable, and stem cells can be guided to differentiate toward specific neuronal subtypes, all ideal for current and future applications. Possible drawbacks include that the resulting neuron cultures are heterogeneous to varying degrees, and lack the complexity of human ganglia with its many neuronal and non-neuronal cell interactions. Both human embryonic stem cells (hESC) and induced pluripotent human stem cells (iPSC) have been developed into neuron cultures for VZV study, and differentiation protocols continuously evolve (Tang et al., 2017). At the time of this review, only hESC-derived neurons have permitted an experimental state of VZV genome persistence to be established that can later be reactivated (Markus et al., 2015; Sadaoka et al., 2016).

Several groups have reported the use of iPSC to generate neuron culture models for VZV infection. Lee et al. (2012) derived their own iPSC line from primary human embryonic fibroblasts using the classic retroviral mediated expression of Oct4, Sox2, cMyc, and Klf4. These iPSC were directed to differentiate into neural progenitors using a combination of small molecule inhibitors of SMAD, GSK and Notch signaling, followed by culture with a combination of neuronal growth factors. The resulting heterogeneous neuron population stained 80% positive for neuronal marker βIII tubulin, with 15% co-expressing βIII tubulin along with the sensory neuronal markers BRN3a and peripherin. Electrophysiological activity was also demonstrated in these cells. The neuron cultures were reported to support a productive VZV infection, cell-to-cell spread, and release of infectious virus, but were not shown to model persistence.

Baird and colleagues report use of a commercially available iPSC-derived neuronal precursor that is immediately plated in defined proprietary media to generate "iCell" neurons (Cellular Dynamics International, Inc.) (Baird et al., 2013, 2014b, 2015; Yu et al., 2013). The supplied mixture consists of post-mitotic neuronal subtypes of mainly of GABAergic and glutamatergic neurons that can be cultured longer than 21 days. Cultures are 95% positive for βIII tubulin expression and show characteristic neurite and axonal projections (Yu et al., 2013). Experimental infection with cell-free VZV leads to extensive transcript and protein expression (Baird et al., 2013, 2015; Yu et al., 2013). While initial reports suggested a complete lack of cytopathic effect (Yu et al., 2013), more recent work reported a fully expressed viral transcriptome, virus production and cytopathic effect (Grose et al., 2013; Baird et al., 2014a,b, 2015). The iCell neuron system was used to show the influence of cytokines IL6, IFNγ and type 1 IFNs in blocking virus growth and gene expression (Baird et al., 2015; Como et al., 2018). It is not yet clear if these cells can host a reactivatable, persistent state.

Using hESCs as the starting material permits some level of reproducibility that can be followed by other groups. At the time of this review, three reports detail their use for study of VZV replication, latency and experimental reactivation. While each differs in the process by which neurons are differentiated, the similarities between the models are more important, as they clearly point to the first bone-fide models of VZV reactivation. The first, detailed in several publications from the laboratories of the Goldstein and Kinchington groups, used the WiCell hESC line WA09 (also known as H9; Thomson et al., 1998). When cocultured with the murine stromal PA6 line, renewable neurosphere precursors are generated that can be maintained in a precursor state on Matrigel or in suspension. Seeding onto laminin-coated plates with neurobasal media containing BDNF, NGF and NT3 for a 2-week terminal differentiation

process leads to cultures consisting predominantly of neurons with extensive neurite projections. Cultures stained 95% positive for βIII tubulin with very few GFAP-positive cells or Ki67-positive dividing precursors. A fraction stain positive for the sensory neuron markers BRN3a and peripherin, indicating some neuron heterogeneity.

These hESC-neurons were used with fluorescent reporter viruses that permitted live cell monitoring of acute infection, lytic gene expression, cell-to-cell spread, and the absence of protein expression during a modeled latent state. In particular, recombinant VZV expressing GFP tagged to the amino terminus of the ORF66 protein kinase, or to the ORF23 capsid protein have been used. The neuron cultures were fully permissive for VZV infection and spread when initiated by cell-associated infection at the soma or axon, or by high levels of cell-free virus at the soma (Markus et al., 2011). Infecting cells fused to neuron soma and axons, delivering not only virus to the neuron, but also intracellular components of the infecting cell (Grigoryan et al., 2015). This may drive the predominantly lytic infections that result. Electron microscopy established that the neurons were productively infected and extensively coated with capsids packaged with DNA on their cell surface. Infected neurons also released infectious virus into the media, a property not shared with VZV replication in most non-neuronal cultures. The platform has also been used to address neurotropism of VZV recombinants lacking VZV genes, and it was demonstrated that ORF7, a protein important for VZV spread in skin culture (Zhang et al., 2010) and in differentiated SH-SY5Y cell infections (Selariu et al., 2012) was critical for neuronal spread.

Culture of neurons in microfluidic chamber devices (**Figure 1**) permitted the separation of neuron soma from axons. When axons were infected with cell-associated VZV, lytic, spreading infections developed on the soma side (Markus et al., 2011). These devices also permitted the first live cell visualization of VZV capsid retrograde transport inside axons using a fluorescent ORF23 capsid protein reporter virus; ORF23 encodes the abundant capsid protein homologous to HSV VP26 (Grigoryan et al., 2012). The motion of VZV capsids was neither continuous nor exclusively retrograde, but capsids migrated toward the neuronal soma at a rate similar to that of the neurotrophic alphaherpesviruses HSV-1 and PRV (Smith et al., 2001; Antinone and Smith, 2010).

The first reactivatable latent infection was demonstrated in this hESC-neuron fluorescent-VZV system (Markus et al., 2015). Persistence was established by infection of neuron cultures in microfluidic devices, either at the soma with cell-free virus in the presence of the antiviral acyclovir, or by axonal infection without use of antivirals. The antiviral approach has been successfully employed to model HSV latency *in vitro* to select against initiating lytic events (Hunsperger and Wilcox, 2003; Kobayashi et al., 2012). It is now recognized that neurons are more sensitive to cell-free VZV infection than other cell types (Sadaoka et al., 2018). Using VZV66GFP, lytic infection in the cultures could be differentiated from non-lytic infected cultures in real time. It was demonstrated that GFP negative cultures still contained VZV genomes in neuronal nuclear puncta, using both qPCR and fluorescent *in situ* hybridization (FISH). FISH showed the viral genome to be localized to single or dual nuclear puncta, similar to that recently reported for HSV latent infections (Catez et al., 2014). Surprisingly, transcriptional analyses by RNA-seq revealed a widespread general suppression of all lytic gene transcripts, but with some ORFs showing relatively higher levels as compared to a lytic infection, particularly ORFs in the repeat region. VLT RNA had not yet been described and was not assessed.

Most importantly, it was demonstrated that disruption of NGF signaling resulted a renewal of GFP positivity and a spreading infection, indicating renewed lytic replication after a long period of GFP absence (Markus et al., 2015). Continuous NGF signaling is required to maintain HSV latency in model systems (Camarena et al., 2010). VZV reactivation, indicated by renewed GFP expression, was achieved by growth factor withdrawal, the inhibition of PI3-Kinase signaling with the inhibitor LY7294002, or the treatment of latent cultures with the type 1 histone deacetylase-inhibitor sodium butyrate. GFP positivity correlated with expression of lytic genes, increased VZV DNA, an increase in the number of puncta by FISH, and renewed virus production capable of infecting ARPE19 cells. Intriguingly, incubation at reduced temperature increased the reactivation frequency and reduced inhibitor toxicity.

The microfluidic chamber system was then used to establish latency without antivirals using axon only infection with cell-free virus. This is more physiologically relevant and reflects infection that would occur in establishing latency from skin vesicles. It had been previously shown that HSV axonal infection preferentially results in a latent infection, most likely due to poor delivery of virion tegument transactivators of lytic infection down the axon to the neuronal nucleus (Hafezi et al., 2012). Even high MOI infections with cell-free VZV failed to initiate GFP-positive (lytic) infected soma in the cell-body chamber, but since soma contained VZV genomes, latency must have been established. Again, reactivation was demonstrated by renewed GFP expression in previously GFP-negative soma chambers stimulated by the PI3K inhibitor. Taken together, these experiments established use of hESC-derived neurons to model an experimentally reactivatable latent VZV infection.

The hESC experimental model was more recently used to explore VZV encoded sncRNAs. While previous studies had not detected miRNA in human trigeminal ganglia latently infected with VZV (Umbach et al., 2009), short miRNA-length RNAs were identified using NGS methods in fibroblasts and hESC-derived neurons lytic infected with VZV (Markus et al., 2017). Unconventional bioinformatic analyses predicted 24 VZV encoded small non-coding RNAs (VZVsncRNA) in NGS reads of productively infected neurons. The presence of one VZVsncRNA was confirmed using stem-loop rt-qPCR, and one was detected in latently infected neurons. These studies established that VZV, like other herpesviruses, makes use of small RNAs that may regulate infection. As noted above, two sncRNAs map to the introns of the VLT transcript (Markus et al., 2017). This work is an area that will likely be expanded in the near future in addressing the contribution of VZVsncRNA to the molecular mechanisms underlying VZV latency.

A second group reported a similar system to host a VZV reactivatable latent state (Sadaoka et al., 2016). Their neuron

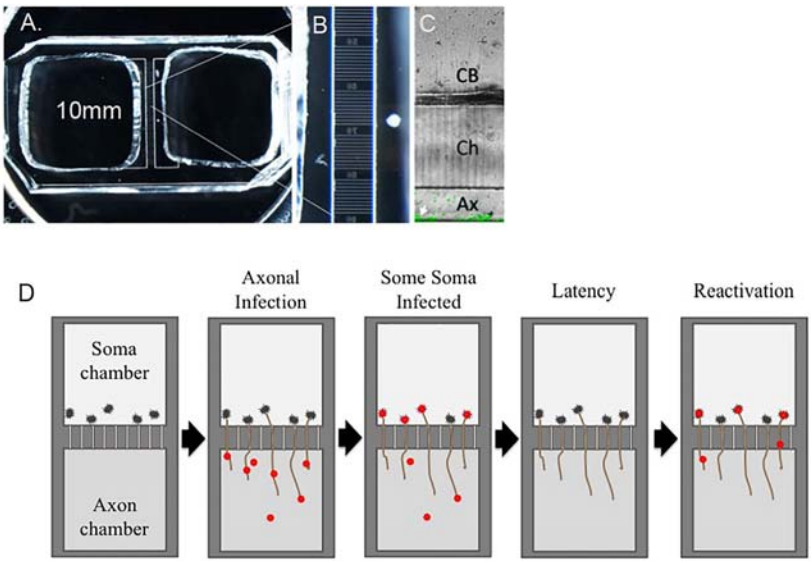

FIGURE 1 | Latent VZV infections established in hESC-neurons in microfluidic devices can be experimentally reactivated. hESC-neurons are infected axonally in microfluidic devices that separate neuronal soma from axons. **(A–C)** Depicts a microfluidic chamber that separates neuronal soma (CB) from axons (Ax). VZV infection is established in the axonal compartment, allowing VZV to be transported through axons into some somata, in which a quiescent infection is established. Upon stimulation with PI3K inhibitor LY294002 and incubation of cultures at 34°C, virus in some latently infected neurons is reactivated and productive infection is re-established. Ch = microfluidic channels that connect the soma and axon compartments. **(D)** A diagrammatic representation shows the process of axonal infection of neurons with VZV, establishment of latency, and reactivation.

platform was differentiated from commercially available hESC-derived neural stem cells (Life Technologies, Inc.), originally differentiated from the same WA09 hESC line used by Markus et al. (2015). The neuron cultures were predominantly βIII tubulin positive, with a fraction of cells also expressing the sensory neuron markers BRN3a and peripherin, as seen by Markus et al. (2015). Only very low levels of cells stained with GFAP, a marker of radial glia, astrocytes and satellite cells. There was no positive staining for microglia or oligodendrocytes in the cultures. Their model predominantly relied on a microfluidic chamber system to separate axons and soma, followed by cell-free VZV infection of the axon or somal compartments. Like Markus et al. (2015), they reported the initiation of lytic events when neuronal soma were infected with cell-free VZV (strain Parent of Oka or POka) at high MOI, but also found that low MOI cell-free VZV infections at the soma could result in VZV DNA positive cultures showing no detectable lytic growth or cytopathic effect. In agreement with Markus et al. (2015), cell-free infection of compartmentalized neurons was not productive, but delivered VZV DNA to the somal compartments. They also saw very low levels of transcription of all VZV ORFs by RNAseq, indicating that most lytic gene expression was silenced. Viral DNA could be detected for up to 70 dpi in the neurons without evidence of replication, and the retained VZV genomes were predominantly circular or endless, as seen for other latent herpesviruses and for latent VZV in human cadaver ganglia (Clarke et al., 1995). This contrasted with the predominantly linear VZV genomes seen in lytic infected cultures. Importantly, reactivation was demonstrated as renewed lytic infections in approximately 25% of latently infected cultures when NGF was depleted using antibodies. Reactivation resulted in spreading productive infections and virus capable of infecting MRC5 cells.

Another intriguing study compared the parent and vaccine strains of Oka for the establishment of latency and reactivation from it. The genetically heterogeneous attenuated vaccine retains the ability to go latent and has caused zoster in vaccinated individuals, albeit at a greatly reduced level compared to wild type strains (see Breuer, 2018 for recent review). The authors found that the vaccine strain could still establish latency in the hESC-neuron model at levels similar to the wild type parent Oka strain, and with a level of genome heterogeneity seen in the vaccine. However, the vaccine virus expressed a considerably reduced level of viral transcripts and was an average of fivefold less efficient at reactivating after the experimental stimulus of NGF removal. Furthermore, the genomic diversity was considerably reduced in the *in vitro* reactivated virus, indicating either there was some clonal selection of genomes more able to reactivate over others in the heterogeneous vaccine strain, or alternatively, there was a stochastic process in which a very low number of genomes are induced to reactivate. This bottleneck may explain the restricted genome diversity seen in breakthrough lesions after vaccine inoculation (Depledge et al., 2014).

A comparison of the two models is warranted. Both systems (Markus et al., 2015; Sadaoka et al., 2016) used axonal infection in microfluidic devices to set up VZV latency without use of antivirals. Both groups showed that initiation of infection at the soma compartment with cell-free virus resulted in lytic infections. Markus et al. (2015) also set up latency using ACV to inhibit lytic infections in non-compartmentalized directly infected neuron cultures. ACV has been used routinely to block HSV lytic

infections in several neuronal model systems to favor establishing a latent state. The use of ACV may be problematic, because any initiated lytic infection will express the deoxypyrimidine kinase and result in the formation of ACV-PPP, which can then become incorporated into DNA and act as a chain terminator. This may render viral genomes as damaged and less able and/or likely to reactivate. As such, latent genomes seen in ACV-treated cultures are probably a mixture of undamaged genomes from infections that enter latency immediately after infection, and ACV-damaged genomes maintained after an initiated lytic infection that becomes repressed after blockade of DNA replication. A minor difference between the two studies is temperature. Sadaoka et al. (2016) reactivated neuron cultures at 37°C, while Markus et al. (2015) reported efficient reactivation at 34°C.

The model of Sadaoka et al. (2016) was more recently exploited to examine the role of c-Jun N-terminal kinase (JNK) in neuronal VZV infection. It was previously indicated that VZV modulates the JNK pathway in human foreskin fibroblasts, increasing JNK and active phospho-JNK. JNK inhibition negatively impacts VZV replication (Zapata et al., 2007), although Rahaus et al. (2004) reported the opposite effect in MeWo cells and suggested blocking JNK was pro-viral. Kurapati et al. (2017) reassessed the role of JNK in VZV infection of neurons, reporting that VZV induced JNK activation and JNK phosphorylation in neuron cultures. The group exploited the microfluidic chamber system to establish persistent VZV infections by axonal infection, and found that chemical inhibition of JNK reduced the efficiency of viral reactivation by up to fourfold. This suggests the potential use of JNK inhibition as a reactivation inhibition strategy.

It is likely that the hESC-neuron platforms will undergo continuous development in the near future. One such development was included in the work by Kurapati et al. (2017), in which they generated cultures highly enriched for sensory neuron phenotypes. These cultures were generated from a genetically modified hESC Wa09 line with a GFP reporter for the neural crest marker SOX10 that allowed selection by flow sorting (Lee et al., 2010). Application of inhibitors of SMAD and canonical WNT signaling to cultures of sorted NC-like cells resulted in efficient (95%) generation of sensory neurons expressing BRN3a and peripherin (Mica et al., 2013). They showed the sensory neuron cultures were fully permissive for VZV and that the JNK inhibitor reduced VZV replication.

QUESTIONS AND PERSPECTIVES ON THE FUTURE OF MODELING VZV LATENCY AND REACTIVATION

(1) The differentiation of hESC into specific subtypes of neurons and lineages is a field of intense interest and continuous development that will impact not only the study of the VZV latent state, but also that of HSV-1 and HSV-2. Evidence is accumulating that suggests some neuronal subtypes are more restrictive for virus replication than others. Work from the human fetal ganglionic implant-SCID-hu model has suggested that peripherin-positive nociceptors are more susceptible to VZV infection as compared to mechanoreceptor neurons marked by the RT97 antibody, which exhibit some restriction to VZV infection (Zerboni and Arvin, 2015). Advances in this area may enable us to address whether the more restrictive neurons host a VZV genome that can eventually reactivate. It may also allow study of the possibility that different subtypes of neurons reactivate in response to different stimuli. While studies have not yet been detailed, we consider it likely that VZV is capable of establishing genomes in many more subtypes of neurons than HSV. HSV does not generally exhibit a viremia and predominantly establishes latency through the infection of axons that infiltrate the periphery and site of infection. This contrasts to VZV, which likely accesses the ganglia by both retrograde axonal transport from the periphery and by direct infection from ganglia-infiltrating VZV infected immune cells. Neurons in ganglia that do not innervate the periphery may be responsible for VZV clinical presentations other than classic zoster, such as zoster without rash (sine herpete) and the numerous enteric, neurological and vascular conditions associated with VZV reactivation. The types of neurons that host VZV genomes and those supplying reactivation is a direction ripe for further exploration.

(2) The discovery of VZV VLT RNA is a recent development that is yet to be included in models of VZV latency, *in vivo* or *in vitro* (Depledge et al., 2018a). The conserved features of VLT with latency transcripts of other neuronal alphaherpesviruses is highly suggestive of important roles that have been functionally retained as alphaherpesviruses have diverged and evolved. In spite of extensive research on the better-studied HSV-1 system, what those conserved functions are is not yet clear. With some further development, we should be poised to determine how the VLT and/or transcripts mapping to ORF63 contribute in the models of latency and reactivation, both *in vivo* and *in vitro* (Depledge et al., 2018a). Are both RNAs expressed in all or only a fraction of VZV latently infected neurons? Do these represent expression in different neuronal subtypes, or is expression of the two transcripts linked? What is the pattern of their expression? It remains a possibility that either RNA is a product of the very early post mortem-induced transcription program, as even minimal PMIs cannot be avoided.

(3) VZV genetic model systems can now be used to probe possible functions of VLT and other genes in the onset of human neuronal infection, latency and reactivation. VZV is readily genetically manipulated through the use of BAC and cosmid systems (Osterrieder et al., 2003; Tischer et al., 2007) and viruses from BACs and cosmids go latent and reactivate in the hESC model platforms (Markus et al., 2015). It should be straightforward to generate VZV VLT mutants, although it may still be quite challenging to evaluate how latency and reactivation is influenced by VLT mutation or deletion. The functions of the more extensively studied HSV LAT are still quite controversial. LAT has long

been speculated to regulate the multifunctional transactivator protein HSV ICP0 (Wagner et al., 1988a,b), a key factor in the establishment of lytic infections, and VLT may act the same on ORF61. The HSV-1 LAT RNA seen during latency is a stable intron from several splice variants of a difficult-to-detect primary 8.3 kb transcript, which accumulates in the nucleus of latently infected neurons (Wechsler et al., 1988; Zwaagstra et al., 1990). HSV-1 LAT has been implicated to influence the regulation of chromatin (Bloom et al., 2010), express miRNAs that influence gene expression (Umbach et al., 2008), regulate apoptosis (Perng et al., 2000), and impact the survival of latently infected neurons (Thompson and Sawtell, 2001) and the efficiency of reactivation (Watson et al., 2018). However, the fact that HSV-1 lacking LAT can still establish persistence and reactivate in all current *in vivo* animal models does imply that LAT roles are not essential. We will likely soon see whether VLT is required for establishing latency and reactivation in the human neuron systems that are now available. It is likely that HSV-1 LAT function will be re-assessed in these human neuron systems.

(4) The *in vitro* human neuron platforms in use do have some limitations that may require a further study of the *in vivo* model systems of persistence. The *in vitro* systems are not yet sufficiently developed to permit studies of how latent infections interact with the adaptive immune system. This is a particularly important issue, given that declining adaptive cellular immunity is a major predictor of zoster incidence, and that vaccination-mediated boosting of immunity reduces rates of zoster. The contribution of adaptive immunity will probably need an *in vivo* system, and the guinea pig model appears to be the most likely permissive *in vivo* system. However, while the guinea pig model has been reported to enter a latent state that is experimentally reactivatable (Gershon and Gershon, 2018), reactivation is not yet fully documented, characterized or optimized. Alternatively, some aspects of the influence of acquired immunity on reactivation may come from further *in vitro* model development, such as by developing MHC-compatible iPSC-derived neuron cultures from the same host in which T cells have been isolated. Alternatively, hESC could potentially be modified to be MHC compatible with a donor immune cell population.

Glia surround and are believed to interact with neurons in both the central and peripheral nervous systems. Thus, satellite glial cells (SGC) and Schwann cells in peripheral ganglia may play a role in establishment and/or maintenance of latent VZV infections. Evidence from the SCID-hu mouse xenografted with fetal human DRG suggests that SGC are infected by VZV and fuse with neighboring neurons (Zerboni and Arvin, 2011). Schwann cells have been generated from hESC and were shown to myelinate human and chick embryo neurons (Ziegler et al., 2011). SGCs have also been implicated in the modulation of neuropathic pain (recently reviewed in Fan et al., 2019). It is therefore likely that additional insights into VZV latency may be obtained by addition of glial cells to the *in vitro* human neuron model for VZV infection.

CONCLUSION

Advances in the development of *in vitro* human neuron systems for modeling VZV latency and reactivation and the recent discovery of the VZV latency-associated transcript have set the stage for a new era in resolving this perplexing persistent state.

AUTHOR CONTRIBUTIONS

As this manuscript is a review, all authors were involved in writing and editing the manuscript. There were no new experiments included in this work.

FUNDING

The authors wish to acknowledge the support of awards R01 NS064022 (PK), R01 AI122640 (PK and RG), P30 EY08098 (PK), and T32 NS073548 (LL) from the National Institutes of Health; Award # 2017259 from the United States-Israel Binational Science Foundation (PK and RG); Award # 254/16 from the Israel Science Foundation (RG); and unrestricted funds from the Research to Prevent Blindness Inc. and Eye & Ear Foundation of Pittsburgh.

REFERENCES

Ambagala, A. P., Krogmann, T., Qin, J., Pesnicak, L., and Cohen, J. I. (2010). A varicella-zoster virus mutant impaired for latency in rodents, but not impaired for replication in cell culture. *Virology* 399, 194–200. doi: 10.1016/j.virol.2010.01.007

Annunziato, P., LaRussa, P., Lee, P., Steinberg, S., Lungu, O., Gershon, A. A., et al. (1998). Evidence of latent varicella-zoster virus in rat dorsal root ganglia. *J. Infect. Dis.* 178(Suppl. 1), S48–S51.

Antinone, S. E., and Smith, G. A. (2010). Retrograde axon transport of herpes simplex virus and pseudorabies virus: a live-cell comparative analysis. *J. Virol.* 84, 1504–1512. doi: 10.1128/JVI.02029-09

Azarkh, Y., Bos, N., Gilden, D., and Cohrs, R. J. (2012). Human trigeminal ganglionic explants as a model to study alphaherpesvirus reactivation. *J. Neurovirol.* 18, 456–461. doi: 10.1007/s13365-012-0123-0

Baird, N. L., Bowlin, J. L., Cohrs, R. J., Gilden, D., and Jones, K. L. (2014a). Comparison of varicella-zoster virus RNA sequences in human neurons and fibroblasts. *J. Virol.* 88, 5877–5880. doi: 10.1128/JVI.00476-14

Baird, N. L., Bowlin, J. L., Yu, X., Jonjic, S., Haas, J., Cohrs, R. J., et al. (2014b). Varicella zoster virus DNA does not accumulate in infected human neurons. *Virology* 45, 1–3. doi: 10.1016/j.virol.2014.04.014

Baird, N. L., Bowlin, J. L., Hotz, T. J., Cohrs, R. J., and Gilden, D. (2015). Interferon gamma prolongs survival of varicella-zoster virus-infected human neurons *in vitro*. *J. Virol.* 89, 7425–7427. doi: 10.1128/JVI.00594-15

Baird, N. L., Yu, X., Cohrs, R. J., and Gilden, D. (2013). Varicella zoster virus (VZV)-human neuron interaction. *Viruses* 5, 2106–2115. doi: 10.3390/v5092106

Baird, N. L., Zhu, S., Pearce, C. M., and Viejo-Borbolla, A. (2019). Current in vitro models to study varicella zoster virus latency and reactivation. *Viruses* 11:103. doi: 10.3390/v11020103

Baringer, J. R., and Swoveland, P. (1973). Recovery of herpes-simplex virus from human trigeminal ganglions. *N. Engl. J. Med.* 288, 648–650. doi: 10.1056/NEJM197303292881303

Bastian, F. O., Rabson, A. S., Yee, C. L., and Tralka, T. S. (1972). Herpesvirus hominis: isolation from human trigeminal ganglion. *Science* 178, 306–307. doi: 10.1126/science.178.4058.306

Bertke, A. S., Swanson, S. M., Chen, J., Imai, Y., Kinchington, P. R., and Margolis, T. P. (2011). A5-positive primary sensory neurons are nonpermissive for productive infection with herpes simplex virus 1 in vitro. *J. Virol.* 85, 6669–6677. doi: 10.1128/JVI.00204-11

Bloom, D. C., Giordani, N. V., and Kwiatkowski, D. L. (2010). Epigenetic regulation of latent HSV-1 gene expression. *Biochim. Biophys. Acta* 1799, 246–256. doi: 10.1016/j.bbagrm.2009.12.001

Breuer, J. (2018). Molecular genetic insights into varicella zoster virus (VZV), the vOka vaccine strain, and the pathogenesis of latency and reactivation. *J. Infect. Dis.* 218(Suppl._2), S75–S80. doi: 10.1093/infdis/jiy279

Brunell, P. A., Ren, L. C., Cohen, J. I., and Straus, S. E. (1999). Viral gene expression in rat trigeminal ganglia following neonatal infection with varicella-zoster virus. *J. Med. Virol.* 58, 286–290. doi: 10.1002/(sici)1096-9071(199907)58:3<286::aid-jmv15>3.0.co;2-e

Camarena, V., Kobayashi, M., Kim, J. Y., Roehm, P., Perez, R., Gardner, J., et al. (2010). Nature and duration of growth factor signaling through receptor tyrosine kinases regulates HSV-1 latency in neurons. *Cell Host Microbe* 8, 320–330. doi: 10.1016/j.chom.2010.09.007

Catez, F., Rousseau, A., Labetoulle, M., and Lomonte, P. (2014). Detection of the genome and transcripts of a persistent DNA virus in neuronal tissues by fluorescent in situ hybridization combined with immunostaining. *J. Vis. Exp.* 83:e51091. doi: 10.3791/51091

Chen, J. J., Gershon, A. A., Li, Z., Cowles, R. A., and Gershon, M. D. (2011). Varicella zoster virus (VZV) infects and establishes latency in enteric neurons. *J. Neurovirol.* 17, 578–589. doi: 10.1007/s13365-011-0070-1

Chen, J. J., Gershon, A. A., Li, Z. S., Lungu, O., and Gershon, M. D. (2003). Latent and lytic infection of isolated guinea pig enteric ganglia by *Varicella zoster* virus. *J. Med. Virol.* 70(Suppl. 1), S71–S78. doi: 10.1002/jmv.10325

Christensen, J., Steain, M., Slobedman, B., and Abendroth, A. (2011). Differentiated neuroblastoma cells provide a highly efficient model for studies of productive varicella-zoster virus infection of neuronal cells. *J. Virol.* 85, 8436–8442. doi: 10.1128/JVI.00515-11

Clarke, P., Beer, T., Cohrs, R., and Gilden, D. H. (1995). Configuration of latent varicella-zoster virus DNA. *J. Virol.* 69, 8151–8154.

Cohen, J. I., Krogmann, T., Bontems, S., Sadzot-Delvaux, C., and Pesnicak, L. (2005a). Regions of the varicella-zoster virus open reading frame 63 latency-associated protein important for replication in vitro are also critical for efficient establishment of latency. *J. Virol.* 79, 5069–5077. doi: 10.1128/JVI.79.8.5069-5077.2005

Cohen, J. I., Krogmann, T., Ross, J. P., Pesnicak, L., and Prikhod'ko, E. A. (2005b). Varicella-zoster virus ORF4 latency-associated protein is important for establishment of latency. *J. Virol.* 79, 6969–6975. doi: 10.1128/JVI.79.11.6969-6975.2005

Cohen, J. I., Krogmann, T., Pesnicak, L., and Ali, M. A. (2007). Absence or overexpression of the varicella-zoster virus (VZV) ORF29 latency-associated protein impairs late gene expression and reduces VZV latency in a rodent model. *J. Virol.* 81, 1586–1591. doi: 10.1128/JVI.01220-06

Cohrs, R. J., Badani, H., Baird, N. L., White, T. M., Sanford, B., and Gilden, D. (2017). Induction of varicella zoster virus DNA replication in dissociated human trigeminal ganglia. *J. Neurovirol.* 23, 152–157. doi: 10.1007/s13365-016-0480-1

Cohrs, R. J., and Gilden, D. H. (2003). Varicella zoster virus transcription in latently-infected human ganglia. *Anticancer Res.* 23, 2063–2069.

Como, C. N., Pearce, C. M., Cohrs, R. J., and Baird, N. L. (2018). Interleukin-6 and type 1 interferons inhibit varicella zoster virus replication in human neurons. *Virology* 522, 13–18. doi: 10.1016/j.virol.2018.06.013

Crosslin, D. R., Carrell, D. S., Burt, A., Kim, D. S., Underwood, J. G., Hanna, D. S., et al. (2015). Genetic variation in the HLA region is associated with susceptibility to herpes zoster. *Genes Immun.* 16, 1–7. doi: 10.1038/gene.2014.51

Cunningham, A. L., Lal, H., Kovac, M., Chlibek, R., Hwang, S. J., Diez-Domingo, J., et al. (2016). Efficacy of the herpes zoster subunit vaccine in adults 70 years of age or older. *N. Engl. J. Med.* 375, 1019–1032. doi: 10.1056/NEJMoa1603800

Dalziel, R. G., Bingham, S., Sutton, D., Grant, D., Champion, J. M., Dennis, S. A., et al. (2004). Allodynia in rats infected with varicella zoster virus–a small animal model for post-herpetic neuralgia. *Brain Res. Brain Res. Rev.* 46, 234–242. doi: 10.1016/j.brainresrev.2004.07.008

Debrus, S., Sadzot-Delvaux, C., Nikkels, A. F., Piette, J., and Rentier, B. (1995). Varicella-zoster virus gene 63 encodes an immediate-early protein that is abundantly expressed during latency. *J. Virol.* 69, 3240–3245.

Decman, V., Freeman, M. L., Kinchington, P. R., and Hendricks, R. L. (2005). Immune control of HSV-1 latency. *Viral Immunol.* 18, 466–473. doi: 10.1089/vim.2005.18.466

Depledge, D. P., Kundu, S., Jensen, N. J., Gray, E. R., Jones, M., Steinberg, S., et al. (2014). Deep sequencing of viral genomes provides insight into the evolution and pathogenesis of varicella zoster virus and its vaccine in humans. *Mol. Biol. Evol.* 31, 397–409. doi: 10.1093/molbev/mst210

Depledge, D. P., Ouwendijk, W. J. D., Sadaoka, T., Braspenning, S. E., Mori, Y., Cohrs, R. J., et al. (2018a). A spliced latency-associated VZV transcript maps antisense to the viral transactivator gene 61. *Nat. Commun.* 9:1167. doi: 10.1038/s41467-018-03569-2

Depledge, D. P., Sadaoka, T., and Ouwendijk, W. J. D. (2018b). Molecular aspects of varicella-zoster virus latency. *Viruses* 10:349. doi: 10.3390/v10070349

Devor, M. (2018). Rethinking the causes of pain in herpes zoster and postherpetic neuralgia: the ectopic pacemaker hypothesis. *Pain Rep.* 3:e702. doi: 10.1097/PR9.0000000000000702

Donahue, J. G., Choo, P. W., Manson, J. E., and Platt, R. (1995). The incidence of herpes zoster. *Arch. Intern. Med.* 155, 1605–1609. doi: 10.1001/archinte.155.15.1605

Edelman, D. A., Antaki, F., Basson, M. D., Salwen, W. A., Gruber, S. A., and Losanoff, J. E. (2010). Ogilvie syndrome and herpes zoster: case report and review of the literature. *J. Emerg. Med.* 39, 696–700. doi: 10.1016/j.jemermed.2009.02.010

Faith, R. E., Montgomery, C. A., Durfee, W. J., Aguilar-Cordova, E., and Wyde, P. R. (1997). The cotton rat in biomedical research. *Lab. Anim. Sci.* 47, 337–345.

Fan, W., Zhu, X., He, Y., Zhu, M., Wu, Z., Huang, F., et al. (2019). The role of satellite glial cells in orofacial pain. *J. Neurosci. Res.* 97, 393–401. doi: 10.1002/jnr.24341

Finnen, R. L., Mizokami, K. R., Banfield, B. W., Cai, G. Y., Simpson, S. A., Pizer, L. I., et al. (2006). Postentry events are responsible for restriction of productive varicella-zoster virus infection in Chinese hamster ovary cells. *J. Virol.* 80, 10325–10334. doi: 10.1128/JVI.00939-06

Fleetwood-Walker, S. M., Quinn, J. P., Wallace, C., Blackburn-Munro, G., Kelly, B. G., Fiskerstrand, C. E., et al. (1999). Behavioural changes in the rat following infection with varicella-zoster virus. *J. Gen. Virol.* 80(Pt 9), 2433–2436. doi: 10.1099/0022-1317-80-9-2433

Gan, L., Wang, M., Chen, J. J., Gershon, M. D., and Gershon, A. A. (2014). Infected peripheral blood mononuclear cells transmit latent varicella zoster virus infection to the guinea pig enteric nervous system. *J. Neurovirol.* 20, 442–456. doi: 10.1007/s13365-014-0259-1

Garry, E. M., Delaney, A., Anderson, H. A., Sirinathsinghji, E. C., Clapp, R. H., Martin, W. J., et al. (2005). Varicella zoster virus induces neuropathic changes in rat dorsal root ganglia and behavioral reflex sensitisation that is attenuated by gabapentin or sodium channel blocking drugs. *Pain* 118, 97–111. doi: 10.1016/j.pain.2005.08.003

Gershon, A. A. (1996). Epidemiology and management of postherpetic neuralgia. *Semin. Dermatol.* 15(2 Suppl. 1), 8–13.

Gershon, A. A., Chen, J., and Gershon, M. D. (2008). A model of lytic, latent, and reactivating varicella-zoster virus infections in isolated enteric neurons. *J. Infect. Dis.* 197(Suppl. 2), S61–S65. doi: 10.1086/522149

Gershon, M., and Gershon, A. (2018). Varicella-zoster virus and the enteric nervous system. *J. Infect. Dis.* 218(Suppl._2), S113–S119. doi: 10.1093/infdis/jiy407

Gilden, D., Nagel, M., Cohrs, R., Mahalingam, R., and Baird, N. (2015). Varicella zoster virus in the nervous system. *F1000Res* 4:F1000FacultyRev–1356. doi: 10.12688/f1000research.7153.1

Goodwin, T. J., McCarthy, M., Osterrieder, N., Cohrs, R. J., and Kaufer, B. B. (2013). Three-dimensional normal human neural progenitor tissue-like assemblies: a model of persistent varicella-zoster virus infection. *PLoS Pathog.* 9:e1003512. doi: 10.1371/journal.ppat.1003512

Gowrishankar, K., Slobedman, B., Cunningham, A. L., Miranda-Saksena, M., Boadle, R. A., and Abendroth, A. (2007). Productive varicella-zoster virus infection of cultured intact human ganglia. *J. Virol.* 81, 6752–6756. doi: 10.1128/JVI.02793-06

Grigoryan, S., Kinchington, P. R., Yang, I. H., Selariu, A., Zhu, H., Yee, M., et al. (2012). Retrograde axonal transport of VZV: kinetic studies in hESC-derived neurons. *J. Neurovirol.* 18, 462–470. doi: 10.1007/s13365-012-0124-z

Grigoryan, S., Yee, M. B., Glick, Y., Gerber, D., Kepten, E., Garini, Y., et al. (2015). Direct transfer of viral and cellular proteins from varicella-zoster virus-infected non-neuronal cells to human axons. *PLoS One* 10:e0126081. doi: 10.1371/journal.pone.0126081

Grose, C., Yu, X., Cohrs, R. J., Carpenter, J. E., Bowlin, J. L., and Gilden, D. (2013). Aberrant virion assembly and limited glycoprotein C production in varicella-zoster virus-infected neurons. *J. Virol.* 87, 9643–9648. doi: 10.1128/JVI.01506-13

Guedon, J. M., Yee, M. B., Zhang, M., Harvey, S. A., Goins, W. F., and Kinchington, P. R. (2015). Neuronal changes induced by Varicella Zoster Virus in a rat model of postherpetic neuralgia. *Virology* 482, 167–180. doi: 10.1016/j.virol.2015.03.046

Guedon, J. M., Zhang, M., Glorioso, J. C., Goins, W. F., and Kinchington, P. R. (2014). Relief of pain induced by varicella-zoster virus in a rat model of post-herpetic neuralgia using a herpes simplex virus vector expressing enkephalin. *Gene Ther.* 21, 694–702. doi: 10.1038/gt.2014.43

Hafezi, W., Lorentzen, E. U., Eing, B. R., Muller, M., King, N. J., Klupp, B., et al. (2012). Entry of herpes simplex virus type 1 (HSV-1) into the distal axons of trigeminal neurons favors the onset of nonproductive, silent infection. *PLoS Pathog.* 8:e1002679. doi: 10.1371/journal.ppat.1002679

Hamza, M. A., Higgins, D. M., and Ruyechan, W. T. (2007). Two alphaherpesvirus latency-associated gene products influence calcitonin gene-related peptide levels in rat trigeminal neurons. *Neurobiol. Dis.* 25, 553–560. doi: 10.1016/j.nbd.2006.10.016

Hanani, M. (2005). Satellite glial cells in sensory ganglia: from form to function. *Brain Res. Brain Res. Rev.* 48, 457–476. doi: 10.1016/j.brainresrev.2004.09.001

Hardy, I., Gershon, A. A., Steinberg, S. P., and LaRussa, P. (1991). The incidence of zoster after immunization with live attenuated varicella vaccine. A study in children with leukemia. Varicella Vaccine Collaborative Study Group. *N. Engl. J. Med.* 325, 1545–1550. doi: 10.1056/NEJM199111283252204

Harpaz, R., and Leung, J. (2017). When zoster hits close to home: Impact of personal zoster awareness on zoster vaccine uptake in the U.S. *Vaccine* 35, 3457–3460. doi: 10.1016/j.vaccine.2017.04.072

Hasnie, F. S., Breuer, J., Parker, S., Wallace, V., Blackbeard, J., Lever, I., et al. (2007). Further characterization of a rat model of varicella zoster virus-associated pain: relationship between mechanical hypersensitivity and anxiety-related behavior, and the influence of analgesic drugs. *Neuroscience* 144, 1495–1508. doi: 10.1016/j.neuroscience.2006.11.029

Hood, C., Cunningham, A. L., Slobedman, B., Arvin, A. M., Sommer, M. H., Kinchington, P. R., et al. (2006). Varicella-zoster virus ORF63 inhibits apoptosis of primary human neurons. *J. Virol.* 80, 1025–1031. doi: 10.1128/JVI.80.2.1025-1031.2006

Hope-Simpson, R. E. (1967). Herpes zoster in the elderly. *Geriatrics* 22, 151–159.

Hunsperger, E. A., and Wilcox, C. L. (2003). Capsaicin-induced reactivation of latent herpes simplex virus type 1 in sensory neurons in culture. *J. Gen. Virol.* 84(Pt 5), 1071–1078. doi: 10.1099/vir.0.18828-0

Jenski, L., and Myers, M. G. (1987). Cell-mediated immunity to varicella-zoster virus infection in strain 2 guinea pigs. *J. Med. Virol.* 23, 23–30. doi: 10.1002/jmv.1890230104

Jones, C. (2013). Bovine Herpes Virus 1 (BHV-1) and Herpes Simplex Virus Type 1 (HSV-1) Promote Survival of Latently Infected Sensory Neurons, in Part by Inhibiting Apoptosis. *J. Cell Death* 6, 1–16. doi: 10.4137/JCD.S10803

Jones, J. O., Sommer, M., Stamatis, S., and Arvin, A. M. (2006). Mutational analysis of the varicella-zoster virus ORF62/63 intergenic region. *J. Virol.* 80, 3116–3121. doi: 10.1128/JVI.80.6.3116-3121.2006

Kennedy, J. J., Steain, M., Slobedman, B., and Abendroth, A. (2019). Infection and functional modulation of human monocytes and macrophages by Varicella-Zoster Virus. *J. Virol.* 93:e01887-18. doi: 10.1128/JVI.01887-18

Kennedy, P. G., Grinfeld, E., Bontems, S., and Sadzot-Delvaux, C. (2001). Varicella-Zoster virus gene expression in latently infected rat dorsal root ganglia. *Virology* 289, 218–223. doi: 10.1006/viro.2001.1173

Kennedy, P. G., Montague, P., Scott, F., Grinfeld, E., Ashrafi, G. H., Breuer, J., et al. (2013). Varicella-zoster viruses associated with post-herpetic neuralgia induce sodium current density increases in the ND7-23 Nav-1.8 neuroblastoma cell line. *PLoS One* 8:e51570. doi: 10.1371/journal.pone.0051570

Kim, J. Y., Mandarino, A., Chao, M. V., Mohr, I., and Wilson, A. C. (2012). Transient reversal of episome silencing precedes VP16-dependent transcription during reactivation of latent HSV-1 in neurons. *PLoS Pathog.* 8:e1002540. doi: 10.1371/journal.ppat.1002540

Knickelbein, J. E., Khanna, K. M., Yee, M. B., Baty, C. J., Kinchington, P. R., and Hendricks, R. L. (2008). Noncytotoxic lytic granule-mediated CD8+ T cell inhibition of HSV-1 reactivation from neuronal latency. *Science* 322, 268–271. doi: 10.1126/science.1164164

Kobayashi, M., Kim, J. Y., Camarena, V., Roehm, P. C., Chao, M. V., Wilson, A. C., et al. (2012). A primary neuron culture system for the study of herpes simplex virus latency and reactivation. *J. Vis. Exp.* 62:3823. doi: 10.3791/3823

Kramer, P. R., Stinson, C., Umorin, M., Deng, M., Rao, M., Bellinger, L. L., et al. (2017). Lateral thalamic control of nociceptive response after whisker pad injection of varicella zoster virus. *Neuroscience* 356, 207–216. doi: 10.1016/j.neuroscience.2017.05.030

Ku, C. C., Besser, J., Abendroth, A., Grose, C., and Arvin, A. M. (2005). Varicella-Zoster virus pathogenesis and immunobiology: new concepts emerging from investigations with the SCIDhu mouse model. *J. Virol.* 79, 2651–2658. doi: 10.1128/JVI.79.5.2651-2658.2005

Ku, C. C., Padilla, J. A., Grose, C., Butcher, E. C., and Arvin, A. M. (2002). Tropism of varicella-zoster virus for human tonsillar CD4(+) T lymphocytes that express activation, memory, and skin homing markers. *J. Virol.* 76, 11425–11433. doi: 10.1128/jvi.76.22.11425-11433.2002

Kurapati, S., Sadaoka, T., Rajbhandari, L., Jagdish, B., Shukla, P., Ali, M. A., et al. (2017). Role of the JNK pathway in varicella-zoster virus lytic infection and reactivation. *J. Virol.* 91:e00640-17. doi: 10.1128/JVI.00640-17

Langley, R. J., Prince, G. A., and Ginsberg, H. S. (1998). HIV type-1 infection of the cotton rat (*Sigmodon fulviventer* and *S. hispidus*). *Proc. Natl. Acad. Sci. U.S.A.* 95, 14355–14360. doi: 10.1073/pnas.95.24.14355

Lee, G., Chambers, S. M., Tomishima, M. J., and Studer, L. (2010). Derivation of neural crest cells from human pluripotent stem cells. *Nat. Protoc.* 5, 688–701. doi: 10.1038/nprot.2010.35

Lee, K. S., Zhou, W., Scott-McKean, J., Emmerling, K. L., Cai, G. Y., Krah, D. L., et al. (2012). Human sensory neurons derived from induced pluripotent stem cells support varicella-zoster virus infection. *PLoS One* 7:e53010. doi: 10.1371/journal.pone.0053010

Lewis, M. E., Warren, K. G., Jeffrey, V. M., and Shnitka, T. K. (1982). Factors affecting recovery of latent herpes simplex virus from human trigeminal ganglia. *Can. J. Microbiol.* 28, 123–129. doi: 10.1139/m82-013

Lowry, P. W., Koropchak, C. M., Choi, C. Y., Mocarski, E. S., Kern, E. R., Kinchington, P. R., et al. (1997). The synthesis and immunogenicity of varicella-zoster virus glycoprotein E and immediate-early protein (IE62) expressed in recombinant herpes simplex virus-1. *Antiviral Res.* 33, 187–200. doi: 10.1016/s0166-3542(96)01014-5

Lowry, P. W., Sabella, C., Koropchak, C. M., Watson, B. N., Thackray, H. M., Abbruzzi, G. M., et al. (1993). Investigation of the pathogenesis of varicella-zoster virus infection in guinea pigs by using polymerase chain reaction. *J. Infect. Dis.* 167, 78–83. doi: 10.1093/infdis/167.1.78

Lowry, P. W., Solem, S., Watson, B. N., Koropchak, C. M., Thackray, H. M., Kinchington, P. R., et al. (1992). Immunity in strain 2 guinea-pigs inoculated with vaccinia virus recombinants expressing varicella-zoster virus glycoproteins I, IV, V or the protein product of the immediate early gene 62. *J. Gen. Virol.* 73(Pt 4), 811–819. doi: 10.1099/0022-1317-73-4-811

Markus, A., Golani, L., Ojha, N. K., Borodiansky-Shteinberg, T., Kinchington, P. R., and Goldstein, R. S. (2017). Varicella-Zoster Virus expresses multiple small noncoding RNAs. *J. Virol.* 91:e01710-17. doi: 10.1128/JVI.01710-17

Markus, A., Grigoryan, S., Sloutskin, A., Yee, M. B., Zhu, H., Yang, I. H., et al. (2011). Varicella-zoster virus (VZV) infection of neurons derived from human embryonic stem cells: direct demonstration of axonal infection, transport of VZV, and productive neuronal infection. *J. Virol.* 85, 6220–6233. doi: 10.1128/JVI.02396-10

Markus, A., Lebenthal-Loinger, I., Yang, I. H., Kinchington, P. R., and Goldstein, R. S. (2015). An in vitro model of latency and reactivation of varicella zoster virus in human stem cell-derived neurons. *PLoS Pathog.* 11:e1004885. doi: 10.1371/journal.ppat.1004885

Masood, I., Majid, Z., Rind, W., Zia, A., Riaz, H., and Raza, S. (2015). Herpes Zoster-induced ogilvie's syndrome. *Case Rep. Surg.* 2015:563659. doi: 10.1155/2015/563659

Matsunaga, Y., Yamanishi, K., and Takahashi, M. (1982). Experimental infection and immune response of guinea pigs with varicella-zoster virus. *Infect. Immun.* 37, 407–412.

McCune, J. M., Namikawa, R., Kaneshima, H., Shultz, L. D., Lieberman, M., and Weissman, I. L. (1988). The SCID-hu mouse: murine model for the analysis of human hematolymphoid differentiation and function. *Science* 241, 1632–1639. doi: 10.1126/science.2971269

Mica, Y., Lee, G., Chambers, S. M., Tomishima, M. J., and Studer, L. (2013). Modeling neural crest induction, melanocyte specification, and disease-related pigmentation defects in hESCs and patient-specific iPSCs. *Cell Rep.* 3, 1140–1152. doi: 10.1016/j.celrep.2013.03.025

Moffat, J. F., Stein, M. D., Kaneshima, H., and Arvin, A. M. (1995). Tropism of varicella-zoster virus for human CD4+ and CD8+ T lymphocytes and epidermal cells in SCID-hu mice. *J. Virol.* 69, 5236–5242.

Moffat, J. F., Zerboni, L., Sommer, M. H., Heineman, T. C., Cohen, J. I., Kaneshima, H., et al. (1998). The ORF47 and ORF66 putative protein kinases of varicella-zoster virus determine tropism for human T cells and skin in the SCID-hu mouse. *Proc. Natl. Acad. Sci. U.S.A.* 95, 11969–11974. doi: 10.1073/pnas.95.20.11969

Mosier, D. E., Gulizia, R. J., Baird, S. M., and Wilson, D. B. (1988). Transfer of a functional human immune system to mice with severe combined immunodeficiency. *Nature* 335, 256–259. doi: 10.1038/335256a0

Myers, M. G., Connelly, B. L., and Stanberry, L. R. (1991). Varicella in hairless guinea pigs. *J. Infect. Dis.* 163, 746–751. doi: 10.1093/infdis/163.4.746

Myers, M. G., Duer, H. L., and Hausler, C. K. (1980). Experimental infection of guinea pigs with varicella-zoster virus. *J. Infect. Dis.* 142, 414–420. doi: 10.1093/infdis/142.3.414

Myers, M. G., Stanberry, L. R., and Edmond, B. J. (1985). Varicella-zoster virus infection of strain 2 guinea pigs. *J. Infect. Dis.* 151, 106–113. doi: 10.1093/infdis/151.1.106

Nagel, M. A., Jones, D., and Wyborny, A. (2017). Varicella zoster virus vasculopathy: the expanding clinical spectrum and pathogenesis. *J. Neuroimmunol.* 308, 112–117. doi: 10.1016/j.jneuroim.2017.03.014

Niewiesk, S., Eisenhuth, I., Fooks, A., Clegg, J. C., Schnorr, J. J., Schneider-Schaulies, S., et al. (1997). Measles virus-induced immune suppression in the cotton rat (*Sigmodon hispidus*) model depends on viral glycoproteins. *J. Virol.* 71, 7214–7219.

Oliver, S. L., Zerboni, L., Sommer, M., Rajamani, J., and Arvin, A. M. (2008). Development of recombinant varicella-zoster viruses expressing luciferase fusion proteins for live in vivo imaging in human skin and dorsal root ganglia xenografts. *J. Virol. Methods* 154, 182–193. doi: 10.1016/j.jviromet.2008.07.033

Osterrieder, N., Schumacher, D., Trapp, S., Beer, M., von Einem, J., and Tischer, K. (2003). [Establishment and use of infectious bacterial artificial chromosome (BAC) DNA clones of animal herpesviruses]. *Berl Munch Tierarztl Wochenschr* 116, 373–380.

Ouwendijk, W. J., Choe, A., Nagel, M. A., Gilden, D., Osterhaus, A. D., Cohrs, R. J., et al. (2012). Restricted varicella-zoster virus transcription in human trigeminal ganglia obtained soon after death. *J. Virol.* 86, 10203–10206. doi: 10.1128/JVI.01331-12

Oxman, M. N., Levin, M. J., Johnson, G. R., Schmader, K. E., Straus, S. E., Gelb, L. D., et al. (2005). A vaccine to prevent herpes zoster and postherpetic neuralgia in older adults. *N. Engl. J. Med.* 352, 2271–2284. doi: 10.1056/NEJMoa051016

Pavan-Langston, D., and Dunkel, E. C. (1989). Ocular varicella-zoster virus infection in the guinea pig. A new in vivo model. *Arch. Ophthalmol.* 107, 1068–1072.

Perng, G. C., Jones, C., Ciacci-Zanella, J., Stone, M., Henderson, G., Yukht, A., et al. (2000). Virus-induced neuronal apoptosis blocked by the herpes simplex virus latency-associated transcript. *Science* 287, 1500–1503. doi: 10.1126/science.287.5457.1500

Pevenstein, S. R., Williams, R. K., McChesney, D., Mont, E. K., Smialek, J. E., and Straus, S. E. (1999). Quantitation of latent varicella-zoster virus and herpes simplex virus genomes in human trigeminal ganglia. *J. Virol.* 73, 10514–10518.

Pugazhenthi, S., Nair, S., Velmurugan, K., Liang, Q., Mahalingam, R., Cohrs, R. J., et al. (2011). Varicella-zoster virus infection of differentiated human neural stem cells. *J. Virol.* 85, 6678–6686. doi: 10.1128/JVI.00445-11

Pui, J. C., Furth, E. E., Minda, J., and Montone, K. T. (2001). Demonstration of varicella-zoster virus infection in the muscularis propria and myenteric plexi of the colon in an HIV-positive patient with herpes zoster and small bowel pseudo-obstruction (Ogilvie's syndrome). *Am. J. Gastroenterol.* 96, 1627–1630. doi: 10.1111/j.1572-0241.2001.03808.x

Quinlivan, M., and Breuer, J. (2014). Clinical and molecular aspects of the live attenuated Oka varicella vaccine. *Rev. Med. Virol.* 24, 254–273. doi: 10.1002/rmv.1789

Quinlivan, M. L., Jensen, N. J., Radford, K. W., and Schmid, D. S. (2012). Novel genetic variation identified at fixed loci in ORF62 of the Oka varicella vaccine and in a case of vaccine-associated herpes zoster. *J. Clin. Microbiol.* 50, 1533–1538. doi: 10.1128/JCM.06630-11

Rahaus, M., Desloges, N., and Wolff, M. H. (2004). Replication of varicella-zoster virus is influenced by the levels of JNK/SAPK and p38/MAPK activation. *J. Gen. Virol.* 85(Pt 12), 3529–3540. doi: 10.1099/vir.0.80347-0

Sabella, C., Lowry, P. W., Abbruzzi, G. M., Koropchak, C. M., Kinchington, P. R., Sadegh-Zadeh, M., et al. (1993). Immunization with the immediate-early tegument protein (open reading frame 62) of varicella-zoster virus protects guinea pigs against virus challenge. *J. Virol.* 67, 7673–7676.

Sadaoka, T., Depledge, D. P., Rajbhandari, L., Venkatesan, A., Breuer, J., and Cohen, J. I. (2016). In vitro system using human neurons demonstrates that varicella-zoster vaccine virus is impaired for reactivation, but not latency. *Proc. Natl. Acad. Sci. U.S.A.* 113, E2403–E2412. doi: 10.1073/pnas.1522575113

Sadaoka, T., Schwartz, C. L., Rajbhandari, L., Venkatesan, A., and Cohen, J. I. (2018). Human embryonic stem cell-derived neurons are highly permissive for Varicella-Zoster Virus lytic infection. *J. Virol.* 92:e01108-17. doi: 10.1128/JVI.01108-17

Sadzot-Delvaux, C., Debrus, S., Nikkels, A., Piette, J., and Rentier, B. (1995). Varicella-zoster virus latency in the adult rat is a useful model for human latent infection. *Neurology* 45(12 Suppl. 8), S18–S20.

Sadzot-Delvaux, C., Merville-Louis, M. P., Delree, P., Marc, P., Piette, J., Moonen, G., et al. (1990). An in vivo model of varicella-zoster virus latent infection of dorsal root ganglia. *J. Neurosci. Res.* 26, 83–89. doi: 10.1002/jnr.490260110

Sato, H., Callanan, L. D., Pesnicak, L., Krogmann, T., and Cohen, J. I. (2002a). Varicella-zoster virus (VZV) ORF17 protein induces RNA cleavage and is critical for replication of VZV at 37 degrees C but not 33 degrees C. *J. Virol.* 76, 11012–11023. doi: 10.1128/jvi.76.21.11012-11023.2002

Sato, H., Pesnicak, L., and Cohen, J. I. (2002b). Varicella-zoster virus open reading frame 2 encodes a membrane phosphoprotein that is dispensable for viral replication and for establishment of latency. *J. Virol.* 76, 3575–3578. doi: 10.1128/jvi.76.7.3575-3578.2002

Schaap, A., Fortin, J. F., Sommer, M., Zerboni, L., Stamatis, S., Ku, C. C., et al. (2005). T-cell tropism and the role of ORF66 protein in pathogenesis of varicella-zoster virus infection. *J. Virol.* 79, 12921–12933. doi: 10.1128/JVI.79.20.12921-12933.2005

Selariu, A., Cheng, T., Tang, Q., Silver, B., Yang, L., Liu, C., et al. (2012). ORF7 of varicella-zoster virus is a neurotropic factor. *J. Virol.* 86, 8614–8624. doi:10.1128/JVI.00128-12

Shipley, M. M., Mangold, C. A., Kuny, C. V., and Szpara, M. L. (2017). Differentiated human SH-SY5Y cells provide a reductionist model of herpes simplex virus 1 neurotropism. *J. Virol.* 91:e00958-17. doi: 10.1128/JVI.00958-17

Smith, G. A., Gross, S. P., and Enquist, L. W. (2001). Herpesviruses use bidirectional fast-axonal transport to spread in sensory neurons. *Proc. Natl. Acad. Sci. U.S.A.* 98, 3466–3470. doi: 10.1073/pnas.061029798

Sorel, O., and Messaoudi, I. (2018). Varicella virus-host interactions during latency and reactivation: lessons from simian varicella virus. *Front. Microbiol.* 9:3170. doi: 10.3389/fmicb.2018.03170

St Leger, A. J., and Hendricks, R. L. (2011). CD8+ T cells patrol HSV-1-infected trigeminal ganglia and prevent viral reactivation. *J. Neurovirol.* 17, 528–534. doi: 10.1007/s13365-011-0062-1

Steain, M., Gowrishankar, K., Rodriguez, M., Slobedman, B., and Abendroth, A. (2011). Upregulation of CXCL10 in human dorsal root ganglia during experimental and natural varicella-zoster virus infection. *J. Virol.* 85, 626–631. doi: 10.1128/JVI.01816-10

Stinson, C., Deng, M., Yee, M. B., Bellinger, L. L., Kinchington, P. R., and Kramer, P. R. (2017). Sex differences underlying orofacial varicella zoster associated pain in rats. *BMC Neurol.* 17:95. doi: 10.1186/s12883-017-0882-6

Tang, Y., Yu, P., and Cheng, L. (2017). Current progress in the derivation and therapeutic application of neural stem cells. *Cell Death Dis.* 8:e3108. doi: 10.1038/cddis.2017.504

Thompson, R. L., and Sawtell, N. M. (2001). Herpes simplex virus type 1 latency-associated transcript gene promotes neuronal survival. *J. Virol.* 75, 6660–6675. doi: 10.1128/JVI.75.14.6660-6675.2001

Thomson, J. A., Itskovitz-Eldor, J., Shapiro, S. S., Waknitz, M. A., Swiergiel, J. J., Marshall, V. S., et al. (1998). Embryonic stem cell lines derived from human blastocysts. *Science* 282, 1145–1147. doi: 10.1126/science.282.5391.1145

Tischer, B. K., Kaufer, B. B., Sommer, M., Wussow, F., Arvin, A. M., and Osterrieder, N. (2007). A self-excisable infectious bacterial artificial chromosome clone of varicella-zoster virus allows analysis of the essential tegument protein encoded by ORF9. *J. Virol.* 81, 13200–13208. doi: 10.1128/JVI.01148-07

Umbach, J. L., Kramer, M. F., Jurak, I., Karnowski, H. W., Coen, D. M., and Cullen, B. R. (2008). MicroRNAs expressed by herpes simplex virus 1 during latent infection regulate viral mRNAs. *Nature* 454, 780–783. doi: 10.1038/nature07103

Umbach, J. L., Nagel, M. A., Cohrs, R. J., Gilden, D. H., and Cullen, B. R. (2009). Analysis of human alphaherpesvirus microRNA expression in latently infected human trigeminal ganglia. *J. Virol.* 83, 10677–10683. doi: 10.1128/JVI.01185-09

van Velzen, M., Jing, L., Osterhaus, A. D., Sette, A., Koelle, D. M., and Verjans, G. M. (2013). Local CD4 and CD8 T-cell reactivity to HSV-1 antigens documents broad viral protein expression and immune competence in latently infected human trigeminal ganglia. *PLoS Pathog.* 9:e1003547. doi: 10.1371/journal.ppat.1003547

Wagner, E. K., Devi-Rao, G., Feldman, L. T., Dobson, A. T., Zhang, Y. F., Flanagan, W. M., et al. (1988a). Physical characterization of the herpes simplex virus latency-associated transcript in neurons. *J. Virol.* 62, 1194–1202.

Wagner, E. K., Flanagan, W. M., Devi-Rao, G., Zhang, Y. F., Hill, J. M., Anderson, K. P., et al. (1988b). The herpes simplex virus latency-associated transcript is spliced during the latent phase of infection. *J. Virol.* 62, 4577–4585.

Wang, L., Oliver, S. L., Sommer, M., Rajamani, J., Reichelt, M., and Arvin, A. M. (2011). Disruption of PML nuclear bodies is mediated by ORF61 SUMO-interacting motifs and required for varicella-zoster virus pathogenesis in skin. *PLoS Pathog.* 7:e1002157. doi: 10.1371/journal.ppat.1002157

Warren, K. G., Marusyk, R. G., Lewis, M. E., and Jeffrey, V. M. (1982). Recovery of latent herpes simplex virus from human trigeminal nerve roots. *Arch. Virol.* 73, 84–89.

Watson, Z. L., Washington, S. D., Phelan, D. M., Lewin, A. S., Tuli, S. S., Schultz, G. S., et al. (2018). In vivo knockdown of the herpes simplex virus 1 latency-associated transcript reduces reactivation from latency. *J. Virol.* 92:e00812-18. doi: 10.1128/JVI.00812-18

Wechsler, S. L., Nesburn, A. B., Watson, R., Slanina, S., and Ghiasi, H. (1988). Fine mapping of the major latency-related RNA of herpes simplex virus type 1 in humans. *J. Gen. Virol.* 69(Pt 12), 3101–3106. doi: 10.1099/0022-1317-69-12-3101

Wilcox, C. L., and Johnson, E. M. Jr. (1987). Nerve growth factor deprivation results in the reactivation of latent herpes simplex virus in vitro. *J. Virol.* 61, 2311–2315.

Wroblewska, Z., Valyi-Nagy, T., Otte, J., Dillner, A., Jackson, A., Sole, D. P., et al. (1993). A mouse model for varicella-zoster virus latency. *Microb. Pathog.* 15, 141–151. doi: 10.1006/mpat.1993.1064

Wu, Q., Rivailler, P., Xu, S., and Xu, W. (2019). Comparison of the whole genome sequence of an Oka varicella vaccine from China with other Oka vaccine strains reveals sites putatively critical for vaccine efficacy. *J. Virol.* 93:e02281-18. doi: 10.1128/JVI.02281-18

Xia, D., Srinivas, S., Sato, H., Pesnicak, L., Straus, S. E., and Cohen, J. I. (2003). Varicella-zoster virus open reading frame 21, which is expressed during latency, is essential for virus replication but dispensable for establishment of latency. *J. Virol.* 77, 1211–1218. doi: 10.1128/jvi.77.2.1211-1218.2003

Yu, X., Seitz, S., Pointon, T., Bowlin, J. L., Cohrs, R. J., Jonjic, S., et al. (2013). Varicella zoster virus infection of highly pure terminally differentiated human neurons. *J. Neurovirol.* 19, 75–81. doi: 10.1007/s13365-012-0142-x

Zapata, H. J., Nakatsugawa, M., and Moffat, J. F. (2007). Varicella-zoster virus infection of human fibroblast cells activates the c-Jun N-terminal kinase pathway. *J. Virol.* 81, 977–990. doi: 10.1128/JVI.01470-06

Zerboni, L., and Arvin, A. (2011). Investigation of varicella-zoster virus neurotropism and neurovirulence using SCID mouse-human DRG xenografts. *J. Neurovirol.* 17, 570–577. doi: 10.1007/s13365-011-0066-x

Zerboni, L., and Arvin, A. (2015). Neuronal subtype and satellite cell tropism are determinants of varicella-zoster virus virulence in human dorsal root ganglia xenografts in vivo. *PLoS Pathog.* 11:e1004989. doi: 10.1371/journal.ppat.1004989

Zerboni, L., Ku, C. C., Jones, C. D., Zehnder, J. L., and Arvin, A. M. (2005). Varicella-zoster virus infection of human dorsal root ganglia in vivo. *Proc. Natl. Acad. Sci. U.S.A.* 102, 6490–6495. doi: 10.1073/pnas.0501045102

Zerboni, L., Reichelt, M., Jones, C. D., Zehnder, J. L., Ito, H., and Arvin, A. M. (2007). Aberrant infection and persistence of varicella-zoster virus in human dorsal root ganglia in vivo in the absence of glycoprotein I. *Proc. Natl. Acad. Sci. U.S.A.* 104, 14086–14091. doi: 10.1073/pnas.0706023104

Zerboni, L., Sen, N., Oliver, S. L., and Arvin, A. M. (2014). Molecular mechanisms of varicella zoster virus pathogenesis. *Nat. Rev. Microbiol.* 12, 197–210. doi: 10.1038/nrmicro3215

Zerboni, L., Sobel, R. A., Lai, M., Triglia, R., Steain, M., Abendroth, A., et al. (2012). Apparent expression of varicella-zoster virus proteins in latency resulting from reactivity of murine and rabbit antibodies with human blood group a determinants in sensory neurons. *J. Virol.* 86, 578–583. doi: 10.1128/JVI.05950-11

Zerboni, L., Sung, P., Lee, G., and Arvin, A. (2018). Age-associated differences in infection of human skin in the SCID mouse model of Varicella-Zoster Virus pathogenesis. *J. Virol.* 92:e0002-e18. doi: 10.1128/JVI.00002-18

Zhang, Z., Selariu, A., Warden, C., Huang, G., Huang, Y., Zaccheus, O., et al. (2010). Genome-wide mutagenesis reveals that ORF7 is a novel VZV skin-tropic factor. *PLoS Pathog.* 6:e1000971. doi: 10.1371/journal.ppat.1000971

Zhu, H., Zheng, C., Xing, J., Wang, S., Li, S., Lin, R., et al. (2011). Varicella-zoster virus immediate-early protein ORF61 abrogates the IRF3-mediated innate immune response through degradation of activated IRF3. *J. Virol.* 85, 11079–11089. doi: 10.1128/JVI.05098-11

Ziegler, L., Grigoryan, S., Yang, I. H., Thakor, N. V., and Goldstein, R. S. (2011). Efficient generation of schwann cells from human embryonic stem cell-derived neurospheres. *Stem Cell Rev* 7, 394–403. doi: 10.1007/s12015-010-9198-2

Zwaagstra, J. C., Ghiasi, H., Slanina, S. M., Nesburn, A. B., Wheatley, S. C., Lillycrop, K., et al. (1990). Activity of herpes simplex virus type 1 latency-associated transcript (LAT) promoter in neuron-derived cells: evidence for neuron specificity and for a large LAT transcript. *J. Virol.* 64, 5019–5028.

Conflict of Interest Statement: The authors declare that the research was conducted in the absence of any commercial or financial relationships that could be construed as a potential conflict of interest.

frontiers in Microbiology

ORIGINAL RESEARCH
published: 11 September 2019
doi: 10.3389/fmicb.2019.02117

Persistence of a T Cell Infiltrate in Human Ganglia Years After Herpes Zoster and During Post-herpetic Neuralgia

*Jeremy P. Sutherland[1], Megan Steain[2], Michael E. Buckland[3], Michael Rodriguez[4], Anthony L. Cunningham[5], Barry Slobedman[2] and Allison Abendroth[2]**

[1] Emergency Department, Westmead Hospital, The University of Sydney, Sydney, NSW, Australia, [2] Discipline of Infectious Diseases and Immunology, The University of Sydney, Sydney, NSW, Australia, [3] Department of Neuropathology, Royal Prince Alfred Hospital, The University of Sydney, Sydney, NSW, Australia, [4] Department of Pathology, The University of Sydney, Sydney, NSW, Australia, [5] Centre for Virus Research, Westmead Institute for Medical Research, Westmead, NSW, Australia

OPEN ACCESS

Edited by:
Randall J. Cohrs, University of Colorado Denver School of Medicine, United States

Reviewed by:
Georges Verjans, Erasmus University Medical Center, Netherlands
Marco Antonio Campos, Fiocruz Research Center Renê Rachou, Brazil
Vicki Traina-Dorge, Tulane University, United States

***Correspondence:**
Allison Abendroth
allison.abendroth@sydney.edu.au

Specialty section:
This article was submitted to Virology, a section of the journal Frontiers in Microbiology

Received: *31 May 2019*
Accepted: *28 August 2019*
Published: *11 September 2019*

Citation:
Sutherland JP, Steain M, Buckland ME, Rodriguez M, Cunningham AL, Slobedman B and Abendroth A (2019) Persistence of a T Cell Infiltrate in Human Ganglia Years After Herpes Zoster and During Post-herpetic Neuralgia. Front. Microbiol. 10:2117. doi: 10.3389/fmicb.2019.02117

Varicella-zoster virus (VZV) is a human herpesvirus which causes varicella (chicken pox) during primary infection, establishes latency in sensory ganglia, and can reactivate from this site to cause herpes zoster (HZ) (shingles). A major complication of HZ is a severe and often debilitating pain called post-herpetic neuralgia (PHN) which persists long after the resolution of the HZ-associated rash. The underlying cause of PHN is not known, although it has been postulated that it may be a consequence of immune cell mediated damage. However, the nature of virus-immune cell interactions within ganglia during PHN is unknown. We obtained rare formalin fixed paraffin embedded sections cut from surgically excised ganglia from a PHN-affected patient years following HZ rash resolution. VZV DNA was readily detected by qPCR and regions of immune infiltration were detected by hematoxylin and eosin staining. Immunostaining using a range of antibodies against immune cell subsets revealed an immune cell response comprising of $CD4^+$ and $CD8^+$ T cells and $CD20^+$ B cells. This study explores the immune cell repertoire present in ganglia during PHN and provides evidence for an ongoing immune cell inflammation years after HZ.

Keywords: herpes zoster (HZ), varicella-zoster virus, ganglia, post-herpetic neuralgia (PHN), immune cell

INTRODUCTION

Varicella zoster virus (VZV) is a highly species specific human herpesviruses responsible for two clinically distinct human diseases. Primary infection results in varicella (chickenpox), during which the virus establishes latency within neurons in the sensory ganglia (Gilden et al., 1983, 1987; Hyman et al., 1983; Lungu et al., 1995; Kennedy et al., 1998; LaGuardia et al., 1999; Levin et al., 2003; Wang et al., 2005). Latency is maintained throughout the life of the host. During latency there is cessation of viral replication and no production of progeny virions (Depledge et al., 2018). Herpes zoster (HZ) also known as shingles is the result of reactivation from latency, and may be followed by a severe neuropathic pain called post-herpetic neuralgia (PHN). PHN is defined as pain lasting longer than 90 days following the onset of the HZ rash (Watson et al., 1988a;

Schmader, 2007; Steiner et al., 2007). PHN affects approximately 10% of all and 30% of elderly patients following HZ. In 30–50% of such patients it persists for more than 1 year, and in some for many years and often has significant negative affects on their quality of life (Coplan et al., 2004; Dworkin et al., 2007, 2008; Kawai et al., 2014).

The underlying pathology and pathogenesis of PHN is unknown, and investigations into PHN are complicated by the rare nature of relevant clinical samples and the non-availability of a suitable animal model. PHN may result from damage to the sensorineural pain pathway during HZ, resulting in malfunctioning of sensory neurons causing the transmission of pain signals (Bennett, 1994; Steiner et al., 2007). An alternate hypothesis is the presence of ongoing viral replication and/or immunopathology within the sensory ganglia resulting from immune infiltration against viral antigens (Steiner et al., 2007). The development of PHN is predicted by the severity of acute HZ pain [reviewed in Kawai et al. (2015)].

Previous studies of human ganglia from PHN-affected individuals have been limited to basic histological examination of rare post-mortem material from PHN-affected patients. To date, there have only been three studies, which have noted infiltrations of inflammatory cells and general cell loss within the dorsal root ganglia (DRG) which innervate the painful area (Smith, 1978; Watson et al., 1988b, 1991a). Our laboratory has developed immunohistochemical and immunofluorescent based assays to investigate immune cell subsets in ganglia months after contracting HZ and during active VZV reactivation. Our previous study of ganglia obtained 1–5 months after contracting HZ revealed a robust immune cell infiltrate is still present following the disappearance of the rash and is comprised largely of non-cytolytic (granzyme B-negative) T cells and macrophages (Gowrishankar et al., 2010). More recently, we examined several ganglia from a patient who died with a HZ rash and demonstrated that $CD4^+$ and cytolytic $CD8^+$ T cells may play an important role in the ganglia during active HZ (Steain et al., 2014). However, to date there have been no detailed studies of ganglia obtained from an individual experiencing clinically defined, prolonged PHN (years after resolution of the HZ rash).

As a result of our very limited understanding of the ongoing pathology of PHN, treatment options are very limited. There is a range of pharmacological, interventional and surgical options available. However, in most cases the pain can often be severe and intractable (Wu and Raja, 2008; Chen et al., 2014) and some patients continue to suffer until death despite the successful introduction of pregabalin, a substantial advance (Snedecor et al., 2014). However, until the mechanism(s) underlying the cause of PHN are better understood, treatment and prevention strategies will remain limited, and patients will continue to develop and suffer from the devastating effects of PHN.

The aim of this study was to investigate VZV antigen expression and nucleic acid levels within ganglion samples from a PHN-affected patient (years following rash resolution) and a HZ-affected patient (presence of HZ rash). These rare clinical samples were also used to define for the first time the nature of the immune cell subsets present within human ganglia years after HZ rash resolution in an individual suffering from PHN.

RESULTS

Description of Cases and Histological Examination of Human Ganglia During Post-herpetic Neuralgia

One of the greatest obstacles to the study of PHN and HZ is the difficulty in obtaining appropriate human ganglia samples. For this study we obtained very rare surgically excised PHN-affected ganglia, as well as post-mortem ganglia from a patient suffering HZ at the time of death, and two control cases consisting of ganglia from individuals without any evidence of VZV disease.

The PHN-affected patient was a 59 year old female who was diagnosed with acute myeloid leukemia, and underwent a bone marrow transplant. During recovery the patient experienced HZ in the right thoracic region (T9–T12), and following the resolution of the rash experienced prolonged pain (>5 years) around the same anatomical site. After exhausting all conservative treatment options a ganglionectomy was performed in an attempt to control the pain, with right thoracic T11 ganglion removed. Nine months later, a second ganglionectomy was performed, with right thoracic T10 removed. Surgery was performed when the patient was 60 years of age. Both of the right T10 and right T11 ganglia (termed PHN1 and PHN2, respectively) were utilized in this study.

The HZ patient was a 93 year old male with frontotemporal dementia who died due to aspiration pneumonia. This patient developed a HZ rash approximately 17 days prior to death. At autopsy there was a hemorrhagic vesicular and ulcerated rash in a left lumbar dermatome. The ganglion innervating the site of the rash (left lumbar L2) was collected, and noted to be inflamed.

The first control patient thoracic ganglion (CON1) was from a 73 year old female who died due to metastatic adenocarcinoma. The second control patient ganglion (CON2) was from a 73 year old female who died due to a head injury. Medical records indicate that these patients experienced no clinical VZV reactivation prior to their death.

Histological examination of ganglia samples utilized a hematoxylin and eosin (HE) stain on 5 μm formal fixed paraffin embedded (FFPE) sections with representative images shown in **Figure 1**. This staining revealed focal infiltrations of small immune-like cells within both the PHN1 and PHN2 ganglia samples (**Figures 1A,B**). There was a greater infiltration of small round immune-like cells spread throughout the HZ ganglion sample (**Figure 1C**). In the sections examined we observed no significant areas of neuronal cell loss. Intact neuronal profiles surrounded by satellite cells were observed in ganglia from the two control patients but there were no apparent infiltration of immune-like cells (**Figures 1D,E**).

Ganglia Samples Were Infected With VZV, but Not HSV-1

Viable DNA was successfully isolated from all ganglion samples. The presence of VZV DNA was confirmed in all PHN and HZ-affected material via PCR, yet the closely related virus HSV-1 was

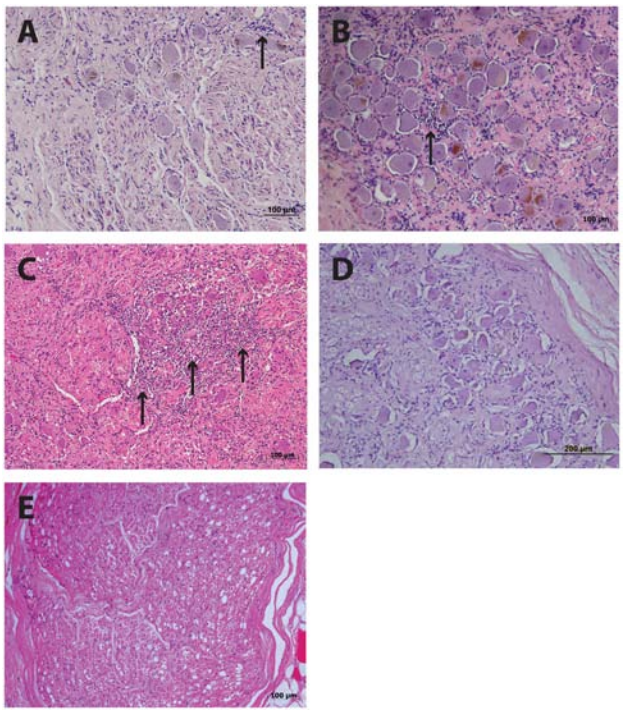

FIGURE 1 | Histology of human ganglia during post-herpetic neuralgia (PHN) and herpes zoster (HZ). Representative images of hematoxylin and eosin staining ganglion sections from PHN ganglia sample 1 **(A)** and sample 2 **(B)** showing infiltrates of small round immune-like cells (arrows). Ganglion sections from a case of active HZ **(C)**, and control ganglia sample 1 **(D)** and 2 **(E)**.

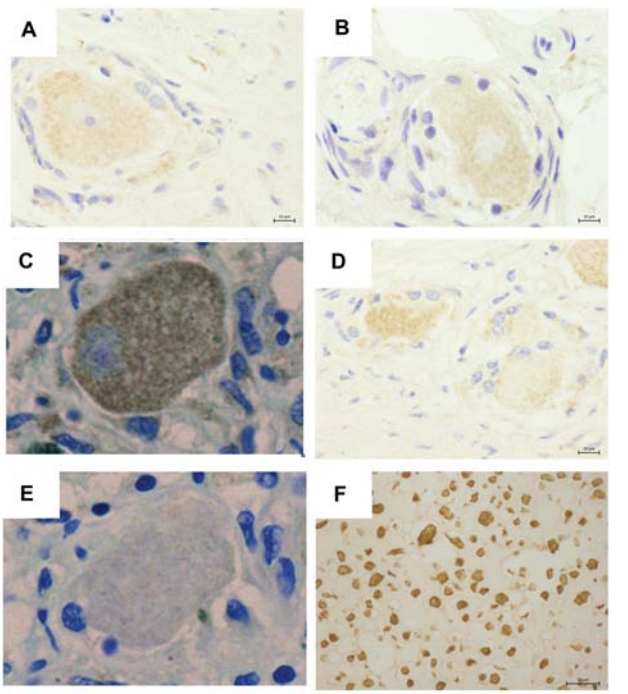

FIGURE 2 | Immunohistochemical detection of VZV antigens in human ganglia from patients experiencing herpes zoster. Representative images of ganglionic sections from PHN1 **(A)** and PHN2 **(B)**, HZ **(C)**, and CON1 **(D)**, as well as a positive control section of infected human fibroblasts stained **(F)** with an anti-VZV IE63 specific antibody. Isotype control antibodies were also applied to a HZ ganglion section **(E)**. Bound primary antibodies were visualized using DAB substrate, and sections were counterstained with Azure B.

not detected (data not shown). Thus, the immune cell infiltration observed in these ganglionic samples was not a consequence of HSV-1 infection.

To further investigate VZV DNA load a real-time PCR approach for VZV open reading frame 28 (ORF28) was employed. Nucleic acids were extracted from sections and the VZV DNA ganglia load calculated. Sufficient DNA was obtained from the PHN2, HZ and CON2 samples only. Human albumin is present in tissue as one copy per cell, and provides a standard against which the copy number of VZV DNA was calculated. There were 2.95×10^5 copies of VZV DNA per 10^5 cells in PHN2 and 4.27×10^4 copies of VZV DNA per 10^5 cells in HZ. No VZV DNA was detected in CON2. This result demonstrates that VZV DNA was readily detectable in ganglia of a PHN-affected patient years after the resolution of their HZ rash and may provide evidence of an ongoing virological process during PHN.

Immunohistochemical Investigation of VZV Antigen Expression in Human Ganglia Samples

Detection of VZV antigen expression in FFPE material has proven to be problematic (Zerboni et al., 2012). Thus we utilized our well-established immunohistochemical (IHC) assay with an antibody against VZV immediate early protein 63 (IE63), to assess VZV antigen expression within ganglionic sections.

Varicella zoster virus IE63 staining was not detected in PHN1 and PHN2 affected ganglia (**Figures 2A,B**). In contrast, VZV IE63 antigen expression was observed at low levels within regions of the HZ ganglia from the site of reactivation (**Figure 2C**). No staining was observed on control ganglionic samples (**Figure 2D**) or ganglionic sections incubated with isotype control antibodies (**Figure 2E**). FFPE human neurons typically show background staining with antibodies via IHC. As expected the positive control VZV infected human fibroblasts (HFs) readily stained for VZV IE63 (**Figure 2F**). IHC and immunofluorescence assay (IFA) was also performed using an antibody specific for the VZV glycoprotein E-glycoprotein I complex and VZV glycoprotein E, respectively and no VZV antigen expression was detected in either of the PHN ganglia (data not shown). Thus VZV antigen expression was not observed in human ganglia during PHN.

Characterization of Infiltrating Immune Cells in Human Ganglia *in vivo*

Previous studies have shown the presence of immune like cells within PHN-affected ganglia material (Vafai et al., 1988; Watson et al., 1988b, 1991a), however, to date there has been

no detailed characterization of the phenotype of these cells. To characterize the immune cells within the ganglia excised from a PHN-affected patient, and the ganglion innervating the site of reactivation of a HZ-affected patient, IFA staining for CD3, CD4, and CD8 to detect T cells, T helper and cytotoxic T cell subsets, and CD20 to detect B cells was performed. Cytotoxic T cells were further identified using the marker TIA-1. Isotype control antibodies were also utilized to establish the level of any non-specific background fluorescence. In both PHN ganglia and the HZ sample there was a large increase in the number of $CD3^+$ T cells present when compared to the control samples but the number of CD3/CD4 lymphocytes was greatest in the HZ sample. Representative images are shown in **Figure 3A**, and frequencies of immune cells are shown in **Figure 3B**. Infiltration of $CD3^+$ T cells was greatest in the HZ sample and these were observed throughout the neuronal regions of the ganglion. The PHN1 sample contained $CD3^+$ T cells and $CD20^+$ B cells in all regions of the ganglion, but with infiltrating cells spread throughout both neuronal and nerve bundle regions of the ganglion. PHN2 ganglion had an infiltration of $CD3^+$ T and $CD20^+$ B cells mainly restricted to the neuronal region. The PHN ganglia showed comparable frequencies of $CD4^+$ and $CD8^+$ T cells. This contrasted to that observed in HZ affected ganglia where there was a predominance of $CD4^+$ T cells over $CD8^+$ T cells (**Figure 3B**). Interestingly when staining for the cytotoxic marker TIA-1, TIA-1^+ cells were readily observed in the HZ affected ganglia, but were less prominent in the PHN affected ganglia (**Figure 3B**). As expected there was limited staining for the various immune cell subsets in the control ganglia samples (**Figures 3A,B**).

Our data demonstrate a B cell and T cell immune infiltrate, with T cells displaying hallmarks of cytolytic T cells within PHN-affected human ganglia material obtained from a patient on long-term immunosuppressive therapy years following the resolution of the HZ associated rash.

DISCUSSION

Despite PHN having a significant impact on patient quality of life, there is a dearth of published studies investigating human ganglia during PHN. Notably only three publications have reported basic histological observations (Smith, 1978; Watson et al., 1988b, 1991b). Our study provides evidence that immune cells infiltrate ganglia during ongoing PHN and $CD4^+$ and $CD8^+$ T cells are a key feature of this process. Interestingly, despite the presence of immune cells a substantial viral DNA load was detected in these ganglia.

The PHN ganglia samples contained similar numbers of $CD4^+$ and $CD8^+$ T cells. Furthermore, there were TIA-1^+ cells readily observed within these ganglia. This is in contrast to previous observations in ganglia from HZ-affected patients, which show a predominance of cytolytic $CD4^+$ T cells during active HZ reactivation (Steain et al., 2014), and non-cytolytic $CD8^+$ T cells in months following HZ reactivation (Gowrishankar et al., 2010). In the current study the number of TIA positive cells exceeded the number of $CD8^+$ T cells. It is possible that this difference may be due to infiltrating cytolytic natural killer (NK) cells, as we have previously reported to be present in ganglia months after VZV reactivation (Gowrishankar et al., 2010).

One of the limitations of our study is the inherent difficulty in obtaining sensory ganglia from individuals who had HZ and suffered from PHN, and thus our sample size is small. This limits the extent to which we can make quantitative comparative analyses, although even with such small sample size, there appear to be differences in the nature of the immune infiltrate across the different patient groups. In addition, FFPE sections are notoriously difficult to unmask and detect antigens by IHC and IFA approaches. Staining for other immune cell markers such as NK cells, mast cells, macrophages, neutrophils and activation markers was not feasible due to technical constraints and the limited amount of ganglionic material available. Nonetheless, with the scarce ganglionic material available our data demonstrate a B cell and T cell immune infiltrate, with T cells displaying hallmarks of cytolytic T cells within PHN-affected human ganglia material obtained from a patient on long-term immunosuppressive therapy years following the resolution of the HZ associated rash. The PHN patient experienced subtotal relief of her neuralgia following both operations. The relief was stable over 2 years of clinical follow-up.

Post-herpetic neuralgia is the result of an as yet unidentified mechanism. In this study we have demonstrated persisting VZV DNA in ganglia during PHN (and years after HZ rash resolution). In the absence of detectable VZV antigen expression this may represent a latent pool of virus. In this respect, previous studies have reported in VZV latently infected ganglia a copy number of 258 of VZV DNA per 10^5 cells (Pevenstein et al., 1999) and from 577 to 55,543 copies of VZV DNA per 10^5 cells (Cohrs et al., 2000), with the latter quantity consistent with our estimate in PHN affected ganglia. It remains to be determined, however, whether reseeding of the latent pool following HZ may drive the immune response we detected in PHN, or whether there are small numbers of cells supporting undetected, persistent low level virus replication that may account for this immune infiltrate. This will be an important component of future studies to detect specific latent and lytic viral transcripts via *in situ* hybridization to further define the nature of viral genome persistence and its contribution to PHN. Irrespective of whether such viral genome persistence reflects true latency or perhaps a mixture of latent and low level productive and/or abortive infection, this study provides evidence of an ongoing immunological process that may contribute to the ongoing pain and pathology of PHN in this patient, years following HZ rash resolution.

MATERIALS AND METHODS

Human Tissue Samples

All patient material was obtained in accordance with ethics guidelines of the University of Sydney and the Sydney Local Health District and informed consent of the donor was obtained where applicable. Post-mortem material were obtained from the

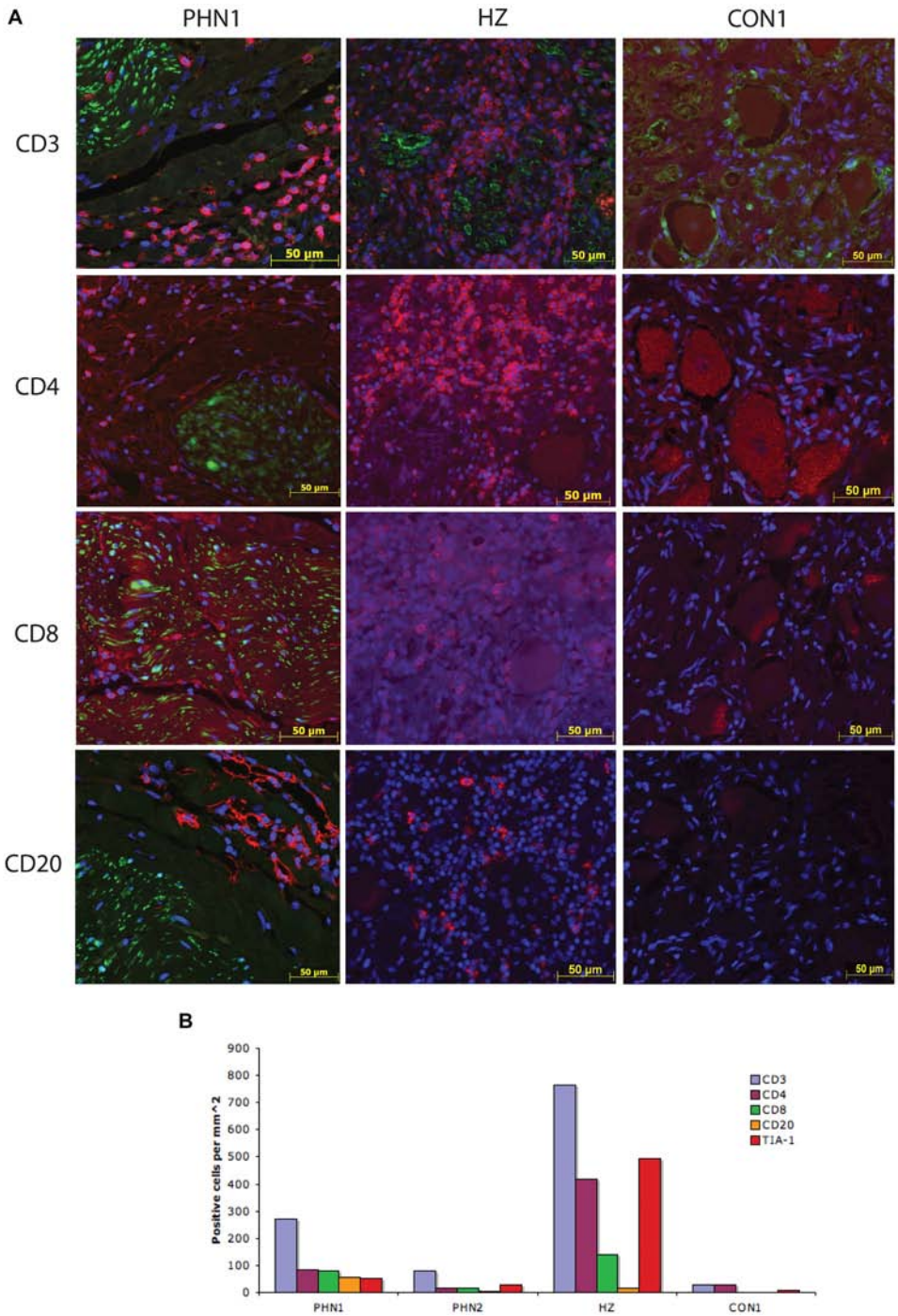

FIGURE 3 | Characterization of the immune response within human ganglia during herpes zoster and post-herpetic neuralgia. **(A)** Representative images are shown for PHN1, HZ, and CON1. Primary antibodies used were specific for CD3, CD4, CD8, and CD20, and were detected using Alexa Fluor fluorescent conjugated antibodies (red). Sections were counterstained with DAPI (blue). All PHN sections were co-stained with all immune cell antibodies, HZ and CON1 with CD3 with an antibody specific for the satellite cell marker S100 (green). **(B)** The number of positive cells per square millimeter for each immune cell marker examined was determined for at least two independent stains and the average is shown.

Department of Forensic Medicine, Glebe, NSW, Australia, by following appropriate ethics approval from University of Sydney, Sydney Local Health District, and the coroner. Trigeminal and DRG fixed in 20% buffered formal were paraffin embedded. A limited number of 5 µm FFPE sections were obtained from each tissue block and mounted onto glass slides.

DNA Extraction

DNA was extracted from FFPE tissue sections using the RecoverAll total nucleic acid isolation kit (Applied Biosystems, United States) as per manufacturer's instructions.

Primers

The human albumin-specific primer pair were as previously published (Douek et al., 2002). The VZV ORF28-specific primer pair sequences were forward CGAACACGTTCCCCATCAA and reverse CCCGGCTTTCTTAGTTTTGG, and the 6-carboxy-fluorescein-linked (FAM) probe sequence was (FAM)-CCA GGTTTTAGTTGATACCA. HSV specific primers for UL42 were forward GCTTTGTGGTGCTGGTT and reverse CTGGT GCTGGACGACAC.

Standard Curve for qRT-PCR

Standard curves were created using serial dilutions of a known amount of linearized plasmid constructs. Plasmid constructs consisted of pGEM-T Easy backbone (Promega, United States) containing small coding regions of human albumin or VZV ORF28 containing the region detected by the corresponding primer pairs.

qRT-PCR Analyses

All samples were processed using a Rotorgene 6000 qRT-PCR machine (Qiagen, Australia). Data was analyzed using Rotorgene 6000 software (Qiagen, Australia). qRT-PCR for human albumin was performed using the SYBR Green system (Invitrogen, United States) as per manufacturer's instructions. Cycling conditions were as follows: 50°C for 2 min, 95°C for 2 min, 45 cycles of 95°C for 10 s, 62°C for 15 s, 72°C for 20 s (acquiring fluorescence levels during this step). qRT-PCR for VZV ORF28 was performed using the Rotor-Gene Probe PCR kit (Qiagen, Australia). Cycling conditions were as follows: 95°C for 3 min, 50 cycles of 95°C for 3 s and 60°C for 10 s (acquiring fluorescence).

Immunohistochemistry and Immunofluorescence Staining

Single and dual immunofluorescence staining was performed as previously described (Gowrishankar et al., 2010).

Antibodies

The following primary antibodies and dilutions were used: mouse anti-human CD3 (Novocastra, Australia) (20 μg/mL), goat anti-human CD4 (R&D Systems, United States) (10 μg/mL), Rabbit anti-human CD8 (Abcam, United States) (2 μg/mL), mouse anti-human CD20 (Novocastra, Australia) (18 μg/mL), mouse anti-human T cell intracellular antigen 1 (TIA-1) (Beckman Coulter, Australia) (20 μg/mL), predilute rabbit anti-cow S100 (Dako, Denmark), rabbit anti-VZV IE63 polyclonal antibody (kindly provided by Prof Ravi Mahalingam, University of Colorado, Denver, CO, United States) and mouse anti-VZV gE:gI (Meridian Life Science, Saco, ME, United States). Isotype controls were mouse IgG_1, mouse IgG_{2a} (Invitrogen, United States), normal rabbit and normal goat IgG (R&D systems, United States), were diluted to match primary antibody concentrations. Secondary antibodies were AlexaFluor labeled antibodies (Molecular Probes, United States) at a dilution of 1:200.

Imaging and Cell Counts

Imaging was performed using a Zeiss AxioPlan 2 upright microscope with an AxioCam camera (Zeiss, Australia). To perform cell counts 5–20 (depending on tissue size) random fields of view were captured and manual cell counting performed using the AxioVision image acquisition software. Counts from at least two independent stains were averaged. Tissue area for each field of view was calculated using the "Measure Outline" function of the AxioVisionLE microscope software. The data represents the average number of positive cells per square millimeter of regions of neuronal cell bodies and regions of nerve bundles.

DATA AVAILABILITY

All datasets generated for this study are included in the manuscript and/or supplementary files.

ETHICS STATEMENT

The studies involving human participants were reviewed and approved by The University of Sydney Ethics approval. Written informed consent for participation was not required for this study in accordance with the national legislation and the institutional requirements.

AUTHOR CONTRIBUTIONS

JS planned, performed the experiments, and analyzed the data. AA, BS, and MS planned the experiments and analyzed the data. MB and MR provided the samples. BS and AA received funding for the study. All authors contributed to writing of the manuscript.

FUNDING

This work was supported by the National Health and Medical Research Council Project grant awarded to AA and BS. JS was a recipient of an Australian Postgraduate award.

ACKNOWLEDGMENTS

We would like to thank Dr. Jane Radford of the Department of Histology, The University of Sydney for assistance with cutting and staining sections, Dr. Louise Cole from the Bosch Institute, The University of Sydney for assistance with microscopy, and Prof. Randall Cohrs of the University of Colorado, Denver for the VZV ORF28-specific primer and probe sequences. Microscopy analysis was performed in the Advanced Microscopy Facility in the Bosch Institute, The University of Sydney.

REFERENCES

Bennett, G. J. (1994). Hypotheses on the pathogenesis of herpes zoster-associated pain. *Ann. Neurol.* 35(Supp l), S38–S41.

Chen, N., Li, Q., Yang, J., Zhou, M., Zhou, D., He, L., et al. (2014). Antiviral treatment for preventing postherpetic neuralgia. *Cochrane Database Syst. Rev.* 6:CD006866.

Cohrs, R. J., Randall, J., Smith, J., Gilden, D. H., Dabrowski, C., van Der Keyl, H., et al. (2000). Analysis of individual human trigeminal ganglia for latent herpes simplex virus type 1 and varicella-zoster virus nucleic acids using real-time PCR. *J. Virol.* 74, 11464–11471. doi: 10.1128/jvi.74.24.11464-11471.2000

Coplan, P. M., Schmader, K., Nikas, A., Chan, I. S., Choo, P., Levin, M. J., et al. (2004). Development of a measure of the burden of pain due to herpes zoster and postherpetic neuralgia for prevention trials: adaptation of the brief pain inventory. *J. Pain* 5, 344–356. doi: 10.1016/j.jpain.2004.06.001

Depledge, D. P., Sadaoka, T., and Ouwendijk, W. J. D. (2018). Molecular aspects of varicella-zoster virus latency. *Viruses* 10:E349. doi: 10.3390/v10070349

Douek, D. C., Brenchley, J. M., Betts, M. R., Ambrozak, D. R., Hill, B. J., Okamoto, Y., et al. (2002). HIV preferentially infects HIV-specific CD4+ T cells. *Nature* 417, 95–98. doi: 10.1038/417095a

Dworkin, R. H., White, R., O'Connor, A. B., Baser, O., and Hawkins, K. (2007). Healthcare costs of acute and chronic pain associated with a diagnosis of herpes zoster. *J. Am. Geriatr. Soc.* 55, 1168–1175. doi: 10.1111/j.1532-5415.2007.01231.x

Dworkin, R. H., White, R., O'Connor, A. B., and Hawkins, K. (2008). Health care expenditure burden of persisting herpes zoster pain. *Pain Med.* 9, 348–353. doi: 10.1111/j.1526-4637.2006.00196.x

Gilden, D. H., Rozenman, Y., Murray, R., Devlin, M., and Vafai, A. (1987). Detection of varicella-zoster virus nucleic acid in neurons of normal human thoracic ganglia. *Ann. Neurol.* 22, 377–380. doi: 10.1002/ana.410220315

Gilden, D. H., Vafai, A., Shtram, Y., Becker, Y., Devlin, M., Wellish, M., et al. (1983). Varicella-zoster virus DNA in human sensory ganglia. *Nature* 306, 478–480. doi: 10.1038/306478a0

Gowrishankar, K., Steain, M., Cunningham, A. L., Rodriguez, M., Blumbergs, P., Slobedman, B., et al. (2010). Characterization of the host immune response in human Ganglia after herpes zoster. *J. Virol.* 84, 8861–8870. doi: 10.1128/JVI.01020-10

Hyman, R. W., Ecker, J. R., and Tenser, R. B. (1983). Varicella-zoster virus RNA in human trigeminal ganglia. *Lancet* 2, 814–816. doi: 10.1016/s0140-6736(83)90736-5

Kawai, K., Gebremeskel, B. G., and Acosta, C. J. (2014). Systematic review of incidence and complications of herpes zoster: towards a global perspective. *BMJ Open* 4:e004833. doi: 10.1136/bmjopen-2014-004833

Kawai, K., Rampakakis, E., Tsai, T. F., Cheong, H. J., Dhitavat, J., Covarrubias, A. O., et al. (2015). Predictors of postherpetic neuralgia in patients with herpes zoster: a pooled analysis of prospective cohort studies from North and Latin America and Asia. *Int. J. Infect Dis.* 34, 126–131. doi: 10.1016/j.ijid.2015.03.022

Kennedy, P. G., Grinfeld, E., and Gow, J. W. (1998). Latent varicella-zoster virus is located predominantly in neurons in human trigeminal ganglia. *Proc. Natl. Acad. Sci. U.S.A.* 95, 4658–4662. doi: 10.1073/pnas.95.8.4658

LaGuardia, J. J., Cohrs, R. J., and Gilden, D. H. (1999). Prevalence of varicella-zoster virus DNA in dissociated human trigeminal ganglion neurons and nonneuronal cells. *J. Virol.* 73, 8571–8577.

Levin, M. J., Cai, G. Y., Manchak, M. D., and Pizer, L. I. (2003). Varicella-zoster virus DNA in cells isolated from human trigeminal ganglia. *J. Virol.* 77, 6979–6987. doi: 10.1128/jvi.77.12.6979-6987.2003

Lungu, O., Annunziato, P. W., Gershon, A., Staugaitis, S. M., Josefson, D., LaRussa, P., et al. (1995). Reactivated and latent varicella-zoster virus in human dorsal root ganglia. *Proc. Natl. Acad. Sci. U.SA.* 92, 10980–10984. doi: 10.1073/pnas.92.24.10980

Pevenstein, S. R., Williams, R. K., McChesney, D., Mont, E. K., Smialek, J. E., Straus, S. E., et al. (1999). Quantitation of latent varicella-zoster virus and herpes simplex virus genomes in human trigeminal ganglia. *J. Virol.* 73, 10514–10518.

Schmader, K. (2007). Herpes zoster and postherpetic neuralgia in older adults. *Clin. Geriatr. Med.* 23, 615–632. doi: 10.1016/j.cger.2007.03.003

Smith, F. P. (1978). Pathological studies of spinal nerve ganglia in relation to intractable intercostal pain. *Surg. Neurol.* 10, 50–53.

Snedecor, S. J., Sudharshan, L., Cappelleri, J. C., Sadosky, A., and Desai, P. (2014). Systematic review and meta-analysis of pharmacological therapies for pain associated with postherpetic neuralgia and less common neuropathic conditions. *Int. J. Clin. Pract.* 68, 900–918. doi: 10.1111/ijcp.12411

Steain, M., Sutherland, J. P., Rodriguez, M., Cunningham, A. L., and Slobedman, B. (2014). Analysis of T cell responses during active varicella-zoster virus reactivation in human ganglia. *J. Virol.* 88, 2704–2716. doi: 10.1128/JVI.03445-13

Steiner, I., Kennedy, P. G., and Pachner, A. R. (2007). The neurotropic herpes viruses: herpes simplex and varicella-zoster. *Lancet. Neurol.* 6, 1015–1028. doi: 10.1016/s1474-4422(07)70267-3

Vafai, A., Wellish, M., and Gilden, D. H. (1988). Expression of varicella-zoster virus in blood mononuclear cells of patients with postherpetic neuralgia. *PNAS* 85, 2767–2770. doi: 10.1073/pnas.85.8.2767

Wang, K., Lau, T. Y., Morales, M., Mont, E. K., and Straus, S. E. (2005). Laser-capture microdissection: refining estimates of the quantity and distribution of latent herpes simplex virus 1 and varicella-zoster virus DNA in human trigeminal Ganglia at the single-cell level. *J. Virol.* 79, 14079–14087. doi: 10.1128/jvi.79.22.14079-14087.2005

Watson, C. P., Deck, J. H., Morshead, C., Van, der Kooy D, and Evans, R. J. (1991a). Post-herpetic neuralgia: further post-mortem studies of cases with and without pain. *Pain* 44, 105–117. doi: 10.1016/0304-3959(91)90124-g

Watson, C. P., Watt, V. R., Chipman, M., Birkett, N., and Evans, R. J. (1991b). The prognosis with postherpetic neuralgia. *Pain* 46, 195–199. doi: 10.1016/0304-3959(91)90076-a

Watson, C. P., Evans, R. J., Watt, V. R., and Birkett, N. (1988a). Post-herpetic neuralgia: 208 cases. *Pain* 35, 289–297. doi: 10.1016/0304-3959(88)90139-x

Watson, C. P., Morshead, C., Van der Kooy, D., Deck, J., and Evans, R. J. (1988b). Post-herpetic neuralgia: post-mortem analysis of a case. *Pain* 34, 129–138. doi: 10.1016/0304-3959(88)90158-3

Wu, C. L., and Raja, S. N. (2008). An update on the treatment of postherpetic neuralgia. *J. Pain* 9(1 Suppl. 1), S19–S30. doi: 10.1016/j.jpain.2007.10.006

Zerboni, L., Sobel, R. A., Lai, M., Triglia, R., Steain, M., Abendroth, A., et al. (2012). Apparent expression of varicella-zoster virus proteins in latency resulting from reactivity of murine and rabbit antibodies with human blood group a determinants in sensory neurons. *J. Virol.* 86, 578–583. doi: 10.1128/JVI.05950-11

Conflict of Interest Statement: The authors declare that the research was conducted in the absence of any commercial or financial relationships that could be construed as a potential conflict of interest.

frontiers in Microbiology

REVIEW
published: 19 May 2020
doi: 10.3389/fmicb.2020.00850

Epigenetic Regulation of Kaposi's Sarcoma-Associated Herpesvirus Latency

Mel Campbell[1†], Wan-Shan Yang[2†], Wayne W. Yeh[2], Chen-Hsuan Kao[2] and Pei-Ching Chang[2]*

[1] UC Davis Cancer Center, University of California, Davis, Davis, CA, United States, [2] Institute of Microbiology and Immunology, National Yang-Ming University, Taipei, Taiwan

Kaposi's sarcoma-associated herpesvirus (KSHV) is an oncogenic γ-herpesvirus that infects humans and exhibits a biphasic life cycle consisting of latent and lytic phases. Following entry into host cells, the KSHV genome undergoes circularization and chromatinization into an extrachromosomal episome ultimately leading to the establishment of latency. The KSHV episome is organized into distinct chromatin domains marked by variations in repressive or activating epigenetic modifications, including DNA methylation, histone methylation, and histone acetylation. Thus, the development of KSHV latency is believed to be governed by epigenetic regulation. In the past decade, interrogation of the KSHV epitome by genome-wide approaches has revealed a complex epigenetic mark landscape across KSHV genome and has uncovered the important regulatory roles of epigenetic modifications in governing the development of KSHV latency. Here, we highlight many of the findings regarding the role of DNA methylation, histone modification, post-translational modification (PTM) of chromatin remodeling proteins, the contribution of long non-coding RNAs (lncRNAs) in regulating KSHV latency development, and the role of higher-order episomal chromatin architecture in the maintenance of latency and the latent-to-lytic switch.

Keywords: Kaposi's sarcoma-associated herpesvirus (KSHV), epigenetic, DNA methylation, histone modification, post-translational modification (PTM), long non-coding RNAs (lncRNAs)

OPEN ACCESS

Edited by:
Louis Flamand, Laval University, Canada

Reviewed by:
Keiji Ueda, Osaka University, Japan
Subhash C. Verma, University of Nevada, Reno, United States

***Correspondence:**
Pei-Ching Chang
pcchang@ym.edu.tw

[†]These authors have contributed equally to this work

Specialty section:
This article was submitted to Virology, a section of the journal Frontiers in Microbiology

Received: *08 January 2020*
Accepted: *08 April 2020*
Published: *19 May 2020*

Citation:
Campbell M, Yang W-S, Yeh WW, Kao C-H and Chang P-C (2020) Epigenetic Regulation of Kaposi's Sarcoma-Associated Herpesvirus Latency. Front. Microbiol. 11:850. doi: 10.3389/fmicb.2020.00850

EPIGENETIC REGULATION OF CHROMATIN

"Epigenetics" refers to a heritable phenotype that changes the chromatin conformation and gene transcription without alteration of DNA sequence. Accurate epigenetic status is essential for normal development and maintenance of tissue-specific gene expression in mammals, and disruption of epigenetic regulation can cause aberrant gene expression and diseases, such as cancer. Different from genetic variation, epigenetics is a reversible mechanism that modifies the genome, and thus, repair of epigenetic lesions has been envisioned to be more feasible than correction of DNA mutations. Epigenetic therapies are therefore emerging as an active area of preclinical and clinical cancer research.

There are three primary interconnected epigenetic mechanisms (**Figure 1**), including (i) DNA methylation and hydroxymethylation, (ii) post-translational modifications (PTMs) of chromatin histone proteins, (iii) regulation by non-coding RNAs (ncRNAs), and a fourth relatively recently identified mode of epigenetic control, (iv) architectural/spatial epigenetics (**Figure 2**).

(i) Methylation of the 5th carbon on cytosine (5-mC) was the first identified, and one of the most well-studied epigenetic marks related to cancer (Bhattacharjee et al., 2016). DNA methylation is maintained by DNA methyltransferase 1 (DNMT1), an enzyme that prefers hemi-methylated DNA substrates, whereas DNMT3A and 3B are responsible for *de novo* methylation. 5-mC within CpG islands in mammalian promoter regions is associated with transcription repression and aberrant DNA methylation is a common lesion related to carcinogenesis (Baylin and Jones, 2011). Cytosine hydroxymethylation (5-hmC), a stable intermediate in 5-mC demethylation, was recently identified as a novel epigenetic modification on DNA in mammals (Richa and Sinha, 2014). 5-hmC seems to promote gene expression during active demethylation (Branco et al., 2011).

(ii) The N-terminal tails of histone proteins are post-translationally modified by acetylation, methylation, phosphorylation, ubiquitination, and SUMOylation, among other modifications (Kouzarides, 2007). The most studied histone modifications include acetylation and methylation. By *acetylating* the ε-amino group of lysine (Lys) using histone acetyltransferases (HATs), acetylation neutralizes the net positive charge on histones, leading to the unfolding of chromatin and exposure of negatively charged DNA to DNA-binding proteins, and consequently activation of gene transcription (Kouzarides, 2007). Histone deacetylases (HDACs) remove acetyl groups from histones and silence gene expression. Disrupting the balance between acetylation and deacetylation is linked to transcription dysregulation.

Histone methylation is more complex than acetylation in that both Lys and arginine (Arg) residues are known to be methylated. Arg can be mono- or di-methylated, with the latter in a symmetrical or asymmetrical manner, by protein arginine methyltransferases (PRMTs) (Pal and Sif, 2007). Lys has the potential to be mono-, di-, or tri-methylated by lysine methyltransferases (KMTs) (Klose and Zhang, 2007). In recent years, histone modification has gained attention due to the discovery of a large family of Jumonji C (JmjC) domain-containing histone lysine demethylases (KDMs) (Klose and Zhang, 2007). Histone methylation status is important in epigenetic regulation of gene expression and has been identified as a contributor to disease development.

(iii) Non-coding RNAs (ncRNAs) are RNA transcripts that do not encode proteins. Based on the length, ncRNAs are divided into two classes, (i) small ncRNAs (sncRNAs), with transcripts shorter than 200 nucleotides (nts), and (ii) long ncRNAs (lncRNAs), with transcripts longer than 200 nts that are devoid of protein-coding potential (Ponting et al., 2009; Fatica and Bozzoni, 2014), though some recent evidence shows that certain lncRNAs are able to encode small functional peptides (Nelson et al., 2016). In general, ncRNAs function to regulate gene expression at either the transcriptional or post-transcriptional level, and this regulation often involves components associated with epigenetic processes. Epigenetic-related ncRNAs include microRNAs (miRNAs) and lncRNAs. miRNAs are a group of sncRNAs of approximately 19–22 nts that inhibit target gene expression by binding to complementary regions of mRNAs and forming the miRNA-induced silencing complex (miRISC) (reviewed in Kim et al., 2009). The development of advanced next-generation sequencing (NGS) technology has revealed the presence of large amounts of lncRNAs in the human transcriptome. These RNAs share many common features with mRNAs, including (Bhattacharjee et al., 2016) 5′-methylguanosine cap, (Baylin and Jones, 2011) polyadenylation, (Richa and Sinha, 2014) RNA polymerase II transcription, and (Branco et al., 2011) splicing (Derrien et al., 2012). However, lncRNAs are generally expressed at a lower level and displayed higher tissue specificity than mRNAs (Fatica and Bozzoni, 2014). Emerging evidence suggests that lncRNAs are involved in regulating multiple biological processes through mechanisms including transcriptional (Dimitrova et al., 2014), post-transcriptional (Yoon et al., 2013; Hu X. et al., 2014), and epigenetic (Khalil et al., 2009; Gupta et al., 2010; Tsai et al., 2010) regulation.

(iv) Architectural/spatial epigenetics considers the three-dimensional (3D) structure of a genome and its impact on gene expression and other nuclear activities. How the 3D organization of a genome operates with the addition of dynamics across time and its relationship to nuclear processes including transcription, DNA replication, and chromosome segregation are included in this class of mechanisms (Dekker and Mirny, 2016; Dekker et al., 2017).

THE KSHV GENOME AND LATENCY

The human γ-herpesvirus Kaposi's sarcoma-associated herpesvirus (KSHV, also known as human herpesvirus type 8, HHV-8) is one of the seven recognized human oncogenic viruses and has been linked to Kaposi's sarcoma (KS) (Scadden, 2003), primary effusion lymphoma (PEL) and Multicentric Castleman's disease (MCD) (Wen and Damania, 2010), and an inflammatory syndrome known as KSHV inflammatory cytokine syndrome (KICS) (Uldrick et al., 2010). KSHV is a linear double-stranded DNA virus with genome size of approximately 165–170 kb consisting of a unique coding region (∼145 kb) that encodes ∼90 viral proteins and many non-coding RNAs and is flanked by long terminal repeats (TRs) (Renne et al., 1996; Russo et al., 1996). After entry into host cells, viral genomes are circularized by joining of GC-rich TRs. The viral genomes associate with cellular histones and form an extrachromosomal circular viral episomes. Establishment of latency in infected cells is a common tactic that herpesviruses employ to prevent elimination by the host immune response and to establish lifelong persistent infections. In order to establish and maintain latency, KSHV has acquired different strategies to hijack the host epigenetic machineries to help viral episomes form a

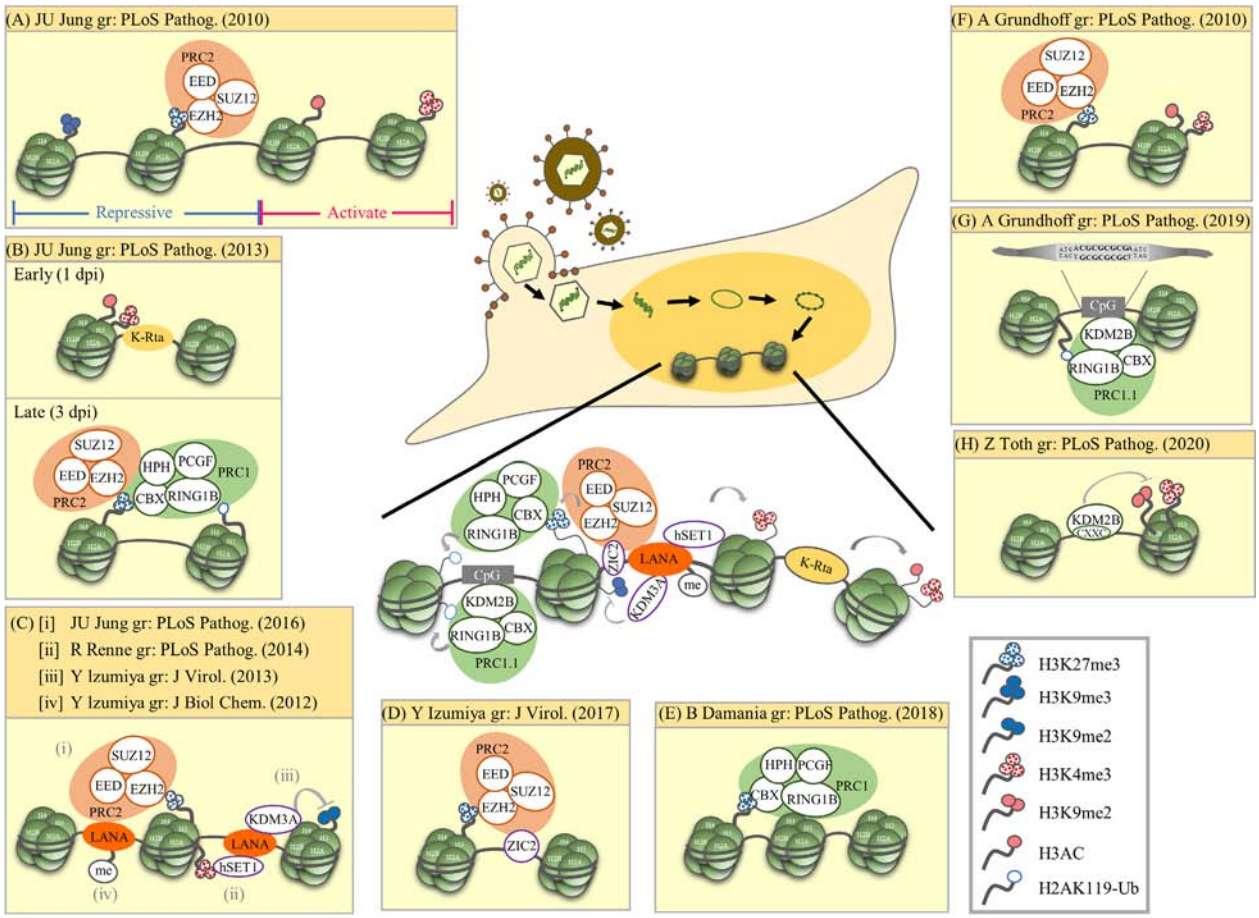

FIGURE 1 | Summary of epigenetic modulation of the latent KSHV genome. The research group (gr) associated with each publication is listed. **(A)** Mutual exclusive localization of histone activation (H3K4me3 and H3-ac) and repressive (H3K27me3 and H3K9me3) marks. The PRC2 complex binds and catalyzes H3K27me3. **(B)** Biphasic euchromatin-to-heterochromatin transition following KSHV infection with initial K-Rta-mediated deposit of active histone marks (H3K4me3 and H3K27-ac). One to three days post-infection (dpi), active histone marks decline and a sequential deposit of H3K27me3 by PRC2, recruitment of PRC1, and deposit of H2AK119-Ub by PRC1. The sequential recruitment of modifying complexes converges to increase repressive histone marks (H3K27me3 and H2AK119-Ub). **(C)** LANA mediated recruitment of histone-modifying enzymes and deposition of corresponding histone marks. (i) LANA recruits PRC2 that potentially increase H3K27me3. (ii) LANA associates with H3K4 methyltransferase hSET1. (iii) LANA associates with H3K9me1/2 histone demethylase KDM3A. (iv) PRMT1-directed methylation of LANA increases its chromatin binding. **(D)** ZIC2 contributes to tethering of PRC2 on the KSHV genome, thus maintaining H3K27me3. **(E)** PRC1 involvement in maintaining nucleosomes on the latent KSHV genome. **(F)** Widespread presence of both active marks (H3K4me3 and H3K9/K14-ac) and repressive marks (H3K27me3) across the latent KSHV genome. **(G)** Direct binding of KDM2B to CpG islands recruits PRC1.1 on the latent KSHV genome. **(H)** KDM2B rapidly binds to the incoming viral DNA and limits the enrichment of activating histone marks on the RTA promoter favoring the downregulation of RTA expression. This early event occurs prior to the polycomb protein-regulated heterochromatin formation on the viral genome. **Summary:** Following *de novo* infection, KSHV K-Rta initiates the acquisition of the active histone marks H3K4me3 and H3K27-ac on the KSHV genome. After LANA is expressed, it mediates the increase of the repressive mark H3K27me3 and the active mark H3K4me3. H3K27me3 consequently recruits PRC1 and increases H2AK119-Ub on the KSHV genome. The cellular protein KDM2B may also help recruit PRCs to the KSHV genome.

heterochromatin structure that restricts viral gene expression to a few genes during latency.

DNA METHYLATION VS. KSHV LATENCY

DNA methylation on CpG islands is associated with gene silencing. It has been shown that the DNA methyltransferase inhibitor 5-Azacytidine (5-AzaC) is a stimulator of KSHV lytic reactivation (Chen et al., 2001), suggesting the involvement of DNA methylation in maintaining KSHV latency. In 2010, Günther and Grundhoff used MeDIP-tiling microarrays to detect global DNA methylation patterns on the KSHV genome following *de novo* infection (Gunther and Grundhoff, 2010). They showed extensive DNA methylation on KSHV latent genomes with the exception of the latency-associated locus. Surprisingly, global viral DNA methylation patterns were shown to develop slower than latency-specific histone modifications (Gunther and Grundhoff, 2010), indicating that DNA methylation is involved in the establishment or maintenance of latency at a later stage relative to histone modifications. Therefore, DNA methylation was proposed to reinforce the inhibition of viral gene expression

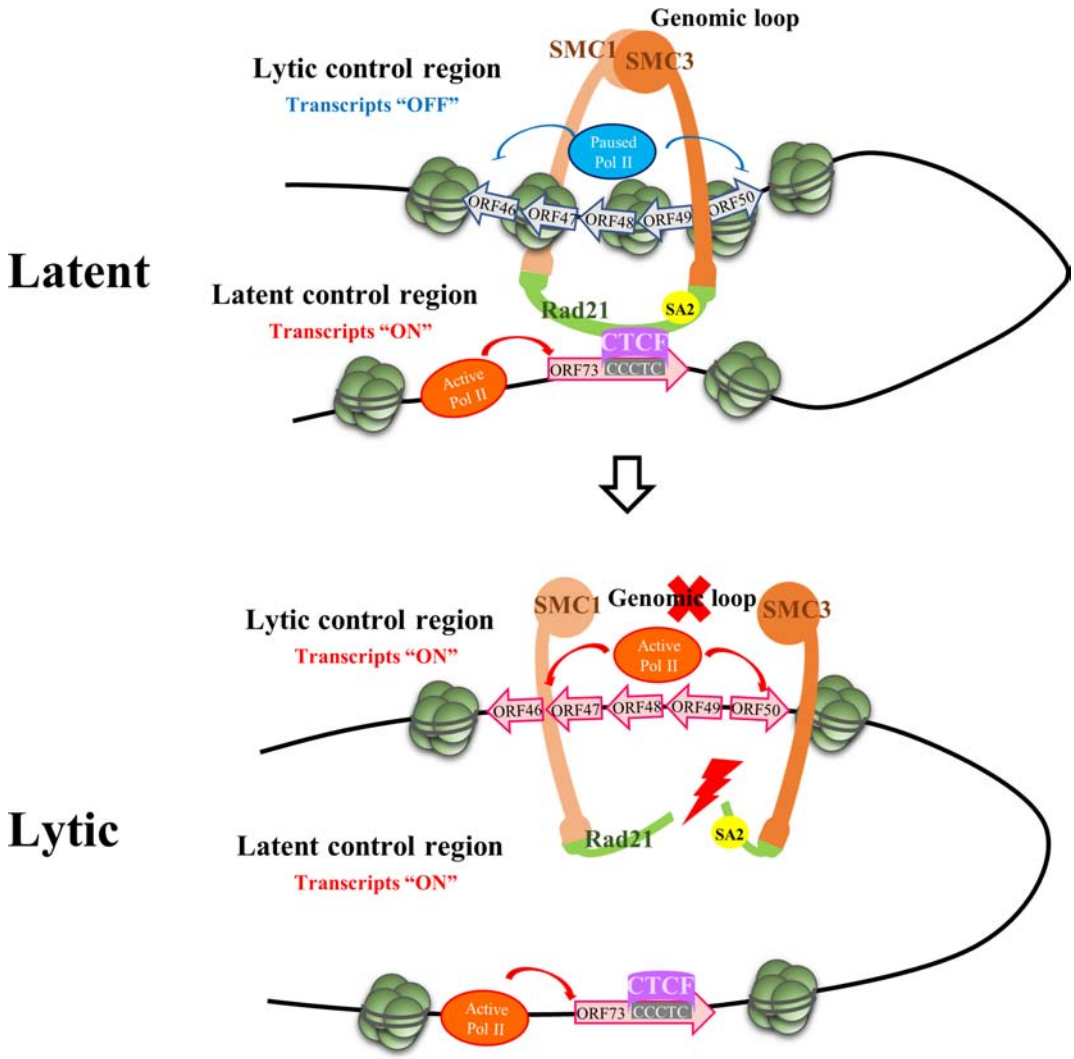

FIGURE 2 | Episome Conformational Control of Latency. The figure depicts the region on the KSHV genome where chromatin contacts implicated in the maintenance of latency and the latent to lytic switch reside. Upper panel: The latency control locus contacts the lytic control region via a CTCF-dependent genomic loop during latency. CTCF sites in the latency control region are clustered within the first intron of ORF73. This looping mechanism permits latent gene expression while early lytic gene expression (i.e., K-Rta) is repressed. Lower panel: Opening of the cohesin ring during lytic reactivation results in loss of the genomic loop and facilitates RNA polymerase II (Pol II) activation at the early lytic locus resulting in K-Rta expression and induction of the lytic phase. The figure depicts RAD21 cohesin complex component (Rad21) cleavage as the initiating factor resulting in opening of the ring with subsequent loss of looping contacts. SMC, structural maintenance of chromosome proteins. CTCF, CCCTC-binding factor.

conferred by repressive histone modifications during *de novo* infection. This notion was supported by a report from Darst et al. (2013). Using methylation accessibility probing for individual templates (MAPit) to map CG methylation on chromatin structure in latent KSHV episomes, these authors suggested that DNA methylation can restrict viral reactivation by chromatin compaction (Darst et al., 2013).

It is important to note that both Gunther and Grundhoff (2010) and Darst et al. (2013) observed that latency could be established independent of DNA methylation at the KSHV replication and transcription activator (K-Rta, ORF50) locus. Although the exact role of DNA methylation and viral latency is unresolved, gradual methylation of the KSHV genome may be important for long-term latency within the host but could also reflect the consequences of a host defense mechanism. These results support an idea originally proposed by Grundhoff and Ganem (2004) for the necessity of infrequent episodes of lytic replication for long-term KSHV persistence in the host.

HISTONE MODIFICATIONS VS. KSHV LATENCY

In 2010, two ChIP-on-Chip studies initiated the analysis of global chromatin marks across KSHV latent genomes (Gunther and Grundhoff, 2010; Toth et al., 2010). In one report, Toth et al.

revealed a mutually exclusive pattern of active and repressive histone marks on the KSHV genome, in which the active marks H3K4me3 and H3-ac are present in some parts of the KSHV genome whereas repressive marks H3K27me3 and H3K9me3 are located in other parts. The same report also showed the colocalization of EZH2, the H3K27me3 methyltransferase of Polycomb repressive complex 2 (PRC2), with H3K27me3 on KSHV latent genomes, suggesting a role of PRC2 in mediating deposition of H3K27me3 on the viral genome during latency (**Figure 1A**; Toth et al., 2010). Following these observations, Toth et al. (2013) found a biphasic euchromatin-to-heterochromatin transition on the KSHV genome upon *de novo* infection. Initially (<1 day post-infection, dpi) with the help of K-Rta, KSHV genomes rapidly acquired the active histone marks H3K4me3 and H3K27-ac. This was followed by (1st to 3rd dpi) sequential deposition of repressive histone marks H3K27me3 by PRC2 and H2AK119-Ub by Polycomb repressive complex 1 (PRC1). It is believed that binding of CBX in PRC1 to H3K27me3 deposited by PRC2 helps recruit PRC1 to the KSHV genome and RING1B in PRC1 ubiquitinated H2A at K119 (**Figure 1B**). In 2016, Toth et al. (2016) further revealed the potential of KSHV latency-associated nuclear antigen (LANA), a KSHV latent protein that is expressed very early after *de novo* infection, in mediating the recruitment of PRC2 onto the KSHV genomes during *de novo* infection (**Figure 1Ci**). Moreover, Hu et al. showed that KSHV LANA interacts and recruits the H3K4me3 methyltransferase hSET1 onto the KSHV genome (**Figure 1Cii**). This result explains the potential underlying mechanism for the deposition of H3K4me3 on latent KSHV genomes (Hu J. et al., 2014). Kim et al. (2013) showed that KSHV LANA also interacts and recruits the H3K9me1/2 demethylase KDM3A onto the KSHV genome (**Figure 1Ciii**). This suggests a mechanism for maintaining low H3K9 methylation on latent KSHV genomes. In addition to LANA, Lyu et al. (2017) also identified ZIC2 as a novel cellular protein that contributes to tethering PRC2 on the KSHV genome, thus maintaining H3K27me3 (**Figure 1D**). In 2018, Hopcraft et al. (2018) showed that ubiquitination of H2A at K119 by PRC1 is essential for prevention of nucleosome depletion on the KSHV genome and for maintaining KSHV latency (**Figure 1E**).

Gunther and Grundhoff (2010) also showed the presence of both the active marks H3K4me3 and H3K9/K14-ac and the repressive mark H3K27me3 on the KSHV genomes following *de novo* infection (**Figure 1F**). Following these observations, Gunther et al. (2014) also found that LANA may increase H3K27me3 deposition by inhibiting soluble Sp100, a negative regulator of PRC2 recruitment, through SUMOylation of Sp100. Recently, this group performed a comprehensive epigenome analysis of the KSHV genome and found the CpG motif as a cis-acting sequence for KDM2B, which consequently recruits Polycomb repressive complexes (PRCs) (**Figure 1G**; Gunther et al., 2019). Interestingly, a recent report from Naik et al. (2020) describes siRNA screening and time course ChIP experiments showing that early deposition of KDM2B on the KSHV genome limits the enrichment of the active marks H3K4me3 and H3K36me2 and helps in the maintenance of viral latency (**Figure 1H**). The binding of KDM2B prior to PRC-regulated heterochromatin supports the potential role of KDM2B in the recruitment of PRCs to viral DNA following *de novo* initial infection.

In summary (**Figure 1**, center), genome-wide studies of histone modifications on the KSHV latent genome revealed a mutually exclusive pattern of active and repressive histone marks, in which active marks, such as H3K4me3 and H3Ac, are located in certain parts of the KSHV genome, whereas repressive marks, such as H3K27me3 and H3K9me3, are located in other parts (Toth et al., 2010; Gunther et al., 2014, 2019). However, a bivalent chromatin structure that consists of both an active mark H3K4me3 and a repressive mark H3K27me3 was also identified in several promoter regions encoding immediate early (IE) (such as K-Rta) and early (E) genes (Gunther and Grundhoff, 2010; Toth et al., 2010; Jha et al., 2014; Lyu et al., 2017). Mechanistically, KSHV K-Rta may help facilitate the initial acquisition of the active histone marks H3K4me3 and H3K27-ac on the KSHV genome (Toth et al., 2013). Since KSHV LANA participates in the maintenance of latency through targeting KSHV K-Rta (Lu et al., 2006), after LANA is expressed, methylation of LANA by protein arginine methyltransferase 1 (PRMT1) may help stabilize LANA on the KSHV genomes (**Figure 1Civ**; Campbell et al., 2012), which consequently recruit PRC2 (Toth et al., 2016) and hSET1 (Hu J. et al., 2014) onto the KSHV genomes and mediate the increase of the repressive mark H3K27me3 and the active mark H3K4me3, respectively. H3K27me3 deposited by PRC2 may consequently aid the recruitment of PRC1, increasing H2AK119-Ub on the KSHV genome (Toth et al., 2013) and maintain nucleosomes on viral chromatin (Hopcraft et al., 2018). In addition to viral proteins, cellular factors may also be involved in recruitment. The direct binding of the PRC component KDM2B to CpG islands may also help in the recruitment of PRCs to the KSHV genome (Gunther et al., 2019; Naik et al., 2020).

PTMS VS. KSHV LATENCY

PTMs, including phosphorylation, ubiquitination, and Small Ubiquitin-related MOdifier (SUMO) modification, were initially identified as reversible protein modifications that regulate signal transduction. Among the PTMs, accumulating evidence suggests that the SUMO system plays an important role in regulating chromatin organization and transcription (Cubenas-Potts and Matunis, 2013). In addition, SUMOylation is also required for the assembly and disassembly of promyelocytic leukemia protein (PML) bodies, a host antiviral system that was found to mediate herpesvirus latency (Sewatanon et al., 2013). It is not surprising that KSHV has exploited the SUMOylation system to modulate its latency. Among viral proteins being SUMOylated, the KSHV IE proteins K-bZIP is a SUMO E3 ligase (Chang et al., 2010) and K-Rta is a SUMO-targeting ubiquitin ligase (STUbL) (Izumiya et al., 2013).

As SUMO modifications regulate chromatin organization, we showed that SUMOylation of the chromatin binding protein Krüppel-associated box domain-associated protein-1 (KAP-1) is essential for its association with the KSHV genome

and for maintaining viral latency. Phosphorylation of KAP-1 by KSHV vPK (ORF36) counteracts KAP-1 SUMOylation-dependent binding and thereby facilitates viral reactivation (Chang et al., 2009). Binding of SUMOylated KAP-1 with LANA through a SUMO-SIM (SUMO interacting motif) interaction maintains KSHV latency (Cai et al., 2013). In addition, inhibition of SUMO/sentrin-specific peptidase 6 (SENP6) expression by LANA was also found to be important in the establishment of latency (Lin et al., 2017). These results together support the potential role of SUMO in maintaining latent KSHV genomes.

In 2015, the genome-wide landscape of SUMO paralog modifications on the KSHV genome was revealed using ChIP-seq assays. The results showed similar SUMO-1 and SUMO-2/3 binding patterns on KSHV latent viral genomes and detailed a significant increase of SUMO-2/3 deposition upon reactivation (Yang et al., 2015). Mechanistically, the KSHV SUMO E3 ligase K-bZIP interacted with (Chang et al., 2011) and SUMOylated (Yang et al., 2017) JMJD2A, a Jumonji domain containing H3K9me3 demethylase. This SUMO modification stabilized JMJD2A on chromatin and therefore maintained the KSHV genome with low levels of H3K9me3 (Gunther and Grundhoff, 2010; Jha et al., 2014; Gunther et al., 2019). This action prevents the formation of heterochromatin on KSHV episomes and maintains the viral genome in a poised state that is prepared for rapid activation (reviewed in Chang and Kung, 2014). These results were supported by a previous report from Hilton et al. (2013) that found open chromatin in both transcriptionally active and inactive loci in latent KSHV episomes. Altogether, these results suggest that PTM of chromatin remodeling proteins is another mechanism that contributes to the epigenetic regulation of KSHV latency.

NON-CODING RNAS VS. KSHV LATENCY

Gene expression profiling of the KSHV life cycle using real-time PCR, oligonucleotide arrays, and Northern blotting (Dittmer, 2003; Chandriani and Ganem, 2010) has detected pervasive transcription throughout the KSHV viral genome, indicative of a complex viral transcriptome. These studies were later confirmed and expanded by comprehensive functional genomic approaches (Arias et al., 2014; Bruce et al., 2017). KSHV transcriptional complexity includes the expression of non-coding RNAs including miRNAs (Cai et al., 2005; Samols et al., 2005; Grundhoff et al., 2006) and lncRNAs (Schifano et al., 2017). A total of 12 KSHV pre-miRNAs that can evolve into 25 mature miRNAs were identified by four groups in the years 2005–2006 [review in (Qin et al., 2017)]. KSHV miRNAs are clustered in the latency-associated locus of the KSHV genome Gottwein et al. (2006). By using a KSHV miRNA deletion mutant, Lu et al. detected several epigenetic changes in the KSHV genome upon loss of KSHV miRNAs. These included a decrease in DNA methylation, a decrease in the repressive mark H3K9me3, and an increase in the active mark H3-ac throughout KSHV genome (Lu et al., 2010). They concluded that KSHV miRNAs are involved in maintaining the latent genome of KSHV by targeting multiple pathways, including an indirect effect on K-Rta and a direct effect on a cellular target Rb-like protein 2 (Rbl2). Rbl2 is known as a regulator of epigenetic reprogramming and loss of Rbl2 resulted in derepression of DNMT3A and 3B that consequently led to an increase in KSHV and host DNA methylation (Lu et al., 2010). Other KSHV miRNAs targeting K-Rta with modest effects on the latent-to-lytic switch have also been reported (Bellare and Ganem, 2009; Ziegelbauer et al., 2009).

A succession of studies using a variety of experimental approaches have described the existence of at least 16 potential KSHV lncRNAs, and these have been nicely summarized by Schifano et al. (2017). KSHV lncRNAs have been characterized to varying levels of detail with the best studied species as the 1.1 kb polyadenylated nuclear RNA (PAN RNA), which was first described in 1996 (Sun et al., 1996; Zhong et al., 1996). The PAN RNA promoter is a direct target of K-Rta (Song et al., 2001, 2002; Bu et al., 2008). Thus, its expression is highly increased (>1000-fold) upon reactivation (accounting for 65% and > 80% of the KSHV reads at 8 h and 24–72 h, respectively, post-induction of reactivation) with early kinetics (Rossetto et al., 2013; Arias et al., 2014; Bruce et al., 2017). PNA RNA persists into the late stage of lytic replication and is packaged into virions (Bechtel et al., 2005). In PEL cell lines, PAN levels are capable of reaching an estimated $1–5 \times 10^5$ copies per cell (Sun et al., 1996; Song et al., 2001) and accumulate as one of the most abundant viral RNA species present in the infected cell during lytic reactivation.

As a lytic transcript, how could PAN RNA affect viral latency? By using chromatin isolation by RNA purification (ChIRP) assay, Rossetto et al. (2013) demonstrated the occupancy of PAN RNA at multiple sites on the KSHV genome, including the K-Rta promoter region. PAN RNA binding was proposed to recruit the cellular factors JMJD3 and UTX, which are H3K27me3 demethylases and the H3K4me3 methyltransferase MLL2. This consequently decreased the repressive mark H3K27me3 and increased the activation mark H3K4me3 on the K-Rta promoter followed by disruption of viral latency (Rossetto and Pari, 2012). The interaction of PAN RNA with KSHV DNA polymerase processivity factor (ORF59) (Rossetto and Pari, 2011) may also contribute to the function of PAN RNA in activation of gene expression during the lytic phase. However, contrasting results were also found by Rossetto et al. (2013) using ChIRP. They demonstrated occupancy of PAN RNA on the KSHV genome and its association with PRC2 components EZH2 and SUZ12, which in turn increased the repressive mark H3K27me3 that acts to repress gene expression. These data together suggest that PAN RNA may function in either positive or negative epigenetic regulation depending on cell context (reviewed in Campbell et al., 2014b; Rossetto and Pari, 2014).

Interaction of PAN RNA with additional viral factors has also been examined. Through direct interaction with LANA, PAN RNA dissociates LANA from the KSHV genome and disrupts viral latency (Campbell et al., 2014a). Using an alternative to ChIRP known as capture hybridization analysis of RNA targets (CHART) and nuclear fractionation studies, Withers et al. showed that KSHV PAN RNA, although nuclear, was not associated with chromatin (Withers et al., 2018). These results

suggested chromatin-independent activities of PAN RNA. Thus, in contrast to results obtained by others (Rossetto and Pari, 2012, 2014; Rossetto et al., 2013; Campbell et al., 2014a), modulation of gene expression at specific viral or host chromatin loci was not considered the pertinent function of PAN RNA. Rather, PAN RNA was proposed to function in nuclear mRNA export of late viral mRNAs. Taken together, current research has suggested several functions for PAN RNA, which can be generally classified as chromatin-associated or chromatin-independent activities, although the exact role of this lncRNA in the viral life cycle is still unclear.

ROLE OF HIGHER-ORDER EPISOMAL ORGANIZATION IN LATENCY

The development of high-resolution chromosome conformation capture (3C)-based methodologies (Dekker and Mirny, 2016) has established that eukaryotic genomes are arranged or folded in a specific manner within the three-dimensional nuclear space. Crucial to this arrangement were the discoveries concerning the roles of CCCTC-binding factor (CTCF) and cohesins (containing structural maintenance of chromosomes; SMC protein subunits) in the dynamics of chromatin organization (Merkenschlager and Nora, 2016; Braccioli and de Wit, 2019). Since circularized KSHV episomes resemble host chromatin in terms of decoration with host histones which are substrates for host chromatin modifiers, it was not too surprising that cellular epigenetic machinery has been implicated in control viral chromatin architecture and viral latency. The genome-wide localization of CTCF and cohesins along the KSHV genome, including the identification of a series of highly enriched sites in the latency control region, was first reported by Stedman et al. (2008). Subsequent studies confirmed the existence of approximately 25 major CTCF binding sites on the KSHV genome, most of which exhibited colocalized cohesin binding although the overall amount of cohesin binding was less (Li et al., 2014). Kang et al. (2011) reported on the existence of a CTCF/cohesin-mediated genomic looping that coordinates KSHV latent and lytic gene expression. 3C and other chromosome conformation assays were used to probe latent KSHV cross-linked chromatin for contacts involving the latency control region and other positions on the KSHV genome. Multiple loops between the latency control region and other KSHV genomic locations were detected, including a high frequency of contacts between a CTCF/cohesin binding site in the latency control region with (i) the 3′ end of the LANA coding region and (ii) the 5′ promoter region of ORF50 (Kang et al., 2011). This pair of loops were suggested to insulate latent and lytic viral gene and coordinate their expression. This arrangement ensures the repression of lytic transcription during latency, while latency transcription occurs efficiently. Moreover, these loops were reduced or eliminated during lytic reactivation, indicating that these contacts are dynamic. Epigenetic changes including RNA Pol II enrichment throughout the early gene locus spanning ORF45–50 transcripts were also noted during cohesin depletion experiments (Chen et al., 2012; De Leo et al., 2017). Additional studies that focused on DNA looping between the latent and lytic control regions found that disruption of this loop also accompanies lytic reactivation induced by ER stress-mediated Rad21 cleavage (De Leo et al., 2017) or lytic induction via Bromodomain and Extended Terminal (BET) protein inhibitor treatment (Chen et al., 2017). Together, these studies have created a model whereby the CTCF/cohesin-dependent genomic linkage between the latency and lytic control regions is necessary for preservation of the latent state. Any structural perturbation to this latent genomic conformation facilitates the switch to the lytic state through locus-specific association and activation of RNA Pol II (**Figure 2**). Although this model highlights effects on gene expression via the topological organization of viral chromatin, local and direct effects of CTCF and cohesion on promoter activity are also likely (Dorsett and Merkenschlager, 2013; Merkenschlager and Odom, 2013). Cohesin may regulate RNA Pol II pausing (Fay et al., 2011) and CTCF binds RNA Pol II may facilitate RNA Pol II recruitment and elongation (Chernukhin et al., 2007; Pena-Hernandez et al., 2015). Together, this complex behavior emphasizes the multifactorial nature of the mechanisms CTCF and cohesin may utilize to regulate KSHV gene expression.

The looping/conformation model described above has only been studied in the context of latently infected cells and, as such, attempts to explain the maintenance of latency and the latent-to-lytic switch. However, it is currently not known how initial episomal chromatin conformations are established following *de novo* infection. Although Toth et al. (2017) have reported that CTCF and cohesin rapidly associate with incoming KSHV genomes following *de novo* infection, detailed mechanisms of the initial high-order structuring and nuclear residences of KSHV episomes are unknown.

CONCLUSION AND FUTURE PROSPECTS

Genome-wide analysis of KSHV episomes have revealed distinct temporal and spatial chromatin modification patterns on the viral genome. In summary, following *de novo* infection, the KSHV IE protein K-Rta may help viral episomes acquire active histone marks (Toth et al., 2013) and cellular factors such as KDM2B may function to limit the enrichment of active histone marks (Naik et al., 2020). The binding of KDM2B to viral episomes may consequently help recruit the PRCs and the deposition of repressive marks. These modifications prevent the virus lytic cycle and promote the establishment of viral latency. Following these events, the latent viral protein LANA is expressed, which helps recruit PRC2 (Toth et al., 2016) and hSET1 (Hu J. et al., 2014) onto the KSHV genomes and mediates the formation of site-specific bivalent chromatin structures. Expression of KSHV miRNAs during latency may also assist with the deposition of DNA methylation and the heterochromatin mark H3K9me3 (Lu et al., 2010). However, the SUMOylation of H3K9me3 demethylase JMJD2A by the KSHV lytic protein

K-bZIP maintains JMJD2A on the KSHV genome and prevents the formation of heterochromatin (Yang et al., 2015, 2017), resulting in maintenance of the latent KSHV episome in a poised state that is ready for rapid reactivation. The expression of the KSHV lncRNA PAN during the early stages of lytic reactivation helps recruit multiple histone modification enzymes to the viral genome and further disrupts viral latency (Rossetto and Pari, 2012). As the switch from latency to lytic replication is essential for viral survival and spread, the role of KSHV lncRNAs in maintaining a balanced viral chromatin state to persist within the host is clearly an important topic for future research. In addition, identifying cellular lncRNAs that are up- or down-regulated during both the lytic and latent states of KSHV infection is also an interesting question to explore in terms of establishing how cellular lncRNAs influence the KSHV life cycle. Spatial and architectural conformation of KSHV episomal chromatin is a relatively understudied feature of KSHV biology; however, episome conformational contacts have been observed to be a dynamic feature of KSHV chromatin at both the focused level of 3C (Kang et al., 2011; Chen et al., 2017; De Leo et al., 2017) and at the global level of Capture Hi-C (Campbell et al., 2018) suggestive of potential roles in the viral life cycle.

The compartmentalization of the epigenetic marks on the KSHV genome might be beneficial for transcription regulation of viral gene expression during its distinct life cycle. The well-organized DNA methylation and different histone modification patterns on the KSHV genome reflects the precise recruitment of cellular chromatin modifying complexes employed by the virus. KSHV latency is essential for persistent infection as well as the development of KSHV-associated malignancies. In recent years, more and more epigenetic modifications and the corresponding modifying enzymes have been identified. Drugs targeting epigenetic modification enzymes have now evolved into a potential viable strategy for controlling persistent viral infections (Nehme et al., 2019). Thus, elucidating the epigenetic regulators involved in establishing KSHV latency may be a new avenue for pharmacological control of KSHV-associated diseases.

AUTHOR CONTRIBUTIONS

MC wrote and edited the manuscript. W-SY helped writing the manuscript. C-HK constructed the figures. P-CC worked on the constructs and the manuscript writing. WY contributed to the final revision with modification of manuscript and **Figure 1** and compose **Figure 2**.

FUNDING

This work was financially supported by grants from the Ministry of Science and Technology (MOST, 105-2320-B-010-007-MY3 and MOST 108-2320-B-010-029-MY3 to P-CC). This work was also supported by the "Cancer Progression Research Center, National Yang-Ming University" from The Featured Areas Research Center Program within the framework of the Higher Education Sprout Project by the Ministry of Education (MOE) in Taiwan.

REFERENCES

Arias, C., Weisburd, B., Stern-Ginossar, N., Mercier, A., Madrid, A. S., Bellare, P., et al. (2014). KSHV 2.0: a comprehensive annotation of the Kaposi's sarcoma-associated herpesvirus genome using next-generation sequencing reveals novel genomic and functional features. *PLoS Pathog.* 10:e1003847. doi: 10.1371/journal.ppat.1003847

Baylin, S. B., and Jones, P. A. (2011). A decade of exploring the cancer epigenome - biological and translational implications. *Nat. Rev. Cancer* 11, 726–734. doi: 10.1038/nrc3130

Bechtel, J., Grundhoff, A., and Ganem, D. (2005). RNAs in the virion of Kaposi's sarcoma-associated herpesvirus. *J. Virol.* 79, 10138–10146. doi: 10.1128/JVI.79.16.10138-10146.2005

Bellare, P., and Ganem, D. (2009). Regulation of KSHV lytic switch protein expression by a virus-encoded microRNA: an evolutionary adaptation that fine-tunes lytic reactivation. *Cell Host Microbe* 6, 570–575. doi: 10.1016/j.chom.2009.11.008

Bhattacharjee, D., Shenoy, S., and Bairy, K. L. (2016). DNA methylation and chromatin remodeling: the blueprint of cancer epigenetics. *Scientifica* 2016:6072357. doi: 10.1155/2016/6072357

Braccioli, L., and de Wit, E. (2019). CTCF: a Swiss-army knife for genome organization and transcription regulation. *Essays Biochem.* 63, 157–165. doi: 10.1042/EBC20180069

Branco, M. R., Ficz, G., and Reik, W. (2011). Uncovering the role of 5-hydroxymethylcytosine in the epigenome. *Nat. Rev. Genet.* 13, 7–13. doi: 10.1038/nrg3080

Bruce, A. G., Barcy, S., DiMaio, T., Gan, E., Garrigues, H. J., Lagunoff, M., et al. (2017). Quantitative analysis of the KSHV transcriptome following primary infection of blood and lymphatic endothelial cells. *Pathogens* 6:E11. doi: 10.3390/pathogens6010011

Bu, W., Palmeri, D., Krishnan, R., Marin, R., Aris, V. M., Soteropoulos, P., et al. (2008). Identification of direct transcriptional targets of the Kaposi's sarcoma-associated herpesvirus Rta lytic switch protein by conditional nuclear localization. *J. Virol.* 82, 10709–10723. doi: 10.1128/JVI.01012-08

Cai, Q., Cai, S., Zhu, C., Verma, S. C., Choi, J. Y., and Robertson, E. S. (2013). A unique SUMO-2-interacting motif within LANA is essential for KSHV latency. *PLoS Pathog.* 9:e1003750. doi: 10.1371/journal.ppat.1003750

Cai, X., Lu, S., Zhang, Z., Gonzalez, C. M., Damania, B., and Cullen, B. R. (2005). Kaposi's sarcoma-associated herpesvirus expresses an array of viral microRNAs in latently infected cells. *Proc. Natl. Acad. Sci. U.S.A.* 102, 5570–5575. doi: 10.1073/pnas.0408192102

Campbell, M., Chang, P. C., Huerta, S., Izumiya, C., Davis, R., Tepper, C. G., et al. (2012). Protein arginine methyltransferase 1-directed methylation of Kaposi sarcoma-associated herpesvirus latency-associated nuclear antigen. *J. Biol. Chem.* 287, 5806–5818. doi: 10.1074/jbc.M111.289496

Campbell, M., Kim, K. Y., Chang, P. C., Huerta, S., Shevchenko, B., Wang, D. H., et al. (2014a). A lytic viral long noncoding RNA modulates the function of a latent protein. *J. Virol.* 88, 1843–1848. doi: 10.1128/JVI.03251-13

Campbell, M., Kung, H. J., and Izumiya, Y. (2014b). Long non-coding RNA and epigenetic gene regulation of KSHV. *Viruses* 6, 4165–4177. doi: 10.3390/v6114165

Campbell, M., Watanabe, T., Nakano, K., Davis, R. R., Lyu, Y., Tepper, C. G., et al. (2018). KSHV episomes reveal dynamic chromatin loop formation with domain-specific gene regulation. *Nat. Commun.* 9:49. doi: 10.1038/s41467-017-02089-9

Chandriani, S., and Ganem, D. (2010). Array-based transcript profiling and limiting-dilution reverse transcription-PCR analysis identify additional latent genes in Kaposi's sarcoma-associated herpesvirus. *J. Virol.* 84, 5565–5573. doi: 10.1128/JVI.02723-09

Chang, P. C., Fitzgerald, L. D., Hsia, D. A., Izumiya, Y., Wu, C. Y., Hsieh, W. P., et al. (2011). Histone demethylase JMJD2A regulates Kaposi's sarcoma-associated herpesvirus replication and is targeted by a viral transcriptional factor. *J. Virol.* 85, 3283–3293. doi: 10.1128/JVI.02485-10

Chang, P. C., Fitzgerald, L. D., Van Geelen, A., Izumiya, Y., Ellison, T. J., Wang, D. H., et al. (2009). Kruppel-associated box domain-associated protein-1 as a latency regulator for Kaposi's sarcoma-associated herpesvirus and its modulation by the viral protein kinase. *Cancer Res.* 69, 5681–5689. doi: 10.1158/0008-5472.CAN-08-4570

Chang, P. C., Izumiya, Y., Wu, C. Y., Fitzgerald, L. D., Campbell, M., Ellison, T. J., et al. (2010). Kaposi's sarcoma-associated herpesvirus (KSHV) encodes a SUMO E3 ligase that is SIM-dependent and SUMO-2/3-specific. *J. Biol. Chem.* 285, 5266–5273. doi: 10.1074/jbc.M109.088088

Chang, P. C., and Kung, H. J. (2014). SUMO and KSHV replication. *Cancers* 6, 1905–1924.

Chen, H. S., De Leo, A., Wang, Z., Kerekovic, A., Hills, R., and Lieberman, P. M. (2017). BET-inhibitors disrupt Rad21-dependent conformational control of KSHV latency. *PLoS Pathog.* 13:e1006100. doi: 10.1371/journal.ppat.1006100

Chen, H. S., Wikramasinghe, P., Showe, L., and Lieberman, P. M. (2012). Cohesins repress Kaposi's sarcoma-associated herpesvirus immediate early gene transcription during latency. *J. Virol.* 86, 9454–9464. doi: 10.1128/JVI.00787-12

Chen, J., Ueda, K., Sakakibara, S., Okuno, T., Parravicini, C., Corbellino, M., et al. (2001). Activation of latent Kaposi's sarcoma-associated herpesvirus by demethylation of the promoter of the lytic transactivator. *Proc. Natl. Acad. Sci. U.S.A.* 98, 4119–4124. doi: 10.1073/pnas.051004198

Chernukhin, I., Shamsuddin, S., Kang, S. Y., Bergstrom, R., Kwon, Y. W., Yu, W., et al. (2007). CTCF interacts with and recruits the largest subunit of RNA polymerase II to CTCF target sites genome-wide. *Mol. Cell. Biol.* 27, 1631–1648. doi: 10.1128/MCB.01993-06

Cubenas-Potts, C., and Matunis, M. J. (2013). SUMO: a multifaceted modifier of chromatin structure and function. *Dev. Cell* 24, 1–12. doi: 10.1016/j.devcel.2012.11.020

Darst, R. P., Haecker, I., Pardo, C. E., Renne, R., and Kladde, M. P. (2013). Epigenetic diversity of Kaposi's sarcoma-associated herpesvirus. *Nucleic Acids Res.* 41, 2993–3009. doi: 10.1093/nar/gkt033

De Leo, A., Chen, H. S., Hu, C. C., and Lieberman, P. M. (2017). Deregulation of KSHV latency conformation by ER-stress and caspase-dependent RAD21-cleavage. *PLoS Pathog.* 13:e1006596. doi: 10.1371/journal.ppat.1006596

Dekker, J., Belmont, A. S., Guttman, M., Leshyk, V. O., Lis, J. T., Lomvardas, S., et al. (2017). The 4D nucleome project. *Nature* 549, 219–226. doi: 10.1038/nature23884

Dekker, J., and Mirny, L. (2016). The 3D genome as moderator of chromosomal communication. *Cell* 164, 1110–1121. doi: 10.1016/j.cell.2016.02.007

Derrien, T., Johnson, R., Bussotti, G., Tanzer, A., Djebali, S., Tilgner, H., et al. (2012). The GENCODE v7 catalog of human long noncoding RNAs: analysis of their gene structure, evolution, and expression. *Genome Res.* 22, 1775–1789. doi: 10.1101/gr.132159.111

Dimitrova, N., Zamudio, J. R., Jong, R. M., Soukup, D., Resnick, R., Sarma, K., et al. (2014). LincRNA-p21 activates p21 in cis to promote Polycomb target gene expression and to enforce the G1/S checkpoint. *Mol. Cell* 54, 777–790. doi: 10.1016/j.molcel.2014.04.025

Dittmer, D. P. (2003). Transcription profile of Kaposi's sarcoma-associated herpesvirus in primary Kaposi's sarcoma lesions as determined by real-time PCR arrays. *Cancer Res.* 63, 2010–2015.

Dorsett, D., and Merkenschlager, M. (2013). Cohesin at active genes: a unifying theme for cohesin and gene expression from model organisms to humans. *Curr. Opin. Cell Biol.* 25, 327–333. doi: 10.1016/j.ceb.2013.02.003

Fatica, A., and Bozzoni, I. (2014). Long non-coding RNAs: new players in cell differentiation and development. *Nat. Rev. Genet.* 15, 7–21. doi: 10.1038/nrg3606

Fay, A., Misulovin, Z., Li, J., Schaaf, C. A., Gause, M., Gilmour, D. S., et al. (2011). Cohesin selectively binds and regulates genes with paused RNA polymerase. *Curr. Biol.* 21, 1624–1634. doi: 10.1016/j.cub.2011.08.036

Gottwein, E., Cai, X., and Cullen, B. R. (2006). Expression and function of microRNAs encoded by Kaposi's sarcoma-associated herpesvirus. *Cold Spring Harb. Symp. Quant. Biol.* 71, 357–364. doi: 10.1101/sqb.2006.71.004

Grundhoff, A., and Ganem, D. (2004). Inefficient establishment of KSHV latency suggests an additional role for continued lytic replication in Kaposi sarcoma pathogenesis. *J. Clin. Invest.* 113, 124–136. doi: 10.1172/JCI17803

Grundhoff, A., Sullivan, C. S., and Ganem, D. (2006). A combined computational and microarray-based approach identifies novel microRNAs encoded by human gamma-herpesviruses. *RNA* 12, 733–750. doi: 10.1261/rna.2326106

Gunther, T., Frohlich, J., Herrde, C., Ohno, S., Burkhardt, L., Adler, H., et al. (2019). A comparative epigenome analysis of gammaherpesviruses suggests cis-acting sequence features as critical mediators of rapid polycomb recruitment. *PLoS Pathog.* 15:e1007838. doi: 10.1371/journal.ppat.1007838

Gunther, T., and Grundhoff, A. (2010). The epigenetic landscape of latent Kaposi sarcoma-associated herpesvirus genomes. *PLoS Pathog.* 6:e1000935. doi: 10.1371/journal.ppat.1000935

Gunther, T., Schreiner, S., Dobner, T., Tessmer, U., and Grundhoff, A. (2014). Influence of ND10 components on epigenetic determinants of early KSHV latency establishment. *PLoS Pathog.* 10:e1004274. doi: 10.1371/journal.ppat.1004274

Gupta, R. A., Shah, N., Wang, K. C., Kim, J., Horlings, H. M., Wong, D. J., et al. (2010). Long non-coding RNA HOTAIR reprograms chromatin state to promote cancer metastasis. *Nature* 464, 1071–1076. doi: 10.1038/nature08975

Hilton, I. B., Simon, J. M., Lieb, J. D., Davis, I. J., Damania, B., and Dittmer, D. P. (2013). The open chromatin landscape of Kaposi's sarcoma-associated herpesvirus. *J. Virol.* 87, 11831–11842. doi: 10.1128/JVI.01685-13

Hopcraft, S. E., Pattenden, S. G., James, L. I., Frye, S., Dittmer, D. P., and Damania, B. (2018). Chromatin remodeling controls Kaposi's sarcoma-associated herpesvirus reactivation from latency. *PLoS Pathog.* 14:e1007267. doi: 10.1371/journal.ppat.1007267

Hu, J., Yang, Y., Turner, P. C., Jain, V., McIntyre, L. M., and Renne, R. (2014). LANA binds to multiple active viral and cellular promoters and associates with the H3K4methyltransferase hSET1 complex. *PLoS Pathog.* 10:e1004240. doi: 10.1371/journal.ppat.1004240

Hu, X., Feng, Y., Zhang, D., Zhao, S. D., Hu, Z., Greshock, J., et al. (2014). A functional genomic approach identifies FAL1 as an oncogenic long noncoding RNA that associates with BMI1 and represses p21 expression in cancer. *Cancer Cell* 26, 344–357. doi: 10.1016/j.ccr.2014.07.009

Izumiya, Y., Kobayashi, K., Kim, K. Y., Pochampalli, M., Izumiya, C., Shevchenko, B., et al. (2013). Kaposi's sarcoma-associated herpesvirus K-Rta exhibits SUMO-targeting ubiquitin ligase (STUbL) like activity and is essential for viral reactivation. *PLoS Pathog.* 9:e1003506. doi: 10.1371/journal.ppat.1003506

Jha, H. C., Lu, J., Verma, S. C., Banerjee, S., Mehta, D., and Robertson, E. S. (2014). Kaposi's sarcoma-associated herpesvirus genome programming during the early stages of primary infection of peripheral blood mononuclear cells. *mBio* 5:e02261-14. doi: 10.1128/mBio.02261-14

Kang, H., Wiedmer, A., Yuan, Y., Robertson, E., and Lieberman, P. M. (2011). Coordination of KSHV latent and lytic gene control by CTCF-cohesin mediated chromosome conformation. *PLoS Pathog.* 7:e1002140. doi: 10.1371/journal.ppat.1002140

Khalil, A. M., Guttman, M., Huarte, M., Garber, M., Raj, A., Rivea Morales, D., et al. (2009). Many human large intergenic noncoding RNAs associate with chromatin-modifying complexes and affect gene expression. *Proc. Natl. Acad. Sci. U.S.A.* 106, 11667–11672. doi: 10.1073/pnas.0904715106

Kim, K. Y., Huerta, S. B., Izumiya, C., Wang, D. H., Martinez, A., Shevchenko, B., et al. (2013). Kaposi's sarcoma-associated herpesvirus (KSHV) latency-associated nuclear antigen regulates the KSHV epigenome by association with the histone demethylase KDM3A. *J. Virol.* 87, 6782–6793. doi: 10.1128/JVI.00011-13

Kim, V. N., Han, J., and Siomi, M. C. (2009). Biogenesis of small RNAs in animals. *Nat. Rev. Mol. Cell Biol.* 10, 126–139. doi: 10.1038/nrm2632

Klose, R. J., and Zhang, Y. (2007). Regulation of histone methylation by demethylimination and demethylation. *Nat. Rev. Mol. Cell Biol.* 8, 307–318. doi: 10.1038/nrm2143

Kouzarides, T. (2007). Chromatin modifications and their function. *Cell* 128, 693–705.

Li, D. J., Verma, D., Mosbruger, T., and Swaminathan, S. (2014). CTCF and Rad21 act as host cell restriction factors for Kaposi's sarcoma-associated herpesvirus (KSHV) lytic replication by modulating viral gene transcription. *PLoS Pathog.* 10:e1003880. doi: 10.1371/journal.ppat.1003880

Lin, X., Sun, R., Zhang, F., Gao, Y., Bin, L., and Lan, K. (2017). The latency-associated nuclear antigen of Kaposi's sarcoma-associated herpesvirus inhibits expression of SUMO/sentrin-specific peptidase 6 to facilitate establishment of latency. *J. Virol.* 91:e00806-17. doi: 10.1128/JVI.00806-17

Lu, F., Day, L., Gao, S. J., and Lieberman, P. M. (2006). Acetylation of the latency-associated nuclear antigen regulates repression of Kaposi's sarcoma-associated herpesvirus lytic transcription. *J. Virol.* 80, 5273–5282. doi: 10.1128/JVI.02541-05

Lu, F., Stedman, W., Yousef, M., Renne, R., and Lieberman, P. M. (2010). Epigenetic regulation of Kaposi's sarcoma-associated herpesvirus latency by virus-encoded microRNAs that target Rta and the cellular Rbl2-DNMT pathway. *J. Virol.* 84, 2697–2706. doi: 10.1128/JVI.01997-09

Lyu, Y., Nakano, K., Davis, R. R., Tepper, C. G., Campbell, M., and Izumiya, Y. (2017). ZIC2 is essential for maintenance of latency and is a target of an immediate early protein during Kaposi's sarcoma-associated herpesvirus lytic reactivation. *J. Virol.* 91:e00980-17. doi: 10.1128/JVI.00980-17

Merkenschlager, M., and Nora, E. P. (2016). CTCF and cohesin in genome folding and transcriptional gene regulation. *Annu. Rev. Genomics Hum. Genet.* 17, 17–43. doi: 10.1146/annurev-genom-083115-022339

Merkenschlager, M., and Odom, D. T. (2013). CTCF and cohesin: linking gene regulatory elements with their targets. *Cell* 152, 1285–1297. doi: 10.1016/j.cell.2013.02.029

Naik, N. G., Nguyen, T. H., Roberts, L., Fischer, L. T., Glickman, K., Golas, G., et al. (2020). Epigenetic factor siRNA screen during primary KSHV infection identifies novel host restriction factors for the lytic cycle of KSHV. *PLoS Pathog.* 16:e1008268. doi: 10.1371/journal.ppat.1008268

Nehme, Z., Pasquereau, S., and Herbein, G. (2019). Control of viral infections by epigenetic-targeted therapy. *Clin. Epigenetics* 11:55. doi: 10.1186/s13148-019-0654-9

Nelson, B. R., Makarewich, C. A., Anderson, D. M., Winders, B. R., Troupes, C. D., Wu, F., et al. (2016). A peptide encoded by a transcript annotated as long noncoding RNA enhances SERCA activity in muscle. *Science* 351, 271–275. doi: 10.1126/science.aad4076

Pal, S., and Sif, S. (2007). Interplay between chromatin remodelers and protein arginine methyltransferases. *J. Cell. Physiol.* 213, 306–315. doi: 10.1002/jcp.21180

Pena-Hernandez, R., Marques, M., Hilmi, K., Zhao, T., Saad, A., Alaoui-Jamali, M. A., et al. (2015). Genome-wide targeting of the epigenetic regulatory protein CTCF to gene promoters by the transcription factor TFII-I. *Proc. Natl. Acad. Sci. U.S.A.* 112, E677–E686. doi: 10.1073/pnas.1416674112

Ponting, C. P., Oliver, P. L., and Reik, W. (2009). Evolution and functions of long noncoding RNAs. *Cell* 136, 629–641. doi: 10.1016/j.cell.2009.02.006

Qin, J., Li, W., Gao, S. J., and Lu, C. (2017). KSHV microRNAs: tricks of the Devil. *Trends Microbiol.* 25, 648–661. doi: 10.1016/j.tim.2017.02.002

Renne, R., Lagunoff, M., Zhong, W., and Ganem, D. (1996). The size and conformation of Kaposi's sarcoma-associated herpesvirus (human herpesvirus 8) DNA in infected cells and virions. *J. Virol.* 70, 8151–8154.

Richa, R., and Sinha, R. P. (2014). Hydroxymethylation of DNA: an epigenetic marker. *EXCLI J.* 13, 592–610.

Rossetto, C. C., and Pari, G. (2012). KSHV PAN RNA associates with demethylases UTX and JMJD3 to activate lytic replication through a physical interaction with the virus genome. *PLoS Pathog.* 8:e1002680. doi: 10.1371/journal.ppat.1002680

Rossetto, C. C., and Pari, G. S. (2011). Kaposi's sarcoma-associated herpesvirus noncoding polyadenylated nuclear RNA interacts with virus- and host cell-encoded proteins and suppresses expression of genes involved in immune modulation. *J. Virol.* 85, 13290–13297. doi: 10.1128/JVI.05886-11

Rossetto, C. C., and Pari, G. S. (2014). PAN's labyrinth: molecular biology of Kaposi's sarcoma-associated herpesvirus (KSHV) PAN RNA, a multifunctional long noncoding RNA. *Viruses* 6, 4212–4226. doi: 10.3390/v6114212

Rossetto, C. C., Tarrant-Elorza, M., Verma, S., Purushothaman, P., and Pari, G. S. (2013). Regulation of viral and cellular gene expression by Kaposi's sarcoma-associated herpesvirus polyadenylated nuclear RNA. *J. Virol.* 87, 5540–5553. doi: 10.1128/JVI.03111-12

Russo, J. J., Bohenzky, R. A., Chien, M. C., Chen, J., Yan, M., Maddalena, D., et al. (1996). Nucleotide sequence of the Kaposi sarcoma-associated herpesvirus (HHV8). *Proc. Natl. Acad. Sci. U.S.A.* 93, 14862–14867. doi: 10.1073/pnas.93.25.14862

Samols, M. A., Hu, J., Skalsky, R. L., and Renne, R. (2005). Cloning and identification of a microRNA cluster within the latency-associated region of Kaposi's sarcoma-associated herpesvirus. *J. Virol.* 79, 9301–9305. doi: 10.1128/JVI.79.14.9301-9305.2005

Scadden, D. T. (2003). AIDS-related malignancies. *Annu. Rev. Med.* 54, 285–303.

Schifano, J. M., Corcoran, K., Kelkar, H., and Dittmer, D. P. (2017). Expression of the antisense-to-latency transcript long noncoding RNA in Kaposi's sarcoma-associated herpesvirus. *J. Virol.* 91:e01698-16. doi: 10.1128/JVI.01698-16

Sewatanon, J., Liu, H., and Ling, P. D. (2013). Promyelocytic leukemia protein modulates establishment and maintenance of latent gammaherpesvirus infection in peritoneal cells. *J. Virol.* 87, 12151–12157. doi: 10.1128/JVI.01696-13

Song, M. J., Brown, H. J., Wu, T. T., and Sun, R. (2001). Transcription activation of polyadenylated nuclear RNA by Rta in human herpesvirus 8/Kaposi's sarcoma-associated herpesvirus. *J. Virol.* 75, 3129–3140. doi: 10.1128/JVI.75.7.3129-3140.2001

Song, M. J., Li, X., Brown, H. J., and Sun, R. (2002). Characterization of interactions between RTA and the promoter of polyadenylated nuclear RNA in Kaposi's sarcoma-associated herpesvirus/human herpesvirus 8. *J. Virol.* 76, 5000–5013. doi: 10.1128/jvi.76.10.5000-5013.2002

Stedman, W., Kang, H., Lin, S., Kissil, J. L., Bartolomei, M. S., and Lieberman, P. M. (2008). Cohesins localize with CTCF at the KSHV latency control region and at cellular c-myc and H19/Igf2 insulators. *EMBO J.* 27, 654–666. doi: 10.1038/emboj.2008.1

Sun, R., Lin, S. F., Gradoville, L., and Miller, G. (1996). Polyadenylylated nuclear RNA encoded by Kaposi sarcoma-associated herpesvirus. *Proc. Natl. Acad. Sci. U.S.A.* 93, 11883–11888. doi: 10.1073/pnas.93.21.11883

Toth, Z., Brulois, K., Lee, H. R., Izumiya, Y., Tepper, C., Kung, H. J., et al. (2013). Biphasic euchromatin-to-heterochromatin transition on the KSHV genome following de novo infection. *PLoS Pathog.* 9:e1003813. doi: 10.1371/journal.ppat.1003813

Toth, Z., Maglinte, D. T., Lee, S. H., Lee, H. R., Wong, L. Y., Brulois, K. F., et al. (2010). Epigenetic analysis of KSHV latent and lytic genomes. *PLoS Pathog.* 6:e1001013. doi: 10.1371/journal.ppat.1001013

Toth, Z., Papp, B., Brulois, K., Choi, Y. J., Gao, S. J., and Jung, J. U. (2016). LANA-mediated recruitment of host polycomb repressive complexes onto the KSHV genome during de novo infection. *PLoS Pathog.* 12:e1005878. doi: 10.1371/journal.ppat.1005878

Toth, Z., Smindak, R. J., and Papp, B. (2017). Inhibition of the lytic cycle of Kaposi's sarcoma-associated herpesvirus by cohesin factors following de novo infection. *Virology* 512, 25–33. doi: 10.1016/j.virol.2017.09.001

Tsai, M. C., Manor, O., Wan, Y., Mosammaparast, N., Wang, J. K., Lan, F., et al. (2010). Long noncoding RNA as modular scaffold of histone modification complexes. *Science* 329, 689–693. doi: 10.1126/science.1192002

Uldrick, T. S., Wang, V., O'Mahony, D., Aleman, K., Wyvill, K. M., Marshall, V., et al. (2010). An interleukin-6-related systemic inflammatory syndrome in patients co-infected with Kaposi sarcoma-associated herpesvirus and HIV but without multicentric Castleman disease. *Clin. Infect. Dis.* 51, 350–358. doi: 10.1086/654798

Wen, K. W., and Damania, B. (2010). Kaposi sarcoma-associated herpesvirus (KSHV): molecular biology and oncogenesis. *Cancer Lett.* 289, 140–150. doi: 10.1016/j.canlet.2009.07.004

Withers, J. B., Li, E. S., Vallery, T. K., Yario, T. A., and Steitz, J. A. (2018). Two herpesviral noncoding PAN RNAs are functionally homologous but do not associate with common chromatin loci. *PLoS Pathog.* 14:e1007389. doi: 10.1371/journal.ppat.1007389

Yang, W. S., Campbell, M., and Chang, P. C. (2017). SUMO modification of a heterochromatin histone demethylase JMJD2A enables viral gene transactivation and viral replication. *PLoS Pathog.* 13:e1006216. doi: 10.1371/journal.ppat.1006216

Yang, W. S., Hsu, H. W., Campbell, M., Cheng, C. Y., and Chang, P. C. (2015). K-bZIP mediated SUMO-2/3 specific modification on the KSHV genome negatively regulates lytic gene expression and viral reactivation. *PLoS Pathog.* 11:e1005051. doi: 10.1371/journal.ppat.1005051

Yoon, J. H., Abdelmohsen, K., Kim, J., Yang, X., Martindale, J. L., Tominaga-Yamanaka, K., et al. (2013). Scaffold function of long non-coding RNA HOTAIR

in protein ubiquitination. *Nat. Commun.* 4:2939. doi: 10.1038/ncomms3939

Zhong, W., Wang, H., Herndier, B., and Ganem, D. (1996). Restricted expression of Kaposi sarcoma-associated herpesvirus (human herpesvirus 8) genes in Kaposi sarcoma. *Proc. Natl. Acad. Sci. U.S.A.* 93, 6641–6646. doi: 10.1073/pnas.93.13.6641

Ziegelbauer, J. M., Sullivan, C. S., and Ganem, D. (2009). Tandem array-based expression screens identify host mRNA targets of virus-encoded microRNAs. *Nat. Genet.* 41, 130–134. doi: 10.1038/ng.266

Conflict of Interest: The authors declare that the research was conducted in the absence of any commercial or financial relationships that could be construed as a potential conflict of interest.

Advantages of publishing in Frontiers

OPEN ACCESS
Articles are free to read for greatest visibility and readership

FAST PUBLICATION
Around 90 days from submission to decision

HIGH QUALITY PEER-REVIEW
Rigorous, collaborative, and constructive peer-review

TRANSPARENT PEER-REVIEW
Editors and reviewers acknowledged by name on published articles

Frontiers
Avenue du Tribunal-Fédéral 34
1005 Lausanne | Switzerland

Visit us: www.frontiersin.org
Contact us: info@frontiersin.org | +41 21 510 17 00

REPRODUCIBILITY OF RESEARCH
Support open data and methods to enhance research reproducibility

DIGITAL PUBLISHING
Articles designed for optimal readership across devices

FOLLOW US
@frontiersin

IMPACT METRICS
Advanced article metrics track visibility across digital media

EXTENSIVE PROMOTION
Marketing and promotion of impactful research

LOOP RESEARCH NETWORK
Our network increases your article's readership